15th AIVC Conference
The Role of Ventilation

held at Palace Hotel, Buxton, UK
27-30 September 1994

Proceedings Volume 2

Preface

International Energy Agency

The International Energy Agency (IEA) was established in 1974 within the framework of the Organisation for Economic Co-operation and Development (OECD) to implement an International Energy Programme. A basic aim of the IEA is to foster co-operation among the twenty-one IEA Participating Countries to increase energy security through energy conservation, development of alternative energy sources and energy research development and demonstration (RD&D). This is achieved in part through a programme of collaborative RD&D consisting of forty-two Implementing Agreements, containing a total of over eighty separate energy RD&D projects. This publication forms one element of this programme.

Energy Conservation in Buildings and Community Systems

The IEA sponsors research and development in a number of areas related to energy. In one of these areas, energy conservation in buildings, the IEA is sponsoring various exercises to predict more accurately the energy use of buildings, including comparison of existing computer programs, building monitoring, comparison of calculation methods, as well as air quality and studies of occupancy. Seventeen countries have elected to participate in this area and have designated contracting parties to the Implementing Agreement covering collaborative research in this area. The designation by governments of a number of private organisations, as well as universities and government laboratories, as contracting parties, has provided a broader range of expertise to tackle the projects in the different technology areas than would have been the case if participation was restricted to governments. The importance of associating industry with government sponsored energy research and development is recognized in the IEA, and every effort is made to encourage this trend.

The Executive Committee

Overall control of the programme is maintained by an Executive Committee, which not only monitors existing projects but identifies new areas where collaborative effort may be beneficial. The Executive Committee ensures that all projects fit into a pre-determined strategy, without unnecessary overlap or duplication but with effective liaison and communication. The Executive Committee has initiated the following projects to date (completed projects are identified by *):

I	Load Energy Determination of Buildings*
II	Ekistics and Advanced Community Energy Systems*
III	Energy Conservation in Residential Buildings*
IV	Glasgow Commercial Building Monitoring*

V Air Infiltration and Ventilation Centre
VI Energy Systems and Design of Communities*
VII Local Government Energy Planning*
VIII Inhabitant Behaviour with Regard to Ventilation*
IX Minimum Ventilation Rates*
X Building HVAC Systems Simulation*
XI Energy Auditing*
XII Windows and Fenestration*
XIII Energy Management in Hospitals*
XIV Condensation*
XV Energy Efficiency in Schools*
XVI BEMS - 1: Energy Management Procedures*
XVII BEMS - 2: Evaluation and Emulation Techniques
XVIII Demand Controlled Ventilating Systems*
XIX Low Slope Roof Systems
XX Air Flow Patterns within Buildings*
XXI Thermal Modelling
XXII Energy Efficient Communities
XXIII Multizone Air Flow Modelling (COMIS)
XXIV Heat Air and Moisture Transfer in Envelopes
XXV Real Time HEVAC Simulation
XXVI Energy Efficient Ventilation of Large Enclosures
XXVII Evaluation and Demonstration of Domestic Ventilation Systems
XXVIII Low Energy Cooling Systems

Annex V Air Infiltration and Ventilation Centre

The IEA Executive Committee (Building and Community Systems) has highlighted areas where the level of knowledge is unsatisfactory and there was unanimous aggreement that infiltration was the area about which least was known. An infiltration group was formed drawing experts from most progressive countries, their long term aim to encourage joint international research and increase the world pool of knowledge on infiltration and ventilation. Much valuable but sporadic and uncoordinated research was already taking place and after some initial groundwork the experts group recommended to their executive the formation of an Air Infiltration and Ventilation Centre. This recommendation was accepted and proposals for its establishment were invited internationally.

The aims of the Centre are the standardisation of techniques, the validation of models, the catalogue and transfer of information, and the encouragement of research. It is intended to be a review body for current world research, to ensure full dissemination of this research and based on a knowledge of work already done to give direction and firm basis for future research in the Participating Countries.

The Participants in this task are Belgium, Canada, Denmark, Germany, Finland, France, Netherlands, New Zealand, Norway, Sweden, Switzerland, United Kingdom and the United States of America.

15th AIVC Conference "The Role Of Ventilation"

Contents Volume 1

Session 1: Ventilation Strategies

Efficiency of Ventilation in Office Buildings
R R Walker, M K White, R Kaleem, N C Bergsøe 1

Annex 27 - Domestic Ventilation , Occupant Habits' Influence on Ventilation Need
L-G Månsson 13

Case Studies of Passive Stack Ventilation Systems in Occupied Dwellings
Lynn Parkins 25

Passive Ventilators in New Zealand Homes: Part 1 Numerical Studies and Part 2 Experimental Trials
M R Bassett 35

Ventilation by the Windows in Classrooms: A Case Study
V Richalet, B Beheregaray, G Guarracino, C Dornier, L Janvier 57

Single-sided Ventilation: A Comparison of the Measured Air Change Rates with Tracer Gas and with the Heat Balance Approach
D Ducarme, L Vandaele, P Wouters 67

Natural Ventilation Through a Single Opening - The Effects of Headwind
G M J Davies, M J Holmes 77

Investigation of Ventilation Conditions in Naturally Ventilated Single Family Houses
N C Bergsøe 93

Session 2: Indoor Air Quality (Posters)

Methods for Investigating Indoor Air Conditions of Ventilated Rooms
H Müller, P Vogel 101

High Quality Ventilation Systems - A Tool to Reduce SBS Symptoms
A Kumlin, J Drakfors, P Emteborg 109

Numerical assessment of thermal comfort and air quality in an office with displacement ventilation
G Gan 119

The Role of Infiltration for Indoor Air Quality - A Case Study in Multifamily Dwelling Houses in Poland
A Baranowski 133

Effectiveness of Various Means of Extract Ventilation at Removing Moisture from a Kitchen
T Shepherd, L Parkins, A Cripps 141

Water Evaporation of 5 Common Indoor Plants Under Various Climate Conditions
B Strickler 151

Role and Tasks of Ventilation in Modern Buildings: A Case Study for Silesian Dwelling Houses
M B Nantka 163

The Role of Ventilation in Controlling the Dispersion of Radon Gas from a Cellar in a Domestic House
I C Ward, F Wang, S Sharples, A C Pitts, M Wolliscroft 173

Detection and Mitigation of Occupational Radon Exposure in Underground Workplaces
P Korhonen, H Kokotti, P Kalliokoski 183

The Mechanical Ventilation of Suspended Timber Floors for Radon Remediation - A Simple Analysis
M Woolliscroft 193

Using Pressure Extension Tests to Improve Radon Protection of UK Housing
P Bell, A Cripps 203

Session 3: Energy Impact of Ventilation, Building Design for Optimum Ventilation

Modelling Fluctuating Air Flows Through Building Cracks
S Sharples, R G Palmer 215

Air-Tightness of U.S. Dwellings
M Sherman, D Dickerhoff 225

Energy Efficient Ventilation of Bathrooms
M Sandberg, C Blomquist 235

The Relative Energy Use of Passive Stack Ventilators and Extract Fans
M Woolliscroft 245

Volume Control of Fans to Reduce the Energy Demand of Ventilation Systems
F Steimle 257

A Design Guide for Thermally Induced Ventilation
C Filleux, S Krummenacher, P Kofoed 263

Air Movement in a Re-clad Medium Rise Building and its Effect on Energy Usage
H G Kula, I C Ward 273

The Performance of Dynamic Insulation in Two Residential Buildings
J T Brunsell 285

Ventilation and Energy Flow Through Large Vertical Openings in Buildings
J van der Maas, J L M Hensen, A Roos 289

Session 4: Ventilation and Energy (Posters)

Survey of Mechanical Ventilation Systems in 30 Low Energy Dwellings in Germany
J Werner, U Rochard, J Zeller 303

Simple and Reliable Systems for Demand Controlled Ventilation in Apartments
S Svennberg 313

Ventilation Concept, Indoor Air Quality & Measurement Results in the "Passivhaus Kranichstein"
W Feist, J Werner 321

Improvement of Domestic Ventilation Systems
J Heikkinen, M-L Pallari 333

The Capenhurst Ventilation Test House
D A McIntyre, S L Palin, R E Edwards 343

Effective Ventilation Strategies Demands Flexible System Design
A Svensson 353

Energy and Environmental Protection Aspects of Desiccant Cooling
F Dehli 361

The Testing and Rating of Terminals used on Ventilation Systems
P Welsh 371

Domestic Ventilation with Variable Volume Flows
K Ulrich Kramm, G Polenskie 381

Contents Volume 2

Session 4:Ventilation and Energy (Posters)(Continued)

Heat Losses from Suspended Timber Floors with Insulation
D J Harris, S J M Dudek 387

Reducing Air Infiltration Losses in Naturally Ventilated Industrial Buildings
P J Jones, G Powell 397

Passive Stack Ventilation
J Palmer, L Parkins, P Shaw, R Watkins 411

Comparing Predicted and Measured Passive Stack Ventilation Rates
A Cripps, R Hartless 421

Ventilation Air Flow Through Window Openings in Combination with Shading Devices
A C Pitts, S Georgiadis 431

Use of Passive Stack Systems in Multi-storey Dwellings: Assessment of Performance
C Irwin, R E Edwards 441

A Study of Various Passive Stack Ventilation Systems in a Test House
L M Parkins 445

A Review of Weather Data for Natural Ventilation
M J M Arif, G L Levermore 455

The Limits of Natural Ventilation in Deep Office Spaces
M White, R Walker 465

Session 5: Calculation, Measurement and Design Tools

The Evaluation of Ventilation Effectiveness Measurements in a Four Zone Laboratory Test Facility
J R Waters, C E Brouns 469

Determination of Local Mean Ages of Air by the Homogeneous Injection Tracer Gas Technique
H Stymne, C Blomquist, M Sandberg 473

Tracking Air Movement in Rooms
D K Alexander, P J Jones, H Jenkins, N Harries 483

Application of a Multi-zone Airflow and Contaminant Dispersal Model to Indoor Air Quality Control in Residential Buildings
S J Emmerich, A K Persily, G N Walton 493

Two-zones Model for Predicting Passive Stack Ventilation in Multi-storey Dwellings
J G Villenave, J-R Millet, J Ribéron 509

Practical Methods for Improving Estimates of Natural Ventilation Rates
I S Walker, D J Wilson 517

A Suggested Standard Methodology for the Assessment of the Performance of Domestic Ventilation Systems
R E Edwards, C Irwin 527

Simulation of Passive Cooling and Natural Facade Driven Ventilation
V Dorer, A Weber 531

Session 6: Measurement and Modelling (Posters)

Dare You Risk Designing Without the Best Tools?
J Littler, M Davies, D Cuckow, A Jarvis, B McCarthy 541

Design Tool for Optimizing the Selection of Ventilation Plants
G Wernstedt 545

Applications of the Air Infiltration and Ventilation Centre's Numerical Database
M S Orme 553

Air Movement Studies in a Large Parish Church Building
I C Ward, F Wang 563

Particle-Streak-Velocimetry for Room Air Flows
F. Scholzen, A Moser, P Suter 573

Thermal Simulation of Ambients with Regard to Ventilated Attics
E L Krüger, O D Corbella 585

Flow Paths in a Swedish Single Family House - A Case Study
B Hedin 593

Determination of k-factors of HVAC System Components Using Measurements and CFD Modelling
Riffat, L Shao, A G Woods 615

Measurement and Modelling of Aerosol Particle Flow in an Environmental Chamber
N Adam, K W Cheong, S B Riffat, L Shao 625

Full Scale Modelling of Indoor Air Flows
F Steimle, J Röben 635

Investigation of Effect of Tracer Species on Tracer Mixing Using CFD
S B Riffat, L Shao 645

Preliminary Ventilation Effectiveness Measurements by a Pulse Tracer Method
M R Bassett, N Isaacs 655

Ventilation and Utility Program Incentives in the Northwest U.S.
D T Stevens, D O'Connor 665

Climate-based Analysis of Residential Ventilation Systems
N E Matson, H E Feustel, J L Warner, J Talbott 673

Measuring Subfloor Ventilation Rates
R Hartless, M K White 687

Standardised Measurements of the Cooling Performance of Chilled Ceilings
F Steimle, B Mengede, K Schiefelbein 697

Air Flow Through Smooth and Rough Cracks
H-G Kula, S Sharples 709

Comparison of the Accuracy of Detailed and Simple Model of Air Infiltration
J-M Fürbringer 719

An Experimental and Theoretical Investigation of Airflow Through Large Horizontal Openings
J S Kohal, S B Riffat, L Shao 729

Algorithm for Interzonal Particle Flow Through Openings
K W Cheong, N Adam, S B Riffat 741

Session 7: Ventilation Strategies

Occupant Satisfaction and Ventilation Strategy - a case study of 20 public buildings
G Donnini, V H Nguyen, J Molina 749

Natural Ventilation Strategies to Mitigate Passive Smoking in Homes
M Kolokotroni, M D A E S Perera 759

Predicted and Measured Air Change Rates in Houses with Predictions of Occupant IAQ Comfort
T Hamlin W Pushka 771

The Air Lock Floor
H J C Phaff, W F De Gids 779

The Role of Ventilation
15th AIVC Conference, Buxton, Great Britain
27-30 September 1994

Heat Losses from Suspended Timber Floors with Insulation

D J Harris, S J M Dudek

Dept of Architecture, University of Newcastle upon Tyne, United Kingdom

Heat Losses From Suspended Timber Floors with Insulation

D.J.Harris, S. J-M. Dudek. Dept of Architecture. University of Newcastle upon Tyne. NE1. 7RU.

Summary

Ventilation of the void below suspended timber floors is necessary to prevent dampness, which leads to wet and dry rot. The air flow beneath such a floor has been investigated for a range of ventilator hole positions, using a full-sized test room. The variations in heat losses with ventilation rate have been measured, for floors with and without insulation. The use of radiation barriers in place of conventional thermal insulation was found to cut down the heat losses significantly at low ventilation rates, but was not so effective at higher rates.

Introduction

It was shown in a previous paper [1] how the rate of heat loss from a suspended floor without insulation increases with the rate of ventilation of the under-floor void. Here, the thermal performance of similar floors, with thermal insulation added, has been measured over the same range of conditions.

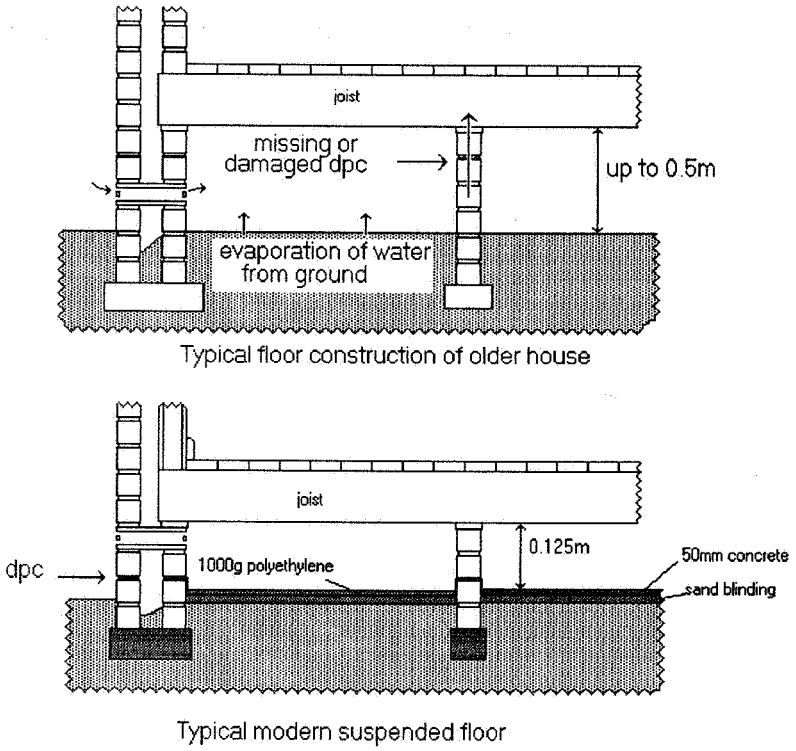

Figure 1. Typical suspended timber floor constructions

Suspended Floors

A number of mathematical techniques to enable the heat loss from solid floors to be predicted have been devised [2-4]. However, the usefulness of these methods in practical situations is limited because they are very sensitive to the properties of the ground beneath the floor. The thermal conductivity of earth can vary by a factor of

three depending on the soil type and conditions, rendering even the most sophisticated methods prone to large errors. The analysis of the heat loss from suspended floors is further complicated by fluctuations in the rate of ventilation in the under-floor cavity, which affect the thermal resistance of the air space. Hence, no attempt has been made here to formulate a mathematical solution to the problem. For most practical purposes, the simple graphical method devised by Anderson, [5] which assumes a fixed ventilation rate, is sufficiently accurate. In this paper we are concerned with ways of minimising the heat losses while maintaining the necessary conditions beneath the floor to prevent rot.

The air in the void below a suspended floor often has a high relative humidity. In modern houses, drying out of the construction water is the main source of moisture, but in older buildings, most of it comes from the evaporation of water from damp earth (Figure 1).

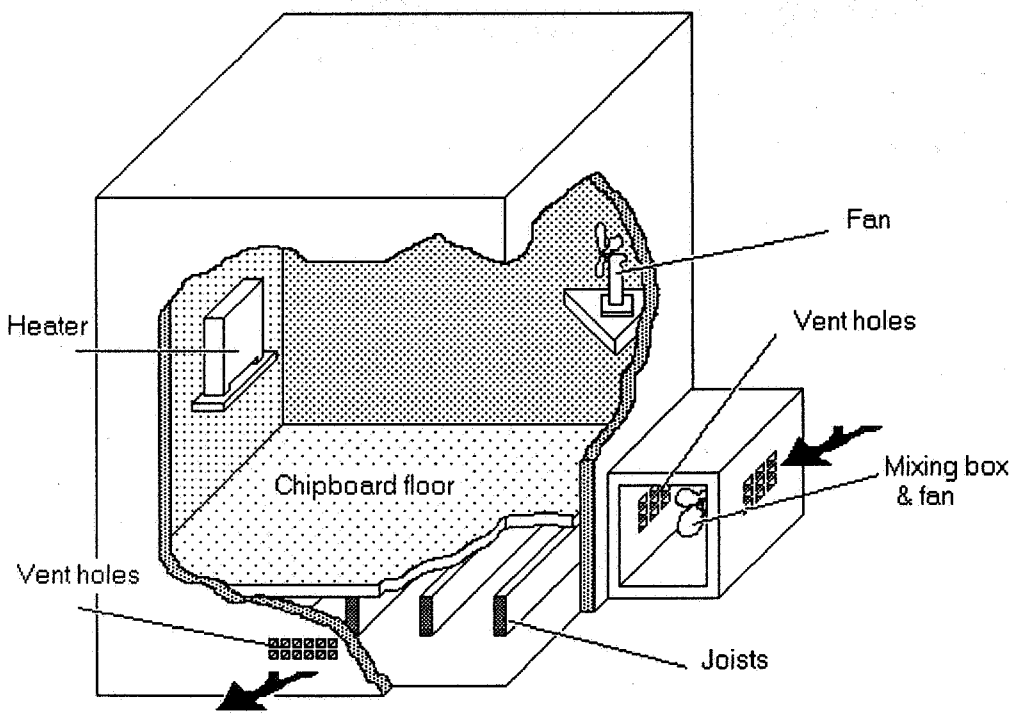

Figure 2. The test room with suspended floor.

Experimental Work - Test Room

A series of measurements were carried out on a 3m by 3m suspended floor with a 0.5m cavity beneath built into a test room situated in an environmental chamber. This has been described in detail elsewhere [1] and is shown in figure 2. Each measurement was made under steady-state conditions over a period of at least eight hours. Ventilation holes, simulating air bricks of the regulation size, were made in the opposite walls of the under-floor space, giving an orifice size equivalent to 4500mm^2 in each wall, and a variable-speed fan was used to force air into the space, simulating the effect of a constant velocity wind perpendicular to the wall. The air

movement was measured using anemometers and a smoke injection technique. The temperatures and heat fluxes were measured using platinum resistance thermometers and heat flow sensor mats

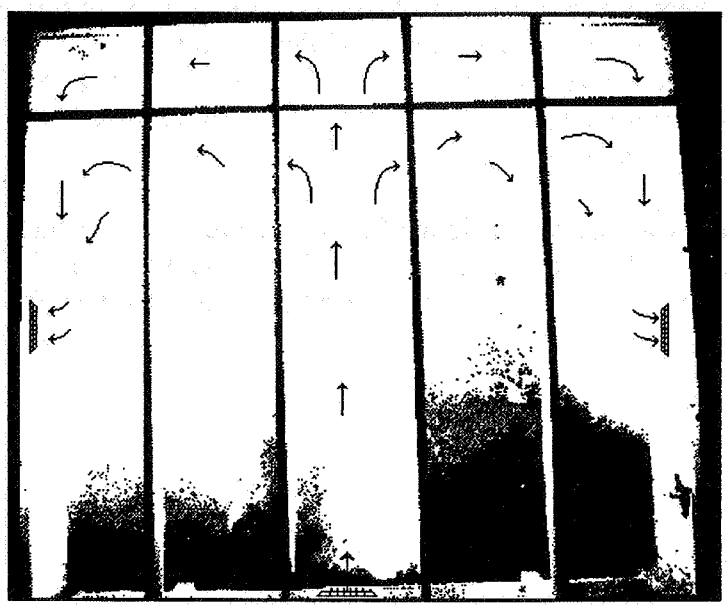

Figure 3. The air flow as shown by smoke tests using a glass floor.

Results - Ventilation patterns

In order to observe the air flow beneath the floor, the timber floor was replaced with glass panels laid upon the wooden joists, and observations were made from above. Smoke was injected into the incoming air stream so that the pattern of air movement could be observed. These were photographed using a still camera (figure 3). A range of inlet and outlet vent positions was used, and the results are shown in figures 4 to 7. They show that the overall pattern is determined principally by the position of the vent on the windward side in relation to the side wall.

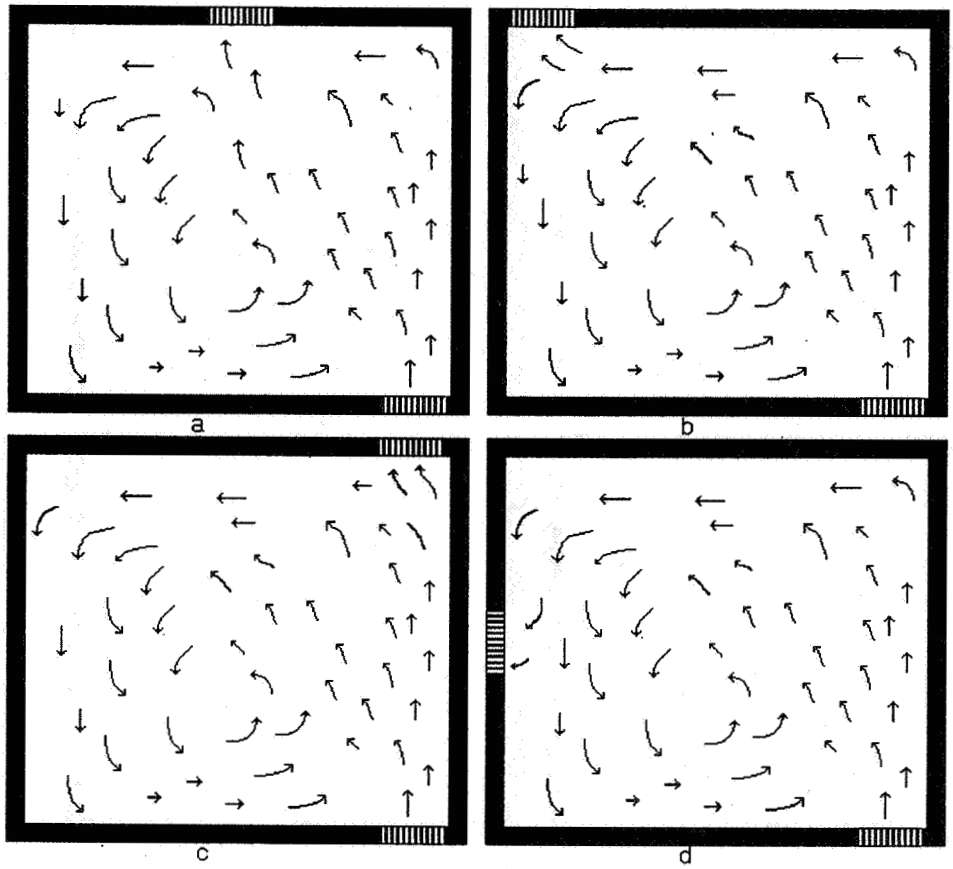

Figure 4.

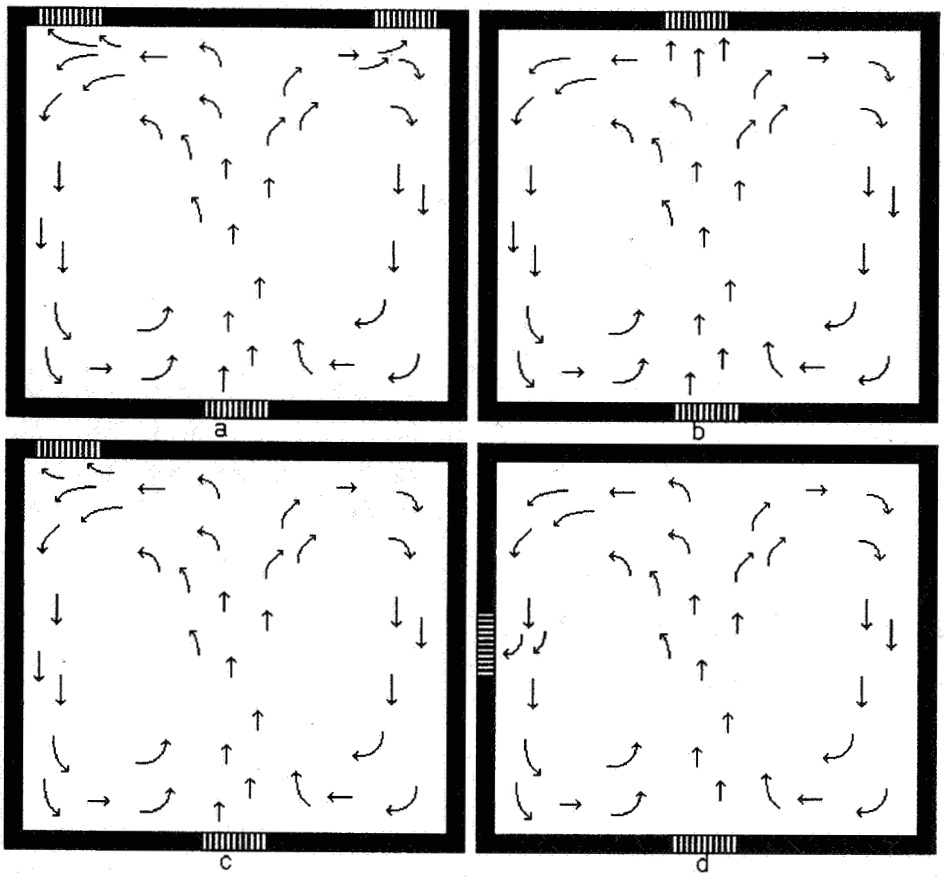

Figure 5.

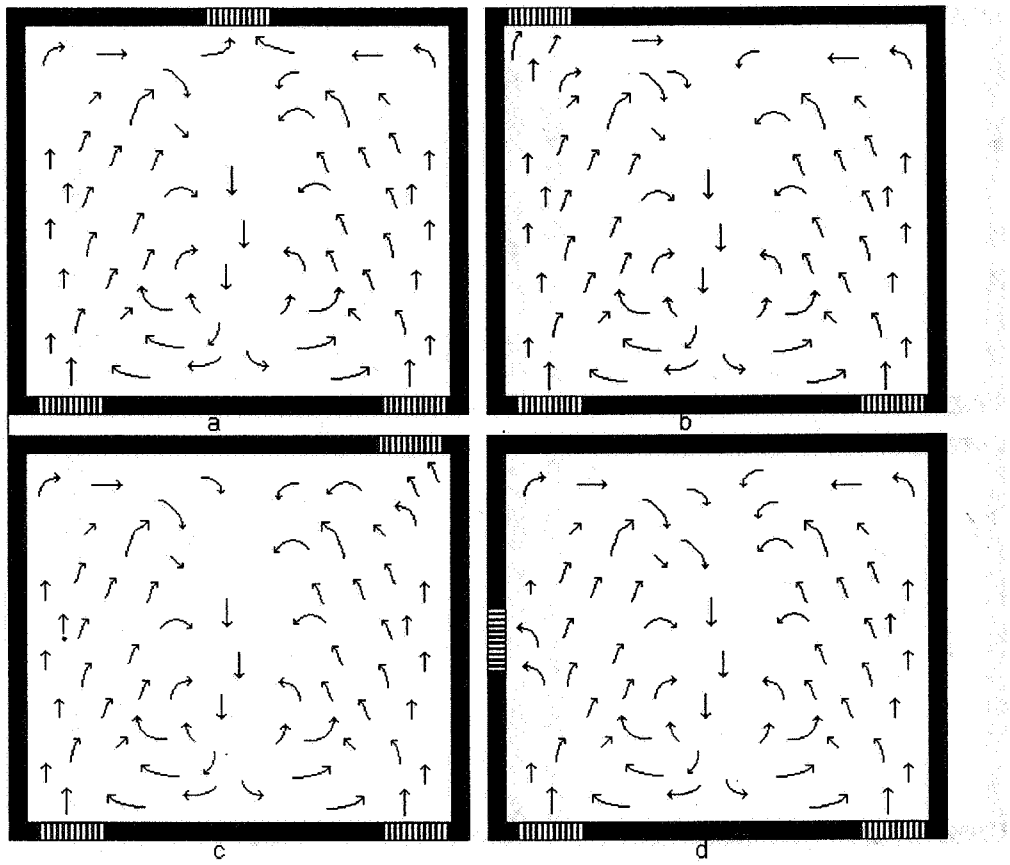

Figure 6.
Figures 4-6. Plans of the under-floor void, showing the air flow for different vent positions.

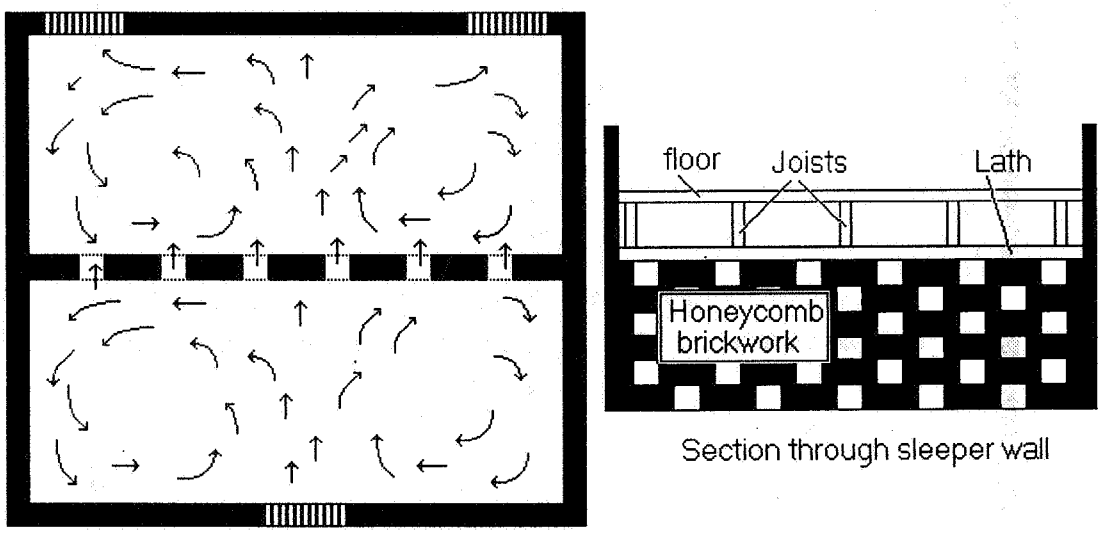

Figure 7. Airflow with sleeper wall present

The location of the vents on the leeward side has little effect upon the general air flow pattern. The addition of a sleeper wall changes the pattern and reduces the velocity of the air beyond it as shown in figure 7. Good mixing is obtained throughout the floor for all vent positions. The principal determinant of the general air flow patterns is the

position of the inlet vent in relation to the corner of the building. The two main patterns, for a single vent on the windward side, are shown in figures 4 and 5. The pattern for two vents on the windward side is shown in figure 6. In reality, of course, there is no "inlet or "outlet" vent. The vents are identical, and whether air enters or leaves by a particular vent depends on the wind direction in the immediate vicinity.

Heat losses

By changing the speed of the fan, the rate of under-floor ventilation was varied from 0 - 1.5 air changes per hour. The heat flux and temperature were measured and the effective U-values calculated (figure 8). Over a range of ventilation rates from 0 - 1.5 air changes per hour (nominal airflow rate at the vent zero to 4m/s) the effective U-value of the floor without insulation increased from 0.62 to 0.87 W/m^2k, an increase of 40%.

The U-value of the floor was measured without insulation, and with 30mm of rigid extruded polystyrene installed as shown in figure 9.

The most effective location for the insulation should be on top of the floor (position a) since most of the heat bridges are eliminated; this proves to be the case, but the difference is small in comparison with the overall U-value. In this position, the effect at zero ventilation rate is to reduce the heat loss to 51.7% of its original value, and at 1.5 air changes per hour the heat loss is 42.2% of that for the uninsulated floor. When located beneath the joists (figure 9b) the heat loss at zero ventilation is 50% of the original, whilst at 1.5 air changes it is 57.4%, i.e. slightly less effective.

Addition of radiation barriers.

The overall heat loss is made up of a number of components - conduction, convection, radiation and ventilation. The ratio of radiation to convection heat loss is about 3:1 with no ventilation. The radiation losses can be reduced by using low-emissivity material adjacent to the air space, thus reducing the level of infra-red radiation to the nearby surfaces. The insulation was removed and thin aluminium foil (ε=0.05) was stapled to the underside of the joists to form a continuous sheet. At low air change rates it was effective, and reduced the heat loss by just over 50% (figure 10), but at 1.5 air changes the reduction in heat loss was just under 30%. This is to be expected, since at higher ventilation rates the radiation heat losses constitute a lower proportion of the total heat loss.

Conclusions

If the rate of ventilation below suspended floors is high, then greater heat losses ensue. The relationship between heat loss and ventilation rate was measured under a range of controlled conditions in a full-size test room, and the heat loss was found to increase by 40% when the ventilation rate increased from zero to 1.5 air changes per hour. When the floor was insulated, the corresponding increase was much lower, and depended on the position of the insulation. Simple radiation barriers provide a much cheaper way of reducing the heat loss, and are effective at low ventilation rates but cease to be as effective at higher rates, the U-value ranging from 0.32 at zero ventilation to 0. 62 at 1.5 air changes. The initial payback period of such foils is considerably less than for polystyrene insulation, but unless the ventilation rate is very low the overall savings over a number of years will be considerably less. When

the floor is insulated the heat loss at high ventilation rates is not significantly greater than under low ventilation. Measurements on occupied houses have shown that the relative humidity below such floors is often dangerously high. If the floor is insulated, then more air vents can be added, increasing the ventilation rate and eliminating problems due to moisture in the void, but without increasing the heat loss unduly.

References

1. Harris, D.J., Dudek, S. J-M., "The variation of heat loss through suspended floors with ventilation rate". 14th AIVC Conference, Copenhagen. September 1993.
2. Anderson, B. R. "Calculation of the Steady-State Heat Transfer Through a Slab-on-Ground Floor." Building & Env. Vol. 26. No. 4. pp 405-415. 1991.
3. Delsante, A.E. "A Comparison Between Measured and Calculated Heat Losses Through a Slab on Ground Floor." Building & Env. Vol 25, No.1. pp25-31. 1990.
4. Hagentoft, C-E, Claesson, J. "Heat Loss to the Ground from a Building - I. General Theory." Building & Env. Vol. 26. No. 2. 1991.
5. Anderson, B.R. "U-values of Uninsulated Ground Floors: Relationship with Floor Dimensions." BSERT. 12(3) 103-105 (1991).

Acknowledgements

The authors wish to acknowledge the financial support of the Science and Engineering Council of the UK. for this work.

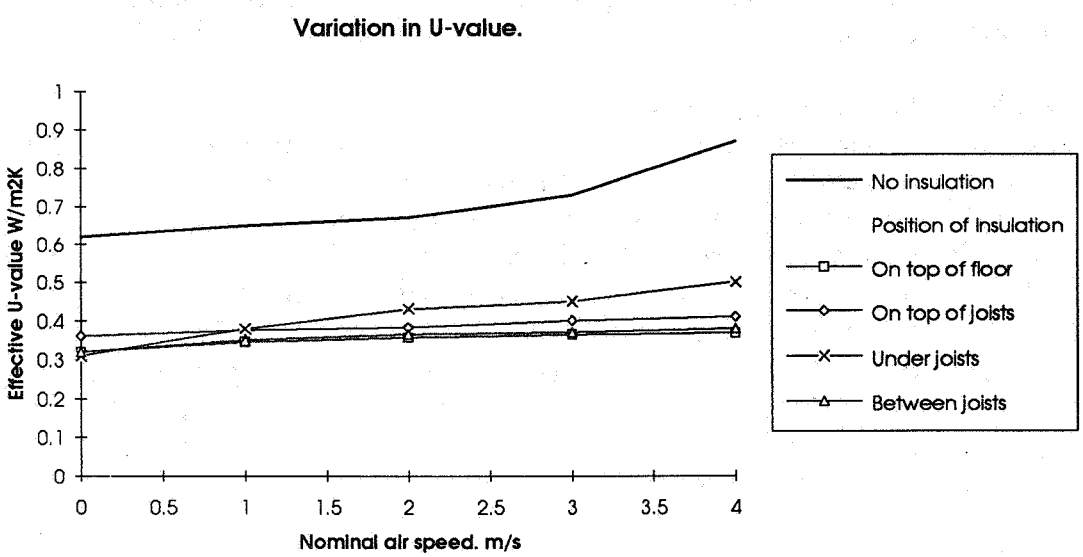

Figure 8. U-values of insulated floors.

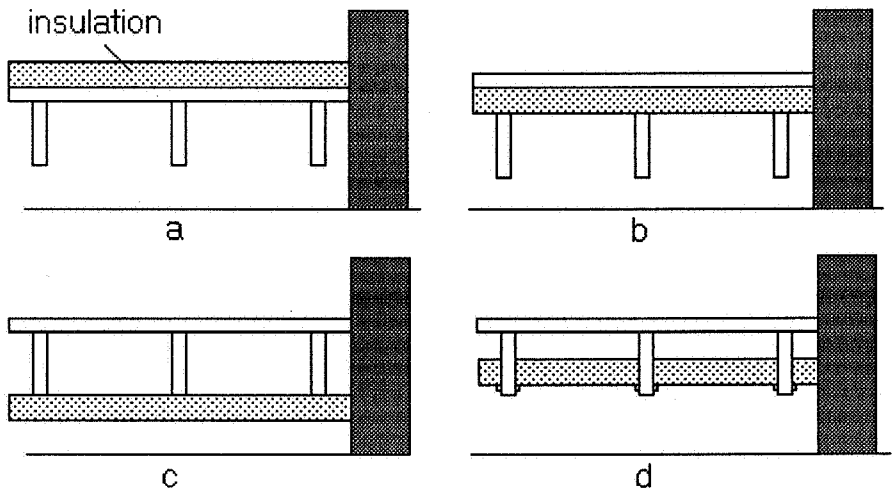

Figure 9. Positions in which the insulation was installed.

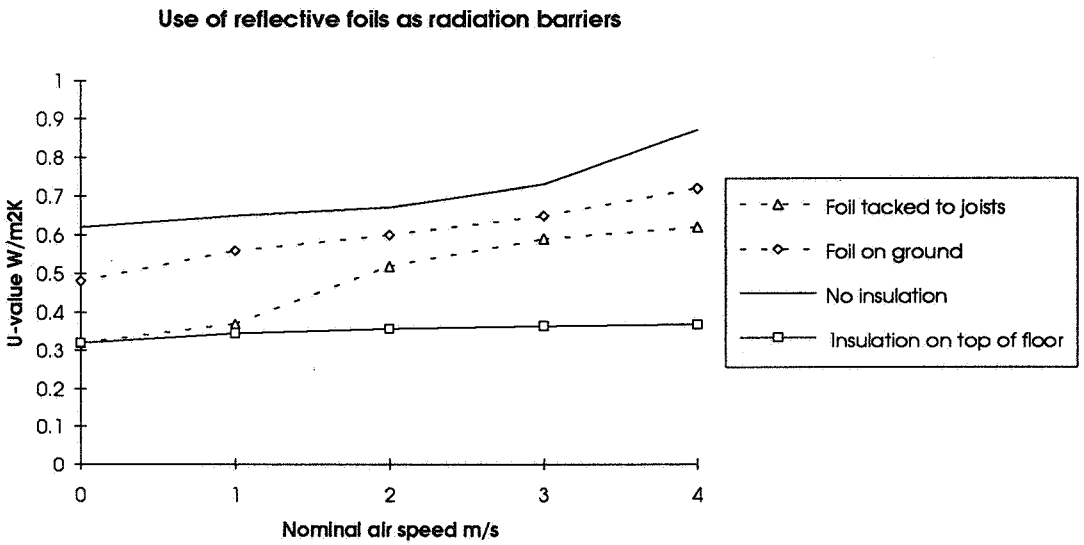

Figure 10. U-values of reflective foils.

The Role of Ventilation
15th AIVC Conference, Buxton, Great Britain
27-30 September 1994

Reducing Air Infiltration Losses in Naturally Ventilated Industrial Buildings

P J Jones, G Powell

The Welsh School of Architecture, University of Wales, Cardiff, Bute Building, King Edward VII Ave, Cardiff CF1 3AP

SYNOPSIS

The UK factory stock is predominantly naturally ventilated. Measurements performed in this class of building have indicated that air infiltration rates in factories are usually excessive in relation to occupants' requirements for health and safety, resulting in an energy penalty.

As part of a project to investigate construction options for energy efficient industrial buildings, three factories of different cladding construction types were designed and then built at Aberaman, South Wales. One of the primary aims of the project was to reduce air infiltration losses and increase air tightness. Attention has been paid to design details in order to achieve these aims. The construction process was observed in order to monitor site practice and workmanship.

Tracer gas tests (primarily constant concentration) tests and air leakage (fan pressurisation) tests have been performed to determine the air infiltration rate and air leakage performance of the factories. A thermographic survey was used to assist the identification of the major air leakage sites. The results have shown that air infiltration rates have been reduced by the order of 40% for the three 'conventional' cladding constructions. Air leakage rates measured at 50 Pa are the lowest achieved in this class of building in the UK, based on published data. The major site for air leakage was found to be the eaves detail.

1.0 INTRODUCTION

Modern factories are predominantly naturally ventilated. In winter, ventilation is mainly provided by natural leakage through the construction. In summer this is often supplemented when necessary by mechanically operated roof ventilators.

Measurements carried out by The Welsh School of Architecture (WSA) in Welsh Development Agency, (WDA) factories [1], have indicated that natural ventilation rates over a range of factories are usually excessive in relation to occupants' requirements for health and safety, resulting in an energy penalty. The potential therefore exists for reducing ventilation rates whilst still maintaining adequate fresh air levels.

Thermographic investigations have indicated that the major locations for air infiltration occur at the various construction details around components, such as roof ventilators, doors, flues, etc. In particular, the eaves and wall details are often major sources of air leakage. Earlier work [2] used a zonal ventilation model to estimate that ventilation rates could be reduced by about half as a result of better sealing of construction details, whilst still maintaining adequate fresh air levels for occupancy.

This paper describes the ventilation performance of three new factories, each of a different cladding construction, that were designed to have 'reduced' air infiltration rates. The three

factories, Units 40, 41 and 42, were constructed at Aberaman Industrial Estate, South Wales by the WDA.

2.0 CONSTRUCTION TYPES AND DESIGN DETAILS

In each factory the eaves height was 5m and the ridge height 7m. Units 40 and 41 had a production space floor area of 840 m^2 whereas Unit 42 was smaller, having a production space floor area of 720 m^2. Rooflights were linear eaves to ridge and of a double skin construction. Each of the three factories had external 'wrap around' office space and a low level (1m high) masonry perimeter wall. The three constructions are described below.

2.1 Sandwich (Lining Panel) Cladding System (Unit 40).

The sandwich construction is detailed in Figure 1. It can be summarised as follows:

> An outer liner sheet of coated steel of thickness 0.55 mm. A breather paper, to separate the ventilation path in the air gap of the external profile from the insulation layer. 80 mm of rock-fibre quilt insulation of density 33 kgm^{-3} and k-value 0.034 $Wm^{-2}K^{-1}$. A vapour barrier on the warm side of the insulation to reduce the risk of interstitial condensation. An inner liner sheet of coated steel of thickness 0.4 mm.
>
> Fixing was by means of Z-spacers onto the cladding rails and purlins, with an adhesive thermal barrier tape (density 175 kgm^{-3}) separating the Z-spacer from the external liner sheet. Ventilated profile fillers were used to control ventilation on the 'cold side' of the insulation between the breather paper and the outer cladding sheet. The design U-value was 0.40 $Wm^{-2}K^{-1}$.

The main disadvantage with this construction is that unless there is a high standard of site supervision, it is potentially more prone to problems of poor workmanship. However, it is a relatively inexpensive system in its construction costs.

2.2 Liner Tray Cladding System (Unit 41)

The liner tray construction is detailed in Figure 2. It can be summarised as follows:

> An outer liner sheet of coated steel of thickness 0.55 mm. A breather paper, to separate the ventilation path in the external profile from the insulation layer. 80 mm of rock-fibre insulation batt of density 33 kgm^{-3} and k-value 0.034 $Wm^{-2}K^{-1}$, fitted into the liner tray. The structural liner tray of steel with a thickness of 1.0 mm, with a tray width of 450 mm and a depth of 80 mm.
>
> Fixing of the external liner sheet to the liner tray was by means a top hat section with a rock-fibre adhesive thermal barrier tape (density 175 kgm^{-3}) separating the top-hat

section from the external liner sheet. The liner trays were fixed to the cladding rails and purlins. A mastic sealant strip was stuck to the side of each tray prior to fixing to prevent air infiltration between adjacent trays. The design U-value was 0.40 $Wm^{-2}K^{-1}$.

This construction was similar to the sandwich cladding system above except that the inner liner sheet and vapour barrier had been replaced by a structural liner tray. This offered the advantage over the sandwich construction that there was less risk of interstitial condensation, as the liner tray itself acted as a vapour barrier. However, there was the disadvantage that each joint offered a potential cold bridge and infiltration path if not properly detailed.

2.3 Composite Cladding System (Unit 42)

The composite construction is detailed in Figure 3. It can be summarised as follows :

The composite panel was 450 mm width and was supplied in lengths of 6 m. The panel incorporated a coated steel of 0.6 mm outer skin and 0.7 mm inner skin. It contained 80 mm of a rock-fibre lamella insulation of density 120 kgm^{-3} and k-value 0.037 $Wm^{-2}K^{-1}$

The U-value for this construction was 0.45 $Wm^{-2}K^{-1}$ which complied with current building regulations.

3.0 AIR INFILTRATION RATE PERFORMANCE

3.1 Introduction

Air infiltration rates were measured using a 10 channel automated tracer gas system developed at WSA. The majority of data was collected under constant concentration although some tracer decay tests were performed. Nitrous Oxide (N_2O) was used as the tracer gas. The continuous measurements were carried out for between 1 and 2 weeks for each factory.

In addition to factory 'as-built' air infiltration rate measurements, further experiments were performed to evaluate the ventilation performance of door opening of the installed summer time cooling fans. There has been concern that cooling or extract fans are not achieving design extraction rates as buildings have become more air tight as insufficient make-up air is allowed to infiltrate through the envelope. This was of particular relevance to the project factories as increased air tightness was one of the primary aims of the exercise.

3.2 Results

The mean values and ranges of measured air infiltration rate are given in Table 1. The effect of door opening and ventilation fans operating either separately or in combination is presented in Table 2.

Table 1: Summary of mean air infiltration rates, wind speed and stack (ranges given in brackets).

Unit Number	Air Infiltration Rate (ach^{-1})	Wind Speed (ms^{-1})	Stack ($°C^{½}$)
40	0.16 (0.05-0.41)	1.8 (0-5.7)	3.6 (2.6-4.4)
41	0.15 (0.07-0.33)	2.4 (0-6.7)	2.6 (1.0-3.4)
42	0.16 (0.04-0.45)	3.2 (0-8.8)	2.3 (0.6-3.4)

Table 2: Summary of mean ventilation rates, wind speed and stack (ranges given in brackets).

Unit Number	Door Open (ach^{-1})	Door Open and Fans On (ach^{-1})	Door Closed and Fans On (ach^{-1})
40	1.2	2.9	2.7
41	1.3	3.7	2.0
42	1.3	1.9*	1.5*

* only one of two fans in operation

3.3 Discussion

The three factories had very similar average air infiltration rates, being 0.16 ach^{-1}, 0.15 ach^{-1} and 0.16 ach^{-1} for Units 40, 41 and 42 respectively. On the recommended basis [3] that 8 ls^{-1} of fresh air per person should be provided in a factory environment, these air infiltration rates would give safe occupancy levels of 28, 26 and 24 people respectively for Units 40, 41 and 42.

Comparison with the results from modelling [2] which indicated that infiltration rates could be reduced to 0.15 ach^{-1} for this type of factory was good. Maximum measured air infiltration rates (corresponding to wind speeds of 7 ms^{-1}) have been reduced from a predicted level of 0.8 ach^{-1} to 0.4 ach^{-1}.

Opening the loading door increased the ventilation rate to either 1.2 or 1.3 ach^{-1}.

Operating the summer time ventilation fans increased the ventilation rate to 2.7, 2.0 and 1.5 ach^{-1} for Units 40, 41 and 42 respectively. In Unit 42 only one fan was operational. The design air change rate of 4 ach^{-1} was not being achieved. Opening the loading door increased the ventilation rate to 2.9, 3.7 and 1.9 ach^{-1} for Units 40, 41 and 42 respectively which provided some indication that there was not sufficient make up air in the factories as-built due to their relatively low air leakage. Opening the door could enable the fans to achieve the design extraction rate if wind conditions were suitable, which implied that directional effects were also present. It would seem likely that the installed fan capacity was not sufficient to provide the design extraction rate under all conditions.

4.0 AIR LEAKAGE PERFORMANCE

4.1 Introduction

Air leakage tests were performed using a fan pressurisation test rig developed at WSA. Each of the tests were performed using a single variable speed fan that had a maximum flow rate of 8.6 m^3s^{-1}.

The main component areas of interest were loading bay doors and roof ventilators. In these cases during the experiment the component was sealed using polythene sheeting and the tests repeated under different levels of sealing, i.e. door only sealed, doors and vents sealed. This enabled the potential for reductions in ventilation losses by the use of high performance components to be estimated.

4.2 Results

The air leakage characteristic curves for each unit are shown in Figures 4, 5 and 6 respectively. The data was fitted to a curve of the following form:

$$Q = C\Delta P^n \quad m^3s^{-1}$$

where:

$Q =$ Air leakage Rate (m^3s^{-1})
$C =$ Flow Coefficient
$\Delta P =$ Internal To External Static Pressure Difference (Pa)
$n =$ Flow Exponent

The unknowns C and n were found from the curve fitting exercise. Then, by putting ΔP equal to 50 Pa the air leakage rate at 50 Pa was be deduced. Table 3 below presents the results obtained at a pressure difference of 50 Pa for each of the factories. The normalised air leakage rate is the absolute air leakage rate at 50 Pa divided by the external envelope area (excluding the floor) of each factory. The experimental error for the fan pressurisation technique was estimated to be of the order of 8%.

Table 3: Absolute and Normalised Air Leakage Rates at 50 Pa

Unit No:		Door And Vents Sealed	Door Only Sealed	As-Built
40	m^3s^{-1}	7.10	7.67	7.72
	$m^3h^{-1}m^{-2}$	13.86	14.94	15.05
41	m^3s^{-1}	7.44	8.15	8.17
	$m^3h^{-1}m^{-2}$	14.51	15.88	15.95
42	m^3s^{-1}	6.21	6.77	6.75
	$m^3h^{-1}m^{-2}$	13.54	14.76	14.72

The air leakage rates measured for each of the factories with roof ventilators and loading door sealed gave a measure of the air leakage performance of the fabric only. From the normalised air leakage rates given in Table 3 above it can be seen that Unit 42 (composite panel) was tightest followed by Unit 40 (conventional sandwich) and finally Unit 41 (liner tray). The difference in normalised air leakage rate performance across construction types was only small. Unit 40 was 2.4% more leaky than Unit 42 and Unit 41 was 7.2% more leaky than Unit 42. It was considered that the liner tray construction was most leaky due to leakage through the butt joints between adjacent panels.

The factory as-built tests show that the same rank ordering of constructions occur even after the addition of components. The percentage differences in normalised air leakage performance are Unit 40 was 2.2% more leaky than Unit 42, Unit 41 was 8.4% more leaky than Unit 42. These relative differences were similar to the relative differences obtained for the factory sealed cases above, showing that the leakage effects of components was similar for each of the three constructions.

Removing the sealing on the roof ventilators increased the absolute air leakage rates for each of the factories. The percentage increases were 8.0%, 9.5% and 9.0% for Units 40, 41 and 42 respectively. These results show that fitting the roof vents into the envelope increased the air leakage by between 8% and 9%. The close agreement of the measured increases in air leakage showed that the leakage effects of roof vents was the same for each of the constructions. A visual inspection of the roof ventilators showed that air leakage could occur around each of the roof ventilators as well as through the closed louvers within the component.

Removing the sealing on each of the loading doors resulted in increases in air leakage rate of 0.65%, 0.25% and -0.003% for Units 40, 41 and 42 respectively. These results implied that there was no real measurable air leakage increase as a result of fitting a loading door in each of the constructions. A greater increase may have been measured if the door sealing had been removed before the roof vent sealing. Time constraints, however, prevented this strategy from being tested.

4.3 Comparison with other UK Factory Data

BSRIA have published work [4] concerning the measurement of air leakage rates in factories. Two of the buildings were of similar construction (cladding sandwich) and size (1300 m^2 floor area) to those at Aberaman.

A bar chart showing the measured air leakage rate for the Aberaman factories and the BSRIA factories is given in Figure 7 using the building code key shown below in Table 4.

Table 4: Building Code Key

Code Number	Building	Sealing Level	Leakage At 50 Pa ($m^3h^{-1}m^{-2}$)
1	BSRIA Building #2	As-Built	24.5
2	BSRIA Building #3	As-Built	26
3	Aberaman Unit 40	As-Built	15.05
4	Aberaman Unit 40	Sealed	13.86
5	Aberaman Unit 41	As-Built	15.95
6	Aberaman Unit 41	Sealed	14.51
7	Aberaman Unit 42	As-Built	14.72
8	Aberaman Unit 42	Sealed	13.54

From the air leakage rates presented above in Table 4 and from Figure 7 it can be seen that the buildings at Aberaman were considerably 'tighter' than similar buildings in terms of air leakage rates. A comparison of the Aberaman factories' recorded air leakage results with results from the authors' unpublished results for a range of factories has shown these constructions to be the most air tight UK factories, based on available data.

5.0 IDENTIFICATION OF AIR INFILTRATION SITES USING THERMOGRAPHIC SURVEYS

The main purpose of a thermographic survey has been to assess the standard of installation of insulation. However, the thermographic equipment can also be used for leakage detection. Leakage detection is assisted if the survey is carried out in conjunction with the fan pressurisation test equipment.

An internal thermographic survey to assess the standard of installation of insulation of each factory had indicated that for the liner tray construction (Unit 41) there were some examples of air infiltrating along the joint between adjacent trays and at the eaves detail for all units.

External thermographic surveys of each factory were carried out in order to locate the main air leakage sites on the external faces of the building envelope. First the survey was performed without the pressurisation fans switched on. The pressurisation fans were then switched on (causing the factories to be pressurised with respect to outside) and the survey repeated. The

assumption was that pressurisation would force warm air through the leakage sites, hence exaggerating the effect that would occur under normal ventilation (infiltration) processes and thereby making the detection of air leakage more pronounced.

For all units, the thermograms indicated that infiltration occurred at the eaves, the verge, around the fire exit door and around the main loading door. As an example, Figures 8 and 9 show air leakage at the eaves of Unit 42, as-built and under pressurisation respectively. Switching on the pressurisation fan exaggerated the heating effect of the air leakage. However, switching on the fan has not identified any new air leakage sites

6.0 CONCLUSIONS

The average infiltration rates of the three factories were measured to be similar at between 0.15 and 0.16 ach^{-1} over the prevailing wind and temperature conditions. This was considered to be about half the average air infiltration rate for typical factories of this size and construction. The average air infiltration rates would give safe occupancy levels of 28, 26 and 24 people for Units 40, 41 and 42 respectively, based on a fresh air requirement of 8 ls^{-1} per person. The results indicated that ventilation rates can be significantly reduced in factories offering the potential for large energy savings. However, at the same time care must be taken to ensure adequate fresh air ventilation for occupants.

Significant increases in ventilation rate were recorded during loading door opening, with ventilation rates increasing to about 1.3 ach^{-1}. The use of summertime roof ventilation fans gave ventilation rates between 2.0 to 2.7 ach^{-1}, and opening the loading doors whilst running the roof ventilators resulted in ventilation rates between 2.9 and 3.7 ach^{-1}. The WDA design for summertime ventilation is 4.0 ach^{-1}, with doors closed. It is likely that the increased sealing measures have resulted in difficulty in providing make-up air through infiltration.

The difference in air leakage performance between the three different constructions was less than 10%, with the composite panel being the most air tight, the conventional lining panel second and the liner tray third. It was considered that the liner tray construction was the most leaky due to leakage through the butt joints between adjacent panels.

The air leakage performance of the three units with doors and vents sealed was 13.86, 14.51 and 13.54 $m^3h^{-1}m^{-2}$ for Units 40, 41 and 42 respectively. Compared with available data from other air leakage measurements performed in the UK, these factories have the lowest recorded air leakage rates.

Incorporation of roof ventilators into the building envelope increased the air leakage rates by 8% - 9% in each case. There was no measurable increase in air leakage attributed to around the closed loading doors.

The thermographic surveys indicated that the main leakage sites identified in this test were at the eaves. Combining thermographic surveys with pressurisation resulted in a more

pronounced thermographic view of air leakage. However, even without pressurisation the major sites were identified. A thermographic survey is therefore appropriate for qualitatively assessing the air leakage as well as the integrity of the insulation.

The main source of air leakage was identified to occur at the eaves detail. This proved to be the most difficult detail to design and construct in relation to air leakage and also to thermal cold bridging. Achieving an airtight eaves detail in all construction types is difficult in practice, due to the angle the roof makes with the wall, the structural penetration of the eaves for gutters, overhangs, and the difficulty in inspecting the workmanship. This is therefore an area that needs to be addressed if further air tightness is required.

This work has demonstrated that low air infiltration rates can be achieved in practice. However, there is also the need to maintain good air quality for the health and safety of the workforce. The ventilation design of factories should be examined, including any provision for summertime ventilation cooling, to ensure that in addition to achieving a good thermal performance, good air quality for occupants must be ensured.

ACKNOWLEDGEMENTS

The work has been funded by the Welsh Development Agency and Rockwool (UK) Ltd.

REFERENCES

1 JONES, P. J. and POWELL, G.
"Monitoring of The Welsh Development Agency's Project to Demonstrate the Efficiency of Low Energy Factories. (ETSU Agreement No. E/5C/2923/904)".
University of Wales Institute of Science and Technology, Cardiff, 1988.

2 JONES P. J. and POWELL, G.
"An Investigation of Insulated Cladding Constructions For Industrial Buildings"
University of Wales, Cardiff, 1993.

3 CIBSE Guide A1. Environmental Criteria for Design.
Chartered Institute of Building Service Engineers, London 1986. ISBN 0 900953 29 2.

4 POTTER , I. N. and JONES, T. J.
"Ventilation Heat Loss in Factories and Warehouses, Technical Note 7/92"
The Building Services Research and Information Association. BSRIA 1992. ISBN 0 86022 2969.

Figure 1: Lining Panel (Sandwich) Construction

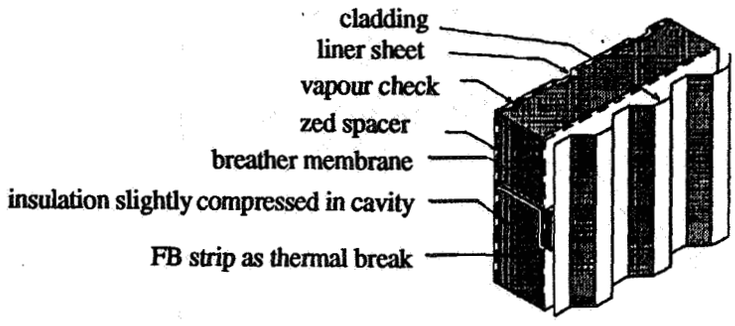

Figure 2: Liner Tray Construction

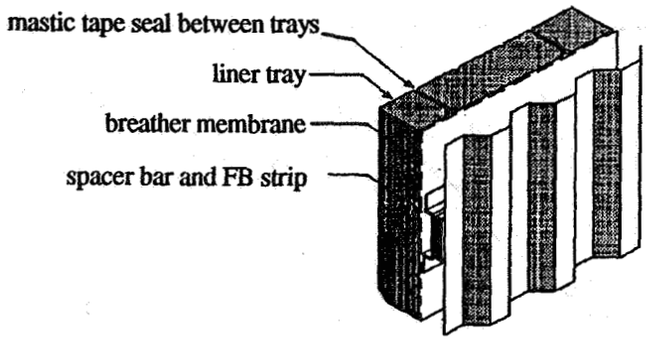

Figure 3: Composite Panel Construction

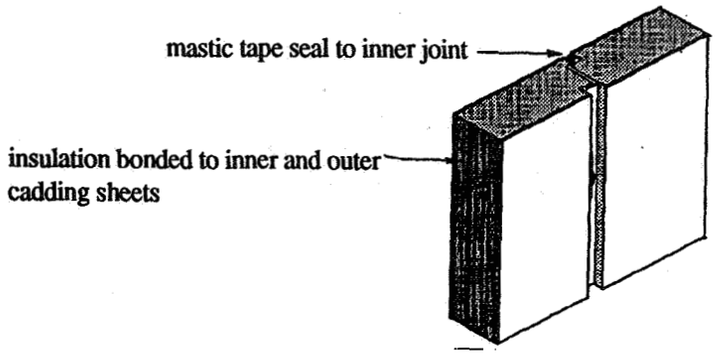

Figure 4: Air Leakage Curve For Unit 40 - Sandwich Construction

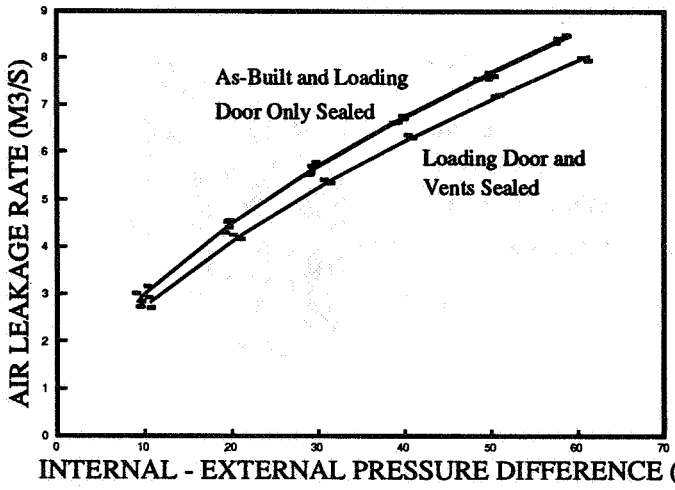

Figure 5: Air Leakage Curves For Unit 41 - Liner Tray Construction

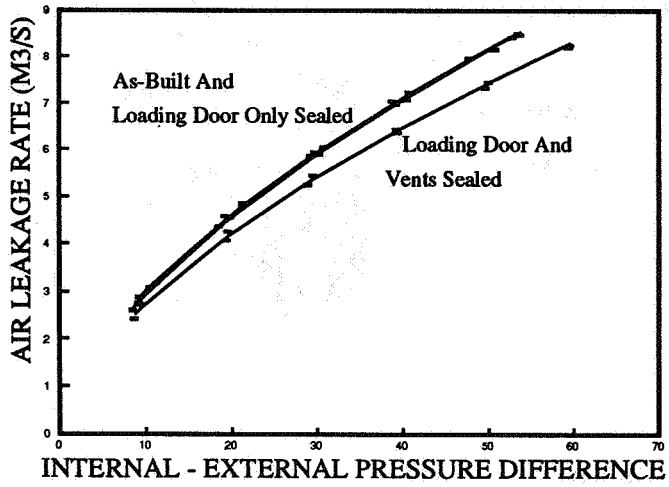

Figure 6: Air Leakage Curve For Unit 42 - Composite Panel Construction

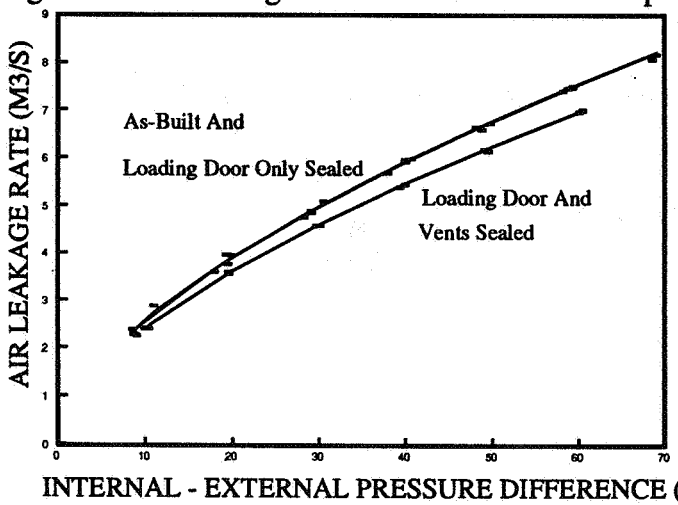

Figure 7: Comparison of Aberaman Air Leakage with Published Data.

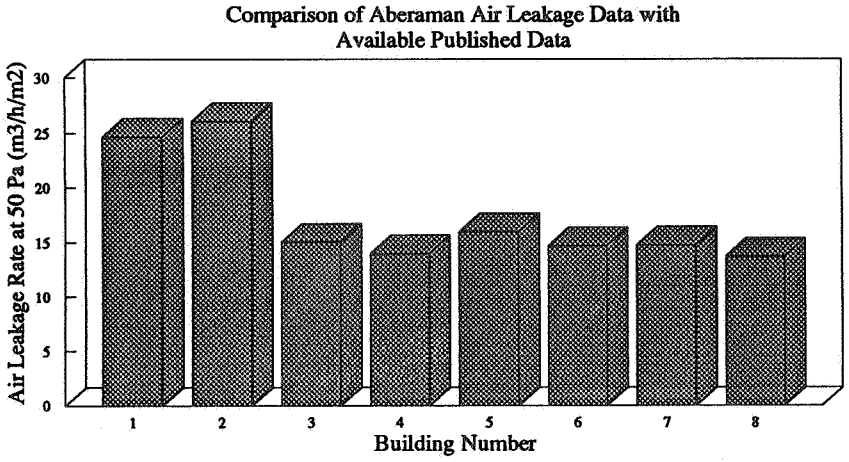

Figure 8: Thermogram of Eaves, Unit 42, Factory Not Pressurised.

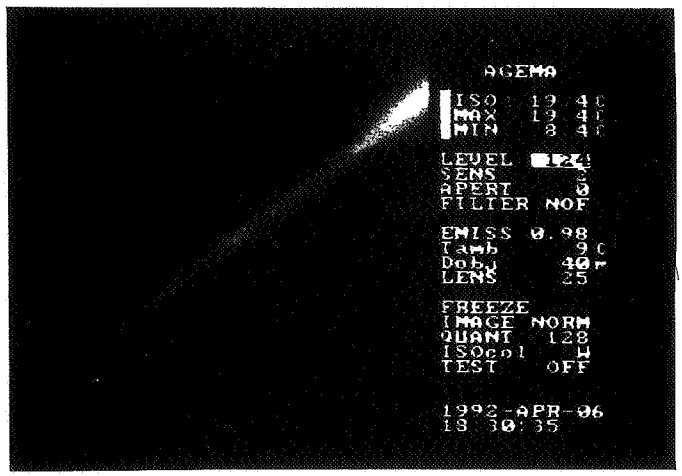

Figure 9: Thermogram of Eaves, Unit 42, Factory Pressurised.

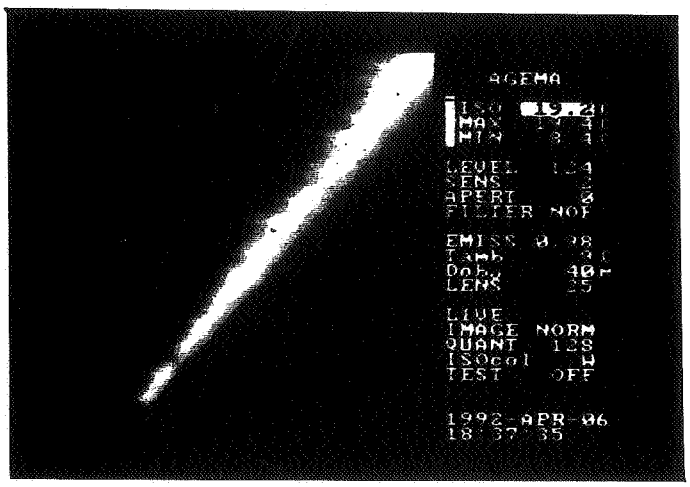

The Role of Ventilation
15th AIVC Conference, Buxton, Great Britain
27-30 September 1994

Passive Stack Ventilation

J Palmer, L Parkins, P Shaw, R Watkins

Databuild, 4 Venture Way, Aston Science Park
Birmingham, B7 4AP, United Kingdom

PASSIVE STACK VENTILATION:
Case Studies of Reverse Flow and Humidity Control

J Palmer, L Parkins, P Shaw, R Watkins.

SYNOPSIS

The adequate ventilation of houses is essential for both the occupants and the building fabric. As air-tightness standards increase, background infiltration levels decrease and extra ventilation has to be designed into the building.

Passive stack ventilation has many advantages - particularly when employed in low cost housing schemes - but it is essential that it performs satisfactorily. This paper give the results from monitoring two passive stack ventilation schemes. One scheme was a retrofit into refurbished local authority houses in which a package of energy efficiency measures had been taken and condensation had been a problem. The other series of tests were conducted on a new installation in a Housing Association development. Nine houses were monitored each of which had at least two passive vents.

Measurements were taken over periods of three weeks in each dwelling and included; wind speed and direction, internal and external temperatures, humidity, and air velocity in the ventilation duct. The data were recorded every quarter hour.

The results show air flow rates by the passive ducts equivalent to approximately 1 room air change per hour. The air flow in the ducts was influenced by both, internal to external temperature difference and wind speed and direction. An important finding was the need to site the vents in the correct location. In those houses where the vents were installed on the roof slope facing the prevailing wind, a location not recommended in current guidance, the air flow was in the reverse direction for the majority of the time due to the design of the terminal. However, in those houses with correctly sited vent terminals of recommended design[1], reverse flow was negligible.

1. Introduction

Too little ventilation in houses often causes excessive condensation and this can lead to problems with both the maintenance of the building fabric and the health of the occupants[2]. This is a particular problem for Local Authorities who have large building stocks, which are often occupied by those least able to afford good heating and ventilation.

As part of an energy efficient renovation programme, undertaken by a Local Authority, passive stack ventilation systems were installed in a number of no-fines houses built in the 1950's. In order to avoid problems of condensation as a result of too little ventilation they incorporated passive stack ventilators in the kitchen and bathroom of each house. The systems were commercially available units and included humidity controlled dampers at the inlet of the passive stack ducts and in the replacement window frames. Mechanical ventilation systems were avoided because it had been observed that these were often over-ridden by the tenants who wished to reduce their electricity costs. Together with the passive ventilation the houses were also fitted with central heating and external insulation.

A Housing Association in Birmingham had similar reasons for specifying passive stack vents in the kitchen and bathroom of three new two-story semi-detached houses. These houses were also monitored.

Guidance has only recently been issued by BRE[3], consequently not all the systems were built to this specification.

2. Monitoring

The ventilation performance of the passive stack systems was monitored in six of the renovated houses: both the bathroom and kitchen stacks. During the tests the houses were occupied in their normal fashion. As in previous studies[4,5] the following parameters were monitored:

Weather:	Wind speed and direction
	External temperature
Stack conditions:	Air speed
	Relative humidity
	Temperature - entrance and exit
Room conditions:	Temperature
	Humidity

The temperature sensors were three wire platinum resistance thermometers. The duct air speed was measured by an omnidirectional hot wire anemometer. All the sensors were connected to a Campbell Scientific data logger. Measurements were taken every 30 seconds and averaged to quarterly hourly data points by the data logger. The monitoring period for each house was approximately three weeks and extended over the period from November 1992 to March 1993 and January 1994 to February 1994. In all 170 days of data were obtained for 15 variables.

3. Results

3.1 Air Flow Rate and Ventilation

The data were analysed to provide the mean air speed in the stack as shown in Table 1.

HOUSE	Kitchen	Kitchen	Bathroom	Bathroom	House
1	0.74	0.78	0.81	2.68	0.25
2	0.81	0.90	0.69	1.76	0.20
3	0.66	0.73	0.53	2.18	0.16
4	0.59	0.63	0.75	3.03	0.24
5	0.55	0.59	0.55	2.26	0.17
6	0.75	0.99	0.35	0.87	0.15

Table 1. Mean air flows and air change rates for all data points.

The air change rates given are based on either the room volume or the house volume and represent the average rate obtained over the whole of the monitoring period. The maximum duct speeds observed tended to be twice the mean value and hence the maximum air change rates achieved would be similarly greater. Whilst the maximum air flows tended to be well above the mean it was seldom that values below 0.2 m/s were recorded. Figure 1 shows a typical distribution of duct air speed. It also indicates that the duct speed has a strong dependency on wind speed. This was seen in 11 out of the 12 stacks monitored.

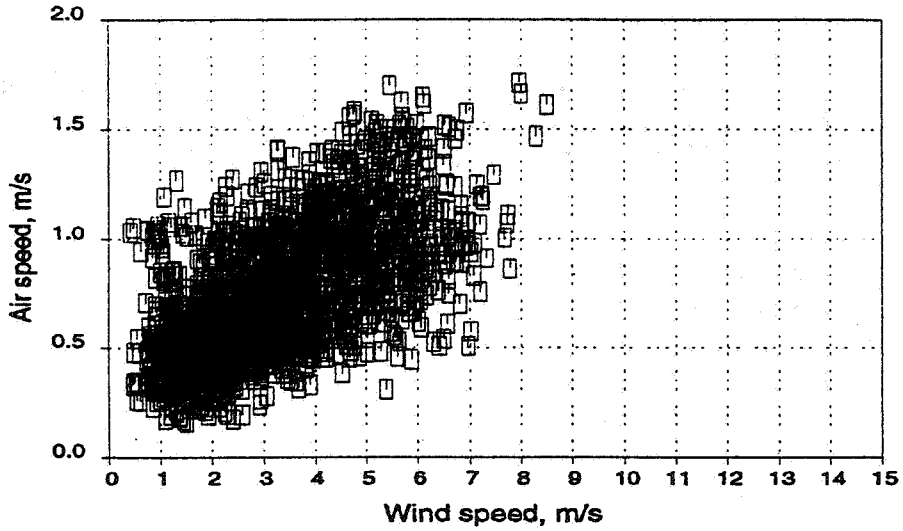

Figure 1. Stack duct air speed related to wind speed - roof pitch termination; house 1 kitchen.

3.2 Reverse Flow

On closer examination of the data it was discovered that there were large periods of time, in some of the houses, when the flow in the duct was in the reverse direction to the expected stack flow. Outside air was entering at roof level and descending down the stack, possibly distributing kitchen or bathroom air around the rest of the house. By selecting occurrences when external conditions appeared at the base of the stack these incidents of reverse flow were isolated. On analysis the reverse flow condition was found to be highly dependent on the wind direction: previous work[6] had implicated wind speed as a cause of reverse flow.

Wind Sector (45^0)	% House 1	% House 3
0-44	18	4
45-89	8	26
90-134	14	58
135-179	53	7
180-224	84	0
225-269	95	1
270-314	94	0
315-359	85	0

Table 2 shows the percentage of reverse flow for the bathroom stack for two of the houses for each 45° sector of wind direction.

Table 2. Occurrence of reverse flow related to wind direction.

These figures are illustrated in Figures 2 and 3 which also indicate that the determining factor was the location of the stack exit, or roof terminal.

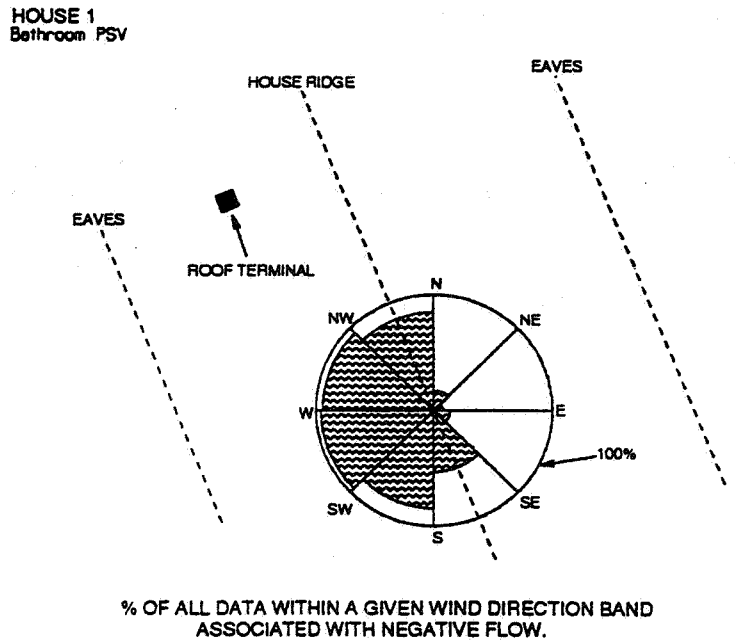

Figure 2. Distribution of incidence of reverse flow against wind direction House 1 - bathroom.

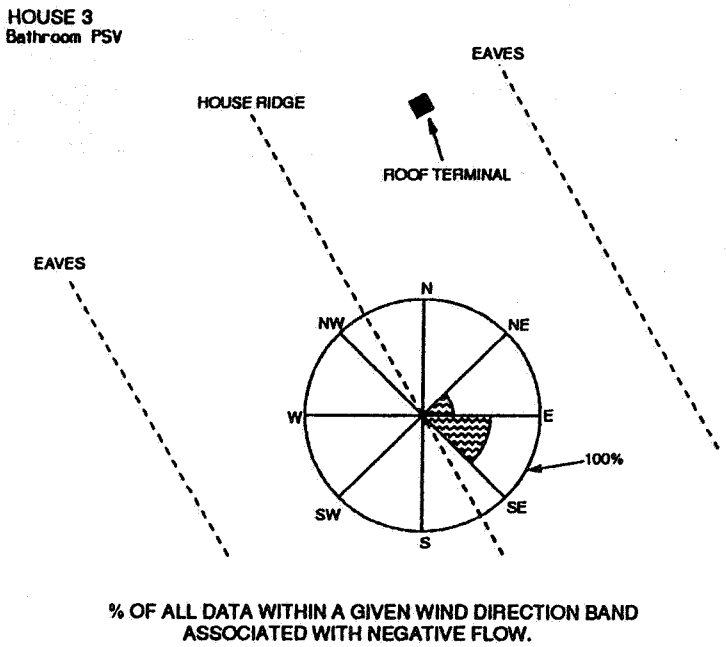

Figure 3. Distribution of incidence of reverse flow against wind direction House 3 - bathroom.

The figures clearly show how the roof terminal installed on the roof pitch facing the prevailing

south-west wind experienced considerable periods of reverse flow. In the house in which the terminal was on the leeward side reverse flow was less frequent and only occurred when the wind was in the appropriate quadrant. This location is contrary to recent guidance, developed as a result of monitoring studies such as these.

3.3 Humidity Control

To allow for an investigation of the humidity control, in two of the houses the monitoring had been carried out without the humidity controlled dampers at the base of the stack.

The humidities measured were within the normal range expected of occupied houses. Mean values were between 40% and 60% RH, with standard deviations of around 6% RH. The maximum values were typically between 60 - 90% RH.

Figure 4 shows the minimum, mean and maximum relative humidities recorded in the kitchen and bathroom of each house.

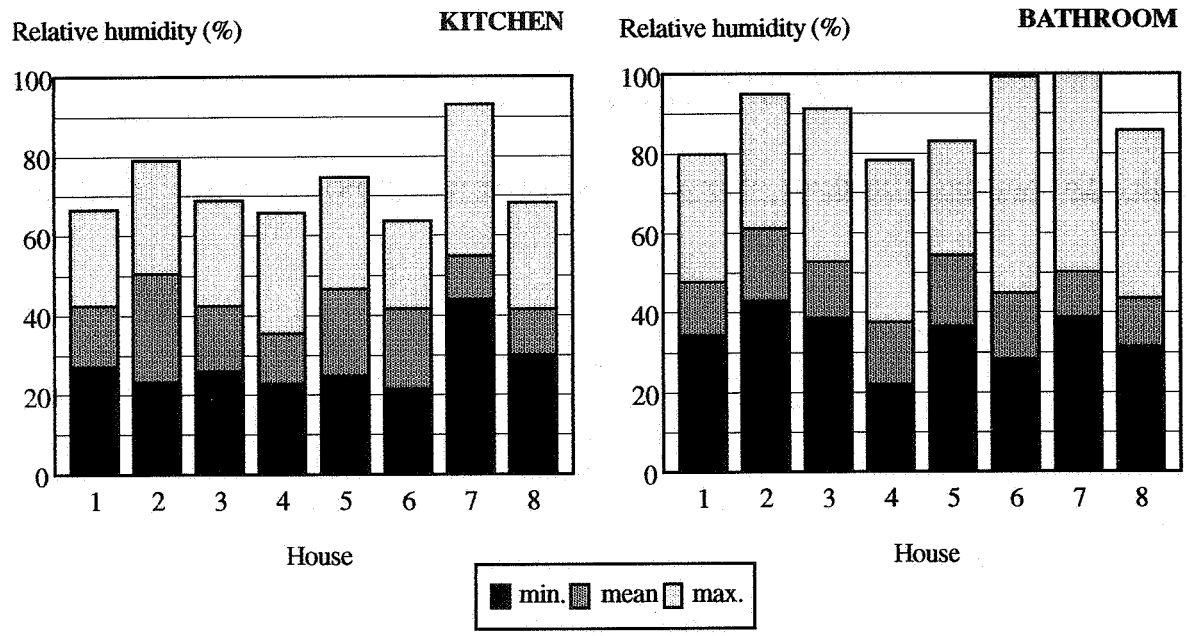

Figure 4. RH levels in the kitchen and bathroom of each house

Visual scanning of the plotted data did not reveal any substantial relationship between duct air speed and humidity in the room it was serving. In order to investigate the data more thoroughly it was decided to try to relate an increase in duct air speed to an increase in the humidity in the room in the previous 15 minute period. In a house with humidity control this should show an increase in the humidity causing the control dampers to open and thereby increase the air flow rate provided other variables affecting the flow rate remain constant and the humidity control device responds fully within the measurement time..
In the uncontrolled house this would not be expected, although it is appreciated that a small increase in speed may be seen because of the reduced density of the moister air. When plotted out the results were as figures 5 and 6.

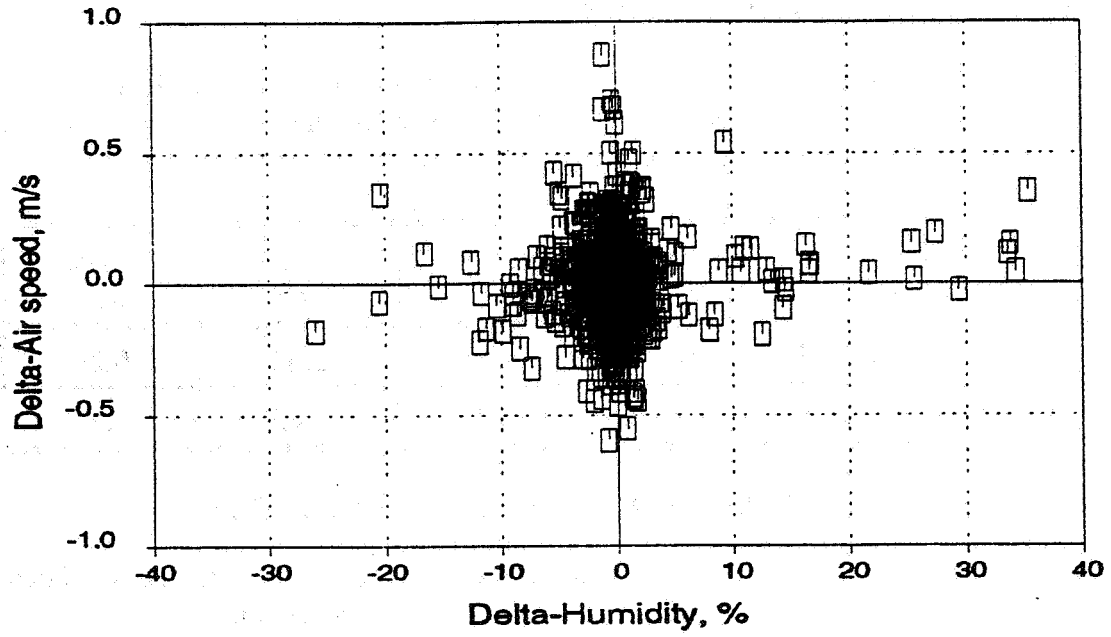

Figure 5. Change in duct air speed against change in humidity with humidity control.

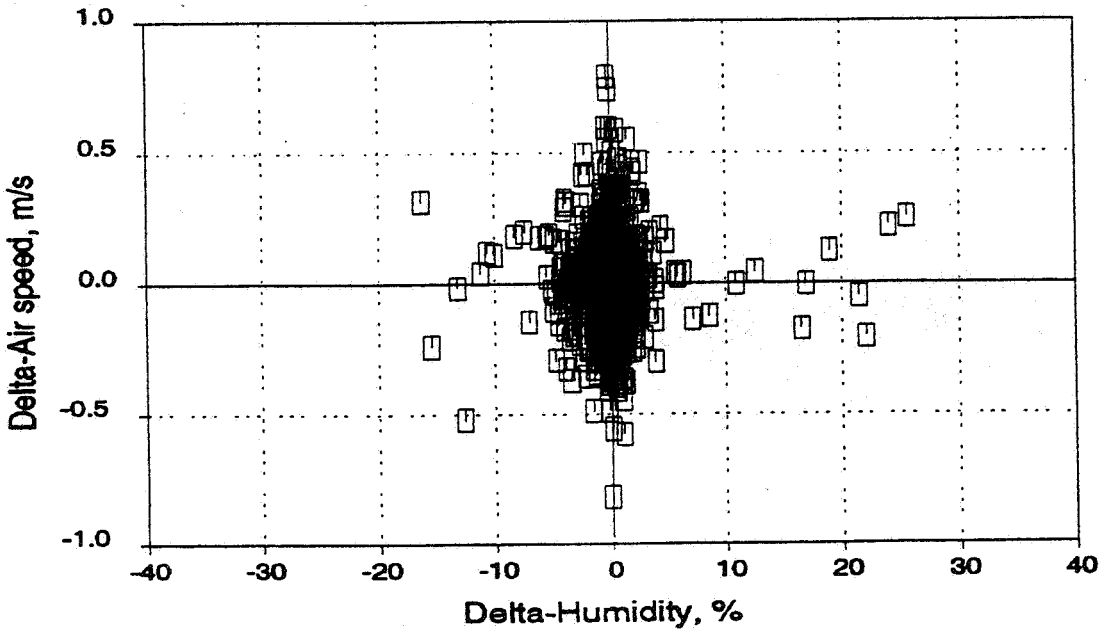

Figure 6. Change in duct air speed against change in humidity with no humidity control.

As can be seen from figures 5 and 6 there is no discernable difference in the air speed in either case, however, the time constant of the humidity device may be of the same order as the averaging time for the humidity and the small changes in humidity are likely to produce small changes in the flow of the same order as random changes produced by the fluctuations in wind speed and temperature.

3.4 Birmingham Housing Association Houses

These houses had the vents terminated correctly[3] at the ridge and this is reflected in the absence of reverse flow. Ridge termination also made the stacks taller, thereby enhancing buoyancy induced air movement. The mean air flows are shown in Table 3.

House	Kitchen m/s	Kitchen ach	Bathroom m/s	Bathroom ach	House ach
1S	1.16	1.72	0.86	2.33	0.26
2S	0.99	1.47	0.61	1.65	0.20

Table 3. Mean air flows and air changes per hour in the Birmingham houses.

Figure 7 shows that the Birmingham houses were less sensitive to wind speed than the Local Authority installations: at wind speeds of up to 4 m/s there was no effect.

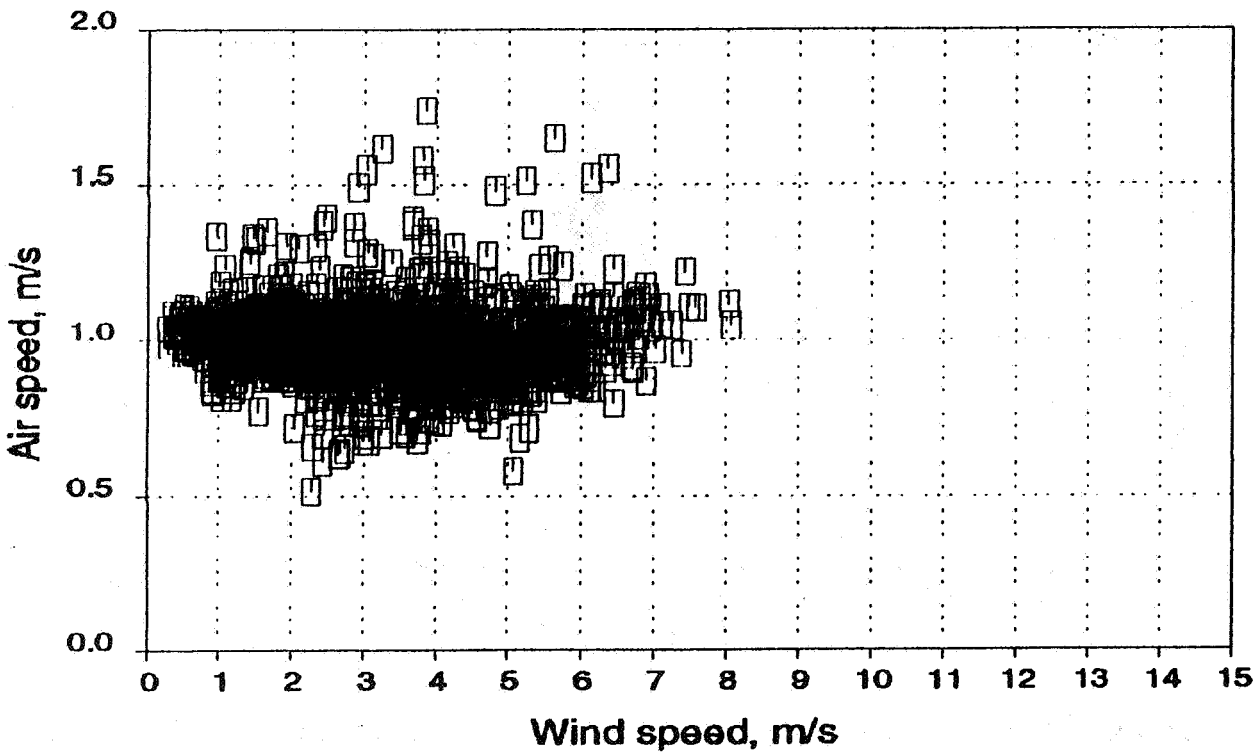

Figure 7. Stack duct air speed related to wind speed - ridge termination.

4. Conclusions

The installation of passive stack ventilation systems can be a useful way to provide good levels of back-ground ventilation in houses. However, good practice must always be observed. Ridge termination of the stacks is recommended and this study shows the degree to which poor performance results from poor location.

However, average humidity levels were below 60% RH in all except one house and below 70% in all houses. With the relatively small changes in RH (generally less than 5%), there seemed to be no relationship between changes in RH and changes in stack velocity but it may be that the changes in relative humidity produce a change in flow indistinguishable from random fluctuations due to temperature and wind variations. In any event it would seem that the levels of ventilation achieved would not be excessive even without the humidity control.

The results from the houses with ridge situated termination are very encouraging with good levels of reliable, and not excessive, ventilation.

ACKNOWLEDGEMENTS

The authors would like to acknowledge the Building Research Establishment for permission to use the data contained in this paper. They would also like to thank the occupants of the houses who so kindly co-operated in the monitoring.

REFERENCES

1. WELSH, P.A. "Testing the performance of free standing ventilation terminals" AIVC Conference, Buxton, Sept 1994

2. MEYRINGER, V. "Ventilation Requirements to Prevent Surface Condensation. Case Study for a Three-person Dwelling." Air Infiltration Review Vol 7 No 1 November 1985.

3. STEPHEN, R.K. PARKINS, L.M.and WOOLISCROFT, M. "Passive stack ventilation systems: design and installation." Building Research Establishment, IP 13/94.

4. PARKINS, L.M. "Experimental Passive Stack Systems for Controlled Natural Ventilation." CIBSE National Conference, Canterbury, 1991.

5. EDWARDS, R.E and IRWIN, C. "Further Studies of Passive Ventilation Systems - Assessment of Design and Performance Criteria." 9th AIVC Conference, Gent, Belgium 1988.

6. EDWARDS, R.E and IRWIN, C. "The Use of Passive Ventilation Systems for Condensation Control in Dwellings, and their Effect on Energy Consumption." 7th AIVC Conference, Stratford on Avon, 1986.

The Role of Ventilation
15th AIVC Conference, Buxton, Great Britain
27-30 September 1994

Comparing Predicted and Measured Passive Stack Ventilation Rates

A Cripps, R Hartless

Building Research Establishment, Garston, Watford, Herts WD2 7JR, United Kingdom

Comparing predicted and measured Passive Stack Ventilation rates

Andrew Cripps and Richard Hartless
Domestic ventilation section
Building Research Establishment
Watford
UK
WD2 7JR
Phone 0923 894040
Fax 0923 664088

Synopsis

BRE have experimental data for the flows found in Passive Stack Ventilation (PSV) ducts from a test house in Garston. These data cover different duct diameters, number of bends and roof terminals, all measured over a variety of weather conditions.

In the first part of this paper the data are analyzed to separate temperature and wind effects, and to see how well they fit well to the expected model of duct flow.

The second part gives a comparison of the same data with predictions from the single zone ventilation model BREVENT. Extensive research at BRE has improved the modelling of PSV ducts within this computer model, and this new information was used to try to calculate the flows in the duct for the measured weather conditions.

The results show good correlation between the predicted and measured duct flow velocities. Care was needed in identifying the effective volume of the building to give this good result. More work is needed on the interaction between PSV flow elements, and whether using a multi-zone model would give better results.

Introduction

Passive Stack Ventilation (PSV) is a method for providing ventilation which does not require any power or action by the user. It consists of a pipe running from a room, upwards to the roof of the building, and extracts air from the room due to the combined effects of the temperature difference between inside and out, and the wind on the terminal of the PSV device. There has been research for some time into how effective it is, and whether it should be being more widely applied [1,2].

In a previous paper Parkins reported on an experiment in a house at BRE Garston to measure the flows through a range of PSV systems. Full details can be found in that paper [3] and another paper at this conference [4], but the velocity in the PSV was measured alongside the weather conditions.

In this paper the results of the earlier experimental study are examined using basic duct flow theory, and the BRE domestic ventilation model BREVENT. This model is a single zone, mass balance model of air flow in buildings, described in full in the manual to BREVENT [5]. It is designed for use in housing, but can be applied to other buildings,

and is available in a 'User-friendly' form. BREVENT models all of the main components of air flow in housing: infiltration, small openings, windows, extract fans, combustion appliances and, of course, PSV.

Experimental data

Figure 1 shows a typical result from the experiments carried out in 1990, with the velocity of air in the duct plotted against the temperature difference. There is considerable scatter in these data, reflecting the fact that flow rates are a function of wind speed, wind direction and temperature difference. In order to make more sense of the data it is helpful to look at the cause of the flow, and whether the temperature and wind effects can be separated out.

The pressure difference ΔP across a PSV is given by [5]

$$\Delta P = \Delta C_p . \tfrac{1}{2} \rho_o U^2 - \Delta\rho\, gh \qquad (1)$$

Where

ΔC_p	$C_{pt} - C_{pI}$ i.e. difference in pressure coefficient between the PSV terminal C_{pt} and inlet C_{pI} calculated from the difference between internal and external static pressures. This is generally negative. ()
ρ_o	density of air outside the building (kgm^{-3})
U	wind speed (ms^{-1})
$\Delta\rho$	$\rho_o - \rho_I$, between internal and external air density (kgm^{-3})
g	acceleration due to gravity (ms^{-2})
h	height of PSV terminal above ground level (m)

The average speed of flow v through the duct is then governed by:

$$v = \left(\frac{2\Delta P}{K\rho}\right)^{\frac{1}{2}} \qquad (2)$$

Where K is the complete loss coefficient for the PSV system, and is discussed fully later. Combining (1) and (2), and using the ideal gas law relationship $\rho_o T_o = \rho_I T_I$ to convert the densities into temperature differences:

$$v^2 = \left(\frac{\Delta C_p}{K} \cdot \frac{T_I}{T_o} \cdot U^2\right) + \left(\frac{2}{K} \cdot \frac{\Delta T}{T_o} \cdot gh\right) \qquad (3)$$

Now the main variables are the wind speed U and the temperature difference ΔT and a comparison of either can be made against the PSV flow speed by manipulation of equation (3). Dividing both sides of (3) by U^2 and then plotting v^2 / U^2 against ΔT is expected to give a straight line if the other values are fairly constant. Similarly, dividing both sides of (3) by ΔT shows that a plot of $v / (\Delta T)^{\frac{1}{2}}$ against $U / (\Delta T)^{\frac{1}{2}}$ gives a straight line as well. An example of the second of these is shown in figure 2. It shows that the data from figure 1 are much clearer in this form than in the original, untreated format, and that stack flow speed is linear with wind speed in the absence of temperature difference.

Figure 1: v vs DT, system 2

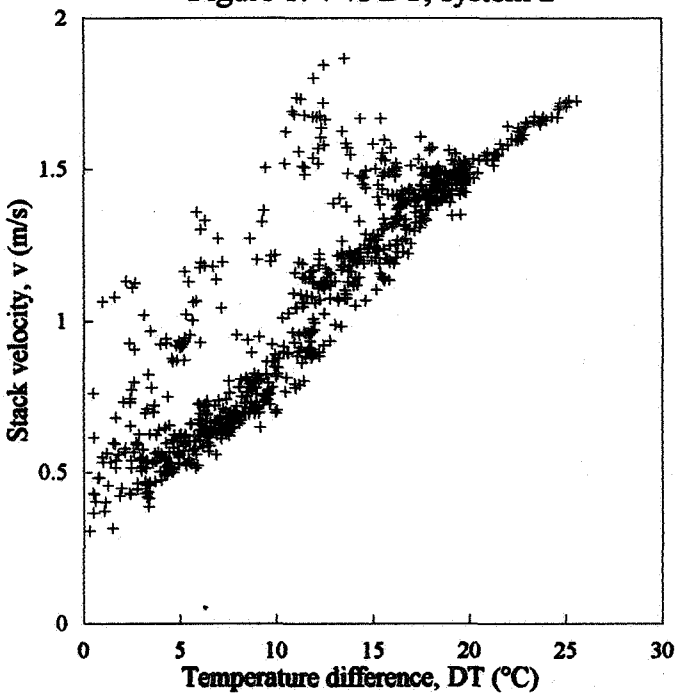

Figure 2: v over U^2 vs DT over U^2

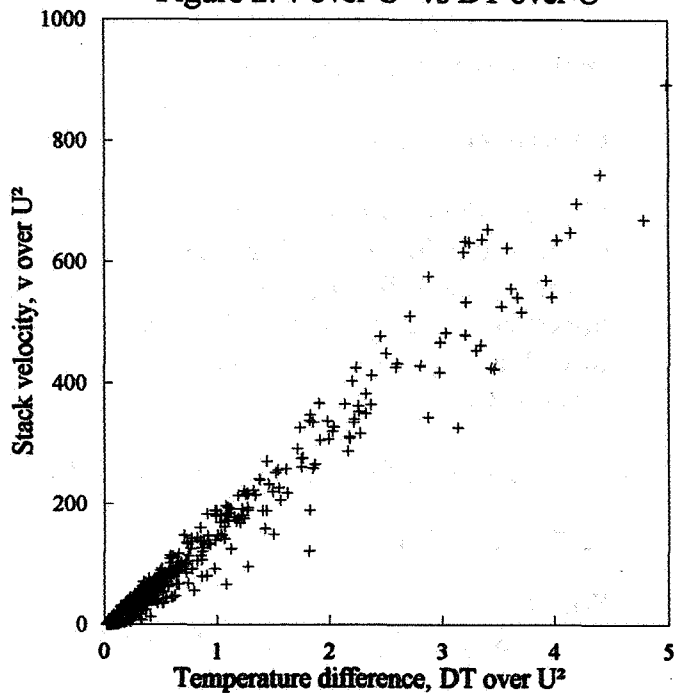

Finding the gradient and intercept from these plots enable us to find a value of the loss factor K. However putting this value into the BREVENT model to be discussed next shows that the values of K predicted are much too high. This is because the simple model of a PSV discussed here ignores the effect of the rest of the building on the PSV flow. This is also discussed in the next sections.

The other significant insight to be gained from equation (3) is when wind effects are expected to dominate over temperature effects and vice versa. If the requirement is for 90% of the contribution to mean one effect is dominating, inserting typical values for the variables in (3) indicates that:

a) If $\Delta T = 10°C$ then U must be greater than 10 ms^{-1} to dominate
b) If $\Delta T = 10°C$ then U must be less than 1 ms^{-1} for ΔT to dominate

These indicate that for most conditions which occur naturally then both effects need to be considered. However it is apparent from experimental data [3] that for wind speeds below 2 ms^{-1} it is the temperature effects which are the most significant.

Because of the variability of the stack flow speeds with wind direction, and the generally large temperature effects observed in these data, the remainder of the analysis in this paper considers low wind speed results only. This simplifies the analysis considerably because we can concentrate on the loss coefficients of PSV systems, and ignore the effect of varying wind direction on the suction coefficients of terminals. These suction effects are discussed by Welsh [6].

BREVENT predictions

The BREVENT model uses an equation equivalent to equation (1) above for flow in a PSV with the dimensionless loss factor K is defined by:

$$K = \left(\frac{4fL}{d} + K_1 + K_2 \right) \quad (4)$$

where

d	diameter of the PSV pipe (m)
f	friction coefficient for the PSV pipe ()
L	length of the PSV pipe (m)
K_1	sum of all bend losses ()
K_2	inlet and outlet losses ()

This paper looks at the results from four of the cases measured by Parkins [3]. These are numbered 1, 2, 5, 6 to match the data in that paper. Systems 1 and 2 had 155 mm diameter pipe, 5 and 6 110 mm diameter pipe, whilst systems 1 and 5 contained two bends and systems 2 and 6 had no bends. The two straight systems emerged within the roof and so had a different type of terminal to the two which emerged at the roof ridge. All of this information is needed to model PSV effectively.

The initial calculation of the loss factors K was as follows:

System	d (m)	Bends	Terminal	Terminal loss	4fL/d	K_1	K_2	K
1	0.155	2	Ridge vent	1	1.42	0.56	1.5	3.48
2	0.155	0	Chinese hat	1.1	1.42	0	1.6	3.02
5	0.110	2	Ridge vent	1	2.0	0.56	1.5	4.06
6	0.110	0	Mushroom	2.1	2.0	0	2.6	4.60

The loss coefficient used in BREVENT can be found by multiplying each K by $8 / \pi^2 d^4$, giving values around 4900 ,4200, 22500 and 25500 (m^{-4}) for systems 1, 2, 5 and 6 respectively. This assumes that the friction coefficient f is 0.008, the inlet loss with no ceiling diffuser is 0.5 in each case, and bends cause a loss of 0.28 each. The terminal data are those now supplied with the BREVENT help pages. These data represented the initial best estimates of the values appropriate for the PSV systems, based on tables [7]. However there is uncertainty remaining over the correct values to be used for bend losses, and particularly the way the interaction of two bends should be calculated.

The airtightness of the house had been measured as 13 air changes per hour (ach) at an applied pressure difference of 50 Pa. The house volume is 205 m^3. This information is needed in the BREVENT model to predict the infiltration rate. There were no significant other sources of ventilation during these experiments. The model was run with a range of temperature differences to match those found during the experiments.

Examples of predicted flows against temperature difference for the four systems considered are shown in figures 3 to 6, labelled as BREVENT initial. It is clear that although the fit to the data is not too bad, the model was over predicting the flow rates for any given temperature difference. This means the model was probably missing out, or under-estimating, some of the loss factors. The possible causes of discrepancy are the subject of the next section. Note that the experimental data is stated as centre line velocity, so that the BREVENT prediction needed to be converted to this from the average velocity.

Figure 3: v vs DT, System 1

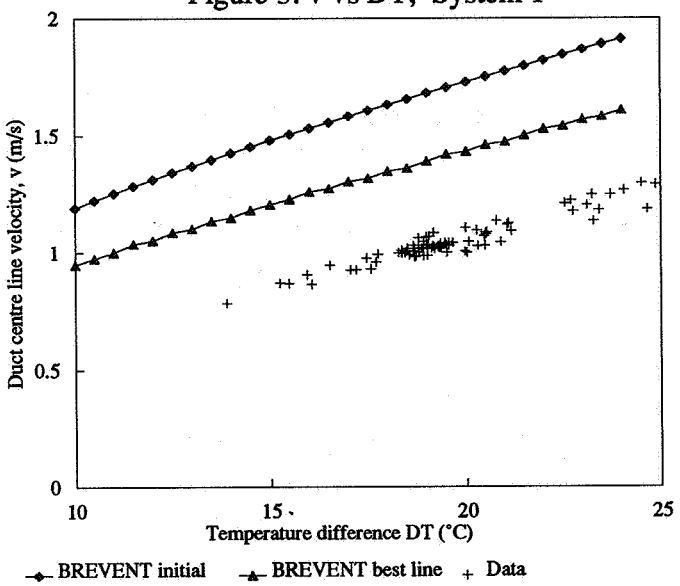

Figure 4: v vs DT, System 2

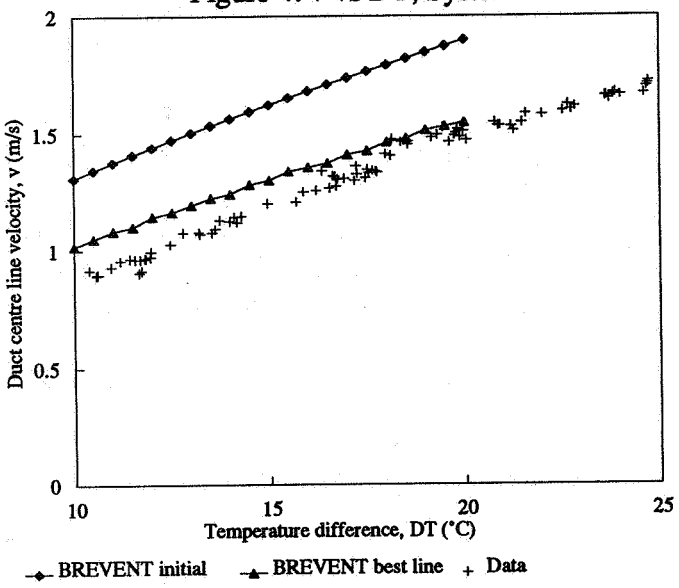

Figure 5: v vs DT, system 5

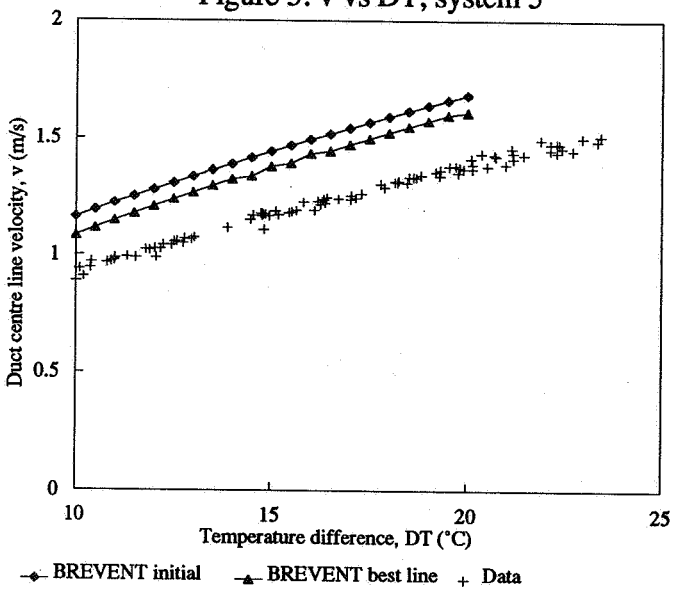

Figure 6: v vs DT system 6

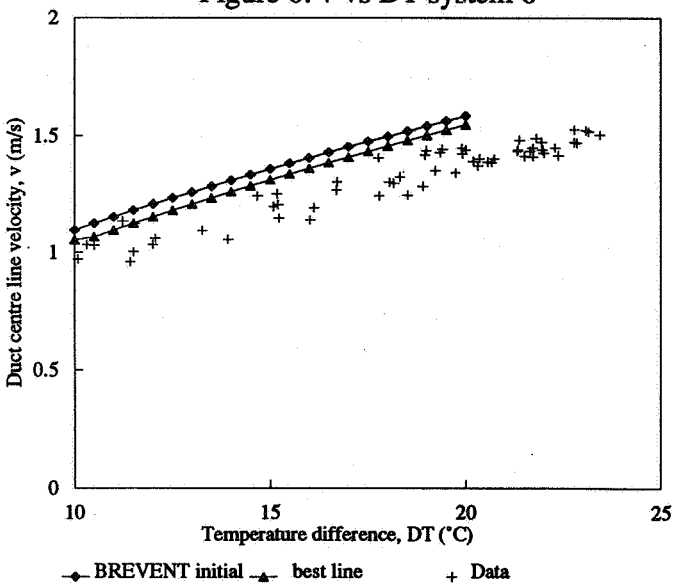

Developments of the model

There were three aspects of the basic model which were felt could be resulting in error. A combination of solutions to all of them was used for the best lines in the figures above.

1) Effect of the kitchen door being closed

In BREVENT all of the inside of a building is assumed to be one well mixed zone. But in these tests, [3] the door to the kitchen where the PSV was sited was closed, so this assumption is not as good as usual. This reduces the effective volume of the house 'seen' by the PSV.

The essential point is that the airtightness of the building is a resistance on the flow up the stack. Closing the kitchen door makes it harder for air from outside the house to reach the PSV, and this reduces the PSV flow. This effect can be well understood by introducing a simple resistance model for air flow. Turbulent air flow can be represented by:

$$Q = \frac{(\Delta P)^{1/2}}{R} \qquad (5)$$

Hence for a PSV system, the Resistance R_D is given by $(\rho_I K \,.\, 8 \,/\, \pi^2 d^4)^{1/2}$. For infiltration the equation needs to be adjusted slightly, since the exponent is usually not 0.5, but nearer to 0.6, reflecting the partially laminar nature of infiltration.

$$Q = Q_T \cdot \left(\frac{\Delta P}{50}\right)^{0.6} \approx \frac{Q_T}{1.3} \cdot \left(\frac{\Delta P}{50}\right)^{0.5} \qquad (6)$$

Where Q_T is the flow rate measured at 50 Pa (m^3h^{-1}). This gives a good approximation to the same flows at pressure differences below 10 Pa, which is the region of most interest. Using this then the R value for infiltration is given by $R_I = (1.3.(50)^{1/2}) \,/\, Q_T$

To show how this can be applied consider the resistance values given in the table below. The values used are those relevant to the BRE test house, so that the volume is either that for the whole house, 205 m^3, or for the kitchen alone, 35 m^3. The total flow resistance is found by adding the two resistances in quadrature $R_{total} = (R_D^2 + R_I^2)^{1/2}$. This is because of the square root in the flow equation (5).

System	K	R_D		Volume	ach	R_I	R_{total} for line
1	3.5	77	House	205	13	13	78
2	3.0	71	Kitchen	35	11	86	111
5	4.1	164	House	205	13	13	164
6	4.6	175	Kitchen	35	11	86	195

From this it is fairly easy to see that the resistance of the PSV is the dominant effect when the whole house is considered. When the kitchen volume alone is taken the infiltration loss becomes significant. Hence by changing the effective volume of the building to

reflect the fact that the kitchen door was closed the total resistance seen by the air flow is increased. This improves the closeness of the modelling fit from BREVENT, particularly for system 2, (figure 4), where the BREVENT best set line is close to that of the data set.

The concept of the resistance model can be useful in predicting expected flows. In fact for the simple situation of the PSV and one other feature in a temperature dominated regime, it can give the same results as BREVENT. However if other flow elements are added then it becomes more complicated, since some elements will be in series, and others in parallel.

This problem shows the limitations of a single zone model, in that a real house is not single zone when internal doors are shut. However, given that this study concerned PSV flow alone it was possible to improve the prediction by treating the kitchen as the only zone of significance.

Other multi-zone effects

In BREVENT the air is either in the building at temperature T_I or outside at temperature T_o. In reality there could well be a temperature difference between zones within the house, and a more advanced multi-zone model of the BREEZE type [8] is needed to model this. Of particular relevance here is the fact that some proportion of the leakage of the kitchen in the test house goes into the other rooms of the house where the temperature difference is less than that to the outside. Hence in a one zone model the leakage taken should be reduced to account for this. However there are no data available for how large this reduction should be, and this remains a problem area.

Applying the reduced leakages to the kitchen gives the effect shown in figure 5. Using the full kitchen leakage for system 5 gives a result almost identical to that for the whole house volume (not shown). For illustration reducing the leakage by 25% produces the improved line on figure 5. This was used for systems 5 and 6 only. More investigation of the multi-zone effects are needed to further improve the closeness of the fit.

2) The bend losses are not well understood

After applying the changes suggested above to the volume in the single zone model the two straight pipe cases give good results compared to the experimental data, both within 20% of measured values, and system 2 within 10%. However the two systems with bends continue to give larger errors, suggesting that the data for bend losses could be an issue. The published data for bend losses shows considerable variation, and this aspect deserves further study. The effect is greater in narrow pipes, so that based on BRE measurements a total value of 0.7 for the two bends is appropriate for system 5, but only 0.4 for system 1. These result in small changes to the predicted flow rates.

An additional feature which has not been addressed is the interaction between the bends and the terminal. These flow elements are not far enough apart in the real PSV system for steady flow profiles to be established by the time the next element is reached, so additional losses may occur.

3) Loss due to reduction of flow area

Changing the bend losses does not bring the system 1 prediction closer to the experimental data. However both systems 1 and 5 used the same terminal, a gas ridge vent. In the BRE laboratory tests this gave a loss factor, better than that of an open pipe. But the spigot on this terminal is fits a 110 mm pipe, and so the wider pipe needed reducing to connect it to the terminal. This gives an additional loss, which has now been included in the model.

In Woods guide [7] the effect of a flow reduction of 50% in area is given as an extra loss of 0.4. This raises the loss factor, but not by enough for the flow to match the data. As with bend losses this does not take any interaction with the terminal into account.

Conclusions

BREVENT is able to predict the passive stack flow in a house to fair accuracy, falling within 10-20% of measurements. Improvements in the given parameters have followed from extra BRE studies into air flow in pipes near the laminar/turbulent transition zone.

The resistance of the building fabric can restrict the flow in a PSV. The loss due to the duct itself may be similar to that due to the rest of the house, especially where the house is airtight, or the assumption of the one zone house is poor. Accounting for this further improves the accuracy of the BREVENT prediction.

Further work on bend losses, and careful consideration of the extra features of a particular system are needed to give detailed assessment of PSV flows.

Acknowledgement

This work was supported by the Building Regulations Division of the Department of the Environment, and is published with their permission. The views expressed are those of the authors and not of the Department.

References

[1] Johnson KA, Gaze AI and Brown DM, *A passive ventilation system under trial in the UK*, published in the proceedings of the 6th AIC conference, 1985.
[2] Stephen RK and Uglow CE *Passive Stack Ventilation in dwellings* BRE Information paper IP21/89, 1989.
[3] Parkins LM, *Experimental passive stack systems for controlled natural ventilation,* published in the proceedings of the CIBSE Technical Conference 1991.
[4] Parkins LM, *A study of various passive stack ventilation systems in a test house,* published in the proceedings of the 15th AIVC Conference, 1994.
[5] Cripps AJ and Hartless RP, *The manual to BREVENT*, BRE report AP21, 1992
[6] Welsh PA, *The testing and rating of terminals used on ventilation systems,* published in the proceedings of the 15th AIVC Conference, 1994.
[7] Daly BB, *Woods practical guide to fan engineering*, Woods of Colchester Ltd, 1978.
[8] *BREEZE,* published as BRE report no AP55, 1992.

The Role of Ventilation
15th AIVC Conference, Buxton, Great Britain
27-30 September 1994

Ventilation Air Flow Through Window Openings in Combination with Shading Devices

A C Pitts, S Georgiadis

Building Science Unit, School of Architectural Studies,
University of Sheffield, P O Box 595 Sheffield, S10 2UJ
United Kingdom

Ventilation air flow through window openings in combination with shading devices

Synopsis

In the UK the increased use of natural ventilation in buildings is being encouraged, particularly during hot weather as an alternative to air conditioning or mechanical ventilation. In order to take advantage of this option building designers need to be able to estimate potential air flows. Conventional calculation methods assume windows to be simple openings, however in practice the situation is more complex since during hot weather the opening is likely to be shielded by some form of solar shading device. This paper reports the results of a laboratory based investigation of the pressure difference-flow relationship for air movement through windows when a venetian blind is also in position. A variety of window opening variations and blind angles have been tested. The results indicate a significant reduction in air flow when blinds are in use in the closed position (angle 85°); the results for partially closed position (45°) show little reduction in flow. The form of the window opening also has an important effect. Care must therefore be taken in setting blind angles so as to avoid reducing beneficial natural ventilation air flow whilst maintaining shading.

1. Introduction

Many modern office buildings suffer the risk of overheating, often during the summer months but also potentially at other times of the year. The causes of this are many: high solar gain; high internal heat production; extensive use of modern office equipment; high densities of occupation. There has however only been one traditional remedy: air conditioning. Air conditioning has a number of negative attributes: it is more costly to install and operate; the refrigerant gases may have the potential to damage the atmosphere if released; and it requires substantial amounts of energy to function with consequent emissions of carbon dioxide from fossil fuels used as the primary energy source. In recent times building designers have become more aware of the potential for overheating caused by large areas of glazing and similar features in buildings and many are attempting to reduce such problems. Even with this change to more climate sensitive design, overheating risk persists and alternatives to air conditioning and mechanical ventilation systems are sought. Clearly one possibility in suitable climates is the increased use of natural ventilation. If the potential of this option is to be fulfilled, designers must have access to calculation/estimation techniques for predicting natural ventilation air flows. The information required is available only for relatively straightforward options at present (plain openings or cracks) and therefore there exists a need for more data, particularly on non-standard openings.

The investigation reported in this study attempts to build on some earlier work and provide help in the specific situation of air flow through partially opened windows which are also shielded against direct solar heat gain by devices such as venetian blinds.

2. Background

Flow relationships for air movement through buildings have been studied for many years. The basic aim of such work being the ability to more accurately predict and assess such flows by calculation and simulation rather than experimentation on every building (though some such experiments do have a role and are valuable in their own right). Knowledge of air flow rates enables more accurate estimation of energy flows and comfort levels.

The power law relationship has been widely used to express the link between pressure differential and volume flow rate with the general form :

$$Q = c\Delta P^n \quad (1)$$

(where Q is the air flow rate, m^3s^{-1}; ΔP is the pressure differential, Pa; n and c are constants). This algorithm is widely used, for example by ASHRAE [1], in the form of equation 1 or in its reciprocal format as $\Delta P = cQ^n$. Studies over many years, going back to the work of Dick [2] have derived this form of empirical relationship for flow through openings other than cracks and have normally found the exponent, n, to take a value of 0.5. The power law relationships of the type of equation 1 have been criticised however for their lack of dimensional homogeneity. Also the square law does not reflect the relationship for flow through narrow cracks. A quadratic relationship of the form :

$$\Delta P = aQ^2 + bQ \quad (2)$$

(where a and b are constants), has been found to be more useful for description of crack flow and more acceptable from a dimensional analysis point of view [3]. More details of air flow algorithms can be found in the work of Liddament [4] for example.

The investigation described in this paper attempts to use such relationships in the case of window openings which are partially blocked by venetian blind shading devices. In this, the work of Yakubu and Sharples [5] which dealt with modulated louvres, is built upon. That study differed in a number of important aspects from the work described here. They were concerned with flow across a louvre system in which the louvres were both thicker (5mm) and wider (100mm) than venetian blinds, with a spacing of 95mm. An attempt was made to apply the flow equations based on the theory of flow through a series of parallel plates; however the experimental results did not substantiate such a theory in the form proposed.

In the reported results of that study, the quadratic form of the flow relationship was found to produce more acceptable results than the power law, however the constant, b, (see equation. 2) took small values with the result that ΔP was almost entirely dependent on the Q^2 term. This would indicate a square law relationship which is characteristic of a turbulent flow. Yakubu and Sharples also found that with louvre inclinations up to about 45° that there was no significant decease in flow for the same pressure difference.

3. Experimental Work

The work described in this study was carried out in a controlled wind tunnel laboratory environment. The situations investigated were chosen to represent a number of commonly found combinations of window opening and venetian blind position. Results reported here deal with the situations of window fully open (100% open surface area) and three variations of partially closed window : 67% open; 50% open and 33% open. Each of these four options was tested in combination with four blind configurations : blind retracted; blind with horizontal fins (angle 0°); blind with fins at 45° (partially closed), and 85° (fully closed). The fins each measured 910mm wide, 50mm depth, 0.25mm thick with a spacing when horizontal of 40mm.

The wind tunnel air flow was controlled by a variable flow axial fan and the flow rate monitored and measured by a vane anemometer centrally positioned and calibrated upstream of the working section. Pressures were measured by means of a high resolution differential pressure manometer which was also calibrated at the start of the investigation. Pressure tapping positions were chosen with care and were situated approximately one "duct" diameter upstream and immediately downstream of the window/blind obstruction. Several options for such positioning were

considered and tested before settling on this regime which appeared to give most accurate and repeatable results. A number of measurements of pressure differential and flow rate (typically 9 or 10) were made for each window opening and blind combination. Flow rates up to about 2.5 ms^{-1} were employed; beyond this physical disturbance to the blinds occurred.

4. Results

The results were analysed with respect to the two principal relationships (see equations 1 and 2) by means of propriety curve fitting packages. Both gave very good correlation coefficients. More details of the results and procedures can be found in Georgiadis[6]. Tables 1 and 2 below summarise the relationships derived.

Table 1 Power Law Flow-Pressure Relationships

Blinds Configuration	Percentage of Open Surface Area 100 %	67 %	50 %	33 %
No blinds	$Q=0.634\Delta P^{0.455}$	$Q=0.354\Delta P^{0.479}$	$Q=0.269\Delta P^{0.481}$	$Q=0.170\Delta P^{0.483}$
Blind angle 0°	$Q=0.636\Delta P^{0.433}$	$Q=0.360\Delta P^{0.474}$	$Q=0.278\Delta P^{0.475}$	$Q=0.185\Delta P^{0.462}$
Blind angle 45°	$Q=0.516\Delta P^{0.441}$	$Q=0.346\Delta P^{0.453}$	$Q=0.280\Delta P^{0.462}$	$Q=0.189\Delta P^{0.452}$
Blind angle 85°	$Q=0.275\Delta P^{0.485}$	$Q=0.212\Delta P^{0.520}$	$Q=0.174\Delta P^{0.486}$	$Q=0.153\Delta P^{0.471}$

Table 2 Quadratic Flow-Pressure Relationships

Blinds Configuration	Percentage of Open Surface Area 100 %	67 %	50 %	33 %
No blinds	$\Delta P = 3.204\ Q^2 - 0.460\ Q$	$\Delta P = 9.502\ Q^2 - 0.786\ Q$	$\Delta P = 15.439\ Q^2 - 0.235\ Q$	$\Delta P = 39.411\ Q^2 - 0.852\ Q$
Blind angle 0°	$\Delta P = 3.560\ Q^2 - 0.790\ Q$	$\Delta P = 9.048\ Q^2 - 0.462\ Q$	$\Delta P = 15.048\ Q^2 - 0.589Q$	$\Delta P = 38.329\ Q^2 - 1.812\ Q$
Blind angle 45°	$\Delta P = 5.336\ Q^2 + 0.878\ Q$	$\Delta P = 11.294\ Q^2 - 1.025\ Q$	$\Delta P = 16.524\ Q^2 - 1.197\ Q$	$\Delta P = 40.758\ Q^2 - 3.234\ Q$
Blind angle 85°	$\Delta P = 13.254\ Q^2 + 0.338\ Q$	$\Delta P = 17.507\ Q^2 + 1.751\ Q$	$\Delta P = 33.790Q^2 + 0.600\ Q$	$\Delta P = 53.174\ Q^2 - 1.951\ Q$

The results are shown in graphical format in Figures 1 to 4 for the power law relationships.

An examination of Table 2 shows that the term bQ has much less significance than the aQ^2 term indicating the square power law relationship to be the predominating factor. This would also be in agreement with the existence of a developed turbulent flow regime for the situation under study (which is as expected from personal observation).

The results are also in agreement with the general finding from the work of Yakubu and Sharples in that the reduction in flow due to the obstruction caused by the blinds is significant only above fin angles of 45°. This is particularly well illustrated by Figures 1 to 4. One unexpected phenomenon was in the apparent increase in flow found when blinds were lowered into position (at 0° and some 45° fin angles) by comparison with the "no blinds" case. This appears to occur in the combinations where the window opening is in a partially closed mode and may be the result of the blinds actually aiding the flow through the window constriction.

5. Conclusions and Recommendations

The study reported in this paper shows that thin cross-section shading devices such as venetian blinds may be used up to fin angles of about 45° without any significant reduction in natural ventilation air flows. Indeed there is some evidence to suggest that the use of suitably angled blinds may actually enhance air flow through partially opened windows. This phenomenon is certainly worthy of further investigation. In this respect it concurs with a previous study which suggested conventional flow equations may be insufficient to explain flow through shading devices where a number of parallel flows occur.

Further work on additional window and blind combinations is currently underway and it may prove useful to attempt to correlate the findings with a computational fluid dynamics analysis.

If shading devices with angled fins are to be used in conjunction with natural ventilation flow openings then care should be taken to ensure that the angle, width of fin and sun altitude are carefully considered to optimise the benefits.

References

1. American Society of Heating, Refrigeration and Air-conditioning Engineers
   Handbook of Fundamentals
   A.S.H.R.A.E., Atlanta, GA, USA, 1993
2. Dick, J.B.
   "The fundamentals of natural ventilation in houses"
   J.I.H.V.E. 18 (179), 1950, pp 123-134
3. Baker, P.H., Sharples, S. and Ward, I.C.
   "Air flow through cracks"
   Building and Environment 22 (4), 1987, pp 293-304
4.. Liddament, M.W.
   "A Review of Building Air Flow Simulation"
   A.I.V.C. Technical Note 33, March 1991
5. Yakubu, G.S. and Sharples, S.
   "Airflow through modulated louvre systems"
   B.S.E.R.& T. 12 , 1991, pp151-155
6. Georgiadis, S
   M.Arch. Stud. Dissertation
   School of Architectural Studies, University of Sheffield, September 1994

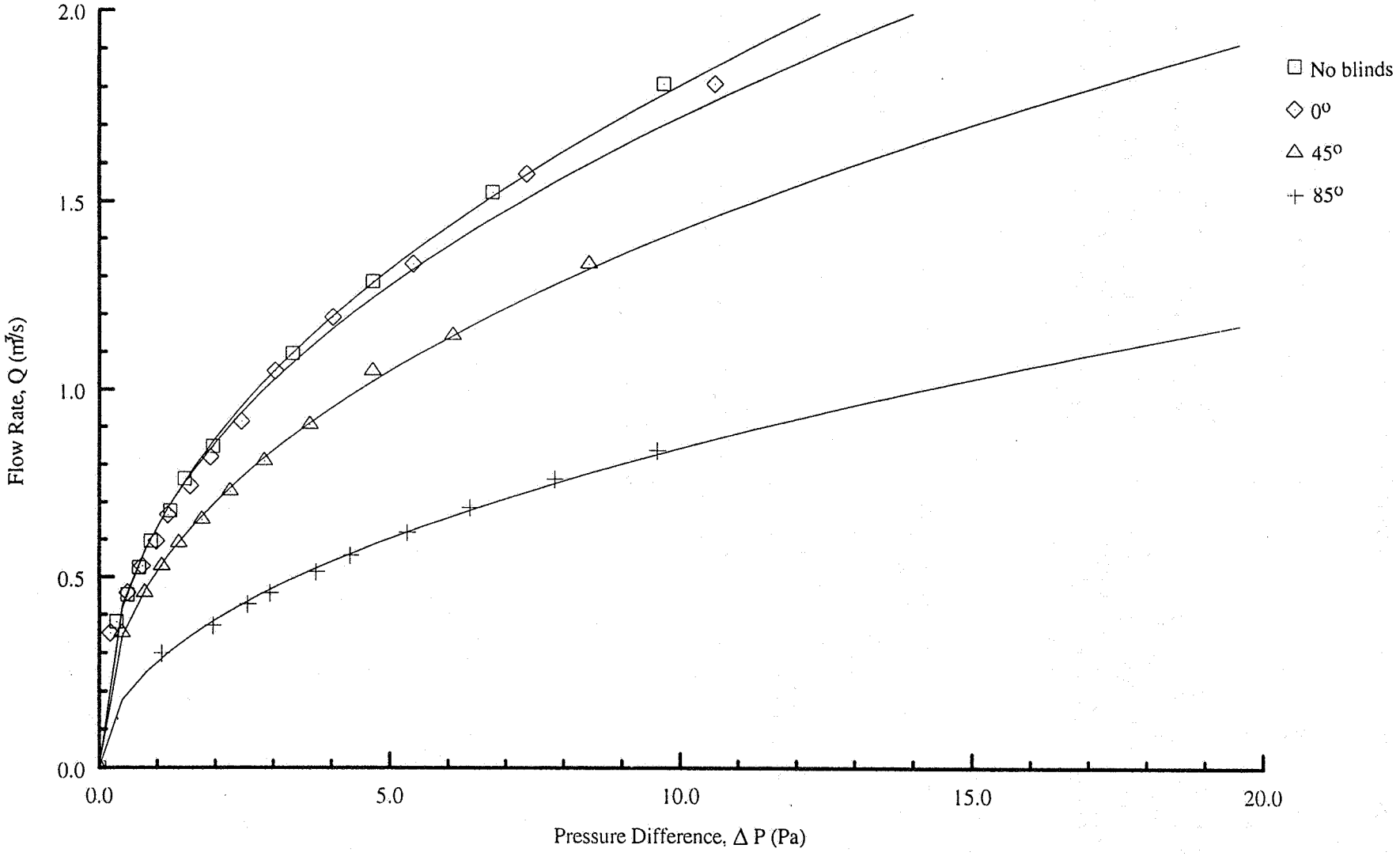

FIGURE 1: RESULTS FOR UNOBSTRUCTED WINDOW (100% FREE AREA)

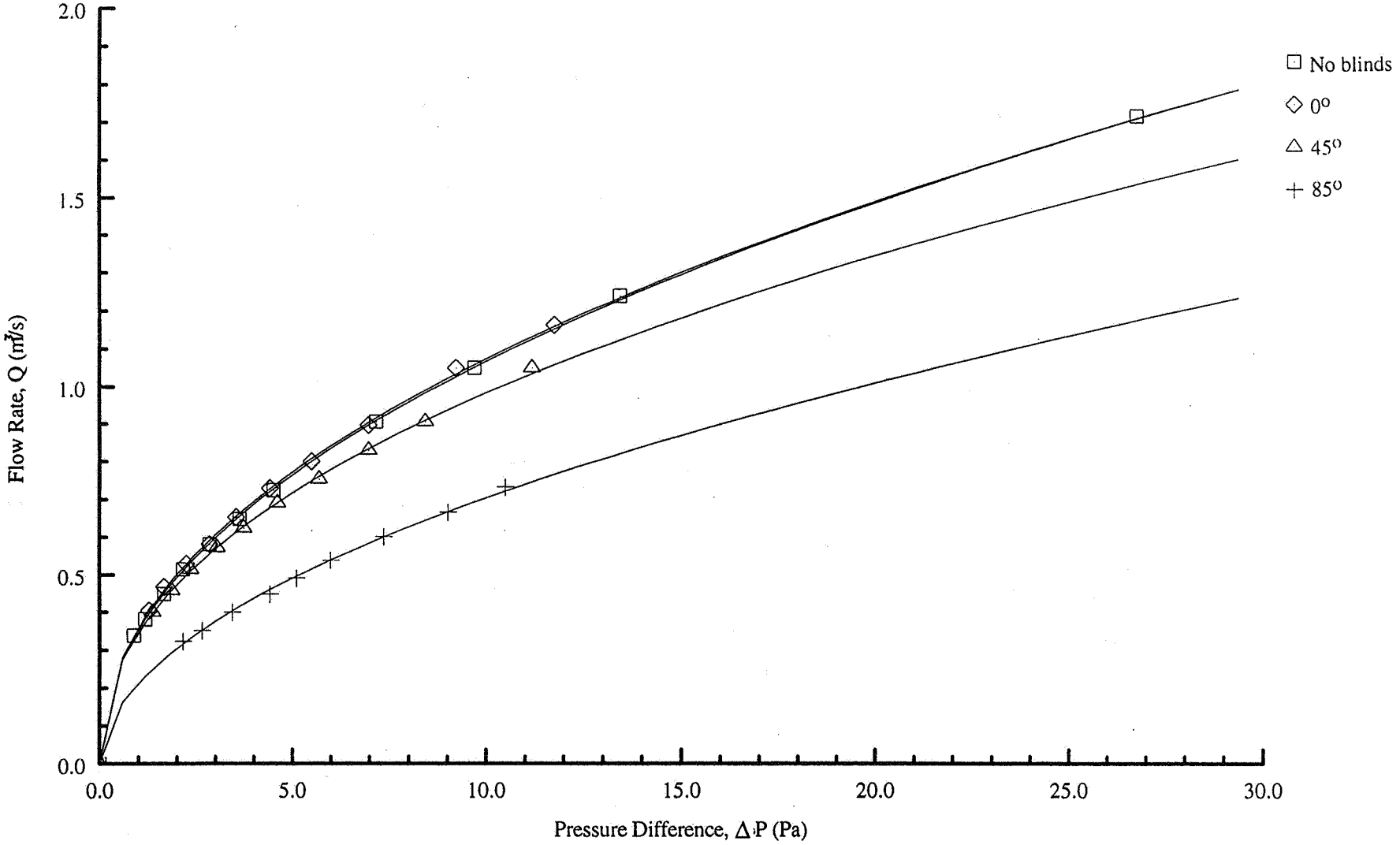

FIGURE 2: RESULTS FOR PARTIALLY OBSTRUCTED WINDOW (67% FREE AREA)

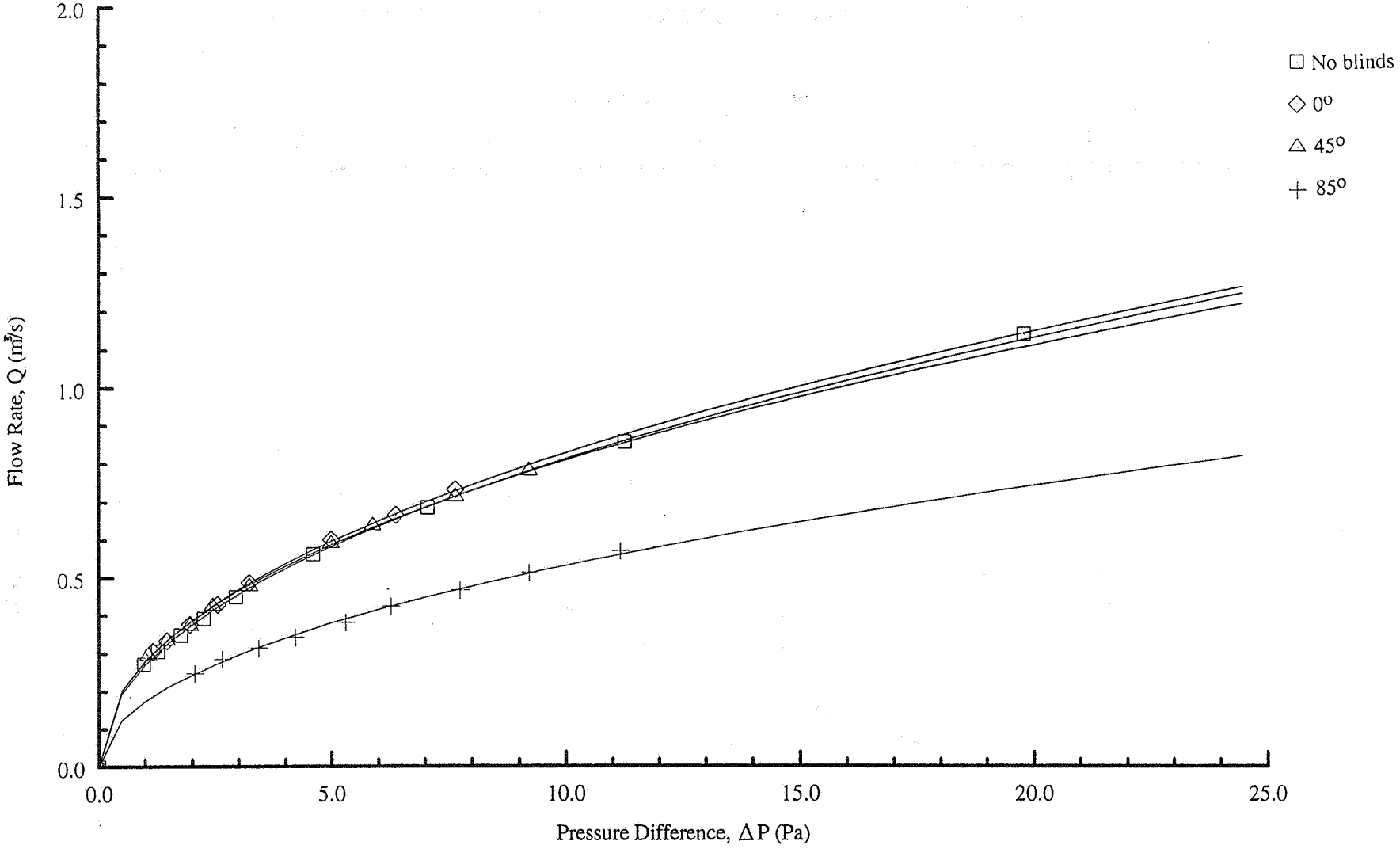

FIGURE 3: RESULTS FOR PARTIALLY OBSTRUCTED WINDOW (50% FREE AREA)

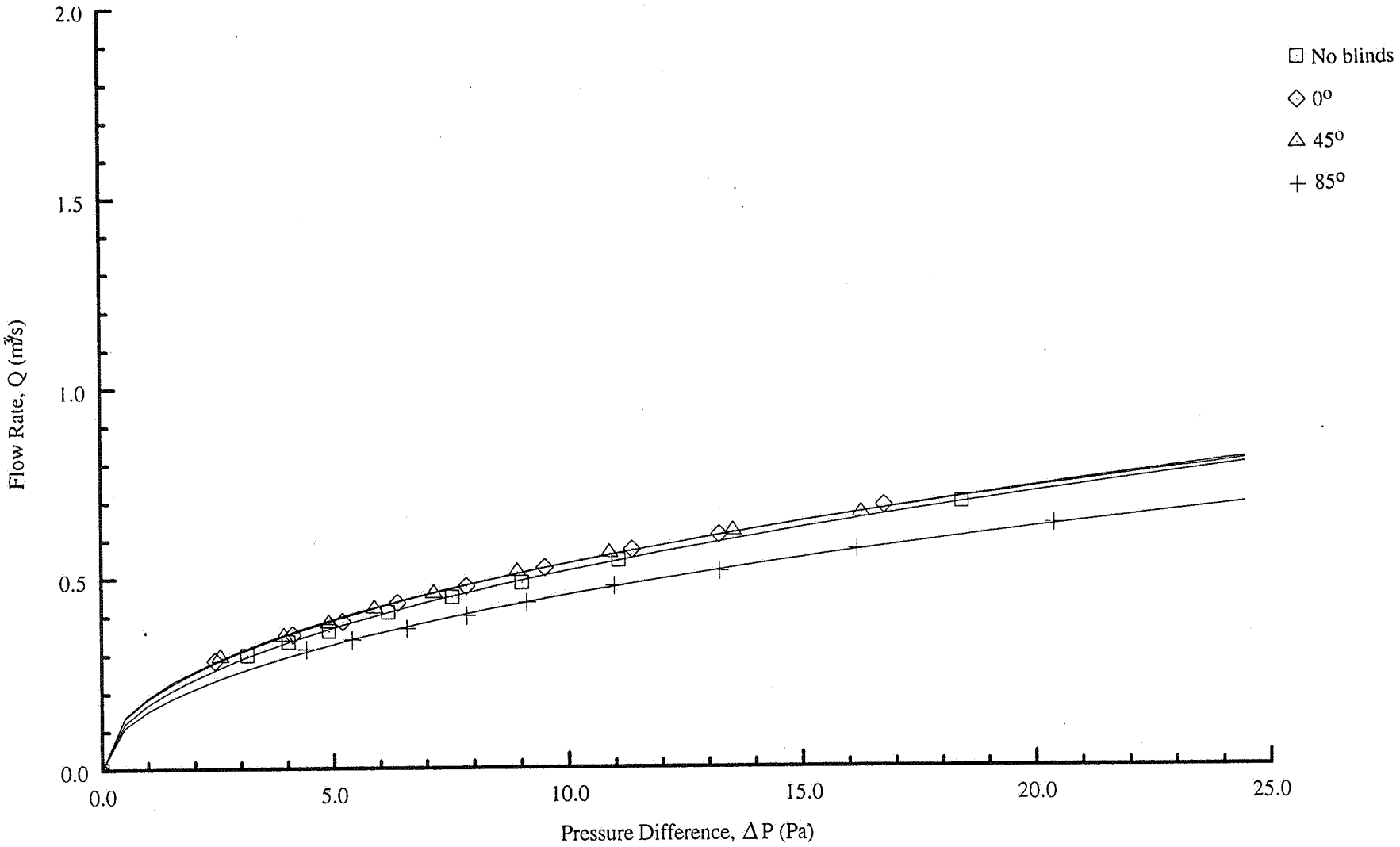

FIGURE 4: RESULTS FOR PARTIALLY OBSTRUCTED WINDOW (33% FREE AREA)

The Role of Ventilation
15th AIVC Conference, Buxton, Great Britain
27-30 September 1994

Use of Passive Stack Systems in Multi-storey Dwellings: Assessment of Performance

C Irwin, R E Edwards

31 Beverley Road, Offerton, Stockport SK2 5AY United Kingdom

Abstract

The use of PSV (Passive Stack Ventilation) systems in two and three storey dwellings is now widely accepted as a method of achieving adequate ventilation levels for indoor air quality control.

However, the application of PSV systems to multiple-storey dwellings is, in the United Kingdom, in its infancy. This paper provides detailed performance data relating to extensive monitoring of PSV systems in multi-storey dwellings in three EC countries (France, Belgium and Holland).

The data presented looks at predicted and actual levels of PSV system performance, variations in internal humidity levels, the influence of buoyancy and wind effects. To remove uncertainties with climatic variations between France, Belgium, Holland and the UK, standard weather years have been used to predict PSV system performance.

The overall aim of the paper is to provide sufficient information to enable PSV system design for optimum performance in UK located multi-storey dwellings.

The Role of Ventilation
15th AIVC Conference, Buxton, Great Britain
27-30 September 1994

A Study of Various Passive Stack Ventilation Systems in a Test House

L M Parkins

Building Research Establishment, Garston, Watford, Herts WD2 7JR United Kingdom

A STUDY OF VARIOUS PASSIVE STACK VENTILATION SYSTEMS IN A TEST HOUSE.

by Lynn M Parkins

SYNOPSIS

The Building Research Establishment has set up various passive stack ventilation systems (PSV) in a test house in order to assess their performance. The test house used was a two storey, end terrace dwelling on the BRE site at Garston.

A PSV was installed in the kitchen of the test dwelling. The duct material, diameter and configuration were varied to determine any differences that they would make to the air flow rates obtained in the duct. In addition, three different ridge terminals were tested and three ceiling inlets.

Air flow rates and temperature in the duct were recorded, together with internal and external temperatures and wind speed and direction. Each system was monitored over several weeks to obtain a spread of climatic data.

Comparisons have been made of the results obtained from each system. Regression analysis has been carried out and predictions of flow rate up the stack, for a typical temperature difference and wind speed, are given for each PSV system.

1. Introduction

Until fairly recently the majority of U.K. houses were built with chimneys and many ventilation problems were with too much rather than inadequate ventilation. The modern trend towards more airtight, energy conserving housing, with no open chimneys or flues, can lead to condensation and indoor air quality problems. Moisture can be removed by mechanical extract fans, but another possible solution could be the use of passive stack ventilation systems (PSV). These are vertical, or near vertical , ducts which run from the moisture producing rooms i.e.. kitchens and bathrooms, to the roof of the dwelling. In this way use is made of the natural stack effect to ventilate these rooms, thereby removing the warm moist air, without the use of mechanical fans. The advantages of using PSV systems are their lack of noise in operation, little maintenance, no direct running costs, no moving parts to break down and, if installed when the dwelling is built, cheapness of installation.
As part of a research programme to test their performance the Building Research Establishment has set up various passive stack ventilation systems in a test house, using different duct materials in a range of diameters and configurations, some of which have been described in an earlier report[1]. This paper describes the performances of all 15 systems.

2. Description of test house and ventilator systems

2.1 Test house

The house used to test the passive stack ventilator systems is an end of terrace, timber framed building with a roof pitch of 42 degrees. It is situated at the Building Research Establishment,

Garston, in a position of fairly open ground to the South and West with trees to the North and office blocks some distance to the East. The room in which the systems were installed is the kitchen/diner, having a volume of 35 m^3. Figure 1 shows the layout of the test house together with the instrumentation positions, table 1 lists the different systems tested.

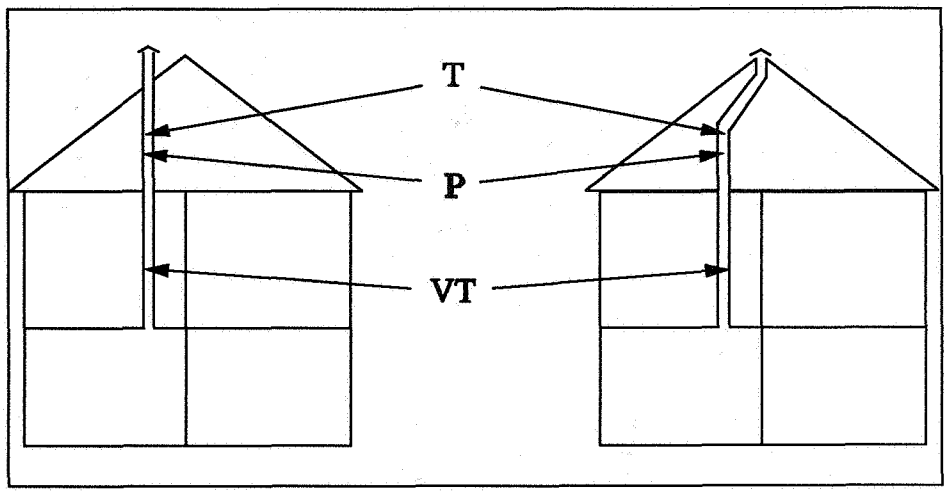

Figure 1: PSV configurations and instrumentation

2.2 Configuration

Two stack ventilator configurations were used, the first was a straight duct from the kitchen ceiling through the bedroom above and the attic, terminating at just above ridge height with a weatherproof terminal. The second configuration had an offset in the attic section to enable the duct to be connected to a ridge terminal see Figure 1.

2.3 Stack diameter and material

Two stack diameters were used, 155 mm and 100 mm, and two different materials, smooth rigid plastic and flexible plastic on a wire spiral. The stack in each case was lagged with fibreglass quilting where it passed through the attic to reduce heat losses and possible condensation problems within the stack.

For two of the systems the stack was cut off at bedroom ceiling height to simulate the shorter stack which would be found in an upstairs bathroom. The same stack was used, rather than monitoring a separate one in the bathroom, to obtain a direct comparison with the longer length stack.

2.4 Terminals

A number of different roof terminals and ceiling diffusers were used. On the straight stack systems a metal 'Chinese hat' shaped terminal was used for the large stack size (SS1) and a plastic 'mushroom' shaped terminal for the small sized stack (SS2). Three types of roof ridge ventilator were used for the systems with an offset and are referred to as (RV1), (RV2) and

(RV3). At the lower end of the duct three ceiling inlets were tested (CT1, CT2, CT3), although of similar design to one another the three inlets had different openable areas.

System no.	Diameter m	Length m	Material	Configuration	Roof terminal	Ceiling terminal
1	0.155	6.88	Rigid	Offset	RV1	-
2	0.155	6.88	Rigid	Straight	SS1	-
3	0.155	6.88	Flexible	Offset	RV1	-
4	0.155	6.88	Flexible	Straight	SS1	-
5	0.110	6.88	Rigid	Offset	RV1	-
6	0.110	6.88	Rigid	Straight	SS2	-
7	0.110	6.88	Flexible	Offset	RV1	-
8	0.110	6.88	Flexible	Offset	RV2	-
9	0.110	6.88	Flexible	Straight	SS2	-
10	0.110	6.88	Flexible	Straight	SS2	CT1
11	0.110	6.88	Flexible	Straight	SS2	CT2
12	0.110	6.88	Flexible	Straight	SS2	CT3
13	0.110	6.88	Flexible	Offset	RV3	-
14	0.110	4.30	Flexible	Offset	RV3	-
15	0.110	4.30	Flexible	Straight	SS2	-

Table 1 Variables for each PSV system

3. Data collection

The following parameters were monitored :
Wind speed, wind direction, external temperature, internal temperature (3 positions), duct temperature (2 positions) and flow velocity in duct. Wind speed and direction were measured adjacent to the test house at a height of 10 metres. External temperatures were taken from inside a Stevenson Screen on the North side of the house. Internal temperatures were taken in the kitchen, bedroom and attic. Duct temperatures and velocity were measured at the positions shown in Figure 1. Duct velocity was measured using a low velocity flow analyzer. This cannot indicate flow direction, so to detect any reverse flow pitot-static tubes were installed in the stack, one facing down to measure upward flow and another facing up to measure downward flow. (No prolonged reverse flow was actually detected by this method). Another method of detecting reverse flow was subsequently installed at the lower end of the stack, this consisted of two adjacent inter-linked thermocouples, one just inside the stack and the other just outside the stack at ceiling height. The datalogger was programmed to monitor temperature differences between the two thermocouples. In the event of the stack temperature being one or more degrees C. below the temperature just outside the stack, the temperature difference and time of occurrence was logged. In this way any prolonged downward flow of cool outdoor air which reached the lower end of the stack could be detected.

Monitoring took place over several weeks for each different system, the duration depending on weather conditions. The data covered as wide a range of wind speeds and directions as possible. In the cases of Systems 10 and 11 it was not possible to cover all wind directions in a reasonable time so only directions 136°- 225° and 226°- 315° are included. A range of temperature differences between inside and outside the house was achieved by the use of electric panel heaters.

Data was collected using a programmable datalogger. With the exception of wind speed, all parameters were scanned once every 10 seconds and then half-hourly averages calculated and logged on magnetic tape. The wind speed recorder works on the 'pulse count' principle and therefore just the half-hourly total count was logged, to give half hour average wind speeds.

4. Analysis of data

The data from each system was analyzed using a spreadsheet computer program.
Initially, graphs were drawn of the stack velocity against temperature difference and wind speed. The stack velocity appeared to be largely dependent on temperature difference although not directly proportional to it. On examination, it was found that the stack velocity is in fact proportional to the square root of the temperature difference, indicating turbulent flow. To see what effect, if any, wind speed and direction had, the stack velocity was divided by the square root of the temperature difference and then plotted again against wind speed. At wind speeds below round 2 m/s the wind had very little effect but had an increasing effect at higher wind speeds. The effect of wind direction for each system was determined by sorting the data into four wind direction quadrants: 045°-135°, 136°-225°, 226°-315°, 316°-045° and then plotting stack velocity divided by the square root of the temperature difference against wind speed for each quadrant. These quadrants approximate to 45° either side of directly onto the four elevations of the test house.

In order to compare the various systems the velocities were converted to flow rates in m^3/h, regressions were then calculated of stack flow with wind speed and square root of temperature difference. From the regressions, predicted flows were calculated for each system for typical conditions of temperature difference of 10°C and wind speed of 4 m/s. Figure 2 shows the results of these calculations.

5. Results

5.1 Effect of configuration and material

5.1.1 Large diameter (systems 1 - 4)

The flows obtained with the straight configurations (2,4) are much higher than those with an offset (1,3), this difference is greater at higher wind speeds. At 4 m/s wind speed and a temperature difference of 10° C the flow rates for the straight stacks are approximately double that for the offset stacks. At wind speeds less than 2 m/s and the same temperature difference the straight stack flow is around 50% higher than the offset stack flow. Material appears to have little effect on stack flow for the offset configurations and although the straight stack systems with flexible ducting produced slightly lower flows at high temperature differences, at a difference of 10°C the flows were very similar.

5.1.2 Small diameter (systems 5 - 7 + 9)
The small diameter stacks showed less variation due to configuration (5+6, 7+9) than the large ones and again material appeared to have very little effect.

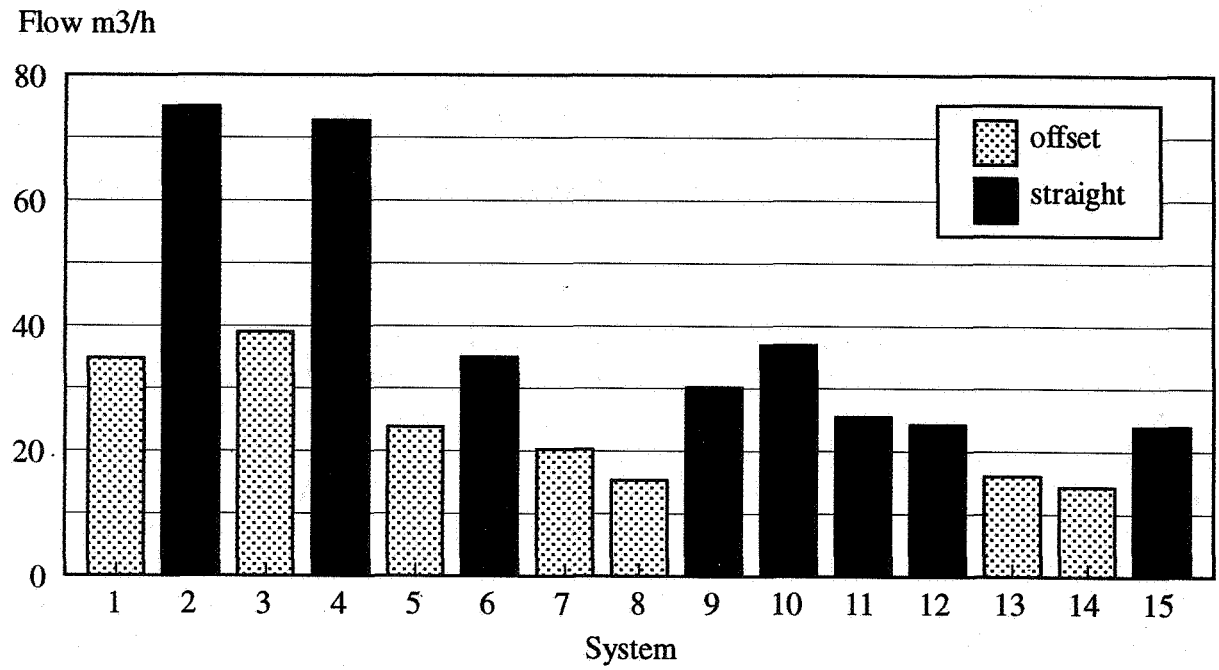

Figure 2: Predicted flow rates for typical conditions
(wind speed = 4 m/s, temperature difference = 10°C)

5.2 Diameter

The flow rates in the larger stacks are, as would be expected, greater than those for the smaller diameter stacks, although the velocities measured are slightly lower. It was thought that this could be due, in part, to the resistance of the room itself, the kitchen door being closed for all tests. Computer modelling of the flows involved carried out by Cripps[2] has shown that this is partly the explanation of the lower velocities in the larger stack ducts. In the case of the straight stacks, the flow rates are roughly proportional to the cross sectional areas of the stacks. For the offset stacks the flows are relatively lower in the larger diameter system, this is probably due to the restricting influence of the ridge terminal. This could also account for the greater difference between straight and offset configurations for the larger diameter systems.

5.3 Length

To find out how much the flow rate would be affected by a different duct length the duct was shortened for systems 14 and 15, being cut off at ceiling height in the bedroom above the kitchen. By comparing the results obtained from systems 13 and 14 it can be seen that there is very little reduction in flow due to a shorter stack length in the offset configuration systems. There is, however, a reduction in flow in the straight system when shortened (9,15).

This difference may be due to the fact that a different room is being ventilated when the duct is shortened and may have different air leakage characteristics from those of the kitchen.

5.4 Terminals

5.4.1 Ridge terminals (7,8,13)

There were variations in flow rates obtained for the three different terminals tested. At low temperature differences there was very little variation in performance but as the temperature difference increased the difference in flow rates between these systems became greater, typically 8.5 m^3 /h at Dt = 20° C.

5.4.2 Ceiling inlets (10,11,12)

The ceiling inlets showed a similar spread of flow rates to the roof terminals ie. little difference at low temperature differences, and 10 m^3/hr. at Dt = 20° C.

The diversity of flow rates obtained with both the ridge terminals and the ceiling inlets is due to the difference in free area and the resistance to flow of each design. These results show the importance of choosing or specifying terminals which do not restrict the air flow: ideally the free area of the terminal should not be less than that of the duct itself. This explains why the differences between the flows in the straight and offset systems was greater with the large diameter ducts than with the small diameter, the same terminals being used for both diameters. In the case of the large duct the ridge terminals were restricting the flow and if a terminal with a larger free area had been used the flows would almost certainly have been greater. This explanation has been reinforced by Cripps[2] with computer simulation of the flows involved.

Wind tunnel tests have been carried out by Welsh[3] on a range of terminals, both for ridge installations and those ducts which pass through the roof slope, this work identifies the terminals most suitable for passive stack ventilation systems.

6 Reverse flow

It was stated earlier that no prolonged periods of reverse flow were detected using the upward facing pitot static tube The alternative method, that of using two thermocouples, did, however, indicate that under certain conditions, reverse flow could occur. This method was not installed until midway through the system 8 testing period so only systems 8 to 15 can be discussed here.

A datalogger was programmed to monitor the temperatures of the two thermocouples once every 5 seconds, in the event of the duct air temperature being one or more degrees lower than near the ceiling just beside the duct, signifying that cooler air was flowing down the duct into the room, the logger would record the time of occurrence and the temperature difference. Subsequently, a note was made of each half hour period when reverse flow had occurred, together with the number of minutes during each half hour in which there had been reverse flow.

System 14 (short offset flexible stack with no ceiling diffuser) showed the greatest amount of reverse flow, with some also indicated for systems 8,11 and 15. Figure 3 shows the distribution of half hour periods containing some reverse flow by wind direction for system

14, it can be seen that this reversal occurs around two particular wind directions and is probably caused by the effects of adjacent trees. The amount of reverse flow in each half hour period, where some occurred, varied between 1 and 50%.

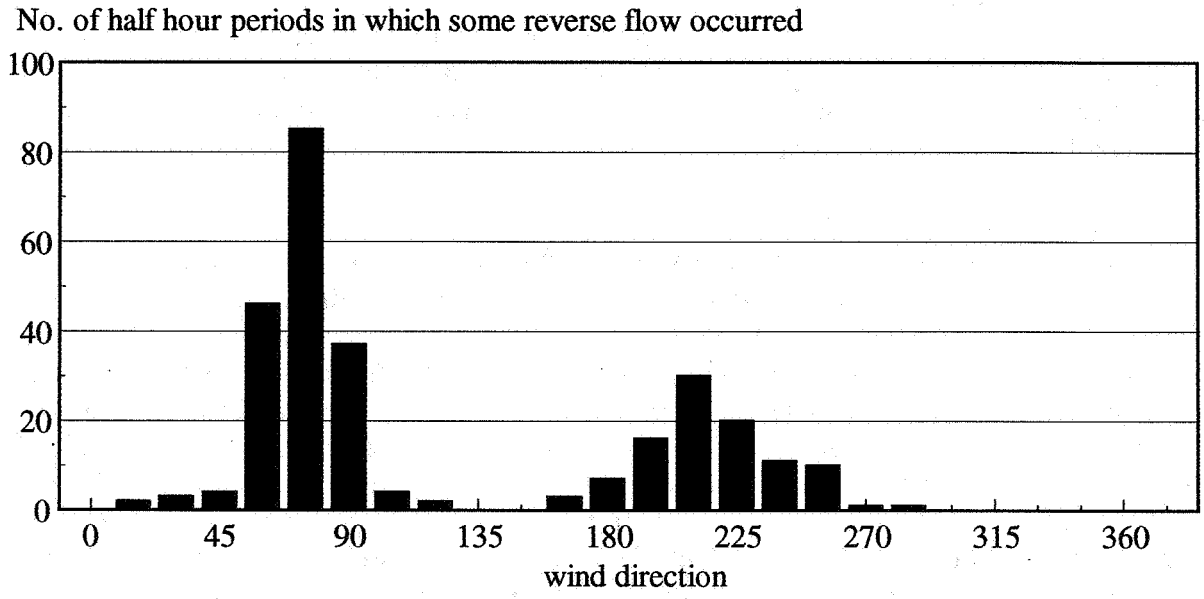

Figure 3: Indications of reverse flow in system 14

The total time during which reverse flow occurred for systems 8 to 15 was 0.7% and for system 14 alone 2.7%.

Reverse flow has only been recorded if it reached the lower end of the stack so the increase noticed in system 14 is probably due to the shorter length of stack, the same system with a longer length stack (System 13) showed no indication of reversal. It is possible that air sometimes flows down the duct for brief periods not long enough to reach the room below, such reversal would not be a nuisance in terms of occupant discomfort although it would reduce the overall flow rate .

7 Discussion

The performance of fifteen different passive stack ventilator systems, using different materials, configuration, diameter, length and terminals, has been monitored in a test house over a range of climatic conditions.

For typical meteorological conditions of 4 m/s wind speed and temperature difference of 10° C, flow rates of 14 - 75 m^3/h were obtained. Thus appropriately sized passive stack ventilation systems could provide adequate ventilation for most kitchens or bathrooms over a 24 h period. Further work carried out by Shepherd et al[5] has shown that over a 24 h period, the air change rate using a PSV system was approximately the same as using an extract fan for 2 h during that period.

An advantage that PSV systems have is that because flow rate increases with temperature

difference, the systems become most effective when the greatest flow is required ie. when cooking is taking place in the kitchen or showering/bathing in the bathroom.

8 Conclusions

Results indicate that :

1) Flow rate measured up the stack was roughly twice as much in the large diameter stack as in the smaller stack for the straight configuration and 50% higher for the stack with an offset.

2) Increasing the diameter of the stack does not necessarily increase the flow rate proportionally, due to the possible restriction of flow by the roof terminal and the resistance caused by the air leakage characteristics of the room.

3) For a given duct diameter, including an offset in the stack can reduce the flow rate by up to 50% depending on type of ridge terminal used.

4) The roughness of the flexible stack material compared with the smooth rigid material, has little or no effect on flow rate.

5) The terminal specified for each end of the duct should have a free area of not less than that of the duct itself.

6) There is an increased risk of reverse flow reaching the room in the case of upstairs bathrooms due to the shorter length of stack involved.

7) There should be sufficient provision for air to enter the room, by means of trickle ventilators or similar, so that the room itself does not act as a restriction to flow.

References

(1) PARKINS, L .M." Experimental passive stack systems for controlled natural ventilation." Proceedings of CIBSE Technical Conference, Canterbury 1991

(2) CRIPPS, A.J. and HARTLESS, R.P." Comparing predicted and measured Passive Stack Ventilation rates." AIVC Conference, Buxton, Sept 1994

(3) WELSH, P." Testing the performance of free standing ventilation terminals." AIVC Conference, Buxton, Sept 1994

(4) DEPARTMENT OF THE ENVIRONMENT AND THE WELSH OFFICE. "The Building Regulations 1985 Approved Document F: F1 Means of ventilation" (1990 edition). Statutory Instrument 1990 No. 2768. London, HMSO, 1990

(5) SHEPHERD, T.A., PARKINS, L. M. and CRIPPS, A.J." Effectiveness of various means of extract ventilation at removing moisture from a kitchen." AIVC Conference, Buxton, Sept 1994

The Role of Ventilation
15th AIVC Conference, Buxton, Great Britain
27-30 September 1994

A Review of Weather Data for Natural Ventilation

M J M Arif, G L Levermore

UMIST, Building Engineering Dept

A review of weather data for natural ventilation

MJM Arif Building Eng Dept UMIST
GJ Levermore Building Eng Dept UMIST

Synopsis

This paper briefly reviews the weather data available for natural ventilation and briefly reviews hourly data for simulation. It starts by reviewing the need for basic data for initial manual calculations. It then discusses the hourly weather data available for example the UK CIBSE Example Weather Years, and the European Community Test Reference Years. These are mostly selected for energy analyses rather than design, but there is still a need for establishing general criteria for weather data for design of HVAC services and natural ventilation. The paper examines weather data for summer conditions and the need to consider solar radiation as well as outside/inside temperatures and wind speed and direction for natural ventilation. A simulation of a typical building is used to demonstrate the importance of solar radiation.

1. Introduction

Extensive effort has been made to reduce energy consumption in buildings through better design of services and building envelopes. In winter, designers are concerned about energy losses through the fabric and the effectiveness of the heating system to provide warmth. Whereas in summer designers make efforts to try to ensure that the cooling system will consume minimal energy whilst maintaining comfort.

One use of energy that has been of arguable concern has been the use of air conditioning in the United Kingdom. It has been proposed that natural ventilation may alone be adequate. However, as this paper discusses, solar gain is a major heat gain after equipment gains in modern offices. So the designer of the natural ventilation system must be aware not only of wind data, and indoor-outdoor temperature differences for stack ventilation but coincident solar radiation must also be considered.

2. Weather Data

It is well understood that the prime agencies for natural ventilation and infiltration are the wind velocity and the stack effect depending on the difference between internal and external air temperatures. In principle the air flow through a building and the ventilation rates of individual spaces within a building can be determined for a given set of weather conditions. However, due to a number of flow paths likely to be present, the calculation can be very complex.

As to the weather data there are a number of sources in the UK including the Meteorological Office and the CIBSE Guide Section A2(1). However, computer simulation is becoming increasingly important in design and Section A2 is primarily for manual design. Example weather years exist for energy analyses, but not design. CIBSE has its Example Weather Years(2,3) for simulation for energy analysis. There are other sources of weather data for energy simulation,(4), as well as the EC's Test Reference Years(5) and ETSU's data(6). Recently a committee of the IEA has developed a further selection method for Designing Reference Years (DRY) but this is oriented mainly towards modelling active solar systems(11). As yet there is no concensus on the period or the extreme values of weather data for the design of naturally ventilated buildings by simulation,(or for mechanically ventilated or air conditioned buildings), although the ETSU EWY work additionally identified three types of "design day"(8). Recently CEN Working Groups have been set up to consider selection methods for sequences of extreme hot, sultry weather for both naturally ventilated and air-coditioned buildings. However, selection criteria are now being discussed in the Wind Data Task Group of CIBSE which is helping rewrite Section A2 as a seperate volume J of the CIBSE Guide. Initial ideas on selection centre on the need for data on coincident wind velocity, direction and the coincident inside/outside temperature difference. But to promote further discussion this paper considers that coincident solar radiation is also an important parameter.

To examine some of these weather parameters the CIBSE Example Weather Year for Kew 1964-65(7), has been analysed. Summer conditions, when natural ventilation will be tested most, have been considered primarily. Fig. 1 shows that in the summer,(taken as June,July and August), the horizontal direct solar radiation generally increases as the outside temperature increases. But Fig. 2 indicates that high wind speeds and high solar radiation do not necessarily tend to coincide. Perhaps this is due to high solar radiation usually occuring in the UK during periods of high atmospheric pressure(anticyclones) when the wind is also generally calm. This does not help natural ventilation. Also the wind speed tends to be lower in the higher temperature periods of the summer as Fig.5 shows.

3. Building Simulation

For this paper the FACET Apache program has been used for the building simulation. In order to illustrate all the varying factors on a consistent basis, a 'typical' commercial building geometry, developed by BRE is used as a reference building(8). Its dimensions are 12.0m length, 5.5m width and 2.65m height.

For this simulation a brick faced wall was choosen with a flat roof and both are insulated to 1990 Building Regulation Standards. The orientation of the building is with the long walls facing north and south. Only the long walls were glazed.
One of the three storeys was considered in the simulation. Results are shown for a 'worst case' day in July.

3.1 Effect of Air Changes

Wind speed and stack effect can affect the rate of air changes in a building. It is important to know how much the rates of air change affect the internal air temperature of the building. By simulating the sample building with 35% glazing, as in Fig. 3, it is shown that higher rates of air changes can reduce its internal air temperature, with significant improvement from 1 ach(air changes per hour) to 10 ach, after which further increases of air changes do not improve the situation very much. The CIBSE Guide(9) gives an empirical average value of 3 ach in Table A8.4 for the normal case of windows open in daytime and closed at night, and a value of 10 ach if the windows are open day and night. Warren and Parkins(10) suggest air change rates of up to 8.8 ach in warm weather with ventilation on one side only when windows are open. It is known that ventilation rates vary considerably under the influence of wind, user operation of blinds and windows, stack effect, etc. but the variations very much depend on the circumstances. With the windows closed the rate could be very low(less than .25 ach) but with cross-ventilation it could be as high as 24 ach(10). Fig. 6 also demonstrates that the pattern of ventilation can lower the internal temperature of the building. For instance allowing ventilation 2 hours earlier in the morning or overnight at 25% of the daytime rate in addition to daytime ventilation, lowers the temperature slightly.

3.2 Effect of Solar Radiation

Solar radiation is often a major source of heat gains in buildings during the summer season, by direct radiation into the room and by conduction through the fabric and windows. Reducing the amount of glazing area and provide shading from direct radiation are the best ways to minimise these gains.

In Fig. 4, the sample building is simulated to have different amounts of glazing from 1% to 100% areas of the long walls. It is found that as the percentage of glazing reduces so the inside temperature reduces. However, even the lowest peak temperature is still high and in practice the solar gains could be reduced by using blinds on the windows.

3.3 Glazing and Air Changes

In Fig.3 and Fig.4 the sample building is simulated with 25% glazing and 10 ach(100% daytime and 25% overnight). It shows that this combination is better than the highest ACH at 35% glazing and as good as 5% glazing at 10 ACH. A summary of these combined effects is plotted in Fig. 7, showing that the rate of air changes is of diminishing effect with increasing air change rates.

Reducing the amount of glazing is the most significant contribution in reducing the inside air temperature. Further reduction in solar radiation is expected when external shadings and blinds are used.

4. Conclusion

This paper shows that coincident solar radiation should be considered when weather data is selected for use in the design of naturally ventilated buildings.

References

1. CIBSE Guide Volume A, Section A2
   "Weather and Solar Data", CIBSE 1986
2. Holmes,M.J, Hitchin, E.R.
   "An Example Year For Calc'ting Energy Demand In Buildings"
   Building Services Engineer, 45,1978, pp 186-9.
3. Hitchin, E.R, Holmes, M.J, Hutt B.C, Irving, S.& Nevrala,D.
   "The CIBSE Example Weather Year"
   BSER & T, 4(3),1983, pp 199-24.
4. Keeble, E.J.
   "Availability of weather data for use in simulation"
   BEPAC Technical Note 90/1
   Building Environmental Performance Analysis Club,1990
5. Lund, H.
   "Test Reference years,Try: Data on magnetic tape for 29 Meteorological Stations in European Community"
   Thermal Insulation Laboratory(Handbook),
   Technical University of Denmark,for CEC,1984
6. Akehurst, P.
   "Passive solar design studies: Provision of weather data"
   FACET Ltd, St Albans, for ETSI, 1990
7. Letherman, K.M. and Wai, F.M.
   "Condensed Statistics on the CIBS Example Year-Kew"
   BSER & T,1980,(1),pp 157-159; BSER & T, 1981, 2, pp 165-173.
8. Leighton, D.J and Pinney, A.A.
   "A set of Standard Office Description for Use in Modelling Studies" BEPAC TN 90/50
9. CIBSE Guide Volume A, Section A8
   "Summertime Temperatures in Buildings"
   Chartered Institute of Building Services, 1986.
10. Warren, P.R. and Parkins, L.M.
    "Window-opening behaviour in office buildings"
    BSER & T, Vol 5(3), 1984, pp 89.
11. Lundh, H.
    "The Design Reference Year"
    Building Simulation 1991, Proc IBPSA Conference,
    Sophia-Antipolis/Nice, 1992-08-20/22, pp 600-606

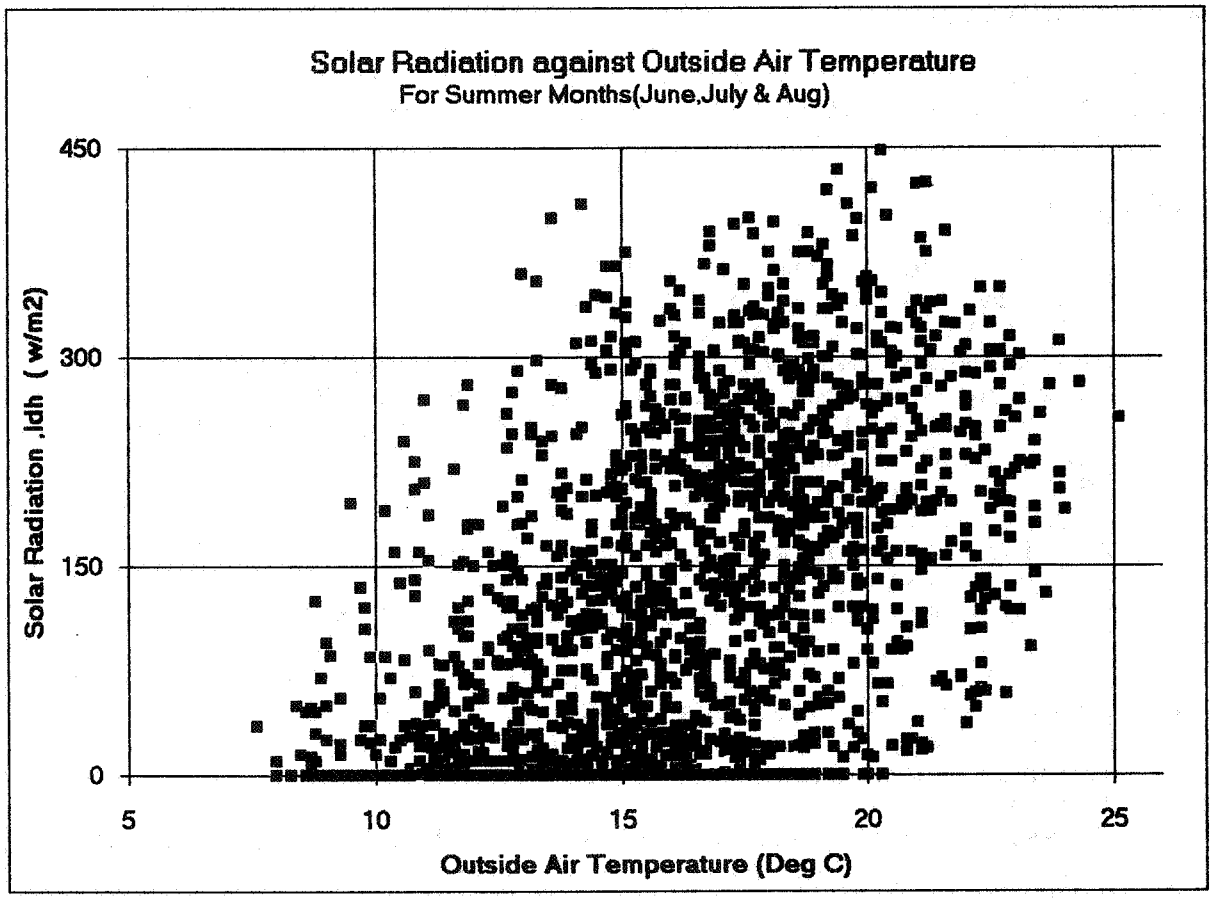
Solar Radiation against Outside Air Temperature
For Summer Months(June,July & Aug)
Solar Radiation ,Idh (w/m2)
450
300
150
0
5
10
15
20
25
Outside Air Temperature (Deg C)

Fig. 1

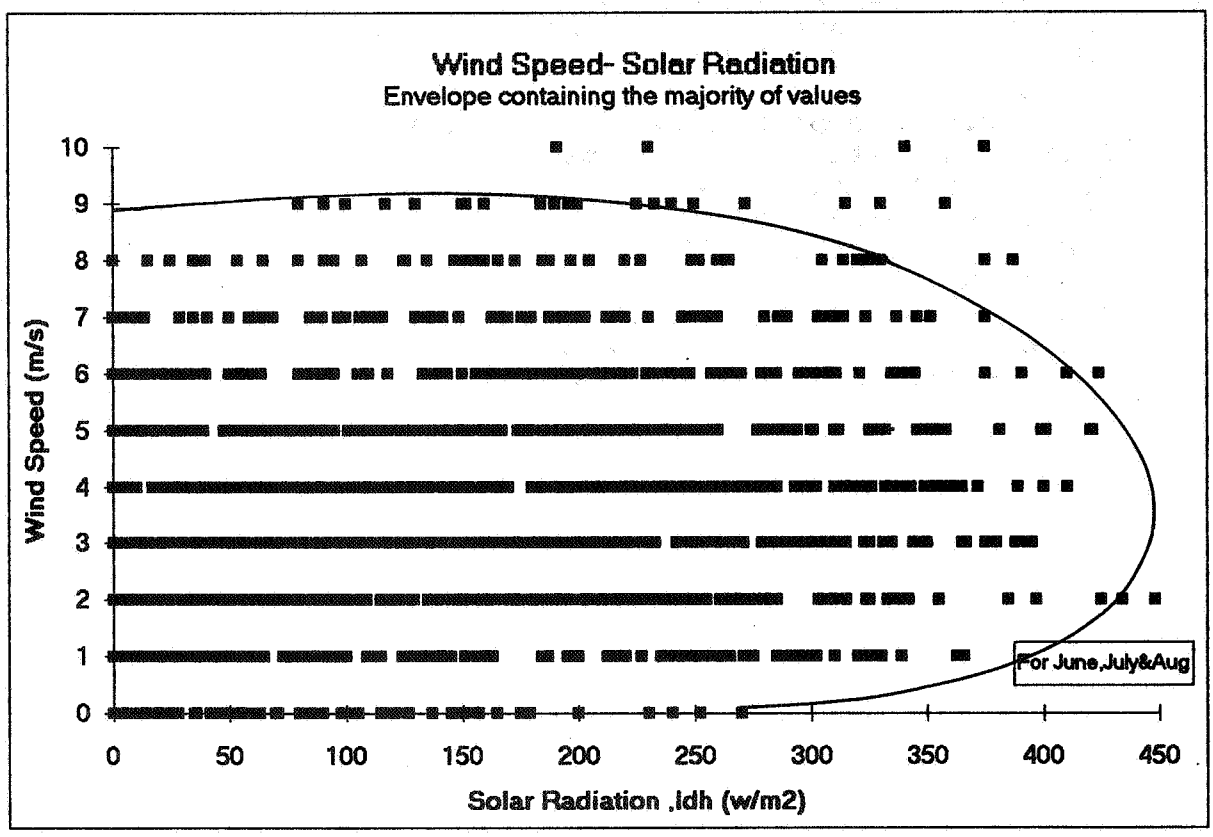
Wind Speed- Solar Radiation
Envelope containing the majority of values
Wind Speed (m/s)
10
9
8
7
6
5
4
3
2
1
0
0
50
100
150
200
250
300
350
400
450
Solar Radiation ,Idh (w/m2)
For June,July&Aug

Fig. 2

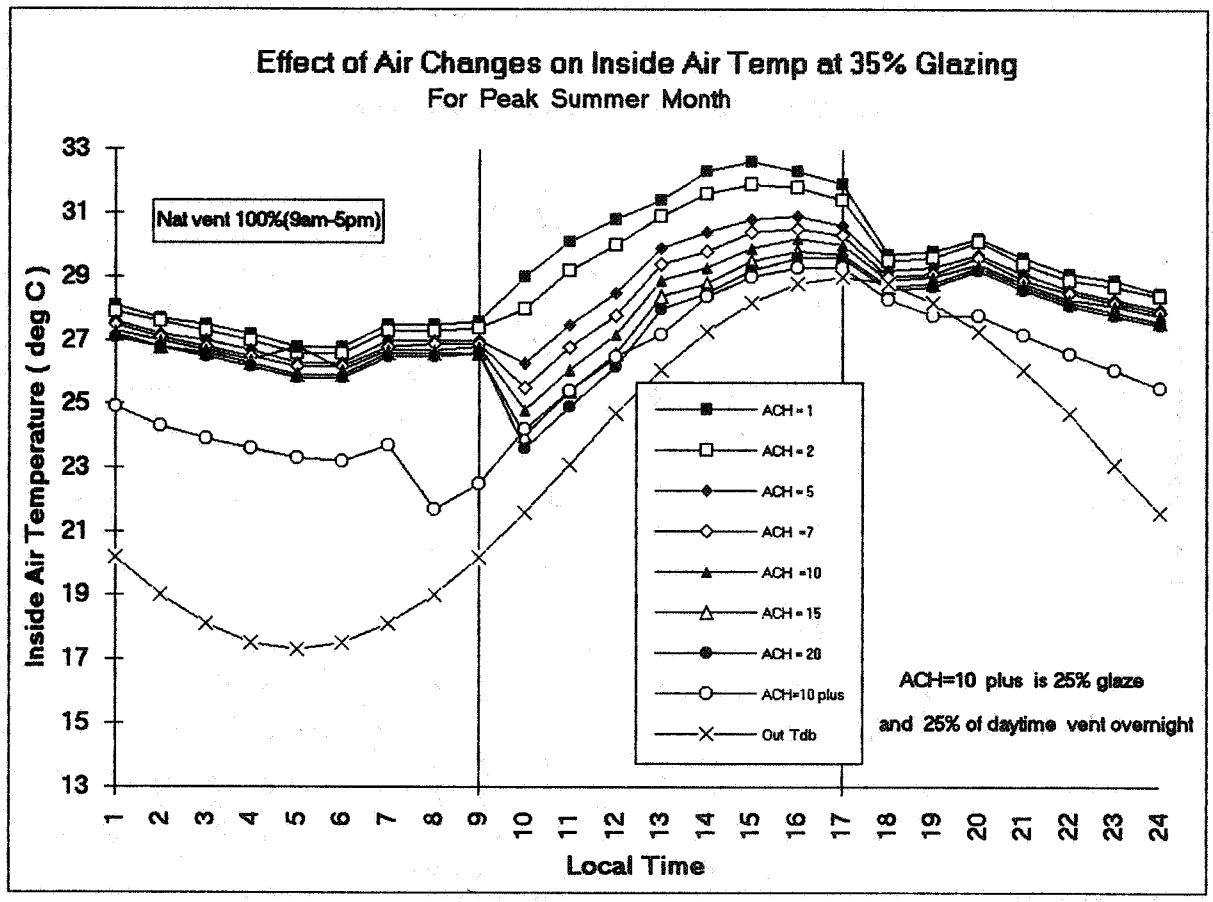
Effect of Air Changes on Inside Air Temp at 35% Glazing
For Peak Summer Month
Nat vent 100%(9am-5pm)
Inside Air Temperature (deg C)
Local Time
ACH = 1
ACH = 2
ACH = 5
ACH = 7
ACH =10
ACH = 15
ACH = 20
ACH=10 plus
Out Tdb
ACH=10 plus is 25% glaze
and 25% of daytime vent overnight

Fig. 3

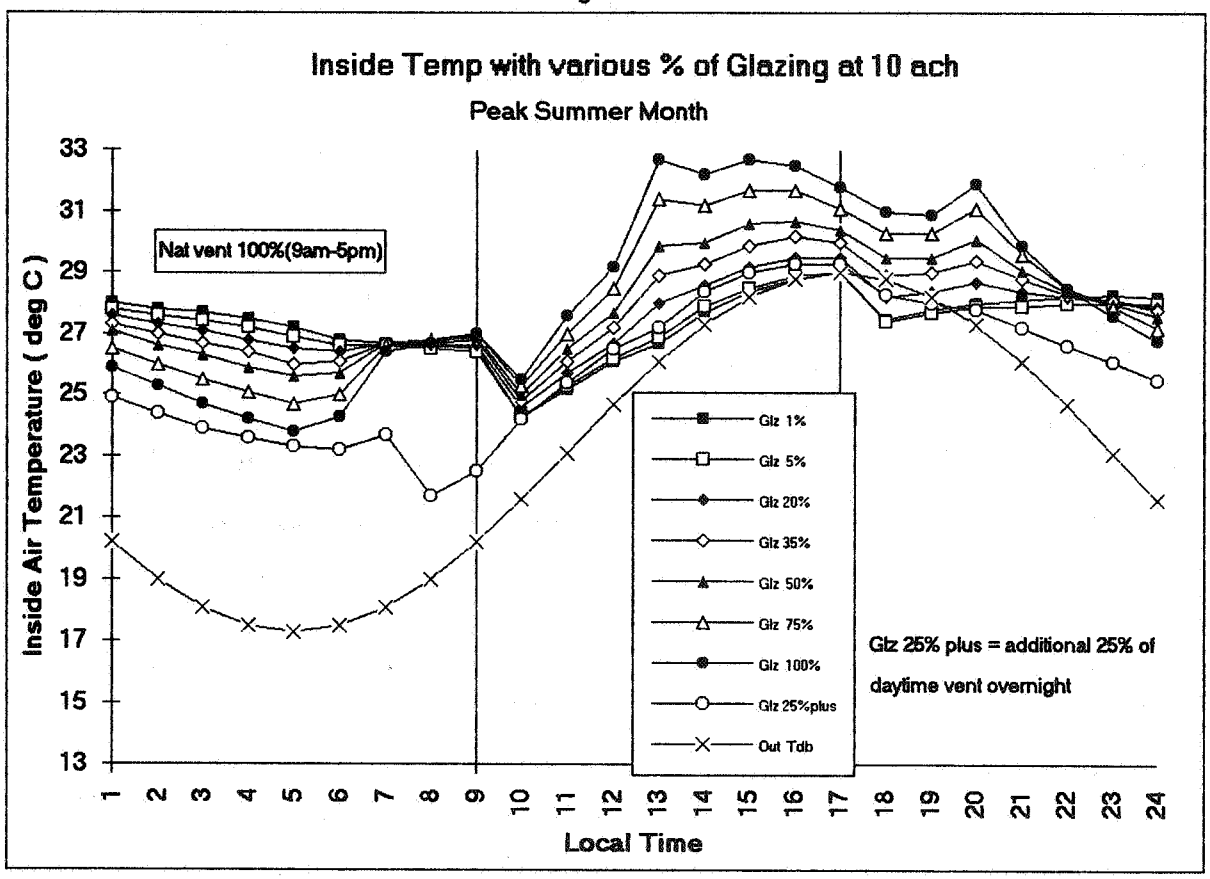
Inside Temp with various % of Glazing at 10 ach
Peak Summer Month
Nat vent 100%(9am-5pm)
Inside Air Temperature (deg C)
Local Time
Glz 1%
Glz 5%
Glz 20%
Glz 35%
Glz 50%
Glz 75%
Glz 100%
Glz 25%plus
Out Tdb
Glz 25% plus = additional 25% of
daytime vent overnight

Fig. 4

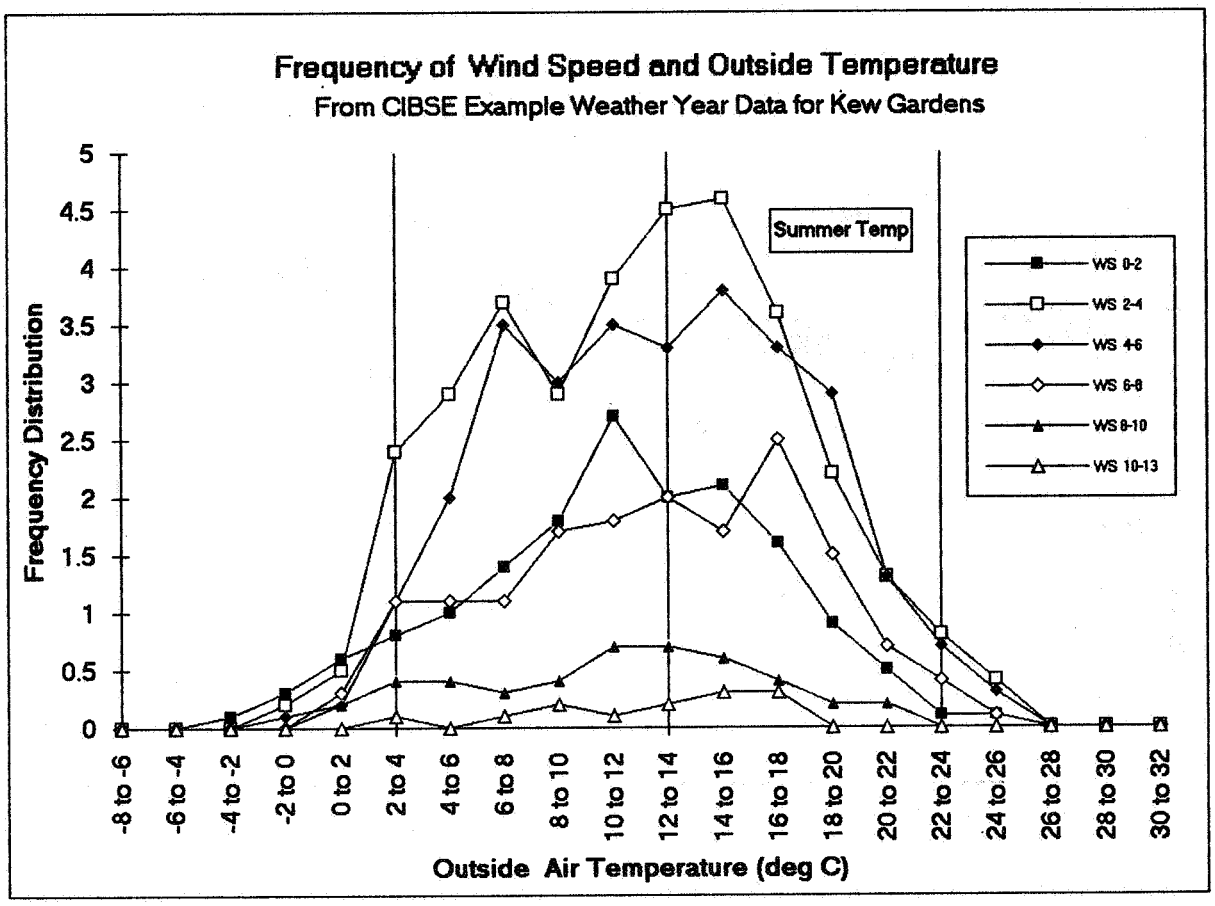
Frequency of Wind Speed and Outside Temperature
From CIBSE Example Weather Year Data for Kew Gardens
Frequency Distribution
Outside Air Temperature (deg C)
Summer Temp
WS 0-2
WS 2-4
WS 4-6
WS 6-8
WS 8-10
WS 10-13
5
4.5
4
3.5
3
2.5
2
1.5
1
0.5
0
-8 to -6
-6 to -4
-4 to -2
-2 to 0
0 to 2
2 to 4
4 to 6
6 to 8
8 to 10
10 to 12
12 to 14
14 to 16
16 to 18
18 to 20
20 to 22
22 to 24
24 to 26
26 to 28
28 to 30
30 to 32

Fig. 5

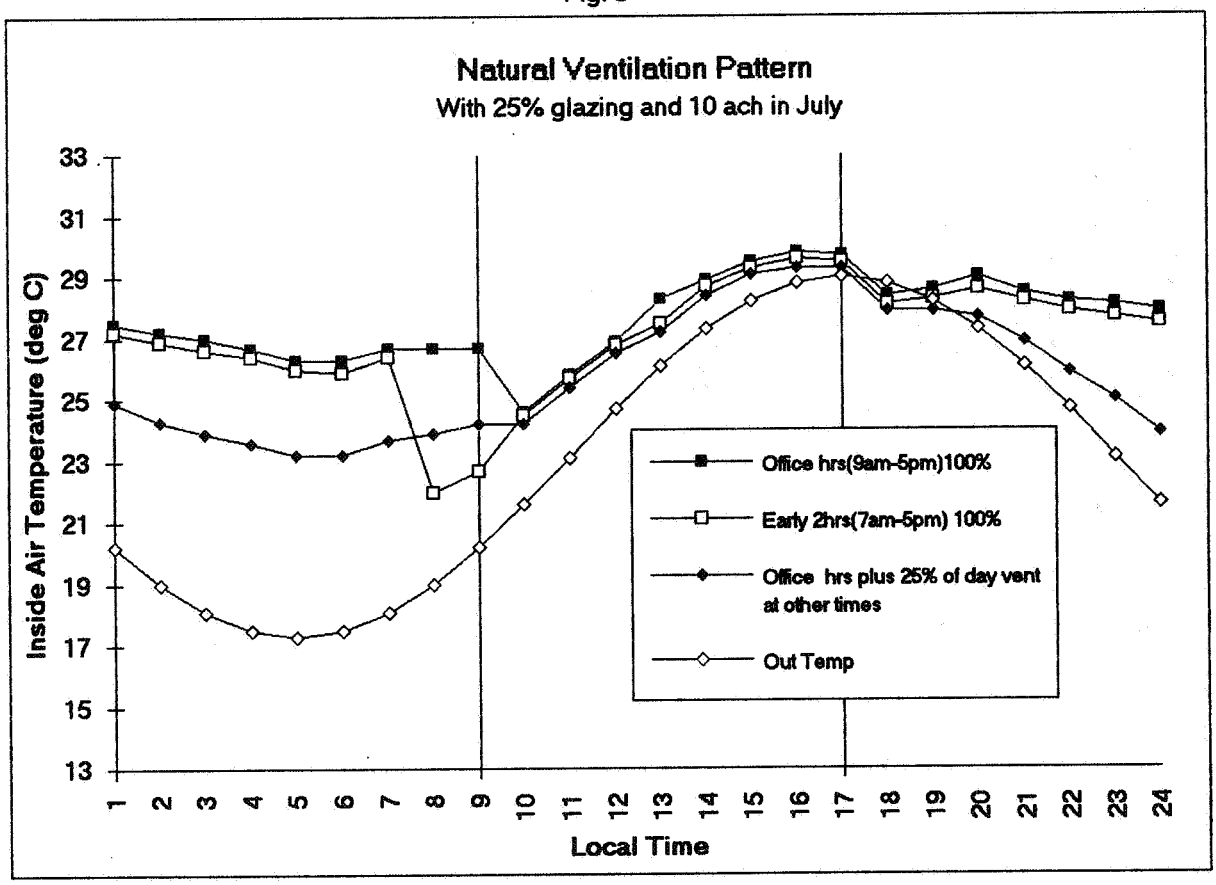
Natural Ventilation Pattern
With 25% glazing and 10 ach in July
Inside Air Temperature (deg C)
Local Time
Office hrs(9am-5pm)100%
Early 2hrs(7am-5pm) 100%
Office hrs plus 25% of day vent at other times
Out Temp
33
31
29
27
25
23
21
19
17
15
13
1
2
3
4
5
6
7
8
9
10
11
12
13
14
15
16
17
18
19
20
21
22
23
24

Fig. 6

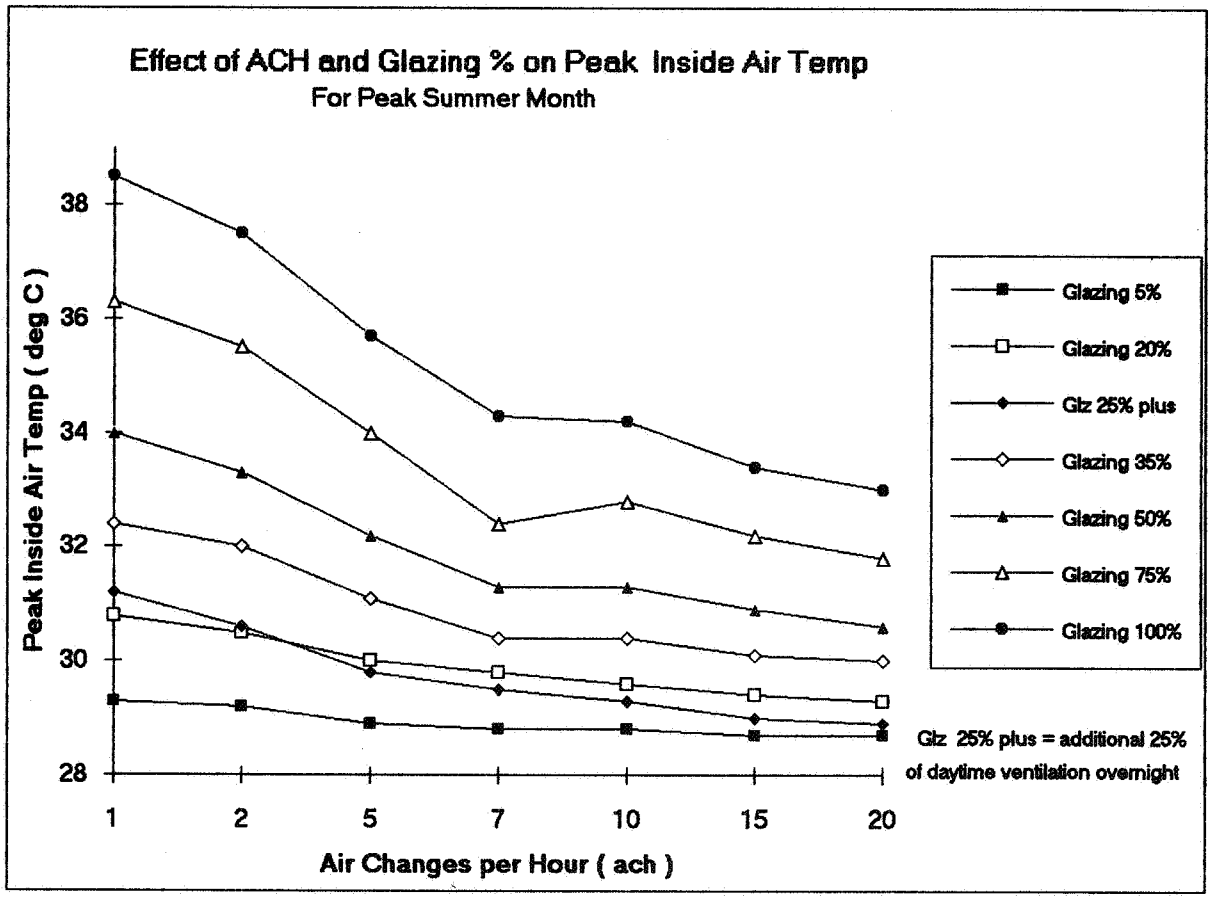
Effect of ACH and Glazing % on Peak Inside Air Temp
For Peak Summer Month
Peak Inside Air Temp (deg C)
38
36
34
32
30
28
1
2
5
7
10
15
20
Air Changes per Hour (ach)
Glazing 5%
Glazing 20%
Glz 25% plus
Glazing 35%
Glazing 50%
Glazing 75%
Glazing 100%
Glz 25% plus = additional 25%
of daytime ventilation overnight

Fig. 7

The Role of Ventilation
15th AIVC Conference, Buxton, Great Britain
27-30 September 1994

The Limits of Natural Ventilation in Deep Office Spaces

M White, R Walker

Building Research Establishment, Garston, Watford, Herts WD2 7JR, United Kingdom

Abstract

Renewed interest is being shown in designing for natural ventilation as a means of avoiding the need for air conditioning. Previous work showed that good distribution of air within a room is achieved up to 10m from a facade containing a window. Draughts and air movement are also important factors in determining the effectiveness of ventilation through windows. High air speeds may cause draught problems near the window whilst at depth the air speed may be uncomfortably low, particularly where the room has many internal partitions. The effect on air movement was investigated for window openings located at different heights in the wall of the room. In addition parallel tests were carried out in two adjacent and identical deep office rooms to compare air movement when internal partitions were added to one room.

These tests showed that the whole room ventilation rates and air distribution are similar for tests with standard windows and tests with high level windows. It was also shown that high level windows reduce the risk of draughts. Comfort conditions for the tests were consistent with an earlier study that suggested that comfort could be maintained most of the time with single-sided ventilation. Preliminary results indicate that partitions do reduce air speeds within the room. The usefulness of ceiling fans to enhance air movement and increase the range of thermal comfort condtions for deep spaces is also addressed.

The Role of Ventilation
15th AIVC Conference, Buxton, Great Britain
27-30 September 1994

The Evaluation of Ventilation Effectiveness Measurements in a Four Zone Laboratory Test Facility

J R Waters, C E Brouns

Coventry University School of Built Environment. Priory Street, Coventry CV1 5FB United Kingdom

Abstract

Improvements to ventilation systems for the purpose of saving energy may also affect the provision of good air quality. Measurement of ventilation effectiveness may be used to determine whether or not good fresh air distribution and satisfactory contaminant removal has been achieved in a specific case. However, for such measurements to be useful, it is necessary to establish recommended values of the parameters, and check the reliability of the measurement procedures. This paper is concerned with the second of these problems. It is well known that both air change efficiency and contaminant removal effectiveness can be easily measured when there are clearly defined supply and exhaust ducts for the ventilating air, and there is no re-circulation. However, measurements become more difficult when these conditions are not satisfied. Also, in all cases, tracer gas measurements often require the estimation of end correction to exponential decay curves, with a possibility of large errors. This paper reports on the first part of a systematic exploration of ventilation effectiveness measurement methods, carried-out in the four zone test facility described by Brouns and Waters. Several different flow patterns and ventilation strategies are tested, and comparisons with some full scale measurements are made.

The Role of Ventilation
15th AIVC Conference, Buxton, Great Britain
27-30 September 1994

Determination of Local Mean Ages of Air by the Homogeneous Injection Tracer Gas Technique

H Stymne, C Blomquist, M Sandberg

Department of Built Environment, The Royal Institute of Technology, P O Box 88, S 80102 Gavle, Sweden

Synopsis

The paper describes the application of a new tracer gas technique for studying ventilation. The technique is called the homogeneous injection technique, since it relies on the continuous injection of tracer gas in all parts of a zone-divided ventilated system, with tracer injection rates, which are strictly proportional to the zone volumes. The steady state concentrations of tracer gas in the different zones are proportional to the local mean ages of air. The technique is demonstrated and compared with other tracer gas techniques in an indoor test house with controlled ventilation under different conditions of air mixing and door opening.

It is shown that the homogeneous injection technique is easy to use and has some attractive advantages, compared to the tracer decay technique. It is shown that reliable results are obtained even without artificial mixing of the air.

1. Introduction

There are several different tracer gas techniques available for studying ventilation, all with their advantages and drawbacks. The most useful ventilation concept, when it comes to air quality and contamination control is the local mean age of air. The local mean age of air tells us how long the air in a local volume has spent on average in the building. A long mean age means that contaminants emitted in the building have accumulated to high concentrations, while a low mean age means a well ventilated space. By mapping the mean age of air in a building, one gets a measure of the distribution of ventilation air. The conventional technique for studying the mean age of air is the tracer gas decay technique. However, there are several drawbacks to the decay technique - the most obvious being: difficulty in achieving a uniform initial tracer gas concentration in a multi-room building, a time-consuming measurement of decay in several rooms and difficulty in following the time dependence of the local mean ages.

Recently a new tracer gas measurement technique (homogeneous emission technique - HET) for studying ventilation was presented by Stymne et al. (1992). This technique relies on the fact that the local steady state concentration of a contaminant, which is homogeneously emitted in a ventilated space is proportional to the local mean age of air. This has been shown in several papers by Sandberg (e. g. 1981, 1984) and has also recently been used for computing distribution of local mean ages from computational fluid dynamics simulations (Han 1992). However, the relationship between the local concentration and the local mean age of air had not been suggested as a basis for ventilation measurement with homogeneously emitted tracer gas until Stymne and Säteri (1991) discussed it in connection with future development of the passive tracer gas technique and Stymne *et al* (1992) demonstrated it, using a passive tracer gas technique in a large laboratory hall. The homogeneous emission technique has recently been validated in a field trial using adjustable passive tracer gas sources (Stymne and Boman, 1994).

In the present paper the technique is demonstrated in an indoor test house, using homogeneous injection of nitrous oxide tracer gas and continuous measurement of the tracer gas concentration. Comparison is made with the tracer decay technique and the constant concentration technique.

2. Theory

Ideally homogeneous injection means that tracer gas should be injected from continuously distributed sources in all parts of the ventilated system, at a constant rate per cubic meter. Perfectly homogenous injection is therefore not practically possible. In the practical application, the system is sub-divided into smaller zones, in each of which tracer gas is injected at a rate, which is proportional to the zone volume. In multi-room environments it is most practical to use rooms of ordinary size as zones, while larger rooms may have to be further divided into several zones. The mixing within a single room is usually good enough compared to the mixing between rooms, to be useful for treatment with the multi-zone theory. In the multi-zone theory the zones are treated as fully mixed (uniform tracer gas concentration), while concentration differences can appear between zones.

In the multi-zone theory the concentration vector $\mathbf{C}$, whose elements are the steady state concentrations in the different zones is:

$$\mathbf{C} = \mathbf{Q}^{-1}\dot{\mathbf{m}} \tag{1}$$

where $\mathbf{Q}^{-1}$ is the so called inverse flow matrix and $\dot{\mathbf{m}}$ is the tracer gas emission rate vector. The mean age vector $\overline{\boldsymbol{\tau}}$ is obtained from the $\mathbf{Q}^{-1}$ matrix and the volume vector $\mathbf{V}$:

$$\overline{\boldsymbol{\tau}} = \mathbf{Q}^{-1}\mathbf{V} \tag{2}$$

If the emission rates are proportional to the zone volumes:

$$\dot{\mathbf{m}} = k \cdot \mathbf{V} \tag{3}$$

the concentrations are proportional to the local mean ages of air:

$$\mathbf{C} = k \cdot (\mathbf{Q}^{-1}\mathbf{V}) = k \cdot \overline{\boldsymbol{\tau}} \tag{4}$$

and the local mean age of air in a zone $\overline{\tau}_p$ can be calculated from the tracer gas steady state concentration:

$$\overline{\tau}_p = \frac{C_p}{k} \tag{5}$$

3. Experiment

3.1 Experimental house

The experiment was carried out in an indoor test house in a laboratory. The house (fig. 1) has five "rooms" - living room, bedroom, hall, kitchen and bathroom. The south wall of the test house is an exterior wall, while the other walls are directed towards the laboratory hall.

In this experiment the house was mechanically extract-ventilated at an air change rate of 1 ACH. The total extract flow rate of 176 m^3/h was equally divided between the extract points in the kitchen and the bathroom. Air was admitted through inlet devices in the walls in the living room (outside air) and bedroom (laboratory air). Some air may also infiltrate into the other rooms from the laboratory hall. The rooms were equipped with oscillating mixing fans (one in each room and two in the living room) directed towards the centre of the rooms away from doorways.

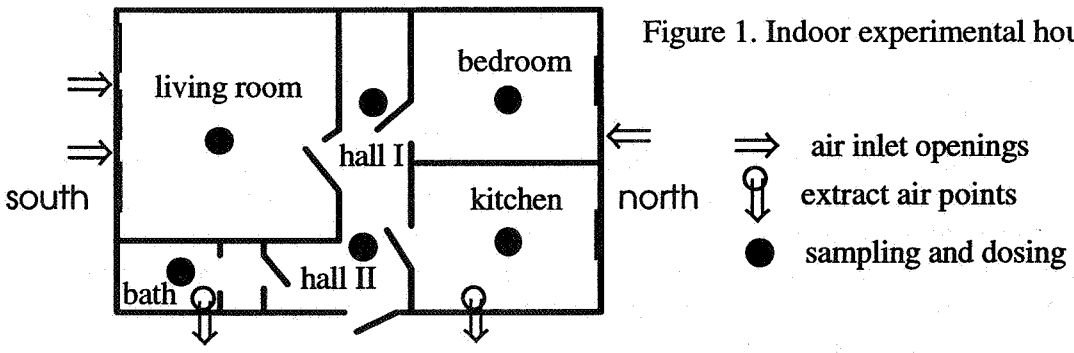

Figure 1. Indoor experimental house

3.2 Experimental layout

Measurements were made during the following conditions:

a) internal doors open (except bathroom)	mixing fans off
b) internal doors open -"-	mixing fans on
c) internal doors closed	mixing fans off
d) internal doors closed	mixing fans on

Tracer gas injection points were at the floor level in the middle of each room. The hall was divided into two zones (hall I and hall II) each with its own tracer gas injection point. The air sampling points were positioned at a height of 1.2 m in the middle of each room (zone). The following nitrous oxide tracer gas measurement scheme was followed for each experiment:

a) Six hours homogeneous injection, with injection rates proportional to the zone volumes.
b) four hours decay period
c) four hours constant concentration period
d) four hours decay period

Continuous measurement of tracer gas concentration at all six measurement points was made during each experiment with a sampling cycle period of approximately 7 minutes.

3.2.1 Homogeneous injection

The approximate injection rates used in the different zones are given in table 1.

Table 1. Approximate injection rates

room	liv. room	bedroom	hall I	hall II	kitchen	bathroom
rate g/h	26.2	15.3	7.9	7.9	16.0	5.0
$g/(h,m^3)$	0.47	0.43	0.44	0.44	0.46	0.33

As can be seen, the emission rates per cubic meter are not exactly equal in all zones. In most zones, this depends on the difficulty in programming an exact rate, while in the bathroom it depends on a calculation error.

3.2.2 Constant concentration

During the constant concentration period the target value was chosen to be 50 ppm.

4. Measurement

The tracer gas measurement and injection was made using a Brüel & Kjær infrared analyzer model 1302 and dosing and sampling unit model 1303, which was programmed to perform all the steps in a measurement cycle, one after the other. The dosing and sampling were made by use of 4 mm polyethylene tubes. During injection the Brüel & Kjær equipment mixes the tracer gas with air in order to avoid density differences between the injected tracer gas and the air. The equipment was checked against a calibration gas mixture (96 ± 2 ppm N_2O in nitrogen), and showed 92.5 ppm. No correction was made for the discrepancy.

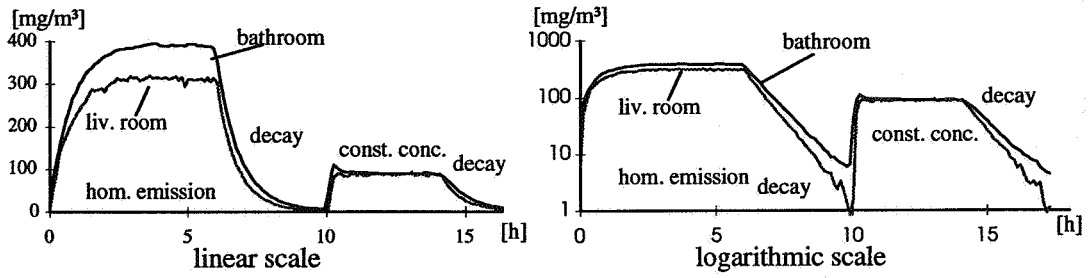

Figure 2. Example of measurement cycle (doors closed - mixing fans on)

5 Calculations

5.1 Mean age of air

5.1.1 Homogeneous emission technique

The time averaged local tracer concentration C_p (mg/m^3) from 3 to 6 hours after the beginning of the injection is calculated for all six measuring points. The total injection rate (mg/h) in the house is calculated and divided by the total volume (176 m^3) to get the average specific injection rate per cubic meter S_t. The local mean age of air is computed through division of the average local concentration with the specific emission rate S_p.

$$\bar{\tau}_p = C_p / S_p \tag{6}$$

S_p is a corrected value of S_t, in order to make a correction of any (small) deviation of local specific injection rate from the average value. It is not possible to make a proper correction for different specific injection rates in the different zones, because this would require knowledge of transfer probabilities between different zones. Here a simplified approach is adopted. Of the excess (or deficit) injection rate in a zone (V_iS_i-V_iS_t), only a volume weighted part (V_i/V_t) is accounted for in that specific zone. Therefore:

$$S_p = S_t + \frac{V_i}{V_t}(S_i - S_t) \tag{7}$$

5.1.2 Constant concentration technique (CCT)

The average dose $\dot{m}_p$ and the average concentration C_p in each zone is calculated for the constant concentration period. The local air supply rate is calculated from:

$$q_p = \dot{m}_p / C_p \tag{8}$$

5.1.3 Decay technique (DT)

The lowest "noisy" part of the decay curve is cut off. The last exponential part of the remaining decay curve is extrapolated to infinity. The area under the curve from the beginning of the decay until the cut off value is computed and corrected with the area under the extrapolated exponential part of the curve. The resulting area is divided by the concentration value at the beginning of the decay curve.

5.2 Accuracy

The accuracy of determination of mean age of air with tracer gas technique depends on four different factors:

- equipment calibration
- initial conditions
- bad mixing in a zone
- evaluation error

these factors are further discussed in the **appendix**.

Table 2 gives approximate estimates of the relative uncertainties, which are taken from informed guesses, equipment data and experimental data for the kitchen in the present experiment. The total inaccuracy of mean age determination is calculated from the square root of the sum of squares of the individual components.

Table 2. Estimated relative uncertainties (in %) from different components

	--------doors open--------				--------doors closed--------			
	---no mix---		----mix----		---no mix---		----mix----	
	HET	DT	HET	DT	HET	DT	HET	DT
calibration	5	3	5	3	5	3	5	3
initial	5	5	5	5	5	5	5	5
mixing	8	8	3	3	3	3	1	1
evaluation	2	11	1	1	1	2	-	2
total	11	15	8	7	6	7	7	6

The uncertainty of the "mixing" component is the relative standard deviation of the concentration during constant emission, which is thought to also reflect the spatial uncertainty in concentration. The "evaluation" component is the relative standard deviation of the concentration divided by the square root of the number of measurements for the homogeneous emission. For the decay technique this component is firstly the inaccuracy in the initial value (which is the standard deviation during the last part of the constant concentration period divided by two) and secondly the inaccuracy of the determination of the area under the first minutes of decay. The "calibration" and "initial" components are reasonable estimates.

6 Results

6.1 Local mean ages of air

The results from the measurements are shown in table 3 and figure 3.

Table 3. Local mean ages of air measured by different techniques.
HET=homogeneous emission technique, DT=decay technique

	liv. room	bed room	hall I	hall II	kitchen	bath	aver. age	extract age
volume[m^3]	55.8	36	17.8	18	34.7	13		
	Doors open - no mixing							
HET [h]	0.74	0.73	0.90	0.80	1.21	0.86	0.86	1.04
DT [h]	0.75	0.53	0.79	0.96	0.94	0.94	0.78	0.94
	Doors open - mixing							
HET [h]	0.73	0.77	0.81	0.85	1.02	0.95	0.83	0.98
DT [h]	0.84	0.85	0.89	0.91	1.10	1.01	0.92	1.06
	Doors closed - no mixing							
HET [h]	0.75	0.19	0.88	0.82	1.08	0.90	0.73	0.99
DT [h]	0.71	0.82	0.85	0.98	1.29	1.13	0.92	1.21
	Doors closed - mixing							
HET [h]	0.70	0.69	0.80	0.80	1.04	0.89	0.80	0.97
DT [h]	0.77	0.84	0.95	0.99	1.33	1.14	0.96	1.24

The average age in the house is calculated from a volume averaged mean of all the local mean ages. The mean age of the extract air corresponds to the nominal time constant and is computed from the mean ages in the extract rooms, weighted with the nominal extract flow rates in those rooms.

6.2 Air distribution patterns

As can be seen in figure 3 there are many similarities between the mean age distribution patterns determined with the two techniques. There is however a tendency for the mean ages determined by the decay technique to be slightly higher, and have a greater variation between the different experimental conditions than those determined by the homogeneous injection technique. It is obvious that the estimated mean ages are not greatly affected by the experimental conditions (door and mixing status). There are two striking exceptions, both occurring in the bedroom. These two low values are obviously erratic. The reason is unknown, but is believed to be caused by an equipment error yielding too low concentration readings. The error does not seem to affect the result in the other zones.

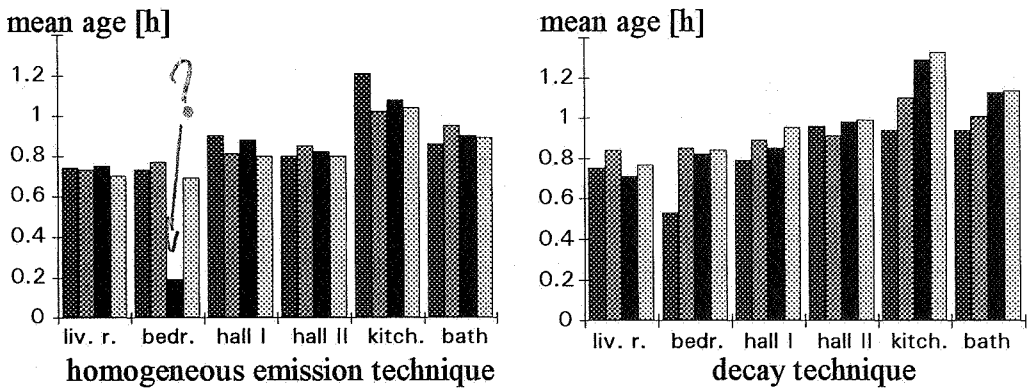

Figure 3. The distribution of mean ages as determined by the two methods. Each group of bars represent a room and the four bars in each group represents from the left to the right a) *open doors - no mixing*, b) *open doors - mixing*, c) *closed doors - no mixing* and d) *closed doors - mixing*.

6.3 Air flow estimates

It is not possible to unequivocally calculate air flow rates from mean ages determined by tracer gas experiments, unless the mean age of the extract air can be measured. However in this controlled experiment, it is known that the extract air is equally divided between the two extract points (kitchen and bathroom). Therefore the mean age of the extract air can be calculated from the average of mean ages of air in the two extract rooms. The total ventilation flow rate can then be calculated from the total volume of the house divided by the mean age of the extract air and compared with the known value (176 m^3/h) or estimates from constant concentration tracer experiment.

It is also possible to calculate the air flow rates in the supply rooms (living room and bed room), when their doors are closed and compare them with estimates made by the constant concentration measurements. Those rooms can be considered isolated, with no inter-zonal flows from the other zones, when their doors are closed. The supply air flow rate in an isolated zone is calculated from the zone volume divided by the local mean age of air. The comparison is shown in table 4.

Table 4. Comparison of air flow estimates with different techniques.

	----------no mixing----------				----------mixing----------			
			-----total*-----				-----total*-----	
	liv. room	bed room	doors closed	doors open	liv. room	bed room	doors open	doors close
HET	74	-**	169	177	80	52	178	181
DT	79	44	186	145	72	43	165	141
CCT	69	69	164	175	80	53	176	171

*true total ventilation flow rate is 176 m^3/h, -** obviously erratic value not included

It can be seen that the estimated total ventilation flow rate closely agrees with the true value in all four cases for the homogeneous injection and the constant concentration technique. The agreement is worse for the decay technique. Also the agreement with the constant concentration determination of supply rates is better for the homogeneous injection technique than for the decay technique.

7 Discussion

The homogeneous emission technique gives essentially the same information on ventilation performance as the tracer decay technique, but has several practical advantages over the latter.

- no demand of a uniform initial tracer concentration, which can be difficult to achieve in multi-room systems.
- a "steady state" technique, which makes it possible to integrate over longer time for increased accuracy.
- possible to monitor variations of ventilation as a function of time.
- easier and more reliable data interpretation and calculation, especially in badly mixed systems.

However there are also some disadvantages:

- long time needed for equilibration before measurement
- adjustable tracer injection units needed for each zone
- continuous injection consumes more tracer gas

All three disadvantages are eliminated using passive tracer gas technique, for which adjustable tracer gas sources are now available. However, further development will also overcome these disadvantages when using "active" techniques. The long equilibration time can for example be appreciably shortened using increased initial injection rates.

8 Conclusions

The homogeneous emission tracer gas technique for measuring local mean ages of air is shown to be easy to use and to yield improved accuracy, compared to the tracer decay technique. The technique has great future potential, either using "active" or "passive" tracer gas techniques and can in most cases substitute the decay technique for ventilation studies.

APPENDIX

Discussion on sources of uncertainty

Equipment calibration
HET: Relative uncertainties in calibration of measurement equipment and injection rate are of importance.
DT: No absolute calibration is necessary, but linearity and zero point deviations are important.

Initial conditions:
HET: Deviation from ideal homogeneous emission rates is important.
DT: Deviation from initial uniform concentration is important

Air mixing:
HET: Bad mixing in a zone results in large variations of concentration as a function of time and may also yield a time averaged concentration at the measuring point which deviates from the room mean value.
DT: Concentration variations due to bad mixing causes difficulty in tracing the true initial value and the important first part of the decay (see evaluation). It may also mean that the measurement point is not representative of the zone.

Evaluation
HET: The inaccuracy in evaluation depends on the standard deviation in the estimate of the time average of the concentration, which is inversely proportional to the square root of measurement time (or number of readings). In the present case it also depends on the inaccuracy in the estimate of injection rates.

DT: There are several difficulties in the evaluation, which cause uncertainties in the estimate of the mean age:

- *extrapolation of measurement from the last measurement point to infinity.* The last part of the curve should always decay exponentially to zero. However, in practice it is often difficult to locate the final exponential part of the curve. A small deviation of the zero setting of the instrument or some background value, will seriously affect the slope of the lowest part of the logarithmic plot of the decay curve. Making a background subtraction afterwards to give a final exponential decay will always be ambiguous.

- Determination of initial concentration

It is very important to get a correct value of the initial concentration since the area under the decay curve is to be divided by this value. This concentration value must be taken before the decay starts, i. e. when there still is a uniform concentration in the whole system. Bad mixing or beginning the decay from a constant concentration measurement (as in the present case) may yield a large uncertainty in the value of the initial concentration.

- Tracing the first part of the decay curve

The differences in the decay in different zones are often concentrated in the first few minutes of decay. After this initial period all curves in a system of coupled zones tend to decay exponentially with the same time constant. A time delay in measurement will make the interpretation of the first part difficult. Even more severe are the concentration fluctuations due to bad mixing in this important part of the decay. Due to the relatively large concentration in the beginning of the decay, this part represents a relatively large portion of the computed area under the decay curve.

Acknowledgements

Financial support from NORDTEST and the Swedish Council for Building Research is gratefully acknowledged.

References

Han H (1992)
"Calculation of ventilation effectiveness using steady-state concentration distributions and turbulent airflow patterns in a half scale office building".
In Murakami *et al.* (editors), Proceedings of the International Symposium on Room Air Convection and Ventilation Effectiveness, Tokyo 1992, pp 187-191.

Sandberg M (1981)
"What is Ventilation Efficiency?"
Building and Environment **16**, pp 123-135, [1981].

Sandberg M (1984)
"The multi-chamber theory reconsidered from the viewpoint of air quality studies"
Building and Environment **19**, 1984, pp 221-233.

Stymne H, Säteri J O (1991)
"The Development of the PFT-Method in the Future."
In Säteri, J.O. (editor): "The Development of the PFT-Method in the Nordic Countries". Swedish Council for Building Research, Document D9:1991, pp 109-120.

Stymne H, Sandberg M and Holmgren O (1992)
"Ventilation Measurements in Large Premises".
Proceedings of Roomvent'92 - Air Distribution in Rooms, Denmark 1992, Vol. 2, pp. 33-47.

Stymne H and Boman CA (1994)
"Measurement of Ventilation and Air Distribution, Using the Homogeneous Emission Technique".
Proceedings of Healthy Buildings '94, International Conference, Budapest, 1994.

The Role of Ventilation
15th AIVC Conference, Buxton, Great Britain
27-30 September 1994

Tracking Air Movement in Rooms

D K Alexander, P J Jones, H Jenkins, N Harries

Welsh School of Architecture, UWCC Bute Building,
Cardiff, CF1 1AD United Kingdom

ABSTRACT
A measurement system is described to record the movement in a room of neutral density balloons or bubbles, and thus the movement of air in that room. It is based on photogrammetric analysis of coincident video recordings made from several view points. Under laboratory conditions, the system was found capable of measuring position to an accuracy of ±3 cm over a range of 8 m, and of measuring 3-D velocities to better than ±0.05 m/s. The system was usable under field conditions, and could be operated in an occupied building. The largest space tested was approximately 30x15x10m. In the course of this work, the applicability of the use of balloons and bubbles for recording air movement was also explored. Balloons were found suited to typical natural room movements, but were unsuited to use within jets; bubbles were more appropriate for those.

1 INTRODUCTION

The air movement within and between rooms of a building is of considerable interest to designers of low-energy and environmentally healthy buildings. Unfortunately air does not always behave as designers would wish, their design tools are limited in scope and prediction techniques are often too complex and difficult to use. Furthermore, there is no easy way of assessing performance during or after the commissioning of a building.

Room air movement can either be measured very accurately through the use of expensive anemometry equipment, or observed easily and inexpensively through the use of smoke, bubbles or balloons. The limitations with the former lie in its' cost and complexity. Due to the high cost, such measurements are generally restricted to a small number of discrete, fixed, points within the space. Due to the complexity and sensitivity of the equipment, they are more suitable to a laboratory based investigation, or to use in an unoccupied building. The limitations of the latter lie in the qualitative nature of the information provided.

This paper describes a relatively low cost measurement system developed to quantify the visualisation of room air movement. The system described uses video recording and computer analysis to convert the recorded motion of neutral density balloons or bubbles into 3-D positions and velocities. As part of the development of the system the characteristics and suitability of various types of balloons and bubbles were explored.

2 THE MEASUREMENT SYSTEM

A number of researchers have used neutral density tracers to visualise air movement in rooms and buildings (1-3). The authors have previously used helium balloons both for qualitative research explorations and for the demonstration of natural ventilation concepts to students.

The analysis of stereo photographs for extraction of 3-dimensional data is well established, for instance in the photogrammetric recording of building dimensions (4). In other fields, such as robotic vision, motion detection and assessment is currently undergoing considerable development (5). There have been a few attempts at 3-D measurement systems (6,7) relating to building problems.

2.1 Measurement System Overview

The mathematical basis of the system is a form of surveying by triangulation (8). If a scene is photographed through several spatially distinct positions, the position of objects within that scene may be calculated from simple geometrical and trigonometric relationships, figure 1.

If the images to be analysed have been made as a time sequence, in synchrony, then the motion of those objects can be estimated from the difference in position between time periods. The motion of a target can be resolved as a true 3-D velocity with u,v,w components.

To establish the position of a target object, at least two views are required. Each pair of views can provide an estimate of position; from a number of such pairs, both position and an estimate of error of that measurement can be calculated. Room clutter (furnishings, structure, people, etc.), and geometry mean that some positions will be obscured from any one view, so the more vantage points the better; the equipment developed allows for three or four views of each area of interest.

In this system, the motion of the tracer objects are captured by a number of domestic quality video recorders and wide-angle cameras placed at fixed vantage points. A desk-top PC computer, with a frame accurate playback deck and a video capture card, provides the means of capturing and analysing the sequences. The recording equipment is simple, portable and robust, and although it is time-consuming to set-up accurately, a site measurement can be carried out within one working day. The system can be used to cover a large zone (a whole room), or it can be focused down onto a small area (e.g. a desktop or outlet grill). The largest space tested during this work was approximately 30x15x10 m; larger dimensions could be perhaps be covered with more viewpoints. The velocities that can be measured could range from <0.05 m/s to >5 m/s.

This system is intended to fill the gap between subjective observation and objective measurements using hot-wire or LDA techniques. Whilst it may not be capable of the high precision of those latter systems, it is simple and robust, is suitable for use in occupied buildings, and is capable of covering large spaces.

2.2 Tracer Objects

Balloons made from metalised polypropylene, filled with helium, were the main balloon type used. No other materials were found to be suitable, as they allowed too fast an escape of helium, and some were prone to static electric forces. The smallest balloon found to be feasible was 22 cm, made from 15μ polypropylene.

Bubbles from a number of sources were also tested, ranging from small seeds (1-2mm diameter) meant for wind tunnel visualisation, through to 5 cm diameter. Bubbles in this size range could be made visible to the cameras, at a distance of 1-2 m, provided that illumination could be controlled.

3 Error Characteristics of System

The overall error characteristics of the system can be identified as having four major components; errors in converting the camera image to direction angles, errors in triangulation positions from those angles, errors in timing or synchrony of the images, and errors introduced by the non-ideal nature of the tracers used.

3.1 Camera Image Errors

A requirement of the analysis is the conversion of the camera view to a digital bitmap image. Each pixel location must be identifiable as relating to a vector (altitude and azimuth) leading

from the optical centre of the camera to the object imaged at that pixel. Each camera system (camera case, CCD, lens, tape recorder, and capture card) was calibrated, using a "gridded" surface (a wall marked off in 5°± 1' steps). After this calibration angular positions could be determined from the images to ±6' (within a 90° horizontal view angle).

3.2 Positional Errors

Practical uncertainties in the position of the viewpoints, the orientations of the cameras, and in the determination of the centre of the targets under varying lighting conditions affect the ability of the system to precisely determine a position. Tests made in controlled conditions within a room sized laboratory (8m maximum range) indicated that high contrast targets could be located to ±3 cm around the room. Tests on a smaller scale (a desk-top set-up of ~1m dimensions) showed a positional accuracy of ±0.5 cm was achieved.

In measuring speed, some error in absolute position may be tolerated if differences between positions can be resolved with higher accurately. This was tested by measuring the distance between two targets, placed at a number of points around the test room. The targets were separated by a fixed amount; 42 cm. The system was able to measure this difference to ±1 cm.

3.3 Errors in Velocity

Velocity determination requires the measurement of the difference in position of a target between two moments in time. The time aspect requires that both the time interval between positions be known accurately and that all images from different viewpoints be synchronous. The time accuracy of the recording and playback equipment was checked and found to be better than 1/25 sec. The individual recorder's frame rates were similar enough such that several minutes of recording could be made before error of that magnitude was found between them. Synchrony in longer recordings was enabled by the use of a periodic electronic flash; each flash lasted less that 1 frame and so provided a unique time point every few minutes.

As a final lab based test of the system, a target was towed along a known path (a wire strung diagonally across the room) at a known speed. The system was able to measure the target velocities to within 5% over the range 0.1 - 0.7 m/s (figure 2).

3.4 Errors in Non-ideal Tracers

The measurement accuracy of the system would be immaterial if the tracer objects could not satisfactorily follow the movement of air. The requirements of an ideal tracer are that it be neutral (i.e. the same density as the surrounding air), be physically small, and have no inertial mass. All physical tracers will vary from this ideal, and each excursion will have a bearing on their accuracy in following air movement. The measurement errors associated with real tracers can be summarised in three subjects; size and visibility, ease of trim and longevity of neutral density, and air resistance or terminal velocity.

3.4.1 Size and Visibility

The larger the target object, the more easily it will be identified and tracked. However the larger the target, the less ideal it becomes as a tracer. The ability of a neutral weight tracer to follow the path of air will depend on its inertial mass; an object with high mass will accelerate slowly and may miss rapid changes of direction. It will also depend on its physical

size; a good tracer should also be smaller than a characteristic dimension of the flow i.e. the width of a jet.

In this work two sizes of balloon were found to be usable, both were made of polypropylene. A standard commercial balloon, with a diameter of approximately 35 cm had a mass of ~10.5 gm. A hand-made balloon, made from thinner material (15μ) could be made neutral down to a diameter of ~22 cm; its' mass then was 4.5 gm. When in a jet or fast rising plume, the smaller balloon showed a markedly faster acceleration. In normal room air currents, of 0.5 m/s or less, their was felt to be little difference between them. When surrounded by smoke, the balloons and smoke were seen to travel coincidentally (although the smoke eventually dissipated through small scale turbulence). Both sizes were visible and identifiable at up to 30m on the captured images.

The generation of suitable bubbles was found to be more problematic than that of balloons. Bubbles in the range 0.2 to 5 cm diameter could be generated by a number of sources, but the quality was always variable; some long-lived, some short-lived and some positively, some negatively buoyant. All sizes were found to be visible in the analysis images when they could be side lit with spot-lights. Image performance was best against a dark plain background. This confirms that bubbles are more suitable for laboratory or controlled environment testing, than for use in occupied buildings.

3.4.2 Longevity of Neutrality

Vitally important to the use of an object as an air following tracer is the ease of achieving, and the longevity of maintaining, neutral buoyancy. Helium is generally the medium through which buoyancy is achieved; it is preferentially lost through the envelope, and so the objects loose buoyancy over time. The buoyancy of bubbles is also be affected by evaporation.

Tests were made of the rate of buoyancy loss for several balloon types and materials. Positively buoyant balloons were tethered, in a draught free cabinet, to an recording electronic scale. The commercial polypropylene balloons performed best, loosing only 3 mg/hour. The handmade polypropylene balloons, when carefully made, lost approximately 6 mg/hour. These rates were sufficiently low so as to allow time to trim to neutral buoyancy and to allow several tens of minutes of recording time between trims. Rubber balloons (of helium grade) on the other hand lost buoyancy at a rate of 230 mg/hour, so fast it was not possible to reliably trim them to neutrality.

The buoyancy loss of bubbles was could not be measured with the equipment available, but in the light of the tests on balloons, the longevity of helium filled bubbles will be small; suitable for only a few seconds, perhaps a few minutes, of use.

3.4.3 Terminal Velocity

The intent in achieving neutral buoyancy is to keep the balloon stationary relative to the surrounding air. However, due to drag it is considered that a certain degree of non-neutrality is acceptable; a tracer will quickly reach a terminal velocity and this may be considered to be the error in the tracer motion. As long as this speed is small compared to the velocity of air movement observed, the resulting error will be small.

Tests were made of the terminal velocity of balloons under various degrees of positive buoyancy, by timing their flights in a draught free cabinet. It was found for the larger balloons that terminal velocities of <0.05 m/s could be achieved if the balloons weight was within ±10mg of neutrality. The smaller balloons, due to their smaller size, showed less drag; their usable range to 0.05 m/s was considered to be ±5mg. This is shown in figure 3.

Standard bubble solutions produced relatively wet, heavy bubbles. Their terminal velocities were estimated to be approximately 0.3 m/s. The use of exotic surfactants allowed significantly lighter bubbles, with corresponding lower terminal velocities; 0.03 m/s was achieved using Hyamine 2389. This is more appropriate for use in typical room flows, but unfortunately this liquid is toxic. The standard bubbles are felt to be useful for the higher velocities found near and within jets.

The information for the buoyancy loss rates and the terminal velocities combine to indicate that the larger balloons, when correctly trimmed, can be considered accurate to 0.05 m/s for up to 3 hours. The smaller balloons can be considered accurate to 0.05 m/s for just under an hour.

All together, the laboratory based tests suggest an estimate for the overall accuracy measurement of velocity of better than 0.05 m/s is achievable when using balloons in typical room air movement (i.e. <1 m/s). The use of balloons within jets is less reliable due to their size and mass, but here bubbles may be more appropriately used.

3.5 Field Trials

The system was tested under field conditions in three circumstances; recording the flow near a small desk fan using bubbles, recording the flow patterns caused by a de-stratification fan in a factory using balloons, and recording the air movement in the glazed atrium of an art gallery, again using balloons. The system performed satisfactorily, though it was noted that due to the effort required to site and accurately survey the positions and orientations of the viewpoints, it was not responsive to changing conditions, i.e. if another area of interest was identified, the equipment could not be quickly or easily moved and re-sited. This means that careful planning is required for its use.

The use in the gallery in particular showed that the system is tolerant to a high degree of "clutter", is capable of handling difficult and changing lighting conditions, and can be operated in an occupied building. Of particular concern to the staff of the gallery, the use of balloons as tracers meant that no damage was possible to the exhibits; the staff would not have permitted the use of smoke or bubbles.

Figures 4 and 5 show the recorded paths of the flow above the desk fan (a soldering station fume extractor; a small axial fan blowing upwards). It displays the swirling flow expected from this type of fan.

Figures 6 and 7 show some of the flow patterns recorded in the art gallery atria. The space is supplied by inlet grills at high level along the top and left hand walls. The air system was in cooling mode at the time of the measurements; the inlet air was approximately 1°C lower than the bulk air of the space. Inlet speeds were approximately 2 m/s; air speeds through the space were generally found to be ~0.5 m/s. The projected section illustrates common

patterns of recirculation found on either side of the inlet jets. Monochrome printing restricts the amount of information that can be shown in these diagrams.

4 CONCLUSIONS

The system described is a suitable method for recording and measuring room air flow patterns. It is capable of measuring 3-D positions and velocities to a reasonable degree of accuracy (±3 cm, ±.05m/s) within large spaces. It can provide a quantified measure of bulk air flow patterns, and is particularly suited to the low velocities found in naturally ventilation buildings. The system is readily transportable and usable in occupied buildings.

The use of balloons in tracking the flow of air is justifiable within air velocities typically found in rooms, that is velocities less than ~1 m/s. When suitably prepared, they can adequately follow the bulk movement of air for a considerable period of time, indicating velocities, areas of recirculation and highlighting problems such as "short circuiting". Balloons are less able to follow the movement of air within small jets, due to their relatively large size and mass. Bubbles, apart from problems associated with their production and with their residue, are better suited for use near or within jets.

REFERENCES

1. Trollope, M., Seager, A., Palmer, J., Watkins, R., Shaw,P., "IEA XI Advanced Case Study: Gateway 2", IEA XI Advanced Case Studies Seminar, April 1991. ETSU Harwell, 1991. 213-236
2. N D Vaughan, P Jones, D K Alexander, H Jenkins, M Fedeski, S Lannon, P Taylor, P E O'Sullivan, "Technical Report: Victoria House: Hampshire Training and Support Headquarters", ETSU 1163/28, ETSU Harwell, 1992
3. Pickering, P.L. , Cucchiara A.L., Gonzales, M. and McAtee, J.L, "Test Ventilation with Smoke, Bubbles and Balloons", ASHRAE Trans. 93, Part 2, 1987, 898-907
4. Ghosh, S.K., "Analytical Photogrammetry", Pergamon Press, New York, 1988. ISBN 0-08-036103-X
5. Shirai, Y. "Three-Dimensional Computer Vision", Springer-Verlag, Berlin, 1986. ISBN 3-540-15119-2
6. Gottschalk, G., Revesz, Z., Suter, P. and Tanner, P., "Experimental Method to Measure 3D Air Velocity", 10th AIVC Conference, Finland, 1989, 251-263
7. Kaga, A., Inoue,Y., Yoshikawa, A., "Velocity Distribution Measurement Through Digital Image Processing of Visualised Flow Images", Proceedings RoomVent '90, Oslo, 1990, B1-14

8 . Allan, A.L. "Practical Field Surveying and Computations", Heinemann, London, 1968.

ACKNOWLEDGEMENTS

The work presented here was funded through the EPSRC.
The authors would also like to acknowledge the interest, information and support provided by:

Jane Porter of The Burrell Collection,
Mr C Boon, Silsoe Research Institute,
ICI,
and the Welsh Development Agency.

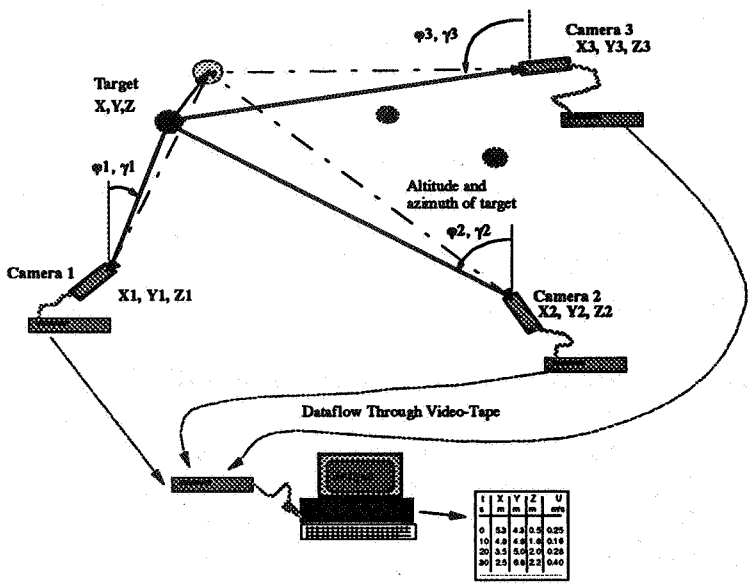

Figure 1 Functional Block Diagram of Measurement and Analysis System

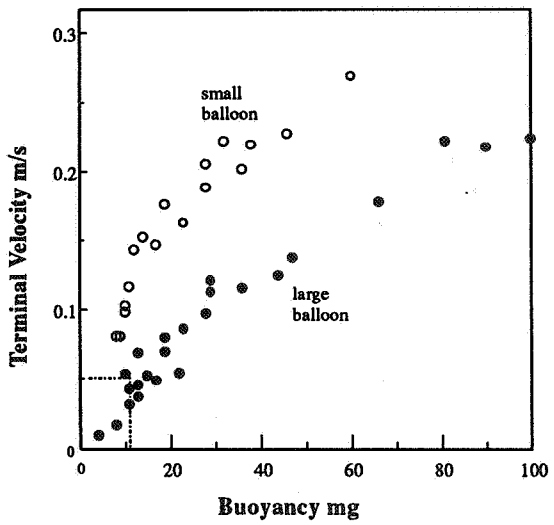

Figure 2 Terminal Velocity of Balloons for Differing Amounts of Buoyancy

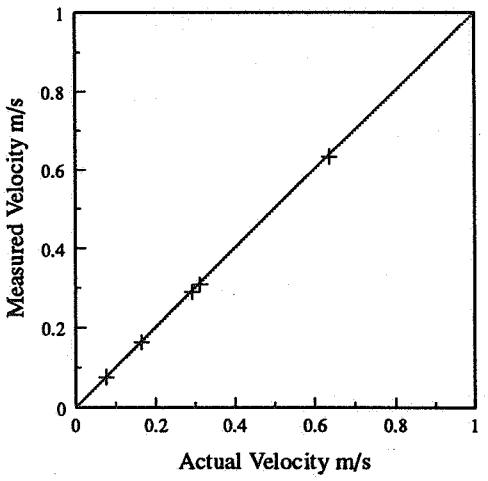

Figure 3 Comparison of Measured and Actual Velocities of Test Targets

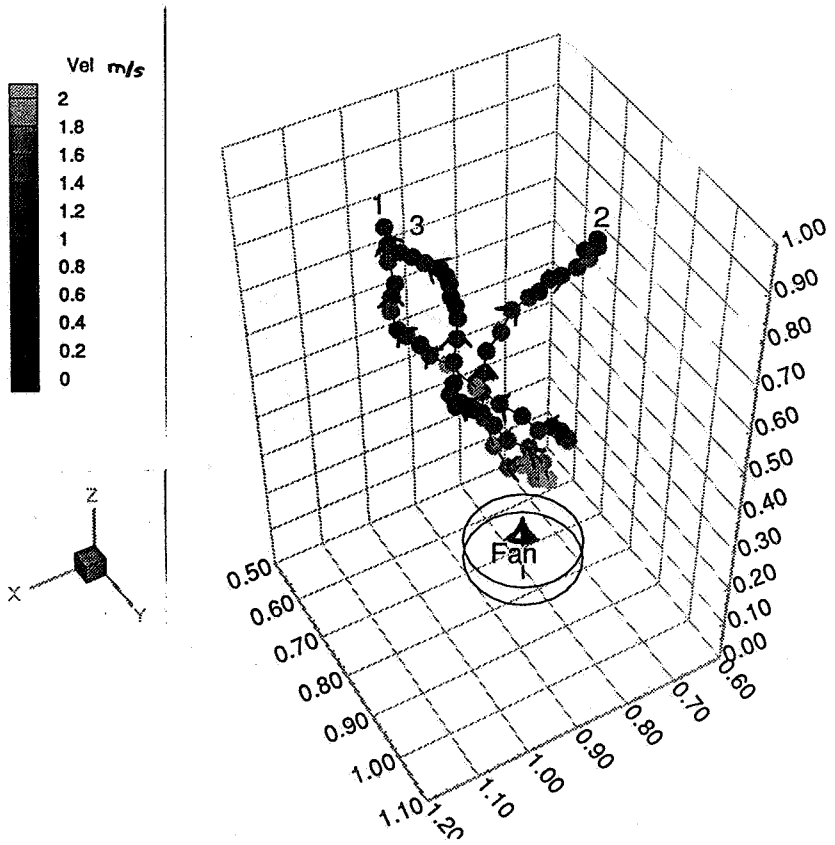

Figure 4 Example Bubble Tracks Produced By An Axial Fan

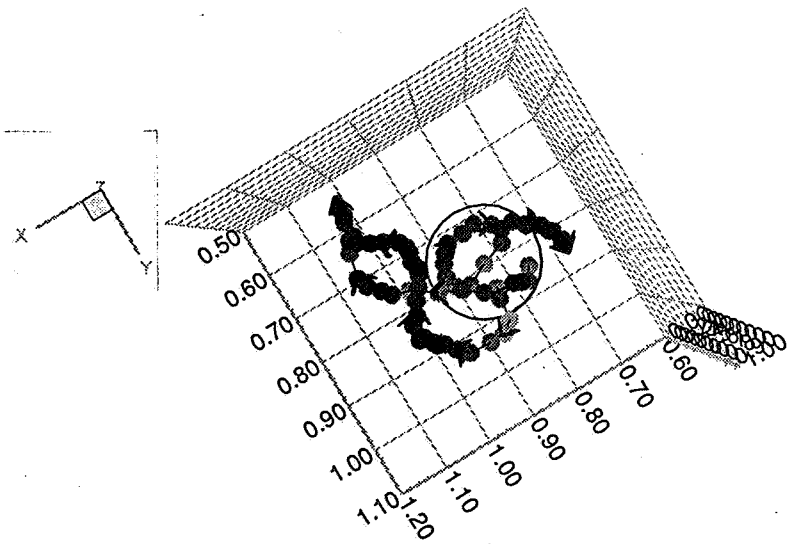

Figure 5 Plan View of Above

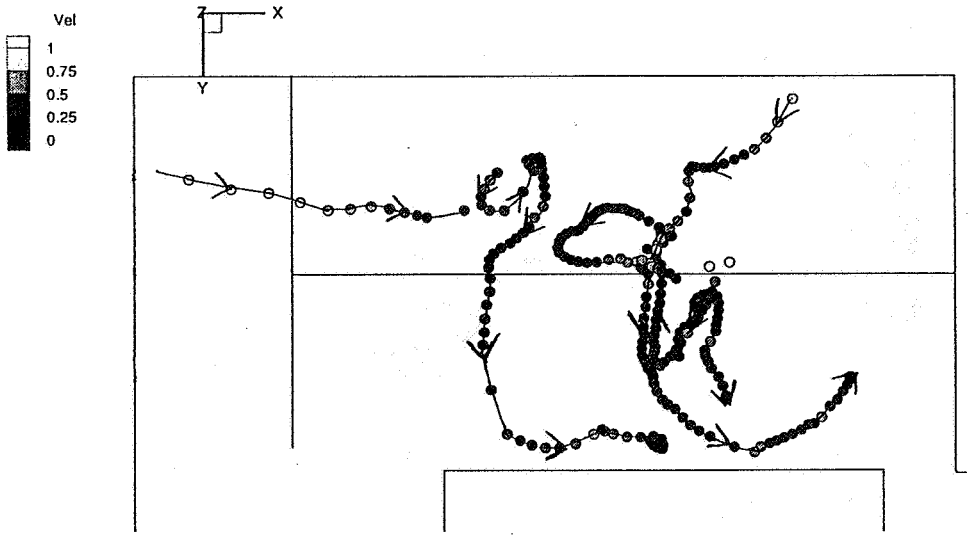

Figure 6 Plan View of Flow Patterns In Large Gallery

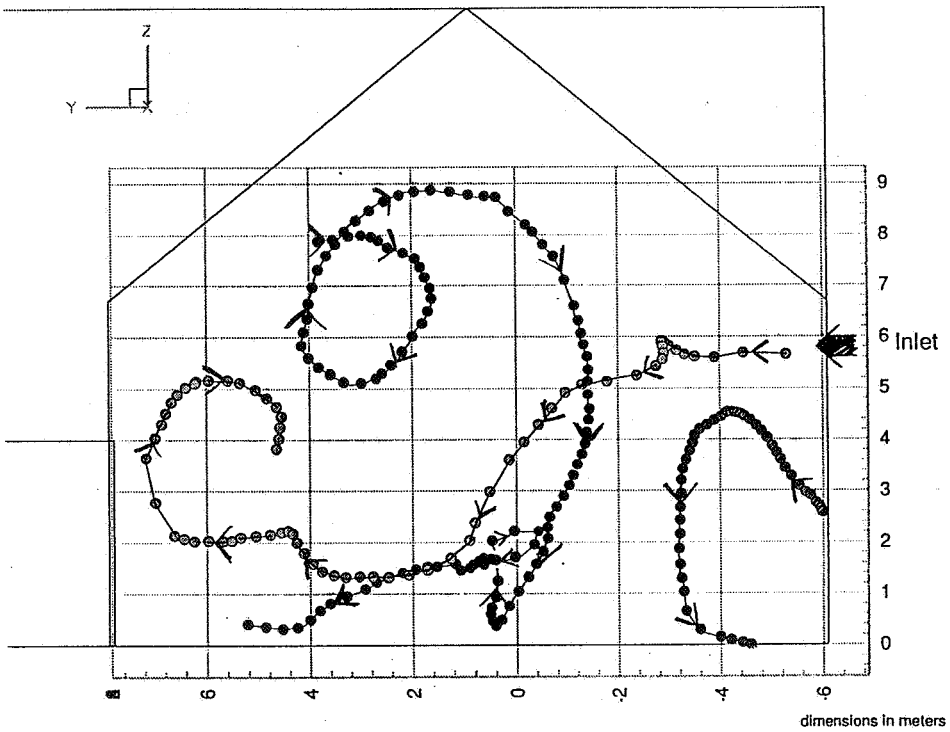

Figure 7 Projected Sectional View of Flow Patterns in Gallery

The Role of Ventilation
15th AIVC Conference, Buxton, Great Britain
27-30 September 1994

Application of a Multi-zone Airflow and Contaminant Dispersal Model to Indoor Air Quality Control in Residential Buildings

S J Emmerich, A K Persily, G N Walton

Bldg 226, Room A313, National Institute of Standards and Technology, Gaithersburg, MD 20899 USA

Synopsis

A new multizone airflow and contaminant dispersal model CONTAM93 is described, along with a demonstration of its application in a study of ventilation and contaminant control in single-family residential buildings. While CONTAM93 is based on existing theory of network airflow analysis and contaminant dispersal, the model employs a unique graphic interface for data input and display. The interface uses a sketchpad to describe the connections between zones and icons to represent zones, openings, ventilation system components, and contaminant sources and sinks. The model, its graphic interface and plans for its further development are described.

As a demonstration of the capabilities of CONTAM93, the paper describes a study of ventilation and contaminant control in eight single-family residential buildings. The overall objective of the effort is to study the impact of residential HVAC systems on indoor air quality (IAQ). This paper describes the study and the use of CONTAM93 to calculate whole building air change rates for a range of weather conditions and to simulate fan pressurization and tracer gas decay tests in the houses.

1. Introduction

Airflow rates in buildings are determined by the interaction of the building structure, its HVAC system, and weather conditions. Indoor pollutant concentrations depend on these airflow rates, pollutant source and sink characteristics, and outdoor concentrations. A whole-building, multizone approach, accounting for all of these factors, is required to study many important issues in building airflow and IAQ and has been implemented in many multizone airflow and IAQ models. A survey of multizone models, all of which provide at least some of the required modeling capabilities, is described by Feustel and Dieris (1). This paper describes a new multizone airflow and pollutant transport program CONTAM93 (2), which is the latest in the series of multizone IAQ modeling programs developed at the National Institute of Standards and Technology (NIST).

To demonstrate the use and capabilities of CONTAM93, its application in a residential IAQ modeling study is also discussed (3). In this study, CONTAM93 is being used to predict contaminant concentrations in a number of single-family dwellings as a function of weather conditions and HVAC system configurations for several contaminant sources. The study design and the use of CONTAM93 in this effort is described, but the results of the contaminant simulations are not presented in this paper. Fan pressurization tests were simulated with CONTAM93 to characterize the airtightness of the houses modeled in the study. The program was also used to calculate whole building air change rates for a range of weather conditions and to simulate tracer gas decay measurements of whole building air change rates. These air change rates were compared to each other and to air change rates calculated with the single-zone LBL infiltration model (4).

2. CONTAM93

2.1 General Description

CONTAM93 is an easily used contaminant analysis program combining the best available algorithms for modeling the airflow and contaminant dispersal in multizone buildings. It employs a graphic interface and is usable on commonly available small computers. Over the past several years, NIST has developed a series of public domain computer programs for calculating airflow and contaminant dispersal in multizone buildings. The earliest such program was ASCOS (Analysis of Smoke Control Systems) (5). Another program, TARP (Thermal Analysis Research Program) (6, 7), used multizone airflow calculations to estimate the portion of building thermal load due to infiltration and perform a simple contaminant migration analysis. Programs developed specifically for the study of contaminant dispersal included CONTAM86 (8) and CONTAM87 (9). NBSAVIS/CONTAM88 (10) added multizone airflow analysis capability, based on the program AIRMOV (11), and a menu-driven interface to CONTAM87. Improvements in the airflow calculation algorithm were implemented in the AIRNET program (12). CONTAM93 combines a new graphic interface with the contaminant simulation capabilities of CONTAM88 and the airflow analysis method of AIRNET.

CONTAM93 requires a 286-class (or higher) PC compatible computer with math coprocessor, VGA graphics, and MS-DOS. CONTAM93 consists of two programs: CONTAM and CONTAMX. CONTAMX is a non-interactive program which computes the airflows and/or contaminant concentrations in a building from information on the building, its HVAC system, ambient conditions, contaminant sources, and contaminant removal mechanisms. CONTAMX can perform steady-state, transient (up to 24 hour), and 24-hour cyclic simulations with a user specified time step. CONTAM is an interactive program for processing the required CONTAMX input and for displaying or exporting the CONTAMX output. Both CONTAM and CONTAMX operate under the 640K-byte memory limit of MS-DOS, which is sufficient for simulating buildings with several hundred zones and multiple contaminants.

2.2 Graphic Interface

When using CONTAM93, the user does not directly access the data files describing the building. All access to the building description is done through the CONTAM program and its graphic interface. The description of the building is created (or modified) in the SketchPad. The SketchPad consists of an invisible array of about 3600 small cells into which the user places various symbols representing building features relevant to the calculation of contaminant dispersal. This produces a simple illustration which has been chosen intentionally to represent the simplicity of the underlying mathematical model. The SketchPad is used to establish the geometric relationships of the relevant building features. It is not intended to produce a scale drawing of the building. Instead, it is used to create a simplified model where the walls, zones, and airflow paths are topologically similar to the actual building. The SketchPad allows the entry and display of the data in an intuitive manner. The SketchPad will bring up various data entry screens needed to define the

mathematical characteristics of the various building features (e.g. leakage areas and contaminant source strengths). After performing the simulation, the flows and pressure drops at each opening are presented on the SketchPad. Transient contaminant concentrations can also be displayed.

The CONTAM93 SketchPad is designed to simplify the data input and analysis processes for a multi-zone airflow and contaminant dispersal simulation. It is still up to the user to decide how best to idealize the building as a multizone system based on the building layout and the objectives of the simulation. The user must also determine which contaminant dispersal processes are important and appropriate input values for the building being simulated. The required input values can be numerous and include the following: airtightness of exterior envelope and interior partition components, ventilation system airflow rates, wind pressure coefficients, ambient weather and contaminant concentrations, indoor contaminant source strengths and sink characteristics, contaminant reaction rates, and filter efficiencies. Values of these quantities can be determined from the published literature and field measurement.

Once the user has decided how to represent the building as a multizone system and has determined appropriate input values, the building data is entered into the SketchPad. Building data is organized by *levels* with data entry beginning at the lowest level. A level would typically be a building floor, but a suspended ceiling acting as a return air plenum or a raised floor acting as a supply plenum may also be treated as a level leading to multiple levels per floor. Each level is divided by *walls* into separate regions of uniform air temperature, pressure, and contaminant concentration called *zones*. Walls include the building envelope and internal partitions with a significant resistance to air flow, and are drawn as either horizontal or vertical lines. There is a set of implicit walls (generally floors) separating the zones on different levels. A default ambient zone surrounds the building. Other zones can be designated as ambient to represent, for example, a courtyard. An airflow *path* indicates some building feature by which air can move from one zone to another. Such features include cracks in the building envelope, open doorways, and exhaust fans. Path symbols placed on the walls are used to represent openings between zones or to ambient; any other placement represents an opening in the floor to the zone on the level below. Contaminant source (or sink) symbols may be placed in any zone. These represent any feature (within the list of available models) which produces or removes a contaminant. A simple model of an air handling system is available with supply and return point symbols placed within the appropriate zones. All supply and return airflows follow user defined schedules.

Figure 1 shows the floor plan of a ranch style house modeled for the residential IAQ study discussed in this paper, and Figure 2 shows the CONTAM93 SketchPad representation of this house. In this case the representation closely mimics the floor plan. Airflow paths are represented by the diamond-shaped symbols on the walls. The zone symbols are squares with X's inside; the contaminant sources are boxes with C's inside. The air handling system, system supply points, and system return points are represented by a bold S, squares with dots inside, and squares with dashes inside, respectively.

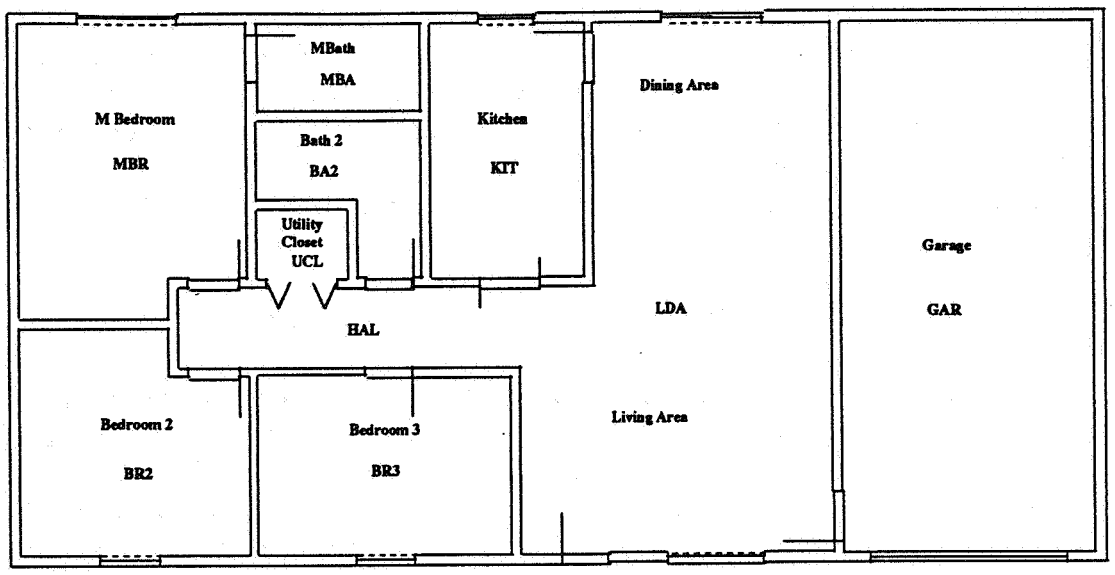

Figure 1 - Miami ranch house floorplan and zones

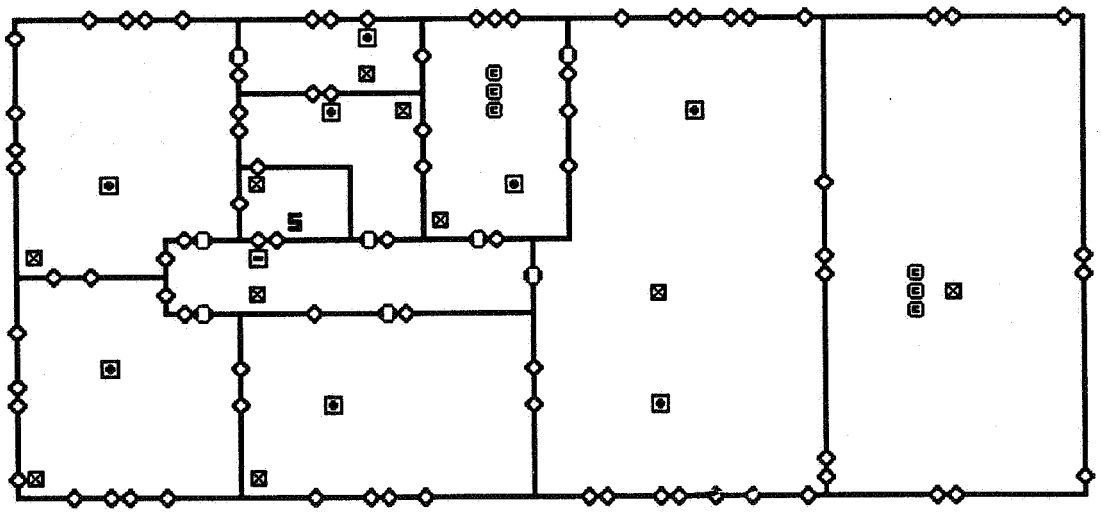

Figure 2 - Miami ranch house in CONTAM93 Sketchpad

2.3 Future Development Plans

Work is presently in progress to improve the user interface and to extend the range of features that can be simulated. The logic of the interface is being made more similar to common graphic interface standards, although the next version of the program will still run

under DOS. A DOS extender is being used to allow merging of the I/O processor and the simulation programs into a single program and to let the size of the SketchPad be user definable with a maximum of about 32,600 cells. This extender will limit the program to 386-class and higher PC's. The program is being modified to include libraries of airflow paths and contaminant source/sink models. Extensions in the simulation capabilities will include ductwork, exposure analysis, non-linear contaminant chemistry. and aerosol transport.

3. Example Application of CONTAM93: A Residential IAQ Study

As a demonstration of the capabilities of CONTAM93, this section describes its application in a study of IAQ in single-family residential buildings (3). The houses are described in terms of how they are represented in CONTAM93. The results of using CONTAM93 to analyze airflow in the houses with three approaches (simulated fan pressurization tests, calculated whole building air change rates, and simulated tracer gas decay measurements of whole building air change rates) are also presented.

3.1 Project Description

As interest and concern about residential IAQ increases, whole building modeling has the potential for improving our understanding of many important issues. Most of the research to date has employed simple models of the building and its systems, ignoring the multizone nature of the airflows involved and some important mechanisms of contaminant transport. Whole building analysis, using multizone approaches, is needed to advance our understanding of the impact of HVAC systems on residential IAQ and the possibility of using these and other systems to mitigate some IAQ problems. This section describes such a study being performed at NIST using CONTAM93. A detailed description of the study plan is contained in reference 3.

The overall objective of the project is to study the impact of residential HVAC systems on IAQ. The study involves simulations in eight single-family residential buildings. The buildings include a ranch house and a two-story house, each located in a hot (Miami, Florida) and a cold (Minneapolis, Minnesota) climate and each modeled with typical and tight levels of envelope air leakage. These houses are described briefly later in this paper and in detail in reference 3.

The pollutant sources used in the study were selected based on a literature review of pollutants relevant to the residential environment. The pollutants include total volatile organic compounds (VOC), nitrogen dioxide (NO_2), carbon monoxide (CO) and fine and coarse particulates. The VOC sources include a constant source with a generation rate proportional to floor area in each room, simulating a flooring material, and so-called burst sources with a constant generation rates lasting 30 minutes, simulating use of a consumer product. An individually identifiable burst source is released in each room, once in the morning and once in the afternoon. CO, NO_2 and fine particulates are generated by an oven in the kitchen area at a constant rate for 30 minutes in the morning and one hour in the evening. These same combustion products are generated by a portable heater in the garage

or basement for a three-hour period in the morning and a two-hour period in the evening. Outdoor concentrations for these pollutants are specified, with the levels of CO and NO_2 becoming elevated in the morning and early evening.

In addition to the airflow component inputs described in this paper, the contaminant modeling required additional inputs. These include numerical values to characterize reversible VOC sinks, NO_2 and particle deposition rates, and HVAC system filter particulate-removal efficiencies. These values were determined based on information available in the literature.

The strategy in the study was to perform 24 hour simulations of airflow and contaminant concentrations for each of the eight houses subject to each of the contaminant sources. These simulations were performed for a typical hot, mild and cold day for each of the two cities. The results of these so-called baseline simulations were concentrations of the simulated contaminants at 15 minute time steps over each day. The simulations are then repeated with one of three IAQ control technologies installed in the HVAC system of each house. These technologies include an electrostatic particulate filter, a heat recovery ventilator and an outdoor air intake damper on the forced-air system return. Although there are many other options for controlling residential contaminants, these particular controls were selected based on their ability to be installed in existing forced-air systems.

3.2 Building Descriptions and CONTAM93 Input

This modeling study involves single-family residential buildings: a ranch house and a two story house, located in two sites (Miami and Minneapolis). Each building is modeled as a multizone airflow system, containing roughly ten zones, with air leakage elements connecting the zones to each other and the outdoors. Figure 1 is a schematic floor plan of the Miami ranch house. The Miami houses are slab-on-grade, while the Minneapolis houses have full basements. Each building was modeled with typical and low values of air leakage, making a total of eight buildings in the study. Reference 3 contains detailed descriptions of the layout and dimensions of each house, including schematic floorplans.

Detailed information on building component leakage of the houses is not available as the houses modeled were not based on real buildings. However, since there is no attempt to match predictions with experimental data, the building leakage modeled needs only to be reasonable in magnitude and distribution. Table 1 shows all of the leakage paths between zones for the Miami ranch house (see Figure 2 for the representation of the Miami ranch house in CONTAM93). Table 2 lists the values for those leakage paths for both typical and tight cases. The Table 2 leakage areas are for a reference pressure difference of 4 Pa and a discharge coefficient of 1.0 and are based on values listed in Table 23-3 of ASHRAE (4) unless otherwise noted. The typical values were generally based on "best estimate" and/or uncaulked entries in the ASHRAE table, while the tight values were based on minimum and/or caulked entries. All doors connecting zones other than closets were modeled as open. The same leakage values were used for the other houses, although the paths connecting the zones differed depending on the house configurations.

Table 1 - Miami ranch house airflow paths

	MBR	BR2	BR3	MBA	BA2	UCL	KIT	LDA	HAL	GAR	ATC
BR2	INTW OUTL										
BR3		INTW OUTL									
MBA	INTD INTW										
BA2	INTW OUTL			INTW OUTL							
UCL	INTW				INTW						
KIT				INTW OUTL	INTW OUTL						
LDA			INTW OUTL				INTW INTD OUTL				
HAL	INTD INTW	INTD INTW	INTD INTW OUTL		INTD INTW	CLD INTW	INTD INTW OUTL	HAD			
GAR								EXTD EXW OUTL			
ATC	CEIL CPEN	CEIL CPEN	CEIL CPEN	CEIL CPEN PIP	CEIL CPEN PIP	CEIL CPEN	CEIL CPEN	CEIL CPEN CPEN	CEIL ATD		
AMB	WIN EXW OUTL	WIN EXW OUTL	WIN EXW OUTL	EXV EXW OUTL	EXV		WIN EXV EXW OUTL	SGD EXTD WIN EXW OUTL		GAD GARF EXW	VNT
	MBR	BR2	BR3	MBA	BA2	UCL	KIT	LDA	HAL	GAR	ATC

The wind pressure distribution on a building's exterior surfaces depends on the wind direction, the building shape, and the location on the building exterior. For this study, the pressure coefficient values used for the building walls were based on Equation 23-8 of ASHRAE (4). The coefficient for the flat garage roof was based on Figure 14-6 of ASHRAE (4).

Each house was modeled with a central forced-air heating and cooling system. Features of the system design for the Miami houses include: equipment in a first floor utility closet, supply ducts in the attic and a central return for the ranch house; and interior supply ducts and one return on each floor for the two-story house. For the Minneapolis houses, features include: equipment located in the basement, interior supply ducts, and a return in each room. Guidelines published by the National Association of Home Builders (15) were used to design the heating and cooling systems. Detailed descriptions of the building HVAC systems are contained in Reference 2 and include the heating and cooling equipment types and descriptions, overall and individual supply and return flow design values for both heating and cooling, and drawings showing the system equipment and duct locations and duct sizes. CONTAM93 also requires information on the HVAC system operation, specifically, an on-off schedule.

Table 2 - Air leakage coefficients

Name	Description	Typical	Tight
ATD	Attic door	30 cm^2/ea	18 cm^2/ea
CEIL	Ceiling [Based on general ceiling]	1.8 cm^2/m^2	0.79 cm^2/m^2
CLD	Closet door (closed) [Based on interior door]	0.9 cm^2/m	0.25 cm^2/m
	Closet door frame [Based on general door frame]	25 cm^2/ea	12 cm^2/ea
CPEN	HVAC ceiling penetration [Based on kitchen vent with damper closed]	5 cm^2/ea	1 cm^2/ea
EXTD	Exterior door [Single]	21 cm^2/ea	12 cm^2/ea
	Door frame [Wood]	1.7 cm^2/m^2	0.3 cm^2/m^2
EXV	Bathroom exhaust vent	20 cm^2/ea	10 cm^2/ea
	Kitchen exhaust vent	40 cm^2/ea	5 cm^2/ea
EXW	Ceiling-wall joint	1.5 m^2/m	0.5 m^2/m
	Floor-wall joint	4 cm^2/m	0.8 cm^2/m
	Wall-wall joint [Based on ceiling-wall joint]	1.5 m^2/m	0.5 m^2/m
GAD	Garage door [Based on general door (2 m x 4 m)]	0.45 cm^2/m	0.31 cm^2/m
	Garage door frame [Wood]	1.7 cm^2/m^2	0.3 cm^2/m^2
GARF	Garage roof [Based on general ceiling]	1.8 cm^2/m^2	0.79 cm^2/m^2
HAD	Hall doorway	2.4 m^2/ea	2.4 m^2/ea
INTD	Interior door (closed) [Based on Table 4.2 of Klote and Milke (13)]	140 cm^2/ea	75 cm^2/ea
	Interior door (open)	2.1 m^2/ea	2.1 m^2/ea
INTW	Interior wall [Based on gypsum board on stud wall (14)]	2.0 cm^2/m^2	2.0 cm^2/m^2
OUTL	Outlet	2.5 cm^2/ea	0.5 cm^2/ea
PIP	Piping penetrations	6 cm^2/ea	2 cm^2/ea
SGD	Sliding glass door	22 cm^2/ea	3 cm^2/ea
VNT	Attic vent [Based on Table 21-1 of 4]	1 cm^2 / 300 cm^2	1 cm^2 / 300 cm^2
WIN	Double hung window	2.5 cm^2/m	0.65 cm^2/m
	Window framing [Wood]	1.7 cm^2/m^2	0.3 cm^2/m^2

Another important consideration for the HVAC systems is duct leakage. In CONTAM93, a leak can be modeled by including an additional system supply or return point and reducing the other supply and return flows by the corresponding amount. For the Minneapolis houses, a 10% return leak was included for the return trunk in the basement. For the Miami ranch house, a 10 % supply leak was included for the supply trunk in the attic. For the Miami two story house, all system ducts are located in a plenum between floors and no leaks were included.

3.2 Airflow modeling results

CONTAM93 was used to analyze airflow in the houses using three approaches: simulated fan pressurization tests, calculated whole building air change rates, and simulated tracer gas decay measurements of whole building air change rates. Based on the the fan pressurization test results, infiltration rates were also predicted using the LBL infiltration model (4).

Fan pressurization tests in the houses were simulated with CONTAM93 by including a constant flow element in the door of each house and adjusting the flow until pressure differences of 4 and 50 Pa was achieved. The airflow rates at 50 Pa were divided by the interior volumes of the houses to determine the 50 Pa air change rates, and the 4 Pa flows

were converted to effective leakage areas using Equation 27 in Chapter 23 of ASHRAE (4). The results of the fan pressurization simulations are shown in Table 3. The difference between the Miami and Minneapolis houses is due primarily to the existence of the basement in the Minneapolis houses. In terms of both measures of airtightness, the tight houses are about 66% tighter than the houses of typical leakage.

Table 3 - Fan pressurization simulation results

House	ach_{50} (hr^{-1})	Leakage area (cm^2)
Typical Miami ranch	13.2	680
Tight Miami ranch	4.1	220
Typical Minneapolis ranch	6.6	720
Tight Minneapolis ranch	2.2	230
Typical Miami 2 story	12.9	1120
Tight Miami 2 story	4.6	390
Typical Minneapolis 2 story	8.8	1170
Tight Minneapolis 2 story	3.1	410

CONTAM93 was used to calculate whole building air change rates for wind speeds from 0 to 10 m/s and indoor-outdoor temperature differences from -10 to 30 °C. The wind direction was held constant throughout the simulations. These simulations were performed with the HVAC systems both on and off. Whole building air change rates were calculated by adding the airflow entering the conditioned space of the house through all leakage paths. The results of these airflow simulations for the Miami ranch house are shown in Tables 4 and 5 for the system off.

Several general trends are shown by these results. Using 'tight' values for the airflow elements vs. 'typical' values reduced the whole building air change rate by up to a factor of four as compared to a factor of three for the fan pressurization results. Also, over the range considered here, the wind speed had a greater impact on the whole building air change rate than the temperature difference. However, the tight airflow elements reduced the impact of the wind speed more than the impact of the temperature difference.

Table 4 - Whole house air change rate for typical Miami ranch house (ach)

Tin - Tout (K)	-10	-5	0	5	10	15	20	25	30
Wind speed (m/s)									
0	0.33	0.21	0.00	0.22	0.35	0.46	0.57	0.67	0.76
2	0.40	0.32	0.33	0.38	0.47	0.54	0.65	0.74	0.84
4	0.75	0.78	0.82	0.85	0.89	0.94	1.00	1.08	1.15
6	1.31	1.34	1.38	1.42	1.46	1.50	1.54	1.61	1.67
8	1.92	1.96	2.01	2.06	2.11	2.16	2.21	2.27	2.33
10	2.57	2.63	2.69	2.75	2.81	2.87	2.94	3.01	3.08

Table 5 - Whole house air change rate for tight Miami ranch house (ach)

Tin - Tout (K)	-10	-5	0	5	10	15	20	25	30
Wind speed (m/s)									
0	0.10	0.07	0.00	0.07	0.11	0.14	0.17	0.20	0.23
2	0.11	0.09	0.08	0.10	0.14	0.17	0.20	0.23	0.26
4	0.18	0.18	0.19	0.21	0.22	0.24	0.26	0.28	0.31
6	0.30	0.31	0.32	0.33	0.34	0.36	0.38	0.39	0.42
8	0.44	0.46	0.47	0.48	0.49	0.51	0.53	0.54	0.57
10	0.60	0.61	0.63	0.64	0.65	0.67	0.69	0.71	0.73

Tables 6 and 7 show the results of the airflow simulations with the HVAC system on. Operation of the HVAC system increased the building air change rate as much as 0.31 ach at zero wind speed and temperature differences due to supply duct leakage in the attic. The effect of the system fan was less than 0.05 ach at high wind speeds (> 4 m/s) and temperature differences (> 10 °C).

Table 6 - Whole house air change rate for typical Miami ranch house with system fan on (ach)

Tin - Tout (K)	-10	-5	0	5	10	15	20	25	30
Wind speed (m/s)									
0	0.45	0.38	0.31	0.39	0.52	0.63	0.73	0.83	0.93
2	0.59	0.52	0.41	0.50	0.63	0.74	0.84	0.93	1.03
4	0.86	0.81	0.85	0.89	0.95	1.02	1.10	1.17	1.24
6	1.34	1.37	1.41	1.45	1.49	1.55	1.61	1.67	1.73
8	1.95	1.99	2.04	2.09	2.14	2.19	2.25	2.30	2.38
10	2.60	2.66	2.72	2.78	2.84	2.91	2.97	3.04	3.11

Table 7- Whole house air change rate for tight Miami ranch house with system fan on (ach)

Tin - Tout (K)	-10	-5	0	5	10	15	20	25	30
Wind speed (m/s)									
0	0.31	0.31	0.31	0.31	0.31	0.31	0.31	0.33	0.37
2	0.32	0.31	0.31	0.31	0.31	0.31	0.32	0.36	0.39
4	0.39	0.37	0.35	0.32	0.32	0.33	0.37	0.41	0.44
6	0.47	0.45	0.44	0.42	0.40	0.41	0.43	0.46	0.49
8	0.56	0.54	0.52	0.51	0.53	0.55	0.57	0.58	0.61
10	0.65	0.63	0.64	0.66	0.69	0.71	0.73	0.75	0.77

CONTAM93 was also used to simulate tracer gas decay tests in the houses by setting an initial tracer gas concentration of 100, in arbitrary units, in all building zones except the garage and attic. Transient tracer gas concentrations were simulated for the same temperature-wind speed grid as above. Air change rates were calculated for each zone from the decay of the tracer gas concentration at 15 minutes after the start of the simulation. The whole house air change rate was calculated as the volume-weighted average of the individual zone air change rates. The simulation time step was chosen such that reducing it by half

resulted in an absolute average change of less than 1% in individual zone tracer gas concentrations at the 15 minute point.

The results of these simulations with the HVAC system off are shown in Tables 8 and 9. These simulations were repeated with the HVAC system on and the results are presented in Tables 10 and 11. The building air change rates based on the simulated tracer gas decay tests are, as expected, very similar to those determined with the building airflow calculations. The average absolute percent difference between the two methods is 5%. The largest differences occur at high temperature differences and high wind speeds due to decreased uniformity in individual zone tracer gas concentrations. These nonuniformities in tracer gas concentration result in an overestimation of the building air change rate as compared to the calculated values in Tables 4 through 7. The overestimation of the air change rates is larger at higher air change rates because the concentrations in the different zones diverge more at the 15 minute time interval. Also, the overestimation is larger at high wind speeds than at large temperature differences because the wind causes greater concentration nonuniformities among the zones.

Table 8 - Tracer gas decay simulation results for typical Miami ranch house (ach)

Tin - Tout (K)	-10	-5	0	5	10	15	20	25	30
Wind speed (m/s)									
0	0.33	0.21	0.01	0.22	0.35	0.46	0.57	0.66	0.76
2	0.40	0.32	0.34	0.39	0.48	0.54	0.65	0.74	0.83
4	0.80	0.84	0.88	0.91	0.96	1.01	1.07	1.14	1.22
6	1.45	1.49	1.53	1.59	1.63	1.67	1.72	1.79	1.86
8	2.18	2.24	2.29	2.35	2.41	2.47	2.54	2.60	2.71
10	3.05	3.12	3.19	3.27	3.35	3.43	3.51	3.60	3.79

Table 9 - Tracer gas decay simulation results for tight Miami ranch house (ach)

Tin - Tout (K)	-10	-5	0	5	10	15	20	25	30
Wind speed (m/s)									
0	0.10	0.07	0.00	0.07	0.11	0.14	0.18	0.21	0.24
2	0.11	0.09	0.08	0.10	0.14	0.17	0.20	0.23	0.26
4	0.18	0.18	0.19	0.21	0.22	0.24	0.26	0.28	0.31
6	0.31	0.32	0.33	0.34	0.35	0.37	0.39	0.40	0.43
8	0.46	0.47	0.48	0.50	0.51	0.53	0.54	0.56	0.58
10	0.62	0.64	0.65	0.67	0.68	0.70	0.72	0.75	0.76

Table 10 - Tracer gas decay simulation results for typical Miami ranch house with system fan on (ach)

Tin - Tout (K)	-10	-5	0	5	10	15	20	25	30
Wind speed (m/s)									
0	0.41	0.35	0.30	0.39	0.52	0.63	0.72	0.82	0.91
2	0.56	0.50	0.40	0.49	0.62	0.73	0.82	0.92	1.00
4	0.88	0.84	0.88	0.93	0.98	1.05	1.13	1.20	1.27
6	1.41	1.46	1.50	1.54	1.58	1.64	1.71	1.77	1.83
8	2.10	2.16	2.21	2.27	2.32	2.38	2.44	2.50	2.58
10	2.92	2.99	3.06	3.14	3.21	3.29	3.37	3.46	3.55

Table 11 - Tracer gas decay simulation results for tight Miami ranch house with system fan on (ach)

Tin - Tout (K)	-10	-5	0	5	10	15	20	25	30
Wind speed (m/s)									
0	0.29	0.29	0.30	0.30	0.30	0.31	0.31	0.31	0.35
2	0.30	0.30	0.30	0.30	0.30	0.31	0.31	0.34	0.38
4	0.37	0.36	0.34	0.33	0.31	0.32	0.36	0.40	0.43
6	0.46	0.45	0.44	0.43	0.41	0.40	0.42	0.45	0.48
8	0.56	0.55	0.53	0.52	0.53	0.55	0.57	0.58	0.61
10	0.65	0.64	0.64	0.66	0.69	0.71	0.73	0.75	0.77

As expected, the zone tracer gas concentrations were more uniform for the simulations with the HVAC system on than for the simulations with the system off. This increased uniformity creates the appearance of decreased air change rates with the system on under certain conditions. For example, at a temperature difference of 30 °C and a wind speed of 10 m/s, turning the system on *reduced* the tracer gas-based estimate of the air change rate by 0.24 ach (from 3.79 in Table 8 to 3.55 in Table 10) while the actual air change rate was *increased* by 0.03 ach (from 3.08 in Table 4 to 3.11 in Table 5).

Whole building air change rates for the houses were also estimated using the single-zone LBL infiltration model described in ASHRAE (4). The airflow rate was calculated using Equation 23-32 of ASHRAE (with the effective leakage areas from Table 3 above and a wind coefficient for moderate local shielding) for the same temperature-wind speed grid as the CONTAM93 simulations above. The results for the Miami ranch house are shown in Tables 12 and 13. The average absolute percent differences between the LBL air change rates and the CONTAM93 air change rates are 32% and 19% for the typical and tight buildings, respectively. However, the LBL model estimates are much closer to the air change rates calculated with CONTAM93 at low wind speeds.

Table 12 - LBL model results for typical Miami ranch house (ach)

Tin - Tout (K)	-10	-5	0	5	10	15	20	25	30
Wind speed (m/s)									
0	0.37	0.26	0.00	0.26	0.37	0.45	0.52	0.59	0.64
2	0.45	0.37	0.26	0.37	0.45	0.52	0.58	0.64	0.69
4	0.63	0.58	0.51	0.58	0.63	0.69	0.73	0.78	0.82
6	0.86	0.81	0.77	0.81	0.86	0.90	0.93	0.97	1.00
8	1.09	1.06	1.03	1.06	1.09	1.12	1.15	1.18	1.21
10	1.34	1.31	1.29	1.31	1.34	1.36	1.39	1.41	1.44

Table 13 - LBL model results for tight Miami ranch house (ach)

Tin - Tout (K)	-10	-5	0	5	10	15	20	25	30
Wind speed (m/s)									
0	0.12	0.08	0.00	0.08	0.12	0.15	0.17	0.19	0.21
2	0.15	0.12	0.08	0.12	0.15	0.17	0.19	0.21	0.22
4	0.21	0.19	0.17	0.19	0.21	0.22	0.24	0.25	0.27
6	0.28	0.26	0.25	0.26	0.28	0.29	0.30	0.31	0.33
8	0.35	0.34	0.33	0.34	0.35	0.36	0.37	0.38	0.39
10	0.43	0.42	0.42	0.42	0.43	0.44	0.45	0.46	0.47

4. Summary and Conclusions

CONTAM93 is an easily used contaminant analysis program combining the best available algorithms for modeling the airflow and contaminant dispersal in multizone buildings with a graphic interface. The models, the program interface, and planned future development were described. Also described was the application of CONTAM93 in a NIST study to assess the potential effectiveness of existing HVAC technology to reduce the levels of selected pollutants in single-family residential buildings with central forced-air heating and cooling systems. This description included the results of simulated fan pressurization tests, building airflow simulations for a range of weather conditions, and simulated tracer gas decay tests.

References

1. Feustel HE and Dieris J. "A Survey of Air Flow Models for Multizone Structures" (1992) Energy and Buildings 18:79-100.

2. Walton GN. *CONTAM93 - User Manual* (1994) NISTIR 5385, National Institute of Standards and Technology.

3. Emmerich SJ and Persily AK. *Indoor Air Quality Impacts of Residential HVAC Systems Phase I Report: Computer Simulation Plan* (1994) NISTIR 5346, National Institute of Standards and Technology.

4. ASHRAE. 1993 Handbook of Fundamentals (1993) American Society of Heating, Refrigerating, and Air-Conditioning Engineers, Inc.

5. Klote JH. *A Computer Program for Analysis of Smoke Control Systems* (1981) NBSIR 80-2157, National Bureau of Standards.

6. Walton GN. *Thermal Analysis Program Reference Manual* (1983) NBSIR 83-2655, National Bureau of Standards.

7. Walton GN. "A Computer Algorithm for Predicting Infiltration and Interroom Airflows" (1984) ASHRAE Transactions, Vol. 90, Part 1.

8. Axley J. *Indoor Air Quality Modeling Phase II Report* (1987) NBSIR 87-3661, National Bureau of Standards.

9. Axley J. *Progress Toward a General Analytical Method for Predicting Indoor Air Pollution in Buildings, Indoor Air Quality Modeling Phase III Report* (1988) NBSIR 88-3814, National Bureau of Standards.

10. Grot RA. *User Manual NBSAVIS CONTAM88* (1991) NISTIR 4585, National Institute of Standards and Technology.

11. Walton, GN. *A Computer Algorithm for Estimating Infiltration and Inter-Room Air Flows* (1983) NBSIR 83-2635, National Bureau of Standards.

12. Walton GN. *AIRNET - A Computer Program for Building Airflow Network Modeling* (1989) NISTIR 89-4072, National Institute of Standards and Technology.

13. Klote JH and Milke JA. Design of Smoke Management Systems (1992) American Society of Heating, Refrigerating, and Air-Conditioning Engineers, Inc. and Society of Fire Protection Engineers.

14. Shaw CY, Magee RJ, and Rousseau J. "Overall and Component Airtightness Values of a Five-story Apartment Building (1991) ASHRAE Transactions, Vol. 97, Pt. 2.

15. Yingling RK, Luebs DF, and Johnson RJ. *Residential Duct Systems - Selection and Design of Ducted HVAC Systems* (1981) National Association of Home Builders of the United States.

The Role of Ventilation
15th AIVC Conference, Buxton, Great Britain
27-30 September 1994

Two-zones Model for Predicting Passive Stack Ventilation in Multi-storey Dwellings

J G Villenave, J-R Millet, J Ribéron

Centre Scientifique et Technique du Bâtiment, Marne La Vallée, France

SYNOPSIS

Proper dimensioning of natural ventilation system for multi-storey buildings is a critical matter, because the air flow rate depends on many parameters as outdoor temperature, wind, distribution of air inlets and envelope air leakage, characteristics of outlets and cowls.

The computer code GAINE BIZONE predicts the ventilation rates in multi-storey dwellings equipped with passive stack ventilation system. Each level is treated as a two-zones configuration, but each zone is linked to the collective ventilation shaft of the building. The model calculates the pressures in every zone of the building and the ducts, using iterative method to balance the mass flows in and out of each zone. One of the both zones represents the kitchen, the other one the rest of the dwelling including the bathroom and the toilets. The kitchen door that links the both zones is represented by an internal transfer opening.

The model takes into account the common cowls used to avoid reverse flow, but also the cowls with motorised device. The latter are very useful, especially to achieve the peak flow rate when cooking or when the stack effect is insufficient because of moderate wind and outdoor temperature. In addition, the model makes it possible to treat a gas appliance linked to the exhaust duct of the kitchen.

The basic modelling method used is known as the 'ping-pong' method because the two-zones model combines two models which are called in turn. In the first step, the ventilation rates are calculated in a stack of storeys representing a part of dwellings, then for the other part. The both models are called in turn until that, for each dwelling, the exchanged flow rate between the two zones are balanced.

Examples of applications conducted with the two-zones model are presented in this paper.

LIST OF SYMBOL

ach	air changes per hour(h^{-1})
C	suction coefficient of the cowl
ΔP	difference of pressure (pascal)
D	diameter of duct (m)
index $_0$	air characteristics at 20 °C
ks	absolute duct material roughness (m)
L	length of duct (m)
Λ	friction factor
m	mass air flow (kg/s)
Q	volume air flow (m^3/s)
ρ	air density (kg/m^3)
Re	Reynolds number
S	duct area (m^2)
V	velocity (m/s)
ζ	local loss factor
ζ_c	pressure drop coefficient of the cowl

1- INTRODUCTION

In France, the regulation on residential building ventilation is based, since 1969, on a general and continuous air renewal ; the fresh air comes into habitable rooms by air inlets and the stale air is drawn out to exhaust vents in the service rooms. [1]

Although the mechanical exhaust systems are now the most commonly used systems, the passive stack ventilation systems called in French 'ventilation naturelle' (different from natural ventilation by opening windows called in French 'aération'), were common in use in the buildings built in the sixties. An important part of the existing building stock have today to be refurbished.

When renovating existing building, air leakage of the envelope is often reduced ; this can lead to an insufficient ventilation if ventilation system is inadequate. A new system is then to be designed, reusing the existing ducts ; the proper dimensioning of system is a critical matter which can be solve using computer models.

2- THE COMPUTER CODE 'GAINE'

GAINE is a model of ventilation in multi-storey dwellings [2]. Each level is treated as a separate zone, but each is linked to a common ventilation shaft. The model calculate the pressure in every level of the building and the duct, using iterative methods to balance the mass flows in and out of each level.

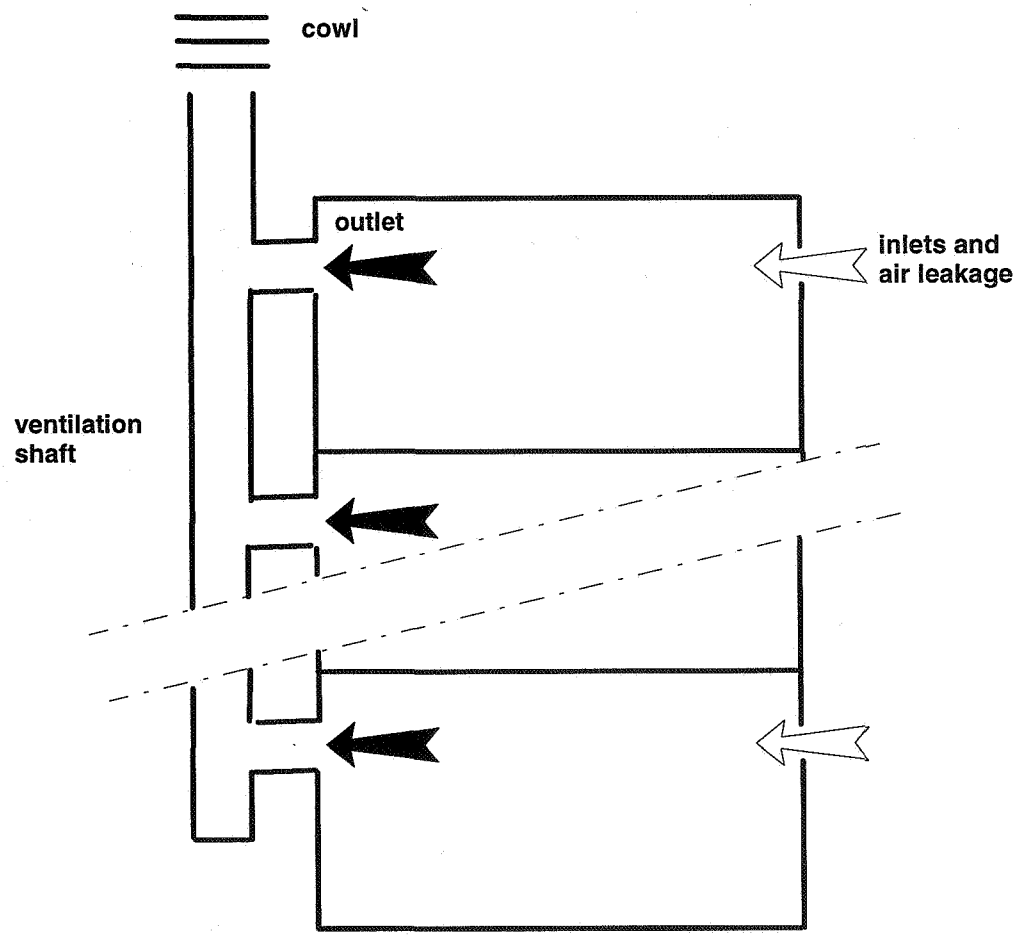

It takes into account the combined effects of driving forces such as wind-induced pressures, thermal buoyancy and mechanical forces due to motorised cowls.

It is a 'mass balance' model, which assume the following :

- an homogeneous air temperature in each room, perfect mixing,
- that air is incompressible,
- steady state conditions,
- the air inlets and extract opening are at the same level,
- infiltration can be represented by a single opening.

The model is described by the following equations :

permeability : $$m = \varepsilon \times m_0 \times \left(\frac{T_0}{T} \times |\Delta P| \right)^{2/3}$$ (ε=+1 if $\Delta P \geq 0$ and -1 if $\Delta P < 0$)

inlets : $$m = \varepsilon \times m_0 \times \sqrt{\frac{T_0}{T} \times \frac{|\Delta P|}{\Delta P_0}}$$ (ε=+1 if $\Delta P \geq 0$ and -1 if $\Delta P < 0$)

outlets : $$m = \varepsilon \times m_0 \times \sqrt{\frac{T_0}{T} \times \frac{|\Delta P|}{\Delta P_0}}$$ (ε=+1 if $\Delta P \geq 0$ and -1 if $\Delta P < 0$)

friction losses in ducts : $$\Delta P = \Lambda \times \frac{L}{D} \times 0.5 \times \rho \times V^2$$

$$\text{with : } \frac{1}{\sqrt{\Lambda}} = -2 \times \log_{10} \times \left(\frac{ks/D}{3.71} \times \frac{2.51}{\text{Re} \times \sqrt{\Lambda}} \right) \quad \text{(Colebrook)}$$

pressure losses in duct branches [3] **:**

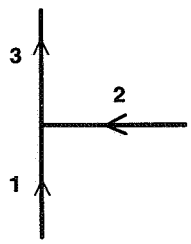

$$\Delta P_{3,1} = \zeta_{3,1} \times 0.5 \times \rho \times V_3^2 \qquad \zeta_{3,1} = 1 + \left(\frac{Q_2}{Q_3} \times \frac{S_3}{S_2} \right)^2 - 2 \times \left(1 - \frac{Q_3}{Q_2} \right)^2 - \frac{S_3}{S_2} \times \left(\frac{Q_2}{Q_3} \right)^2$$

$$\Delta P_{3,2} = \zeta_{3,2} \times 0.5 \times \rho \times V_3^2 \qquad \zeta_{3,2} = 1 - \left(1 - \frac{Q_2}{Q_3} \right)^2 - 1.41 \times \frac{S_3}{S_2} \times \left(\frac{Q_2}{Q_3} \right)^2$$

cowls : $$\Delta P = \frac{T}{T_0} \times \left(-\Delta P_X + \Delta P_0 \times \left(\frac{m}{m_0} \right)^2 \right)$$

where : ΔP_x is the available pressure for motorised cowls (ΔP_x=0 for static cowls)

The air pressure on the exterior of the envelope due to wind are expressed by the dynamic pressure in a free-flowing wind stream multiplied by an dimensionless pressure coefficients. Wind velocity and direction are assumed constant (stationary conditions). The dimensionless pressure coefficients used in the model were derived from pressure distribution measurements performed in a boundary layer wind tunnel on a scale model [4].

GAINE has been used to improve the knowledge of the operating of ventilation systems, and in particular for dimensioning passive stack ventilation systems [5], for assessing the performance of mechanical ventilation systems [6], and for studying the passive stack ventilation in summer [7]

3- THE COMPUTER CODE 'GAINE BIZONE'

In GAINE only one ventilation shaft is modelled : it is not possible to study the reciprocal action between ducts and particularly the problem of siphoning. So we developed the code GAINE BIZONE.

Each level is treated as a two-zones configuration, but each zone is linked to the collective ventilation shaft of the building. The model calculates the pressures in every zone of the building and the ducts, using iterative method to balance mass flows in and out of each zone. One of the both zones represents the kitchen, the other one the rest of the dwelling including the bathroom and the toilets. The kitchen door that links the both zones is represented by an internal transfer opening.

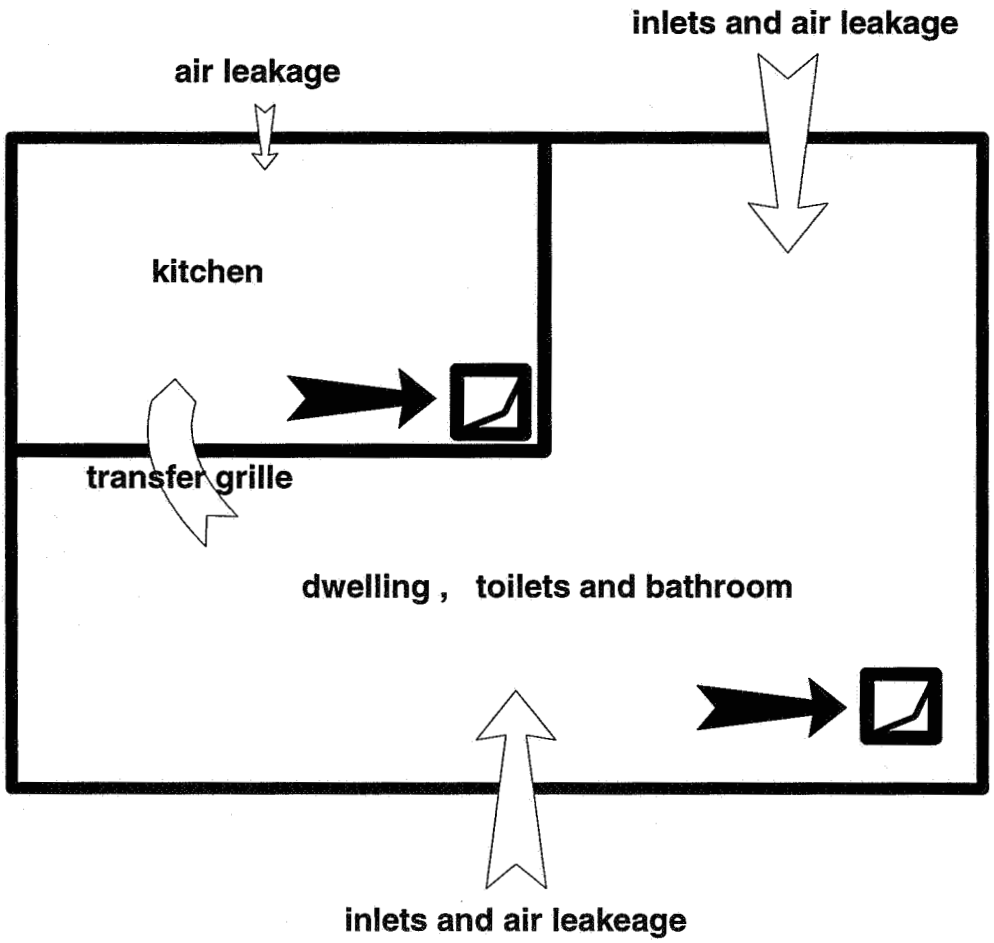

The model takes into account the common cowls used to avoid reverse flow, but also the cowls with motorised device. The latter are very useful, especially to achieve the peak flow rate when cooking or when the stack effect is insufficient because of moderate wind and outdoor temperature. In addition, the model makes it possible to treat a gas appliance linked to the exhaust duct of the kitchen.

The basic modelling method used is known as the 'ping-pong' method because the two-zones model combines two models which are called in turn. In the first step, the ventilation rates are calculated in a stack of storeys representing a part of dwellings, then for the other part. The both models are called in turn until that, for each dwelling, the exchanged flow rate between the both zones are balanced.

The code GAINE BIZONE is linked with EXCEL® which manages the inputs and outputs : running under WINDOWS® the code makes it possible to study one case on about 10 seconds (PC 486DX33).

4 - EXAMPLES OF RESULTS

Retrofitting makes the building envelope more airtight and can lead to an insufficient air change rate in passive stack ventilated buildings : the existing ventilation system has therefore to be redesigned in order to insure an adequate indoor air quality.

4.1 - Before retrofitting

The building is five floor high. Each dwelling has four habitable rooms.

The dwellings are not airtight ; the air leakage rate is 4 ach under 50 pascal.

Inlets are installed in each habitable rooms (30 m^3/h under 20 pascal for each inlet).

Outlets (grilles of 100 cm^2) are installed in the service rooms.

Two shunt ducts (20 × 20 cm) serve the kitchen and the toilets/bathroom (ventilation system using one collective shaft and two individual ducts for toilets and bathroom are very common in France).

The ducts are covered by a concrete cowl ($\zeta_c = 2.5$ $C = -0.3$)

The table hereafter presents the results of calculation (in m^3/h) for the dwelling underprivileged (1) and the dwelling favoured (2) with regard to air renewal.

	outdoor temperature 0 °C				outdoor temperature 10 °C			
	wind 0 m/s		wind 5 m/s		wind 0 m/s		wind 5 m/s	
	(1)	(2)	(1)	(2)	(1)	(2)	(1)	(2)
extract flow in the kitchen	14	66	29	63	10	45	29	45
extract flow in toilets and bathroom	12	69	19	64	9	47	21	45
total flow (extract + cross ventilation) in the dwelling	26	135	194	245	19	92	190	216

The underprivileged dwelling is under ventilated in windless outdoor conditions.
When the wind is blowing all the dwellings are over ventilated by cross ventilation

4.2 - After retrofitting

Single glazing windows have been replaced by double glazing ; the dwellings are airtight ; the air leakage represent only 0.4 ach under 50 pascal.

When the ventilation system is not modified the table hereafter presents the results of calculation (in m^3/h) for the dwelling underprivileged (1) and the dwelling favoured(2).

	outdoor temperature 0 °C				outdoor temperature 10 °C			
	wind 0 m/s		wind 5 m/s		wind 0 m/s		wind 5 m/s	
	(1)	(2)	(1)	(2)	(1)	(2)	(1)	(2)
extract flow in the kitchen	16	43	14	42	11	29	12	24
extract flow in toilets and bathroom	15	50	11	48	10	34	11	26
total flow (extract + cross ventilation) in the dwelling	31	93	65	90	21	63	65	74

With regard to the previous situation the cross ventilation has sharply decreased and the underprivileged dwelling continued to be under ventilated. The ventilation system has to be redesigned.

We give here an example

Inlets are installed in each habitable rooms (30 m^3/h under 20 pascal for each inlet).

Self regulated outlets are installed in the service rooms (45 m^3/h between 5 and 30 pascal in the kitchen, 30 m^3/h between 5 and 30 pascal in the toilet and the bathroom).

Two shunt ducts (20 × 20 cm) serve the kitchen and the toilets/bathroom.

The ducts are covered by cowls ($\zeta = 1.5$ $C = -0.65$) ; these cowls are motorised and can give an additional pressure (15 pascal) when necessary.

The table hereafter presents the results of calculation (in m^3/h) for each dwelling.

	outdoor temperature 0 °C		outdoor temperature 10 °C	
	wind 0 m/s	wind 5 m/s	wind 0 m/s	wind 5 m/s
extract flow in the kitchen	45	45	45	45
extract flow in toilets and bathroom	60	60	60	60
total flow (extract + cross ventilation) in the dwelling	105	105	105	105

This system makes it possible to ensure a satisfactory indoor air quality and to save energy and the same flowrate in dwelling whatever the floor.

5- CONCLUSION

The computer code GAINE BIZONE makes it possible to design and to dimension the passive stack ventilation systems in particular for the renovation of buildings with existing shafts.

The examples above mentioned show that it is possible :

- to ventilate correctly the dwellings when external conditions (temperature and wind) are insufficient,
- to save energy when the outdoor temperature is low or when the wind is blowing.

Actual studies are carried out to improve the code in order to take better into account the individual duct which link the dwelling to the collective shaft and to validate the results by laboratory and field measurements.

REFERENCES

[1] Villenave JG, Ribéron J, Millet JR, "French Ventilation in dwellings", Air Infiltration Review, vol 14, n°4, pp 12-15, September 1993

[2] Mounajed R, "La modélisation des transferts d'air dans les bâtiments : application à l'étude de la ventilation", thèse de doctorat de l'Ecole Nationale des Ponts et Chaussées, Noisy le Grand, October 1989.

[3] Idel'cik IE "Memento des pertes de charge" Eyrolles éditeur, Paris, 1969

[4] Gandemer J, "Ecoulements et charges induites par le vent sur les bâtiments", Cahiers du CSTB n°2045, livraison 265, Paris, December 1985

[5] Ribéron J, Mounajed R, "Dimensionnement des installations de ventilation naturelle", CSTB GEC 88-4457, 1988

[6] Ribéron J, Villenave JG, Millet JR, "Evaluation of mechanical domestic ventilation systems : the French approach", Indoor Air, Helsinki, July 1993

[7] Cripps AJ, Millet JR, Villenave JG, Bienfait D, "Operation of passive stack systems in summer", 13th AIVC conference on ventilation for energy efficiency and optimum indoor air quality, Nice, September 1992

The Role of Ventilation
15th AIVC Conference, Buxton, Great Britain
27-30 September 1994

Practical Methods for Improving Estimates of Natural Ventilation Rates

I S Walker, D J Wilson

Department of Mechanical Engineering, University of Alberta, Edmonton, Alberta, Canada

Synopsis

This paper discusses four concepts that have been found useful in improving estimates of ventilation rates in residential buildings. These concepts are improved methods for describing leakage distribution and wind pressures:

1. Separation of large, well defined "local" leakage sites from the background building leakage.
2. Changing surface pressure coefficients to account for the effect of upwind obstacles.
3. Making wind pressures (in terms of pressure coefficient and wind shelter) continuous functions of wind direction.
4. Development of a wind shadow shelter model specifically tailored for buildings in urban locations.

The effectiveness of the implementation of these four concepts was examined by comparing predicted ventilation rates using a computer model (LOCALEAKS) that incorporates these concepts to several thousand hours of ventilation measurements from the Alberta Home Heating Research Facility (AHHRF). The houses at AHHRF have been tested in several leakage configurations to evaluate the model performance over a wide range of parameters. For brevity, a single leakage configuration is discussed in this paper that shows the success and failures of the model in predicting ventilation rates for complex leakage and shelter configurations. The above methods for improving ventilation calculations can be applied to other models and are not restricted to use in the ventilation model used for this study.

1 LOCALEAKS Ventilation Model

This ventilation model was specifically developed to incorporate the methods for improving ventilation rate estimates outlined above. LOCALEAKS balances the flow in and out through the building leaks by applying the power law pressure flow relationship, given below, to each leakage site,

$$M = \rho C(\Delta P)^n \tag{1}$$

where M is the mass flow rate [Kg/s], C is the flow coefficient [m^3/sPa^n], n is the leakage exponent, ρ is the air density [Kg/m^3] and ΔP is the pressure difference [Pa] across the leak. The flow coefficient is split into distributed and localised leakage, and the pressure difference is due to a combination of stack and wind effects, and the pressure that acts to balance the inflow and outflow.

1.1 Pressure Differences For Flow Through House Leaks:

The total pressure difference across each leak can be written in terms of a reference wind parameter, P_U, and stack effect parameter, P_T, common to all leaks:

$$P_U = \rho_{out} \frac{U_H^2}{2} \tag{2}$$

$$P_T = g\rho_{out}\left(\frac{(T_{in}-T_{out})}{T_{in}}\right) \quad (3)$$

where ρ_{out} is the outdoor air density, U_H is the eaves height wind speed [m/s], g is the gravitational constant (9.81m/s^2), T_{in} is the indoor temperature [K] and T_{out} the outdoor temperature [K]. The total pressure difference is due to a combination of the wind and indoor-outdoor temperature difference effects and the pressure that acts to balance the inflows and outflows ΔP_I.

$$\Delta P = CpS_U^2 P_U - ZP_T + \Delta P_I \quad (4)$$

Equation 4 is applied to every leak for the building with the appropriate values of pressure coefficient (Cp) wind shelter factor (S_U) and Z (the height above grade). Thus, each leak is defined by its height, shelter and pressure coefficient.

2 Leakage Site Separation

2.1 Distributed Leakage

The unintentional "background" leakage through cracks and holes is distributed in six separate locations: ceiling, floor, and each of the four walls. The flow coefficient C_{dist} for the distributed leakage and exponent n_{dist} are found from a fan pressurization test, or estimated from similar construction types. The same value of n_{dist} is used for all sites, and the flow coefficient is given by Equation 5, with wall, ceiling and floor level leaks specified as a fraction of the total.

$$C_{dist} = C_{ceiling} + C_{floor} + C_{wall1} + C_{wall2} + C_{wall3} + C_{wall4} \quad (5)$$

2.2 Local Leakage Sites

Local leakage sites may be at floor level, in the ceiling, and in the walls. The default assumption for these sites is that they act like sharp edged orifice holes with $n_{local} = 0.5$ and an effective flow area of $C_d A_{local}$, where C_d (typically 0.6) is the discharge coefficient and A_{local} is the flow area of an opening. Alternately, the flow coefficient C_{local} and n_{local} may be specified for each local leakage site. For wind pressures each local leak is given the same pressure coefficient and wind shelter as the surface it is located in. LOCALEAKS uses a single averaged wind pressure coefficient for each wall of the building, so that only the height above grade of each local leakage site needs to be specified, rather than its horizontal location on a wall.

3 Changing Pressure Coefficients to account for Upwind Obstacles

The wind pressure coefficients, Cp, are taken from wind tunnel tests. It is assumed that there is no specific horizontal location for a leak on a wall and so extremes of pressure coefficients occurring at corner flow separations, for example, are not included. This assumption allows the simplification of using wall averaged pressure coefficients.

A set of comprehensive wind tunnel tests that cover many different wind directions have been presented by Akins, Peterka and Cermak [1]. Their Cp's are representative of isolated houses but it has been found in the development of LOCALEAKS that a change of side wall Cp is necessary for houses in a row. For an isolated building the side wall is about Cp = -0.65

based on Akins, Peterka and Cermak's measurements. For houses in a row with the wind along the row, the upwind houses change the flow pattern around the building so that large flow separations do not occur on the sidewalls. This requires a reduction in magnitude of the side wall pressure coefficient to about Cp = -0.2. This value was found by Wiren [2] in tests of row house shelter and is suggested by model errors in passive ventilation studies performed by Wilson and Walker [3]. Analysis of Wiren's data by Walker [4] has shown that for a house to be considered to be in a row only one upwind house is necessary because the closest obstacle dominates the wind flow pattern. The wind pressure coefficients for the other walls are taken directly from Akins, Peterka and Cermak. For wind perpendicular to the upwind wall they are: Cp = 0.6 for the upwind wall and Cp = -0.3 for the downwind wall.

4 Making Pressure Coefficients a Continuous Function of Wind Direction

When the wind is not normal to the upwind wall the above pressure coefficients do not apply. An harmonic trigonometric function was developed to interpolate between these normal values to fit the variation shown by Akins, Peterka, and Cermak and Wiren. For each wall of the building the harmonic function for Cp was empirically developed in the following form:

$$Cp(\theta)=\frac{1}{2}[(Cp(1)+Cp(2))(\cos^2\theta)^{\frac{1}{4}}+(Cp(1)-Cp(2))(\cos\theta)^{\frac{3}{4}} +(Cp(3)+Cp(4))(\sin^2\theta)^2+(Cp(3)-Cp(4))\sin\theta] \quad (6)$$

where Cp(1) is the Cp when the wind is at 0° (+0.60)
Cp(2) is the Cp when the wind is at 180° (-0.3)
Cp(3) is the Cp when the wind is at 90° (-0.65 or -0.2)
Cp(4) is the Cp when the wind is at 270° (-0.65 or -0.2)
and θ is the wind angle measured clockwise from the normal to the wall.
This function is shown in Figure 1 together with data from Akins et. al. for a cube. The error bars on the data points in Figure 1 represent the uncertainty in reading the measured values from the figures of Akins, Peterka and Cermak. Equation 6 fits the measured data within about Cp = ±0.02 except at about 150 degrees and 210 degrees (which are the same by symmetry) where the equation overpredicts the Cp by about 0.1. Figure 2 shows Equation 6 with Cp's from another data set from ASHRAE [5](Chapter 14) which it also fits well.

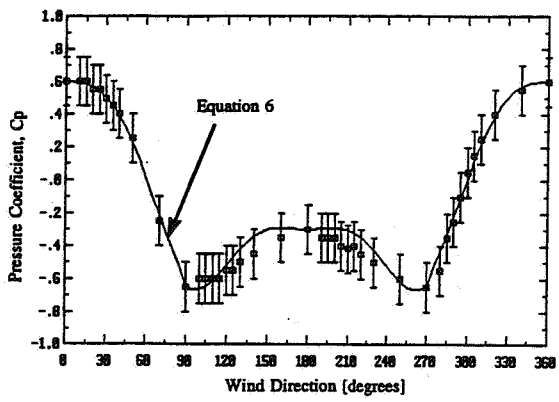

Figure 1. Wind Angle Dependence of measured (data from Akins et.al. (1979)) and predicted wall pressure coefficients for isolated buildings

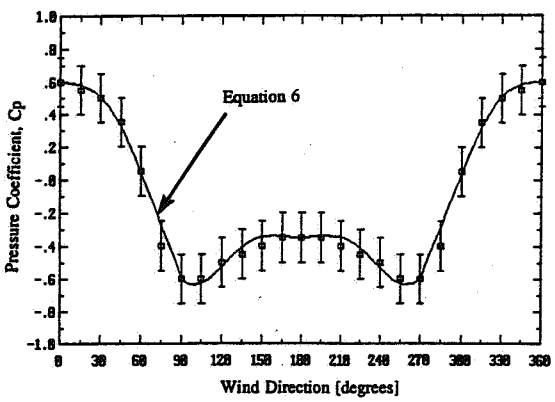

Figure 2. Wind Angle Dependence of measured (data from ASHRAE (1989)) and predicted wall pressure coefficients for isolated buildings

The function in Equation 6 was chosen to have the above form so that if a different data set were to be fitted then only the values for when the wind is normal to one wall are required and the function will estimate the intermediate values for different wind directions. Equation 6 is shown in Figure 3 for the row pressure coefficients where the sidewall Cp is -0.2. There are no intermediate measured values but this figure shows that Equation 6 produces reasonable pressure coefficients for this case. The value for pressure coefficient at the top of the furnace flue is Cp=-0.5, based on measurements by Haysom and Swinton [6].

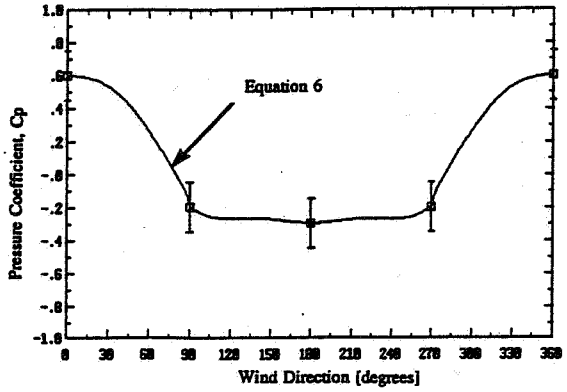

Figure 3. Wind Angle Dependence of Wall Pressure Coefficients for Houses in a Row.

5 Wind Shadow Shelter

To improve shelter estimates the wind shadow shelter method was developed to calculate numerical values for the reduction in velocity caused by an upwind obstacle. The shelter method is based on work by Walker and Wilson [7]. The shelter factor, S_U, is used to reduce the eave height wind speed, U_H, in the flow approaching the building to produce an effective wind speed U, such that

$$U=S_U U_H \tag{7}$$

U calculated from Equation 7 is used to calculate the wind pressure on each wall in Equation 4. When the walls are not sheltered, $S_U = 1.0$ and complete shelter corresponds to $S_U = 0$. Wind shadow wake shelter uses self-preserving three dimensional wake theories of Counihan, Hunt and Jackson [8] and Lemberg [9] to determine the rate of recovery of wind speed in the wake of an upwind obstacle. The theories are combined with wind tunnel measurements of Peterka, Meroney and Kothari [10], Lemberg [9] and Wiren [2] to develop appropriate relationships for wind shelter factor (or windspeed multiplier), S_U, to be used in the near wakes of interest in building shelter problems.

The wind shadow concept is analogous to the shadow produced by an obstacle in front of a light source that is cast onto another surface. The projection of the wake downstream of the sheltering obstacle is the "wind shadow". If a surface is partially covered by the wind shadow of the projected wake, then the shelter factor is weighted by the amount of wall area covered by the wind shadow to obtain the average shelter factor for the wall.

For this study, a computer programme was used to calculate S_U for all four walls of the test buildings at AHHRF every one degree of wind angle. The houses are in an east-west row, and are exposed for north and south winds and shelter each other for east and west winds. The calculated values of S_U are illustrated in Figures 4 and 5. Figure 4 is for the North facing wall and shows the symmetry of its shelter with a maximum wind speed reduction

factor of $S_U = 0.43$ for winds from 110 and 250 degrees. Figure 5 is for the East facing wall where the shelter is asymmetric because the sheltering building is closer for east winds than west winds. For East winds (90 degrees) the shelter is maximum with $S_U = 0.25$. For West winds the shelter is less with $S_U = 0.61$. The furnace flue protrudes above the houses and is assumed to be unsheltered, and $S_U = 1.0$ for the flue.

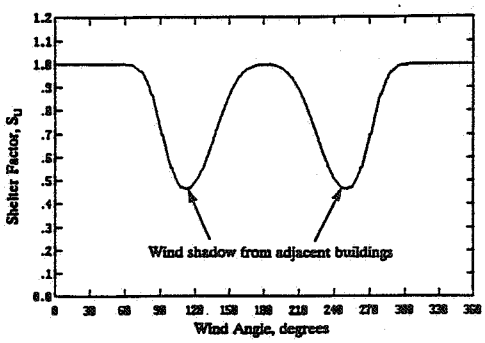

Figure 4. Wind Angle Dependence of Shelter Factor, S_U, for the North Wall of a House at AHHRF.

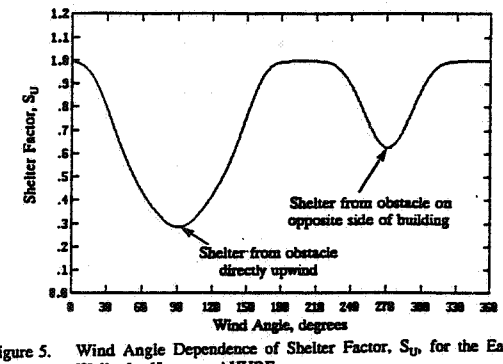

Figure 5. Wind Angle Dependence of Shelter Factor, S_U, for the East Wall of a House at AHHRF.

6 Validation of Improved Leakage Distribution and Wind Pressure Estimates

A detailed description of the measurement facility is given by Wilson and Walker [3]. The house with the most complex leakage distribution is examined here because it is the most difficult to model. In addition to the background leakage of the house (86 cm^2) there is a furnace flue (34 cm^2) , a passive ventilation pipe into the basement (59 cm^2) and an open window (30 cm^2).

To separate the effects of the improvements to ventilation predictions from the behaviour of the rest of the model, the measured data will be compared to predictions with and without the improvements. Without the improvements, the window and basement passive vent leakage were included in the distributed leakage of the walls and floor, the wall and floor leakage were evenly distributed over the four walls, and the flue was included in the ceiling leakage. The shelter factor used was the average for all four walls over all wind directions ($S_U = 0.79$), and the pressure coefficients did not vary with wind angle.

The predictions are evaluated using two parameters - the bias and the absolute error. The bias is the mean of the differences between individual pairs of predicted and measured data. Thus the bias indicates the difference between measurements and predictions over long time periods. The absolute error is the mean of the absolute differences between measurements and predictions. In this case positive and negative errors do not cancel and this provides an estimate of the typical model error for an individual hour. The results are presented in Air Changes per Hour (ACH) using a house volume of 220 m^3. The measured data are sorted into wind and stack dominated parts so that the wind and stack dependence of the predicted and measured ventilation rates may be examined separately.

The computer model used the measured wind speeds, wind directions and indoor and outdoor temperatures to calculate ventilation rates corresponding to every measured ventilation rate, both with and without the improvements. For stack dominated conditions, Figure 6 shows how the model with improvements gives better estimates of the ventilation rate. The upper figure shows every measured data point and the lower figure shows the measured data in bins every 5K of temperature difference, with the error bars representing the standard deviation of the measured data within the bin. For the model, the ventilation rate is calculated for each point, but for clarity, the calculations are also binned every 5K and the average value in each

bin is connected by a line. In this case the bias changed from -19% to -1% (negative errors indicate underprediction) and the absolute error from 19% to 8% by including the improved ventilation estimation methods discussed in this paper. These results illustrate the benefit of allowing the large localised leakage sites (the flue, basement pipe and window) to have their own height above grade instead of being included in the distributed leakage.
For wind dominated conditions the measured and calculated data are shown in Figure 7. In this case, the differences are much less clear than for stack dominated ventilation. However, including the leakage distribution and wind pressure calculation improvements decreased the bias from -12% to -4% and the absolute error from 21% to 12%.

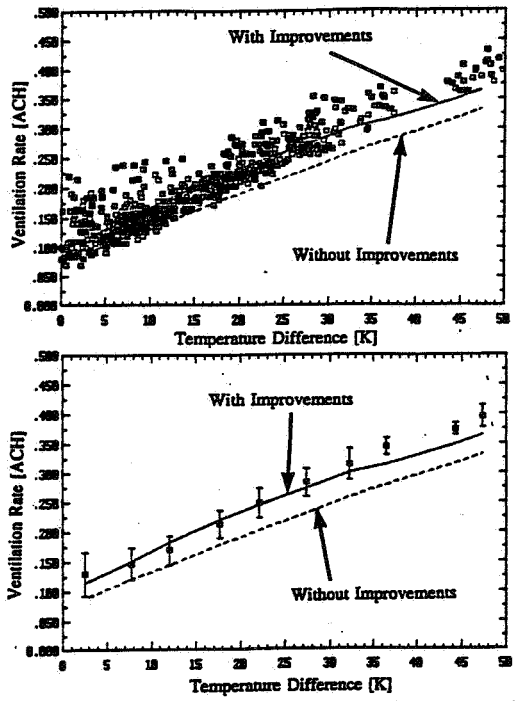

Figure 6. Comparison of Measured and Predicted Stack Dominated Ventilation Rates for House 5 at AHHRF, with a Furnace Flue, Passive Vent and an open Window (659 hours, Mean Temperature Difference = 15.6K, Mean Windspeed = 1.4 m/s).

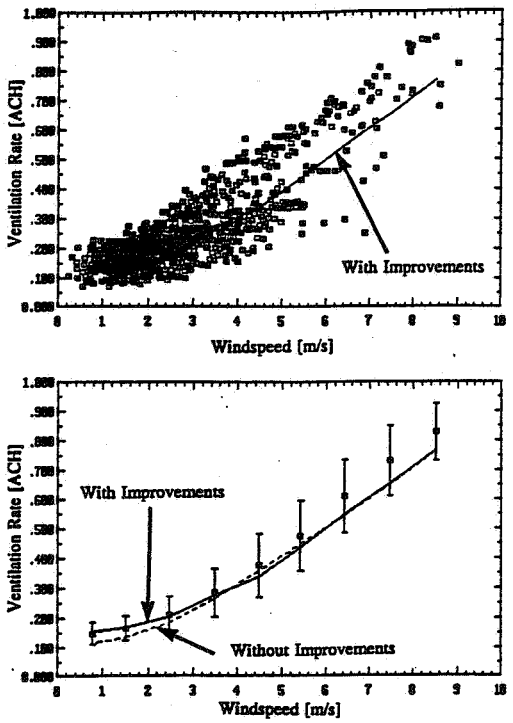

Figure 7. Comparison of Measured and Predicted Wind Dominated Ventilation Rates for House 5 at AHHRF, with a Furnace Flue, Passive Vent and an open Window (1042 hours, Mean Temperature Difference = 9.6K, Mean Windspeed = 2.7 m/s).

To obtain a clearer interpretation of the effects of allowing the shelter and pressure coefficients to vary with wind direction, this data set was replotted to show the variation with wind angle in Figure 8. Figure 8 shows binned data only, where the measured data has been binned every 20 degrees of wind direction. As with the other figures the error bars represent the standard deviation of the measured data for each wind direction bin, and the predicted infiltration rates are shown by a straight line connecting their mean values in each bin. Figure 8 shows that constant shelter and pressure coefficients result in underprediction for south winds (when the building is exposed) and over prediction for east and west winds (when the building is sheltered and the pressure coefficients change). The results of the above data comparisons are summarised in Table 1.

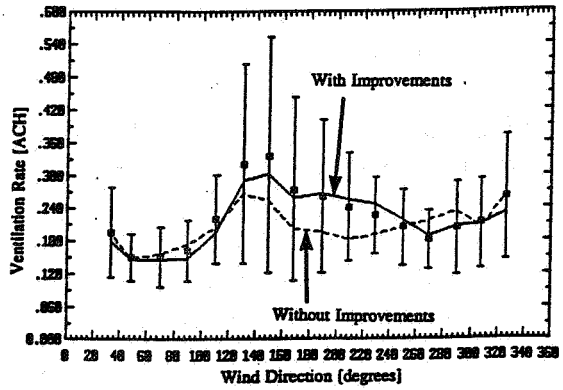

Figure 8. Wind Angle Dependence of Measured and Predicted Wind Dominated Ventilation Rates for House 5 at AHHRF, with a Furnace Flue, Passive Vent and an open Window (1042 hours, Mean Temperature Difference = 9.6K, Mean Windspeed = 2.7 m/s).

Table 1. Summary of Differences Between Measured Data and Model Predictions

	Wind Dominated		Stack Dominated	
	With Improvements	Without Improvements	With Improvements	Without Improvements
Number of points	1042		659	
Mean ΔT	9.6 K		15.6 K	
Mean U	2.7m/s		1.4 m/s	
Mean Measured Ventilation Rate	0.249 ACH		0.202 ACH	
Mean Predicted Ventilation Rate	0.238 ACH	0.220 ACH	0.200 ACH	0.160 ACH
Bias Error	-0.011 ACH -4%	0.030 ACH -12%	-0.002 ACH -1%	-0.038 ACH -19%
Absolute Error	0.031 ACH 13%	0.052 ACH 21%	0.017 ACH 9%	0.038 ACH 19%

8 Summary

Four concepts have been introduced to improve estimates of ventilation rates in houses. These improvements have been incorporated into a ventilation model (LOCALEAKS) whose predictions have been validated by comparison to several hundred hours of measured ventilation rates and flows through individual leaks. LOCALEAKS was also used without localised leakage and changing shelter and pressure coefficients in order to illustrate the effect of these concepts. In every case the improvement produced ventilation rate predictions that were significantly improved (by 10% or more).

The ideas about shelter and pressure coefficients introduced here may be used as input to other ventilation models, and are not restricted to use in LOCALEAKS, because they are parameters that are normally input to a model rather than the functional form of the model itself.

References

1. Akins, R.E., Peterka, J.A., and Cermak, J.E.
"Averaged Pressure Coefficients for Rectangular Buildings"
Vol.1, Proc. Fifth International Wind Engineering Conf., Fort Collins, U.S.A., July 1979, pp. 369-380.
2. Wiren, B.G.
"Effects of Surrounding Buildings on Wind Pressure Distributions and Ventilation Losses for Single Family Houses : Parts 1 and 2"
National Swedish Institute for Building Research, 1985.
3. Wilson, D.J. and Walker, I.S.
"Feasibility of Passive Ventilation by Constant Area Vents to Maintain Indoor Air Quality"
Proc. Indoor Air Quality '92, ASHRAE/ACGIH/AIHA Conf., San Francisco, October 1992.
4. Walker, I.S.
"Pressure Coefficients on Sheltered Buildings"
Air Infiltration Review, Vol.13, No.4, 1992, Air Infiltration and Ventilation Centre, Coventry, U.K.
5. ASHRAE
Handbook of Fundamentals, ASHRAE, 1989, Atlanta, Georgia.
6. Haysom, J.C., and Swinton, M.C.
"The Influence of Termination Configuration on the Flow Performance of Flues"
Canada Mortgage and Housing Research Report, 1987.
7. Walker, I.S. and Wilson, D.J.
"The Wind Shadow Shelter Model"
Manuscript in review.
8. Counihan, J., Hunt, J.C.R., and Jackson, P.S.
"Wakes Behind Two-Dimensional Surface Obstacles in Turbulent Boundary Layers"
J. Fluid Mech., Vol.64, Part 3, 1974, pp.529-563.
9. Lemberg, R.
"On the Wakes Behind Bluff Bodies in a Turbulent Boundary Layer"
University of Western Ontario Report BLWT-3-73, 1973.
10. Peterka, J.A., Meroney, R.N., and Kothari, K.M.
"Wind Flow Patterns About Buildings"
J. Wind Eng. and Ind. Aero., Vol. 21, 1985, pp.21-38.

The Role of Ventilation
15th AIVC Conference, Buxton, Great Britain
27-30 September 1994

A Suggested Standard Methodology for the Assessment of the Performance of Domestic Ventilation Systems

R E Edwards, C Irwin

Dept of Building Engineering, UMIST, Manchester United Kingdom

Abstract

The monitoring of the performance of domestic ventilation systems is quite a complex exercise. A wide variety of parameters must be taken into account in order that a suitable assessment of performance may be made - in many cases, insufficient data is collected. Even when the data has been collected, it is often the case that comparison of results from different studies is made very difficult due to variations in the treatment and presentation of the data. At worst, it may even be the case that a meaningful comparison may be impossible on the basis of the form in which the results are presented, even though sufficient raw data exists for a more satisfactory comparison to be made, given an alternative analytical treatment.

This paper presents a suggested methodology for a standard assessment procedure suitable for the collection and processing of data which is intended to demonstrate the performance of domestic ventilation systems. The process is illustrated by means of a simple example.

The Role of Ventilation
15th AIVC Conference, Buxton, Great Britain
27-30 September 1994

Simulation of Passive Cooling and Natural Facade Driven Ventilation

V Dorer, A Weber

EMPA Section 175, Building Equipment, CH 8600 Duebendorf Switzerland

Simulation of passive cooling and natural façade driven ventilation

V. Dorer and A. Weber

EMPA, Swiss Federal Laboratories for Materials Testing and Research
Section 175 Building Equipment
CH- 8600 Duebendorf, Switzerland

Synopsis

In many design cases, energy as well as occupant comfort are the relevant criteria which are studied using computer simulation programs. Comfort evaluations cover air quality, thermal, visual and acoustical comfort. For all these individual aspects, specific simulation programs are available today, but very few programs allow for the integrated evaluation of several or all relevant parameters. The more, heat transport, ventilation as well as lighting are physically coupled and therefore must be integrally modelled in the simulation process.
This paper gives a short description of the concept used for the coupling of the air flow simulation code COMVEN with the building and systems simulation code TRNSYS. Then, two application examples typical for a building design study situation are presented.
The first example shows a multi-storey school building which is passively cooled at night-time due to natural stack airflow. The influence of the operation of the openings on the maximum room temperatures is discussed for a hot summer period case.
The façade of the building of example 1 shall be retrofitted with a glazed outer façade. In example 2 the natural ventilation of this building is studied. Ventilation is provided by naturally driven shaft ventilation through the façade spaces. Control strategies for the openings and the blinds are discussed in respect to overheating risk and minimum air flow rates.

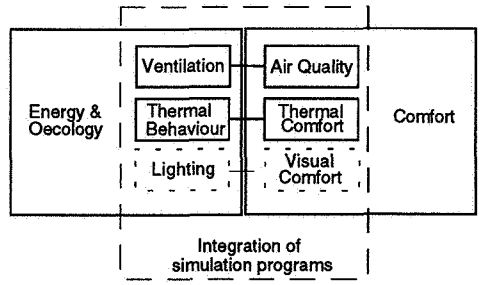

***Figure 1**: Evaluation of energy and comfort aspects*

Keywords: Multizone air flow modelling, building simulation, coupling, COMIS, TRNSYS, passive cooling, façade driven ventilation

1 COMV-TRNS: Integration of COMVEN as a TRNSYS Type

1.1 Combined modelling of heat, air and contaminant transport

Many building simulation models are not very well adapted to the simulation of natural ventilation. On the other hand, multizone air flow models normally require the room air temperatures as input values. Therefore the modelling of thermally induced driving forces is limited because in many applications the room air temperatures are not known a priori. In such cases, the coupling of a thermal and an air flow model is needed. This can be established according to

several different concepts, ranging from user directed parameter transfer to a complete merging of the two model codes.
Quite a few attempts to integrate an air flow model into a thermal model have already been made [1]. This paper describes the integration of the multizone air flow and contaminant transport model COMIS into the building and systems simulation code TRNSYS [2].

1.2 The multizone air flow simulation code COMIS

COMIS is a multizone air flow and contaminant transport simulation code which development started in the frame of the one-year COMIS workshop and presently is continued in the frame of the IEA-ECB Annex 23 'Multizone Air Flow Modelling' [3]. COMERL, an user interface with an integrated database is available for PC. A graphical, more sophisticated user interface is developed in the frame of Annex 23. The actual simulation code, written in Fortran77, is named COMVEN.

1.3 Integration of COMVEN into TRNSYS

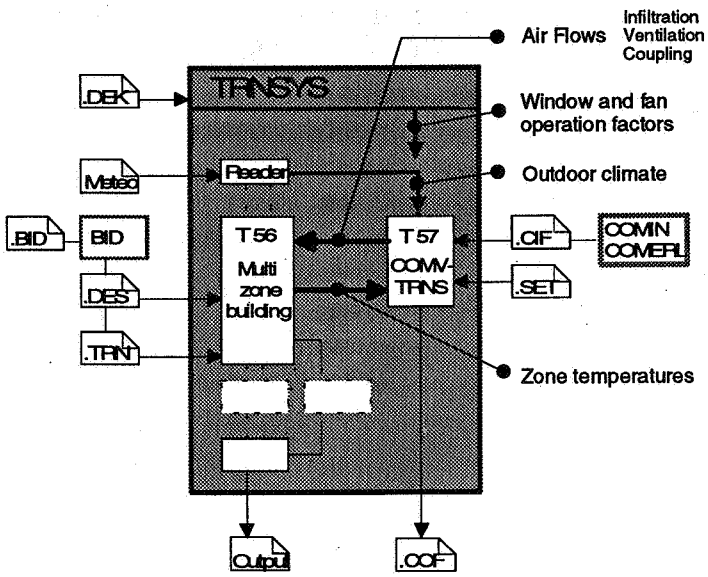

Figure 2: Integration of COMVEN as Type 57 into TRNSYS, data transfer, related files and pre-processor programs

The simulation program COMVEN has been adapted as Type 57 COMV-TRNS for the building systems simulation code TRNSYS, to be used in combination with the TRNSYS multizone building Type 56 [4]. This allows for the integral determination of the heat fluxes due to transmission, radiation and convection. Interactions between the building masses, the plants and the air flows due to natural and mechanical ventilation can be studied.

Figure 2 shows the TRNSYS program with the two Types mentioned, the parameters of their data connection, as well as the related input and output files and the respective pre-processor programs.

2 Example 1 : Passive night cooling by natural ventilation

2.1 Description of the building and the simulation cases

For a four-storey school building, the effect of passive cooling by natural night ventilation was studied. Figure 3 shows a section of the building with the respective air flow paths through the gap in the always closed internal room door and the bottom hung openable windows to outside.
Two operation modes are compared: In mode 1 the windows are fully opened at night and during the breaks, and in a tilted position during the lessons, in mode 2 the windows are closed at night, tilted during the lessons and fully opened only for one hour before the morning and the afternoon lessons respectively.

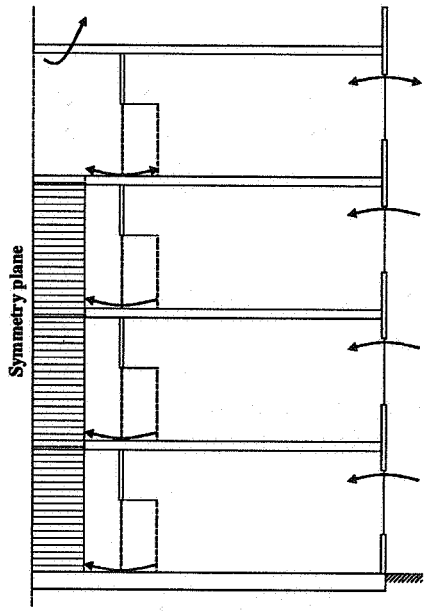

Figure 3: Cross section of the building and the air flow paths for natural ventilation

2.2 Simulation results

For one typical room during a hot summer period in Lucerne, central Switzerland, Figure 4 shows for mode 1 and 2, respectively, the outside and room air temperature as well as the outdoor air exchange together with the window opening schedule.

The full opening of the windows in the morning brings the room temperature rapidly down to the outside temperature, but due to the higher building mass temperature, in mode 2, the room temperature rises quickly again during the lesson, while in mode 1 the temperature remains on a moderate level. Peak room temperatures differ about 4°C from mode 1 (night cooling) to mode 2.

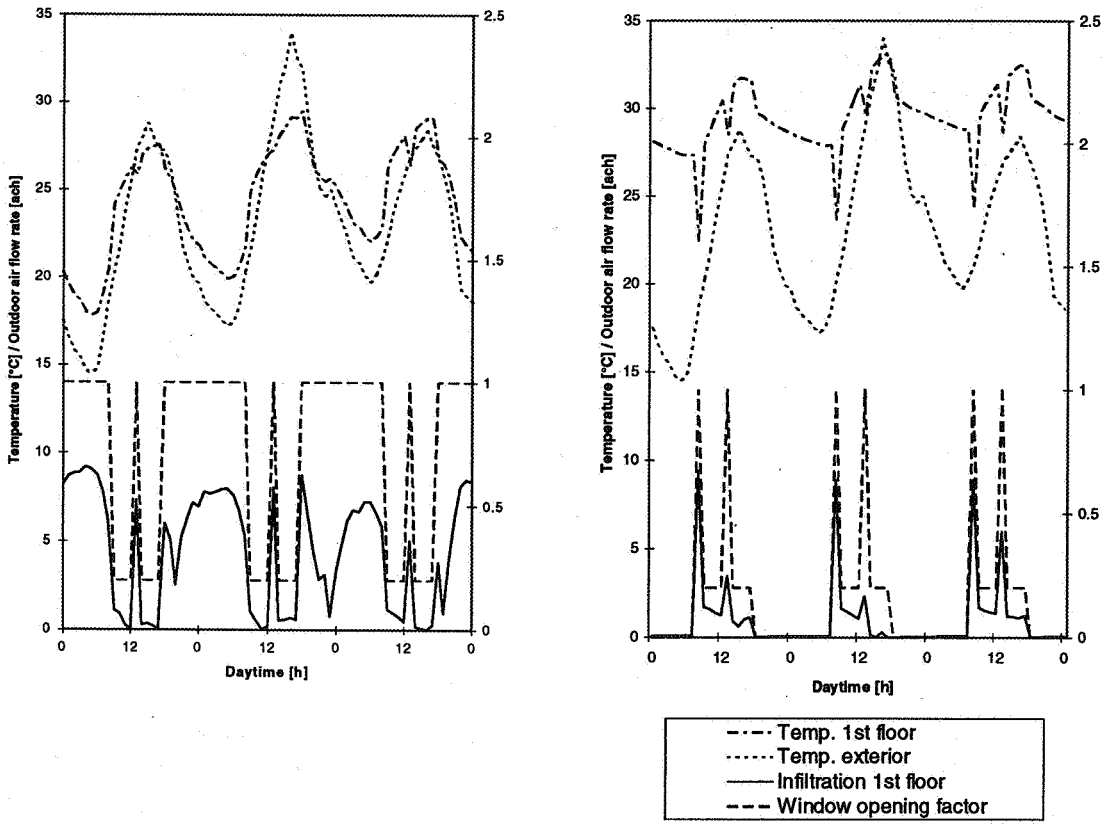

Figure 4: Outside and room air temperature, the outdoor air exchange together and the window opening factor for mode 1 (night ventilation, left) and for mode 2 (no night time ventilation, right)

3 Example 2: Retrofit with a glazed double façade

For the same building, retrofit concepts have been worked out on the basis of a glazed double façade, built up over the original structure which remains practically unchanged. This approach is effective in respect to construction costs and to ecological aspects. Figure 5 shows one of the proposed constructions. On each side of a room, the double façade spaces are open in vertical direction, acting thus as a ventilation shaft. In the middle section, the original window is removed and replaced by a window in the outer façade.
While the potential for reduced transmission losses in winter time is quite obvious, more concern was related to the overheating risk in summer and thus to the possibilities to cool and ventilate the building satisfactorily.

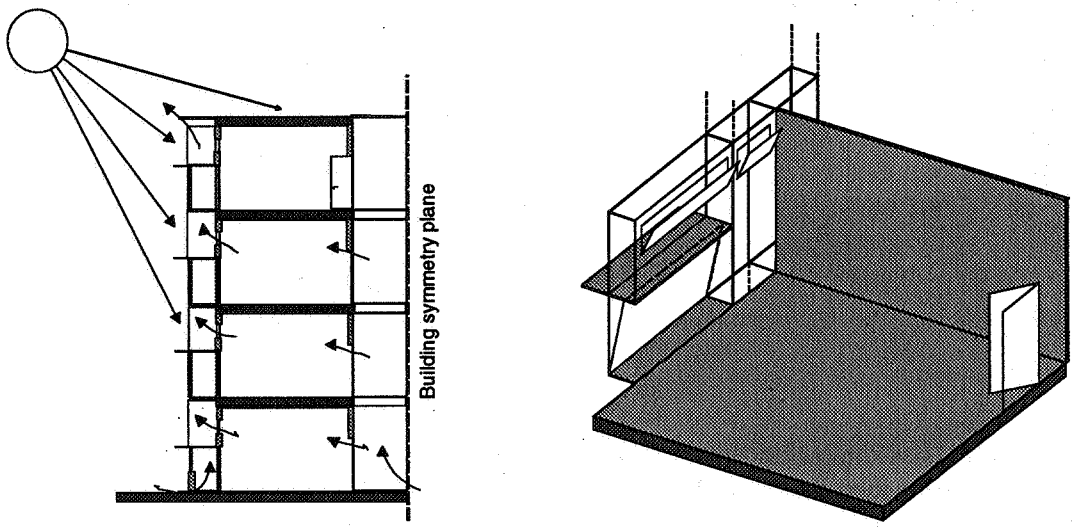

Figure 5: Cross-section of the building section modelled and isometric drawing of one room with the double façade spaces.

The aim of the simulation study presented in this paper was to provide data on the thermal comfort and the respective ventilation situation in the different rooms for a typical hot summer period, and to establish strategies for the operation of the different windows and openings for optimum indoor environment.

3.1 Modelling of the building

A section over the entire building height of the southern half of the building is modelled with its double façade and the adjacent rooms using the TRNSYS Type 56 multizone building.

Type 56 (TRNSYS version 13.1) is not very well suited to model this specific building configuration due the following limitations:

- Solar radiation is considered only for windows and external walls. This means that radiation through the double façade zone into the rooms behind cannot be modelled without applying some modelling tricks.
- The model for windows in Type 56 is quite limited as it does not allow for specific glazing types with specific spectral characteristics. The more, blinds are only considered as a geometrical aperture factor. Thus the energy transport aspects must be modelled by the user.

The double facade and the adjacent room are modelled as follows:

- The energy flows into the double facade space and the room are modelled by equations which are set up specifically for this case. The type 56 model is used only for the calculation of the radiative and convective energy distribution within the two zones.
- The outer glazing and the blind are considered as a wall (TRNSYS wall with known boundary condition), with a very low resistance in order to get literally the same surface temperature on both sides of this wall. The optical properties according to the glazing and the blind are considered in specifically set up energy flux equations.
- Also the inner double glazing is modelled as a wall (TRNSYS wall between zones).

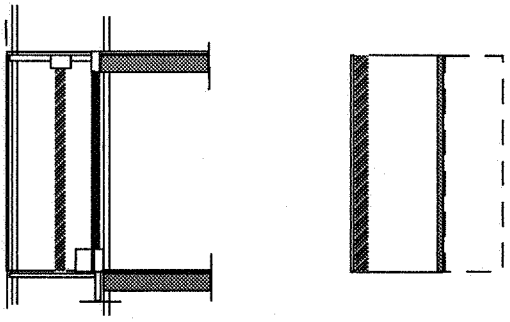

***Figure 6:** A section of the double façade zone with the blind, left, and the respective model with the outer wall and the inner wall, right.*

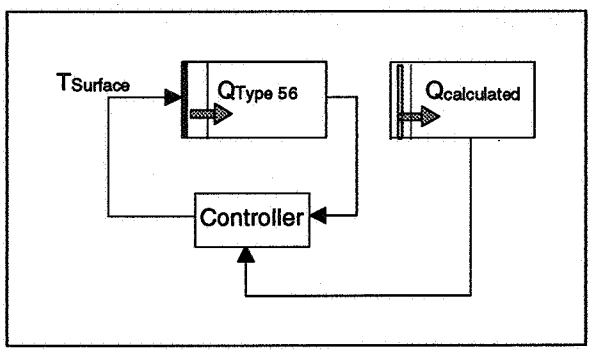

***Figure 7:** The control loop for the surface temperature of the outer wall.*

The correct heat flux into the double façade zone due to solar radiation, radiative and convective emission from the blind and the heat transfer through the external wall cannot be determined explicitly but has to be determined iteratively by balancing out

a) the energy flux $\dot{Q}_{Calculated}$ as determined explicitly as the difference between the incoming radiation energy and the heat exchange from the blind to the outside surface
b) the energy flux $\dot{Q}_{Type56}$ as determined by the room star network model in type 56

The free parameter for this iteration is the surface temperature of the outer (external) wall. The iteration is realized by a control loop (see Figure 7). This approach has to be made due to the fact that no direct gains to walls can be defined in Type 56. The modelling of the glazed double façade is described in more detail in [5].

It has to be mentioned however that in the new release TRNSYS 14.1, Type 56 has been improved and individual wall gains can now be defined, making the above described modelling approach obsolete in some parts.

3.2 Simulations

Simulations have been made for the same hot summer period as used in example 1. The result parameters are the air flows per opening in the room as well as the temperatures in the individual zones. Thermal comfort parameters can be checked taking into account also the wall surface temperatures. The air quality aspects are covered by mean age of air values per room or by defining CO_2 sources according to the occupant presence and checking the resulting concentrations. Wind effects as well as the influence of the second, north oriented building half have not been considered in the simulations.

Within the iterative solution process, oscillations may occur in stack (boyancy) dominated driving force conditions. In such cases, changes in the air temperatures and thus in the stack pressures lead to reversed flow directions in a critical zone and in consequence the room temperatures change again significantly. These oscillations from one iteration step to the next may lead to numerical convergence problems, which can be overcome by introducing an element which numerically damps the air flow data connection between Type 56 and Type 57 (COMV-TRNS).

3.3 Simulation results

Figure 8 shows for the same three-day period as in Figure 4 the calculated temperatures and air flows for the room and the double façade space of the second floor as well as for the staircase, together with the opening schedules for the windows, the openings to the double façade space and the openings in the staircase to outside.

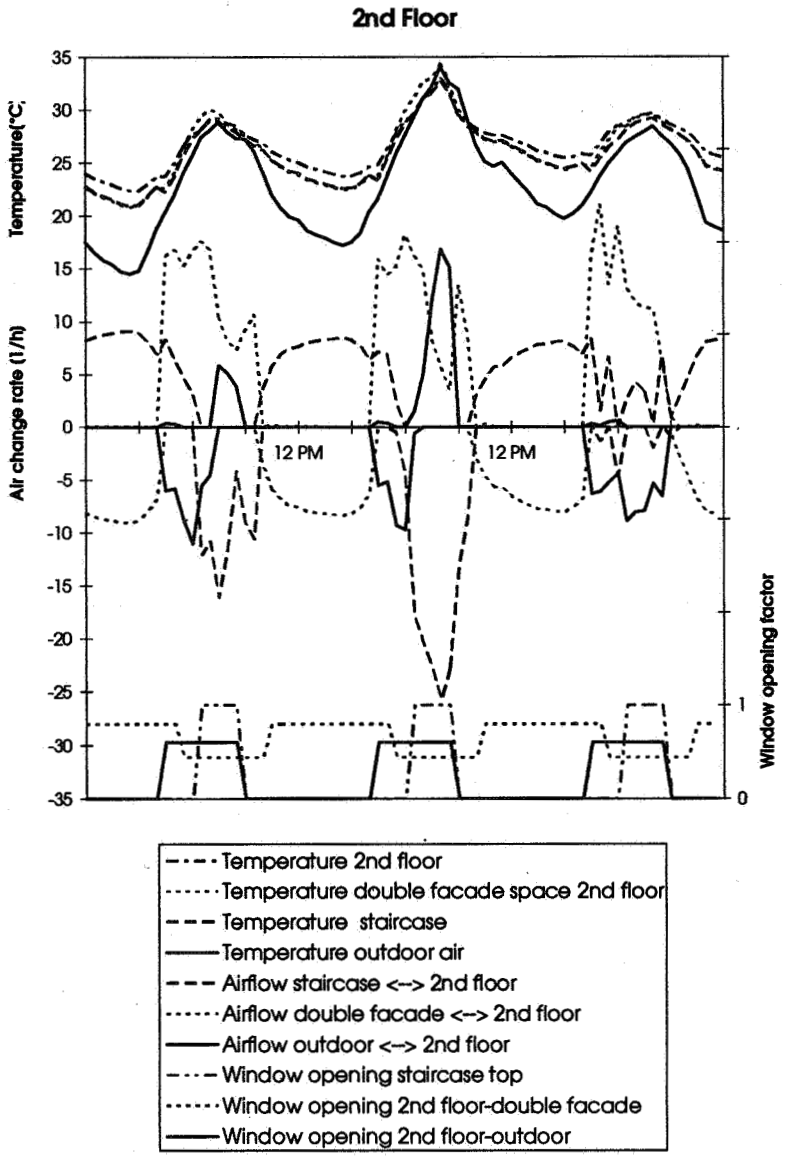

***Figure 8**: Temperatures and air flows to and from the 2nd floor room and opening schedules for the different openings. The bottom staircase opening is opended as soon as the top opening is closed (and vice-versa).*

Figure 9 shows the air temperatures and the air flows of the individual openings in the section of the building modelled for two typical daytimes during the second day: Early in the morning at 6 AM when the windows to outside in the room are closed and at 4 PM (at peak outside temperature) when the room windows to outside are opened.

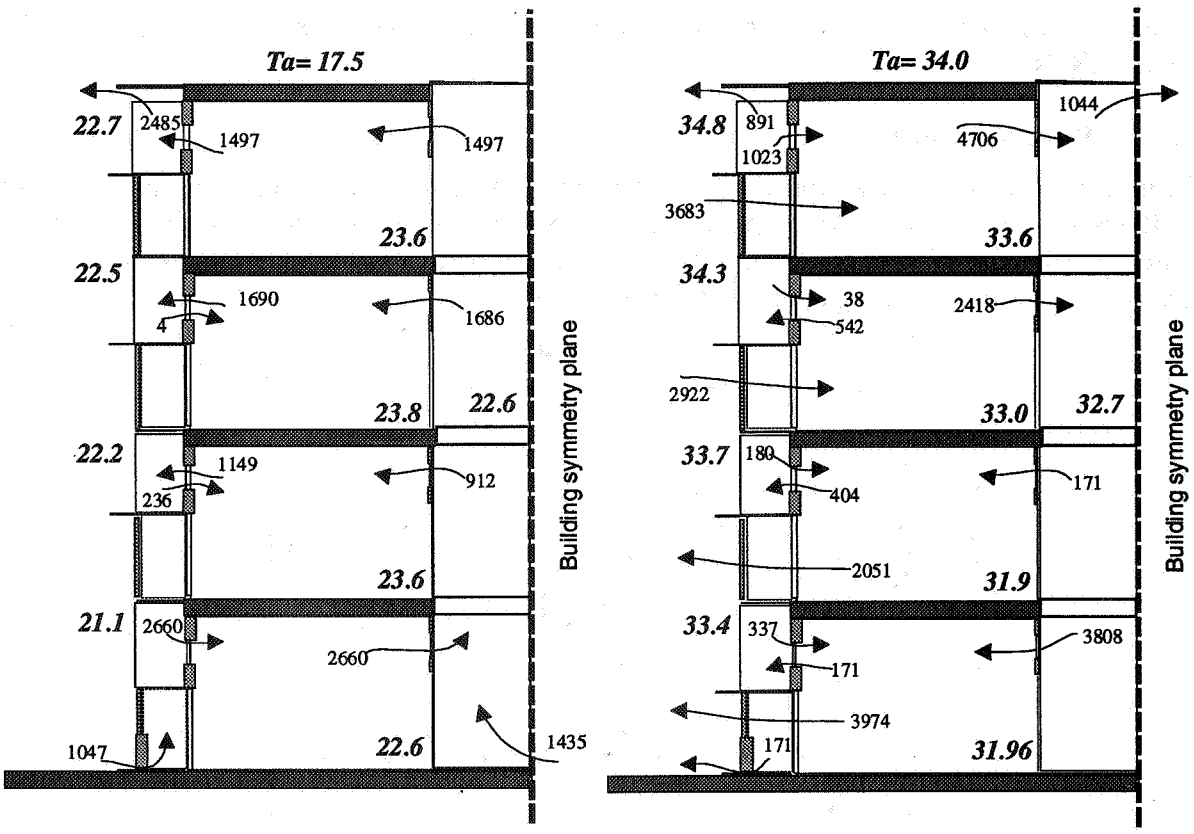

Figure 9: Outdoor and zone temperatures [°C] (in italics), and the respective air flows per opening [kg/h] at two typical daytimes for the building section modelled
(left at 6 AM, right at 4 PM corresponding to peak outdoor temperature, see Figure 8)

3.4 Discussion

The room windows are closed during night and the rooms are ventilated only through the façade space. Quite large openings to either the staircase and the double façade space are needed in order to cool the building sufficiently by night-time ventilation. In the rooms, windows openable directly to outside can supply cooler outside air for most of the time during the day and significantly increase the ventilation rate.

Most of the time the air flow pattern for the rooms is quite satisfactorily, only for a short period at peak outside temperatures the supply of the uppermost room is from the façade space, which should be avoided.

Additional simulations were performed in order to study optimum opening control strategies. Simulations showed that there is a potential to use the staircase space as a storage of cool air during peak outside temperatures. In this case all external openings in the staircase and in the upper floors the openings to the façade space must be closed. Consequently, at the upper

floors, the doors between the room and the staircase should be open in order to achieve an acceptable ventilation.

4 Conclusions

The evaluation of design concepts for naturally ventilated and cooled buildings can be greatly improved by simulation, considering the coupled effects of the thermal behaviour of the building and the naturally driven air flows.

Numerical problems during the iterative solution process which may occur in stack dominated driving force conditions, may be overcome by numerical damping of the data transfer from the air flow model to the thermal model.

Due to the complex nature of the physical phenomena and the great variety of possible ventilation control strategies, the amount of simulation runs needed to cover a reasonable parametric range may not be underestimated.

5 Acknowledgements

This work was financially supported by Swiss National Energy Research Fund (NEFF, project 'Energierechengruppe'), the Swiss Federal Office of Energy (BEW, project 'IEA-ECB Annex 23'), and the EMPA.
Thanks to Frederik Huck for his contributions to Example 1 and to Markus Koschenz for his advice on how to model the double façade.

6 References

1. KENDRICK J: *An Overview of Combined Modelling of Heat Transport and Air Movement* AIVC TN 40, February 1993
2. *TRNSYS, A Transient System Simulation Program*, Solar Energy Laboratory, University of Wisconsin Madison, USA
3. *COMIS User Guide*, Version 1.3 or newer, available form the Lawrence Berkeley Laboratory, Berkeley, USA.
4. DORER, V. and WEBER, A: *Multizone Air Flow Model Comven-Trnsys, TRNSYS Type 57 Documentation*, IEA-ECB Annex 23 technical report, EMPA 175, 1994
5. DORER V, KOSCHENZ M, WEBER A: *Modelling of a glazed double façade with TRNSYS 13.1 Type 56*, EMPA internal report, 1994

The Role of Ventilation
15th AIVC Conference, Buxton, Great Britain
27-30 September 1994

Dare You Risk Designing Without the Best Tools?

J Littler*, M Davies*, D Cuckow**, A Jarvis**, B McCarthy**

* University of Westminster, 35 Marylebone Road, London NW1, United Kingdom

** 12 Flitcroft Road, London EC1, United Kingdom

ABSTRACT FOR
"THE ROLE OF VENTILATION"
AIVC CONFERENCE SEPTEMBER 27-30 1994, BUXTON

"Dare you risk designing without the best tools?"

by
John Littler and Michael Davies
University of Westminster
35 Marylebone Road, London NW1
and
David Cudow and Andrew Jarvis, Battle McCarthy
12 Flitcroft Road, London EC1

The authors will present calculations concerning proposals to cover, with a highly glazed roof, the 80 m gap between an existing railway station and a long rail tunnel in Lisbon.

The extension will provide a covered area for new platforms. The design-risk was mainly in the potential for overheating.

Readily available climatological data (mean daily temperatures) and an assumed indoor temperature, allowed a rough estimation of the temperature difference between indoors and outdoors, namely 5 °C. Initially this temperature was used to calculate the cooling available by air change.

However, simulation quickly showed that simplistic assumptions vastly overestimated the cooling potential.

Simulation, using hourly weather data for Lisbon (kindly supplied by E Maldonado of the University of Porto), and APACHE (Facet Ltd of St Albans UK), shows that much smaller temperature differences will prevail at the critical time of day:

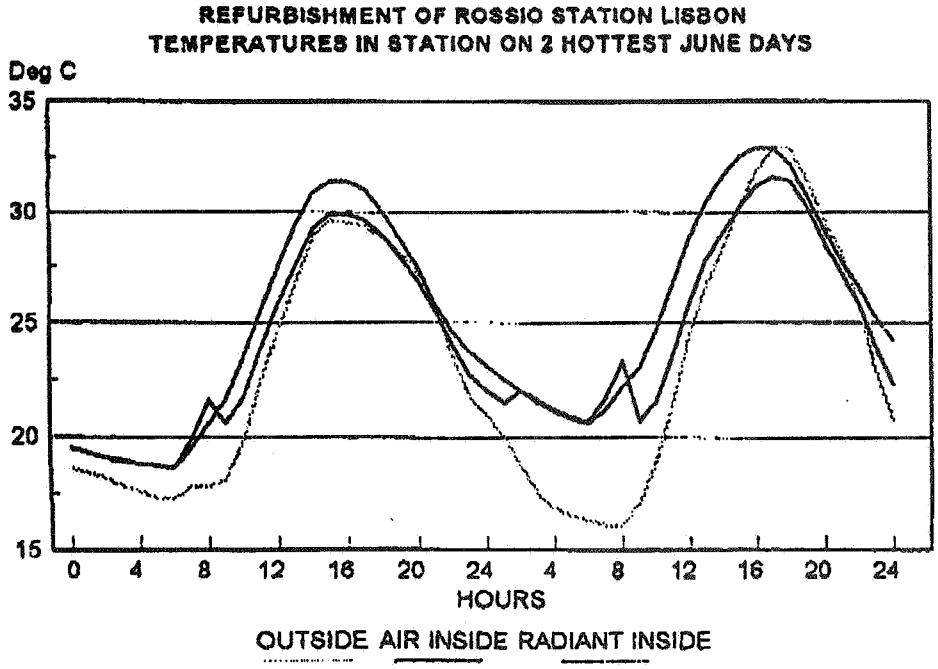

Originally the design assumed that the major cooling resource is the (lower) outside air; but modelling suggests two more important cooling resources, namely the mass of the platforms and walls surrounding the station and the cool tunnel air. Both of these resources rely on the lag in

earth temperature to carry away surplus heat and thus the modelling itself relies on a good description of the ground conditions.

The authors' first modelling exercise illustrated the small effect of the ambient air (even for night ventilation) and the probable importance of the cooling by the earth.

Algorithms describing the 3-D heat propagation through the ground (or any other massive element) have recently been added to APACHE by one of the authors (MD) and detailed results of the modelling of the station will be presented at the AIVC meeting describing the performance with the benefit of the 3-D model.

The Role of Ventilation
15th AIVC Conference, Buxton, Great Britain
27-30 September 1994

Design Tool for Optimizing the Selection of Ventilation Plants

G Wernstedt

Stockholm Konsult, Stockholm, Sweden

DESIGN TOOL FOR OPTIMIZING THE SELECTION OF VENTILATION PLANTS

Gunnar Wernstedt, Stockholm Konsult Sweden 13 July 1994

Introduction

The selection of ventilation plant and it's level of energy efficiency is often done without economic calculations. The reason could be lack of time or knowledge.
The result will be the selection of the plant of lowest investment cost, which means' a small plant of inefficient type. This normally includes a fan-wheel of the "sirocco type" followed by a large electric motor. The motor should be large enough to stand for the rise in power due to increased fan power if the calculations of the ductwork systems pressure-drop show up to be wrong or the flow rate must be increased because of too large ductwork system leakage. In other cases the selection in the end will be the same in spite of a god selection from the beginning. This could be the case when the total cost of the whole building show up to be larger then calculated. The first cost to cut will often be the installation cost. The cut will, in many cases, be made by reducing the size of the ventilation plants and selecting more energy demanding equipment.
The economic consequences of such a selection are seldom analysed. This paper describes a tool to improve the knowledge of the economic consequences and help the designer to make the wright choice.

Synopsis

The main goals for this design tool are:

- A powerful, but simple to use, technical and economic tool for selecting a ventilation plant.
- Guide and control the consultants in accordance with the owner's economic preferences.
- The long run extra cost, if one is forced not to follow the guidelines of the method is calculated in order to get the economic backgrounds for a decision.
- Creating a key-value for the cost of ventilation that can be understood by engineers and people with economic education.

The three most important parts of the selection of this design tool are:

1. The representative or equivalent parameters called "the equivalent working condition". This operating condition has the same electric energy consumption as the sum of all running condition of the selected ventilation plant will run at. VAV system is transformed to a CAV system running at a fixed air flow rate.
2. Selecting key-values are presented, for the pressure drop in the plant, fan efficiency and the efficiency of the heatrecovery equipment and optimal specific fan power, to guide the designer.
3. When the selection is made the "specific total cost" of the selected plant is calculated and compared with the optimal cost. This "specific total cost" describes the cost for operation,

maintenance and capital cost for the ventilation-function.

* The kernel of this design tool (selection method) is " the database of performance and investment cost for manufactured ventilation plants" , " The general economic evaluation key-values stipulated by the owner " and "the equivalent conditions ". This kernel make it possible to find the best set of performance key-values similar to the ventilation plants that have the lowest Life Cycle Cost in the database.The performance sets with lowest Life Cycle Cost in the database, modified to suite "the equivalent working condition", are chosen to derive performance key-values diagrams.

Description of the design tool from the user point of view.

The flowchart fig. 1 shows the basic steps of this method. Here are some more details of the different parts of this method.

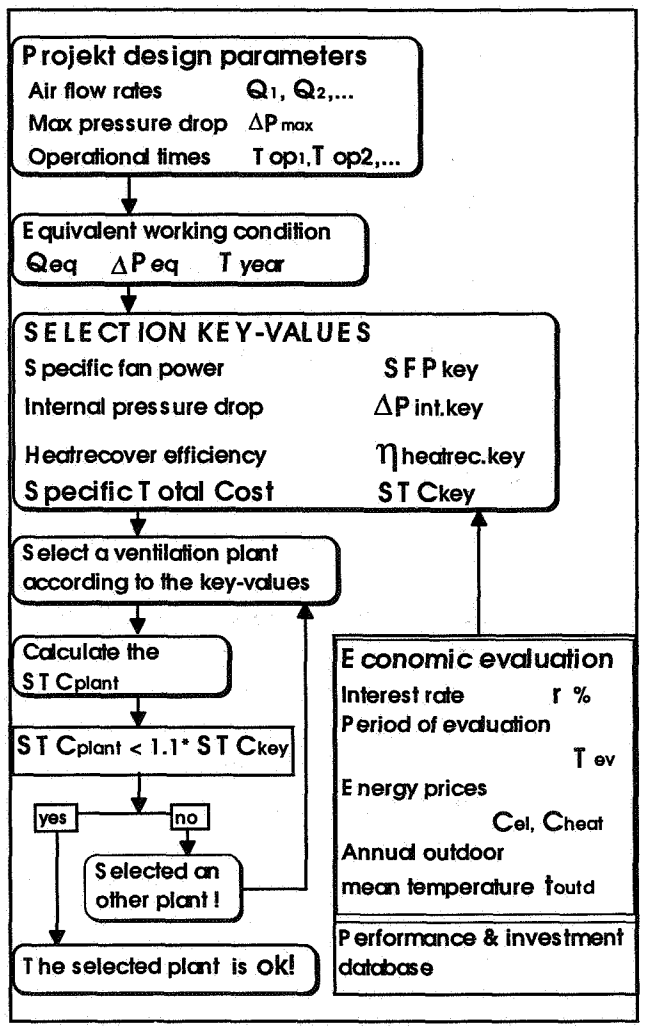

fig 1

The first things to do when selecting a ventilation plant is to document the design parameters of the project.

1. *Project design parameters*

The specific project design parameters as working conditions and operational time are specified under this header.
Working conditions used by this design tool is:

The different air flow rates to be used.

$Q_1, Q_2, \ldots$ [m^3/s]

In case of Variable Air Volume system (VAV) an approximation with a number of fixed flow rates are used.

The pressure drop for the largest air flow rate

ΔP_{max} [Pa]

Exhaust air temperature

t_{exh} [°C]

Supply air temperature

t_{sup} [°C]

The operational time for the specified flow rates

$T_{op1}, T_{op2}, T_{op3}, \ldots$ [hours]

2. *Calculation of one equivalent working condition*

From the project design parameters one equivalent working condition and the total annual operational time are calculated.

The parameters of the equivalent working condition are:

Equivalent air flow rate	$\mathbf{Q_{eq}}$	[m^3/s]
External pressure drop for the system at the equivalent air flow rate	$\mathbf{\Delta P_{eq}}$	[Pa]
Total annual operational time	$\mathbf{T_{year} = \sum (T_{op1}, T_{op2}, T_{op3}, \ldots)}$	[hours]

During the selection procedure the ventilation plant is assumed to be a constant air volume system, CAV. system, with the equivalent flow rate, Q_{eq}, and the equivalent pressure drop, ΔP_{eq} and operating time, T_{year}, equivalent to the sum of the operating time of the all working conditions. The equivalent working condition is chosen to have the same electricity consumption with the operating time, T_{year}, as the sum of all the different working conditions under the ventilation plant will operate.

Performance and investment cost database

The kernel of this design tool (selection method) is " the database of performance and investment cost of manufactured ventilation plants" together with " The general economic evaluation key-values" these parts makes it together with "the equivalent conditions " possible to find the best set of performance key-values. This set of key-values is similar to the ventilation plants that have the lowest Life Cycle Cost in the database. The ventilation plants have different kind of heatrecovers and transmission(f or instance belt transmission or direct drive including equipment modulating the current frequency).
The data in the database describes the performance of a number of ventilation plants from three manufactures (minimum, could be increased to a arbitary number) in three different working conditions. The air flow rate is 1, 3 and 5,4 m^3/s in the three different cases. The pressure drop is 500 Pa in all three cases. The energy demands for these three cases are calculated at three different running times. This makes nine " performance sets" for each ventilation plant.

General economic evaluation key-values

The owner, or the one in charge instead of him, declare his economic preferences by setting up a couple of key-values that should be used by the consultant in the evaluation procedure of this method. These key-values will be used in the Life Cycle Cost (LCC) calculation that will be used to evaluate the selection of ventilation plants.
These economic key-values should be reconsidered, for instance once a year.

Interest rate (excluding inflation)	$\mathbf{r}$	[%]
Period of evaluation	$\mathbf{T_{ev}}$	[year]
Energy prices (mean value under the evaluation period, excluding the inflation)		
Specific electricity price	$\mathbf{C_{el}}$	[Ecu/kWh]
Specific heat price	$\mathbf{C_{heat}}$	[Ecu/kWh]
Annual outdoor mean temperature of the building site	$\mathbf{t_{outd}}$	[C°]

Life Cycle Cost calculation

With data from the performance database and the "general economic evaluation key-values the Life Cycle Cost (LCC) are calculated for all " performance sets".
The amount of air V [m^3] passing through the ventilation plant each year is calculated by multiplying the running time with the largest of the support air and the exhaust air flow rate.

$$\mathbf{V = T_{year} * Q} \quad [m^3]$$

Specific Total Cost (STC)

In order to get a key-value for the total functional cost for the air transportation (including capital costs) the LCC for each performance set is divided with the air volume (V) multiplied with the number of years the LCC calculation is made for.

$$\mathbf{STC = LCC/(V * T_{ev})} \qquad [ECU/m^3]$$

Key-values diagram

The performance sets in the database, modified to suite "the equivalent working condition", are grouped by working conditions as running time and air flow rate, type of heatrecover and type of transmission.The performance sets from the ventilation plants with lowest **STC** for each group are chosen to derive performance key-values diagrams. These diagrams should be used to find a recommendation of performance sets for ventilation plants with low LCC. Choosing a ventilation plant with performance similar to the recommended performance set should give a ventilation plant with low LCC. In fig. 2 is an exampel of key-value diagram (SFP)

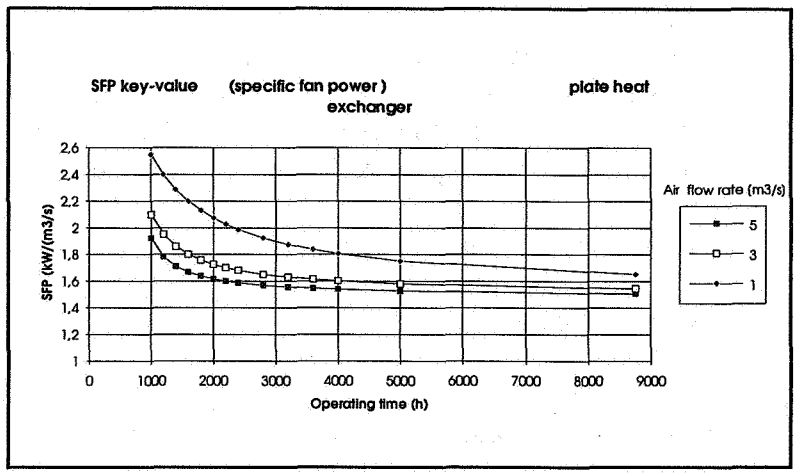

fig. 2

Selecting a ventilation plant

Select the ventilation plant that best suits "the selection key-values". The one you choose must not meet all the key-values, they are just meant to be guidelines. The only thing that counts in the end is that the Life Cycle Cost of selected plant is low.

Calculate the Specific Total Cost of the selected ventilation plant

Now is the time to calculate the STC of the selected plant.
To your help there is a tool making it easy to calculate the heat and electricity demand of the selected plant. From the diagram in **fig. 3** you can find the mean supplementary energy demand percentage. per volume [m^3]. The input to the diagram is the temperature of the exhaust and supply air and the heatrecovers temperature efficiency reduced with a factor due to lower efficiency in the future when the heatrecover is old and dirty.

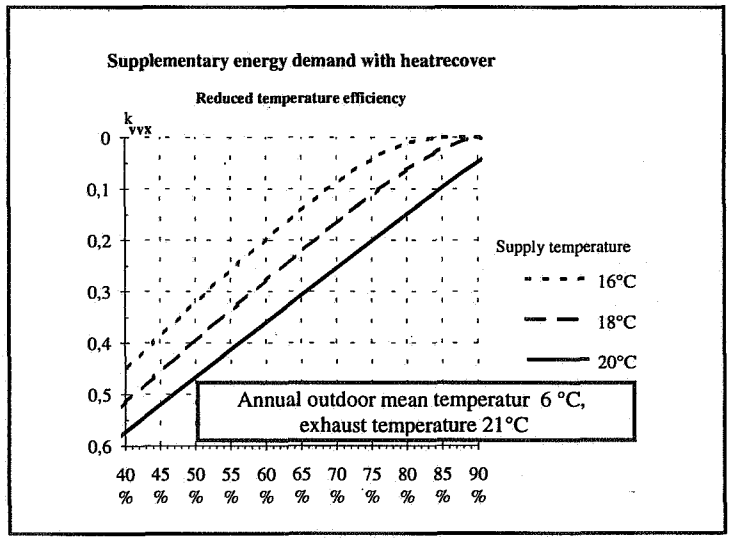

fig. 3

Evaluation of the selected plant

If the selected plants $\mathbf{STC}_{plant}$ not exceeds the $\mathbf{STC}_{key}$ with more than **10%** it is accepted and the selection procedure is finished. Otherwise one has to go back again and try with an other ventilation plant.

Restrictions in the size of the plant room space and other selection restrictions

If thera are any kind of restrictions, as restricted hight or floor area, of the selection of the ventilation plant choice, the method compare the extra cost for not selecting the plant with lowest LCC with the extra cost for removing the restriction.

Documentation
All the steps in this method are documented in a special form. This make it possible in the future to go back and see what parameters used, and the reason a certain plant was chosen.

Further development

To make this tool even more powerful a computor data program version will be developed in 1995. The program will shorten the time of selection and make it easier to compare different alternatives. The key-values sensitivity to changes in "the general economic parameters" will easiely be analysed.

List of Symbols

$Q_1, Q_2, \ldots$	[m^3/s]	The different air flow rates to be used.
ΔP_{max}	[Pa]	The pressure drop for the largest air flow rate
t_{exh}	[°C]	Exhaust air temperature
t_{sup}	[°C]	Supply air temperature
$T_{op1}, T_{op2}, T_{op3}, \ldots$	[hours]	The operational time for the specified flow rates
Q_{eq}	[m^3/s]	Equivalent air flow rate
ΔP_{eq}	[Pa]	External pressure drop for the system at the equivalent air flow rate
$T_{year} = \sum (T_{op1}, T_{op2}, T_{op3}, \ldots)$	[hours]	Total annual operational time
r	[%]	Interest rate (excluding inflation)
T_{ev}	[year]	Period of evaluation
C_{el}	[Ecu/kWh]	Specific electricity price (excluding the inflation)
C_{heat}	[Ecu/kWh]	Specific heat price (excluding the inflation)
t_{outd}	[C°]	Annual outdoor mean temperature of the building site
$V = T_{year} * Q$	[m^3]	The amount of air V [m^3] passing through the ventilation plant each year is calculated by multiplying the running time with the largest of the support air and the exhaust air flow rate.
LCC	[Ecu]	Life Cycle Cost
$STC = LCC/(V*T_{ev})$	[ECU/m^3]	Specific functional cost for the air transportation

13 July 1994 \aivcför.ed1\

The Role of Ventilation
15th AIVC Conference, Buxton, Great Britain
27-30 September 1994

Applications of the Air Infiltration and Ventilation Centre's Numerical Database

M S Orme

Air Infiltration and Ventilation Centre, University of Warwick Science Park, Coventry CV4 7 EZ, United Kingdom

Applications of the Air Infiltration and Ventilation Centre's Numerical Database

Synopsis

Building airtightness data are essential for design and model evaluation. An attempt has been made with the Numerical Database to compile data appropriate to infiltration and ventilation studies. These cover the air leakage characteristics of building components, the characteristics of buildings themselves and data on wind pressure distributions.

AIVC Technical Note 44 (*Orme, Liddament, and Wilson, 1994*), contains detailed summary tables and graphs of the information stored in the computer Database, together with a complete list of references. Technical Note 44 also discusses wind pressure distributions on buildings.

This paper outlines some potential applications of the Numerical Database and illustrates one of these with a worked example. It also briefly discusses how airtightness is represented in the Database.

1. Introduction

The Air Infiltration and Ventilation Centre's Numerical Database has been developed in order to establish a core of numerical data suitable for design purposes and model validation, and to provide a focus for data derived from related International Energy Agency projects. Source information is contained within a computerised database from which direct searching for specific material is possible. The purpose of this paper is to present some potential areas of application of the Database.

Data have been derived from as wide a range of sources as possible, including many organisations who have contributed both expertise and experimental results. By combining information from these sources, it has been possible to consider a far wider range of operating conditions than would have been possible if only a single set of measurement results had been used.

Users are cautioned that the data presented are based on measurements published in the literature or provided by various institutions for inclusion in the Numerical Database. Therefore, there is no guarantee that it is suitable for any specific design application. Wherever possible, applicable standards or airtightness recommendations should be applied to new and retrofit construction.

The nature of the representation of airtightness used by the Numerical Database is shown in Section 3. Determination of ventilation rate and its applications are briefly outlined in Section 5, whilst Section 6 discusses airtightness.

2. About the Numerical Database

The AIVC's Numerical Database is contained in Idealist for DOS software and, in order to ensure ease of operation, a User Guide (*Orme and Limb, 1994*) is supplied. AIVC Technical Note 44 (*Orme, Liddament, and Wilson, 1994*), contains detailed summary tables and graphs

of the information stored in the computer Database, together with a complete list of references. This Technical Note also discusses wind pressure distributions on buildings.

The Numerical Database includes typical data (from both laboratory and field test experiments) for individual components and whole buildings, and wherever possible, relevant standards and recommendations for building or component airtightness performance have been incorporated. The appropriate standards and recommendations are described in detail in AIVC Technical Note 43 (*Limb, 1994*).

3. How Airtightness Characteristics are Described in the Numerical Database

3.1 Building Components

The Power Law equation is given by:

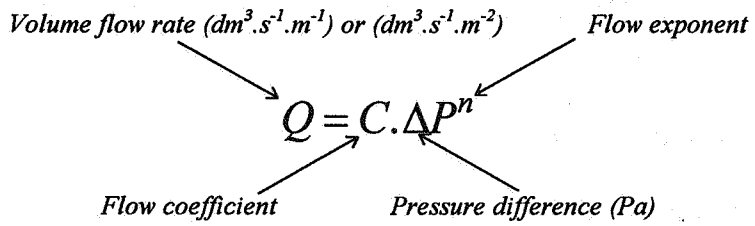

The Power Law equation is essential for understanding the contents of the Numerical Database. This equation is empirically based and it relates the pressure drop across components to the volume flow rate of air passing through them. Building component characteristics collected in the Numerical Database are in the form of flow coefficients, C, together with their associated flow exponents, n. Every flow coefficient has been normalised by dividing, either by the length of crack, or where more appropriate, by the area of the permeable surface. This enables direct comparison between components of different physical dimensions and also more general application of the collected data.

The following types of component are covered in the Database:

- Windows
- Doors
- Interfaces of window and door frames with walls
- Wall construction, ceilings and floors
- Ceiling/wall/floor interfaces
- Wall to wall interfaces
- Penetrations
- Roofing
- Fireplaces and flues
- Trickle ventilators and vents

3.2 Whole Buildings

In the case of whole building records, airtightness values have been normalised by dividing the volume flow rate at 50 Pa pressure difference by the internal building volume to give air changes per hour at 50 Pa. Expressing airtightness in this way allows the leakage of buildings of different volumes to be compared. The basis of the artificially induced 50 Pa pressure difference, is that it is sufficiently large to prevent naturally occurring pressure differences from significantly influencing the result. On the other hand it is not so large that cracks and gaps are distorted by the applied pressure. The flow exponents, and in most cases the building

volumes, have also been included so that conversion to other pressure differences is still possible, by using the Power Law. (See Section 3.1.)

4. Determination of Ventilation Rate Using the Numerical Database

Part of the information needed to estimate the ventilation rate of existing or planned buildings is located within the Numerical Database. Ventilation rate is expressed in terms of volume air changes per hour (ach) and is the fundamental quantity involved when considering aspects of occupant comfort, indoor air quality, contaminant dispersal and energy use. The airtightness value of a building can be approximately derived from the Database, either by dealing with the structure as a single item, or as a combination of components. The latter of these approaches forms the basis of Section 7. Theoretically these two approaches should coincide. The airtightness of previously investigated real buildings or components can then be used in order to predict the ventilation rate obtained under certain internal and external climatic conditions, for the test configuration. This can be achieved with, for example, an air flow mass balance model.

5. Ventilation Rate Applications

5.1 Design Studies and Ventilation Strategies

As a consequence of its application in determining ventilation rates, the Numerical Database can be used to provide some of the initial data which are necessary for the evaluation of different ventilation strategies. Design studies are needed to derive an indication of typical expected airtightness values for a building specification, as well as ensuring the building is adequately, but not excessively, ventilated. For these reasons it is anticipated that designers will find the Numerical Database a useful tool.

5.2 Model Evaluation

For the purpose of evaluating air flow models, it is desirable that the airtightness characteristics of buildings, either considered as combinations of components, or as single structures, are represented in a realistic manner. This includes making certain that the magnitudes of leakages are within the appropriate commonly measured ranges. The Numerical Database allows the identification of such data, so that models can be configured to accurately represent the real world.

6. Airtightness

6.1 Effectiveness of Standards

Another area in which the Numerical Database may be beneficial is the effectiveness of national standards. It can be used to judge the proportion of components or whole buildings in a particular country that conform to the relevant standard(s). For instance, Figure 1 shows such data from the Netherlands, which approximately indicates the proportion of dwellings

complying with existing recommendations. A major assumption made here is that the airtightness distribution is representative of the building stock of the entire country.

Figure 1 Dwelling Airtightness (All Building Types) for The Netherlands

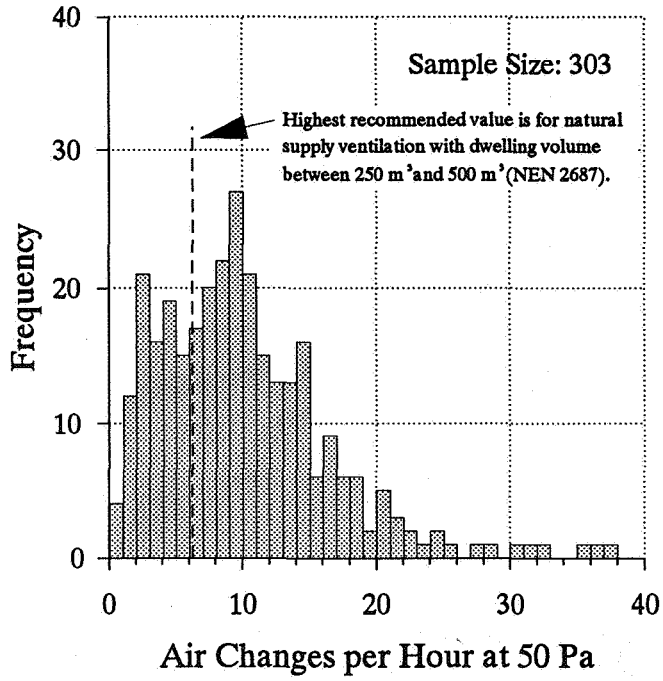

Data Source: TNO Air Leakage Database

6.2 Assessment of Airtightness

It is possible to search the computer Database for specific types of construction, and as such, an investigation of factors which influence airtightness can be made and different constructional techniques examined. This enables an assessment of the effect of retrofit or replacement on component or whole building leakage. It is also possible to explore the impact of climatic conditions by considering the measured range of airtightness encountered in different countries.

7. How to Derive the Airtightness of a Building from the Airtightness of its Individual Components - A Worked Example

The worked example illustrated in Figure 2 calculates the airtightness of a building from its component data. Estimations of the air change rate of this building, with an inside to outside pressure difference of 50 Pa, are given in Table 1. These are based on the building being of (i) high construction standard (lower quartiles), (ii) good construction (medians), or (iii) poor construction quality (upper quartiles).

Table 1 Worked Example - Estimation of Whole Building Airtightness

Component	Dimension /m²	Lower quartile				Median				Upper quartile			
		C /dm³.s⁻¹.m⁻².Pa⁻ⁿ	n	Leakage at 50 Pa /m³.h⁻¹	Percentage	C /dm³.s⁻¹.m⁻².Pa⁻ⁿ	n	Leakage at 50 Pa /m³.h⁻¹	Percentage	C /dm³.s⁻¹.m⁻².Pa⁻ⁿ	n	Leakage at 50 Pa /m³.h⁻¹	Percentage
Ceiling	59	0.042	0.81	212	10.5	0.11	0.75	439	17.0	0.20	0.72	710	17.9
Brickwork	138.8	0.016	0.86	231	11.5	0.018	0.85	250	9.7	0.021	0.84	281	7.1
	Dimension /m	C /dm³.s⁻¹.m⁻¹.Pa⁻ⁿ	n	Leakage at 50 Pa /m³.h⁻¹	Percentage	C /dm³.s⁻¹.m⁻¹.Pa⁻ⁿ	n	Leakage at 50 Pa /m³.h⁻¹	Percentage	C /dm³.s⁻¹.m⁻¹.Pa⁻ⁿ	n	Leakage at 50 Pa /m³.h⁻¹	Percentage
Service pipe	0.63	0.63	0.60	15.0	0.7	0.74	0.60	17.3	0.7	0.84	0.60	19.9	0.5
Ceiling hatch	4	0.64	0.60	96.5	4.8	0.68	0.60	102	4.0	0.75	0.60	113.0	2.9
Ceiling to wall joint (upper)	32	0.45	0.60	542	26.9	0.49	0.60	590	22.9	0.53	0.60	638	16.1
Ceiling to wall joint (lower)	16	0.45	0.60	271	13.4	0.49	0.60	295	11.4	0.53	0.60	319	8.1
Wall to floor joint (upper)	16	0.45	0.60	271	13.4	0.49	0.60	295	11.4	0.53	0.60	319	8.1
Window frame to wall	52	0.053	0.60	104	5.2	0.061	0.60	120	4.6	0.067	0.60	131	3.3
Door frame to wall	12	0.053	0.60	24.1	1.2	0.061	0.60	27.5	1.1	0.067	0.60	30.1	0.8
Window opening	66	0.086	0.60	214	10.6	0.13	0.60	324	12.5	0.41	0.60	1018	25.7
Door opening	12	0.082	0.60	36.7	1.8	0.27	0.60	122	4.7	0.84	0.60	379	9.6
Total				2018	100			2582	100			3958	100
Air changes per hour at 50 Pa				7.5				9.6				14.7	

Figure 2 Worked Example - Building Layout

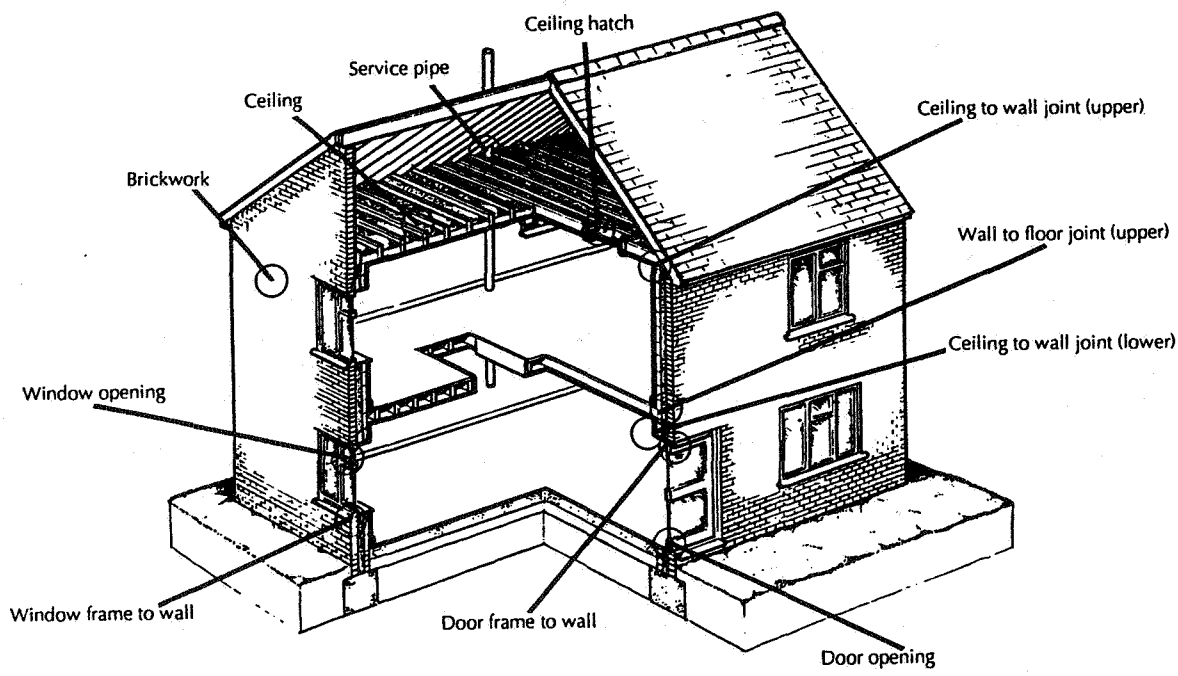

7.1 Construction Information

A two storey building of insulated cavity brick construction has internal floor dimensions of 8 m x 6 m and a ceiling height of 2.8 m on each storey. The ground floor is of solid concrete construction, which is perfectly sealed to the interior brick leaf. The ceilings are of plaster board construction and the interior walls are plastered and painted. The ceiling to wall joints are uncaulked. The floor of the upper storey is of suspended timber construction which only penetrates the inner leaf of each 8 m wall.

Door and window frame to wall joints are uncaulked. The net (internal) building volume approximately equals 269 m^3.

The upper storey ceiling is penetrated by:

(i) a non-weatherstripped roof hatch of dimension 1.0 m x 1.0 m, and

(ii) a service pipe of 200 mm diameter.

Each of the 8 m walls is penetrated by:

(i) a door of dimension 2 m x 1 m on the lower storey,

(ii) a window frame of dimension 1.0 m x 1.5 m on each storey, and

(iii) a window frame of dimension 1.0 m x 1.0 m on each storey.

Each of the 6 m walls is penetrated by a window frame of dimension 1.0 m x 1.0 m on each storey.

All windows and doors are of timber construction with weatherstripped opening sections.

The large window frames each have:

(i) 2 x side hung openers of dimension 1.0 m x 0.5 m, and

(ii) 1 x top hung opener of dimension 0.25 m x 0.5 m.

The small window frames each have:

(i) 1 x side hung opener of dimension 1.0 m x 0.5 m, and

(ii) 1 x top hung opener of dimension 0.25 m x 0.5 m.

Figure 3 Guidance on Interpreting Component Airtightness Distributions

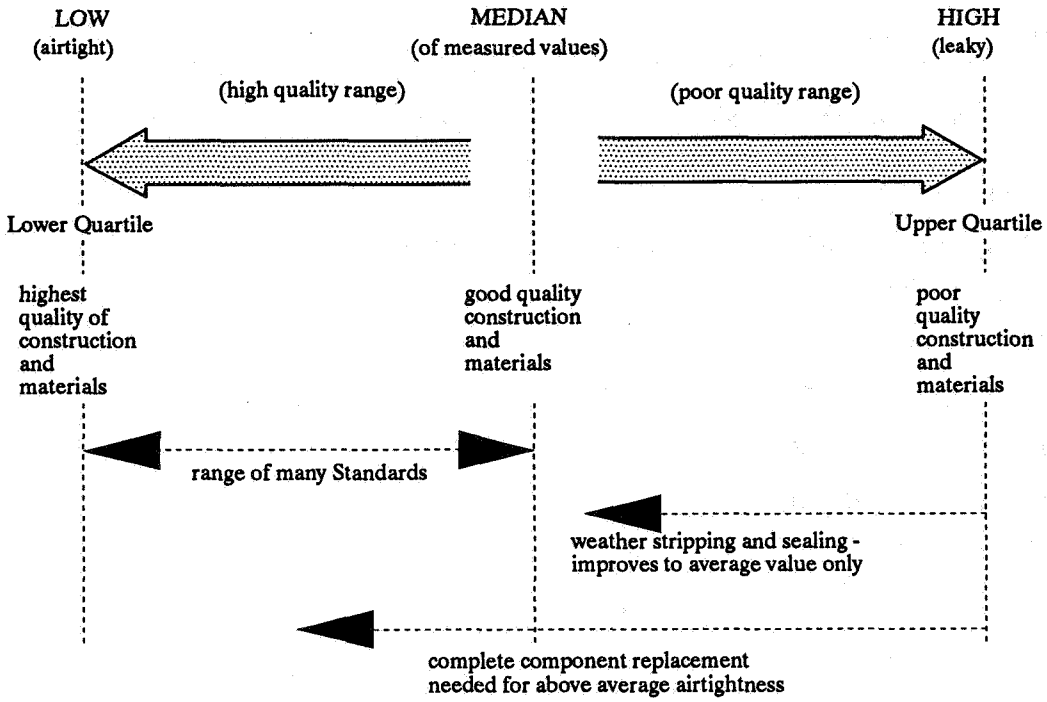

7.2 Selecting Suitable Default Component Leakage Data

Data tables presented in Technical Note 44 (*Orme, Liddament, and Wilson, 1994*) summarise the building component records of the Numerical Database. These tables provided suitable values to describe the construction in the worked example. Figure 3 gives guidance on interpreting the quartile values of the distribution of component flow coefficients, as default leakage data.

7.3 Calculations and Assumptions

The flow coefficient, C, and the flow exponent, n, together with the dimensions of the components have been used to give volume flow rates at 50 Pa pressure difference (noting that the quantities have now been expressed in terms of units $m^3.h^{-1}$). The sum of these flow rates was then divided by the internal building volume to give the airtightness for each of the three standards of construction. A simplification was made by assuming that the inside of the roof space was at the same absolute pressure as the outdoor air.

In practice, a uniform pressure difference throughout is achieved by fully opening all internal doors during pressurisation tests. A discrepancy can occur between the airtightness value measured when a building is pressurised compared to when it is depressurised by the same amount. Pressurisation airtightness and depressurisation airtightness were assumed to be identical for the purposes of this example.

It should be emphasised that the component data contained within the summary tables in Technical Note 44 (*Orme, Liddament, and Wilson, 1994*) have originated from many different countries, where construction techniques sometimes differ. On the other hand, it

was considered that the sample sizes were too low to distinguish between items from these countries.

8. Conclusions

Data are essential for design and model evaluation. An attempt has been made with the Numerical Database to compile data appropriate to infiltration and ventilation studies. These cover the air leakage characteristics of building components, the characteristics of buildings themselves and data on wind pressure distributions.

Component leakage data have been summarised in Technical Note 44 (*Orme, Liddament, and Wilson, 1994*), in terms of median values with upper and lower quartiles and their appropriate usage. Additionally, this Technical Note also presents whole building data in the form of graphs and as a series of data sheets for generic types of building construction.

It is essential that measurement data collected during individual tests should be compiled since, collectively, they may be used to identify trends in the performance of construction techniques. Much more can be accomplished in producing information about the leakage performance of the existing building stock by analysing the key structural components and the corresponding air leakage performance of measured buildings.

Further information on wind pressure coefficients are needed to accommodate a wider range of building shapes. These would enable basic design calculations to be accomplished without the need for excessive modelling or expensive wind tunnel exercises.

9. Acknowledgements

Valuable assistance and data were given to the AIVC by numerous individuals and research organisations during the preparation of the Numerical Database. Contributors are listed in the analytical review of the Database (*Orme, Liddament, and Wilson, 1994*).

10. References

1) LIMB, M.J.
"Ventilation and Building Airtightness: an International Comparison of Standards, Codes of Practice and Regulations"
Air Infiltration and Ventilation Centre Technical Note 43, February 1994.

2) ORME, M.S., LIDDAMENT, M.W. and WILSON, A.J.
"An Analysis and Data Summary of the AIVC's Numerical Database"
Air Infiltration and Ventilation Centre Technical Note 44, March 1994.

3) ORME, M.S. and LIMB, M.J.
"Numerical Database User Guide *Idealist for DOS format*"
Air Infiltration and Ventilation Centre, 1994.

The Role of Ventilation
15th AIVC Conference, Buxton, Great Britain
27-30 September 1994

Air Movement Studies in a Large Parish Church Building

I C Ward, F Wang

Building Science Research Unit, School of Architectural Studies, The University of Sheffield S10 2UJ

ABSTRACT

This paper presents a trial of applying a CFD package into an air movement study in an old English church. The possibility of adopting computational modelling in a complex shaped building has highlighted the problem encountered due to the large difference in scale between thermal elements and building enclosure. The results have demonstrated that there are still significant problems to be overcome in using CFD models in such situations.

1. INTRODUCTION

For several years there has existed thermal and ventilation problems in old English Parish Churches. Unsuitable heating systems and cold air currents experienced in these buildings are regarded as being the two main problem areas which result in uncomfortable internal thermal conditions being experienced by the occupants [1]

Solutions to these problems have not yet been fully established partly due to a lack of financial support and also to the difficulty of applying new technology to buildings of historical value. Mainly because of the second reason it is important to understand the air flows and temperature patterns prevailing in such buildings and to investigate a range of solutions using computing tools prior to installing new system systems or altering the building fabric.

This study into the air movement patterns found in an old English Parish Church, is an attempt to understand the problems faced by such buildings and to develop a CFD Model which is capable of dealing with them.

The CFD software chosen was FLOVENT as this particular model was specifically designed to deal with buildings.[2] FLOVENT is a commercially available programme and it is not intended in this paper to deal in detail with the theory behind the model. Issues regarding setting up the building will be explained in the following sections.

2 SPECIFYING THE PROBLEM

The building being modelled is the Parish Church in Dronfield Derbyshire which was founded in 1135 AD. This Church is unusual in that it has a large Chancel compared to the Nave. From the modelling standpoint, the interior of the church can be divided into two spaces connected by an arch 6 metres high. The Chancel has an area of 145m^2 with a pitched roof 14 m high. The other main space consists of the Nave, South Aisle and North Aisle. The highest point of the Nave roof is 11.5 metres. The aisles have shallow pitch lean-to roofs which are 6 metres high on average. There is no apparent thermal insulation anywhere on the roofs. The stone external walls have a thickness of 0.3 m . Except for six upper clerestory windows, all other windows are 1.2 m in width and 3.6m in height, the largest is in the east end of Chancel which is 5.5m wide and about 8.9m high. The heating system is a single pipe radiator system using cast iron pipes. A schematic layout of the church is shown in Fgure 1.

2.1 SETTING THE GRID

As it was intended to simulate the building operating under the influence of wind pressure, it was necessary to include in the grid structure the small cracks around the windows.[3] This meant that the grid structure had to be very fine at specific points, which resulted in the body of the church having a mixture of fine and course grids.

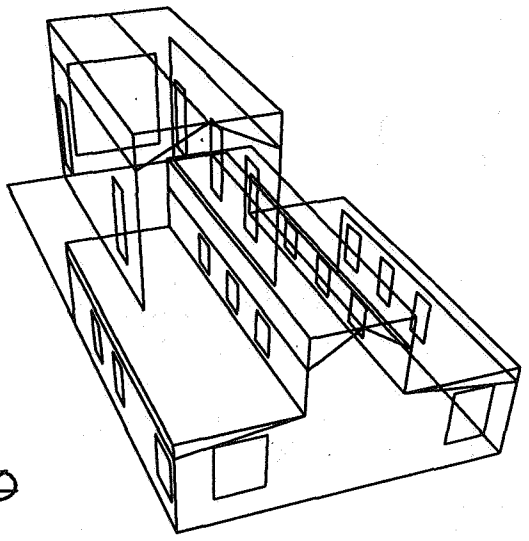

Figure. 1 The Final Model of the Church

The 3D grid structure used to simulate the performance of the Church had some 104,448 cells which took a significant amount of time to reach convergence. The finer the grid structure the greater the accuracy in establishing the temperature and flow fields. This is also true of the boundary conditions which require a fine mesh to give accurate solutions.

2.1.1 Grid Sizes

In order to investigate the effect of grid size on the accuracy of the solution three grid systems varying cell sizes were used in a 2D model of part of the Church. The section chosen included a radiator and a window. The cell sizes in the three grid systems used were $2.00*10^{-2}m^2$, $1.33*10^{-2}m^2$ and $1.00*10^{-2}m^2$

Figure 2 shows the results of the analysis for mesh size $1.33*10^{-2}m^2$ and $1.00*10^{-2}m^2$. It can be clearly seen that with the fine mesh size a more accurate solution can be found . The small grid size allows a more accurate solution of the convective heat transfer at the radiator surface to be achieved[4].

Figure 3, which shows the effect of grid size on the air velocity also indicates that a fine mesh size appears more accurate.

3. RESULTS OF THE FULL ANALYSIS

3.1 THE EFFECT OF WIND SPEED

The 2D model of the building was simulated for two different wind speeds, 2 and 4 m/s in order to establish the likely temperature and flow patterns. The wind direction used was the prevailing direction (south west). The cracks around the windows were simulated by openings with very small value of FAR (free area ratio) within FLOVENT. For a solution to be reached it was necessary to convert the wind speed into an equivalent pressure drop across the openings.

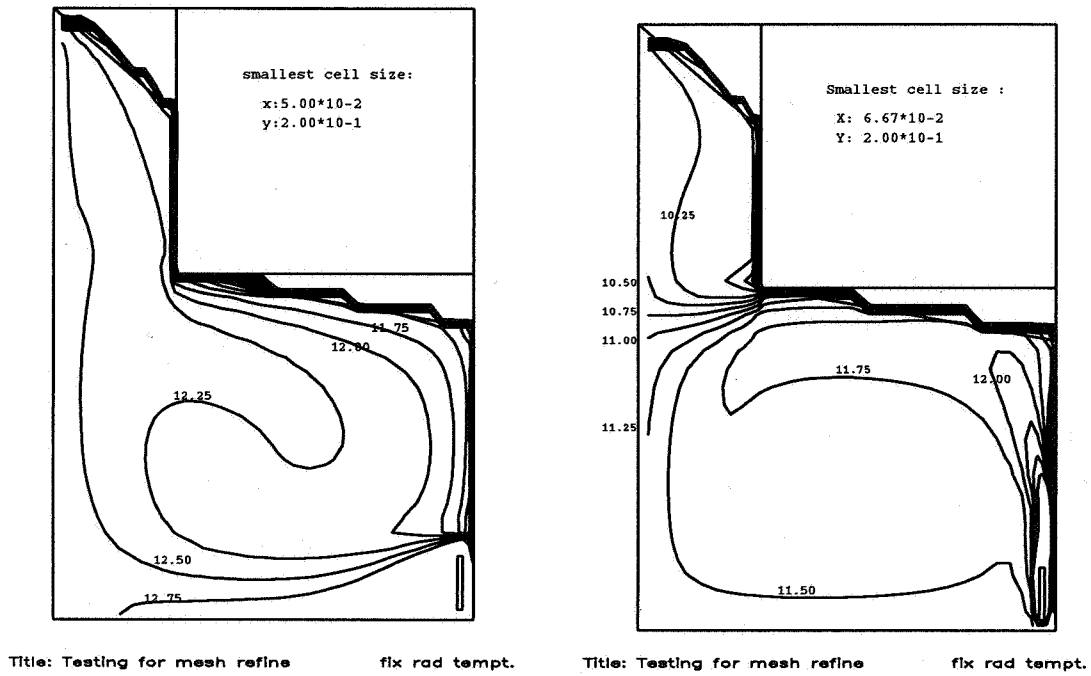

Figure. 2 Solutions of temperature field in 2D half-section from two different grid system
a) Temperature contour using medium size cells b) Temperature contour using fine grid.

Table 1 shows the results of this analysis. It can be clearly seen that as the wind speed increases the air flows across the window increased which was consistent with what would be expected.

Crack location	ΔP=0.48	ΔP=1.92	ΔP=4(lower), 8(upper)*
Upper right	$-2.3*10^{-3}$ / 8.3	$4.8*10^{-3}$ / 5.0	$1.2*10^{-2}$ / 5.0
Lower right	$4.7*10^{-3}$ / 5.0	$9.2*10^{-3}$ / 5.0	$1.5*10^{-2}$ / 5.0
Upper left	$-4.9*10^{-3}$ / 8.4	$-7.1*10^{-3}$ / 8.2	$1.3*10^{-2}$ / 8.0
Lower left	$-4.2*10^{-3}$ / 10.8	$9.0*10^{-3}$ / 10.5	$1.4*10^{-2}$ / 10.3 **

* Unit of Pas and WPC are set to different values, hence higher pressure difference value for crack on upper windows.
F.A.R (free area ratio)= 0.002

** Air flow rate(kg /m^2 s) / air temperature (°C)

Table 1 Air Flow Rates and temperature of the air through the cracks when pressure difference varies due to wind speed.

3.2 THE EFFECT OF WIND ON 3D MODEL

3.2.1 Input Parameters

A complete 3D model of the church was set up including all existing windows and radiators. As the flow field is subject to indoor temperature distribution and outdoor infiltration. Two typical cases were simulated to study the field dominated by either infiltration influence due to a high wind speed or buoyancy forces due mainly to free natural convection. For the former condition, the pressure difference across the six upper clerestory windows was set to 8.0 Pa

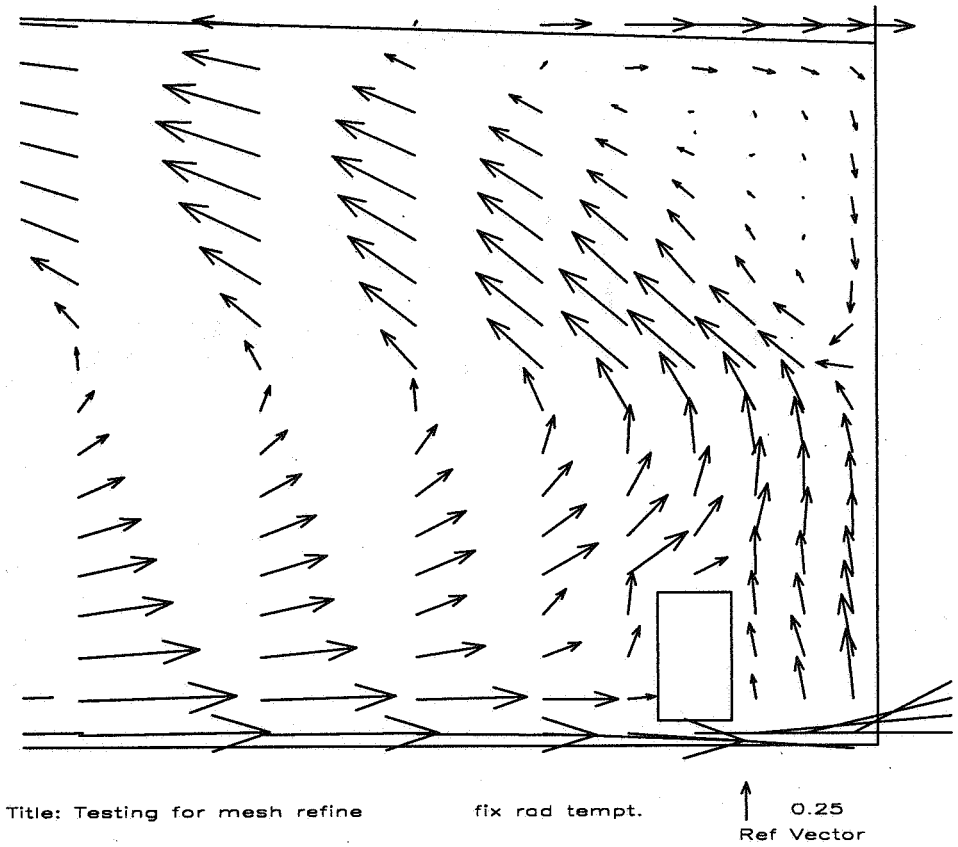

a) Air-movement around radiator, grid system with medium size cell

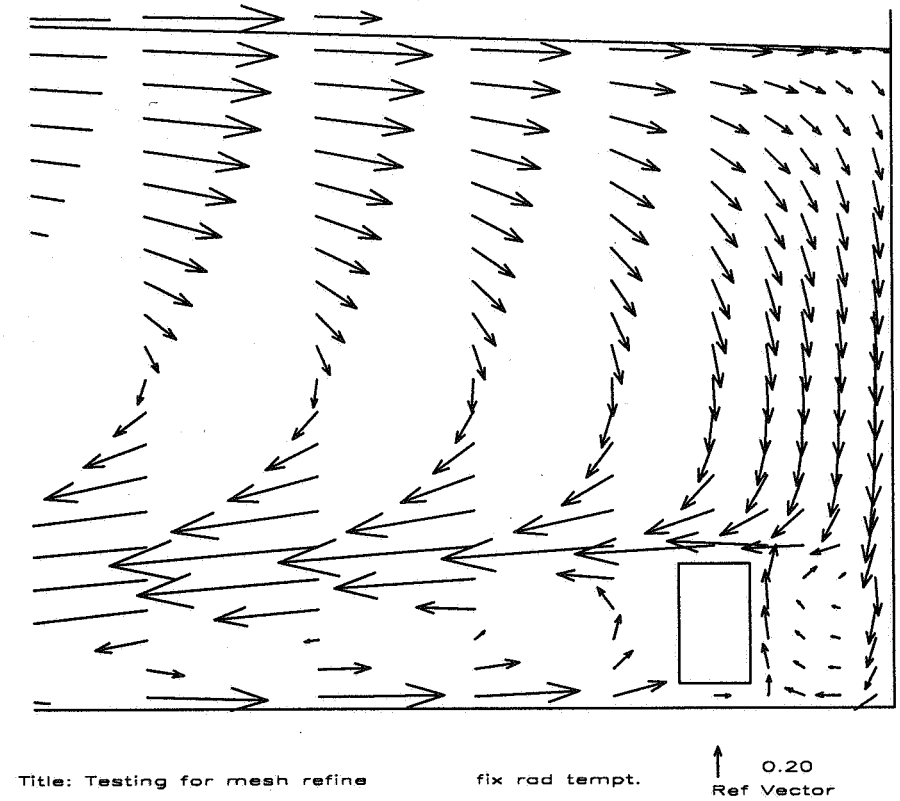

b) details around radiator when finer grid applied

Fig. 3 Solutions of vector field in 2D half-section from two different grid sustem

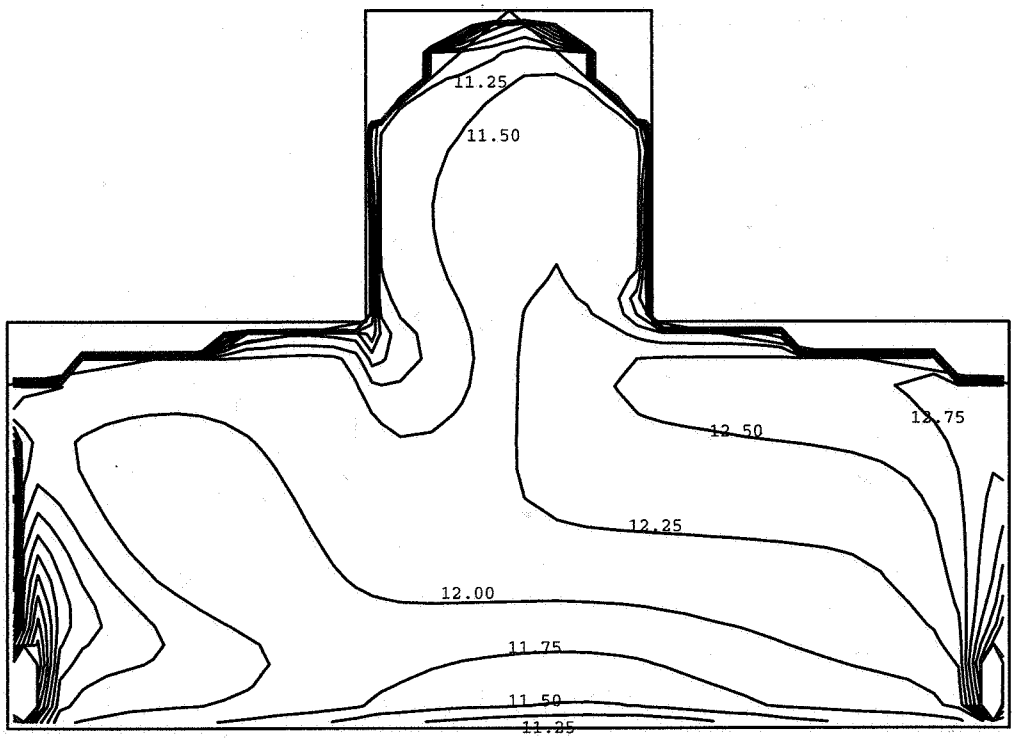

Title: RF U=2; WD U=5.6 DPu=8;DP=4 FAR=0.001

a) Temperature contour

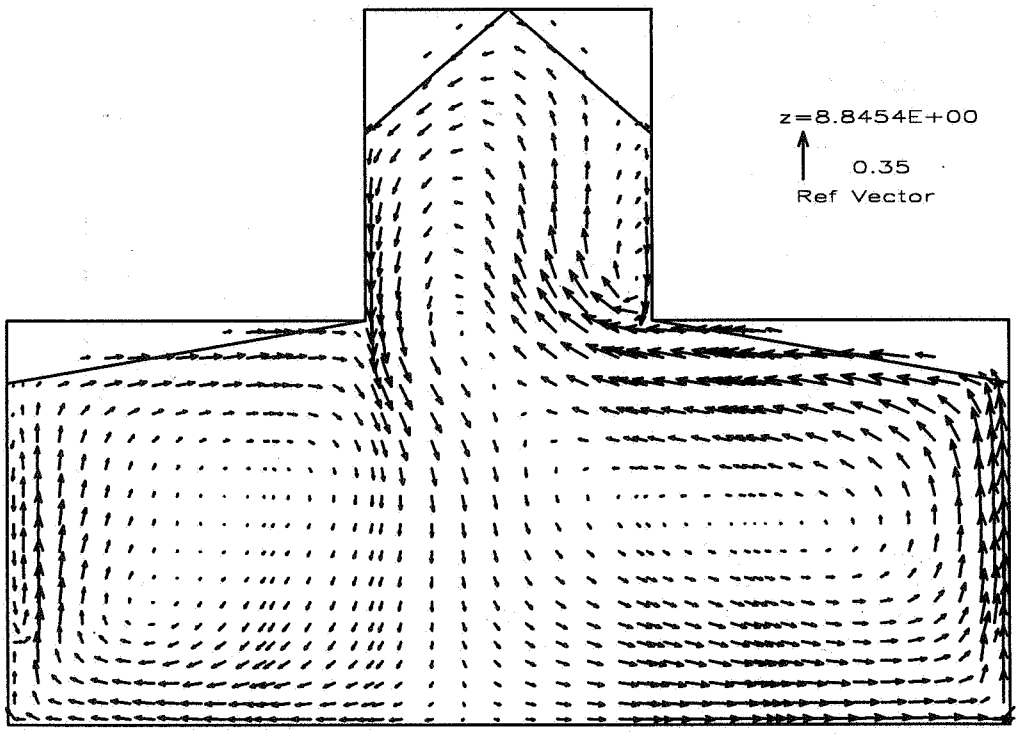

Title: RF U=2; WD U=5.6 DPu=8;DP=4 FAR=0.001

b) Air movement, vector field

Fig. 4 Solutions on plane XY, z=8.5m. A cross section of aisles and nave . Side radiators, windows and upper clerestory windows are included.

and other windows to 4.0 Pa. The wind at speed chosen had a velocity of 2.0m/s. from the south-west:

3.2.2 Results

The calculated temperature is higher in the case when there was less infiltration than when the wind was strong. The average difference in temperature at the monitor points was 0.3°C. Table 2, shows air flow rates through cracks and their temperature under the two condition. Although the buoyancy effects always exist, infiltration due to wind pressure will become a more important factor which affects both temperature and velocity.

	Crack location	Buoyancy Dom. Air flow $*10^{-3}$ kg/s	Temp. °C	Wind Pres. Dom. Air flow $*10^{-3}$ kg/s	Temp °C
1	S. lower	4.60	11.2	-11.37	5.0
2	S. upper	4.20	11.5	-7.36	5.0
3	N. upper	5.35	11.8	9.74	11.6
4	N. lower	8.46	12.6	14.20	12.4
5	west window	13.17	12.3	-30.83	5.0
6	East wd	68.33	10.0	122.11	9.83
7	S. of Chancel	11.84	9.6	-21.89	5.0
8	N. of Chancel	18.82	9.7	29.99	9.5

1,2,3 & 4 on Plane XY, Z= 8.5m. 7,8 on plane XY, Z= 22m

Table 2 **Mass flow across cracks driven by the force dominated by natural convection and by natural convection and infiltration caused by wind pressure together. Air flow in(+) and out(-) of cracks and its temperature.**

Figures 4 and 5 shows both the temperature and velocity field in two cross sections including side and clerestory windows and radiators. It can be easily seen that the air near to the window on the left side was cooled by infiltration. The radiator underneath the window creates an up-draught which improves the temperature at ground level. Unfortunately in the real church not all windows have radiators installed underneath, thus unpleasant cold draughts are inevitable in winter. There is also flows from the Chancel to Nave at low level (which has been noted in the church)

4 CONCLUSION AND FURTHER WORK

The trial mentioned above has shown that installing radiators right under the windows is more likely to solve the problem of cold down-draught in winter, consequently improving the indoor thermal environment. The promising result indicates that further research and development in the area of thermal remedial measures for old buildings by computer simulation is worthwhile.

The most interesting point to be gained from the work is to improve the software's grid generating function. Although it is possible to establish a uneven mesh in calculation domain with FLOVENT, all grid lines dividing the domain into cells are required to extend across the whole solution domain (Figure. 6a-b). This grid system is quite capable in dealing with most

common problems such as rooms in offices, hotels and houses where there is simple enclosure and not significant difference in scale due to heat emitters and other elements.

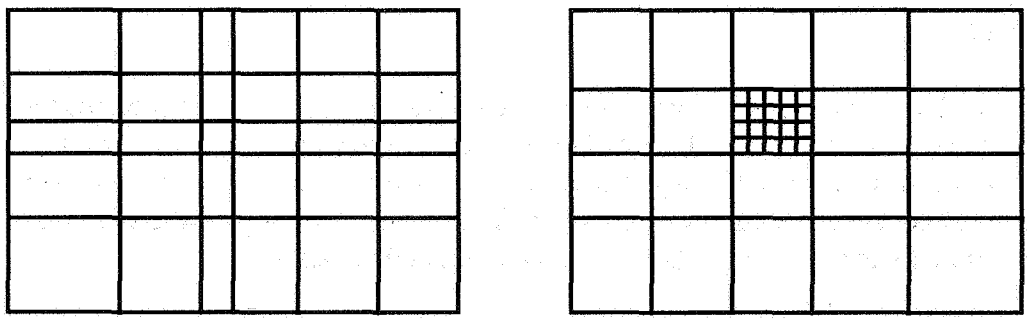

Figure .6 a) Grid in Domain of FLOVENT b) Grid in Local Grid-refinement System

However, for large enclosures such as described above a finer mesh is necessary for accurate flow and natural convection calculations. To avoid generating too many cells to solve within a tolerant time period, two alternatives for conventional single-grid system have been studied in, Grid Patching and the Local Grid Refinement Method. The main idea behind the methods is that the whole domain can be divided into several sub domains where grids with different sizes can be adapted according to the either object's size or Rayleigh number in the area. Finer grids can result in more accurate solution and reveal more flow details in the sub domain while coarse grids given to other area save calculating time[5]. These method benefit such problems when an irregular shape is involved and spaces are required to represent outdoor ambient environment. If one of the above methods were to be applied to FLOVENT, then the program way be more versatile and powerful.

Acknowledgement. The authors wish to thank Mr. M. Broady for his prompt help on computing and Ivor Capsey and Paul Rose, Flomerics Support for their helpful advice and information. The help of Garry Palmer and others in Building Science Unit are acknowledged. The financial support for one of the authors from Sino-British Friendship Scholarship Scheme is gratefully acknowledged.

Reference

1 Bemrose C R, Smith I E, Thermal Stratification In Intermittently Heated Heavyweight Buildings, *Building Serv. Eng. Res. Technol.* 13(3) 119-131 (1992)

2 FLOMERICS, *FLOVENT User's Guide for software version 1.3,ppv.*

3 Gosman A D, Nielson P V, Restivo A and Whitelaw J H The flow properties of rooms with small ventilation openings *Journal of Fluids Engineering* **102** 316-323 (1980).

4 Bejan A, *Convection Heat Transfer,* John Wiley & Sons New York (1984)

5 Li Y, Holmberg S, Paprochi A, Tang Y-Q, Simulation Of Room Flows With Small Ventilation Openings By A Local Grid-refinement Technique, *Building Serv. Eng. Res. Technol.* **15**(1)1-10 (1993).

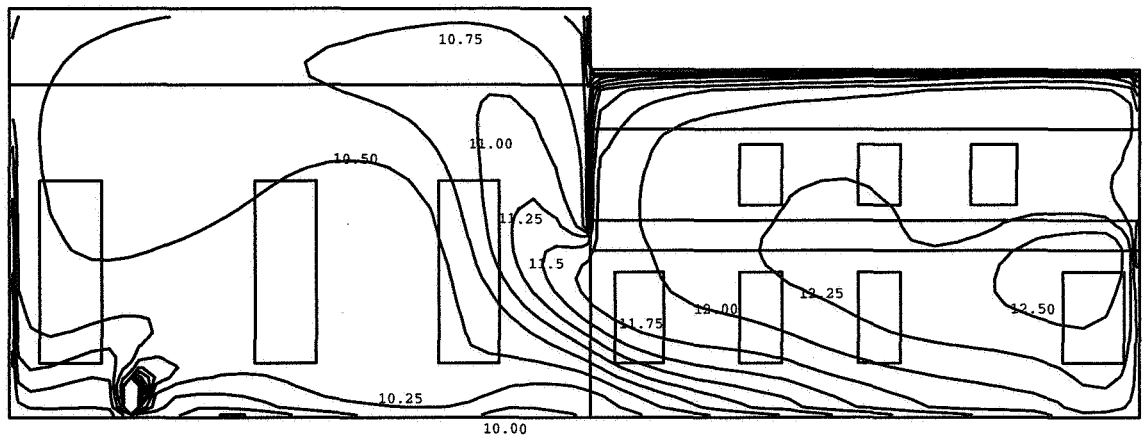

7 Title: RF U=2; WD U=5.6 DPu=8;DP=4 FAR=0.001

a) Temperature contour

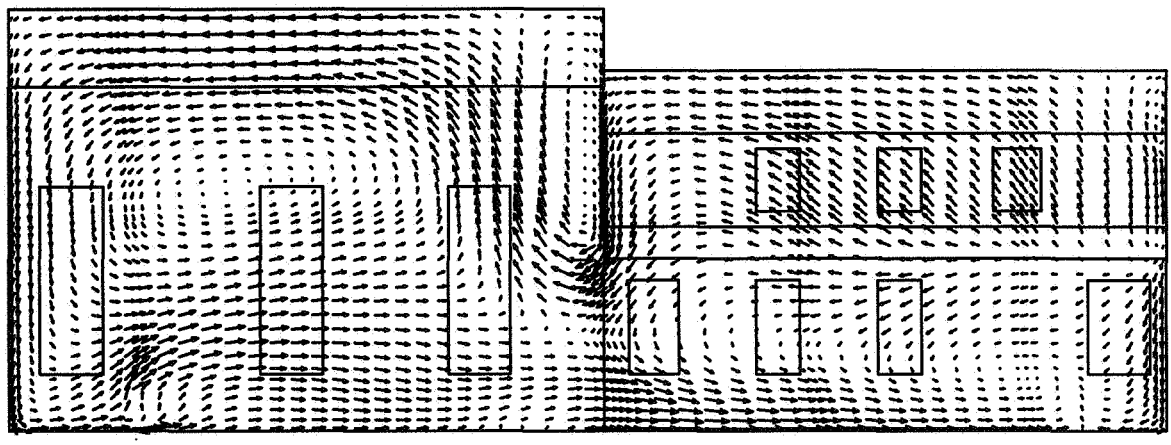

Title: RF U=2; WD U=5.6 DPu=8;DP=4 FAR=0.001 0.35 Ref Vector

b) Air movement.

Fig. 5, Solutions on the plane YX, X=8.0m, the central sector paralle to the symmetric axial.

The Role of Ventilation
15th AIVC Conference, Buxton, Great Britain
27-30 September 1994

Particle-Streak-Velocimetry for Room Air Flows

F. Scholzen, A Moser, P Suter

Energy Systems Laboratory, Swiss Federal Institute of Technology Zurich, CH 8092 Zurich, Switzerland

Synopsis

This paper presents a measurement technique to perform quantitative visualization of room air flows. The visualization is done by discrete particles, namely helium-filled soap bubbles, illuminated in a plane light sheet generated by a point light source in combination with a special lens. The recording is done stereoscopically with 3 standard cameras by streak photography. The scanned negatives are analysed digitally.
The method is able to give the three-dimensional instantaneous velocity field of room air movements, also in real-scale.

Introduction

The aim of the presented work is to realise a measurement technique for performing quantitative flow visualisation of room air flow patterns, in laboratory rooms as well as in field studies. Solid tracers, here helium-filled soap bubbles, are added to the flow and transported with the air streams. Supposing the tracer's movement to be identical to the one of the ambient air, a whole velocity vector field can be extracted at one instant by recording the tracer trajectories on photographic film.

1. Experimental Technique

1. 1. Method

The air stream together with the tracer particles is photographed using relatively long exposure times. This results in thin elongated streaks on the negative, see Fig. 1 & 2.

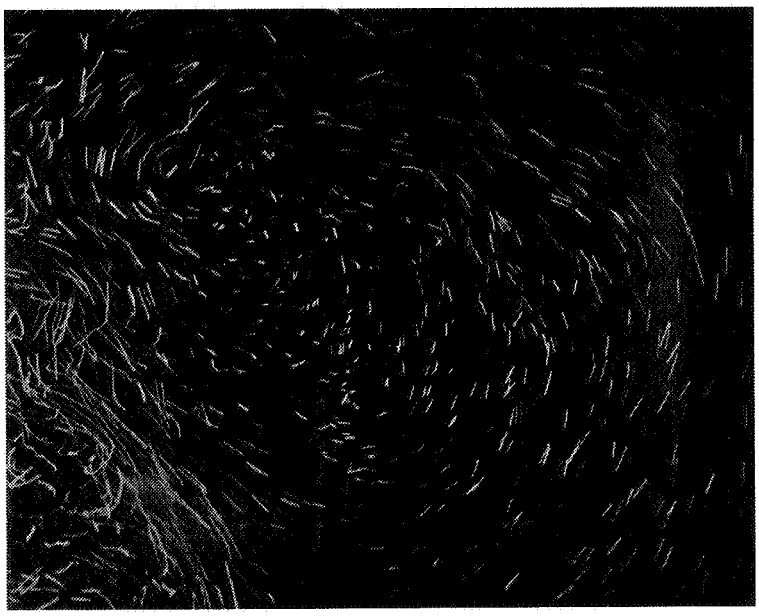

Fig. 1 : example of tracer streaks; a vortex in a room, 1.0 x 0.8 m extract of an image covering 2.5 x 1.7 m

Assuming that during the exposure the velocity vector of the particle is constant, the instantaneous velocity can be regarded as the ratio of length to exposure time.
As with this simple principle neither the third velocity component nor the direction of the flow can be extracted, the photographic set-up is extended to three cameras (see sect. 1.3 & 3.5)

1.2. Lighting

A halogen metal vapour arc lamp (250 W) in combination with a special biconvex, cylindrical lens, is used to generate a planar light sheet of a constant thickness of 12 cm. Just the bubbles situated in the light sheet are visible on the film. The lamp is air-cooled to avoid disturbance of the air flow situation by this heat source.

1.3. Photographic technique

Standard reflex cameras (36 x 24 mm) are used, with black and white film (3200 ASA).
The use of standard non-metric cameras instead of special metric cameras for this photogrammetric investigations reduces the cost of the set-up while requiring more computational calibration effort to give adequate results.
To reconstruct the three-dimensional coordinates out of two-dimensional images, at least two simultaneous recordings are necessary. But the information on the flow direction cannot be extracted out of two views of a (non chopped) particle trajectory since the order in time is lost on the photographic film.
To solve this directional ambiguity, a third image is recorded with another camera. This third camera is triggered simultaneously with the two others. But the exposure time is different, so that the streaks on that film have just one of their two endpoints in common with the recordings of the cameras right and left. This common end point correspond to the beginning of the recorded movement.

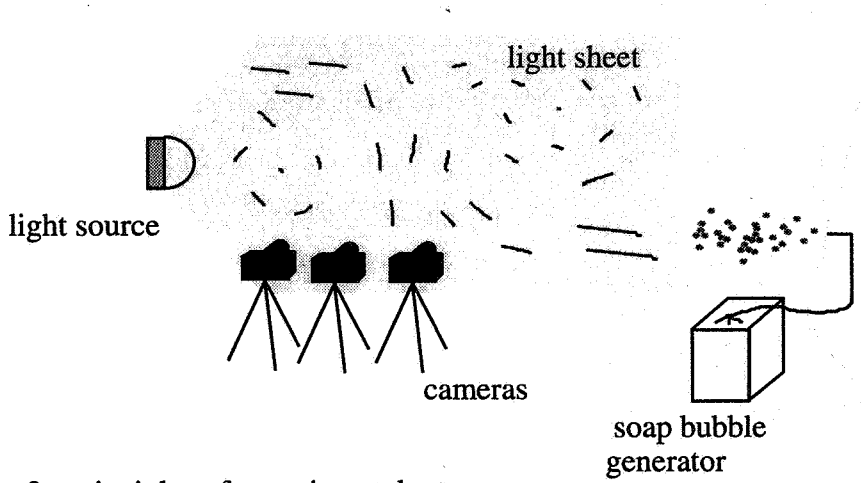

Fig 2 : principles of experimental set-up

2. Image digitization and pre-processing

The negatives are digitized using a slide scanner connected to a Macintosh Computer. The resolution is about 1000 dpi, giving a 1520 x 1024 pixel, 256 greyscales image out of a 36 x 24 mm negative.

The resulting digital images are analysed separately. Depending on the specific scene, digital enhancement of the images is necessary. So a high-pass filter is used to eliminate uneven illumination of the measurement zone.
The segmentation (separation of image information, namely the particle streaks, and image background) is done by applying a single threshold to the filtered image.
On the resulting binary image, all objects are analysed to determine their position, size, length, width and orientation. Only possible particle streaks, namely long and slender objects are retained and the coordinates of their endpoints are calculated.
At this stage, still many objects survive that do not represent a particle movement but are due to light reflections or any kind of background objects.
These 'wrong streaks' are eliminated in a later stage by the combined analysis of the three pictures.

3. Stereophotogrammetric Analysis

3.1. Basics

The ideal photographic recording is a central projection which transforms an object point P (X,Y,Z) to its image point p' (x', y'), as shown in Fig. 3. The mathematical description is given by the collinearity equations :

$$x' = -c\frac{a_{11}(X-X_0)+a_{12}(Y-Y_0)+a_{13}(Z-Z_0)}{a_{31}(X-X_0)+a_{32}(Y-Y_0)+a_{33}(Z-Z_0)}$$

$$y' = -c\frac{a_{21}(X-X_0)+a_{22}(Y-Y_0)+a_{23}(Z-Z_0)}{a_{31}(X-X_0)+a_{32}(Y-Y_0)+a_{33}(Z-Z_0)} \qquad (1)$$

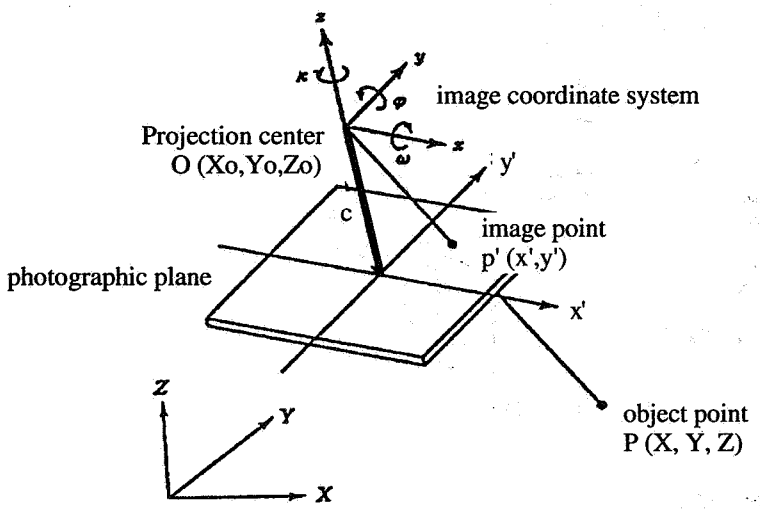

Fig. 3 : photographic recording

For a more accurate modelling several terms have to be added to this equation. Lens distortion effects and an offset (x_h, y_h) of the principle image point (intersection point of the optical axis and the image plane) compared to the image coordinate system are considered by extending the collinearity equations to :

$$x = x_h + x' + \Delta x \qquad y = y_h + y' + \Delta y \qquad (2)$$

In the present work a two-parameter lens distortion model is used to correct for radial-symmetric distortion (see also [Brown], [Wolf], [Maas]):

$$\Delta x = x' (k_1 r'^2 + k_2 r'^4) \qquad \Delta y = y' (k_1 r'^2 + k_2 r'^4) \qquad (3)$$
$$r'^2 = x'^2 + y'^2$$

x,y	image coordinates
x',y'	image coordinates without lens distortion and offset correction
X,Y,Z	global coordinates
X_0, Y_0, Z_0	global coordinates of the projection centre
c	image distance (distance projection centre to film plane)
a_{ij}	coefficients of the rotational matrix (functions of ω, ϕ and κ)
x_h, y_h	image coordinates of the principal point
Δx, Δy	lens distortion terms

3.2. Calibration

Due to the unknown exact orientation (Xo,Yo,Zo, ω, ϕ κ) of the camera, of the film in the camera (c,x_h,y_h), as well as of the unknown lens distortion parameters (k_1, k_2), a calibration is necessary for each recording ("photo-variant").
The "on-the-job" calibration consists in recording object points of known position (X,Y,Z), finding their image coordinates (x,y), and calculating all unknown parameters by combining equations (1), (2) and (3) . Due to the non-linearity of these equations, an iterative solution is necessary.
A set of 44 light-emitting diodes is placed in the room to serve as calibration points.

3.3. Stereo-pair matching

To perform the calculation of the three room coordinates of any point of a particle trace, first the matching between the extracted traces in the right and in the left picture has to be done.
The matching is done just considering the geometric set-up of the cameras. Having the image of the trace in the first picture, all possible locations of the trace image in the second picture can be calculated. Each trace in the second picture fulfilling this geometric condition is considered to be a possible partner.

3.4. Calculation of the 3D coordinates.

Having the information for each endpoint of a trace in both pictures the three-dimensional location (X,Y,Z) of that point in room coordinates can be reconstructed by equations (1), (2),(3).
The particle trajectory is now known by the three coordinates of its two endpoints. Knowing the used exposure time, one can calculate the three velocity components.
But the positive direction of this velocity vector cannot be extracted by having just two views of the whole streak. For this purpose, the image of the third camera is used.

3.5. Solving the directional ambiguity

The particle traces, reconstructed from the pictures of the left and the right cameras, as described in 3.4, are projected virtually into the third image. In this step the calculated calibration parameters of that camera are used. These virtual traces correspond to a different exposure time as used for the third image. All three images having been triggered simultaneously, one of the endpoints of this virtual trace will correspond with one of the endpoints of the real trace in image 3, the other will not. This common endpoint is the starting point of the movement.

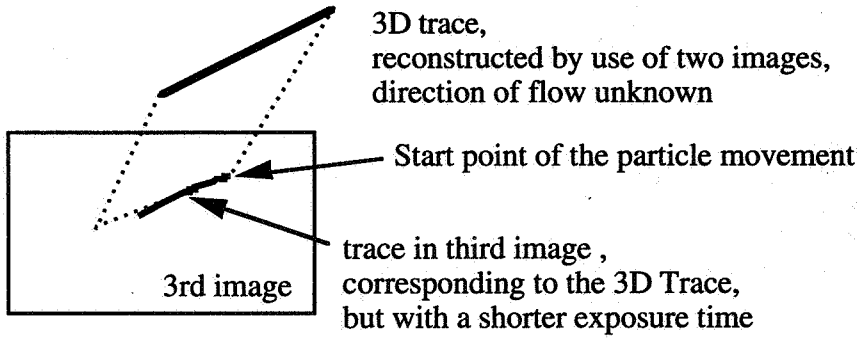

Fig. 4 : elimination of the directional ambiguity; in the example shown, the flow would be from upper right to lower left. Traces start at their right ends.

4. Interpolation

The scattered data can be interpolated to any point within the surveyed domain. Based on [Shepard], a two-dimensional interpolation function is used to interpolate independently the u,v, and w components of the velocity vectors. Due to the small extent in Z direction (the light sheet is just 12 cm thick, compared to X and Y extensions of several meters) the variations of u,v and w in Z direction are neglected and all vectors are transposed to the middle Z-plane.
To improve the interpolation, it is useful to add known boundary velocities to the measurement data, as for example the zero velocity at fixed walls.

5. Example

5.1. Set-Up

The following situation has been set up to test the presented method:

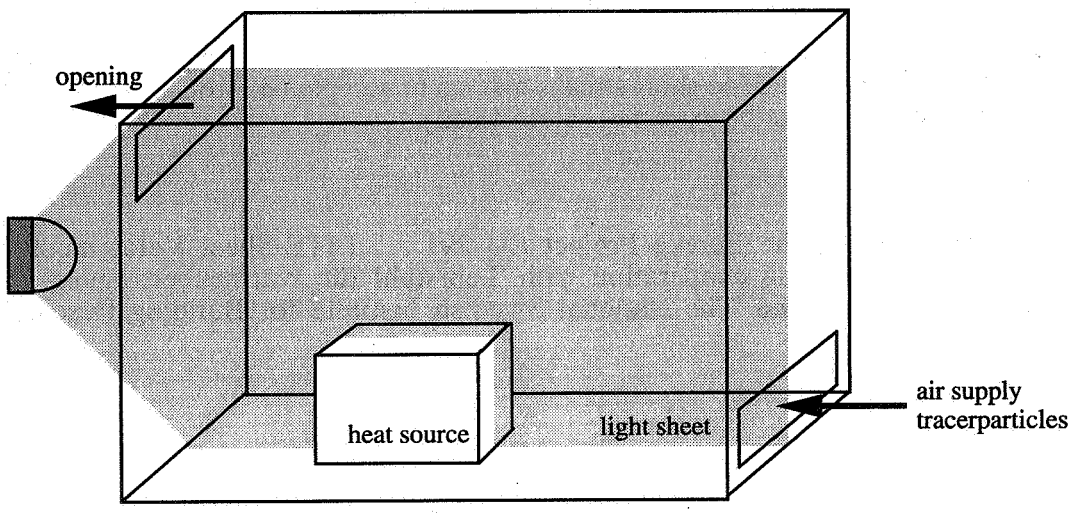

Fig. 5: test situation: heat source 300 W, overall dimensions 2.4 x 1.7 x 1.2 m

The frontside and the left side of the test room are made of glass to permit the optical access for the cameras and for the light sheet.

5.2. Results

Figures A1.1 to A1.3 show the digized images for one set of three pictures. The exposure time is 0.25 seconds for the right and the left cameras and 0.176 for the middle one.

Figure A2 shows the velocity vectors extracted out of this set. The (grey) colour scale illustrates the third velocity component w.

The flow field shown in the previous figure is completed by additional vectors (Fig. A3). These vectors result from a supplementary analysis focused on the inlet. The exposure times (0.06, 0.06 and 0.03 sec.) were shorter, better suited to the higher velocities near the inlet.

Figure A4 shows the interpolated velocity field. The interpolation is based on the data of Fig. A3 and on boundary data.

6. Conclusions

Digital stereophotogrammetric particle streak velocimetry is possible for room air flows.

It combines flow visualization and quantitative measurements. The area that can be analysed within one measurement covers several square meters and can be further extended by a suitable

combination of the parameters light (increasing intensity, minimizing reflections) , tracer (size, light scattering properties) and image resolution.

For the analysis, the necessary image filtering and segmentation steps (sect. 2) depend on the lighting conditions. For complex flow situations or bad lighting conditions special appropriate image processing algorithms or more user interaction may be necessary.
The three-dimensional photogrammetric analysis (sect. 3) works correctly for all situations.

The dynamic range (ratio of the highest to the lowest measurable velocity within one recording) is expected to be of the order of ten. Too short streaks give an unacceptable error, while too long streaks do not reflect enough light to be extracted automatically.

Acknowledgements

The presented work is part of the Eureka Project EU 291 : " LITE-Sheet Velocimeter ", supported by KWF Nr. 2577.1, in cooperation with 'Lehrstuhl für Wärmeübertragung und Klimatechnik, RWTH Aachen' and 'The National Swedish Institute for Building Research, Gävle, Sweden'.

References

Brown D.
Close-Range Camera Calibration,
Photogrammetric Engineering, Vol. 37, No. 8, pp 855 - 866 , 1971

Maas H.G.
Digitale Photogrammetrie in der dreidimensionalen Strömungsmesstechnik,
Institut für Geodäsie und Photogrammetrie, ETH Zürich, Mitteilungen Nr. 50,
1992

Wolf Paul R.
Elements of Photogrammetry, Ed. 2
Mc Graw - Hill, New York, 1983

Shepard, D.
A two dimensional interpolation function for irregularly-spaced data
23 rd ACM Nat. Conf. Proceed., 1968, pp 517 - 524.

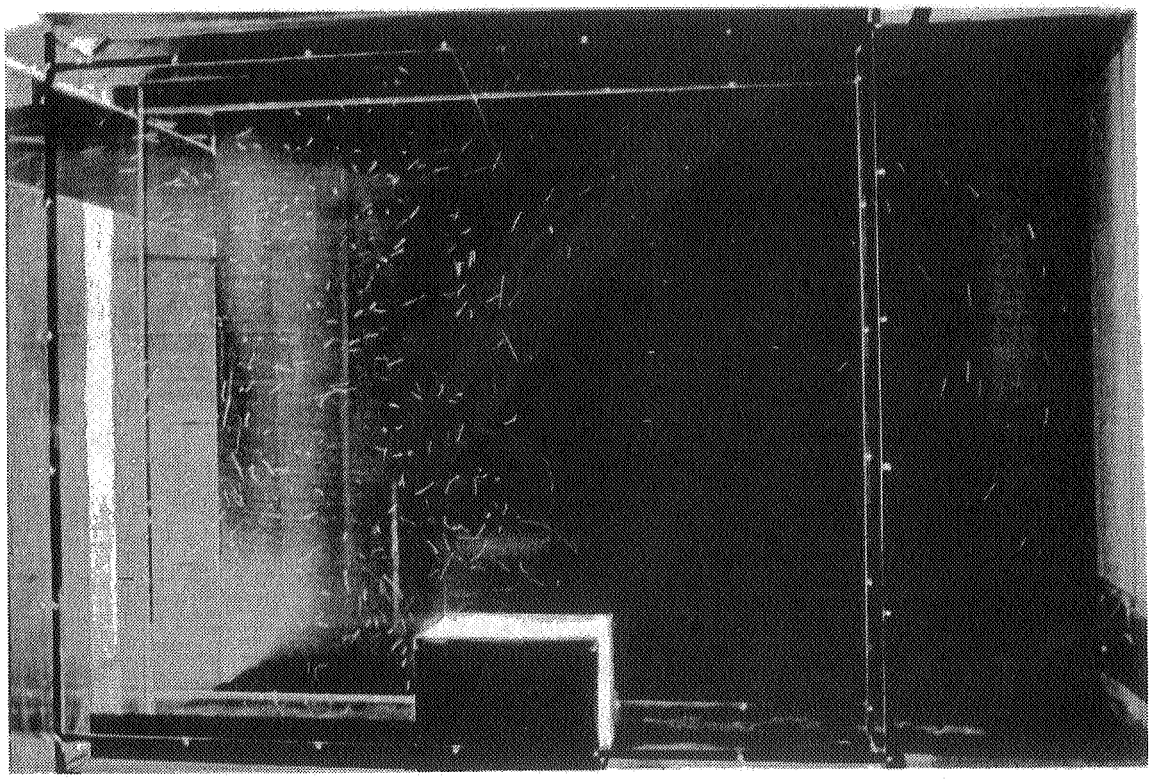

Fig. A1.1 Image of the right camera

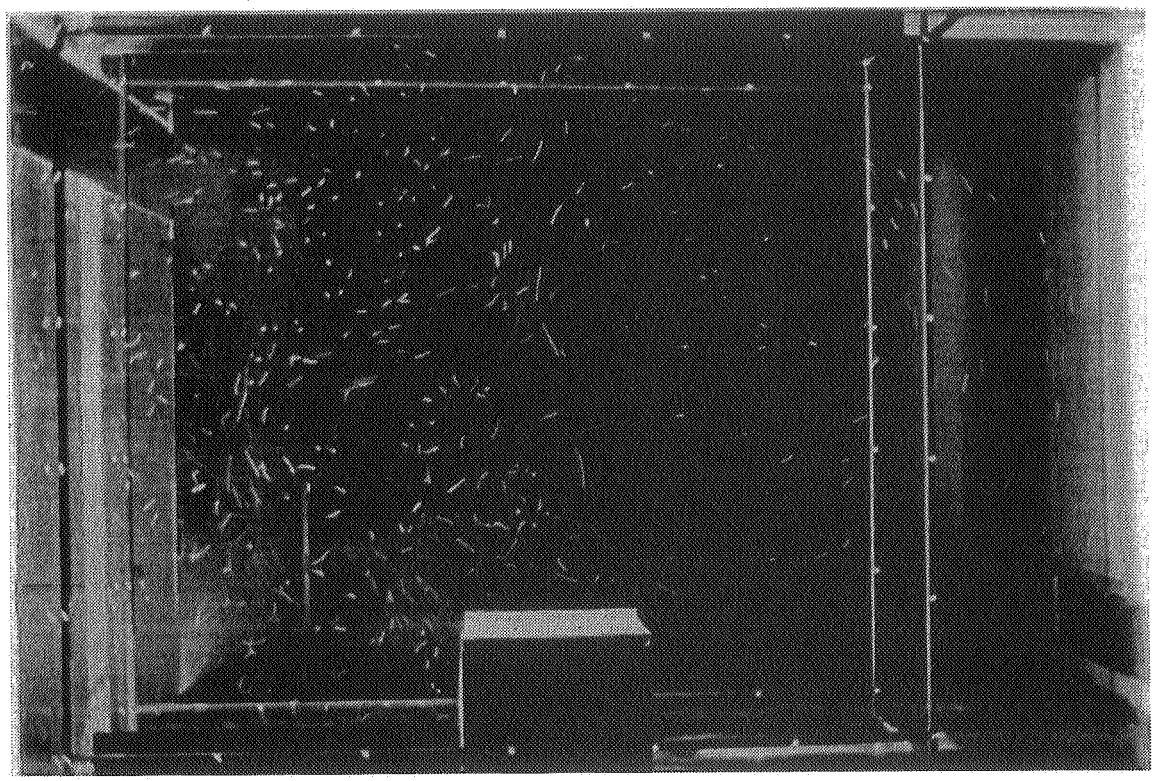

Fig. A1.2 Image of the left camera

Fig. A1.1 - A1.3 Set of three digital images :
exposure times (0.25, 0.25 and 0.18 seconds)

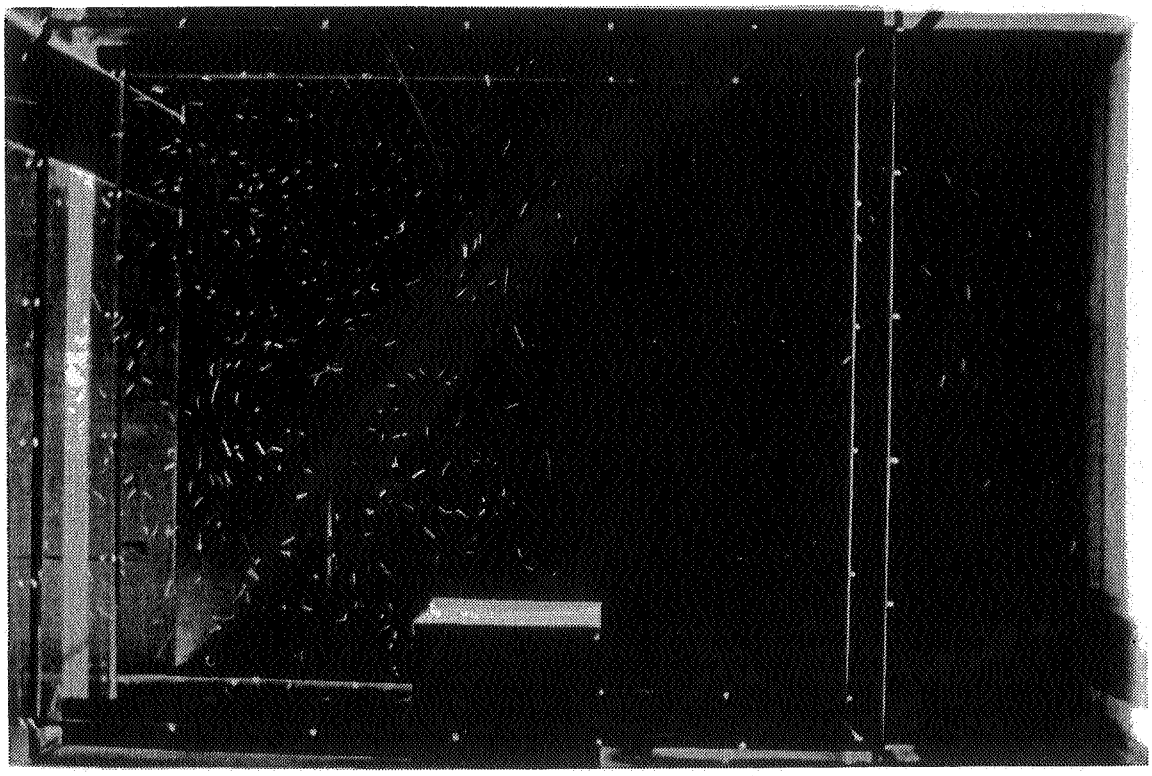

Fig. A1.3 Image of the middle camera

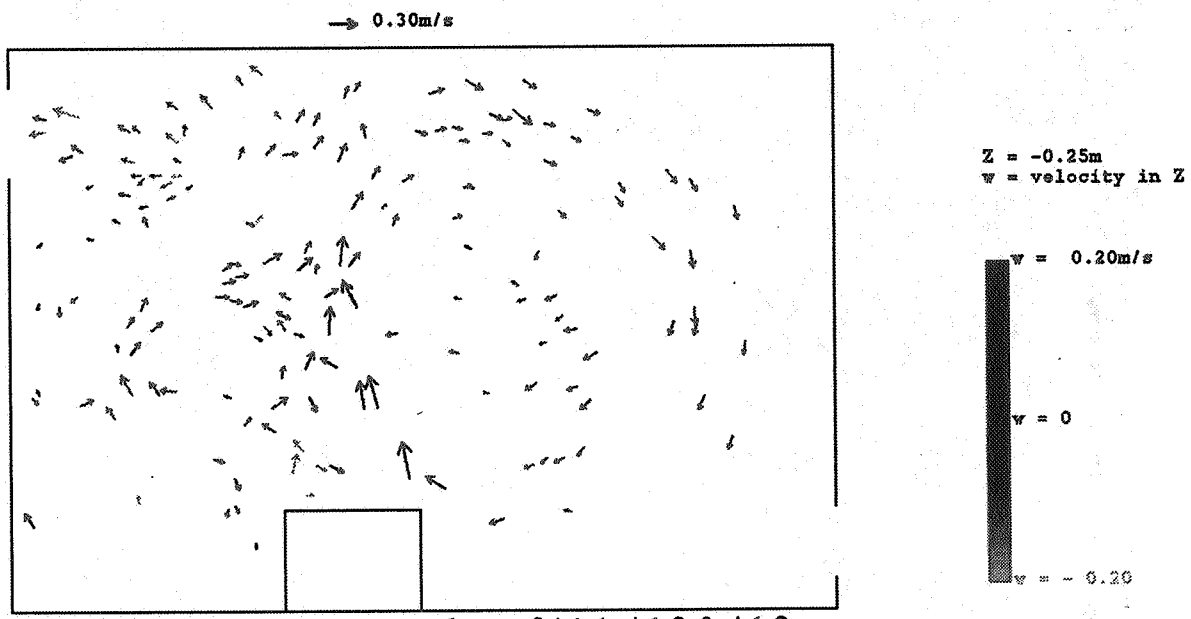

Fig. A2 Velocity vectors extracted out of A1.1, A1.2 & A1.3

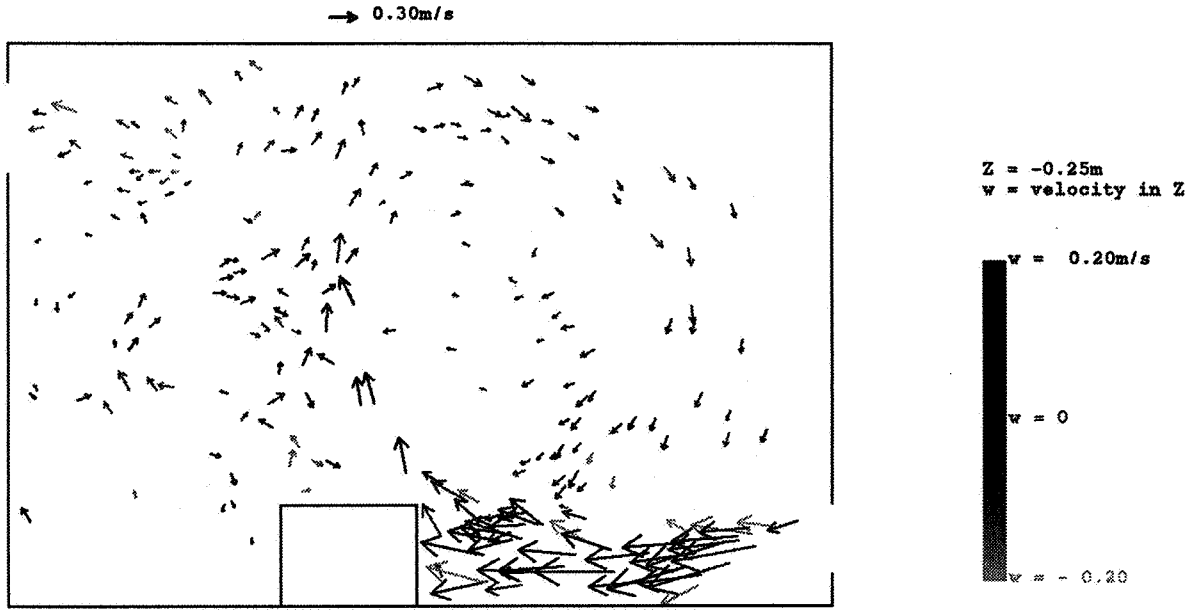

Fig. A3 Velocity Field : completed by measurements of the inlet region

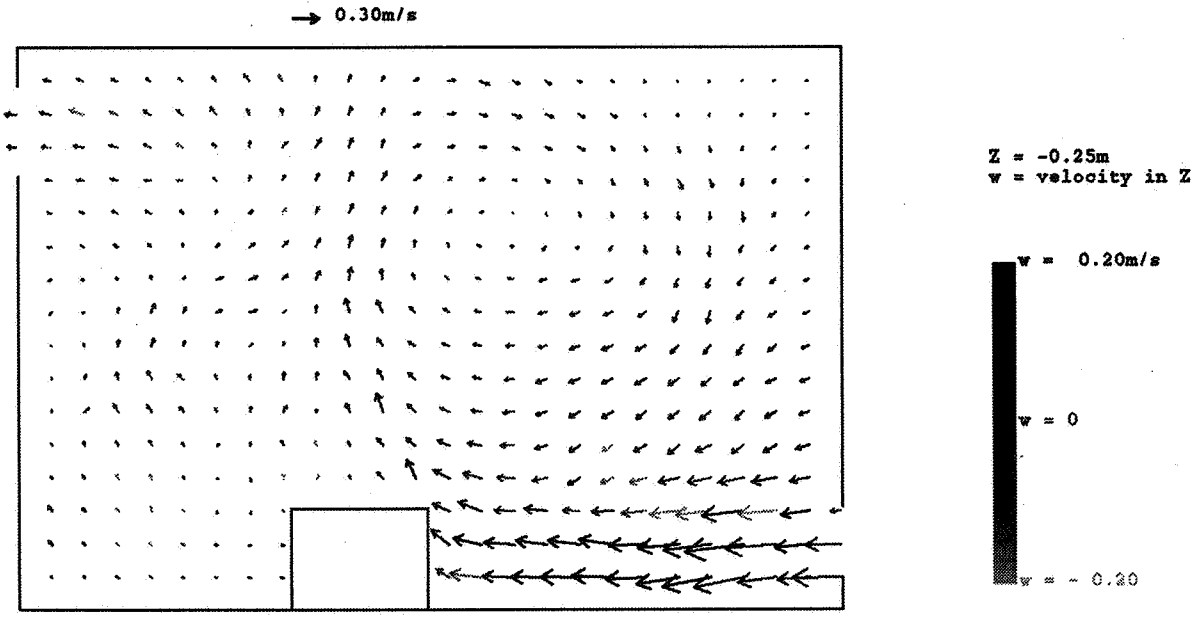

Fig. A4 Interpolated velocity field

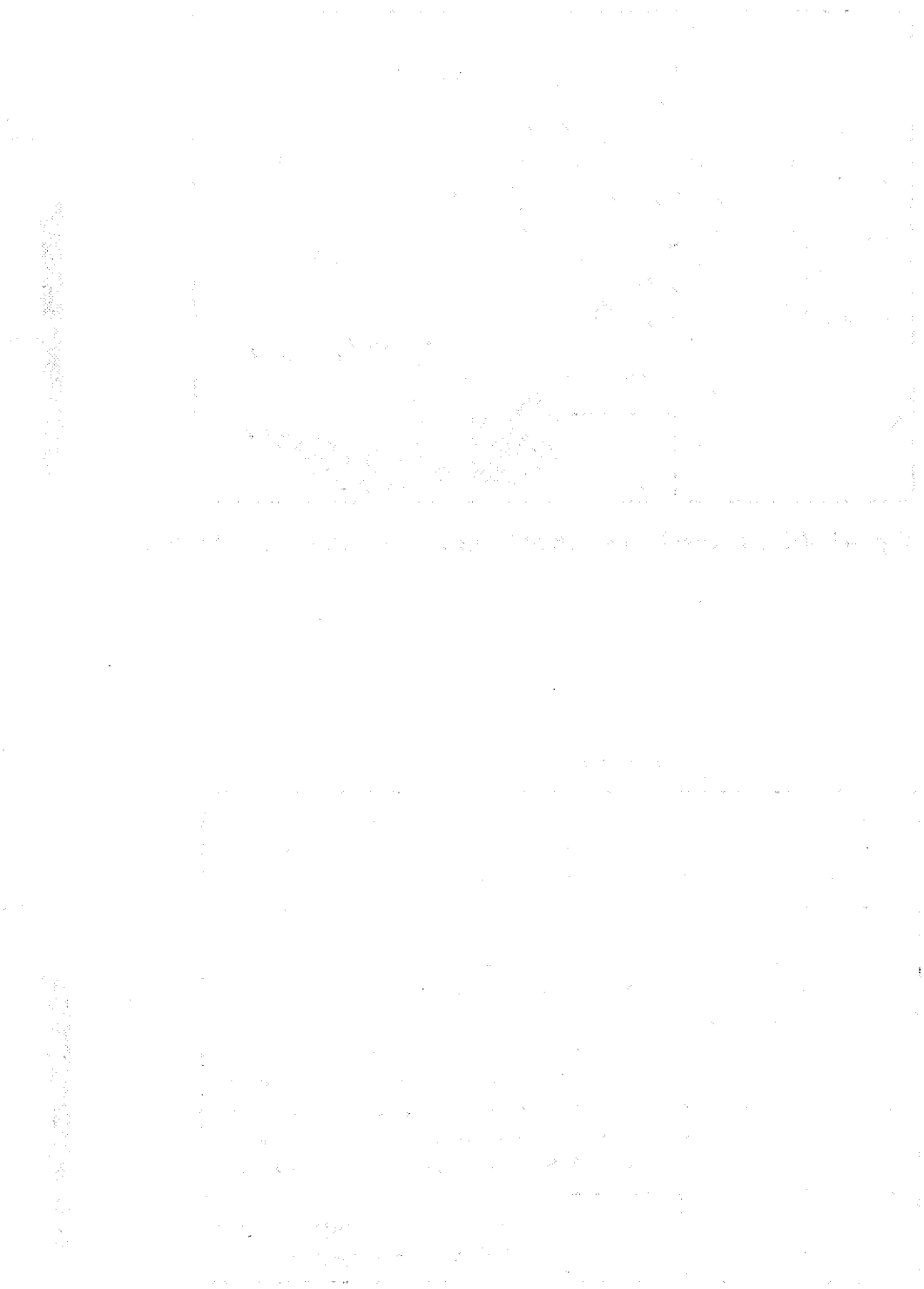

The Role of Ventilation
15th AIVC Conference, Buxton, Great Britain
27-30 September 1994

Thermal Simulation of Ambients with Regard to Ventilated Attics

E L Krüger*, O D Corbella**

* M.SC. Energy Planning - COPPE/UFRJ, Rio De Janeiro, Brazil, Student at the Institut für Industrialisierung des Bauens Hannover, Germany

** Full Professor at the Architecture School of the Federal Univ of Rio De Janeiro, FAU/UFRJ, Predio da Faculdade de Arquitetura - 4 Andar, Sala 433 Cidade, Rio De Janeiro, Brazil

Thermal Simulation of Ambients with Regard to Ventilated Attics

by Eduardo L. Krüger (Ph.D. Student at the *Institut für Industrialisierung des Bauens* - Universität Hannover, Germany) and Oscar D. Corbella (Full Professor at the Architecture School of the Federal University of Rio de Janeiro, FAU/UFRJ, Brazil)

ABSTRACT

The idea that internal temperatures can be reduced by ventilating the air-space between the ceiling and the roof (the attic) of a house, is widely acknowledged by Civil Engineers and Architects. This phenomenon was evaluated through three softwares (CASAMO-CLIM, COMFIE and SPIEL) which were designed for the analysis of the thermal performance of buildings, by comparing the results of all three. The prototype of a popular house in three different locations in the State of Rio de Janeiro (Brazil), at Ilha do Governador, Jacarépaguá and Teresópolis, was used for the evaluation of summer conditions.

It is understood that thermal comfort in hot climates is related to the energy consumption required for the artificial climatization of ambients, thus a reduction of this consumption can be attained if building techniques, aimed at the proper adaptation of the building to the local climate, are used, i.e. those employing passive solutions to achieve thermal comfort in the built environment.

The ventilation of attics for the three climatic situations studied resulted in a small reduction of the inside temperatures. It was verified, during this research, that this reduction was about tenths of a degree centigrade, for the most extreme climatic condition, at Governador. However, the utilisation of ventilated attics can help promoting an expressive reduction in residential energy consumption, if used alongside the adoption of other solutions of Bioclimatic Architecture, thus contributing to energy conservation in this area.

1. INTRODUCTION

The necessity of providing thermal comfort to the built environment is based on one of the prime tasks of architecture, i.e. the provision of shelter against the external conditions. At the very beginning of the History of Architecture, the idea was to have some kind of protection against rain, wind, cold or heat next to the obvious protection against wild animals and enemy tribes. Indeed, by the time of Ancient Greece, Aristotle (382-322 B.C.), Xenophon (430-350 B.C.) and Hippocrates (460-380 b.C.) had already incorporated the climatic factor within the existent building-code. Later on, Vitruvius, in the 1st Century B.C., proposed several guide-lines concerning the proper adequacy of constructions to the local climate. Thus, it could be said that the climatic factor is a decisive parameter for architectural design.

But somehow during the 20th Century the traditional examples of the vernacular architecture were put aside, when a widespread adoption of an internationalised architecture occurred, in places of different climatic conditions. One can observe the same building being built in New York, Rio de Janeiro or Jakarta. The cause for these discrepancies can not be simply summarised. Among many factors, cheap energy prices until the first oil crisis in the 70's, guaranteed the general use of artificial climatization of ambients.
This is particularly true of office-buildings, but average one-family houses in tropical conditions also show a lack of interest in the vernacular designs. The consequent favouring of imitations of foreign solutions also lead to "climate alienated" constructions, which normally result in uncomfortable

solutions also lead to "climate alienated" constructions, which normally result in uncomfortable ambients. In low-cost houses, the use of artificial climatization by air-conditioners remains a luxury. Furthermore, as a consequence of improper architectonic design, already unfavourable climatic conditions outside, are substantially worsened inside the ambient.

For warm-humid climates (which characterise the greatest part of the Brazilian territory, including the States of Rio de Janeiro and São Paulo), the most common passive solutions to achieve thermal comfort internally consist of reducing heat gains through solar radiation by protecting the openings of the envelope and promoting a good ventilation rate [1].

In this research, the effects of the ventilation of the attic of the prototype of a low-cost house were evaluated. The air-space between the ceiling and the roof of a house becomes a substantial heat trap, as a result of the transmitted long-wave radiation of the roof elements. By the ventilation of this air-space, the heat can mostly be dispersed. In this case, by reducing the air-temperature inside the attic, a lower amount of heat will reach the space below. This phenomenon was analysed by using computer programmes, which were designed for the evaluation of the thermal performance of buildings. For that purpose, the climatic conditions of three different locations at the State of Rio de Janeiro were considered.

This paper will firstly give a brief description of the mechanisms related to the natural ventilation of ambients, concerning the achievement of thermal comfort standards. Secondly, the conditions for the simulations with the softwares are presented, followed by the simulations themselves and their results. Finally, some comments regarding the simulation results and the utilisation of the softwares are expressed.

2. NATURAL VENTILATION AND THERMAL COMFORT

There are two main goals related to the ventilation of internal spaces:
- the removal of excessive heat from the interior space (heat stored in walls and internal surfaces and the removal of internal hot air itself);
- ventilation for hygienic reasons, in which fresh air is permanently provided through openings at the building envelope.

However, under tropical climatic conditions, the natural ventilation of ambients is connected to the former, i.e., the removal of excessive heat and improvement of thermal comfort conditions internally. This is in general not easily achieved when high temperatures are to be found outside. In that case, selective ventilation may normally be the best solution.

The ventilation of the attic aims at a different objective. The primal task is neither increasing air movements in the ambient for immediate body cooling nor removing stored heat of internal surfaces by convection, but that of indirectly reducing the heat gains which are transmitted to the ambient through the ceiling.

---

[1] As the temperature ranges remain considerably low in a daily and yearly schedule, i.e., permanently above comfort standards, the use of thermal inertia does not offer many advantages. In this respect, light constructions are mostly recommended, as these allow sufficient airflow (air-permeability) and do not absorb and retain heat.

Especially in one-storied houses, the roof is the building element which receives the highest amount of solar radiation throughout the year. If there is also an attic, the converted solar radiation into long-wave radiation is transmitted through the roof-elements and a heat trap is formed between the roof and the ceiling. When no ventilation is provided for this air-space, the inside temperatures rise far above the outside ones.

Through the ventilation of the attic, it is supposed that the inside temperatures of the attic may be reduced to a level the same as the rates of the outside air temperatures. This is partially achieved by renewing the inside air through the openings at the attic and partially by cooling the internal surfaces by convection and interfering at the radiation heat exchanges. After this temperature reduction is achieved, the heat transfer from the attic to the ambient below it is somewhat softened, thus a slight drop of the internal air temperatures is to be expected, increasing comfort conditions in the ambient.

Although the system is quite simple, its efficiency depends on the location and size of the openings. Furthermore, next to the natural ventilation by wind effect, one could take advantage of the stack effect, which consists of the natural upwards movement of hot air, if openings at different heights are provided. In this case, the heated air trap would also be slightly dissolved by the permanent air current from the lower to the upper openings.

3. THE PROTOTYPE: CASA-MODELO

The prototype (CASA-MODELO) which was used for the simulations consists of a low-cost house with an internal area of 12 m² and 3 m high, based on a proposed model by *Instituto de Pesquisas Tecnológicas de São Paulo* for similar studies [2].

The CASA-MODELO (figure 1) constitutes average brick walls (20 cm thick) which form only one ambient with an attic, separated by a 3 cm wooden ceiling. The roof is formed by ceramic tiles (1.5 cm thick) which offer a good thermal resistance. Wooden boards (3 cm thick) are used fo the floor. For a permanent ventilation of the ambient, two wooden venetian blinds (4.00x2.00 m) are provided at 2.70 m above the floor. At the same facades of this blinds, there is a wooden door and a single-glass window with wooden venetian blinds as well. External surfaces receive white finishes (including the roof). As for the internal surfaces, only the attic surfaces and the floor remain unpainted.

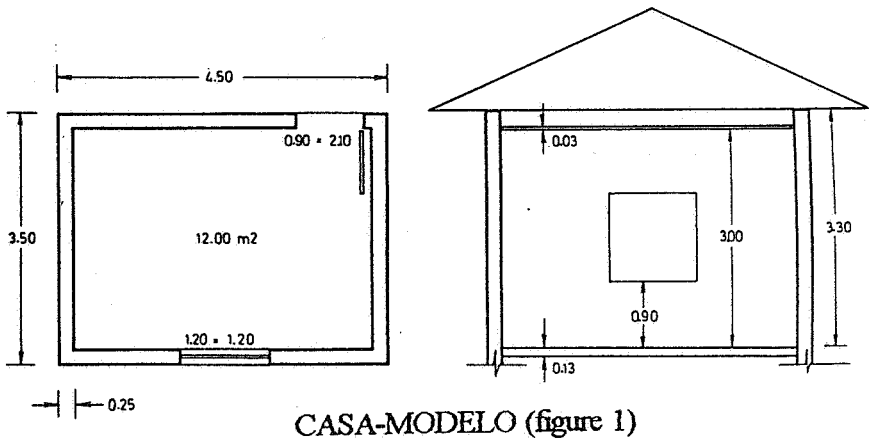

CASA-MODELO (figure 1)

[2] As this study is related to computer simulations, only the building data is considered as a basis for the simulations. It is not an experimental research, and no building has actually been built.

In the case of the attic, three situations were considered: firstly, without ventilation, and secondly and thirdly, with respectively two and four air-openings, protected by mosquito-nets.

With consideration of the climatic parameters, the adopted building orientation was preferentially North-South. However, for the best use of the wind effect (according to the existent average rates of wind currents), both wind- and sun-orientation were considered, allowing for heat losses by ventilation and less solar gains.

The occupation and utilisation of the CASA-MODELO are typical of a working-class couple, being basically nocturnal.

Three different locations were considered, representative of the basic climates of the State of Rio de Janeiro: Ilha do Governador (typical urban climate), Jacarépaguá (seaside climate) and Teresópolis (mountain climate). For these three locations, the basic climatic factors such as air temperatures, relative humidity, wind and solar radiation were collected for February (summer conditions).

4. SIMULATIONS

The three computer softwares which were used (CASAMO-CLIM, COMFIE and SPIEL) have been developed for the analysis of the thermal performance of buildings. They are run in small personal computers (PC's XT or AT) and are aimed at the design phase of the building activity and are aligned for the use of architects and civil engineers. The simulation results enable the planner to have a general idea of the building before it has actually been built. The main advantage of this evaluation method is allowing several variants of the same building to be tested, with regard to their thermal performance.

The basic data for the three programs have been summarised as follows:
- geographical data (latitude, hemisphere, height);
- meteorological data (radiation, albedo, wind direction and velocity, air temperature, relative humidity);
- building data (orientation, volume, areas, shadowed surfaces, materials, internal heat gains, ventilation rates, transmission, absorption and emissivity values).

After providing the program with these values, the simulation is run by finite differences and its results are offered as tables, diagrams and graphics, which make it possible for the architect to evaluate the comfort standards in the built environment.

4.1 CASAMO-CLIM

CASAMO-CLIM was developed by the *Centre d'Energetique de l'Ecole des Mines de Paris,* and its primal objectives are the evaluation of comfort conditions and the calculation of the existent charges of artificial climatization.

After the climatic and building data has been entered, the simulation is run for the desired time period and the results are shown in graphics (Givoni's Comfort Diagram and temperature curves) or in numbers (hourly values of the air temperatures, resultant temperatures -considering the heat wave emitted by the internal surfaces- and relative humidity for the studied ambient).

Considering the three situations (attic without ventilation and with two or four openings), for the three climatic zones, the results are summarised in the following tables.

table 1: CASAMO-CLIM Results for Governador

Zone: Governador Latitude: 22° 49' S minimal external temperature: 25.1°C maximal external temperature: 34.7°C		
variant	max. int. temperature (°C)	mean int. temperature during occupation (°C)
without ventilation at the attic	32.90	30.79
with 2 air-openings at the attic	32.90	30.76
with 4 air-openings at the attic	32.90	30.76

table 2: CASAMO-CLIM Results for Jacarépaguá

Zone: Jacarépaguá Latitude: 22° 59' S minimal external temperature: 23.4°C maximal external temperature: 31.4°C		
variant	max. int. temperature (°C)	mean int. temperature during occupation (°C)
without ventilation at the attic	29.70	26.89
with 2 air-openings at the attic	29.80	26.88
with 4 air-openings at the attic	29.80	26.91

table 3: CASAMO-CLIM Results for Teresópolis

Zone: Teresópolis Latitude: 22° 27' S Height: 874 m minimal external temperature: 18.2°C maximal external temperature: 28.6°C		
variant	max. int. temperature (°C)	mean int. temperature during occupation (°C)
without ventilation at the attic	27.70	26.35
with 2 air-openings at the attic	27.70	26.31
with 4 air-openings at the attic	27.60	26.28

Apart from an unexpected rise of the internal temperatures when the attic was ventilated in Jacarépaguá, the average tendency which was observed is a slight reduction of the internal air temperatures during the occupation of the ambient. These reductions are nevertheless insignificant and the program is not sensitive to variations of the air flow in the attic. In the case of Governador, for instance, the daily ventilation rate of the attic is risen from 73 up to 143 vol/h while nightly from 20 to 41 vol/h, which means an increase of 100%, and no temperature reduction was observed.
Though this program does not allow a precise understanding of the thermal behaviour inside the attic (for it presents the temperature curves and values only for the studied ambient), one may draw as a conclusion that a reduction is to be found, although not a very significant one.

5.2 COMFIE

COMFIE is also a product of *Centre d'Energetique de l'Ecole des Mines de Paris* and it was designed for the thermal analysis of multizonal buildings.

As this program offers the possibility of studying several zones simultaneously, its results concerning the thermal performance of the attic allow a more precise understanding. However, the results are presented in form of temperature means and maximal and minimal values for each zone.

For the three climatic zones considered and for the three situations concerning the ventilation of the attic, the results are shown below:

table 4 : COMFIE Results for Governador

variant	mean int. temperature (°C)	mean int. temperature during occupation (°C)
without ventilation at the attic	30.87	30.81
with 2 air-openings at the attic	30.76	30.69
with 4 air-openings at the attic	30.72	30.67

table 5: COMFIE Results for Jacarépaguá

variant	mean int. temperature (°C)	mean int. temperature during occupation (°C)
without ventilation at the attic	28.00	27.20
with 2 air-openings at the attic	27.90	27.12
with 4 air-openings at the attic	27.88	27.12

table 6: COMFIE Results for Teresópolis

variant	mean int. temperature (°C)	mean int. temperature during occupation (°C)
without ventilation at the attic	24.50	24.18
with 2 air-openings at the attic	24.38	24.06
with 4 air-openings at the attic	24.33	24.03

The first thing to be noticed is a better sensitivity of this program towards the ventilation of the attic. Although the reduction of the ambient temperatures is still not very significant, through higher ventilation rates in the attic, the reduction of its internal temperatures is quite expressive, as it is shown in the following table.

table 7: COMFIE Results for Governador - Internal Temperatures in the Attic

variant	min. int. temperature in the attic (°C)	max. int. temperature in the attic (°C)
without ventilation at the attic	27.46	36.82
with 2 air-openings at the attic	25.93	35.29
with 4 air-openings at the attic	25.70	34.81

Thus, through these results, it can be concluded that the ventilation of the attic is not as effective as the ventilation of the ambient itself, though, an attic when present should be preferentially ventilated.

4.3 SPIEL

SPIEL was designed by *Ecothec Design Ltd.* (Sheffield, UK) for the analysis of the thermal performance of buildings and the calculation of the energy charge for the climatization of ambients.

The input data is similar to that of CASAMO-CLIM and COMFIE and the results consist of the daily temperature development and of the correspondent energy consumption during occupation (for lighting and climatization).

For the first situation (the unventilated attic), at Governador, the temperatures of the ambient and of the attic were practically identical. Allowing for the fact that the program had not considered the heat gains from solar absorption on the roof, several tests were conducted to verify this assumption.

In order to try to solve this problem, a fictitious "glass envelope" that is perfectly transparent and with a thermal conductance equal to that of the external surfaces was introduced to the model. For the most extreme situation, the unventilated attic at Governador, the temperatures of the ambient remained below those of the attic. However, when the attic was ventilated, the internal temperatures of the ambient rose, even though the attic presented lower temperatures than before.

It was then assumed that this program was designed for northern part of the northern hemisphere, where milder solar radiation is to be found. In this case, the great temperature differences between in- and outside (due to heating systems and insulated walls) turn the solar gains in opaque elements into an almost negligible factor.

5 CONCLUSIONS

While admitting that computer simulation by PC's is still a rudimentary tool to predict the precise performance of a physical phenomenon (an experimental analysis would be more recommendable), one can nevertheless infer what happens in reality.

In this research, small reductions of the internal temperatures were observed by the utilisation of two softwares (CASAMO-CLIM and COMFIE) when the attic was ventilated. Though the exact decrease of the ambient temperatures was left undetermined, it was noticed that this reduction is insignificant.

Nevertheless, as one of the various means to achieve thermal comfort in buildings using Bioclimatic Architecture, the ventilation of the attic could be efficient when applied alongside others such as shadings, building finishes with low absorption and cross-ventilation.

REFERENCES

1. Centre d'Energetique de l'Ecole des Mines de Paris *CASAMO-CLIM: Cahier Scientifique.* Paris: Agence Française pour la Maitrise de l'Energie, 1990.
2. Centre d'Energetique de l'Ecole des Mines de Paris *CASAMO-CLIM: Exemples d'Utilization.* Paris: Agence Française pour la Maitrise de l'Energie, 1990.
3. Centre d'Energetique de l'Ecole des Mines de Paris *CASAMO-CLIM: Manuel d'Utilization.* Paris: Agence Française pour la Maitrise de l'Energie, 1990.
4. GREEN, C. WELLS, J. *Spiel: Manual of Utilisation.* Sheffield: Ecotech Design, 1991.
5. KRÜGER, E.L. *Ventilação de Áticos como Instrumento de Conservação de Energia em Edificações: Análise Comparativa de Respostas de Programas de Simulação Térmica de Ambientes.* Rio de Janeiro: COPPE/UFRJ, 1993 (M.Sc. Dissertation).
6. MARKUS, T.A. MORRIS, E.N. *Buildings, Climate and Energy.* London: Pitman, 1980.
7. PEUPORTIER, B. SOMMEREUX, I.B. *Comfie: User's Manual.* Paris: Centre d'Energetique de l'Ecole des Mines de Paris, 1991.

The Role of Ventilation
15th AIVC Conference, Buxton, Great Britain
27-30 September 1994

Flow Paths in a Swedish Single Family House - A Case Study

B Hedin

Lund Institute of Technology, Dept of Building Science/Building Services, P O Box 118, S 22100, Lund Sweden

Synopsis

The ventilation of a Swedish single family house is investigated by means of tracer gas and pressurization techniques. The ventilation flow plays an important role in this house as it enters through a dynamic loft insulation and exits via the crawl space. This design is said to give preheated and clean supply air, warm floors and good energy efficiency. But to meet these promises, it is essential that the air really flows in the intended paths.

A single tracer gas technique is used to determine the air flow rates. The measurements show that actually too much of the supply air by-passes the dynamic insulation by direct infiltration. The measurements also detect an unintended flow from the crawl space to the living area. If there exists radon in the ground ~~soil~~ such a flow must be avoided.

Pressurization tests are used to build a pressure drop-flow model. This model describes *intended flows*, i.e. supply air through dynamic insulation, extract air to crawl space and exhaust air from crawl space to the outside, as well as the *unintended flows*, i.e. infiltration to living area and the two leakages from outside to crawl space and from crawl space to living area. The model is used to explain the present flows and then to tell how to change them. This is done by simulating the model when one of the parameters (e.g. a size of a leakage) is changing. One conclusion is that the crawl space must be made considerably more airtight.

Introduction

The aim of this paper is to show how tracer gas and pressurization measurements have been used to study the ventilation system of the Skanska "Optima' house at Dalby in southern Sweden.[1] To a large extent, the idea underlying the Optima house is to try and make optimal use of the ventilation air flow. Since the paths taken by ventilation flow through the house have such central importance, it is natural that a thorough measurement of the function and effectiveness of the ventilation system should be made.

If all the air flows of interest were confined to ducts and terminals, it would have been sufficient to make measurements by conventional techniques (i.e. pressure drop or hot wire anemometer measurements). But this is not the case. Not all air flows take the desired paths; a considerable proportion of the supply air infiltrates into the house, some of the supply air passes - as intended - through the dynamic insulation but then passes around the terminals, and an unintended portion of the extract air flow recirculates from the crawl space foundation back into the dwelling.

[1]The presented work is part of a larger measurement project 'Optimät' in which an evaluation is made of the energy consumption and occupant comfort in the Optima house and on which a report will be submitted by Elmroth and Fredlund (1994). A full report on the ventilation study is also available (Hedin, 1994b).

This necessitates the use of the tracer gas method to determine the flows and flow paths through the Optima house. In the tracer gas method, an easily detectable tracer gas (in this case laughing gas, N_2O) is injected, the resulting concentration process is measured and a model is fitted to the measured data, with the sought unknown flows (and possibly the volumes) as the parameters. It is a special characteristic of the tracer gas method that all flows which influence the tracer gas concentrations - i.e. the 'diffuse' infiltrations also - can be determined. Two unique properties are that with tracer gas it is possible to determine measures of effectiveness such as air change efficiency and air quality measures such as air change time. The latter two are however only possible for well defined flow paths, i.e. not for infiltration.

The arrangement of the paper is as follows:

Section 1 describes the Optima house from the standpoint of ventilation. In Section 2, the air leakage flow between the dwelling and the crawl space foundation is determined by steady state analysis of a simple tracer gas test. Next, in Section 3, an idealised flow model is determined for the dwelling with the assistance of other tracer gas measurements.

Tracer gas measurements clearly demonstrated some problems due to air leakage from the crawl space foundation into the dwelling. In Section 4, a pressure drop and flow model is determined for the dwelling and the crawl space on the basis of pressure test data. This model is used to analyse how the Optima house ought to have been constructed to perform as intended.

The paper ends by a short summary and a list of symbols.

1 The Optima house

The Optima house is a single family house built with one storey, see the layout in Figure 1. Some of the more important ventilation data and measured values have been summarised in Table 1.

The supply air is taken in through a dynamic insulation, and exhaust air is removed through the foundation. This is described in greater detail in the next two subsections.

The supply side

The house has loose fill insulation in the attic floor. Outside air is drawn in from the attic and slowly passes through the insulation which extends over the whole ceiling. On its passage through the insulation, supply air is filtered and is also preheated according to the dynamic insulation principle. Insulation is terminated at the bottom by a non woven fabric about 5 cm above the gypsum board ceiling, and a plenum is thus formed over the whole ceiling through which the supply air can pass unhindered. Further preheating of the supply air takes place here due to transfer of heat via the ceiling from the dwelling to the supply air. Supply terminals can be sited anywhere by making holes in the ceiling up into the plenum. The house in question has five supply terminals, one in each bedroom and two in the sitting room. The supply terminals are described below in greater detail.

The supply air system is a passive one and is thus dependent on the negative pressure created by the extract air system and on the uncontrolled infiltration which occurs.

The dynamic insulation and the plenum replace a traditional supply air system. There are no supply ducts here which must be cleaned, or filters which must be changed. The filter constituted by the loose fill insulation is assumed to have the same service life as the house. Owing to preheating of the supply air, large quantities of supply air can be admitted into the house without the risk of draughts. □

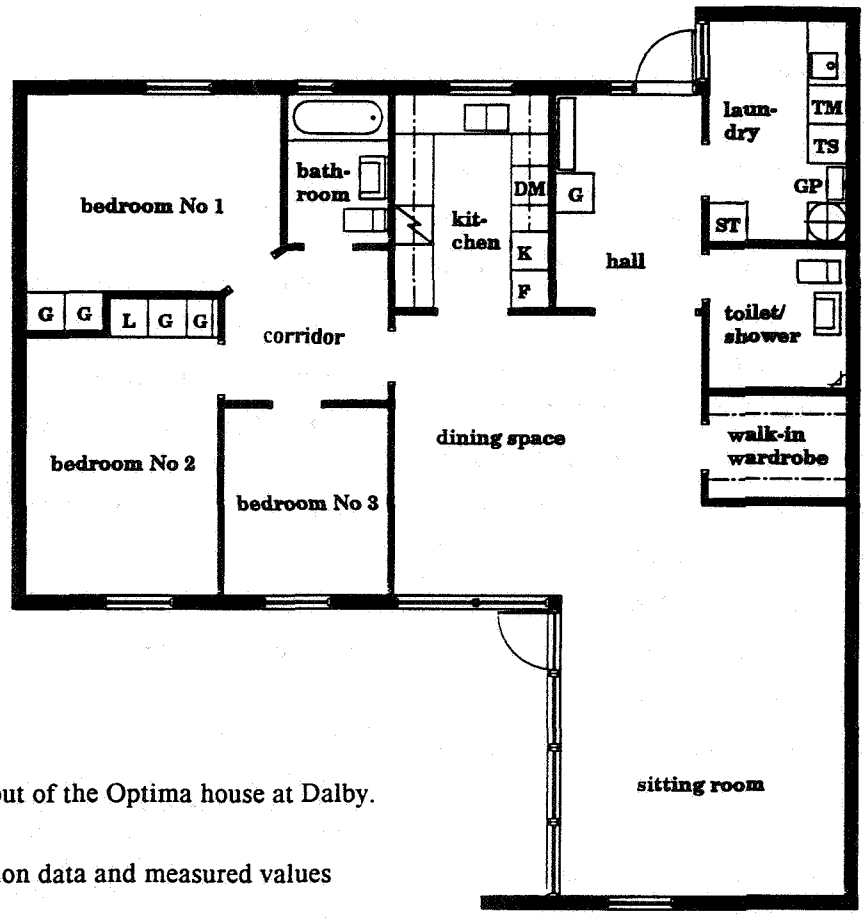

Figure 1 Layout of the Optima house at Dalby.

Table 1 Ventilation data and measured values

Data for the Optima house Living area 116 m², ceiling height 2.4 m, volume 277 m³ + approx. 60 m³ in the crawl space, air change rate n_{nom} = 0.78 ach

room→ ↙ quantity [unit]	bed-room No. 1	bed-room No. 2	bed-room No. 3	corri dor	bathr oom	kitch en	dining space + sitting room + hall = living room	laund ry	toilet	walk-in ward-robe	Total
living area [1] [m²]	10.4	12.0	7.6	4.9	3.7	7.9	19.8+23.6+7.3 = 50.7	6.3	4.0	2.9	111
volume [1] [m³]	26	31	18	12	9	17	47+57+18 = 122	14	10	7	266
supply air flow, design [l/s]	12	12	12				0+(2•12)+0 = 24				60
corrected. [2] [l/s]	9	9	9				0+(2• 9)+0 = 18				45
meas. normal [3a] [l/s]	5.2	4.9	5.8				0+(6.4+5.0)+0 = 11.3				27
meas. open [3b] [l/s]	6.9	7.8	7.8				0+(8.2+8.3)+0 = 16.4				39
extract air flow, design. [l/s]					15	10		15	15	5	60
measured [4a] [l/s]					14	9		15	16	4	58[4b]

[1] From the drawing, corrected volume

[2] Design flow, but corrected with 75% of the total supply air passing through the dynamic insulation

[3a] Normal supply air terminals, measured with the bag method. [3b] As 3a), but with opened (taped) supply terminals.

[4a] Measured in the extract air terminal with a funnel and hot wire anemometer, unreliable measurements.

[4b] Total extract air flow measured across the adjustment device by pressure drop measurement: 60 l/s

The extract side

Initially, the extract system[2] has a normal design, with an extract fan, duct system and extract terminals in the kitchen, bathroom, toilet (with shower), laundry room and walk-in wardrobe. But the collected extract air is then blown down into the crawl space foundation and is exhausted from there with a fan to an exhaust air heat pump before it leaves the house. The foundation has no insulation on the underside of the floor, but is insulated along the ground. ❑

The advantages of this design are said to be that it provides clean, i.e. filtered, and preheated supply air, without the use of a traditional balanced mechanical system with a heat exchanger. The intention is that the ventilated foundation would make the floor warmer, prevent moisture problems in the crawl space and prevent the entry of soil radon into the dwelling. One precondition for the latter function is that the negative pressure in the crawl space should be higher than in the dwelling. Finally, the overall design should make for good utilisation of energy.

Too few supply terminal devices

Even before the tracer gas measurements were made, we knew from measurements in terminals that the flow of supply air through the supply terminals was low. The measurements in Table 1 show 27 l/s which is less than half the extract air flow of 60 l/s. (On the other hand, we did not know if there was any leakage around the terminals or where the remaining supply air came into the house).

The low level of supply air flow was found to be in good agreement with available data for the supply air terminals, and may thus be blamed on a simple - but fatal - design fault:

Supply terminals

The supply terminals were developed to suit the Optima house. Their special feature is that they have a nonreturn valve consisting of two plastic flaps which open and admit supply air if the pressure in the dwelling is lower than that in the plenum. If, for instance, a window is opened and the negative pressure in the room is eliminated, the valve shuts to prevent room air entering the dynamic insulation and causing condensation in the colder insulation material.

The design of the terminal gives it an almost linear characteristic, but there is a bend between 0 and 2 Pa corresponding to its opening pressure

$$q \approx constant\,(\Delta p - \Delta p_{open})$$

see Figure 2. At a negative pressure of 10 Pa, each terminal gives 4 l/s. Measured flows through the actual terminals are a little higher, around 4-5 l/s at 10 Pa. ❑

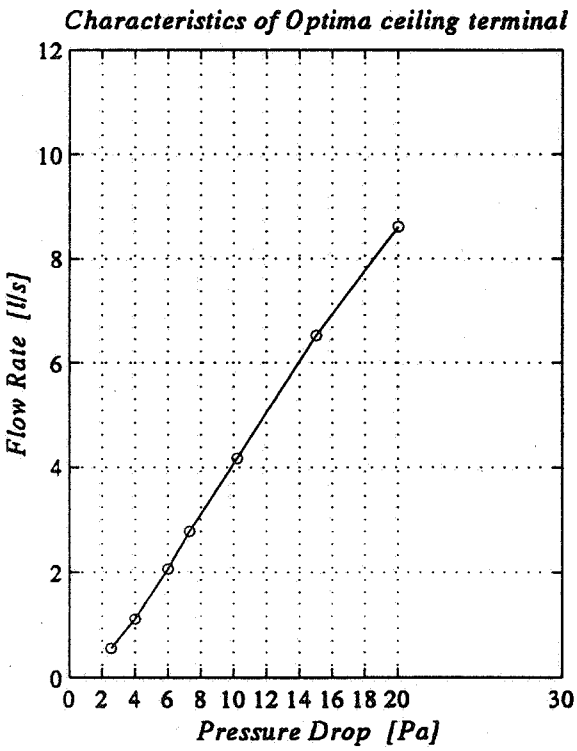

Figure 2. Pressure drop-flow curve for a fully open Optima ceiling terminal (redrawn from the data sheet)

It is obviously desirable - from the standpoint of both filtration and preheating - that as much as

[2] The ventilation air flow will be called 'extract air' between dwelling and crawl space and 'exhaust air' after leaving the crawl space.

possible of the total supply air flow should really pass through the dynamic insulation. This means that the negative pressure in the dwelling shall be small so that air does not enter through leakage paths in the walls and floor. Two factors which militate against the use of far too low a negative pressure is that it must be higher than the opening pressure of the nonreturn valve and that a higher negative pressure provides better stability against wind pressures.

A reasonable pressure in the dwelling may be somewhere around -10 or preferably -5 Pa. On the basis of this - as an initial estimate without consideration of infiltration - between 15 and 30 supply terminals of the chosen size would be needed. But, naturally, it would be more appropriate to choose a larger size.

In contrast to this, the house has only 5 supply terminals. If all the design supply air flow of 60 l/s, i.e. 12 l/s per terminal, were to pass through the supply terminals, the negative pressure would have had to be about -30 Pa, see Figure 2 (outside the range of measurements). In order for this to work, a very airtight house would have been necessary, but such a design can hardly have been the intention. A more accurate analysis of how many supply terminals are needed is given in Section 6.

2 A tracer gas test which demonstrates leakage flows to and from the crawl space

Figure 3 shows an experiment in which tracer gas has been injected into the extract air (a few metres downstream from an extract terminal) and the resulting tracer gas concentration was recorded at the following measurement points.

tracer gas conc.	*measurement point*
c_f	total extract air (into the crawl space)
c_a	total exhaust air (out from the crawl space)
c_{i1}-c_{i5}	extract air in bathroom, kitchen, laundry, toilet and walk-in wardrobe
other data: p = 18.9 μm³/s T_c= 280 s, T_g=35 s, N = 182 samples start: 05.2.93 12:30 hrs fans: no doors: closed	

The expected result - in the absence of leakage to and from the crawl space - would be the same steady increase in concentration in the extract and exhaust air flows and no increase in concentration in the dwelling, i.e.

$$c_f(\infty) = c_a(\infty) \quad (= p / q_f)$$

and

$$c_{i1}(\infty) = c_{i2}(\infty) = c_{i3}(\infty) = c_{i4}(\infty) = c_{i5}(\infty) = 0$$

The results in Figure 3 are different. The tracer gas concentration in the extract air is just under 300 ppm when injection of tracer gas commences, and gradually rises to 350 ppm. This shows that all extract air does not leave the house with the exhaust air but some, a flow q_{ik}, recirculates from the crawl space back into the dwelling. The exhaust air also has a lower steady concentration than the extract air. This shows that there is a leakage flow q_k from the outside to the crawl space which dilutes the extract air.

Analysis of leakage flows with a simple steady state model

For the determination of the magnitudes of these two leakage flows, we need a model. It is easiest to make a simple steady analysis, i.e. to make use of .

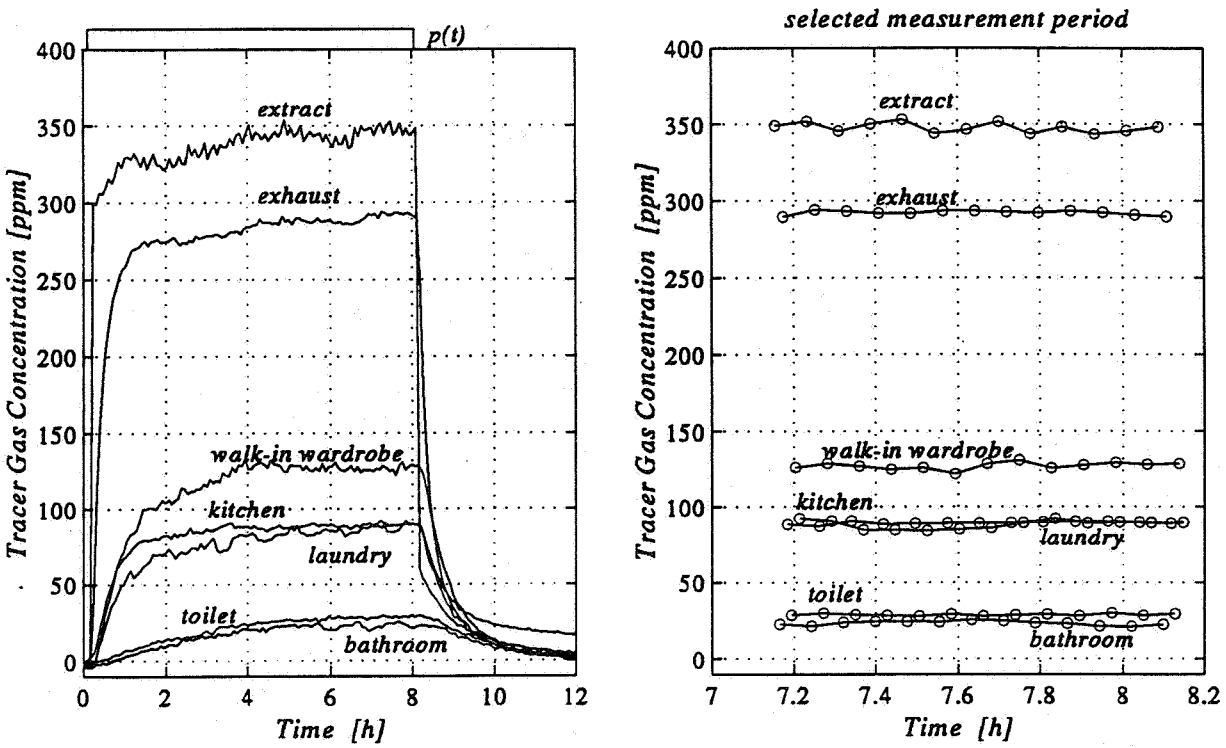

Figure 3. LHS: Tracer gas test with constant injection of tracer gas into the extract air for about 8 hours.
RHS: Period selected for steady analysis

the relationship which applies under steady conditions. The advantage of such an analysis is that the requirements on the model are less stringent, e.g. the requirement for complete mixing can be omitted. The drawbacks are.that it gives less information - for instance, volumes cannot be determined - and that only the steady portion, i.e. only a fraction of the experiment, can be used as measured data.

One problem is that we do not know the (mean) concentration c_{ik} of the flow q_{ik} which leaks into the dwelling from the crawl space. This concentration depends on where this leakage is situated, or rather on the extent to which the concentration in the extract air has been diluted by the flow q_k of outside air before it returns to the dwelling.

An upper and lower bound can however be given. No dilution gives $c_{ik} = c_f$, and complete dilution or ideal mixing in the crawl space gives $c_{ik} = c_a$. In the first case there is in actual fact no recirculation of "crawl space air" at all since there has been no time for mixing to occur. Figure 4 shows a model in which these two cases occur as extreme cases for the parameter values $a = 0$ and $a = 1$. By calculating with these two cases, we also obtain an upper and a lower bound of the sought flows q_k and q_{ik}. Since it is found that the upper and lower bounds are situated near one another, we can ignore the intermediate cases where $0 < a < 1$.

Note that we cannot determine the value of a from the measurements presented. We can only assume a certain value of a and comment on the results thus obtained.

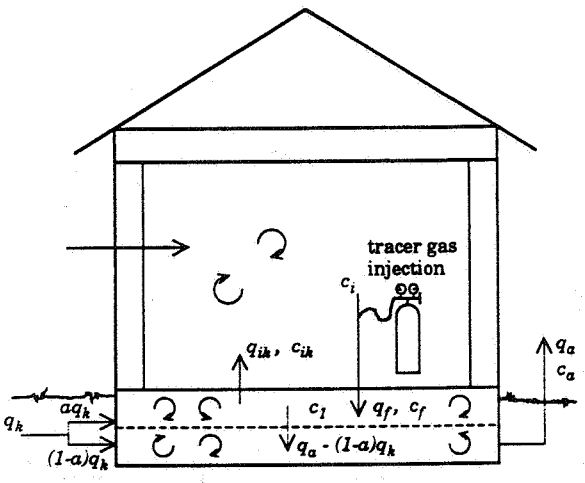

Figure 4. Three cell model which describes the flow system dwelling - crawl space foundation. The crawl space is divided into two cells. $0 \leq a \leq 1$ is that proportion of the outside-crawl space leakage flow which is mixed in the upper of these two cells.

Calculation of steady flows

The fundamental steady relationship in appropriate units is

$$c = \frac{p}{q} + c_0$$

where

c	is tracer gas concentration	[ppm]
c_0	background concentration	[ppm]
p	tracer gas supply	[µm^3/s]
q	air flow	[m^3/s]

The model in Figure 4 has six unknown parameters:

q_f, q_a, q_{ik}, q_k, c_i and c_1

but only four known measured data:

c_{ik}, c_f, $c_2 = c_a$, p

and one constraint:

$$q_f + q_k = q_a + q_{ik}$$

One more measured data or constraint is therefore required.

One possibility would be to require that $q_f = q_a$, which we think is true on the basis of pressure drop measurements across the balancing device. But we decide instead to make use of the measured data relating to the extract air flows, see Table 1, and to calculate with the help of these, using the expression below, the mean concentration in the extract air as a weighted mean of the five extract air concentrations.

$$c_i = \frac{\sum_{j=1}^{5} c_{i_j} q_{f_j}}{\sum_{j=1}^{5} q_{f_j}}$$

The five steady extract air concentrations c_{i_j} are calculated from the measured data.

The other known relationships are as follows: The increase in the concentration of the extract air when the tracer gas flow p is injected is given by p / q_f. We then have:

$$c_f - c_i = p / q_f$$

i.e. the extract air flow is given by

$$q_f = p / (c_f - c_i)$$

Furthermore, according to the model, the tracer gas injected will sooner or later be removed with the exhaust air, i.e. $p = c_a q_a$. The exhaust air flow is thus given by.

$$q_a = p / c_a$$

If $c_{ik} = c_f$ (case a = 0), the following mass balances apply in the dwelling and in the upper crawl space cell:

$$c_f q_{ik} = c_i q_f$$

and

$$c_f q_f = c_f (q_a - q_k) + c_f q_{ik}$$

Rewriting these relationships, we have

$$q_{ik} = \frac{c_i}{c_f} q_f \quad \text{and} \quad q_k = q_a - q_f + q_{ik}$$

If, instead, $c_{ik} = c_a$ (case a = 1), the last two relationships are replaced by the following two mass balances in the dwelling and the crawling space cells:

$$c_a q_{ik} = c_i q_f$$

and

$$c_f q_f = c_a (q_a + q_{ik}) = c_a (q_f + q_k)$$

When these are rewritten, we have

$$q_{ik} = \frac{c_i}{c_f} q_f \quad \text{and} \quad q_k = \frac{c_f}{c_a} q_f - q_f$$

The results of the steady state analysis:

From the measured data in Figure 3 we calculate the following mean values for the selected measurement period:

Steady concentrations [ppm]						
ex-tract	ex-haust	bath-room	kitchen	laun-dry	toilet	wardr obe
348	292	23	89	88	29	127

After substitution of these values into the above equations, the following results are obtained:

Results from steady state analysis
$(c_i = 60$ ppm$)$
$q_f = 65.7\ l/s,\ \ q_a = 65.5\ l/s$
$10.5\ l/s \le q_k \le 12.5\ l/s$
$10.7\ l/s \le q_{ik} \le 12.8\ l/s$

The lower bounds apply for a = 0 and the upper ones for a = 1. The steady concentration in the extract air before injection of tracer gas, c_i = 60 ppm, is in good agreement with the value of c_f just when the injection of tracer gas is turned off; see Figure 3.

Distribution of the crawl space - dwelling leakage flow

We can also estimate the way in which the leakage flow q_{ik} divides between the different spaces. One source of uncertainty is that we do not know the infiltrations in each room. However, the influence of these is not very large.

All doors were closed during the test. It is therefore reasonable to assume that the transmitted air to the five rooms with extract terminals is directed only into these rooms. It is further assumed that there is no leakage from the crawl space to the bathroom and toilet. This is reasonable in view of the watertight floor of these rooms (with heat welded plastics mats which are drawn up onto the walls). This is also reflected by the time curve for the concentrations in these two rooms, with a slow rise and decay, see Figure 3. This means that the concentrations in these two rooms are equal to those in the corridor and living room respectively. In particular, $c_{living\ room} = c_{toilet}$. The further rise in the kitchen, laundry room and walk-in wardrobe, all of which have extract terminals and, in the same way as the toilet, receive their supply air in the form of transmitted air from the living room, can therefore be considered to be due to leakage flows in these rooms. We therefore have the following type of mass balance for e.g. the kitchen:

$$c_{kit}\, q_{f_{kit}} = c_{living}\, q_{kit\ living} + c_{ik}\, q_{kit\,k} =$$
$$= c_{living}\,(q_{f_{kit}} - q_{kit\,k} - q_{kit\ inf}) + c_{ik}\, q_{kit\,k}$$

or

$$q_{kit\,k} = \frac{(c_{kit} - c_{living})\, q_{f_{kit}} + c_{living}\, q_{kit\,inf}}{(c_{ik} - c_{living})}$$

The infiltration into the kitchen, $q_{kit\,inf}$, is unknown and its influence can be written as a (relatively small) correction term:

$$q_{kit\,k} = \frac{(c_{kit} - c_{living})}{(c_{ik} - c_{living})} q_{f_{kit}} + q_{corr}\, q_{kit\,inf}$$

In the same way as before, the concentration in the crawl space, c_{ik}, is replaced by c_f or c_a (depending on the parameter a), and the leakage flow from the crawl space to the kitchen can thus be calculated.

The flow from the crawl space to the laundry room and the walk-in wardrobe can be calculated in the same way. The following results are obtained:

Distribution of leakage flows from the crawl space into the dwelling according to the steady analysis. If there is infiltration, these values are increased by: $q_{korr}\, q_{x\,inf}$	
$q_{toilet\,k} = q_{bathroom\,k} \approx 0\ l/s$	(assumed value)
$2.2\ l/s \le q_{kitchen\,k} \le 2.7\ l/s$	
$2.3\ l/s \le q_{laundry\,k} \le 3.0\ l/s$	
$1.8\ l/s \le q_{wardrobe\,k} \le 2.2\ l/s$	
$4.4\ l/s \le q_{other\,k} \le 4.9\ l/s$	
$0.09 \le q_{corr} \le 0.11$	

Although the leakage in the walk-in wardrobe is smaller than the others despite being most apparent in Figure 3, it is nevertheless the largest leakage as a proportion of the extract air flow.

The above calculations locate more than half the leakage flow from the crawl space. Most of the services entries for ventilation, water and drainage are also situated in these three rooms. The remainder passes into the living room and the hall, and, to judge from the difference between the bathroom and the toilet, to a lesser extent to the bedrooms. ❑

4 Determination of an idealised flow model

Even though the steady analysis is easy to use and to understand, the common idealised flow model utilises the whole test and yields more exhaustive results. The latter describes cell volumes, the air flows between different rooms, infiltration and the leakage flow to and from the crawl space foundation.

It is not the intention here to describe the determination of such models. For this, reference is to be made to Chapter III of AIVC TN 34 or more specific to Hedin (1989, 1994b). Here we just give the final results, see Table 2. These confirm the leakage paths from crawl space to dwelling and also shows that only less than half, or about 27 l/s, of the total air flow into the house passes through the supply terminals. The flow which proceeds the right way (through the dynamic insulation) is not quite so small since about 5 l/s leaks from the plenum into the dwelling around the supply terminals. The remaining supply air flow breaks down into about 17 l/s infiltration and 12 l/s recirculated air from the crawl space.

Obviously, the fact that such a large proportion of the supply air flow bypasses the dynamic insulation reduces the filter function of the system and lowers the coefficient of heat recovery ε_{dyn} for the dynamic insulation. Simple estimates, according to Jensen (1993), are that $\varepsilon_{dyn} < 33/53 \times 0.5 \approx 0.3$, and in view of the insulation thickness $\varepsilon_{dyn} \approx 33/53 \times 0.23 \approx 0.14$, which can hardly be said to be 'optimal'. ❑

Table 2. Identified flows and volumes for the Optima house.
The absolute values along the diagonal represent the total flow into and out of the cell concerned.

Flow matrix Q [l/s]

air flow from→ / ↙ air flow to	bed-room1	bed-room2	bed-room3	cor-ridor	bath-room	living room	kitche n	laun-dry	toilet	wardr obe	crawl space	supply air	infil-tration
bedroom 1	-7.9										0.6	5.2	2.0
bedroom 2		-6.1										6.1	
bedroom 3			-6.8								0.3	5.7	0.8
corridor	7.9	6.1	6.8	-22.5							0.9		0.8
bathroom				13.9	-14.6								0.7
living room				9.7		-28.8					2.0	12.8	4.2
kitchen						5.5	-11.0				1.4	0.2	3.9
laundry						7.1		-15.3			3.8	1.0	3.3
toilet						14.9			-15.7			0.9	
walk-in wardrobe						1.3				-5.5	2.6	0.7	0.9
crawl space				0	14.6		11.0	15.3	15.7	4.3	-78.1	0.9	17.1
exfiltration										1.1	68.3		
											Σq_{ik} =11.6	Σq_t =32.6	Σq_i =16.6

Active volumes [m^3]

cell	bed-room1	bed-room2	bed-room3	cor-ridor	bath-room	living room	kitche n	laun-dry	toilet	wardr obe	crawl space	total volume
cell volume	26	31	18	14	9.2	114	17	10	9.3	7.2	68	68+257

optima id

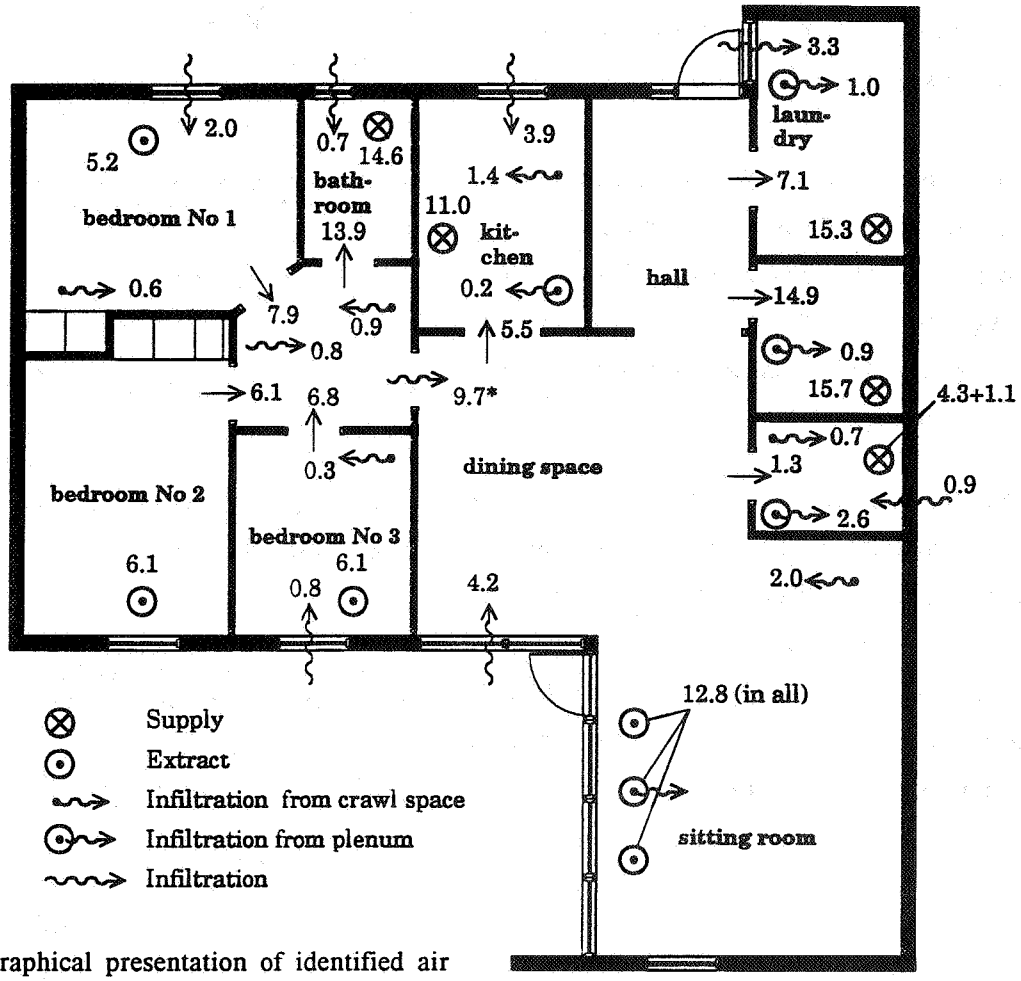

Figure 5. Graphical presentation of identified air flows [l/s] from table 2

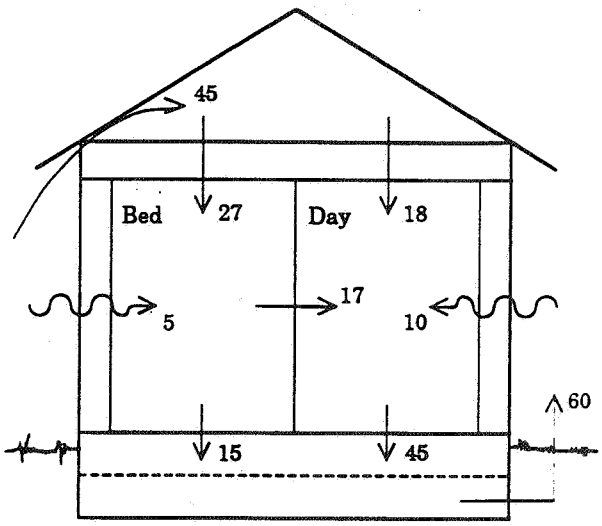

Figure 6a Overview of design flows [l/s], corrected, with 25% infiltration. Bedroom section = bedrooms + corridor, Daytime section = the rest of the house.

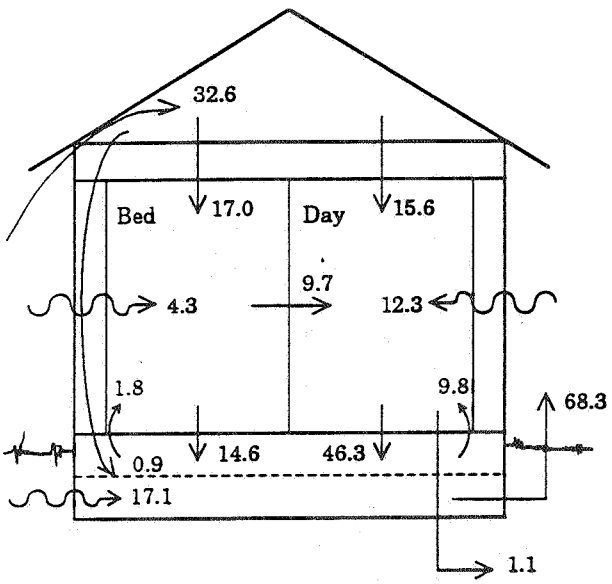

Figure 6b Overview of identified flows [l/s].

6 Analysis of air flow with a pressure drop-flow model

In order to analyse why air leaks in from the crawl space and how this is to be prevented, we now introduce a simple pressure drop-flow model for the Optima house. The model is shown in Figure 7a, and only the resistance network has been reproduced in Figure 7b.

The model describes *the supply air* q_t, *the infiltration* q_i (outside-dwelling), *the leakage flows* q_{ik} (crawl space-dwelling) and q_k (outside-crawl space), *the extract air system* which removes extract air q_f from the dwelling down into the crawl space, and *the exhaust air system* which removes exhaust air q_a from the crawl space to the external air.

Detailed description

The model comprises two pressure nodes p_i for pressure in the dwelling, and one, p_k, for pressure in the crawl space. These are measured in relation to the pressure outdoors which is put equal to 0 Pa. The intended flow path passes along the right of the resistance network and is described by the flow resistances R_t, R_f, R_a and the pressure rises P_f, P_a.

The fans are assumed to have quadratic characteristics (see Note 2 below), with the pressure rises $P_f - R_f^* q_f^2$ for the extract air fan and $P_a - R_a^* q_a^2$ for the exhaust air fan. R_f is modelled as a pure turbulent flow resistance for the extract air duct and its components (i.e. for the extract air terminals, the fan parameter R_f^* and the balancing device). We then have

$$p_i - p_k = R_f q_f^2 - P_f \qquad (1)$$

In the same way, R_a is assumed to be a pure turbulent flow resistance which describes the exhaust duct and its components (i.e. heat pump, , the fan parameter R_a^* and the balancing device). We then have

$$p_k - 0 = R_a q_a^2 - P_a \qquad (2)$$

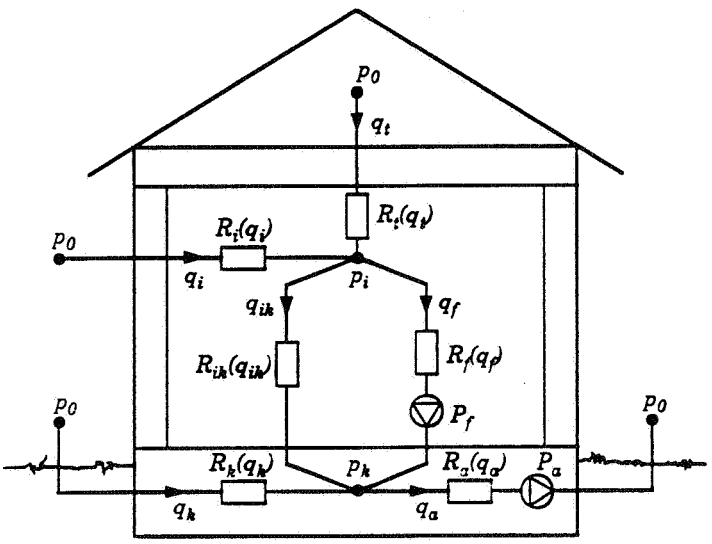

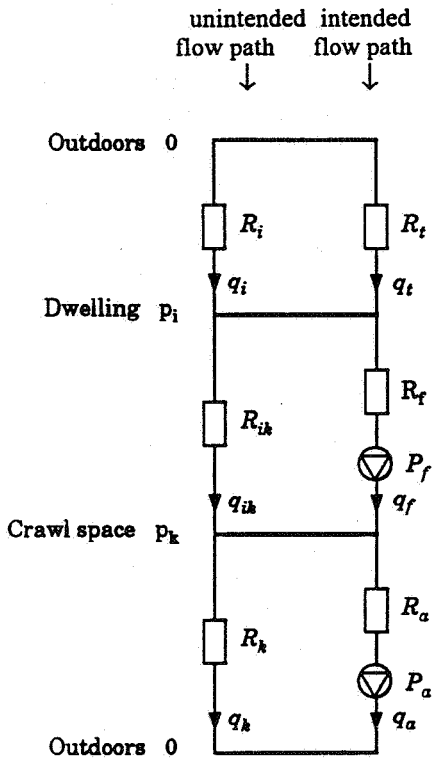

Figure 7a. Pressure drop flow model for the Optima house Figure 7b The corresponding resistance network.

The flow resistance R_t describes the - possibly nonlinear - relationship between the supply air flow q_t and the pressure p_i in the dwelling:

$$0 - p_i = R_t(q_t)\, q_t \tag{3}$$

Apart from the intended flow paths, the model contains three leakage flows/infiltrations with the resistances R_i, R_{ik}, R_k. These describe the outside-dwelling infiltration, the crawl space-dwelling leakage flow and the outside-crawl space leakage flow respectively, as follows:

$$\begin{aligned} 0 - p_i &= R_i(q_i)\, q_i \\ p_i - p_k &= R_{ik}(q_{ik})\, q_{ik} \\ 0 - p_k &= R_k(q_k)\, q_k \end{aligned} \tag{4}$$

Remark 1: Note that all flows are defined as positive when they are directed downwards in Figure 7b. Normally, all flows apart from q_{ik} and $q_k \geq 0$. In the initial stage, when the house has been balanced before the tracer gas measurements, q_{ik} and $q_k \leq 0$, but the direction of these two flows may be reversed depending on how the system has been balanced, i.e. on the values of R_f and R_a, assuming however that the fans are sufficiently powerful. q_k, however, can be only positive if there is positive pressure in the crawl space, which is hardly a desirable operating case. ❑

Remark 2: The fact that R_f and R_a are modelled as pure turbulent resistances may be open to discussion, for instance in view of the possible fan curves and the fact that they include a filter. In actual fact, however, this choice is of no significance when, as below, we chiefly consider balanced cases, i.e. when R_f and R_a have been adjusted to yield a certain intended flow. It is instead the choice of the other four resistances which is important. These are all modelled as arbitrary, monotonically increasing and convex functions. ❑

Remark 3: Above, we use the general pressure-flow relationship $p = R(q)q$, where $R(q)$ is a flow-dependent resistance. Certain relationships can however be written more simply in the inverse form $q = k(p)p$ where $k(p)$ is a pressure drop-dependent flow conductance, sometimes referred to as the (flow-pressure) characteristic. Both methods of notation are used. ❑

Data from pressurization tests

The problem of determining appropriate values of the flow resistances $R_t(q_t)$, $R_i(q_i)$, $R_{ik}(q_{ik})$ and $R_k(q_k)$ for the supply air, infiltration and the two leakage flows to/from the crawl space respectively, has been solved by making use of measured data from pressurization tests carried out before. The primary object of these measurements, which were made by Lundberg and Lundh (1993), was to determine the airtightness of the house and the crawl space in the form of the leakage factor n_{50}. The leakage factor is measured as the specific air change, the unit being number of room volumes per hour or more simply air changes per hour (ach) at a pressure difference of 50 Pa across the building envelope, but measurements are also done for lower pressure differences. Intended openings such as supply and extract terminals are normally sealed during these measurements. Luckily, the authors had the foresight to make several additional measurements, for instance with and without supply air and with and without a pressure difference between the dwelling and the crawl space. In the latter case, the measurements were made by simultaneously using two pressurization test equipments. All four nonlinear flow resistances will be determined below from these measurements. Typically, this is done by forming the difference between different pressure drop measurements.

The determined characteristics consist of tables which set out the flows for each whole Pascal pressure difference. These have been fitted to the measured data, with the constraint that they shall be monotonically increasing and convex, but, on the other hand, they need not have the form $q = k\, p^{1/n}$, with a fixed exponent n, but the exponent can increase from 1 (laminar) for small pressure drops to 2 (turbulent) for large pressure drops.

Owing to the convexity condition, the exponent is not permitted to decrease at higher pressure drops. The determined characteristics are shown in Figure 8.

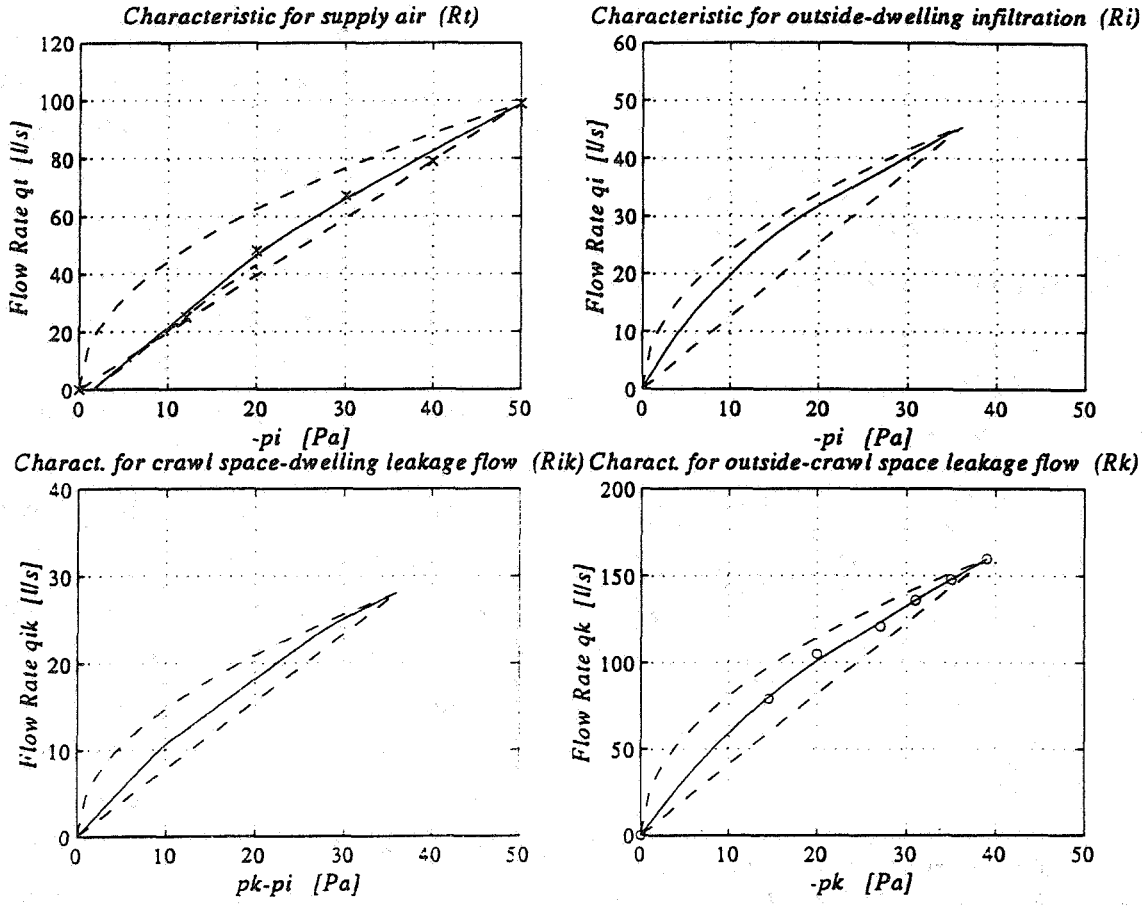

Figure 8. Measured relationships between flow and pressure drop for supply air, infiltration and the crawl space-dwelling and outside-crawl space leakage flows. The dashed curves show a linear and a quadratic characteristic up to the maximum value. The markings o and x denote measured data or the difference between measured data in those cases when these are measured at the same pressure difference.

Owing to the convexity condition, the exponent is not permitted to decrease at higher pressure drops. The determined characteristics are shown in Figure 8.

Adjustment to eliminate the leakage flow from the crawl space to the dwelling

Since both q_f and q_a can - within certain limits - be adjusted, we start with the way these flows are to be selected. The condition for all nodes is at all times $\sum q = 0$, or in this case:

$$q_f = q_t + q_i - q_{ik} \quad (5)$$

$$\Delta q = q_a - q_f = q_{ik} - q_k \quad (6)$$

the notation Δq being introduced for the extra exhaust air flow which is removed from the crawl space in addition to the extract air flow.

By making Δq sufficiently large, the negative pressure in the crawl space can be made greater than that in the dwelling, i.e. $p_i > p_k$. The leakage flow between the crawl space and the dwelling is then in the desired direction, i.e. down into the crawl space, and according to our definition q_{ik} is positive. The magnitude of Δq required depends, according to (6), on the outside-crawl space leakage flow at the prevailing pressure. In the limiting case, $p_i = p_k = p_{lim}$, we have $q_{ik} = 0$ and, according to (5), the prevailing pressure is given by the pres-

sure in the dwelling when $q_f = q_t + q_i$. This can be easily calculated by summating the characteristics for supply flow and infiltration and reading off the pressure p_{lim} which corresponds to q_f. With p_{lim} known, Δq is calculated according to (6), and the characteristic for the outside-crawl space leakage flow as

$$\Delta q = -q_{k_{lim}} = k_k(p_{lim})\, p_{lim} \qquad (7)$$

Note that the magnitude of the leakage flow between the crawl space and the dwelling, R_{ik}, has no effect on the condition for the change in direction of the flow. After all, the flow q_{ik} is zero in the limiting case.

Equation (7) can also be rewritten as a more formal relationship between the characteristics.

$$\Delta q = -q_{k_{lim}} = \frac{k_k(p_{lim})}{k_t(p_{lim}) + k_i(p_{lim})}\, q_f \qquad (8)$$

If the above calculations are made with the measured/calculated values of the parameters of the pressure drop-flow model, the pressure $p_i = p_k \approx$ -15 Pa and the outside-crawl space leakage flow is as much as 81 l/s, while q_a is 141 l/s compared with q_f which is 60 l/s. Naturally, the existing exhaust air fans do not have such a large overcapacity. This explains why it was not possible to attain a lower pressure in the crawl space than in the dwelling when the house was taken into use - in spite of the fact that attempts were made.

In order that these figures may be brought down to more reasonable levels, the crawl space must be made considerably more airtight. Figure 9 shows how the necessary exhaust air flow decreases towards the extract air flow when the magnitude of the leakage flow (i.e. q_k at a certain value $-p_k$) decreases.

In the absence of better information, we assume that such a more airtight crawl space has the same flow characteristics as now. In view of the fact that it is more likely for the few large and "turbulent" leakage paths to be found and put right and for the many small and more "laminar" leakage paths to remain undetected, this is not quite realistic.

There are several reasons why the exhaust air flow should not be allowed to become too large: higher energy consumption and noise from the exhaust fan, and also a drop in temperature in the crawl space, so that the floor is cooler and the operating conditions of the heat pump deteriorate.

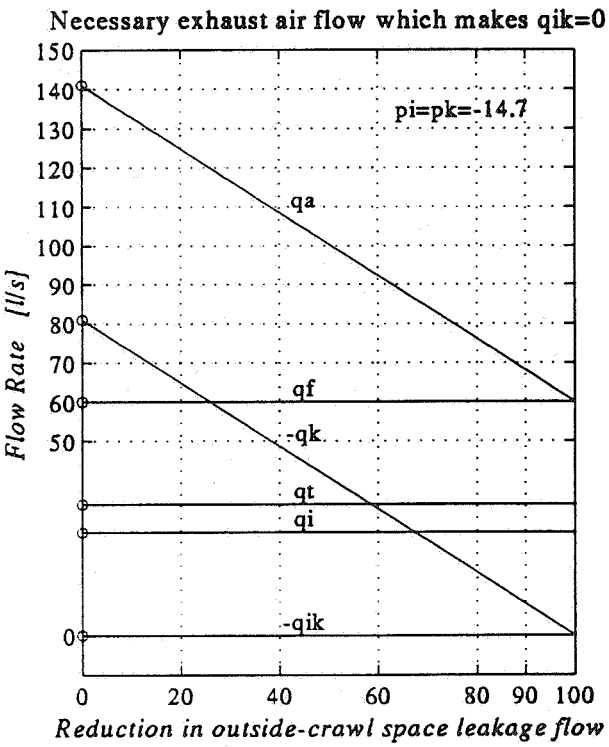

Figure 9. Exhaust air flow required if the outside-crawl space leakage flow can be reduced. The circles at 0% airtightness denote the present situation.

If, as an example, we regard 10% of the nominal flow - i.e. 6 l/s - as a reasonable additional flow q_a- q_f, the leakage flow must be reduced to about 6/81) 7% of the present leakage flow. If we instead select 5% additional flow as reasonable, the requirement is made more stringent and equal to half this value.

By increasing the negative pressure $p_i = p_k$ towards zero, however, these requirements can be reduced. If, for instance, the number of supply terminals is increased from the existing 5 to 30, so that the value of p_i is about -5 Pa instead of -15 Pa as above, the leakage flow also will diminish, but not by a factor of 3 but 2.5 because of the somewhat nonlinear characteristic of R_k. The requirement for the crawl space then remains that it must be made just over 5 times more airtight, or the leakage flow reduced to 18% of the existing flow.

In view of the fact that the existing crawl space - constructed as a normal one - is very leaky, this is no unreasonable improvement. If the characteristic for R_k in Figure 8 is extrapolated to $-p_k$ = 50 Pa, the leakage flow becomes approximately 190 l/s and, with the volume of the crawl space put at 60 m^3, the present value of the leakage factor for the crawl space will be n_{50} = 11.4 ach and the requirement regarding the airtightness of the crawl space will be 18% of this or n_{50} = 2.2 ach, while increasing the airtightness to about 7% of the remaining leakage flow corresponds to the stringent requirement of n_{50} = 0.84 ach.

Further values with some other assumptions are given in Table 3.

One comment on the above calculations is that in the limiting case $p_i = p_k$ and q_{ik} = 0. In order to ensure that no air from the crawl space enters the dwelling, it may be advisable to increase Δq by a few more l/s so that a small flow $q_{ik} > 0$ takes place in the desired direction. The check for this is that p_k is a few Pa lower than p_i.

Table 3. Required airtightness of the crawl space to prevent air leakage flow from the space to the dwelling, for different numbers of supply terminals and different accepted additional flows. The present leakage factors are n_{50} = 11.4 ach for the crawl space and n_{50} = 0.75 ach for the dwelling.

Extra exhaust air flow, Δq [l/s]	6	6	6	6	6	3	3	3	3	3
100 $\Delta q/q_f$ [%]	10	10	10	10	10	5	5	5	5	5
Number of supply terminals [-]	5	10	20	30	40	5	10	20	30	40
Pressure in dwelling, p_i [Pa]	-14.7	-9.6	-6.1	-4.8	-4.0	-14.7	-9.6	-6.1	-4.8	-4.0
Required airtigtness, n_{50} [ash]	0.84	1.2	1.8	2.2	2.6	0.42	0.60	0.89	1.1	1.3

Further simulations with the pressure drop-flow model

In order to further illustrate how the flow system functions, on the following two pages we present some simulations with the pressure drop-flow model which show what happens when the following natural action is taken:

Action: Increase in	Adjustment [l/s] q_a	q_f
1. number of supply terminals	60	60
2. outside-dwelling airtightness	60	60
3. crawl space-dwelling airtightness	60	60
4. crawl space-dwelling airtightness	66	60

Figure 10 shows that about 30 supply air terminals of the existing type are required to attain the moderate aim that 75% of the total supply air should go the right way, i.e. through the dynamic insulation.

The small circles at the beginning of the curves indicate the existing values according to the model. (The same for Figure 11-13).

Figure 11 shows that the same results can be achieved if all infiltration between the outside and the dwelling is eliminated. The remaining 25% of the extract air is then taken from the crawl space.

Figure 12 shows that the leakage flow decreases but that the driving force $p_k - p_i$ increases when the airtightness between the crawl space and the dwelling is increased. There is however no point in this if the leakage flow between the outside and the crawl space is instead eliminated.

Figure 13 shows what we want to achieve, namely to make the leakage flow between the outside and the crawl space sufficiently small so that $p_k - p_i$ is less than zero and the crawl space-dwelling leakage flow is in the correct direction, down into the crawl space. Since the simulation refers to the case in which only Action No 4 is carried out, without the simultaneous execution of Action No 1, according to the figure an increase in airtightness to about 7% of the existing leakage flow is required.

Action to make the house function as intended is not sufficient; the minimum requirement is both a more airtight crawl space and larger supply terminals. In the following two simulations we assume an Optima house with a more airtight crawl space (n_{50} = 2 ach). Figure 14 illustrates what happens when we increase the number of supply terminals from 5 up to 40. Let us assume that we decide on 40 terminals (i.e. in practice terminals with a flow 8 times as high for the same pressure drop). Figure 15 shows what benefit is gained from a further increase in airtightness. (The small x's at the beginning and end of the curves in Figure 14 and 15 denote associated values).

Summary

While the new ventilation solutions in the Optima house may have a development potential, they also impose more stringent requirements on the construction of the house in order that it should function as intended. The investigated house has two serious shortcomings in this respect: due to a fatal design fault, the supply air terminals are too small, and the airtightness of the walls of the crawl space and its airtightness towards the soil are insufficient, which results in a pressure distribution such that air from the crawl space leaks into the dwelling.

Leakage of air from the crawl space into the dwelling can be prevented by making the negative pressure in the crawl space greater than that in the dwelling. What is required is for the exhaust air flow to exceed the extract air flow by at least the prevailing outside-crawl space leakage flow. The prevailing leakage flow is a function of the size of the leakage path, infiltration and the number of supply air terminals. The conditions governing this were determined, and the result is that the airtightness between the outside and the crawl space must be considerably improved, from the existing value of n_{50} = 11.4 ach at 50 Pa down to about 2 ach; see Table 3. This presupposes that there are six times as many supply terminals as before, otherwise a crawl space of even greater airtightness is required. If this can be achieved, there is no reason to improve airtightness between the crawl space and the

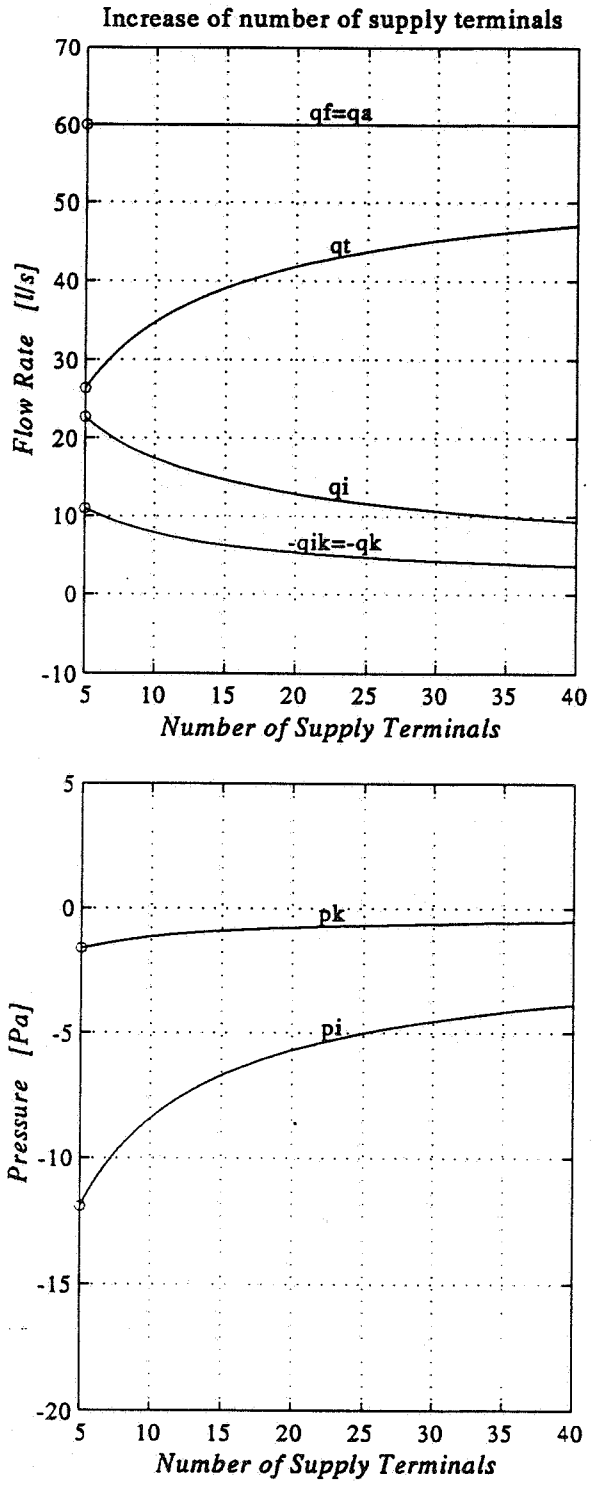

Figure 10. Changes in flows and pressures if the number of supply terminals is increased.

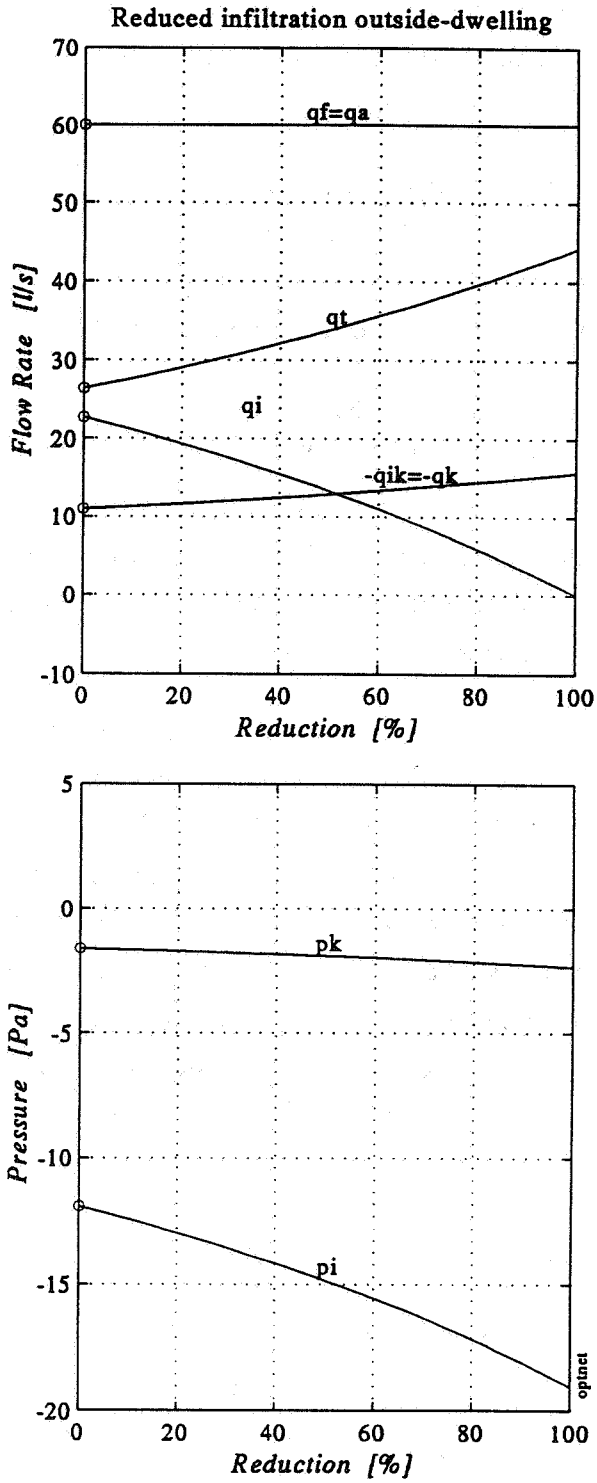

Figure 11. Changes in flows and pressures if the airtightness between the outside and the dwelling is increased.

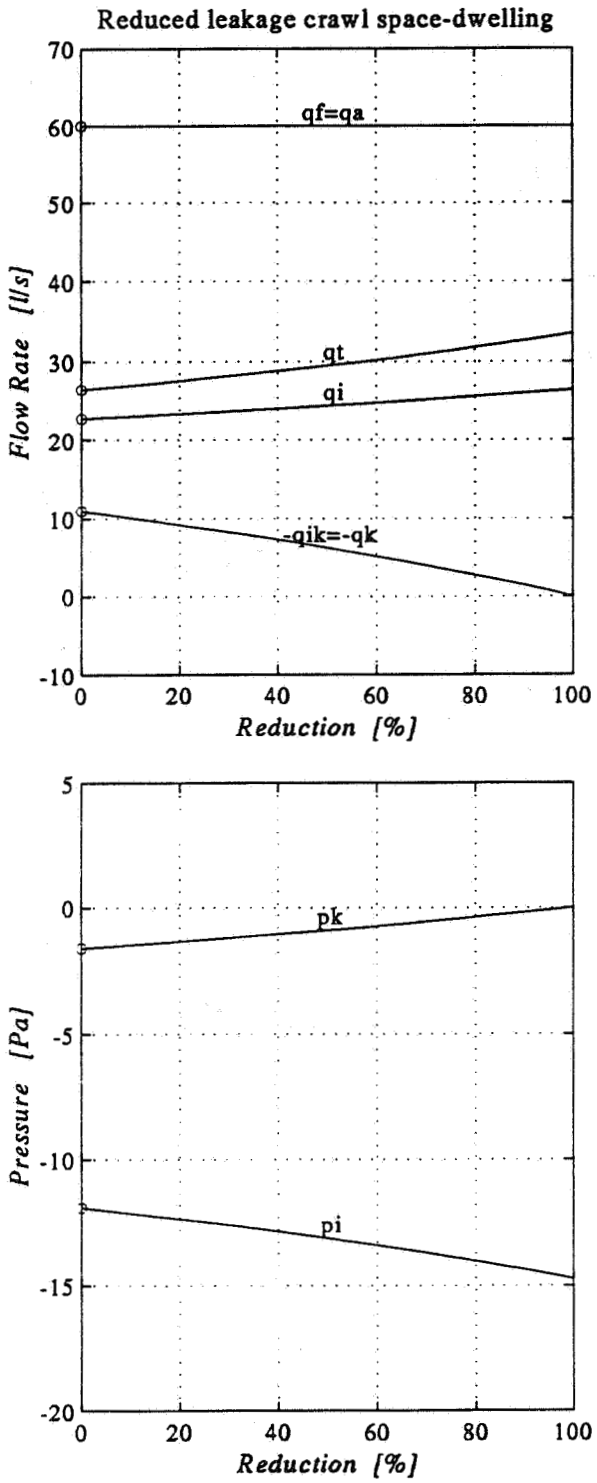

Figure 12. Changes in flows and pressures if the airtightness between the crawl space and the dwelling is increased.

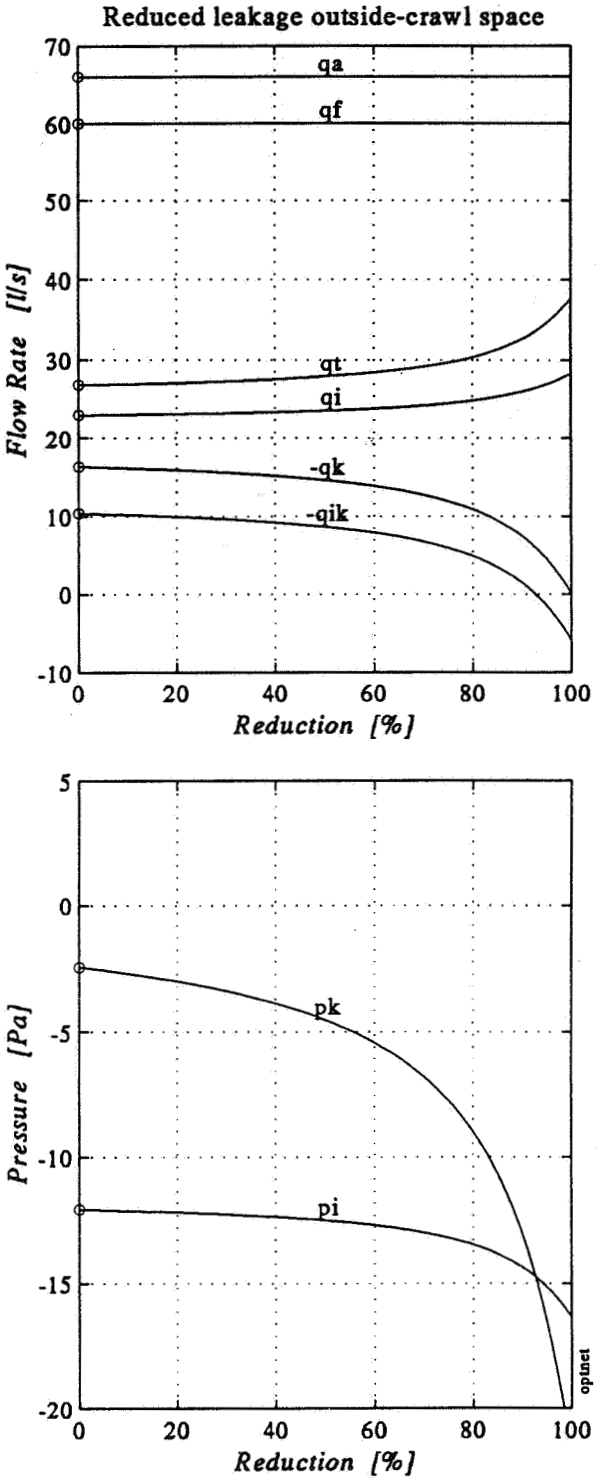

Figure 13. Changes in flows and pressures if the airtightness between the outside and the crawl space is increased.

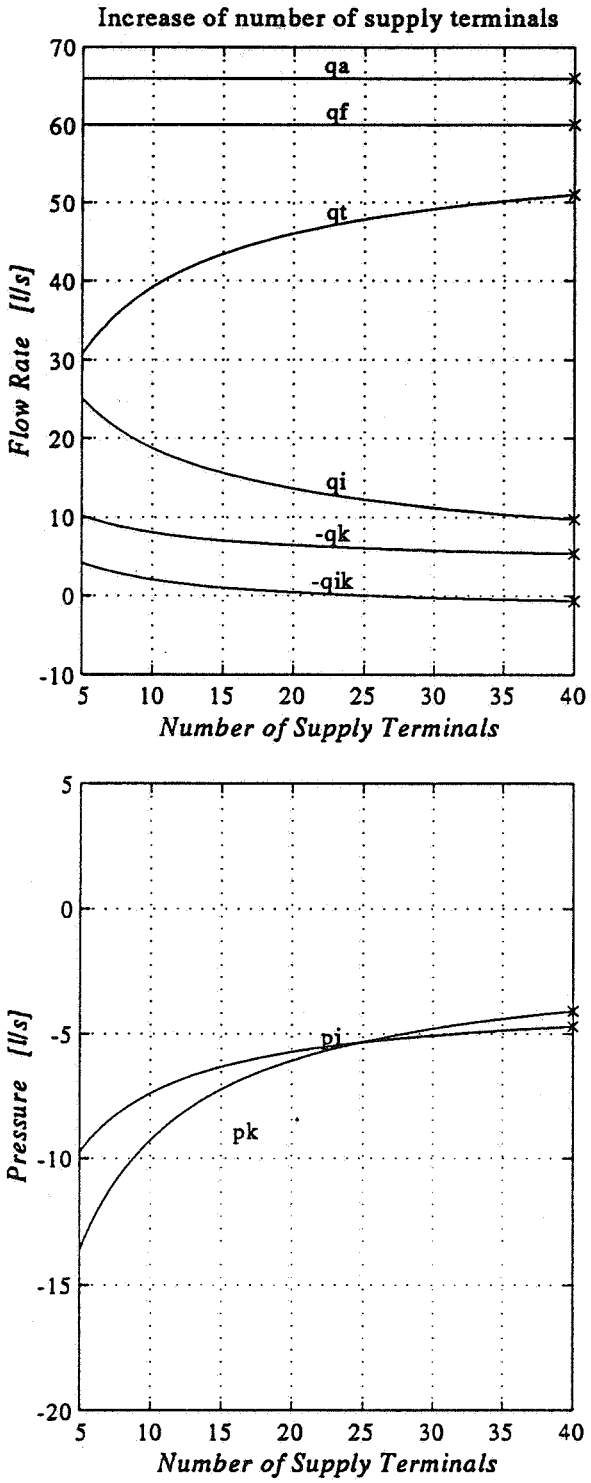

Figure 14. Changes in flows and pressures if the number of supply terminals is increased. (Crawl space constructed to give n_{50}=2ach.)

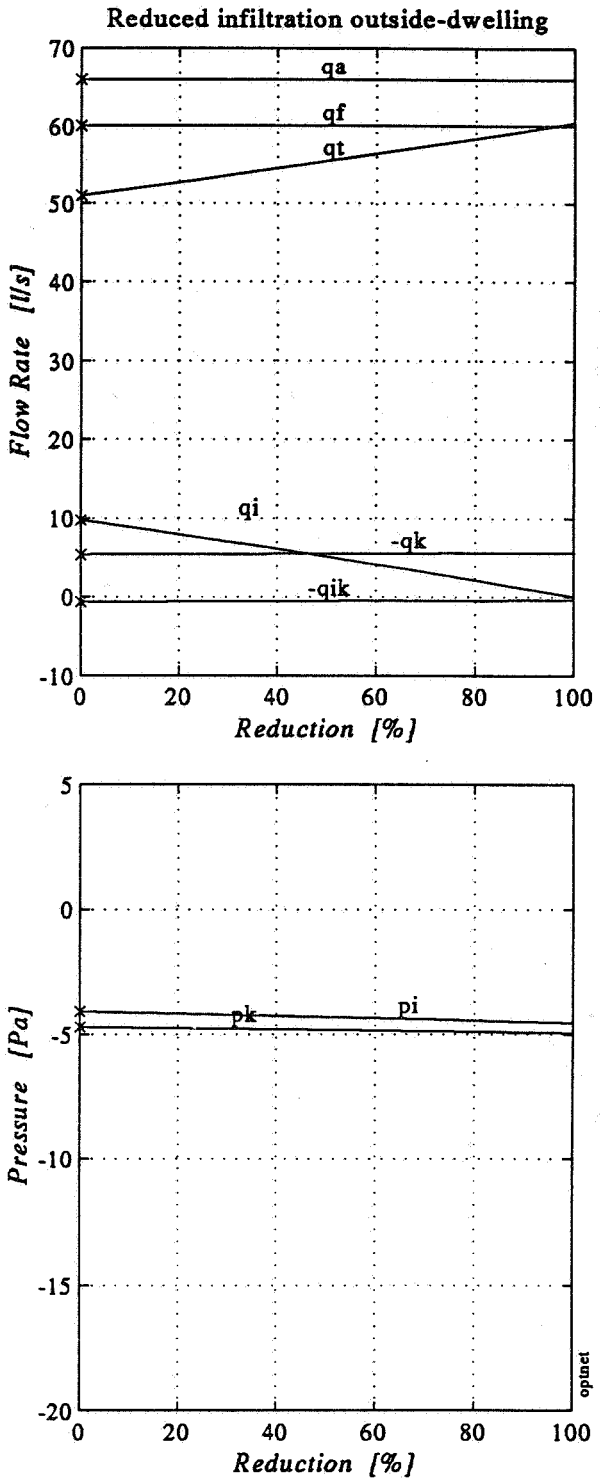

Figure 15. Changes in flows and pressures if the airtightness between the outside and the dwelling is increased. (Crawl space constructed to give n_{50} = 2 ach, number of supply terminals = 40).

dwelling. Note that the required airtightness of the crawl space approaches the same order as that required for the remainder of the house. This can be formulated as follows:

- From the standpoint of airtightness, the crawl space of the Optima house is to be regarded as part of the house rather than a traditional crawl space foundation.

It is easy to put the design fault right and it should be possible to avoid both these faults when new houses are built. It is considered that these faults are due to defective construction of this house and not to the underlying ideas for the Optima house.

Concerning the methods used: the tracer gas method has proved to be very useful to uncover and quantify the leakage paths. In combination with the analysis based on pressurization data it has been possible to reach both a qualitative and quantitative understanding of the ventilation system of the Optima house.

A more thorough discussion of the measurements in the Optima house - including impulse response tests and determination of air change times and efficiencies for different flow paths - is given in Hedin (1994b).

References

AIVC Tn 34 (see Roulet)

Elmroth, A., Fredlund B. (1994) (Unknown title). Building Physics and Department of Building Science, LTH (Forthcoming Report)

Hedin, B. (1989) Identification Methods for Multiple Cell Systems. Proc. 10th AIVC Conference, Espoo, Finland, 1989, p209-232

Hedin, B. (1994) Mätteknik med spårgas - Aktiva metoder för bestämning av volymer, luftflöden, flödesvägar och strömningssätt i småhus. (Tracer Gas Measurement Techniques - Active Methods for Determination of Air Volumes, Flow Rates, Flow Paths and Flow Patterns in Detached Houses) Department of Building Science, Building Services, LTH

Hedin, B. (1994b) Ventilation Measurements in the 'Optima' House. Department of Building Science, Building Services. LTH

Jensen, L. (1993) Energy Impact of Ventilation and Dynamic Insulation. Proceedings of the 14th AIVC Conference, 1993, p251-260

Lundberg, R., Lundh, U. (1993) Mätningar för projektet Optimät. Material under bearbetning, (Measurements for the project 'Optimät'). Department of Building Science, LTH

Roulet, C-A, Vandaele L. (1991): Air Flow Patterns Within Buildings Measurement Techniques. Technical Note AIVC 34. International Energy Agency, Air Infiltration and Ventilation Centre 1991.

(LTH = Lund University, Institute of Technology)

Symbols

Most of the symbols are explained where they occur in the text. Some are summarised below.

c	tracer gas concentration
$c(\infty)$	steady state concentration
h	ceiling height (2.4 m)
N	number of samples
p	tracer gas injection flow rate
$\Delta p, p$	pressure(drop)
q	air flow rate
T_c	sampling period (time period between measurement in the same cell)
T_g	time period between measurement in consecutive cells)

The following subscripts are used (the names of rooms - abbreviated - are also used as subscripts).

a	exhaust (out from crawl space)
f	extract (into crawl space)
i	extract from the dwelling
i_j	extract from room No j, j=1,2,...
ik	to dwelling from crawl space
k	infiltration to crawl space

A double subscript, e.g. $q_{kit\,k}$, is to be interpreted as a flow to the kitchen from the crawl space, i.e. from subscript 2 to subscript 1.

The Role of Ventilation
15th AIVC Conference, Buxton, Great Britain
27-30 September 1994

Determination of k-factors of HVAC System Components Using Measurements and CFD Modelling

Riffat, L Shao, A G Woods

Building Technology Group, School of Architecture,
University of Nottingham, NG7 2RD United Kingdom

SYNOPSIS

Indoor air quality, comfort and energy use in buildings are largely dependent on the performance of HVAC systems. However, the pressure loss factors available to the designer show large discrepancies depending on the source of the data. In particular there are very few data regarding the effect on k-factors of interactions between duct components in close proximity. This paper describes measurement and computational fluid dynamics (CFD) modelling of pressure loss in HVAC system components. The results were compared with those data given in the ASHRAE and CIBSE guides.

LIST OF SYMBOLS

A	Area of the duct [m^2]
C	Concentration of tracer-gas [ppm]
ΔP_m	Measured pressure difference across the duct fitting [Pa]
ΔP_s	Actual pressure difference [Pa]
k	k-factor
P_k	Kinetic pressure [Pa]
q	Tracer-gas injection rate [m^3/s]
ρ	Density of air [kg/m^3]
V_1	Air velocity before duct fitting [m/s]
V_2	Air velocity after duct fitting [m/s]
V	Air velocity in the duct [m/s]

1.0. INTRODUCTION

Indoor air quality, thermal comfort and energy use in buildings are largely dependent on the performance of HVAC systems. The pressure loss of ductwork supplying air to various zones can be calculated using computer models which incorporate pressure loss factors (k-factors) for duct fittings based on data given in the CIBSE guide "Reference Data" (1), and ASHRAE handbook "Fundamentals" (2). However, there are significant discrepancies concerning these data which can result in inaccurate sizing of fans used in HVAC systems and wastage of fan energy.

There are differences of up to several hundred percent between values quoted in the CIBSE and ASHRAE guides. In addition, they do not consider the interaction of duct fittings and they do not include many duct fittings used in HVAC systems. Designers are forced to make "intelligent guesses" for some k-factors used in their calculations. There is clearly a need for an expanded and accurate guide for k-factors of HVAC system components.

Data given by the CIBSE and ASHRAE guides have been determined experimentally using traditional instrumentation such as pitot tubes and orifice meters. These measurements can be greatly distorted by the size or geometry of ductwork, obstructions to the airflow or a high level of turbulence. Tracer-gas techniques offer an alternative approach for measuring airflow in ducts and can be used to provide accurate measurement of flow rates over a wide range of velocities without the requirement for a long duct length for the development of fully developed flow. The techniques are easy to use and have been successfully applied to airflow measurements in HVAC systems (3, 4).

The experimental approach for obtaining k-factors requires that ducts and duct fittings are built and assembled for each test; this could be costly if a wide range of fittings is to be tested. Computational fluid dynamics (CFD) can simulate duct flows accurately using the k-ε

or Reynolds stress models commonly employed in existing CFD packages (5). Furthermore, the numerical simplicity associated with modelling the components, which have relatively regular shapes and simple boundary conditions, also assists the accurate application of CFD.

This work examines the application of tracer-gas and CFD methods for estimation of k-factors of HVAC system components.

2.0 THEORY

2.1 k-Factors

When a fluid, such as air, flows through a duct containing duct fittings there is inevitably an energy loss due to factors such as friction and turbulence. The energy loss is manifested as a loss of static pressure across the duct component, ΔP_s. The magnitude of the static pressure loss can be shown to be proportional to the kinetic pressure in the duct, P_k. The k-factor (k) is defined such that:

$$\Delta P_s = k\, P_k \qquad (1)$$

In order to determine the k-factor for any given fitting both ΔP_s and P_k need to be determined experimentally for a range of flow rates.

In cases where there is a change in area between the two static pressure tappings, the resulting change in kinetic pressure must be accounted for as follows:

$$\Delta P_s = \Delta P_m - 0.5\rho(V_2^2 - V_1^2) \qquad (2)$$

2.2 Tracer-Gas Techniques

Throughout the experimental work the constant injection technique was used. In this method tracer gas is released at a constant rate, q. The concentration, C, of tracer gas is then measured downstream of the injection point. The flow velocity, v, can then be calculated using:

$$v = q/CA \qquad (3)$$

where A is the area of the duct. The kinetic pressure can then be determined from:

$$P_k = \rho V_2^2/2 \qquad (4)$$

where ρ is the density of air. The value of ΔP_s can be determined directly by the use of a manometer. The k-factor for the given component can then be calculated from (1).

2.3 Pitot Tube Technique

A pitot static tube in conjunction with a manometer can also be used to measure the flow velocity, although a traverse is needed in order to achieve an accurate value for the mean flow velocity. The pitot tube measurements were carried out at standard positions following the method described by CIBSE guide (1). The k-factor can then be calculated in the same way as for the tracer-gas technique.

3.0 EXPERIMENTAL

Fig. 1 shows a schematic diagram of the experimental set-up for use of tracer gas techniques. The injection rate of SF_6 was governed by the mass flow controller to be 1 litre per minute during the experiments. The use of a reservoir allowed the flow to be consistent. A sampling tube was placed into the duct to pump a sample from the duct through the gas analyser. The flow rate was controlled and filtered in order to allow the gas analyser to work accurately. An analogue manometer was used to measure the pressure difference between 8 pressure tappings across the double bend. For the pitot tube measurements a simple traverse was used, and a

mean value for the flow velocity was calculated using the same values from the static pressure tappings as for the gas analyser method.

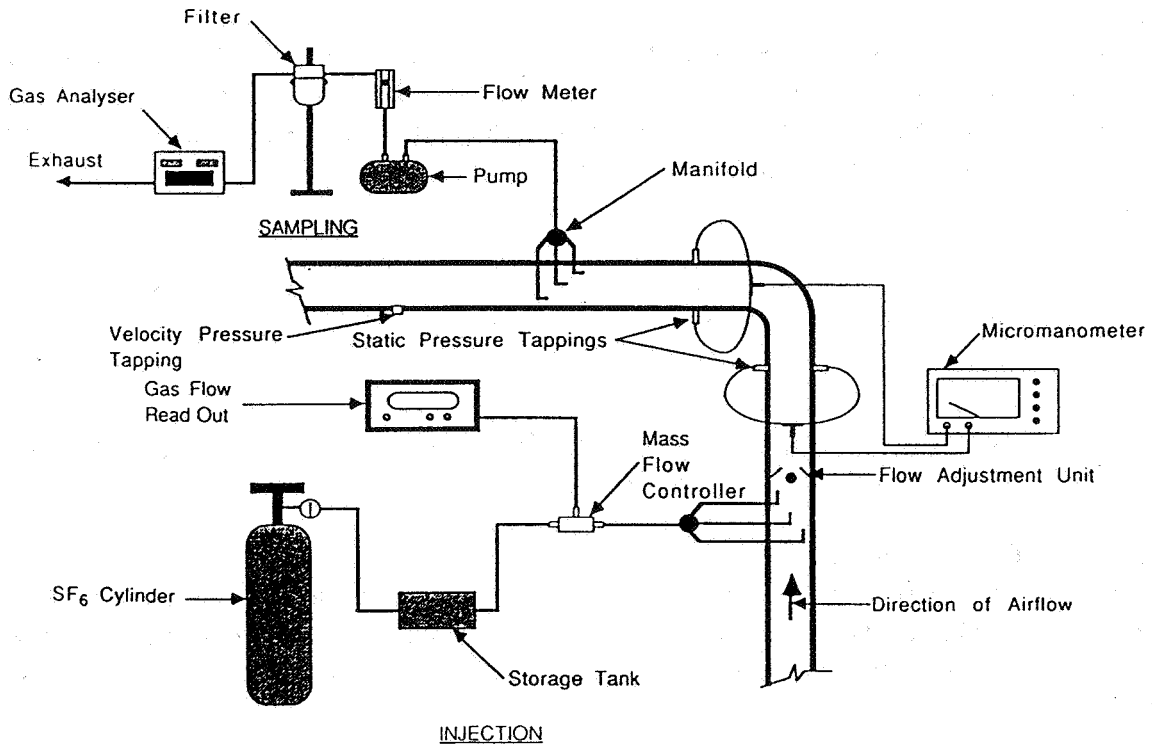

Fig. 1 Instrumentation for the constant-injection tracer-gas technique

4.0 RESULTS AND DISCUSSION

A large number of experiments were carried out to assess the effect of the distance between two 90-degree bends on the overall k-factor. Both the pitot tube and the tracer-gas technique were employed to provide a comparison between the two methods.

Figures 2 shows the relationship between ΔP_s and P_k over a range of duct flow rates for distances between the bends of 1.0m. The results from the pitot tube and the tracer-gas technique are displayed together in each case. In each case the value for ΔP_s is the mean value for the tappings at 25mm, 40mm, 55mm and 70mm from the bend. These points were selected since closer to the bend the flow is separated from the inside wall of the duct causing a lowering of the static pressure, and hence an error in the k-factor calculated. Further away from the bend the effect of friction from the duct would start to become important, and entrance effects might also cause errors if readings were taken closer to the inlet.

It can clearly be seen that the relationship between ΔP_s and P_k is linear, and passes through the origin, as the theory for k-factors suggests. Least squares regression has been

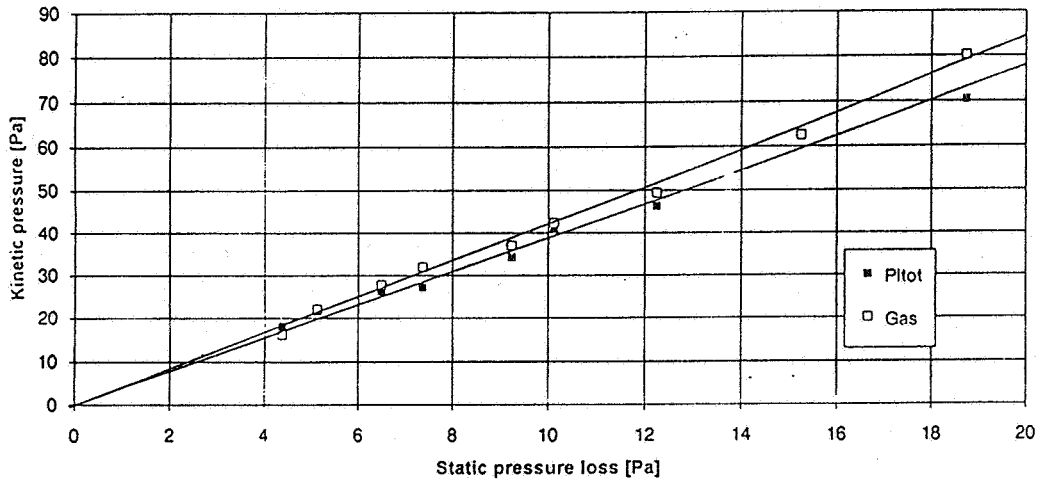

Figure 2. Pressure loss for two 90 degree bends 1.0m apart.

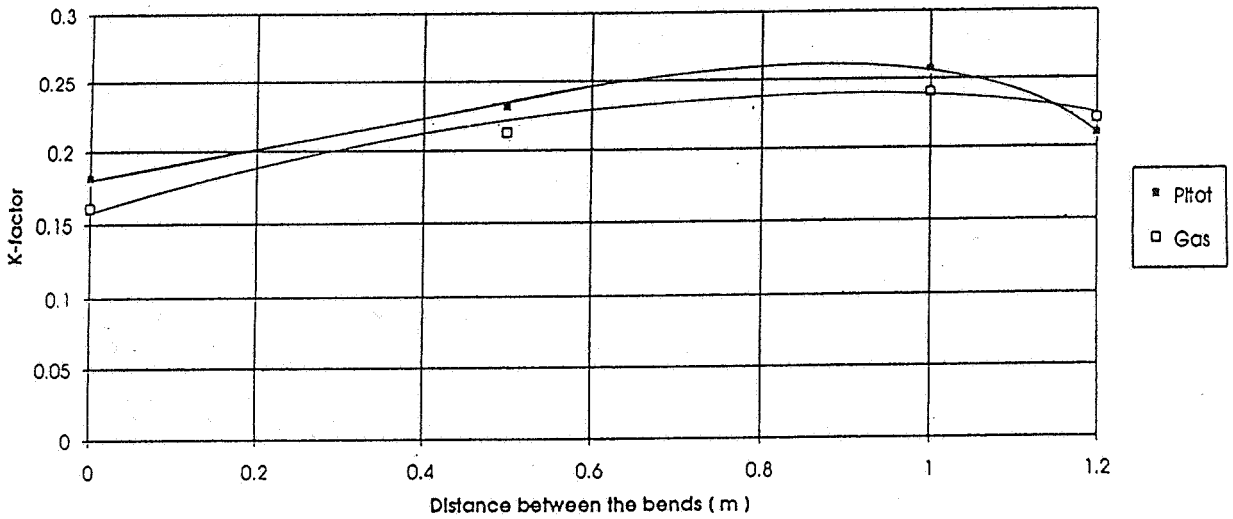

Figure 3. Variation of k-factors with distance between two 90 degree bends.

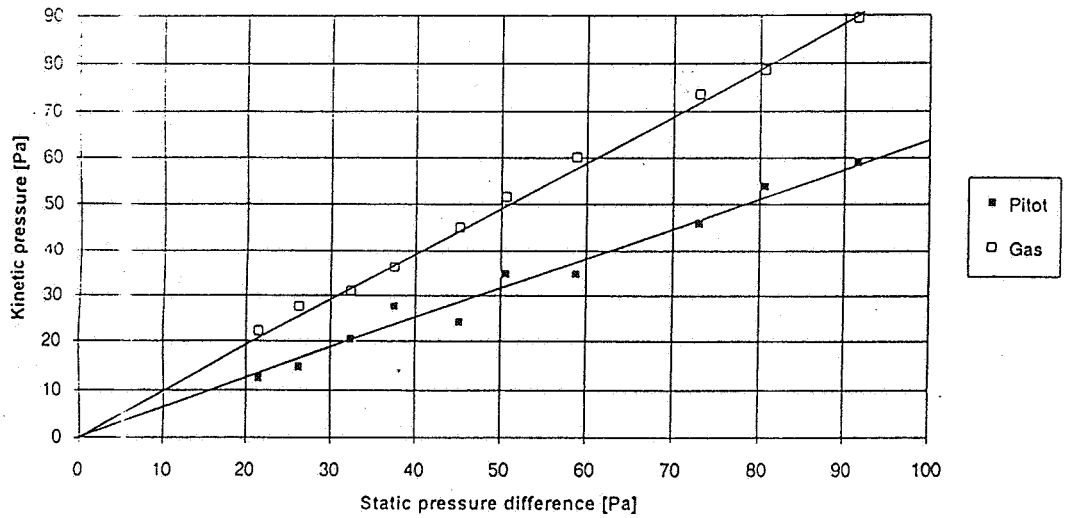

Figure 4. Pressure loss for a contraction followed by an expansion 1.0m apart.

applied to the data for each experiment in order to determine the k-factors. Figure 3 shows a chart of the variation of k-factor with distance between the two bends and Table 1 shows these results in tabular form along with the values quoted in the CIBSE and ASHRAE guides. The product moment rank correlation coefficient, R^2, is also shown as an indication of the closeness of the experimental data to the given straight line.

Figures 4 shows the relationship between ΔP_s and P_k over a range of duct flow rates for a contraction followed by an expansion respectively. In each case the reduction in area was of 50%. As for the 90 degree bends a mean value for the pressure drop was assumed. Although the actual pressure drop needed to be calculated as shown in section 2.1. The same pressure tappings were also used.

Table 1. k-factors from the measurement and ASHRAE and CIBSE guides

Distance apar	Gradient		K-factor				R squared	
of bends	Pitot	Gas	Pitot	Gas	CIBSE	ASHRAE	Pitot	Gas
0	5.507426	6.213388	0.181573	0.160943	0.25	0.24	0.977	0.985
0.5	4.33172	4.70437	0.230855	0.212568	0.23	0.26	0.941	0.96
1	3.886418	4.163717	0.257306	0.24017	0.23	0.26	0.994	0.995
1.2	4.76345	4.535674	0.209932	0.220474	0.23	0.26	0.921	0.987

From the experimental data it can be seen that:

i) The distance between two 90 degree bends does have an effect on the overall k-factor for the bend. This effect is of a parabolic nature. Neither the CIBSE or ASHRAE guides give a different value for the k-factor in this range, except for a full 180 degree bend with no separation, where ASHRAE give a small reduction in the k-factor, and CIBSE a small increase.

ii) The tracer-gas method gives a closer fit to a straight line than the pitot tube technique. It is therefore likely that the tracer gas results are more accurate. This is probably due to the fact that the tracer gas levels can be averaged over a long time period giving more reliable results while the pitot tube measures the velocity at 9 points and these are averaged.

iii) The tracer-gas method give a lower value (between 3.5 to 10% lower) for the k-factor than the pitot tube method. This is most likely due to the error caused from placing the pitot tube into the air flow, thus increasing the air flow rate locally around the pitot tube.

iv) Both the pitot tube and the tracer gas methods show that the k-factor is significantly reduced when there is no separation between the bends. Neither CIBSE or ASHRAE quote such a reduction, CIBSE even quote an increase. The error between the experimental tracer gas results and the value quoted by CIBSE is 36%. This is significantly large, especially considering it is only for a single component. It is true, however, that both the CIBSE and ASHRAE values are quoted for all bend geometries and are therefore an average of the k-factors for a large number of bend sizes. The experimental data presented here is only for a single geometry (that of a bend radius 1.5 times the duct width). Further experimentation would be required to ascertain whether the CIBSE and ASHRAE mean values are sufficiently accurate.

v) For the contraction the CIBSE value takes no account of the reducer angle; the k-factor is therefore at best only an approximation. The ASHRAE value for the particular geometry used in the experiments is similar to that obtained.
vi) Neither CIBSE or ASHRAE provided tables on the interactions between reducer and enlargement components. The best table available is the one used for interactions between two bends.

5.0 COMPUTATIONAL FLUID DYNAMICS SIMULATION

The computations were performed using the commercial flow simulation software FLUENT. The Reynolds stress terms in the averaged Navier-Stokes equations were computed using the standard two-equation k-ε model and in the region of low Reynolds number close to the walls, wall-functions were used instead. Most HVAC ducts have aspect ratios between 1 and 4, in which case, all sides of the duct exert significant influence on the character of the duct flow. It is therefore necessary to treat the simulation as a three-dimensional problem. The duct fittings examined in this CFD study are identical to those used in the experimental study described above. The assumption was made that during the computation, air velocity distribution at the entrance of a duct is uniform (6m/s) and that the flow direction is normal to the inlet cross-section. As the air enters and moves along the duct, the uniform velocity distribution gradually changes into a fully developed profile. The length over which this change is completed is referred to as the entrance length, where the friction and pressure loss are larger than in the fully developed parts of the duct. To avoid the entrance length effect interfering with the effect of the bend, the section of duct upstream of the bend must be long enough to allow the velocity profile to develop fully. An upstream duct length of 20 duct widths was used. A three-dimensional body-fitted co-ordinate (BFC) grid was used to allow accurate representation of the smooth curved bends, the axis of which form an arch with a radius of 0.3m, in the computational domain. Using the Cartesian grid system in such cases would mean that the curved duct walls be approximately modelled by a series of steps, which would cause great distortion of the flow patterns and pressure loss characteristics of the bend. The Navier-Stokes equations were discretised by a finite volume method and solved using the SIMPLE algorithm.

Fig. 5 shows the pressure contours in the double-bends described previously. The separation between the bends are, for the assemblies from top to bottom, 1.2m, 1.0m, 0.5m and 0m, respectively. Each contour line along the duct marks a further amount of pressure fall which is approximately 2 Pa. Clearly, the pressure drop in the vicinity of the bend is far greater than anywhere else in the duct. As can be seen, the pressure contour patterns in the two bends for the 1.2m-separation case are very similar to that of the 1.0m case. As the separation reduces to 0.5m, some of the contour lines in the two bends join together, but other parts of the contour patterns, including that before the upstream bend and that after the downstream bend, remain largely unchanged. This indicates that the pressure loss in the double bend is not affected by the shortening of the separation. As the separation falls to zero, more contour lines join together but the contour pattern before the upstream bend and that after the downstream bend are still relatively unaffected. Obviously, the pressure loss across the four double bends would be rather similar, which is borne out by examination of the detailed pressure loss data in the flow fields. The relative difference between the largest and smallest of the four pressure losses is less than 6%, which agrees quite well with the experimental results for double bends with separations 1.2m, 1.0m and 0.5m. The measured pressure loss of the double bend with 0m separation is, however, much smaller than the other

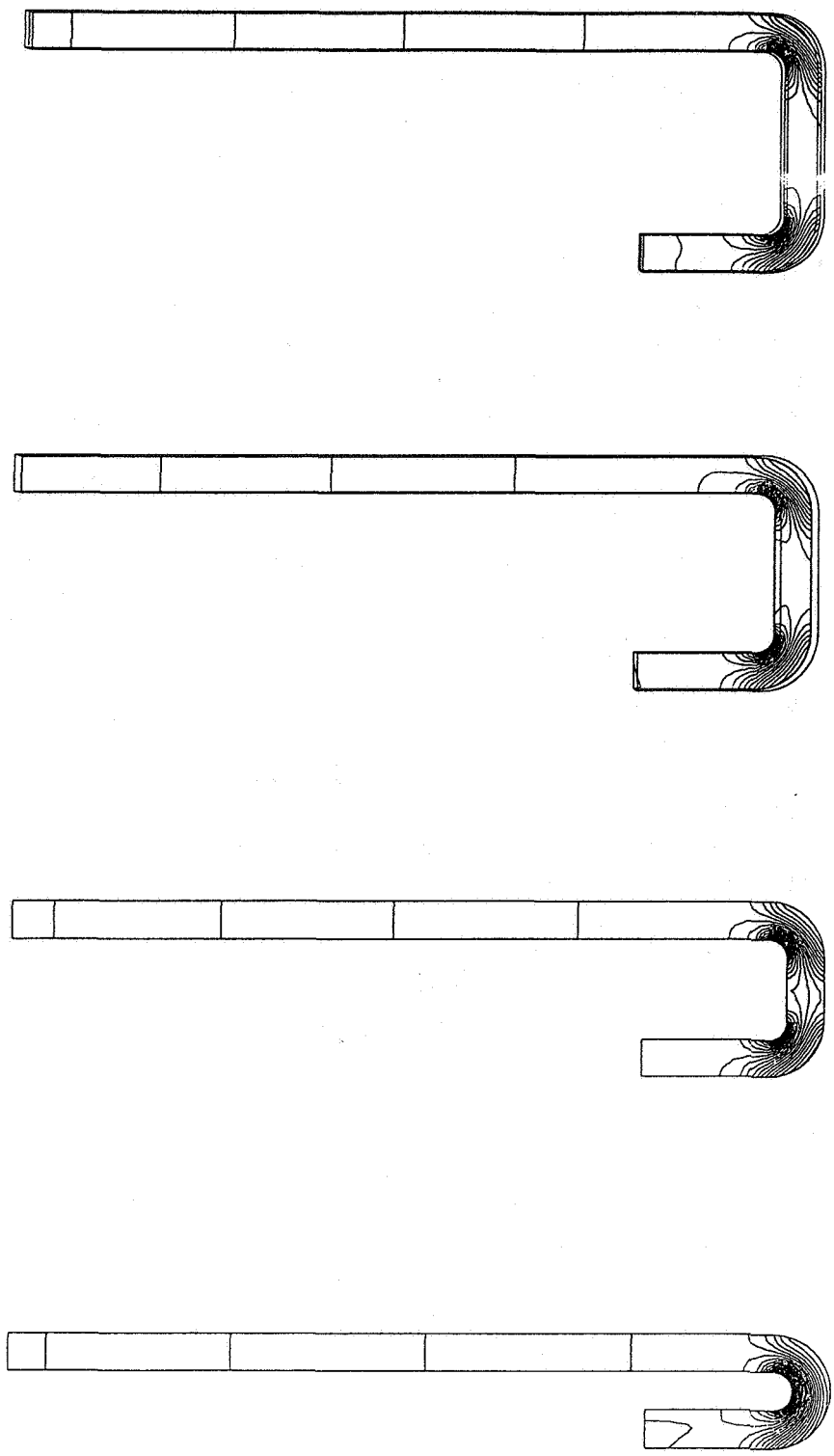

Figure 5. Pressure contour patterns in double-bends

three, with relative difference of about 33% based on the largest pressure loss at 1.0m separation. The trend predicted by CFD is in very good agreement with the CIBSE and ASHRAE data, as shown in the sixth and seventh column of Table 4.1.

6.0 CONCLUSIONS

The experimental data acquired thus far show that there is a relationship between the k-factor and the separation between two 90 degree bends. Furthermore, there is a significant reduction of the k-factor as the distance between the bends becomes small. Although the ASHRAE and CIBSE data do give an allowance for this reduction, it appears that the change is greater than that quoted in the guides. Further work would be required to ascertain whether this is true for all configurations, or just those used in the current experiments.

The experiments with the reducer-enlarger combination have demonstrated that there is considerable interaction between duct components, and that this interaction can have a large effect on the overall k-factor. Neither ASHRAE or CIBSE give data on such effects. The interaction effect between reducers and enlargements is significantly different from that for two 90 degree bends. Further work would be required to determine how individual components are affected by the proximity of other components.

The CFD method has been used to predict k-factors of double bends of various separation distances. Flow fields in duct fittings were simulated by solving the three dimensional Navier-Stokes equations with body-fitted co-ordinate grids, the k-ε model and a finite volume method. It was found that variation of the separation distance between the double bend causes only minor changes (6%) in its k-factor. This result agrees well with the CIBSE and ASHRAE data and, except for one measurement point (zero separation), also agrees well with the experimental data reported above. It should be pointed out however, that the accuracy of CFD and the consistency of the agreement need to be verified by studying interactions of other types of duct fittings.

7.0 REFERENCES

1. The Chartered Institution of Building Services Engineers (1986). *CIBSE Guide "Reference Data"*, London, CIBSE.
2. American Society of Heating, Refrigeration and Air Conditioning Engineers (1989). *ASHRAE Handbook "Fundamentals"*, Atlanta, ASHRAE.
3. Riffat, S.B., Cheong, K.W. and Holmes, M. (1991) 'Measurement of entrance length and friction factor of ducts using tracer-gas techniques', *Proceedings of 12th AIVC Conference*, 321-334.
4. Cheong, K.W. and Riffat, S.B. (1992). 'A new method for determination of velocity pressure loss-factors for HVAC system components', *Proceedings of 13th AIVC Conference*, 549-561.
5. Shao, L. and Riffat, S.B. (1993) ' CFD for prediction of k-factors of duct fittings', *International Journal of Energy Research*, (in press).

ACKNOWLEDGEMENTS

The authors wish to thank the Engineering and Physical Science Research Council (EPSRC) for their financial support.

The Role of Ventilation
15th AIVC Conference, Buxton, Great Britain
27-30 September 1994

Measurement and Modelling of Aerosol Particle Flow in an Environmental Chamber

N Adam, K W Cheong, S B Riffat, L Shao

Building Technology Group, School of Architecture,
University of Nottingham, NG7 2RD United Kingdom

SYNOPSIS

This paper is concerned with measurement of air and aerosol particle exchange efficiency in a single zone chamber. Aerosol particles and tracer gases were injected into the chamber and their concentrations were monitored as a function of time. The chamber was provided with supply and exhaust terminals which allowed various airflow and particle patterns (e.g. piston flow, displacement flow) to be investigated. The effect of airflow pattern on deposition rate of aerosol particles on the surfaces of the chamber was determined. This paper also describes the application of computational fluid dynamics (CFD) modelling for the prediction of particle flow in the chamber. The CFD model, FLUENT, was used for this investigation and results were compared with particle and tracer-gas measurements.

LIST OF SYMBOLS

a_1, a_2, a_3	constants
A	surface area of chamber, (m^2)
C_D	drag coefficient
d	diameter of particle, (μm)
F_D	drag force, (N)
F_X	force acting on a particle due to virtual mass and pressure gradient in a fluid, (N)
I	tracer-gas exchange rate, ($\mu g/m^3h$ or h^{-1})
P	particle-exchange rate, ($\mu g/m^3h$ or h^{-1})
Re	relative Reynolds number
t	time, (s)
u	component of velocity in the x direction, (m/s)
V	velocity, (m/s)
V_Z	volume of zone, (m^3)
α	particle deposition rate, ($\mu g/m^2h$)
η_a	average air exchange efficiency
η_p	average particle exchange efficiency
ρ	density, (kg/m^3)
τ_{TE}	age of air at the exhaust terminal, (min)
τ_{Ti}	age of air at point i in the chamber, (min)
τ_{PE}	age of particle at the exhaust terminal, (min)
τ_{Pp}	age of particle at point p in the chamber, (min)
μ	molecular viscosity of air, (kg/ms)
∞	local air
p	particle

1. INTRODUCTION

Particulate pollutants in buildings can have damaging effects on the health of occupants. Studies have shown that indoor aerosol particles influence the incidence of sick building syndrome [1]. Some airborne particles are associated with allergies because they transport viruses and bacteria. Particulate pollutants can be transported between zones; this can have serious effects in hospitals and buildings used by the micro-electronic and pharmaceutical industries [2]. Deposition of airborne particles in museums and galleries may lead to perceptible soiling within a short period and ultimately result in damage to works of art [3].

The concentration of indoor aerosol particles can be reduced by using different ventilation strategies such as displacement and perfect mixing. However, there are insufficient data to quantify the effectiveness of these methods, as removal of particles is influenced by particle deposition rate, particle type, sizes, sources and concentrations.

This work aims to study various ways of removing aerosol particles from a mechanically-ventilated room and determine the effectiveness of each technique. This study also looks at the distribution of particles at four different locations in the chamber. Computational fluid dynamics (CFD) was also used to model the particle movement.

2. EXPERIMENTAL WORK

Measurements were carried out in a tightly-sealed chamber (3m x 2.5m x 2.4m) as shown in Figure 1. A variable-speed axial fan supplies fresh air to the chamber via a 0.3m diameter ductwork and 2m x 0.5m diffusers. Air is removed from the chamber via three diffusers which allows different ventilation strategies (shown in Figure 2) to be examined. The chamber was used for measurement of air exchange efficiency and particle exchange efficiency.

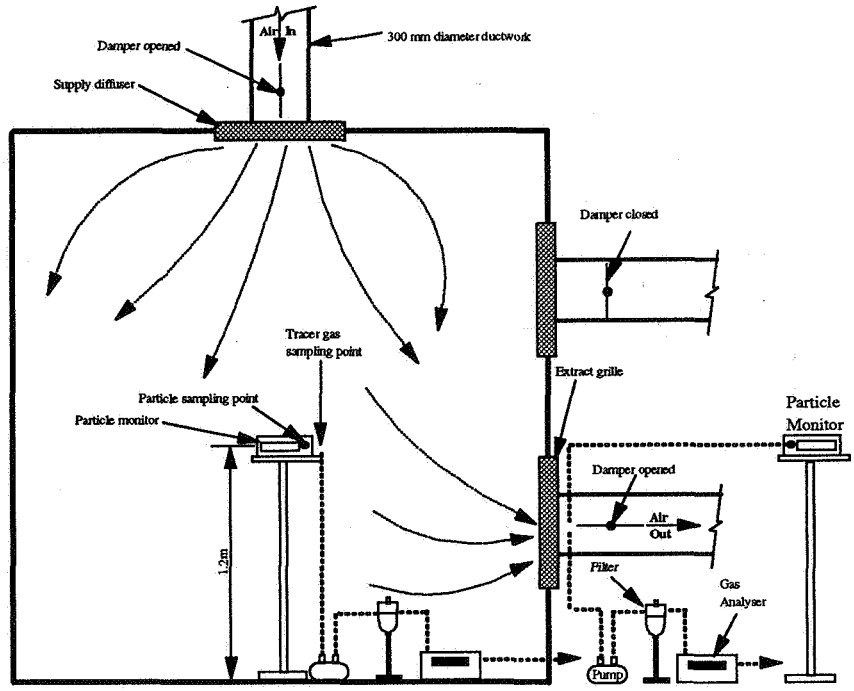

Figure 1 Schematic of the chamber and instrumentation

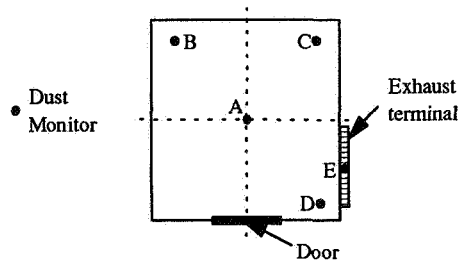

Figure 1a Location of dust monitors in environmental chamber, (Plan)

The experimental procedure involved injecting SF_6 tracer-gas and oil-smoke particles into the chamber with all dampers shut and all fans off. A desk fan was used to assist mixing. After a mixing period of 10 minutes, the desk fan was switched off. Once a uniform concentration of tracer-gas and smoke particles was achieved in the chamber, dampers at respective diffusers were opened and the axial fans were switched on. At the same time, simultaneous monitoring of the concentration of tracer-gas and smoke particles ($0.5\ \mu m < d < 2\ \mu m$) commenced at the exhaust terminal, in the centre of the chamber and three other locations (see Figure 1a). An infra-red gas analyser type BINOS 1000 made by Rosemount Ltd., U.K. and an infra-red particle monitor type Grimm 1.100 manufactured by Grimm Ltd., Germany were used to monitor the concentrations of tracer-gas and particles, respectively. A series of five different airflow rates was used for each condition.

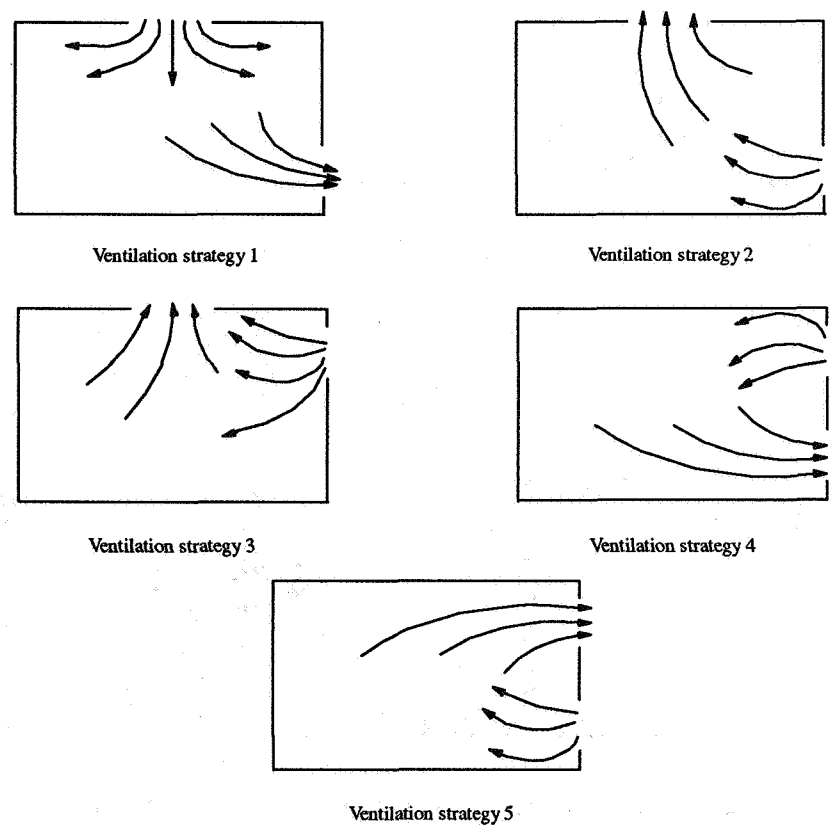

Figure 2 Ventilation strategies for experiment

3. RESULTS AND DISCUSSION

Experimental work was carried out in the chamber to determine average air exchange efficiency for various ventilation strategies using the tracer-gas decay method, defined as:

$$\eta_a = \frac{\tau_{TE}}{\tau_{Ti}} \quad (1)$$

and average particle exchange efficiency defined as:

$$\eta_p = \frac{\tau_{PE}}{\tau_{P_p}} \quad (2)$$

Results are given in Table 1. Location D gives the lowest average particle efficiency. Short circuiting may give $\eta_p > 1.0$ for strategies 3, 4 and 5. Strategy 2 gives a higher overall η_p than strategy 1. The particle exchange rates were found to be higher than tracer-gas exchange rates. The difference in tracer-gas and particle exchange rates is due to deposition (or adsorption) of particles on the surfaces of the environmental chamber. This was estimated using the following equation:

$$\alpha = (P - I) \times \frac{V_z}{A} \quad (3)$$

Strategy 1 gives deposition 0.10 - 2.09$\mu g/m^2h$ only at 17 h^{-1}. Strategy 2 gives deposition 0 - 1.80$\mu g/m^2h$ for all ventilation rates. Strategy 3 gives deposition 0.09 - 3.69$\mu g/m^2h$ for 17 - 25.4h^{-1}. Strategy 4 gives deposition 0 - 4.98$\mu g/m^2h$ for all ventilation rates. Strategy 5 gives deposition 0 - 1.16$\mu g/m^2h$ for all ventilation rates.

Strategy	Air change rate, (h^{-1})	τ_{PA}(mins) (η_A)	τ_{PB} (mins) (η_B)	τ_{PC}(mins) (η_C)	τ_{PD}(mins) (η_D)	τ_{PE} (mins)	τ_{TA}(mins) (η_a)	τ_{TE} (mins)
1	25.4	3.53 (0.90)	3.34 (0.95)	3.45 (0.92)	3.72 (0.85)	3.18	1.66 (0.91)	1.52
	17	4.46 (0.81)	3.37 (1.07)	3.98 (0.91)	4.98 (0.73)	3.61	2.18 (0.80)	1.74
	14.1	9.68 (0.75)	8.48 (0.85)	9.57 (0.75)	18.15 (0.40)	7.21	3.76 (0.96)	3.61
	7.1	23.90 (0.38)	10.37 (0.86)	11.32 (0.78)	11.92 (0.75)	8.88	5.20 (0.88)	4.55
	4.2	23.40 (0.68)	16.99 (0.93)	21.80 (0.73)	24.02 (0.66)	15.82	11.01 (0.90)	9.88
2	25.4	2.92 (0.84)	3.74 (0.66)	3.55 (0.69)	3.28 (0.75)	2.46	0.74 (1.16)	0.85
	17	4.33 (1.08)	4.74 (0.98)	4.67 (1.00)	5.27 (0.89)	4.67	1.86 (1.07)	1.98
	14.1	4.89 (1.10)	5.00 (1.07)	4.94 (1.08)	5.73 (0.93)	5.35	2.43 (1.01)	2.44
	7.1	10.16 (1.03)	10.39 (1.00)	10.53 (0.99)	11.47 (0.91)	10.42	6.07 (0.98)	5.93
	4.2	69.13 (0.50)	48.05 (0.72)	57.43 (0.60)	59.78 (0.58)	34.51	25.39 (1.00)	25.35
3	25.4	2.33 (1.01)	2.59 (0.91)	2.83 (0.83)	3.01 (0.79)	2.36	0.79 (1.02)	0.81
	17	4.96 (1.03)	4.62 (1.11)	5.23 (0.98)	5.41 (0.95)	5.11	1.53 (1.03)	1.58
	14.1	12.96 (0.86)	11.98 (0.92)	12.23 (0.91)	12.42 (0.89)	11.07	3.61 (0.95)	3.44
	7.1	17.65 (1.00)	15.47 (1.14)	17.18 (1.03)	18.55 (0.95)	17.67	7.96 (2.57)	20.45
	4.2	15.62 (1.12)	18.50 (0.95)	22.38 (0.78)	19.34 (0.90)	17.49	9.11 (1.25)	11.41
4	25.4	2.31 (1.11)	2.73 (0.94)	2.91 (0.88)	3.13 (0.82)	2.56	1.12 (1.00)	1.12
	17	3.72 (0.96)	4.25 (0.84)	4.67 (0.77)	4.63 (0.77)	3.58	1.34 (0.81)	1.09
	14.1	3.79 (0.99)	3.83 (0.98)	4.16 (0.90)	4.47 (0.84)	3.76	1.59 (0.91)	1.45
	7.1	5.92 (1.21)	5.35 (1.34)	5.23 (1.37)	7.98 (0.90)	7.16	3.46 (0.60)	2.06
	4.2	16.05 (0.70)	27.38 (0.41)	22.24 (0.51)	28.94 (0.39)	11.24	12.59 (0.75)	9.39
5	25.4	2.91 (1.17)	4.63 (0.74)	4.92 (0.69)	5.42 (0.63)	3.41	0.92 (0.88)	0.81
	17	4.74 (1.14)	6.29 (0.86)	6.20 (0.87)	7.09 (0.76)	5.41	1.98 (0.83)	1.65
	14.1	6.91 (0.98)	6.77 (1.00)	6.90 (0.98)	7.62 (0.89)	6.77	3.03 (0.97)	2.92
	7.1	12.58 (0.87)	10.59 (1.03)	11.40 (0.96)	11.95 (0.92)	10.95	6.14 (1.19)	7.29
	4.2	35.55 (0.81)	33.15 (0.87)	35.50 (0.81)	37.05 (0.78)	28.71	20.28 (0.96)	19.40

Table 1 Experimental results

4. CFD MODELLING

The CFD code FLUENT was used to simulate three-dimensional, isothermal and non-reacting particle movement in the previously described, ventilated single zone, by solving the Navier-Stokes equations and equations governing the dynamic behaviour of particles. The particle equations, in Lagrangian formulation as shown below, take into account the effect on particle movement of particle inertia, aerodynamic drag and gravitational force:

$$\frac{du_p}{dt} = F_D(u_p - u_\infty) + \frac{g_x(\rho_p - \rho_\infty)}{\rho_p} + F_x \qquad (4)$$

$$F_D = \frac{18\mu}{\rho_p D_p^2}\frac{C_D Re}{24} \qquad (5)$$

$$Re = \frac{\rho D_p |V_p - V_\infty|}{\mu} \qquad (6)$$

$$C_D = a_1 + \frac{a_2}{Re} + \frac{a_3}{Re^2} \qquad (7)$$

These are the equations for the x-coordinates in a Cartesian system and those for the other two axes are in similar forms. The 3-D computation domain used in this CFD analysis is shown in Figure 3 and it has the same dimensions, opening positions and opening sizes as discussed in the previous section. The amount of air supplied to the room through the inlet and that extracted via the outlet are both 254m^3/h, giving rise to an average flow velocity of 0.14m/s at the openings. Particles are assumed to rebound from solid boundaries with a coefficient of restitution of 1. It is also assumed that the particles are spherical, which is reasonable, considering that the particles used in corresponding experiments are tiny droplets, shaped by the force of surface tension. The density of the oil used for smoke generation and thus that of the particles is 865kg/m^3. One thousand particles of identical diameter (2μm) and properties were uniformly distributed in the domain at the beginning of the test and their tracks and time of escape through the outlet were monitored. The number of particles remaining in the domain and thus the average particle concentration at any given moment was recorded. This was then compared with corresponding experimental results to determine the accuracy of the CFD simulation.

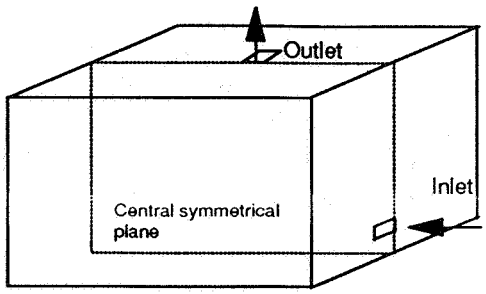

Figure 3 Schematic of building zone used in computation

Figure 4 shows the predicted (squares) and measured (short line sections) particle concentration histories. The normalised concentrations enable direct comparison between the two histories although greatly different number of particles were involved in the prediction and the tests because computing resources impose practical limits on the number of particles that can be traced. Both the predicted and the measured concentrations were assumed to have a relative concentration of unity at 60 seconds. This time lag allows the flow in the test chamber to be reasonably established and stable from 0 second. As can be seen, particle concentrations decreased sharply indicating rapid removal of particles from the test chamber through the outlet by the ventilating flow. In both experiment and simulation, the concentration is close to zero at 20 minutes, although the decrease in the former is slower than that in the latter. This discrepancy is probably due to the rather uncertain boundary conditions, in terms of particle deposition and resuspension, for the test chamber walls. Two particle sizes were used, 2μm (the same as that used in the experiments) and 10μm, but no difference in particle behaviour were observed in the simulation results under the conditions adopted in this study.

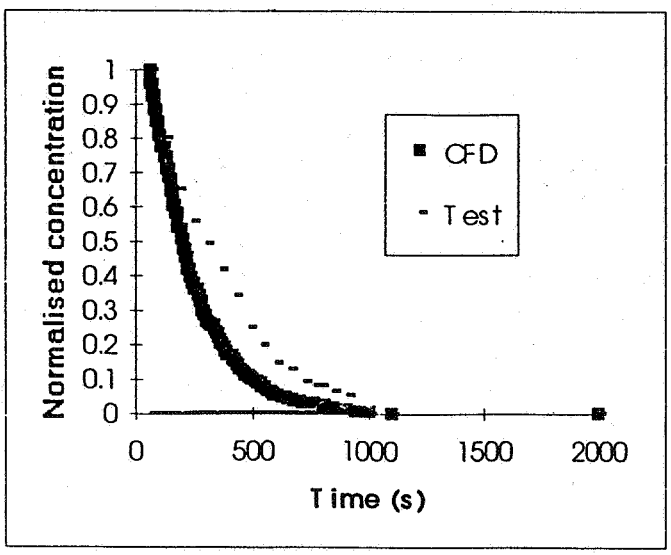

Figure 4 Histories of average particle concentration obtained from CFD and tests

5. CONCLUSIONS

i) Displacement flow has high values of average particle effectivenes and average air effectiveness compared with other flow strategies used for this study.

ii) The distribution of particles in the environmental chamber is not uniform, the corner away from the door (Point D) has the lowest age-of-particle.

iii) CFD simulation of particle movement has been carried out using the CFD code FLUENT. The history of particle concentration was predicted by monitoring 1000 particles uniformly distributed in the computation domain at the beginning of the tracking excercise. Comparison of the predicted history with that obtained from experiments shows reasonable agreement, which could be further improved by adopting more realistic boundary conditions in the CFD simulation.

ACKNOWLEDGEMENTS

The authors wish to thank the financial support of the Engineering and Physical Sciences Research Council (EPSRC).

REFERENCES

1. BERGLUND, B., BRUNEKREEF, B., KNOPPEL, H.,LINDVALL,T.,MARONI, M.,MOLHAVE and SKOV, P.
"Effects of Indoor Air Pollution on Human Health"
Report No. 10, European concerted action "Indoor Air Quality and Its Impact on Man" 1991

2. FARRANCE, K. and WILKINSON, J.
"Dusting Down Suspended Particles"
Building Services 12, 1990, pp45-46.

3. NAZAROFF, W.W. and CASS, G.R.
"Protecting museum collections from soiling due to the deposition of airborne particles"
Atmospheric Environment, Vol 25A, No. 5/6, 1991, pp841-852.

The Role of Ventilation
15th AIVC Conference, Buxton, Great Britain
27-30 September 1994

Full Scale Modelling of Indoor Air Flows

F Steimle, J Röben

Universität Essen, Angewandte Thermodynamik und Klimatechnik, Universitätsstrasse 15, 45141 Essen, Germany

Synopsis

As a result of the "Sick Building Syndrome" (SBS) the confidence of operators of office buildings into HVAC technologies has suffered a considerable drop. One of the most urgent questions before reconstructing or renovating old office buildings is, therefore, whether the air conditioning system to be installed will lead to increasing complaints on behalf of the occupants and how to prevent them. As for indoor air flows, one possibility is given by full scale model experiments leading to results which are very much like the future effective values.

The poster presents the modelling of indoor air flows in an office room. The model chamber, and the monitoring of the measurements are explained. The measured parameters are temperature and air velocity during an extremely hot summer day and an extremely cold winter day, respectively. All measurements were carried out under almost real conditions, i.e. the model chamber was equipped with office furniture and thermal loads were introduced into the room.

An additional advantage of this kind of experiments is that operators, architects, designers, work committee members etc. can have a look at the office rooms in the planning stage so that possible changes can easily be decided and carried out.

1 Introduction

During the last 20 years ventilation systems, mainly air conditioning systems, have gained more and more importance for large buildings. In many branches of production the use of an air conditioning system is vitally necessary, because it has very often a substantial influence on the quality of products. But the air conditioning of office buildings is also important. Correctly air conditioned working areas arrange thermal comfort and can increase the productivity at the place of work and also prevent absence by illness.

In line with increasing numbers of air conditioned buildings the complaints of the building owners and the employees have also increased. The complaints were mainly related to: low or high indoor temperature, low or high humidity, draughts, unpleasant noise level and high ernergy costs. Above all mistakes are made again and again with the air distribution in the rooms. But especialy the air distribution in the room decides about the physiological feeling of the people and the energy consumption of the air conditoning system.

The so-called "Sick Building Syndrome" describes how feel increasing disturbed people by wrong air conditioned rooms.

To avoid mistakes it is useful to make investigations about the air conditioning system in combination with the geometry of the rooms in an early planning stage. The losses by possible bad investment through wrong choice of the air conditioning system and high absenteeism are so big that such investigations are often profitable.

2 Experimental arrangement

The Institute of Applied Thermodynamics and Air Conditioning, University of Essen, possesses a laboratory with a test room to investigate the indoor air flows. In this test room all modes of operation can be simulated on the scale of 1:1. It is possible to investigate different air distribution systems and the figures 1 to 4 show schematicly most of the systems used in practice.

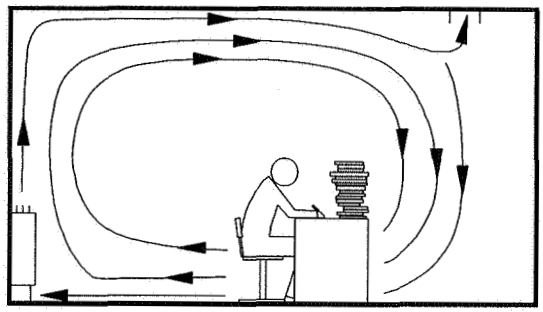

Fig. 1: Air distribution by tangential air circulation (Induction unit)

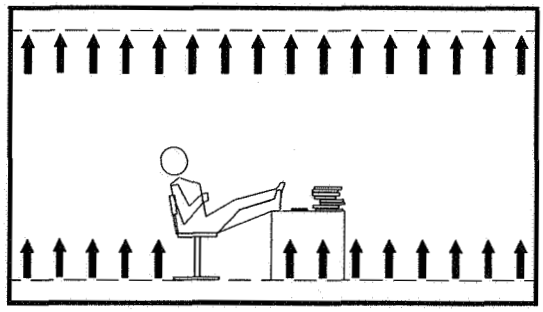

Fig. 3: Displacement flow by air circulation from buttom to top

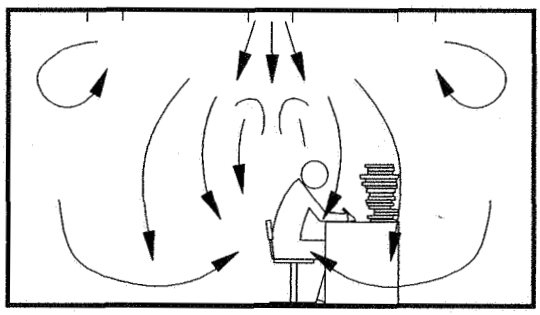

Fig. 2: Air distribution by diffused air circulation

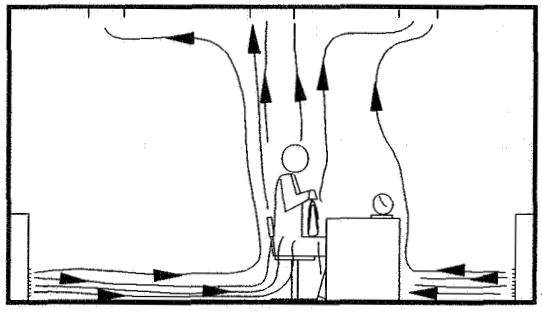

Fig. 4: Displacement flow by displacement ventilation

The test room which is described in the next chapter is equipped with induction units placed under the windows and a specific room ceiling. The room is a replica of a real office in a building which e.g. is to be renovated, and the investigation is made by using the original office furniture.

2.1 Test room

The test room is equipped with four walls, a floor, and a ceiling to avoid disturbing influence from the laboratory. Figure 5 shows the test room with its dimensions in the side view. Two of the walls are painted black and a $0.5 \cdot 0.5$ m grid is stuck on them with a white adhesive tape to get a better contrast when visualizing the flow by smoke.

One of the walls is built true to scale of the original building facade. The window legde is in its geometry and its heat transfer attitude the same as in the original building. The overall coefficient of the heat transfer of the windows in the test room corresponds to the original windows. The front wall (Fig. 6) is made of glass to have a control of the measurements and the experiments with smoke during a special operating condition.

The floor consists of a thick layer of bottom plates and it is built on stilts. The complete test room with exception of the parapet is surrounded by constant air conditions, so that there is no influence of the walls or the floor of the laboratory.

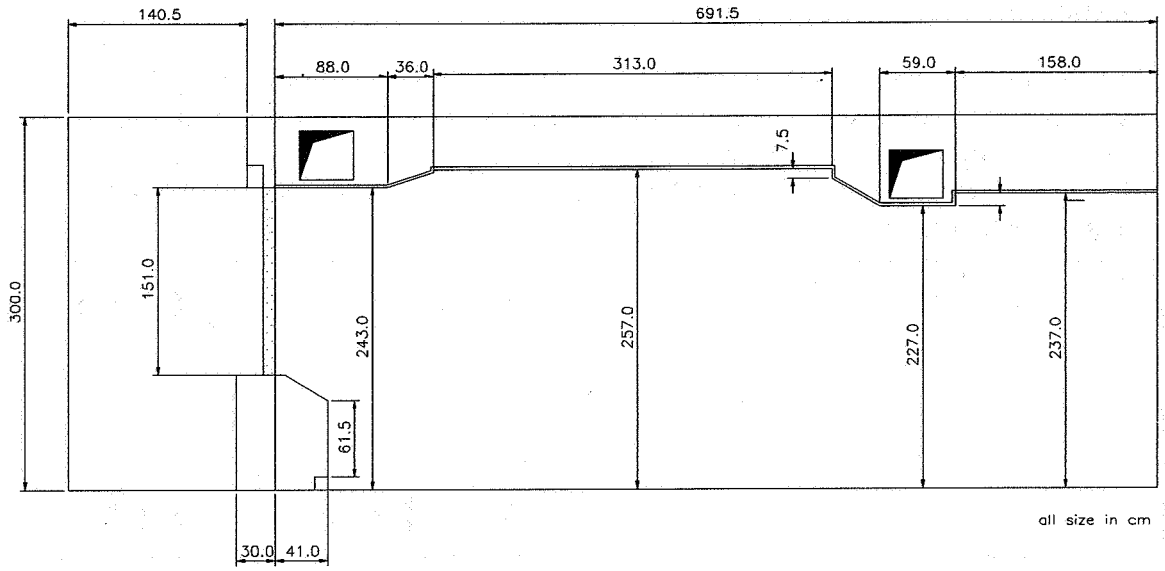

Figure 5: Side view of the test room

2.2 Climatic chamber

The climatic chamber is situated on the window legde of the test room (Fig. 6). The chamber is well insulated to the laboratoy and it is possible to adjust different weather conditions.

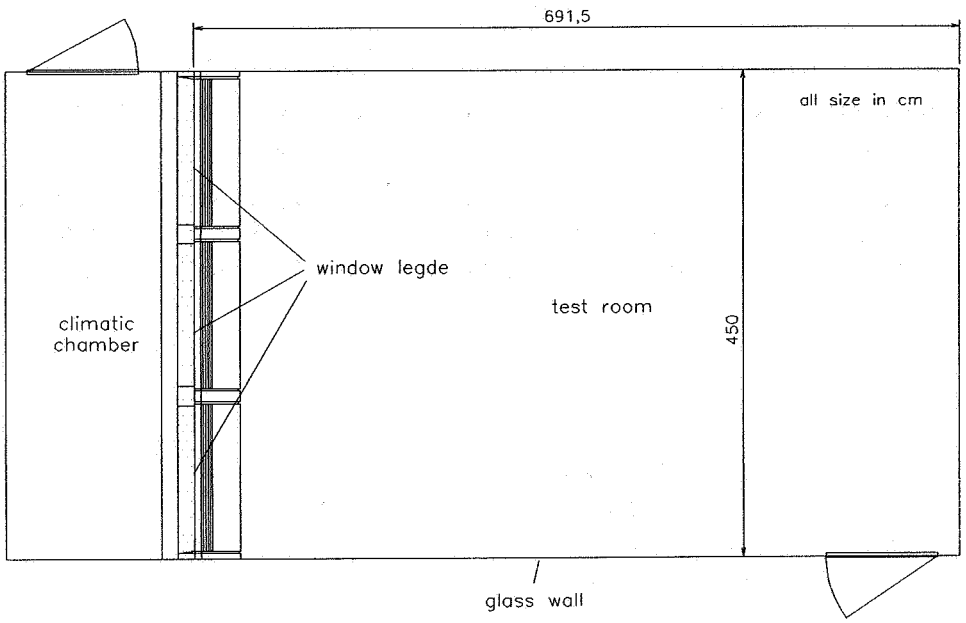

Figure 6: Setup of the test room and the climate chamber

By a refrigerating machine it is possible to get winter conditions with temperatures of -15°C and with a heater fan we get summer conditions (+32°C) in the climate chamber. This range of temperature corresponds to the German standard DIN 4701 (Rules for the calculation of the heat requirement of buildings) and VDI 2078 (Calculation of the cooling load of air conditioned rooms).

3 Measuring device

For the evaluation of the indoor air climate referring to the thermal comfort the following quantities are primarily important and have therefore to be measured in the test room and the climate chamber:

- Flow of the cold water
- Flow of the warm water
- Supply air flow
- Extract air flow
- Supply nozzle presurre (Induction unit)
- Temperature of the cold and warm water supply
- Temperature of the cold and warm water return
- Supply air temperature
- Extract air temperature
- Surface temperature of the windowpane and windowframe
- Indoor air temperatures
- Temperatures in the climate chamber
- Air velocities in the test room

3.1 Equipment

Figure 7 gives a schematic survey of the fundamental setup of the measuring device. To connect peripheral instruments like a sensor with a computer an additional circuit, a so-called interface, is nessesary. They adapt the computer and peripherial instruments.

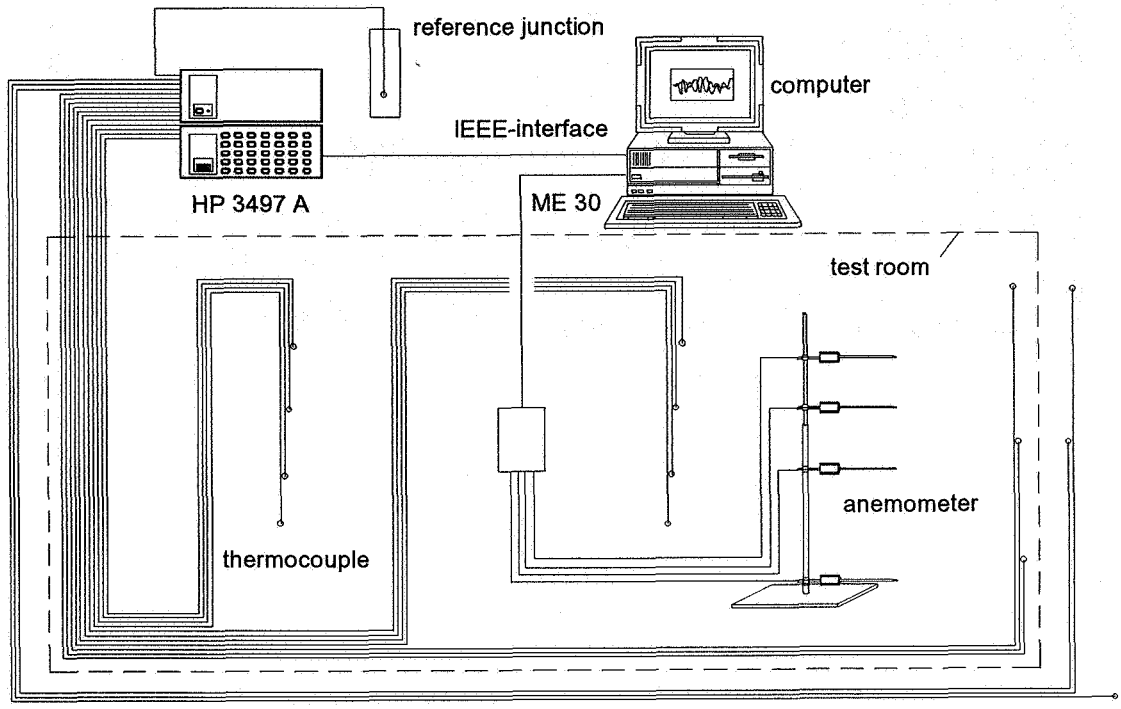

Figure 7: Setup of the measuring device

The measuring device needs a lot of single instruments and interfaces. The following instruments are used by the measurement of the air flow in the test room:

- One AT-80286-12 MHz Computer with 1 MByte RAM, MS-Dos 5.0 operating system and 40 MByte hard disk
- One high resolution monitor with VGA-graphic-card

- One Hewlett Packard HP 3497 A Scanner
- One IEEE-488 interface
- One Meilhaus ME30 multifunction-card

3.2 Control of the measurements

Before the actual measurement can be started the conditions must be constant. Therefore a permanent control of the temperatures is very important. Figure 8 shows the monitor display during the contol measurement.

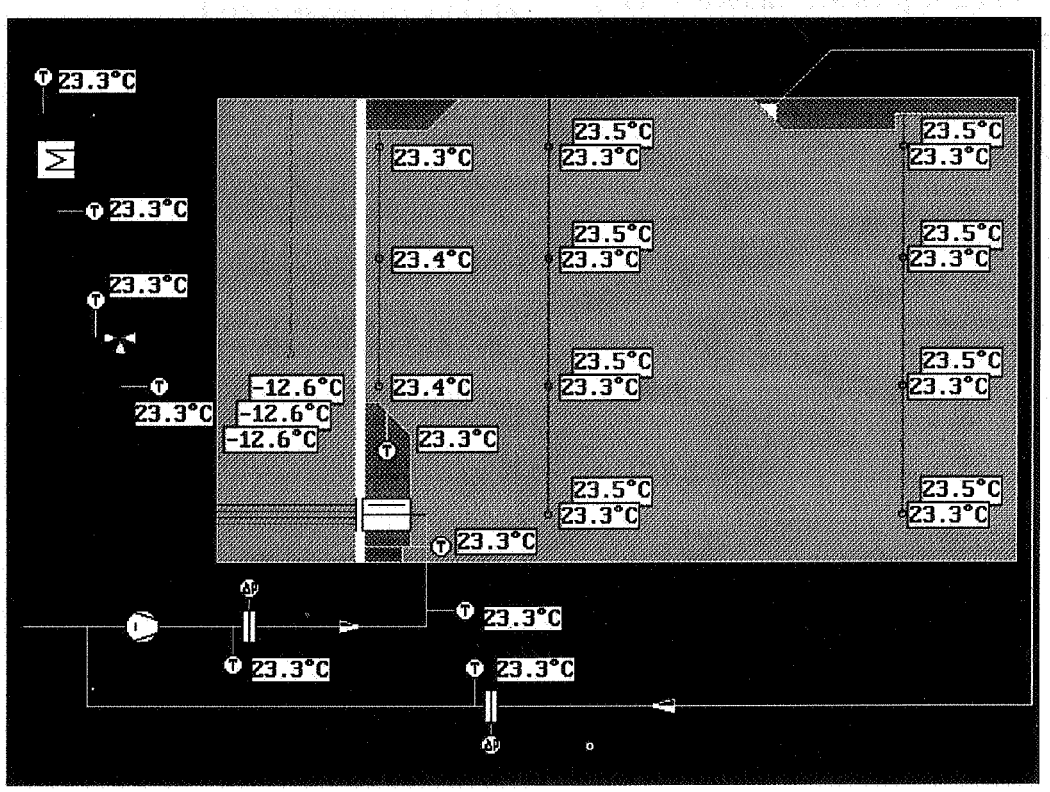

Figure 8: Control-graphic of the testing plant

The graphic shows the test room and the climate chamber and also water and air supply for the induction units. All temperatures are indicated in the graphic at those places where they are measured the temperature in the testing plant. If there is a defect or an error in the test plant, it is shown directly on the screen and can be repaired adequatly. The vertical line in the test room and the climate chamber represents the thermocouples hanging from the ceiling. The temperatures which are very close together on the screen are in the test plant next to each other. If the conditions are constant the investigation of the air flow in the test room can be started.

The air velocity is measured by thermal anemometers and every measured value is shown on the computer screen (Fig. 9). The velocity-graphic is permanently updated. All measuring points of one anemometer are connected by a line and indicated with the same colour, so that it is easy to differentiate the four anemometers. The real air velocity is not represented in this picture. If the maximum of the shown measuring time in the picture is reached (30 seconds in Fig. 9), the graphic and the time axis will be updated.

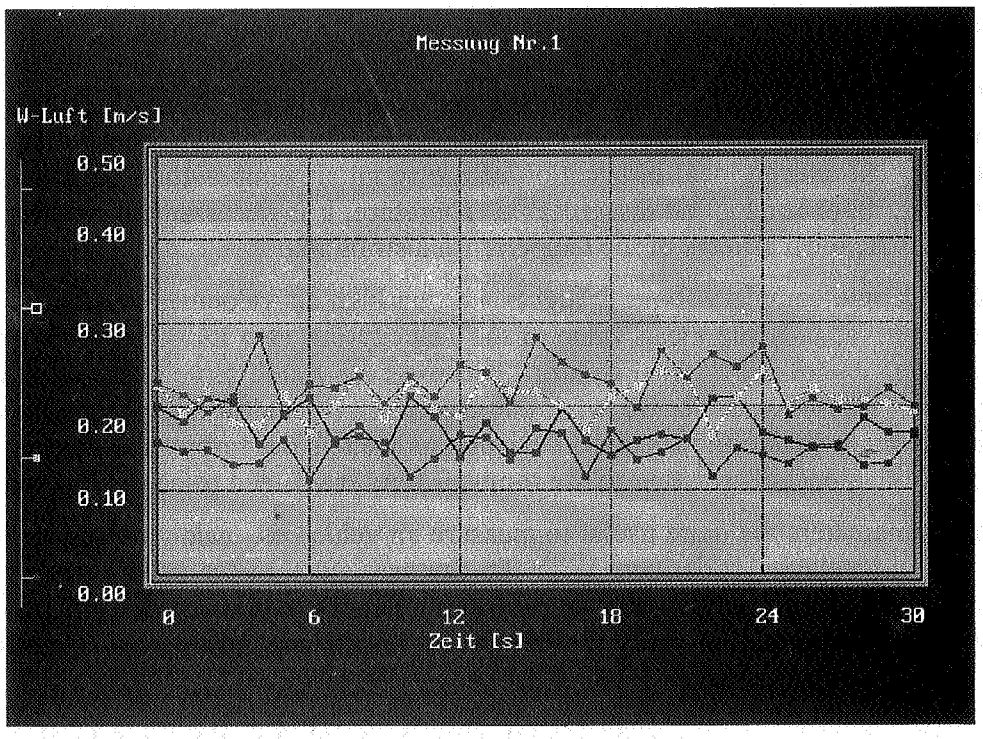

Figure 9: Graphic during the measurement of the air velocity

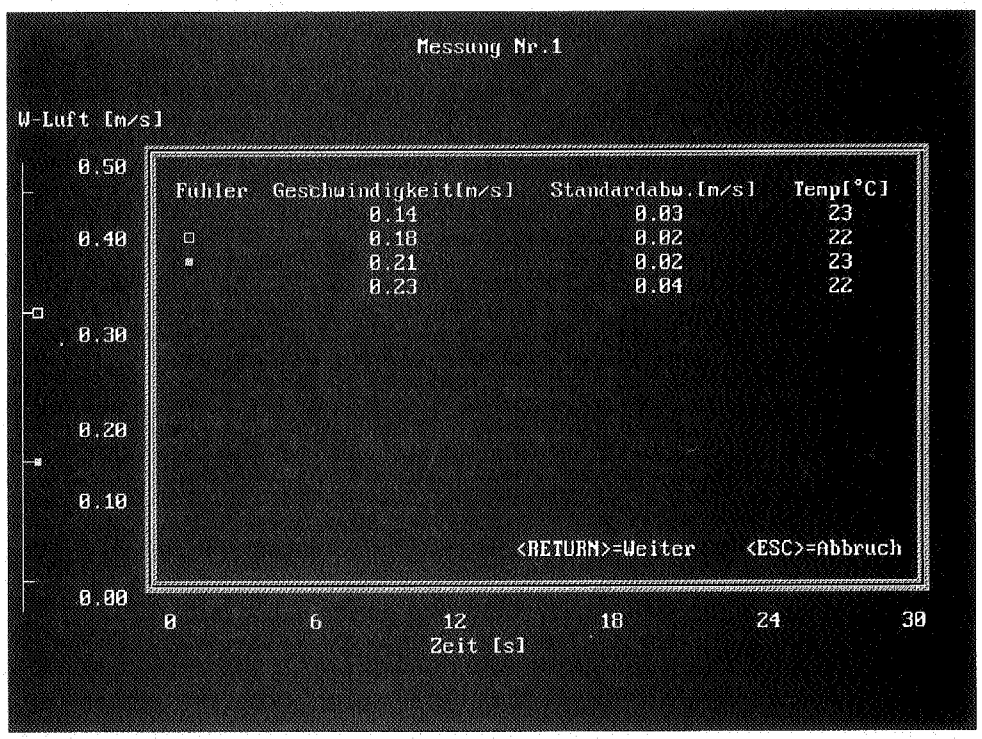

Figure 10: Graphic after finishing the measurement of air velocity

If the measurement of the air velocity is finished, the graphic will be replaced by the table of the results (Fig.10). In this table the following results are shown:

- Air velocity : The arithmetic average of the velocity over the measuring time
- The standard deviation : The standard deviation of the velocity
- Temperature : The arithmetic average of the temperature

4 Test methods

One of the most important criteria with thermal comfort is the room air temperature, its distribution and its occurence. Strongly varying temperatures quickly cause discomfort. In the same way an uneven local distribution of the room air temperature, such as a zone of cold air above floor level is felt disagreeable. Therefore, it is necessary to monitor both the temporal and the local aspects of the temperature distribution.

Very often people complain about draughts, i.e. too high air velocities at often too low air temperatures. Not only the mean value of the velocity but also its variation is of decisive importance in view of the thermal comfort, because even at the same mean value of the air velocity highly turbulent air flows are felt disagreeable. To monitor the mean value of the air velocities and to evaluate the standard deviation as well as the turbulance degree, both the temporal and the local distribution of the room air flow rates need to be determined.

Thermal anemometers are quite useful to measure air velocities, mainly at low air flow rate, and to monitor velocity variations. With the thermal anemometer used here both the air velocity and the air temperature can be measured. Thanks to a computer integrated multi-function-card (analog/digital-card) the measured results are transferred directly to the computer for quick processing.

Velocity and temperature measurements are always executed at the same locations, i.e. at the air outlet of the grille, above floor level as well as below the ceiling and mainly in the breathing area. A brief description of the testing method is given to show the connection between the monitoring programme and the examination of the room air flows.

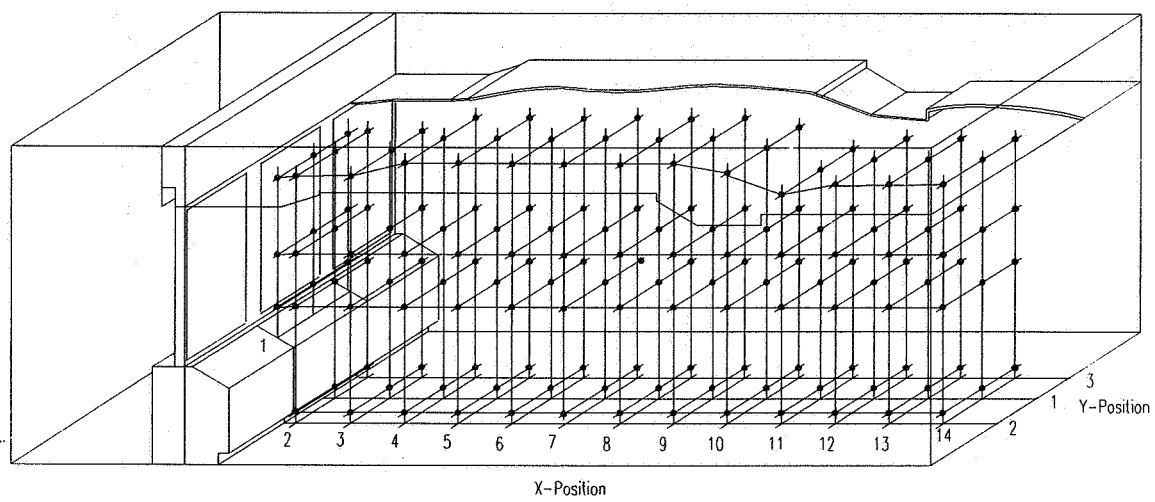

Figure 11: Arrangement of the air velocity meterring points in the test room.

To evaluate the room air flows the room was divided into a three-dimensional grid (Fig. 11). The measurements were executed along three room axes: the center line and two parallel axis at 0.5 m each on the left and on the right from the centre line. Each of these axes is divided into 14 metering points, with the first metering point above the blower aperture of the induction units and the second located at the end of the induction unit cover and with the others following at a distance of 0.5 m each.

At each metering point (with the exception of point 1 of each axis) the air velocity and the air temperature was measured at four different heights.

- 0.1 m (above the floor level)
- 1.1 m (upper part of the body when sitting)
- 1.65 m (upper part of the body when standing) and
- 0.1 m (below the ceiling)

It was the aim of each measurement to determine a velocity profile at each metering point at a certain operating state. For this reason the anemometers had to be transported to the next metering point after each measurement. To do this, however, it was necessary to open the test room. Disturbances going hand in hand with the required opening could hardly be avoided.

The following conditions need to be fulfilled for the series of measurements to be valid:

- The running state must remain stable over a long period of time
- All other parameters (such as the arrangement and kind of the furniture) of the series of measurements must not be changed.
- After changing the metering point a short break has to be kept to allow the flow conditions to be soothed and the disturbances (human body as a heat source, air turbulence due to movements, etc.) to be levelled.

Several measurement series at different operating states and with different furniture arrangements were executed. Moreover, the temperature was measured at four different heights at each velocity metering point and at five other metering points in order to detect possible cold air zones or temperature layers.

5 Summary

With the the test room it ispossible to make different full scale investigations. Following a few advantages of this test plant are presented:

- Quick and relatively simple changes of the room geometry and the equipment (e.g. ceiling, walls, furniture, etc.)
- Investigation of the indoor air flow under different outdoor air conditions (climatic chamber)
- Investigation of the influence of the furniture of the indorr air flow
- Investigation of original facade including windows (e.g. condensation, heat losses, etc.)
- Examination of the thermal comfort with respect to temperature and air velocity

An additional advantage of this kind of experiments is that operators, architects, designers, work committee members etc. can have a look at the office rooms in the planning stage so that possible changes can easily be decided and carried out. It is also possible to use the measurement results from the test room for the examination of the data from computer fluid dynamic programs (CFD).

The Role of Ventilation
15th AIVC Conference, Buxton, Great Britain
27-30 September 1994

Investigation of Effect of Tracer Species on Tracer Mixing Using CFD

S B Riffat, L Shao

Building Technology Group, School of Architecture,
University of Nottingham, NG7 2RD United Kingdom

SYNOPSIS

Tracer-gas techniques are widely used for measurement of airflow in buildings and their accuracy depends critically on the uniformity of tracer/air mixing. However, tracer mixing is still an unsolved problem and the effect of many factors remains unclear. This paper presents a study of the effect on mixing of tracer species. The investigation concentrated on tracer mixing involved in the decay technique, which is the most widely used version of the tracer gas method. The distribution and history of tracer concentration during air flow measurements were examined using Computational Fluid Dynamics (CFD). It was found that for single-zone tracer decay tests, three tracer gases, sulphur hexafluoride, nitrous oxide and carbon dioxide have virtually identical mixing patterns and thus there is no difference between them in terms of flow rate measurement results. However, for multi-tracer gas tests where there is interzonal tracer movement, the three tracer gases with different binary diffusivities exhibit significantly different mixing behaviour. In these situations, the choice of tracer will impact the accuracy of air flow measurement.

LIST OF SYMBOLS

A, B	Components A and B
C	Tracer concentration (%)
D	Molecular diffusivity (m^2/s)
k	Boltzmann's constant, 1.3805×10^{-25} (J/K)
M	Molecular weight (g/mol)
P	Pressure (Pa)
t	time (second)
T	Temperature (°C)
T_b	Normal boiling point (°C)
V	Velocity
V_b	Liquid molar volume at boiling point (m^3/mol)
ε	Characteristic energy parameter
Ω_D	Diffusion collision integral (dimensionless)
μ_p	Dipole moment (debyes)
σ	Collision diameter (m)

1. INTRODUCTION

Tracer-gas techniques[1-5] are widely used for building airflow measurements. However, they have a potential problem, i.e. the discrepancy between the less than perfect tracer mixing achieved in practical tests and the theoretical requirement of uniform tracer concentration within the test zone during the test. This requirement implies that the supply air entering the zone must instantly achieve uniform mixing with the air-tracer mixture in the zone. This is physically unsound and tracer mixing is still, in general, an unsolved difficulty.

The accuracy of tracer-gas methods has been the subject of much research. However, until recently it has been predominantly along the line of analysing the effect of measurement errors on the flow rate results. Such work provided information on acceptable measurement errors and elucidated the most error tolerating algorithm for flow rate derivation. These studies, by accepting the algorithms, implicitly assume that the tracer concentration is uniform

and errors arise solely from equipment or operators. They therefore did not address the crucial problem of mixing. More recently, the focus of research is starting to switch to the more fundamental study of factors affecting tracer mixing[6-9]. These are necessary in order to provide insight into the mixing mechanisms, based upon which, better mixing enhancement methods may be devised in the future. It has been shown that smaller building zones, lower air change rates and higher inlet airflow velocities have positive effects on tracer/air mixing and that there does not exist a universal critical value of air change rate below which satisfactory mixing is guaranteed. Nevertheless, many more questions regarding tracer mixing remain unanswered.

This paper presents a study of the effect of tracer species on mixing. It is usually assumed[1, 6] that tracer mixing is independent of the tracer species, which appears reasonable, given the always small proportions of tracer-gas in tracer-air mixtures. However, there is recent experimental evidence[8, 9] to contradict this assumption. In both studies, three different tracer-gases were used and these gave rise to different flow rate results for the same flow. This study examines this problem using an analytical/computational approach and the results were used to compare with previously obtained experimental findings.

2. COMPUTATION PROCEDURES

The CFD code FLUENT was used to solve the three dimensional Navier-Stokes equations and time dependent simulations were carried out to predict the transient tracer concentration variation.

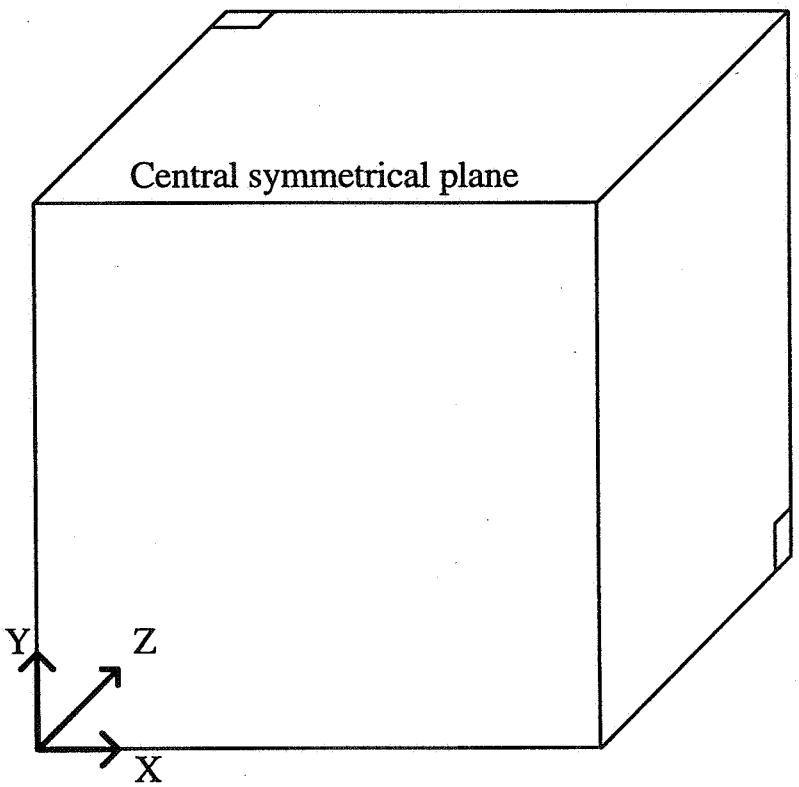

Fig. 1 Schematic of the computation domain.

The building zone used in this study is of cubic shape and measures 3m×3m×3m. The three-dimensional computational domain was selected in preference to the two-dimensional one, despite the penalty in CPU processing time. It is felt that in a two-dimensional domain, the air-stream from the inlet to the outlet will divide the domain into separate areas, isolating them from each other, resulting in mixing being artificially obstructed. The zone used in the computation is symmetrical about its central symmetrical plane. This fact was utilised to reduce the amount of computer storage and calculation required by including only one half of the zone in the computation domain (Fig. 1). As a consequence, the central symmetrical plane becomes one of the boundaries and the symmetrical boundary conditions were imposed, which assumes that the velocity component perpendicular to the plain is zero and all scalar gradients are zero. The supply air inlet for the room, as shown in Fig. 1, has a cross section 0.15m × 0.3m. The supply air stream enters the room perpendicular to the inlet at a uniform speed of 0.01 m/s. This resembles the magnitude of stack-driven natural convection between building zones and provides a bulk airflow rate of 1/3 ach. This velocity was selected to enable the computational assessment of tracer mixing in zones that are not saturated with fully developed turbulence. In situations where fully developed turbulence prevails, the mixing between air and different species of tracer will be identical. This is because molecular mixing which is species-dependent is several orders of magnitude weaker than turbulent mixing, the latter being dependent only on the flow properties. However it is rare to find fully developed turbulence in building air infiltration and ventilation. In the vast majority of cases, there is co-existence of turbulent areas and laminar areas or the flow is completely laminar. Thus there could be differences in terms of mixing between different species. The outlet for the exhaust air has the same shape and dimensions as the inlet and only half of both were included in the computation domain as is the case for the building zone.

Three tracer-gases, sulphur hexafluoride, nitrous oxide and carbon dioxide, were used to examine the effect of tracer species on mixing. Diffusion of one gaseous species into another is governed by

$$J = -D\frac{dC}{dx},$$

for one-dimensional diffusion and the equivalent equation for three-dimensional diffusion is very similar. Here J is the diffusion flux across unit area normal to the x-direction, $\frac{dC}{dx}$ is the concentration gradient and D is binary diffusivity. Binary diffusivity data for the three tracer-gases used in this computation were calculated based on molecular kinetics[10] as outlined in the following. The binary diffusivity of a two gaseous species (A and B) system is given by:

$$D_{AB} = 1.858\times10^{-3} T^{3/2} \frac{(\frac{1}{M_A} + \frac{1}{M_B})^{1/2}}{P\sigma_{AB}{}^2\Omega_D},$$

where

M = molecular weight, g/mol

D_{AB} = binary diffusivity, cm^2/s

T = temperature, K

P = pressure, atm

Ω_D is diffusion collision integral (dimensionless) which can be calculated using

$$\Omega_D = \frac{A}{T^{*B}} + \frac{C}{e^{DT^*}} + \frac{E}{e^{FT^*}} + \frac{G}{e^{HT^*}} + \frac{0.19\delta_{AB}^{\ 2}}{T^*} \qquad (1)$$

where A = 1.06036, B = 0.15610, C = 0.19300, D = 0.47635, E = 1.03587, F = 1.52996, G = 1.76474, H = 3.89411;

$$\delta_{AB} = (\delta_A \delta_B)^{1/2}$$

$$T^* = \frac{kT}{\varepsilon_{AB}}$$

$$\frac{\varepsilon_{AB}}{k} = (\frac{\varepsilon_A}{k}\frac{\varepsilon_B}{k})^{1/2}$$

$$\frac{\varepsilon}{k} = 1.18(1+1.3\delta^2)T_b$$

$$\delta = \frac{1.94\times10^3 \mu_p^{\ 2}}{V_b T_b}$$

σ_{AB} in equation (1) is defined by

$$\sigma_{AB} = (\sigma_A \sigma_B)^{1/2}$$

where σ is collision diameter with unit Å and is evaluated by

$$\sigma = (\frac{1.585V_b}{1+1.3\delta^2})^{1/3}$$

The binary diffusivities for sulphur hexafluoride-air, nitrous oxide-air and carbon dioxide-air at the temperature of 288K were calculated as 8.8532×10^{-6}, 1.35566×10^{-5} and 1.50348×10^{-5} m^2/s.

Single-tracer or multiple-tracer decay tests can be classified into two groups. Consider the simplest multiple-tracer decay tests: Two zones, A and B, are injected with tracers "a" and "b" respectively. During the test, fresh air from the outside environment and flow from zone B will mix with the tracer "a" and air mixture in zone A, diluting tracer "a". On the other hand flow from zone B also carries tracer "b" into zone A, increasing the "b" concentration there. These two distinct mixing situations occur in a similar way to zone B. Indeed, the two groups of mixing situation can be identified in all multiple tracer tests. The first type is referred to as type "aA" mixing and the second "bA" mixing. Mixing in all single-tracer decay tests and mixing of tracer "a" in zone A belong to the first type and mixing of tracer "b" in zone A belongs to the second.

In light of the above discussion, two groups of a total of six cases of tracer mixing were examined. In the first group, which corresponds to the "aA" type described above, the room was injected with one of the three tracers described above which then is mixed with the air in the zone to achieve a uniform concentration of 0.1%. As the test starts, fresh air enters the zone and the variation of tracer concentration distribution with time is recorded; The computation is halted when the accumulative air change reaches 1/3 ac. The same procedure is repeated for the other two tracer-gases and the three set of results are then compared to determine the effect of tracer species. The second group, corresponding to the "bA" type

mixing, of three cases was computed in a similar manner. The only difference is that the air in the zone at the start of the tests is fresh (free from tracers) while the supply air entering the zone had a uniform tracer concentration of 0.1%.

3. RESULTS AND DISCUSSION

Figs. 2, 3 and 4 are results from the first group of three cases. Fig. 2 shows the sulphur hexafluoride concentration distribution, by means of concentration contours, across the central symmetrical plane. This is a "snap-shot" at the end of the test when 1/3 air change has been accumulated. The concentration is measured as the ratio of the mass of the tracer to the mass of air. The values for the contours, in the order from upper-right to lower-left are, in equal steps, 9.93×10^{-4}, 9.41×10^{-4}, 8.89×10^{-4}, 8.36×10^{-4}, 7.84×10^{-4}, 7.32×10^{-4}, 6.80×10^{-4}, 6.27×10^{-4}, 5.75×10^{-4}, 5.23×10^{-4}, 4.70×10^{-4}, 4.18×10^{-4}, 3.66×10^{-4}, 3.14×10^{-4}, 2.61×10^{-4}, 2.09×10^{-4}, 1.57×10^{-4}, 1.05×10^{-4}, 5.23×10^{-5}, respectively. Figs. 3 and 4 are interpreted in the same way except that they show the concentration distribution of nitrous oxide and carbon dioxide, respectively. The distribution patterns show remarkable similarity. At any particular point on the plane the differences in concentration between the three tracer-gases are smaller than 5%. In fact, the similarity is repeated across the complete zone. These results show that the mixing between air and each of the three tracer-gases is virtually identical and that all three tracer-gases would yield the similar results when used in flow rate measurement.

Very different results emerge from the second group of three cases which correspond to the "bA" type mixing. The supply air has a uniform tracer concentration of 0.1% and the zone contains no tracer-gas at the start of the test. Fig. 5 shows the tracer concentration histories for sulphur hexafluoride, nitrous oxide and carbon dioxide at a spatial point with co-ordinates in x, y and z axes of 1.5, 1.5 and 1.0, respectively. The definition of the co-ordinate system is shown in Fig. 1. Large differences in concentration, especially between sulphur hexafluoride and the other two tracers, is evident and maintained for most part of the test duration. These differences are consistent with the fact that the binary diffusivities of nitrous oxide and carbon dioxide are much larger than that of sulphur hexafluoride. Obviously, the mixing performances of the three tracer-gases are significantly different, which is closely related to their widely differing molecular diffusion capacity.

The histories of concentration variation of the three tracer-gases at 19 other points, positioned throughout the domain, were also examined. The twenty points are classified into three groups according to the gaps between the concentration curves for the three tracers. In the first group, the curves for the three tracers virtually coincide; Sampling points where the gap, in terms of relative difference in concentration, averages up to 10% are assigned to the second group and those with gaps over 10% form the third group. For example, the sampling point for Fig. 5 belongs to group three. Among the 20 sampling points, there are 4 in group one, 7 in group two and 9 in group three. These results indicate that tracer-air mixing for sulphur hexafluoride, nitrous oxide and carbon dioxide are significantly different for "bA" type situations.

It has been explained previously that all single-zone tracer decay tests are associated with "aA" type tracer mixing and all multi-zone or multi-tracer decay tests involve "bA" as well as "aA" type mixing. It follows from the above results concerning the two mixing types that for single-zone tracer decay tests, there is no difference between the three tracer-gases, sulphur hexafluoride, nitrous oxide and carbon dioxide, in terms of results of flow rate

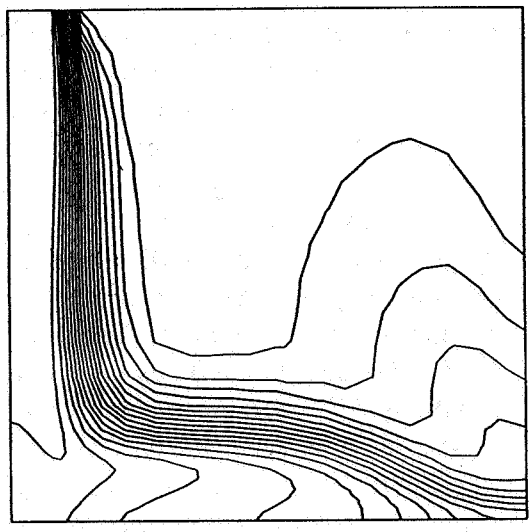

Figure 2. Concentration contours for SF_6 in the central symmetrical plane.

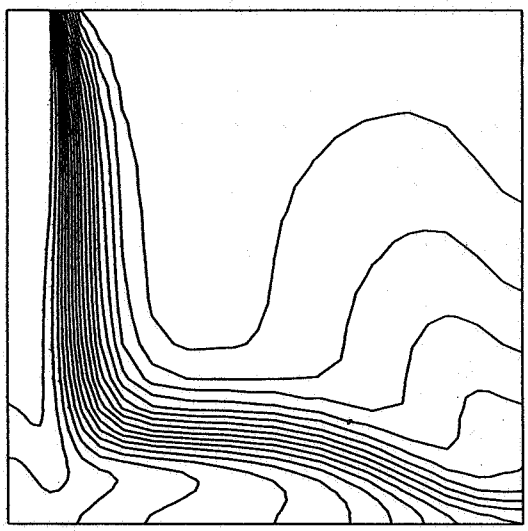

Figure 3. Concentration contours for N_2O in the central symmetrical plane.

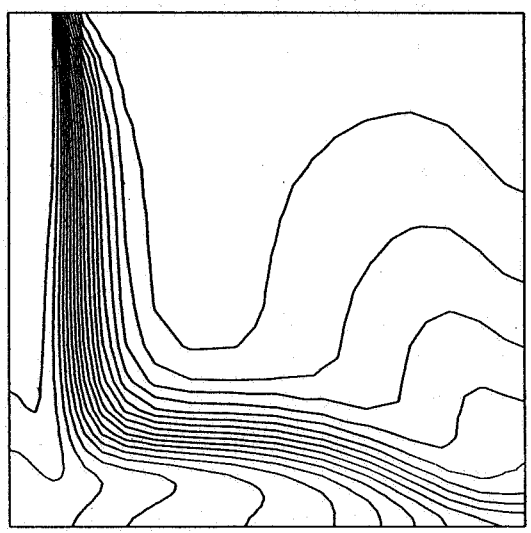

Figure 4. Concentration contours for CO_2 in the central symmetrical plane.

measurements. However, for multi-tracer-gas tests, the choice of tracer will impact the result of airflow measurement. This conclusion supports recent experimental findings by Kohal and Riffat[9] who revealed the significant effect of tracer species on flow rate measurement results. They revealed that nitrous oxide tends to perform better than sulphur hexafluoride, which is in line with the fact that the binary diffusivity of the former is significantly higher and that tracer concentration distribution results from this study show greater uniformity for the former. The results from this study also show that carbon dioxide tends to have better mixing than nitrous oxide and sulphur hexafluoride, as it has the highest binary diffusivity of the three tracer-gases. However, significant and variable background concentration and relatively poor detectability of carbon dioxide discourage its use as a tracer-gas. The level of detectability of carbon dioxide is around 3 and 7 orders of magnitudes lower than those of nitrous oxide and sulphur hexafluoride[1], respectively. As a result, 100 litres of carbon dioxide may need to be injected into a modest sized (3m×3m×3m) zone. Heating, cooking and breathing contribute to oscillation in background carbon dioxide concentration, causing uncertainty and inaccuracy in flow rate measurements. As a result, carbon dioxide may not perform as well as the other two tracers despite of its high diffusivity. This is borne out by recent experimental results[9].

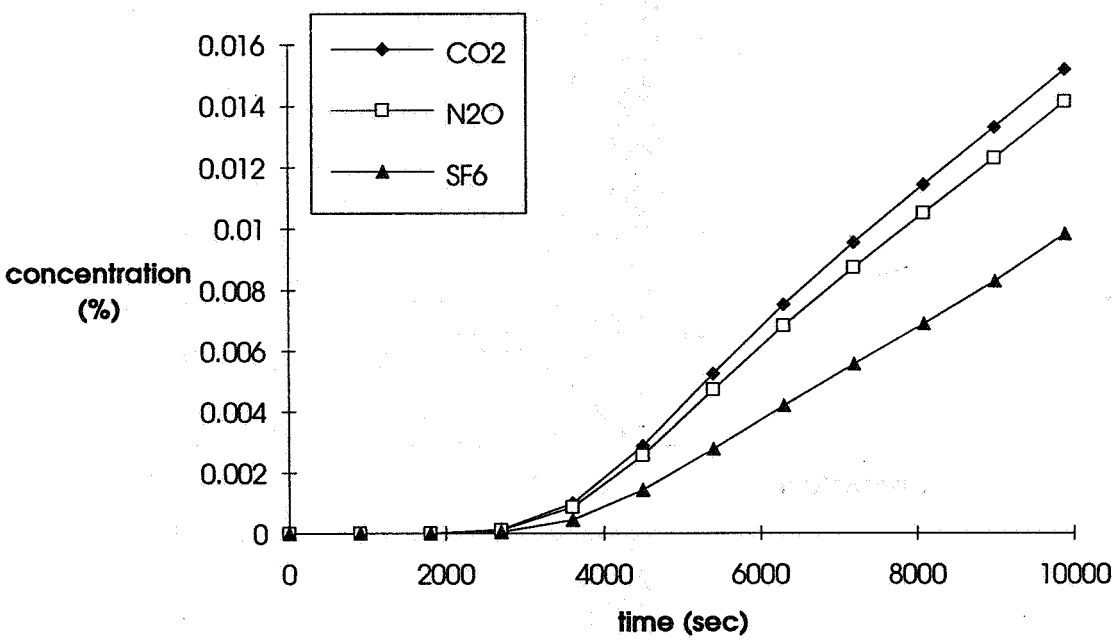

Figure 5. Concentration history for three tracer-gases.

4. CONCLUSIONS

The effect on mixing of tracer species has been examined using computational fluid dynamics. It was found that for single-zone tracer decay tests, three tracer-gases, sulphur hexafluoride, nitrous oxide and carbon dioxide have virtually identical mixing patterns and thus there is no difference between them in terms of flow rate measurement results. However, for multi-tracer-gas tests where there is interzonal tracer movement, the three tracer-gases with different binary diffusivities exhibit significantly different mixing behaviour. In these situations, the choice of tracer will impact the accuracy of airflow measurement. These conclusions support

recent experimental findings concerning the significant effect of tracer species on flow rate measurement results.

The sequence of the tracers, in the order of descending mixing power, is carbon dioxide, nitrous oxide and sulphur hexafluoride, which is a result of their different diffusivities, also in the same order. However, mixing power should be considered together with other practical factors when making a choice of tracer-gas. Use of carbon dioxide should be avoided despite of its high diffusivity because of its significant and variable background concentration and relatively poor detectability.

REFERENCES

1. Roulet, C. -A. & Vandaele, L., Airflow patterns within buildings: Measurement techniques. AIVC TN-34 (1991).
2. Wouters, P., l'Heureux, D. & Voordecker, P. The determination of leakages by simultaneous use of tracer gas and pressurisation equipment. *Air infiltration Review* **8**(1) 4-4 (1986).
3. Shao, L. & Howarth, A. T. Air infiltration through background cracks due to temperature difference. *BSER&T* **13**(1) 25-30 (1992).
4. Cheong, K. W. & Riffat, S. B., Perfluorocarbon tracer (PFT) for measurement of airflow in ducts. *BSER&T*, **17**(1) (1994).
5. Sherman, M. H. & Dickerhoff, D. J., A multi-gas tracer system for multizone air flow measurements. *ASHRAE/DOE/BTECC Symp. on Thermal Performance of External Envelopes of Buildings, Atlanta, USA* (1989).
6. Shao, L., Sharples, S. & Ward, I. C., Tracer gas mixing with air. *BSER&T*, **14**(2) (1993).
7. Alevantis, M. S. & Hayward, S. B., The feasibility of achieving necessary initial mixing when using tracer gas decay for ventilation measurement. *Proc. 5th Int. Conf. on Indoor Air Quality and Climate, Toronto, Canada,* 349-354 (1990).
8. Niemela, R., Lefevre, A., Muller, J.-P. & Aubertin, G., Comparison of three tracer gases for determining ventilation effectiveness and capture efficiency. *Roomvent'90, Oslo*, C-44 (1990).
9. Kohal, J. S. & Riffat, S. B., Computer modelling and measurement of airflow in an environmental chamber. *Proc. 14th AIVC Conference, Copenhagen, Denmark,* 421-431 (1993).
10. Fahien, R. W., *Fundamentals of transport phenomena.* McGraw-Hill, (1983).

The Role of Ventilation
15th AIVC Conference, Buxton, Great Britain
27-30 September 1994

Preliminary Ventilation Effectiveness Measurements by a Pulse Tracer Method

M R Bassett*, N Isaacs**

* Building Research Association of New Zealand

** Centre for Building Performance Research, Victoria University of Wellington, New Zealand

Synopsis

Workers in 'white collar' jobs continue to complain about air-quality problems. Although there is a growing commercial interest in the measurement of gaseous and solid pollutants, there is no information on the effectiveness of New Zealand office ventilation systems. A set of baseline data is necessary to develop an understanding of the effectiveness with which air is provided in office spaces. This paper describes the results of preliminary ventilation effectiveness measurements made in mechanically ventilated spaces using a pulse tracer gas method.

Electron-capture tracer-detection equipment was modified to release a single pulse of sulphur hexafluoride (SF_6) into the fresh air supply duct and to monitor the concentration increase and decay in a matrix of breathing zone locations. A pulse approach was chosen on the basis of equipment suitability but it was found to have some drawbacks in terms of dependence on calibrations and long data-recording times.

The local mean age-of-air was determined at a matrix of locations in the largely un-partitioned zones of two unoccupied spaces of each of two large office buildings. A numerical approach was developed to allow the data acquisition to be truncated at a practical time and the remainder of the integration to infinity to be determined by extrapolation.

The paper discusses the practicalities of this approach to measuring air change efficiency and, in the course of discussing the results, makes recommendations for further work.

1. Experimental details

The tracer gas-detection system used in this study has been derived from equipment described [1] for multi-zone tracer studies in residential buildings. It consists of a gas chromatograph (GC) and electron-capture detector with a tracer delivery and sampling system automated to step through a sequence of eight independent local mean-age measurements. Air samples can be taken from eight points through small-bore PVC tubes through which sufficiently high air flows can be maintained to ensure that up-to-date tracer concentrations are seen by the GC. In the buildings examined in this study, dosing the fresh air inlet with tracer gas was achieved with a system that released discrete shots of tracer from a small pressure vessel connected between two solenoid valves to a cylinder of pure SF_6. The solenoid valves were switched in a sequence that opened first the supply solenoid to charge the pressure vessel with SF_6 at 80 kPa. The supply solenoid was then closed and, thirdly, the pressure was allowed to relax to atmospheric pressure through the exhaust solenoid into the return air stream, where it was carried to the fresh air duct. The time taken to dose the inlet was typically 5 seconds and the volume of pure SF_6 delivered in each shot was 50cc.

For local mean age-of-air (LMA) measurements, it is important that the calibration of the detection equipment is well established. For this electron-capture detector and peak-area integration software, it is known that the calibration depends on the carrier gas pressure but that the response is linear over the normal working range of 1 to 100ppb [1]. Certified reference tracer gases at 5 and 20 ppb were used to fit a linear relationship between the integrated output from the gas chromatograph and tracer concentration. This calibration process was carried out each time the equipment was moved.

For pulse tracer measurements of the local mean age of air in mechanically ventilated buildings, the system configuration was as shown in Figure 1.

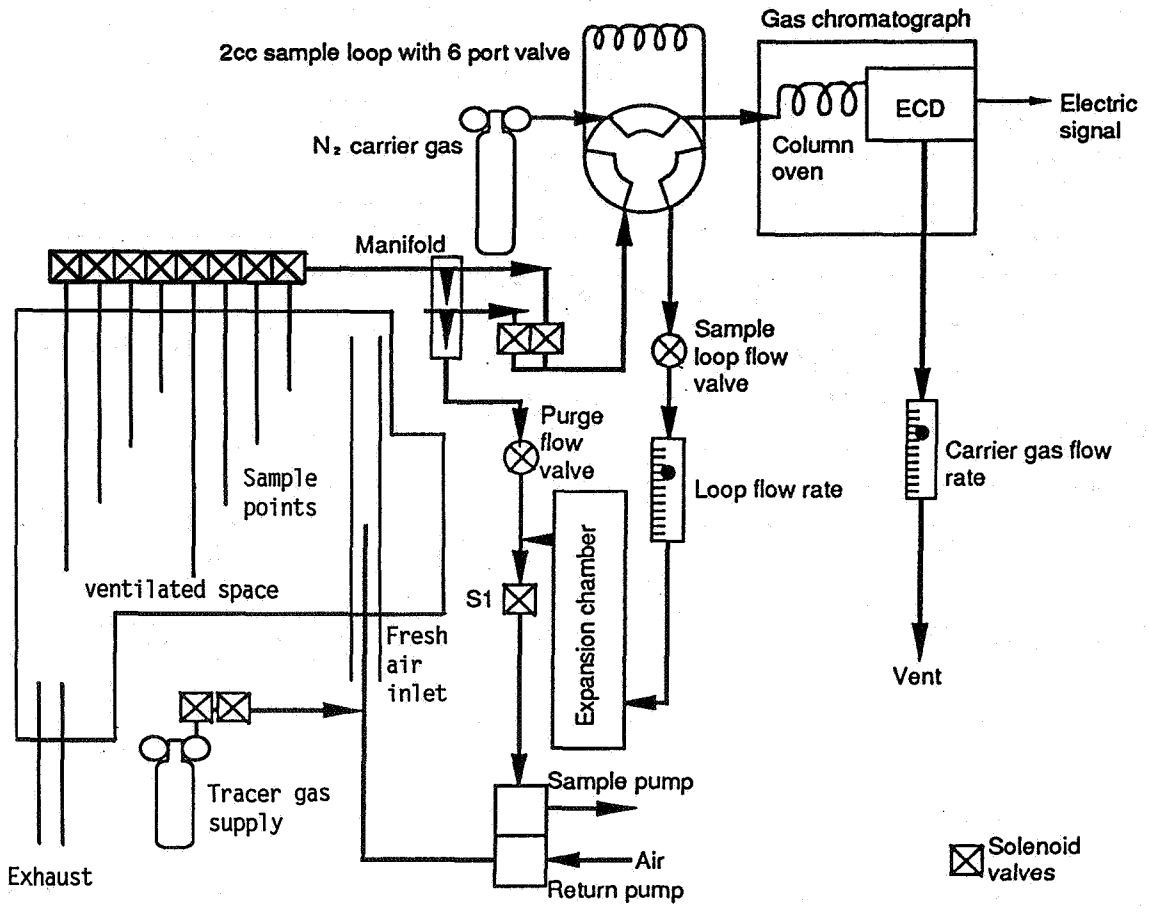

Figure 1: Tracer gas delivery and detection system for pulse local mean-age measurements.

2. Building descriptions

The two buildings examined in this study included both open-plan and partitioned zones. The important floor plan and air handling system details are presented in Table 1. Building A was originally designed as the city base for a national airline and consisted of office spaces (the top floor) and freight handling areas (middle floor). The air handling systems for each floor were independent but in practice there was some interaction between zones, because the fresh air and exhaust air flow rates were not balanced. Building B was a 7-level office building with each floor supplied with fresh air from a central duct. Exhaust air was removed through the plenum area into a central ventilation shaft. Fresh air was delivered into the breathing zones by plenum-mounted fan coil units cooled from a central chilled water plant. Each unit recirculated a proportion of exhaust air from the plenum area but there was no significant mixing of air between floors. Level 3 was mostly open plan but with about one third of the floor area partitioned into offices. Level 2 consisted of a single office with the remainder open plan.

Building A Top Floor	
Floor area (effective test space) 1,526 m²	**Volume** (including plenum) 4,731 m³
Air handling - Two roof air handlers delivering heated fresh air, return air ducted through the plenum	
Fresh air delivery - Not able to be measured	**Exhaust air removal** - Not able to be measured
Building A Middle Floor	
Floor area (effective test space) 521 m²	**Volume** (including plenum) 2,553 m³
Air handling - Internal air handler with exposed duct running centrally at ceiling level. Internal extract from exposed duct following the external wall at ceiling level	
Fresh air delivery - 1,826 m³/h	**Exhaust air removal** - 3,219 m³/h
Building B Second Floor	
Floor area (effective test space) 454 m²	**Volume** (including plenum) 1,438 m³
Air handling - Fresh air ducted to local heat pump air conditioners in the plenum area. Exhaust carried from plenum area into an extract shaft exhausting at roof top.	
Fresh air delivery - 1750 m³/h	**Exhaust air removal** - Not able to be measured
Building B Third Floor	
Floor area (effective test space) 469 m²	**Volume** (including plenum) 1,486 m³
Air handling - Fresh air ducted to local heat pump air conditioners in the plenum area. Exhaust carried from plenum area into an extract shaft exhausting at roof top.	
Fresh air delivery - 1573 m³/h	**Exhaust air removal** - Not able to be measured

Table 1: Building descriptions and air handling system capacities.

3. Data analysis

The pulse method for determining the local mean age of air entering a room requires a shot of tracer gas to be injected into the airstream over a time period that is short compared to the nominal time constant of the room. It also requires that it be fully mixed in the ventilation duct before entering the room. When these conditions are satisfied, it has been shown [2] that the local mean age of the air at a point p can be determined from tracer concentration as follows:

$$\bar{\tau}_p = \frac{\int_0^\infty t\, C_p(t)\, dt}{\int_0^\infty C_p\, dt} \qquad (1)$$

Where $C_p(t)$ = The concentration of tracer gas at point p at time t

$\bar{\tau}_p$ = The local mean age in units of t

This expression requires that the integration be continued to infinity but, in practice, the tracer concentration decays to low levels after 2 to 3 hours. A procedure developed here allows the data taking to be truncated to about two hours and a small (about 5%) correction term applied to approximate the required integration to infinity.

Figure 2 is an example of the tracer concentration variation with time at one of the sample points in building B. It shows that the concentration has fallen from a maximum of 50 ppb to around 1ppb after 3 hours, suggesting that truncating the integration at this point might give a satisfactory estimate of the local mean age of air. Also indicated on Figure 2 is a running total of the mean age integral, which is clearly still increasing at the end of the data-taking period of 3 hours.

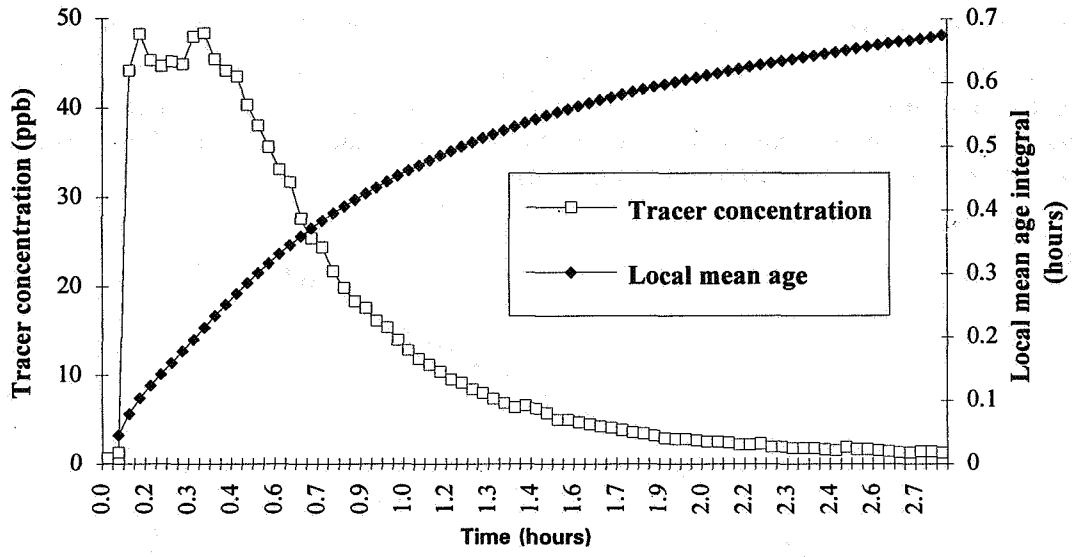

Figure 2: A typical tracer concentration record and developing local mean age of air integral.

One way of estimating the local mean age of air from data of this type is to assume that the concentration decay characteristics established in the last hour or so of results can be determined by curve fitting and extrapolation to infinity. The data gathered in this paper has been extrapolated using an exponential decay function of the following form:

$$C_p = C_0 e^{-nt} \qquad (2)$$

Where n = An exponent

C_0 = A constant (ppb)

There is no fundamental reason for expecting an exponential equation of this type to always be suitable (with displacement ventilation it would clearly not be suitable), but in the buildings investigated in this study the long tail decay has been found to approximate an exponential decay function. In these circumstances, equation 1 can be evaluated in two parts, the first determined from experimental data up to time t' and the second from values of C_0 and n determined from data recorded immediately prior to t'.

$$\bar{\tau}_p = \frac{\int_0^{t'} tC_p(t)dt + \left[\int_{t'}^{\infty} tC_0 e^{-nt} dt\right]}{\int_0^{t'} C_p dt + \left[\int_{t'}^{\infty} C_0 e^{-nt} dt\right]} \qquad (3)$$

This takes the following form

$$\bar{\tau}_p = \frac{\int_0^{t'} t\, C_p(t)\, dt + \frac{C_0}{n} e^{-nt'} \left[t' + \frac{1}{n} \right]}{\int_0^{t'} C_p\, dt + \frac{C_0}{n} e^{-nt'}} \qquad (4)$$

A similar procedure can be used to compensate for data taken over a finite time when the room mean age of air is determined from tracer concentrations measured at the exhaust duct. In this case, the correction is rather more important because of the t^2 term in the numerator of equation 5. Figure 3 shows the tracer concentration measured at the exhaust of the middle floor of building A. The developing integral of the room mean age of air is plotted on the same time scale, where it is clearly seen to have not converged after 3 hours of data recording.

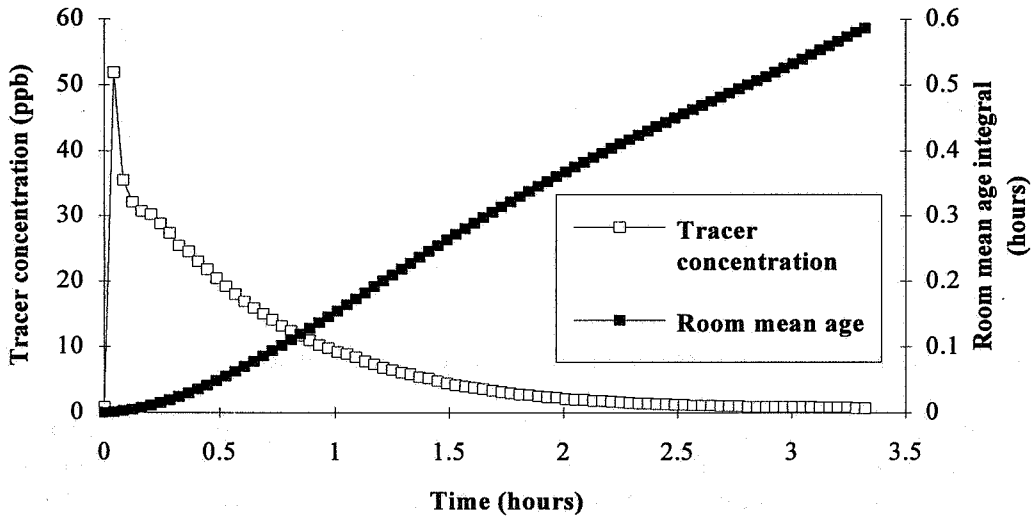

Figure 3: A typical tracer concentration record and developing room mean-age integral.

The equation for the room mean age determined from the exhaust [1] is shown expanded here into two parts:

$$\langle \bar{\tau} \rangle = \frac{Q}{2V} \frac{\int_0^{\infty} t^2 C_e(t)\, dt}{\int_0^{\infty} C_e(t)\, dt} = \frac{Q}{2V} \left[\frac{\int_0^{t'} t^2 C_e(t)\, dt + \frac{C_0 e^{-nt'}}{n} \left[t'^2 + \frac{2t'}{n} + \frac{2}{n^2} \right]}{\int_0^{t'} C_e(t)\, dt + \frac{C_0 e^{-nt'}}{n}} \right] \qquad (5)$$

Where $\langle \bar{\tau} \rangle$ = The room mean age of air

$C_e(t)$ = The tracer concentration at the exhaust duct at time t

Q = The airflow rate into the zone m³/h

V = The zone volume m³

Integrating the room mean age of air from extrapolated exhaust concentration measurements measured in this study has shown that the integration beyond 3 hours may add as much as 30% to the final result. The room mean age of air measured this way therefore rests heavily on assumptions made in extrapolating the data, as well as on the linearity of tracer detection equipment (in this case close to its detection limit). This reduces the practicality of pulse-method room mean age-of-air measurements by exhaust air tracer analysis.

4. Results

The local mean ages (in hours) measured in the four building floors are marked out on floor plans in Figures 4 to 7. Each local mean age of air has been determined using equation 3, which has compensated for the finite measurement period by adding between 2-7% to the result. A measure of the repeatability of these results has been determined from measurements carried out in five locations on the middle floor of building A. Lumped into this uncertainty will be experimental errors as well as the effect of infiltration changes and supply air temperature fluctuations. The pooled relative standard deviation of this data is 4%. There are, of course, systematic errors and errors of interpretation that add further to the overall uncertainty. The systematic error has been estimated to be about 20%, which is similar to the 95% confidence interval suggested by Fisk [3] for breathing-level air-exchange effectiveness and air diffusion effectiveness measurements.

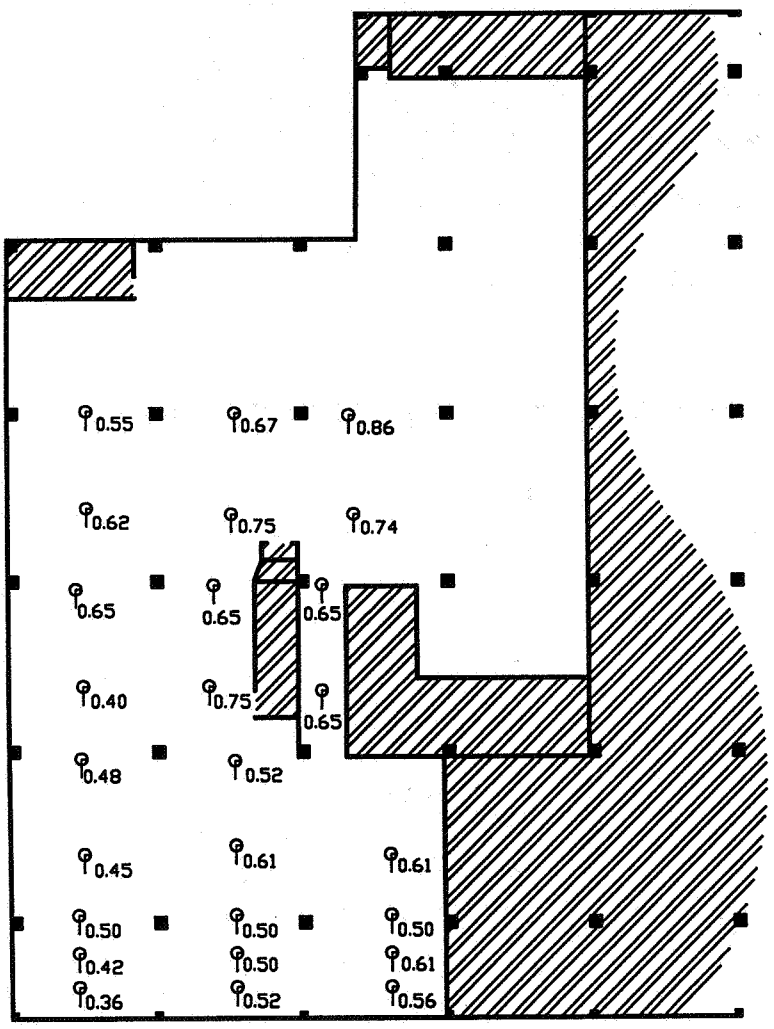

Figure 4: Local mean age-of-air data (in hours) for building A top floor

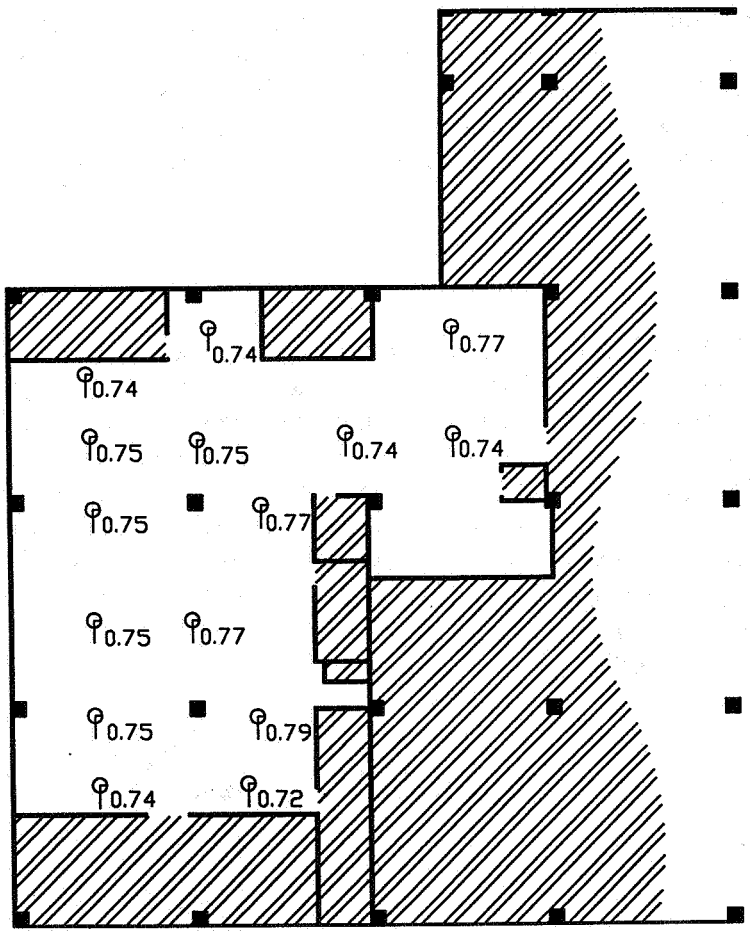

Figure 5: Local mean age-of-air data (in hours) for building A middle floor.

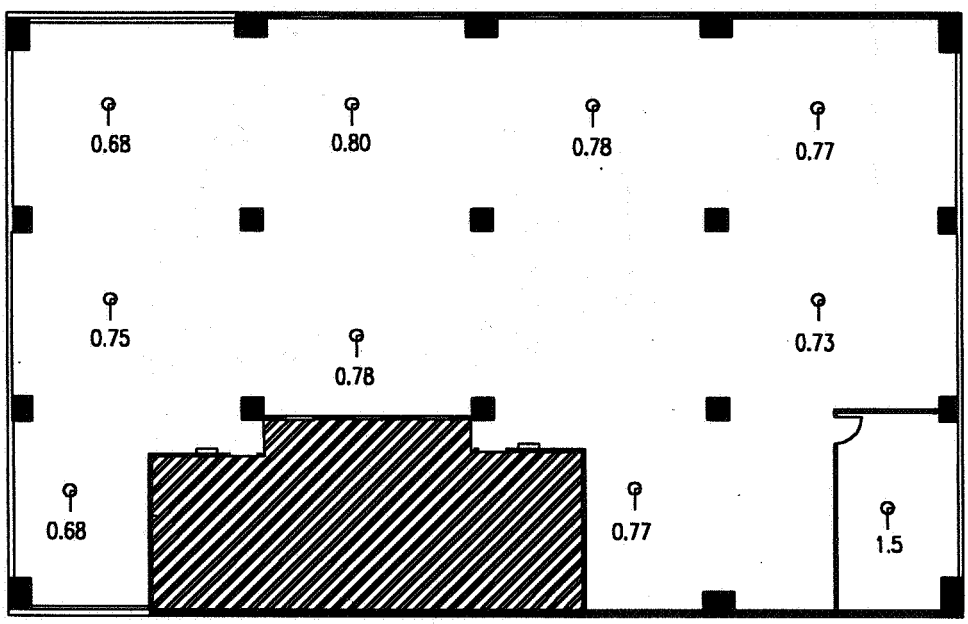

Figure 5: Local mean age-of-air data (in hours) for building B second floor

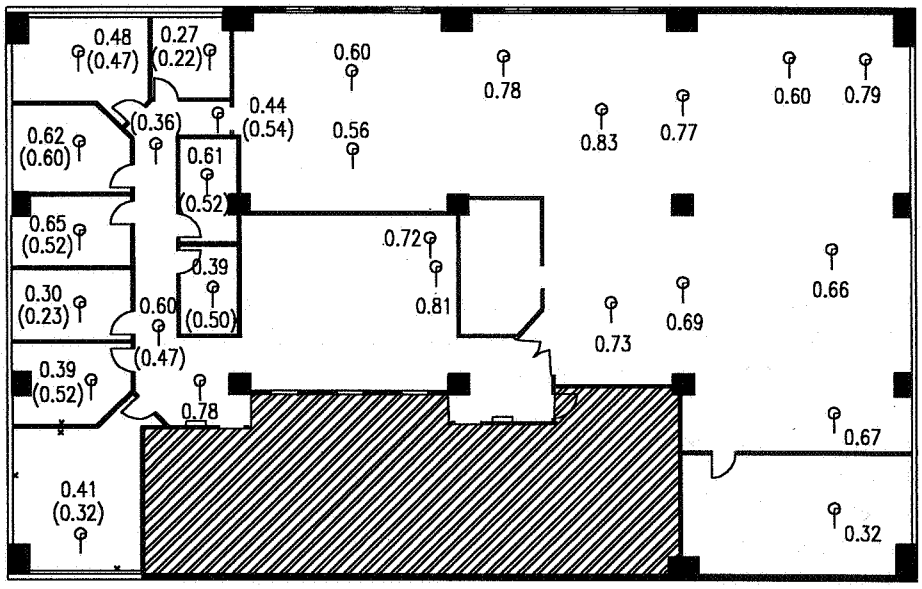

Figure 7: Local mean age-of-air data (in hours) for building B third floor (values shown in brackets measured with all doors closed).

The breathing-zone local mean age-of-air data has been averaged to give an estimate of the room mean age of air. These averages, along with the nominal time constants and the room mean age of air determined using exhaust air analysis, are given in Table 2.

Ventilation parameter	Building A middle floor	Building A top floor	Building B floor 2	Building B floor 3
Room mean age of air (space averaged) in hours	0.75	0.60	0.76	0.64
Room mean age of air (analysed at exhaust duct) in hours	0.76	-	0.79	0.60
Nominal time constant (hours)	0.79	-	0.82	0.95
Space averaged air change efficiency %	53%	-	54%	74%

Table 2: Ventilation effectiveness parameters measured in four building ventilation zones.

Where it was possible to measure the nominal time constant, the air change efficiency measured in the breathing zones has fallen between 50%-75%, indicating a pattern of ventilation somewhere between uniform internal mixing and displacement flow. The short local mean ages in some of the partitioned areas may be attributed to the high density of inlet and exhaust registers leading to shorter nominal time constants in the rooms. Other workers, e.g. [3], have measured ventilation-effectiveness parameters in mechanically ventilated buildings and developed a picture of the effectiveness of systems in a range of buildings. It is too early to form similar conclusions about the effectiveness of ventilation systems in New Zealand office spaces, but further measurements are planned.

In the partitioned areas of the third floor of building B the local mean age of air was found to depend to some extent on whether the doors were open or closed. Data for doors open and closed is given in Figure 7 (doors closed in brackets). All of these spaces contained fresh air inlets and outlets, whereas the room isolated from the open-plan area on the second floor contained only an inlet. The LMA in this zone was difficult to measure but appeared to be at least twice that of adjacent open-plan areas.

5. Conclusions

This study has developed pulse tracer equipment and analysis procedures for measuring the local mean age of air in the breathing zones of mechanically ventilated buildings in New Zealand. The following key points and limitations are identified:

- One problem often encountered was that of measuring all of the inlet and exhaust air flows. In the buildings studied here, there was either a significant imbalance between inlet and exhaust air flows leading to inter-zone air movement, or there were practical difficulties in measuring inlet or exhaust air flow rates using conventional velocity scanning methods. Tracer-dilution measurement methods will have to be used to measure air flows in further work.

- The limitation imposed by finite data-taking times has been addressed with a small correction (about 5%) applied to local mean age of air measurements made using the pulse method. The same problem arises with room mean age-of-air measurements determined from tracer concentrations measured at exhaust points. Unfortunately, the tracer concentration history that has to be determined by extrapolation forms a significant part (30%) of the mean age integral, and this limits the usefulness of room mean ages of air measured this way.

The air-change efficiencies reported in this paper lie in the range 50%-75%, indicating a pattern of ventilation somewhere between uniform internal mixing and displacement flow. In partitioned areas (building B third floor) the local mean ages were generally lower than in the open-plan areas. This was thought to be a result of the higher density of fresh air and exhaust registers in the partitioned areas, leading to shorter nominal time constants in the rooms. Further measurements are planned in order to develop an understanding of ventilation effectiveness achieved in New Zealand buildings.

6. Acknowledgements

This work was funded by the Building Research Levy and the Foundation for Research, Science and Technology. We acknowledge the assistance of the building owners for access to the buildings, and the staff of BRANZ and the Centre for Building Performance Research for conducting the measurements.

7. References

1 Bassett, M.R. and Beckert, H. M. (1989). *Automated tracer equipment for air-flow studies in buildings*. Proceedings of the 10th AIVC Conference, "Progress and Trends in Air Infiltration and Ventilation Research". Depoli, Finland.

2 Sutcliffe, H. (1990). *A guide to air change efficiency*. Air Infiltration and Ventilation Centre, Technical Note 28. Coventry.

3 Fisk, W. J. and Faulkner, D. (1992). *Air change effectiveness in office buildings: Measurement techniques and results*. Proceedings of the International Symposium on Room Air Convection and Ventilation Effectiveness, pp282-294. Tokyo.

The Role of Ventilation
15th AIVC Conference, Buxton, Great Britain
27-30 September 1994

Ventilation and Utility Program Incentives in the Northwest U.S.

D T Stevens*, D O'Connor**

* Stevens and Associates, 1800 Pacific Avenue, P O Box 398 Keyport, Washington, USA 98345

** Pacific Power and Light Co/PacifiCorp, 920 SW Sixth Ave, Portland, Oregon, USA 97204

1. Synopsis

Residential ventilation has at least two energy penalties that must be considered when addressing the ventilation levels recommended in ASHRAE Standard 62.

- Energy is required to heat the fresh outside air used for ventilation. In cold climates with high heating costs, an air-to-air heat exchanger can lessen the operating expense.
- Energy is needed for the fan motor used to introduce fresh outside air and/or to exhaust stale indoor air.

This paper will explore the residential ventilation experience in the Pacific Northwest states of the United States regarding the use of heat recovery versus non-heat recovery ventilation systems. It will also discuss the experience of one large private electric utility (1.6 million customers in seven states) in determining utility ventilation program design and incentive programs based on Demand Side Management. It will trace the analysis by the authors of the energy penalties of several ventilation strategies and the level of incentive for low-energy fans that is supportable by the utility in the rate-making process. (Private utilities in the United States are regulated monopolies that must seek approval of state utility regulatory boards for rates, energy conservation programs, and program incentives.)

2. Introduction

The Pacific Northwest region of the United States includes the states of Washington, Oregon, Idaho, and western Montana. The coastal area has a temperate, damp, maritime climate west of the Cascade Mountains; the interior area east of the Cascades and west of the Rockies has a dry, cold, high mountain climate. Approximately 80% of the Pacific Northwest's population lives in the coastal area.

Residential ventilation has been a component of electric utility and governmental agency programs in the Northwest since about 1984 and has been required in residential energy and ventilation codes since 1991. The major complaint from occupants of houses built early in the programs was that the ventilation fans were too loud. Follow-up surveys showed that occupants would not operate a noisy fan even if disabling the fan caused condensation and mold growth in the home. As we have gained experience in residential ventilation, quieter fans have been introduced, and the length of recommended daily operation has grown. But better fans and longer operating times raised concerns about the energy cost of ventilation. This paper will explore one utility's attempts to address these concerns.

History of Ventilation in Utility Energy Efficiency Programs

The northwestern United States is an area with energy codes exceeding almost all other parts of the country. As residential energy codes and electric utility energy efficiency programs became more stringent, ventilation and indoor air quality (IAQ) became critical issues. Unfortunately, due to a lack of consumer knowledge and questionable installation and performance in many ventilation fans and heat recovery ventilation (HRV) units, adequate ventilation levels were often not maintained. Electric utilities marketing energy efficient thermal shell programs often faced customer complaints about stuffy homes and mold growing on walls. Often the problem was customers disconnecting the ventilation systems in their homes due to excessive fan noise. Quite often disconnecting the ventilation system was done despite specific utility guidelines requiring a certain amount of ventilation system run time per day to ensure adequate air exchange and indoor air quality.

The concept of using a controlled, mechanical ventilation instead of natural ventilation was not understood by the majority of consumers and contractors. Many contractors and consumers could not understand the idea of building a house tight and then "punching holes in the walls" to allow fresh air to come in. This lack of education on the part of both consumers and contractors led to inadequate ventilation and unacceptable indoor air quality in many homes. Clearly, a solution was needed.

Importance of Ventilation in Marketing Energy Efficiency

The solution was a combination of increased education for consumers and contractors, as well as the introduction and marketing of new and improved ventilation technologies in the residential marketplace. The increased education component focused first on in-depth technical training on ventilation for utility representatives managing the energy efficient thermal shell programs. This training was supported by a technical booklet on ventilation written for general contractors, with separate sections developed for single family construction and multi-family construction. Explanations of both HRV and non-HRV ventilation systems were provided to address the needs of different climates.

Finally, a less technical consumer brochure was developed to explain the importance of home ventilation and its relation to indoor air quality. Ventilation is a dry topic in residential construction and often not understood well by consumer or contractor. Typically, consumers are more interested in the carpet colors and the type of decorative tile to be installed in the home, while contractors are interested in what helps them sell their homes as fast as possible. Here was another dilemma facing utility marketers: how to make ventilation an integral part of the home construction and buying process. Enter indoor air quality as the marketing tool to ensure adequate ventilation. The elements of ventilation education segued into a successful marketing message for promoting energy efficient home programs to both consumers and contractors. Everyone can relate to concerns about living in a stuffy, stinky, or polluted indoor environment. No one wants to live in an unhealthy indoor environment; no contractor wants the liability of building an unhealthy home. Ventilation is the solution to the IAQ problem.

While utility program technical specifications were changed to require quieter fans, they were still not quiet enough for some customers. The new technical specifications also required longer ventilation system run times, raising the specter of energy penalties. To address the energy penalty and quietness issues, we explored the concept of a nominal utility incentive paid to contractors who installed quiet, energy efficient ventilation fans and HRV systems. The goal was to encourage market transformation so that quiet, energy efficient ventilation fans and HRV systems would become commonplace in the residential home construction marketplace.

3. Research and Analysis of Fan Energy Considerations

In analyzing the costs of providing adequate ventilation for reasonable indoor air quality, we looked at both the energy penalty for heating outside air drawn into the structure and for the fan energy for operating the fan. The cost of electrical energy in the Pacific Northwest averages approximately $.05 per kilowatt-hour, while the United States national average cost is over $.10 per kWh. Given that the majority of the housing in the Northwest is located in a climate that requires less than 5000 heating degree days (°F) per year, the energy penalty for bringing in fresh air typically does not justify the added cost of heat recovery ventilation. In areas where the energy cost is greater and/or the climate is more severe, HRV systems deserve more consideration than we have given them in the maritime Northwest.

Most residential ventilation systems currently installed in the Pacific Northwest use negative pressure ventilation strategies with one or more exhaust fans to pull stale air out of the building. Typically, a quiet (1.5 sone or less), surface-mounted bath fan or a remote-mounted bath fan is controlled by a 24-hour time-of-day timer to provide general ventilation for at least eight hours a day. We refer to this as "whole house ventilation". While ASHRAE Standard 62-1989 generally requires ventilation at 0.35 ACH whenever the house is occupied, we have adopted a setting of eight hours a day as a program- or code-minimum setting for the automatic control.

All the houses built in the Northwest are of fairly tight construction, with a target leakage rate of about 7 air changes per hour at 50 Pascals. Consequently, the houses need mechanical ventilation with a specific strategy for bringing in outside fresh air. Fresh air is introduced either through passive air inlets located in bedrooms and the living space or through an outside air connection to the return air plenum of the forced air furnace. The air inlets are generally Swedish or French through-the-wall inlets or American inlets built into the window frames. The outside air connection to the return air plenum of the forced air furnace relies on negative pressure created by the air handler to pull in outside air and on the air handler fan to move the mixture of household air and outside air to all the rooms of the house.

The major emphasis of our research was to analyze the energy cost of using the air handler in the forced air system, compared to the use of an exhaust fan with inlets, and

then to determine if the energy savings of low energy fans could support an incentive from the utility. A major issue addressed was the energy used by the furnace. When the forced air furnace's air handler is used to bring in outside air and deliver it to habitable rooms, the air handler fan's energy use must be analyzed. Field surveys by the authors on behalf of Pacific Power and Light and by Ecotope for the Bonneville Power Administration and the Washington State Energy Office under Cycle III of the Residential Construction Demonstration Program have shown an average wattage of 500 watts for air handler fans in a sample of nearly 30 houses. Wattage ranged as high as 740 watts for a half-horsepower fan and as low as 310 watts for a quarter-horsepower fan. When the air handler is used to supply the outside air, an average load of 500 watts is placed on the home's electrical system with an additional load of 15-100 watts for the exhaust fan.

Some builders and HVAC contractors have tried using variable speed heat pumps to minimize this fan energy penalty. Some of the true variable speed motors can slow down to under 100 cfm, resulting in fairly low wattages. However, as the cfm decreases, the pressure in the duct available for supply and return air movement is reduced as well. In fact, when the cfm is dropped to one-quarter of its former rate, the pressure available in the ducts drops to one-sixteenth, leaving virtually nothing to draw in air from the outside. These systems in fact do not introduce any measurable fresh air at low speed.

When using the furnace air handler to supply outside air for ventilation, it is reasonable to assume that some portion of the eight hours of daily ventilation operating time will coincide with a call for heating. The amount of overlap time will depend on the UA of the house, the climate, the system size, and the thermostat setting. If we assume that over the year one to two hours of the ventilation operating time will in fact coincide with the call for heat, then a conservative estimate is that the air handler would operate for at least six hours a day for ventilation only. At 500 watts, this represents a load of 1,095 kilowatt hours per year just for the air handler operation. The typical 60 watt, whole house fan consumes an additional 175 kwh, resulting in a cost of operation for fan energy alone of 1,270 kwh per year. On the basis of this analysis, Pacific Power and Light stopped allowing the use of the furnace air handler to introduce and distribute outside air for the ventilation system.

If a quiet bath fan controlled by a timer is used with wall or window inlets for passive introduction of fresh outside air, only the exhaust fan energy must be counted. For the typical 60 watt fan, this represents approximately 175 kwh per year. However, over the past year several manufacturers have introduced low energy fans that draw only 12-25 watts. In multifamily buildings, central remote-mounted fans can deliver similar energy savings when one fan ventilates several units in the same building. Pacific Power and Light decided to investigate the potential for offering an incentive to builders who installed low energy fans. One of the considerations was whether the energy savings were worth enough to support an incentive to move builders to the more efficient (and more expensive) fans. The following data summarizes the analysis:

Manu-facturer	Model Number	Cfm at .1" w.g.	Cfm at .25" w.g.	Sone Rating	Wattage	kWh/Yr for 8 hr	kWh/Yr for 24 hr
Surface mounted fans:							
Broan	S90	90	75	1.5	50 w	146 kWh	438 kWh
	314	128	106	1.5	70 w	204 kWh	613 kWh
	360	100	84	1.5	80 w	234 kWh	701 kWh
Fan America	SMV80	80	60	0.8	35 w	102 kWh	307 kWh
	SMV100	100	80	1.2	37 w	108 kWh	324 kWh
	SMV140	120	120	1.5	40 w	117 kWh	350 kWh
NuTone	QT-80	80	63	1.5	60 w	175 kWh	526 kWh
	QT-90	90	85	1.5	75 w	219 kWh	657 kWh
	QT-130	130	100	1.0	120 w	350 kWh	1,051kWh
Panasonic	05VQ	50	31	0.5	12 w	35 kWh	105 kWh
	07VQ	70	52	0.5	15 w	44 kWh	131 kWh
	08VQ	90	70	1.0	17 w	50 kWh	149 kWh
	11VQ	110	88	1.5	19 w	55 kWh	166 kWh
	12VQ	110	60	1.0	20 w	58 kWh	175 kWh
	20VQ	190	130	1.5	31 w	91 kWh	272 kWh
Remote single pickup fans:							
Broan	SP100	120	107	--	50 w	146 kWh	438 kWh
	SP140	160	145	--	85 w	248 kWh	745 kWh
Fantech	F-100	150	140	--	70 w	204 kWh	613 kWh
Kanalflakt	K4	105	90	--	48 w	140 kWh	420 kWh
	K5	143	125	--	50 w	146 kWh	438 kWh

Remote multipoint fans:
Assume 2 story building with 2 bedroom units with 850 square feet (85 square meters) and 1 bath that needs 45 to 50 cfm (21-24 l/s) of whole house fan ventilation.

Manu-facturer	Model Number	Cfm at .25" w.g.	Cfm at .40" w.g.	Number of units	Wattage	kWh/Yr for 24 hr operation
ALDES	VMPK	110 low	110 low	2	72 w	315/unit
		180 high	180 high	3	120 w	350/unit
	MPV200	75-230	75-230	4	90 w	197/unit
	MPV300	200-330	200-330	6	120 w	175/unit
Broan	MP100	106	98	2	50 w	219/unit
	MP140	149	141	2	85 w	372/unit
	MP200	210	200	4	140 w	307/unit
Kanalflakt	EQ180	178	150	2	69 w	302/unit
	EQ375	290	280	4	152 w	333/unit

In the Pacific Northwest, we use the rated flow at 0.25 inches of water gauge (62 Pascals) for surface-mounted fans and 0.4" w.g. (100 Pascals) for remote multipoint fans. When comparing ventilation strategies for buildings, it is obvious that the use of low energy fans has a significant impact on the energy use of the building. For a four bedroom house being ventilated at 80-120 cfm for eight hours a day, the choices might be a NuTone QT-130 or a Panasonic 20VQ to provide the ventilation at 1.0 sones of noise level. The NuTone fan would use 350 kWh per year while the Panasonic fan would use only 91 kWh per year, a savings of 259 kWh. If the ventilation in a multifamily apartment building were being compared, then the choices for two bedroom apartments being ventilated continuously at 50-75 cfm might include a Broan S90 or a NuTone QT-80 in each apartment or a central multipoint fan such as the ALDES MPV300 ventilating six apartments. The Broan fan would use 438 kWh, the NuTone fan would use 626 kWh, and the ALDES multipoint fan would use 175 kWh per apartment. This gives a savings of 263-451 kWh per year per apartment, with the added incentive of no fan noise in the apartment. As can be seen, the low energy fans from Panasonic offer the lowest fan energy cost on a per unit basis. A central multipoint fan such as the ALDES MPV300 fan that ventilates several apartments at once is also quite efficient when compared to the more typical quiet, surface-mounted fan.

On the basis of this analysis of fan energy, Pacific Power and Light Company determined that the current value of the potential saved energy over the life of an exhaust fan operating for at least eight hours daily supported a $50 incentive payment to encourage a builder to install a low energy fan. Because the private electric utility operates as a regulated monopoly in its service area, Pacific Power was required to show the state regulatory commissions in its several-state service area that the avoided

cost of the saved energy was greater than the added cost of the ventilation upgrade. Pacific Power was successful in making this case, and the incentive is now in place in four states. For a utility with higher electric rates, a higher incentive could be justified.

4. Summary:

Our experience in the Pacific Northwest is that passive ventilation strategies do not provide adequate ventilation at the time it is needed and that mechanical ventilation is much more dependable and predictable. Electric utilities and government agencies should approach mechanical ventilation with an eye to both the energy penalty of heating the fresh air (or reheating the house) and to the energy penalty for fan motor energy. If energy rates are low and the climate is moderate, the reheat energy penalty is low and therefore the use of heat recovery ventilation is not warranted. The fan energy consideration can be addressed either by requiring a low energy or shared fan or by providing an incentive to encourage the use of low energy fans or shared fans to reduce the fan energy penalty for ventilation. The savings by using low energy fans is significant and should be considered in calculating program, code, and incentive costs.

The Role of Ventilation
15th AIVC Conference, Buxton, Great Britain
27-30 September 1994

Climate-based Analysis of Residential Ventilation Systems

N E Matson*, H E Feustel*, J L Warner*, J Talbott**

* Energy Performance of Buildings Group, Indoor Environment Program, Lawrence Berkeley Laboratory, Berkeley, California USA

** U.S. Dept of Energy, Washington, DC, USA

CLIMATE-BASED ANALYSIS OF RESIDENTIAL VENTILATION OPTIONS: NEW YORK ANALYSIS*

Nance E. Matson, Helmut E. Feustel and Jeffrey L. Warner
Energy Performance of Buildings Group
Indoor Environment Program
Lawrence Berkeley Laboratory
Berkeley, California, USA

John Talbott
U.S. Department of Energy
Washington, DC, USA

A study has been undertaken to (1) evaluate airtightness in recent construction dwellings in New York State, (2) evaluate the effectiveness of various strategies in providing adequate ventilation, and (3) study the use of various ventilation options by residential builders and heating, ventilation and air-conditioning (HVAC) contractors. Ventilation provided by infiltration and installed mechanical ventilation systems was analyzed in 97 New York post-1980 single-family dwellings, including 50 houses built to recent building standards (control houses) and 47 houses constructed to standards set by NYSE-Star, an energy-efficient residential building program. These houses were analyzed using RESVENT, which incorporates the LBL infiltration model and the ASHRAE Standard 136 air change rate calculation methodology. Based on the building characteristics of these houses and those of other data sets of U.S. residential buildings, quantitative descriptions of prototypical houses were developed to be used in evaluating the effectiveness of ventilation strategies. COMIS, a multizone air flow model, was used to evaluate hourly air change rates of a base case and three mechanical ventilation strategies in Buffalo, New York. Results of a survey of residential builders and HVAC contractors are presented. The survey explored the use of various residential ventilation strategies in New York State, the frequency of information requests from homeowners and developers regarding ventilation systems, comfort and health issues, and the influence of various factors on decisions about installing ventilation strategies.

Keywords: Ventilation, Infiltration, Ventilation Strategies, Modeling

LBL Report #36003, UC350

---

*The research reported here was co-sponsored in part by the New York State Energy Research and Development Authority and the California Institute for Energy Efficiency. Additional related support was provided by the Assistant Secretary for Energy Efficiency and Renewable Energy, Office of Building Technologies, Building Systems and Materials Division of the U.S. Department of Energy under Contract No. DE-AC03-76SF00098. Publication of research results does not imply NYSERDA or CIEE endorsement of or agreement with these findings, nor that of any CIEE sponsor.

Introduction

This study has been undertaken to (1) evaluate airtightness in recent construction single-family dwellings, (2) evaluate the effectiveness of various strategies in providing adequate ventilation, and (3) study the use of ventilation strategies by builders and heating, ventilation and air-conditioning (HVAC) contractors. This study is part of a larger ongoing effort, by many researchers, to quantify and understand the relationship and delicate balance between building tightness, energy efficiency, ventilation strategies, and adequate ventilation. To add to this understanding, a research project is ongoing, focusing on single-family detached dwellings in the states of California and New York. In order to provide a full picture of the process and results of this project, we have focused solely on the New York portion of our work in this paper.

Evaluation of Building Tightness and Ventilation Rates

Two leakage data sets were examined in order to evaluate airtightness and corresponding ventilation rates. One data set consists of 50 post-1980 construction houses (control houses) in New York State[1], while the other data set consists of 47 houses from the NYSE-Star energy-efficient residential building program[2]. The NYSE-Star program is a builder incentive program sponsored by a consortium of New York State utilities and energy agencies. The program requires that the houses be built to allow a maximum air change rate of 7 h^{-1} at 50 Pa pressurization. Mechanical ventilation systems are recommended but not required by the program.

Building and Leakage Characteristics

General building and leakage characteristics for the two data sets are given in Table 1. The NYSE-Star program houses are generally slightly larger than those of the control houses (240 m^2 vs. 212 m^2 of floor area). Most of the houses in each data sets are two-story houses with basements. Approximately 1/3 of the houses in each data set have heated basements.

TABLE 1: House and Leakage Characteristics - New York

Characteristics	NYSE-Star Houses	Control Houses
Average Air Change Rate @ 50 Pa	4.42 h^{-1}	6.81 h^{-1}
Average Normalized Leakage	0.30 (-)	0.42 (-)
Average Floor Area	240 m^2	212 m^2
Stories (predominant)	Two	Two
Foundation Type (predominant)	Basement	Basement
Houses with Heated Basements	33 %	32 %
Average Ceiling Height	3.0 m (9.7 ft)	2.5 m (8.1 ft)

The NYSE-Star houses, with an average ACH_{50} of 4.42 (std. dev. = 1.70), are tight compared to other U.S. residences that have been measured[3,4]. The control houses tend to be somewhat looser, but still relatively tight, with an average ACH_{50} of 6.81 (std. dev. = 2.50). The average normalized leakage, the equivalent leakage area per unit area of

building envelope area is 0.30 (std. dev. = 0.16) for the NYSE-Star houses and 0.42 (std. dev. = 0.16) for the control houses. The ranges for the two data sets overlap and are similar.

The RESVENT Model

In order to analyze infiltration and ventilation and their energy and indoor air quality impacts, an hourly simulation model, RESVENT, was developed. RESVENT is an enhancement of VENTNRG[3], an hourly simulation model incorporating the LBL infiltration model[5] and calculation of infiltration-related space-conditioning loads. RESVENT incorporates the ability to schedule and model various ventilation strategies and the flexibility to perform multiple simulations using different combinations of houses and weather data.

Three input files are used with RESVENT, generically named "house," "fan," and "site." The "house" input file includes building and leakage characteristics. The "fan" input file includes the fan types (supply or exhaust), flow rates, and on/off times for the ventilation systems modeled. The "site" input file contains references to the weather data files to be used and general site information. Weather data files developed for use in RESVENT simulations were derived from existing DOE-2[6] weather files.

RESVENT outputs include (1) identification of the peak- and low-infiltration days (based on a 24-hour average) of the infiltration-only air change rates calculated using the LBL infiltration model, (2) air change rates calculated based on ASHRAE Standard 136[7] as well as by using the LBL infiltration model, and (3) infiltration and ventilation-related space-conditioning loads, and (4) ventilation-related electrical requirements.

RESVENT Modeling Assumptions

RESVENT was used to analyze both the NYSE-Star and control data sets. Input files were developed based on information provided by the data sources. In all cases, the houses were modeled with bathroom and kitchen exhaust fans (85 m^3/h and 170 m^3/h respectively), running for one hour at 6:00 a.m. and 5:00 p.m., respectively. Each house was modeled using the most appropriate available weather data, with respect to location and climate.

RESVENT Modeling Results

RESVENT results of interest section include the identification of minimum and maximum daily average infiltration air change rates and the combined effective air change rate calculated using the ASHRAE Standard 136 calculation methodology. For both data sets on the low-infiltration day, the average hourly air change rates, derived using the LBL infiltration model, are below the 0.35 h^{-1} minimum set by ASHRAE Standard 62[8]. The average hourly air change rates on the low-infiltration day range from 0.02 h^{-1} to 0.14 h^{-1} (mean = 0.07, std. dev. = 0.03) for the NYSE-Star houses and from 0.05 h^{-1} to 0.34 h^{-1} (mean = 0.15 , std. dev = 0.06) for the control houses.

For the peak-infiltration day, the average hourly air change rates are higher, but not always high enough to meet Standard 62. The average hourly air change rates on the peak-infiltration day range from 0.08 h^{-1} to 1.08 h^{-1} (mean = 0.45, std. dev. = 0.21) for the NYSE-Star houses and from 0.33 h^{-1} to 2.10 h^{-1} (mean = 0.93, std. dev. = 0.40) for the control houses.

The combined effective air change rates, based on ASHRAE Standard 136, for individual houses range from of 0.07 to 0.82 (mean = 0.28, std. dev. = 0.16) for the NYSE-Star houses and from 0.15 to 0.77 (mean = 0.39, std. dev. = 0.15) for the control houses. Figure 2 shows the combined effective air change rate as a function of the measured air change rate at 50 Pa for the two data sets. While the NYSE-Star houses have lower values of combined effective air change rates and measured air change rates at 50 Pa, there is no significant difference between the two data sets in terms of the correlation between the measured and combined effective air change rates. Due to high normalized leakage values, two of the NYSE-Star houses have much higher combined effective air change rates than the others.

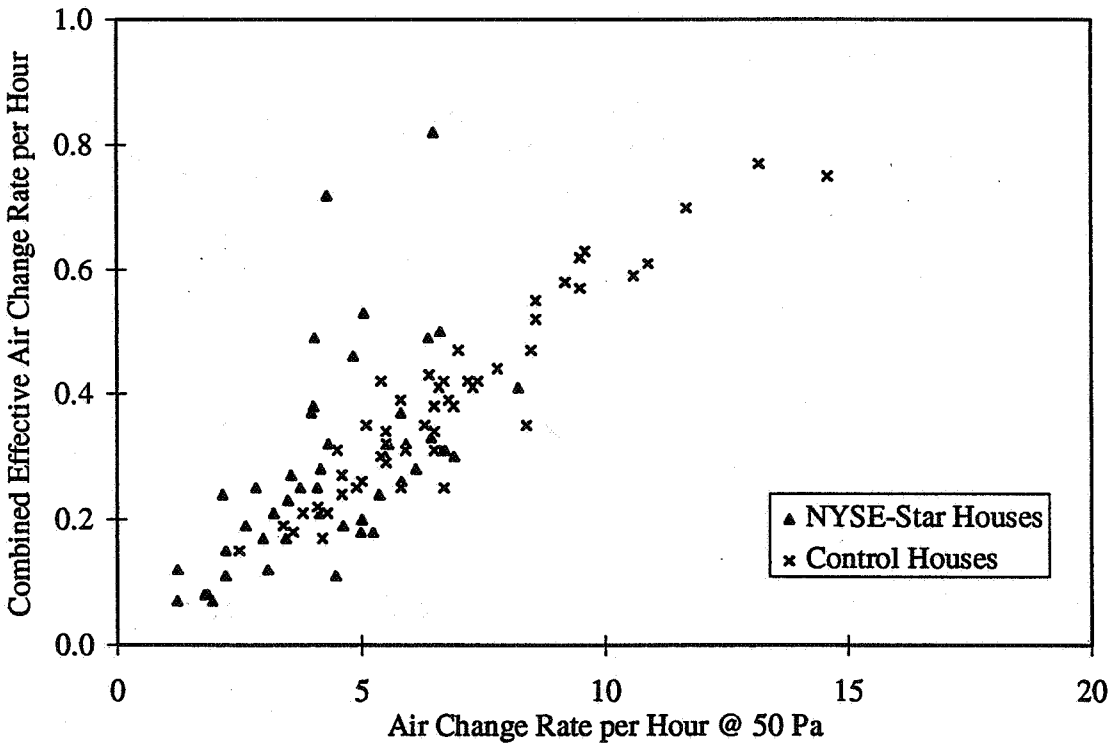

Figure 2: Calculated Air Change Rate (ASHRAE Standard 136) vs. Measured Air Change Rate (ACH_{50})

To determine compliance with the ASHRAE ventilation and tightness standards (Standards 62[8] and 119[9], respectively), the combined effective air change rates and the normalized leakage values were compared to the requirements of the relative standards. To meet Standard 62, a house must have a minimum air change rate of 0.35 h^{-1}. Standard 119, the tightness standard, specifies maximum normalized leakage values, taking into account climate and location. The percentage of the houses meeting the standards are

shown in Table 2. Only 23% of the NYSE-Star houses meet the ventilation standard, while 79% meet the tightness standard. This suggests that adequate ventilation is sacrificed in tightening the houses and lowering the infiltration-related space-conditioning loads.. On the other hand, the control data set has a higher percentage of houses (56%) meeting the ventilation standard, while 52% of the houses meet the tightness standard. Only a small percentage, 2% of the NYSE-Star data set and 8% of the control data set, are able to meet both standards, suggesting that it is difficult to strike a balance between airtightness and adequate ventilation.

TABLE 2: Compliance with ASHRAE Ventilation and Tightness Standards - New York

ASHRAE Standard	NYSE-Star Houses	Control Houses
Standard 62 Only	21 %	48 %
Both Standards (62 & 119)	2 %	8 %
Standard 119 Only	77 %	44 %
Neither Standard	0 %	0 %

Evaluation of Residential Ventilation Strategies

As shown in the analysis above, supplemental ventilation may be necessary to provide adequate ventilation. In order to explore the effectiveness of various ventilation options, a prototypical house was developed for use in modeling efforts. COMIS, a multizone air flow model[10], was used to evaluate the air change rates of a base case and three ventilation strategies in the prototypical house on peak- and low-infiltration days in Buffalo, New York. The appropriate peak- and low-infiltration days for the air flow simulations were determined using RESVENT.

Prototypical House

The prototypical house was developed to represent current construction practices for residential buildings in New York. The building was a 144 m^2, one-story house with a full unconditioned basement and attached garage.

For air flow simulation purposes, the prototypical building was divided into zones: a common living space, a laundry room, three bedrooms, two bathrooms, a garage, an attic, and a basement. The modeled background leakage between the conditioned building and the exterior or unconditioned spaces (around window and door perimeters and through joints in framed surfaces) was based on an air change rate of 7 h^{-1}, determined at an induced pressure difference of 50 Pa. Proportionate leakage rates were assigned to the surfaces between zones and to the exterior. Equally sized cracks were specified at 1/4, 1/2, and 3/4 of the heights of all walls to the exterior and between conditioned and unconditioned zones to model the stack effect.

Air flow between the basement and the exterior was assumed to occur around the perimeters of the basement windows. Attic vents were also modeled as effective leakage areas. Interior doors were modeled as large openings.

Eight supply ducts ran from the supply plenum in the basement to floor registers in the conditioned rooms. A single return duct also ran through the basement to a central floor return grille. It was assumed that 8.5% of the supply air leaked from the ducts and supply plenum, while 12% leakage occurred at the return plenum.

The flow exponent, n, for leaks through the building envelope was taken to be 0.67. Open interior doors and ducts were assumed to have orifice flow with a flow exponent of 0.5. For the leakage from the ducts, a value of 0.65 was assumed for n.

The prototypical house was located in a suburban area. Wind pressure coefficients for a building surrounded by obstructions of equal height were used[11]. The weather data used in the COMIS simulations were the same as those used with RESVENT.

Ventilation Strategies

Four ventilation scenarios were modeled using COMIS, as explained below. Hourly space-conditioning loads were determined by summing the ventilation-induced loads and the loads simulated using DOE-2.1D. Oversizing factors of 175% for heating and 125% for cooling were applied, and the part-load-ratios were determined based on the peak load results from DOE-2.

1) *Base case*: a 2040 m^3/h rated central heating and air-conditioning system with intermittent bathroom, kitchen, and laundry exhaust fans with design flow rates of 85 m^3/h, 170 m^3/h, and 425 m^3/h, respectively, running one hour per day, at 6:00 a.m., 5:00 p.m., and 8:00 p.m., respectively.
2) *Central exhaust system with an outside air duct*: the base case with a 140 m^3/h rated single-port central exhaust fan, running 24 hours per day. An air duct with a motorized damper supplied outside air to the return plenum of the furnace. The outside air damper was closed from 75% to 25% when the furnace fan was in operation to counter higher pressure differences and higher flow rates.
3) *Central exhaust system with room intake louvers*: the base case with a 140 m^3/h rated single-port central exhaust fan, running 24 hours per day. Intake louvers were located in the exterior walls of each bedroom and the common living space to provide make-up air for the exhaust fan.
4) *Balanced ventilation system with heat recovery*: the base case with a 130 m^3/h rated cross-flow heat recovery ventilator, running 24 hours per day with a 70% heat recovery efficiency. Supply air was provided to the return plenum of the furnace, while exhaust was drawn from a separate grille in the common living space.

COMIS Modeling Results

Figure 3 shows the peak-infiltration day hourly air change rate profiles for the four scenarios modeled. In all four cases, the hourly average air change rates are roughly constant, with the exception of the hours when intermittent fans are operating. Due to HVAC system impacts, total air change rates fluctuate within the hour in cases when an outside air duct or air-to-air heat exchanger is connected to the central HVAC system.

On the peak-infiltration day, the base case shows air changes on the order of 0.25 h^{-1}. As the ASHRAE Standard 62 specifies a minimum air change rate of 0.35 h^{-1}, the need for supplemental ventilation is indicated.

The central exhaust system with an outside air duct, on the peak-infiltration day, provides ventilation rates of approximately 0.40 h^{-1} when the HVAC system fan is on and 0.47 h^{-1} when the system fan is off. The performance differences are a consequence of the air duct damper setting, which allows more air to enter during the furnace fan off time. The central exhaust system with intake louvers shows a steady ventilation rate on the order of 0.50 h^{-1}. Only the operation of additional exhaust fans increases this rate.

On the peak infiltration day, the balanced ventilation system with heat recovery provides a slightly higher ventilation rate than the central system options, on the order of 0.52 h^{-1}. Due to the balanced character of the system, the influence of additional exhaust fans is less pronounced than in the central exhaust fan cases.

On the low-infiltration day (Figure 4), the base case system provides ventilation of approximately 0.10 h^{-1}. The central exhaust fan with an outside air duct increases the ventilation rate to 0.30 h^{-1}. Since the furnace fan is off most of the time, the damper is in its open position (75% open) most of the time as well. The central exhaust fan with intake louvers increases the ventilation rate to 0.40 h^{-1}. The balanced system with heat recovery provides 0.35 h^{-1}, slightly less than the central exhaust fan with intake louvers.

Based on this analysis, on both the peak- and low-infiltration days, the base-case house does not have adequate ventilation as required by ASHRAE Standard 62. The central exhaust/outside air duct option, while providing adequate ventilation on the peak-infiltration day, does not provide sufficient ventilation on the low-infiltration day. This standard is met using two options, the central exhaust fan with intake louvers and the air-to-air heat exchanger.

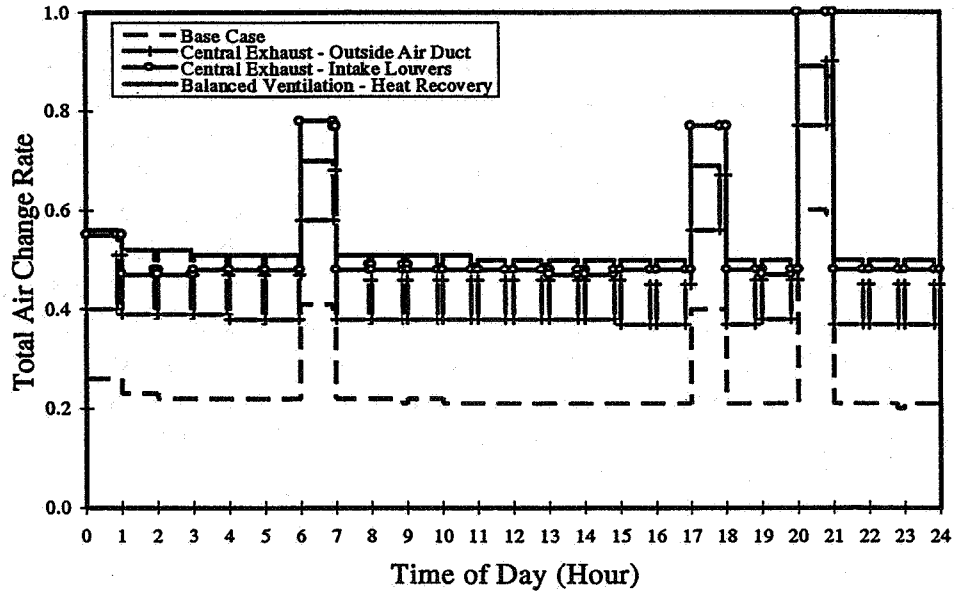

Figure 3: Hourly Air Change Rates on the Peak-Infiltration Day, January 26th (heating season), for the Prototypical House in Buffalo, New York

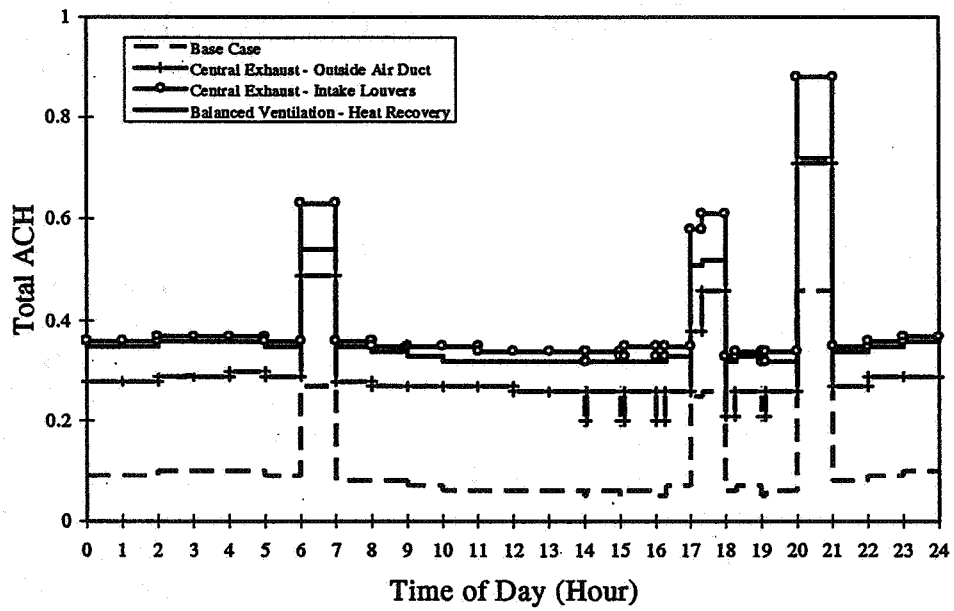

Figure 4: Hourly Air Change Rates on the Low-Infiltration Day, June 13th (cooling season), for the Prototypical House in Buffalo, New York

Residential Ventilation Surveys

As was discussed in the previous sections of this paper, when houses have been constructed to airtightness standards, supplemental ventilation is often required. We have also evaluated the effectiveness of various ventilation options and have discovered that, between infiltration and ventilation systems, adequate ventilation can be provided. However, the familiarity of builders and contractors with ventilation options and the commercial availability of residential ventilation equipment has not been known. To answer these questions, two surveys on residential ventilation systems and equipment availability are currently being conducted. One survey focuses on residential builders and HVAC contractors, while the other survey focuses on equipment distributors and retailers. Synertech Systems Corporation and Syracuse University in Syracuse, New York, are administering these surveys. While these surveys are being conducted in both New York and California, only the New York results are presented here.

Builder / Contractor Survey

The builder and contractor survey respondents consisted of a pool of residential builders and HVAC contractors who may or may not have had experience with residential ventilation systems beyond bathroom and kitchen exhaust fans. The survey sample includes 60 builders and 40 HVAC contractors per state, with the stipulation that a minimum of 50% of the respondents have had at least some experience with advanced residential ventilation systems. The survey sample was also split evenly between respondents who have participated in utility or public agency incentive or rebate programs and those who have not participated in such programs. The builder and contractor survey covers the number and types of residential ventilation strategies installed, system-specific issues, and perceived market barriers.

Types of Ventilation Strategies Installed

Table 3 summarizes the number of respondents (builders and contractors) surveyed who have installed each specific ventilation strategy during the past year. Also summarized for each strategy, based on the number of respondents who have reported installing that strategy, are the total number of systems installed in the past year as well as the range, average and median number of each strategy installed per respondent. Most of the respondents (80%) have experience with the basic systems (bathroom and kitchen exhaust fans), which was to be expected. Over half of the respondents (53%) have installed outside air ducts into a central system. Whole-house fans (18%), central exhaust fans (14%), and intake louvers (13%) were installed by fewer respondents. Only a few of the respondents have installed economizers (7%), located windows for optimum ventilation (6%), and installed ventilation shafts (2%). The total number of systems installed is impressive, but a comparison of the average and median number of systems shows that only a handful of respondents have installed the bulk of the systems reported. Most of the builders and contractors have installed only a few of the advanced ventilation strategies.

TABLE 3: Number of Ventilation Strategies Installed - 100 New York Builders and HVAC Contractors Surveyed					
Ventilation Strategy	Number of Respondents	Total Systems per Year	Range per Respondent	Average per Respondent	Median per Respondent
Bathroom and Kitchen Exhaust Fans	80	3,457	1-496	43	20
Whole-House Fans (High Volume)	18	266	1-100	15	5.5
Central Exhaust Fans (Single- or Multi-Port)	14	285	1-100	20	5
Ventilation Shafts	2	15	5-10	8	7.5
Wall Inlet Louvers	13	241	1-200	18	2
Locate Windows for Optimum Ventilation	6	131	2-100	22	7
Outside Air Ducts into a Central HVAC System	53	1,650	1-688	31	10
Air-to-Air Heat Exchangers	23	370	1-100	16	3
Residential Economizers	7	150	1-100	21	2

Requests for Advanced Ventilation Systems

Respondents were asked how often homeowners and developers asked about advanced ventilation systems (e.g., central exhaust, air-to-air heat exchangers, or economizers). A few of the respondents stated that homeowners (8%) and developers (15%) always or often asked about advanced systems. The majority of the respondents indicated that homeowners (78%) and developers (58%) seldom or never asked about advanced ventilation systems. While only a few homeowners or developers tended to ask about advanced ventilation systems, these percentages indicate that there is some level of understanding about ventilation and indoor air quality issues.

Homeowner Questions about Comfort and Health

Respondents were asked how often homeowners asked about general comfort and health issues. Only a small percentage of respondents indicated that homeowners always or often asked about these issues, ranging from a high of 15% for comfort and 10% for health to a low of 3-4% for more air flow and fresh air. 20-25% of the respondents stated that homeowners sometimes asked about these issues, with the bulk of the respondents (53-67%) stating that homeowners seldom or never ask about these issues.

Importance of Factors in Installing Systems

The factors that directly affected the ability of the builder or contractor to complete their work easily and profitably rated highest and were deemed more important than those that would probably be of more importance to the homeowner, such as ease of operation and operating costs. Of the six factors given, system price was most important to the respondents, followed by product availability, ease of installation, ease of maintenance, ease of operation, and, occasionally important, system operating costs.

Overall Impressions

The builders and contractors who had experience with specific ventilation strategies felt at ease with the systems, stating that the systems were relatively easy to install and that they had very few callbacks to make repairs. Obtaining ventilation system equipment did not seem to be a problem to these builders and contractors, who ranked obtaining equipment as somewhat to very easy. Similarly, system installation was often ranked as somewhat to very easy.

Conclusions

We have shown that there is often a need to provide some type of supplemental ventilation when building houses tight. Only in a few cases is it possible to tighten buildings while still allowing sufficient air change rates without providing supplemental ventilation. However, supplemental ventilation, either through enhanced natural ventilation or mechanical ventilation, may be necessary to provide adequate indoor air quality.

We looked at three ventilation options for a prototypical house in Buffalo, New York, including a central exhaust fan with an outside air duct into the central HVAC system, a central exhaust fan with wall intake louvers, and an air-to-air heat exchanger. While all three options increased the building air change rates on the peak-infiltration day sufficiently to exceed the minimum required air change rate of 0.35 h^{-1}, the central exhaust fan with an outside air duct was not able to meet this requirement on the low-infiltration day.

Our survey shows that, while builders and contractors have had experience with various ventilation strategies, on average they have installed very few of these systems. Only a handful of builders and contractors stated that homeowners or developers ask about advanced strategies, and very few homeowners ask questions regarding comfort and health. As with other construction-related decisions, we found that system price, availability, and ease of installation and maintenance are more important to the builders and contractors than ease of operation and operating costs.

In conclusion, we found that there is a definite need to consider ventilation when building a tight house. Our analysis of ventilation strategies show that central exhaust with intake louvers and air-to-air heat exchangers are effective in providing sufficient ventilation. And, while builders and contractors do have experience with various ventilation strategies, homeowners and developers do not ask very often about installing such systems.

Future Work

The work on this project is continuing, including evaluation of building tightness and ventilation rates for post-1980 California dwellings and climate-based COMIS simulation of ventilation strategies in the one-story as well as a two-story prototype. The California and New York surveys are nearing completion and are expected to provide vital information on the use of residential ventilation systems in the building sector. A ventilation guidebook for New York contractors and builders is also being developed. A proposed phase II of the New York work includes a demonstration project, consisting of installing and monitoring various ventilation strategies in New York houses, to verify and fine-tune the effectiveness of residential ventilation strategies.

References

1. STRUNK, P.R., "Air Leakage and the Effects of Mechanical Ventilation: Measurements in Fifty Newer Homes in New York State," Synertech Systems Corporation for NYSERDA, Syracuse, NY, February 1994.

2. CARVER, B., Data Collection of NYSE-Star Building and Leakage Characteristics for LBL Project (Personal Communication), New York State Energy Research and Development Authority, Albany, NY, January 1994.

3. SHERMAN, M.H. and N.E. MATSON, "Ventilation-Energy Liabilities in U.S. Dwellings," 14th Annual AIVC Conference Proceedings, Copenhagen, Denmark, 1993.

4. DICKERHOFF, D.J., personal communication, August 1994.

5. SHERMAN, M.H. and M.P. MODERA, "Infiltration Using the LBL Infiltration Model," Special Technical Publication No. 904, Measured Air Leakage Performance of Buildings, pp. 325-347. ASTM, Philadelphia, PA, 1984. Lawrence Berkeley Laboratory Report, LBL-17487.

6. BIRDSALL, B., W.F. BUHL, K.L. ELLINGTON, A.E. ERDEM, and F.C. WINKELMANN, "Overview of the DOE-2 Building Energy Analysis Program, Version 2.1D," LBL-19735, Rev. 1, Lawrence Berkeley Laboratory, Berkeley, CA, 1990.
7. -, "Standard 136: A Method of Determining Air Change Rates in Detached Dwellings," American Society of Heating, Refrigeration and Air-Conditioning Engineers, Atlanta, GA, 1993.

8. -,"Standard 62: Ventilation for Acceptable Indoor Air Quality," American Society of Heating, Refrigerating and Air-Conditioning Engineers, Atlanta, GA, 1989.

9. -, "Standard 119: Air Leakage Performance for Detached Single-Family Residential Buildings," American Society of Heating, Refrigerating and Air-Conditioning Engineers, Atlanta, GA, 1988.

10. FEUSTEL, H.E. and A. RAYNER-HOOSON "Fundamentals of the Multizone Air Flow Model - COMIS," Air Infiltration and Ventilation Centre, TN 29, 1990, LBL-28560, Lawrence Berkeley Laboratory, Berkeley, CA, 1990.

11. LIDDAMENT, M.W., "Air Infiltration Calculation Techniques - An Applications Guide," Air Infiltration and Ventilation Centre, Bracknell, Berkshire, Great Britain, 1986.

The Role of Ventilation
15th AIVC Conference, Buxton, Great Britain
27-30 September 1994

Measuring Subfloor Ventilation Rates

R Hartless, M K White

Building Research Establishment, Garston, Watford, Herts WD2 7JR, United Kingdom

SYNOPSIS

This paper reports on ventilation measurements taken beneath a suspended timber floor of a BRE/DoE energy and environment test house. Sulphur hexafluoride was introduced into the subfloor void at a constant rate and the resulting concentration measured. Wind speed, wind direction, and internal, external and subfloor temperatures were also recorded. A range of air brick locations were used for each run which lasted two to three days. Analysis of the data shows that subfloor ventilation rates in this test house fluctuated widely, ranging from about 3 air changes per hour (ach) to over 13 ach. Also, the subfloor ventilation rate for this house seems to be heavily influenced by the subfloor/external temperature difference rather than the wind speed, particularly when air bricks are located on sheltered subfloor walls. The main reason for this stack dependence is that there is a significant leakage path at the wall/floor junction with air moving from the subfloor void to the gap behind the plasterboard lining.

1. INTRODUCTION

In the UK naturally ventilated floors are used to control water vapour from the ground. Building Regulations for England and Wales recommend that for suspended timber floors air bricks be distributed over the subfloor walls with a minimum open area of 1500mm^2 per meter run of wall and a vapour barrier be provided [1]. Suspended concrete floors can be used to control water vapour as well as gaseous contaminants (e.g. radon and landfill gas) in which case they should be ventilated to the above provision. To control water vapour, BS5250 [2] recommends that the void beneath a suspended concrete floor should be ventilated. Further, the void beneath a suspended timber floor should be ventilated with an area of 1500mm^2 per meter run of wall or 500mm^2 per m^2 of floor area whichever is the greater, as well as having a vapour barrier [2]. However, the subfloor air change rate that these ventilation provisions will give is unknown. The purpose of this work, therefore, is to measure the air change rates beneath a suspended floor of a house with these ventilation provisions and to relate these measurements to the two driving forces for natural ventilation: stack effect and wind speed.

2. THEORY

The subfloor ventilation rate (Q_V) depends on wind speed (U), wind direction (ϕ) and temperature difference (ΔT) as well as other factors such as air brick area, degree of local shelter, leakiness of floor etc. The two driving pressure differences for (subfloor) ventilation are stack, ΔP_B, and wind, ΔP_W, which, to a good approximation, can be treated separately and simply added together to give a total driving pressure difference [3]:

$$\Delta P_T = \Delta P_B + \Delta P_W = k_B \Delta T g h + k_W U^2 \qquad (1)$$

where, h is the stack height (approximated by the depth of the subfloor void), g is the acceleration due to gravity and k_B and k_W are both constants encompassing all of the factors such as floor tightness etc. Now, leakage measurements of buildings have shown that the volume flow rate, Q, through the building envelope can be related to the pressure drop, ΔP, across it using the equation [4]:

$$Q = K\Delta P^n \qquad (2)$$

where K is a constant and n is a flow exponent (range 0.5 to 1) both of which are determined from the leakage measurement. Using this means that the total ventilation rate can be expressed as the combined stack and wind induced ventilation rates [3], i.e.

$$Q_V = (Q_B^{1/n} + Q_W^{1/n})^n \quad (3)$$

However, for subfloor ventilation much of the air flow is likely to be through air bricks which have a measured flow exponent of about 0.5. Therefore, equation (3) can be simplified to:

$$Q_V = (Q_B^2 + Q_W^2)^{1/2} \quad (4)$$

Combining equations (1), (2) and (4) gives the subfloor ventilation rate as:

$$Q_V^2 = K_B\Delta T + K_W U^2 \quad (5)$$

where K_B and K_W are both constants. (The above method can also be used to model passive stack ventilation systems [5].) Equation (5) can be rewritten in two other forms by dividing through either by U^2 or ΔT. Using these forms it is possible to plot ventilation measurements to determine the relative importance of the wind and stack driven terms. For example, plotting $(Q_V/U)^2$ against $\Delta T/U^2$ will give a straight line with gradient K_B and intercept K_W. It is likely that there will be a certain amount of scatter when plotting $Q_V^2/\Delta T$ against $U^2/\Delta T$ due to the dependence of subfloor ventilation on wind direction.

3. EXPERIMENTAL

3.1 DoE/BRE energy and environment test houses

The house used for the subfloor experiments was one of the DoE/BRE energy and environment test houses constructed at BRS Garston. They are a row of four detached houses constructed so as to be two matched pairs: one pair built to just beyond current UK Building Regulations (houses 1 and 2), the other built to Swedish standards (houses 3 and 4). For a layout of the site see figure 1. House 2 was used for all experiments.

The floor construction of all four houses is suspended timber above a concrete oversite of thickness of about 100mm, and the ground floor area of each is 42m^2. In houses 1 and 2 the floor consists of carpet on 22mm chipboard supported on 150mm joists set 400mm apart. The insulation is 75mm thick and supported between joists on 50 x 50mm treated softwood battens fixed to the joists. The depth of the subfloor void (i.e. height of the bottom of the joists above the concrete oversite) is on average 22cm (figure 2). This gives a total subfloor void volume of 10.19m^3 (void plus air spaces between the joists beneath the insulation). In addition there is a foundation (sleeper) wall running E-W through the middle of the subfloor void. To assist cross ventilation this wall has slots (5 x 30cm) at about 2m centres. Four floor hatches (one in each room) provide access to the void which helped us to position equipment. The void was ventilated using plastic air bricks fitted with a cavity sleeve for which air flow rate measurements gave an equivalent area of 4420mm^2. Sixteen of these air bricks are evenly located around the perimeter of each house to give a ventilation provision of about 2450mm^2 per metre run of external wall.

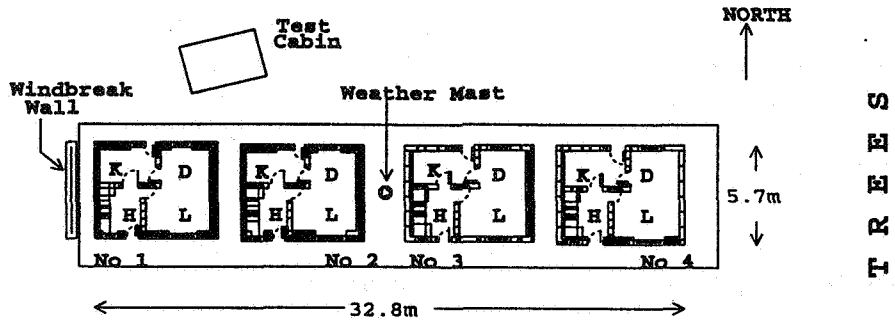

Fig 1 The DoE/BRE Energy and environment test houses

Fig 2 Cross section through floor

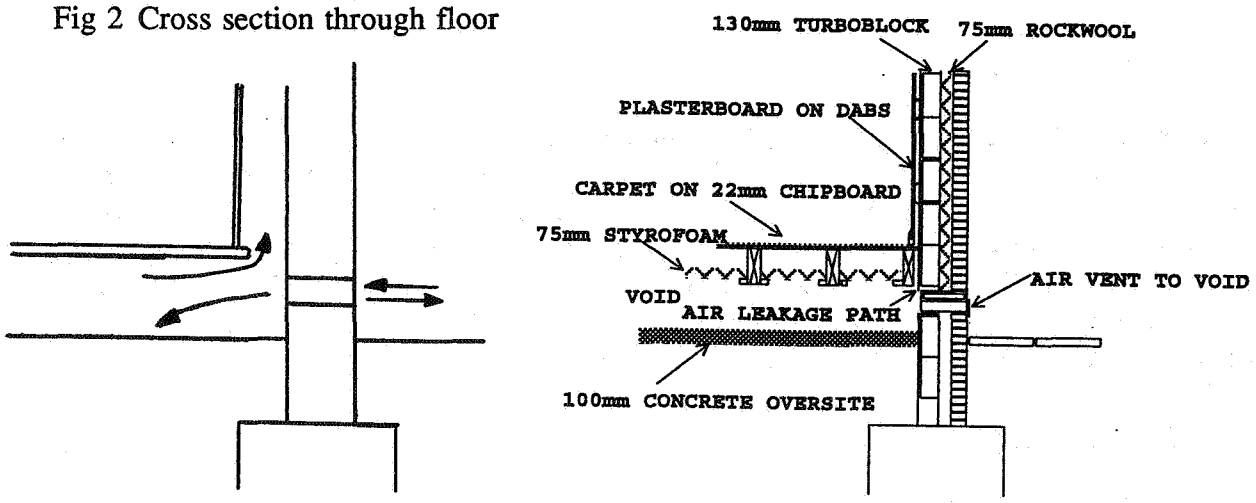

3.2 Equipment to measure subfloor ventilation

The constant emission technique was chosen to measure the subfloor ventilation rate [6]. For the purposes of this experiment the subfloor void of house 2 was divided into four comparably sized zones. Into the middle of each of the four zones the selected tracer gas, sulphur hexafluoride (SF_6), was injected at a constant flow rate from a gas cylinder by way of a mass flow controller and its associated control unit. Using data on likely subfloor ventilation rates from other studies [7], the flow rate chosen was 6 ml/minute into each half so that the resulting SF_6 concentration within the void would fall within the detection range (0-50ppm) of the infra-red analyser that was used. By using four injection points it was hoped to ensure an even distribution of tracer gas throughout the void without the need for mixing fans. However, preliminary results showed that mixing fans were necessary.

In each of the four zones was also a gas sampling point. Air from each point was drawn back from each point using a gas handling unit on a six minute cycle. A data logger was used to record SF_6 concentration as well as the subfloor temperature, measured using thermistors. All of the above equipment was housed in a test cabin (see figure 1). A 15m mast was used for wind speed and direction, and a Stevenson screen for external temperature. Thermistors were also used to obtain an average internal temperature. These data were recorded every ten minutes: the wind speed as an average over the preceding ten minutes, the wind direction and all temperatures as spot measurements. The subfloor ventilation rate was an average of the

four zones, and linear interpolation was used to calculate a 10 minute average.

4. MEASUREMENTS OF SUBFLOOR VENTILATION

Half of the air bricks were always blocked to give a ventilation provision of 1230mm^2 per meter run of wall. Using two pairs of 6-inch fans (one pair in each half of the void) ensured good mixing but results indicated that they might be affecting the subfloor ventilation rate. Using one fan in each half still gave good mixing whilst not affecting the ventilation rate. Therefore, for subsequent runs only two fans were used and these were directed to blow away from open air bricks. The gas analyser was zeroed using nitrogen and the span established using cylinders of 50ppm SF_6 in air. It was also necessary to check the filter regularly because the subfloor void was dusty. As each run lasted between one and three days the zero and span of the gas analyser was re-checked to see how much they had drifted. If they had changed, all concentration readings were corrected assuming a linear drift from the start to the end of the run. This drift was generally quite small though.

In all six runs were carried out each lasting two to three days. However, because of the large quantity of data that this generated, only two of the runs are summarised here. For Run 1 air bricks were open on the East and West facing walls, and for Run 2 they were open on the North and South facing walls. Graphs 1a and 1b show the average subfloor ventilation rate plotted with wind speed and subfloor/external temperature difference respectively for Run 1. Graphs 2a and 2b show the same data for Run 2. Graphs 3a and 3b are plots of equation (5) for Run 1. Graphs 4a and 4b are the equivalent for Run 2.

A variable not so far considered is wind direction. This is likely to be very important if air bricks are only located on subfloor walls which are sheltered from the wind. To bring wind direction into the analysis we resolved the wind velocity vector into two perpendicular components, one along an axis for which the ventilation rate would be maximised (i.e. wind blowing directly onto air bricks) and the other along an axis for which the ventilation rate would be minimised or, preferably, zeroed. For Run 2 this means that the minimum axis runs E-W and the maximum axis runs N-S. For Run 1 the maximum axis was assumed to run NE-SW. Graphs 5 and 6 are duplicates of graphs 1a and 2a respectively except that wind speed is replaced by component wind speed and the data are 30 minute averages.

5. DISCUSSION

Overall, the subfloor ventilation rate measured for this house fluctuated widely over time ranging from 3 to as high as 13ach. Graphs 1a and 1b show that the subfloor ventilation rate for Run 1 is heavily influenced by temperature difference and is negatively correlated with wind speed. This is not the case for Run 2. Graph 3a shows good correlation between subfloor ventilation and subfloor/external temperature difference except when this difference becomes negative. (A better correlation is achieved using the internal/external temperature difference which was always positive.) Graph 3b is for negative temperature differences only and shows a reasonable correlation between subfloor ventilation rate and wind speed. The equivalent graphs for Run 2 show a similar pattern except the wind speed correlation is better. Finally, graphs 5 and 6 show that for Run 1 the subfloor ventilation rate still does not appear to follow changes in component wind speed whereas it does for Run 2 for part of the time.

The most important observation from the data is that temperature difference appears to play a major role in the subfloor ventilation rates seen in this house. Whilst the internal and external temperatures moved through their usual daily cycles the subfloor temperature remained constant at about 16°C because the subfloor air is primarily warmed by the large concrete slab whose temperature is only likely to change on a seasonal basis. (Subfloor temperature measurements in April and May support this.) As a result, the subfloor/external temperature difference becomes negative in the early morning reaching a peak at midday; thereafter it rises becoming positive again in the evening reaching a peak after midnight. Conversely, the wind speed falls to relatively low levels (0-2m/s) in the night, with generally higher levels during the day. This means that subfloor ventilation in this test house is influenced by the wind during the day but is dominated by temperature difference during the night. This is clearly shown in graph 6. When the air bricks are located on the sheltered walls though the wind speed appears to have little effect on subfloor ventilation (graph 5).

However, even though a temperature difference exists this will not drive air flow unless there is a height difference between subfloor air bricks. Therefore, there must be a flow path through the floor: infra-red thermography shows that air is moving up from the subfloor void into the gap behind the plasterboard (figure 2). This problem has been observed in a number of UK houses [8], and it could help to explain the high subfloor ventilation rates seen here.

Further work in this area is planned. This will include repeat measurements of subfloor ventilation now that the wall/floor junction has been sealed using expanding polyurethane foam. Tests with all of the air bricks closed are also planned so that the floor tightness can be assessed. A wider range of air brick configurations and areas will also be tried.

ACKNOWLEDGEMENTS

This work was funded by DoE Building Regulations and is published with their permission. Many thanks to Robert Rayment for giving us access to the DoE/BRE test houses and to Derek Whiteside for providing the weather data.

REFERENCES

(1) **Department of the Environment (DoE)** "Site preparation and resistance to moisture". Approved Document C, The Building Regulations 1991, HMSO.
(2) **British Standards Institution** "Control of condensation in buildings". BS 5250: 1989.
(3) **Walker,I.S. & Wilson,D.J.** "Evaluating models for superposition of wind and stack effect in air infiltration". Building and Environment, Vol.28, No.2, pp.201-210, 1993.
(4) **Stephen,R.K.** "Determining the air tightness of buildings by the fan pressurisation technique: BRE recommended procedure". BRE Occasional Paper, 1988.
(5) **Cripps,A. & Hartless,R.P.** "Comparing predicted and measured passive stack ventilation rates". AIVC conference, Buxton, Derbyshire, September 1994.
(6) **Charlesworth,P.S.** "Air exchange rates and airtightness measurement techniques - An applications guide". AIVC, Document AIC-AG-2-88, ISBN 0 946075 38 7, 1988.
(7) **Edwards,R.E., Hartless,R.P. & Gaze,A.** "Measurement of subfloor ventilation rates - comparison with BREVENT predictions". AIVC conference, Italy, September 1990.
(8) **Millett,C.** "Draughtproof drylinings". Building Today, pp.26-27, June 14, 1990.

(1a) Subfloor ventilation and wind speed
Run 1: 6-9th August 1993
Subfloor ventilation rate (ach)
Wind speed (m/s)
Time (hours)
— Ventilation rate — Wind speed

(1b) Subfloor ventilation and temperature difference
Run 1: 6-9th August 1993
Subfloor ventilation rate (ach)
Subfloor/External temperature difference (°C)
Time (hours)
— Ventilation rate — Temperature

(2a) Subfloor ventilation and wind speed
Run2: 18-20th August 1993
Subfloor ventilation rate (ach)
Wind speed (m/s)
Time (hours)
— Ventilation rate — Wind speed

(2b) Subfloor ventilation and temperature difference
Run 2: 18-20th August 1993
Subfloor ventilation rate (ach)
Subfloor/External temperature difference (°C)
Time (hours)
— Ventilation rate — Temperature

(3a) DEPENDENCE OF SUBFLOOR VENTILATION ON TEMPERATURE DIFFERENCE
Run 1: 6-9th August 1993

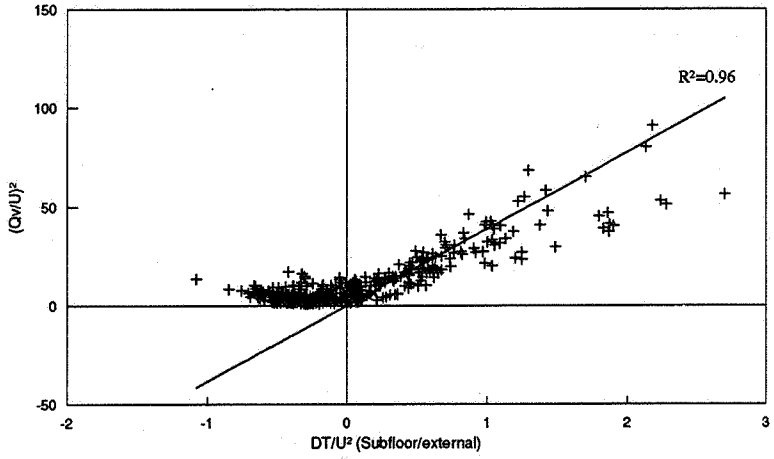

(4a) DEPENDENCE OF SUBFLOOR VENTILATION ON TEMPERATURE DIFFERENCE
Run 2: 18-20th August 1993

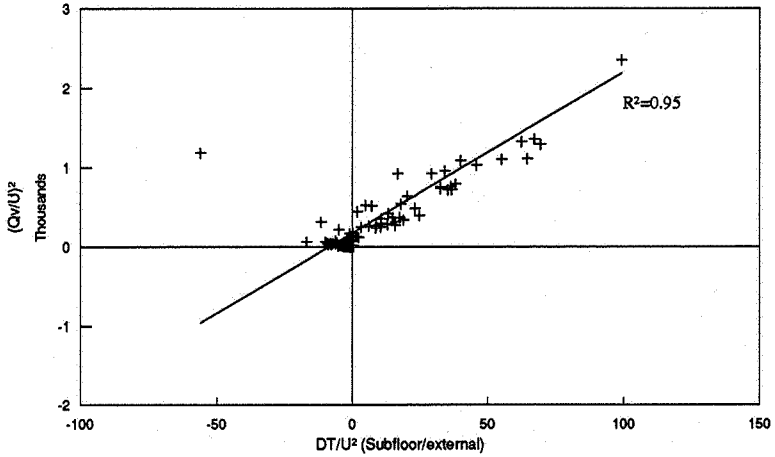

(3b) DEPENDENCE OF SUBFLOOR VENTILATION ON WIND SPEED
Run 1: 6-9th August 1993

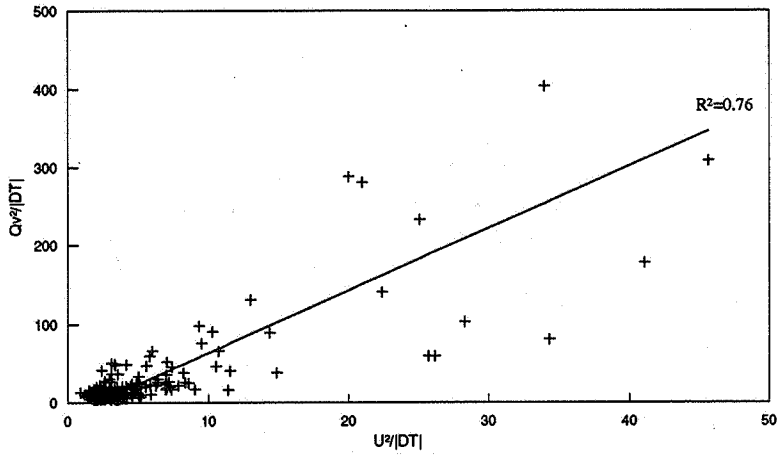

(4b) DEPENDENCE OF SUBFLOOR VENTILATION ON WIND SPEED
Run 2: 18-20th August 1993

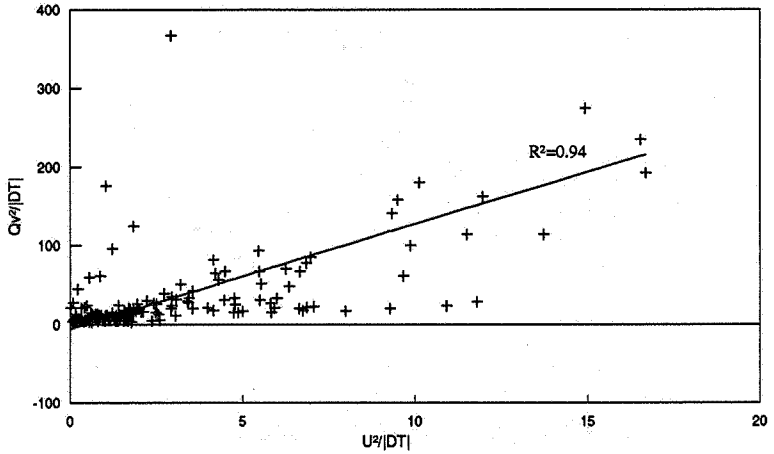

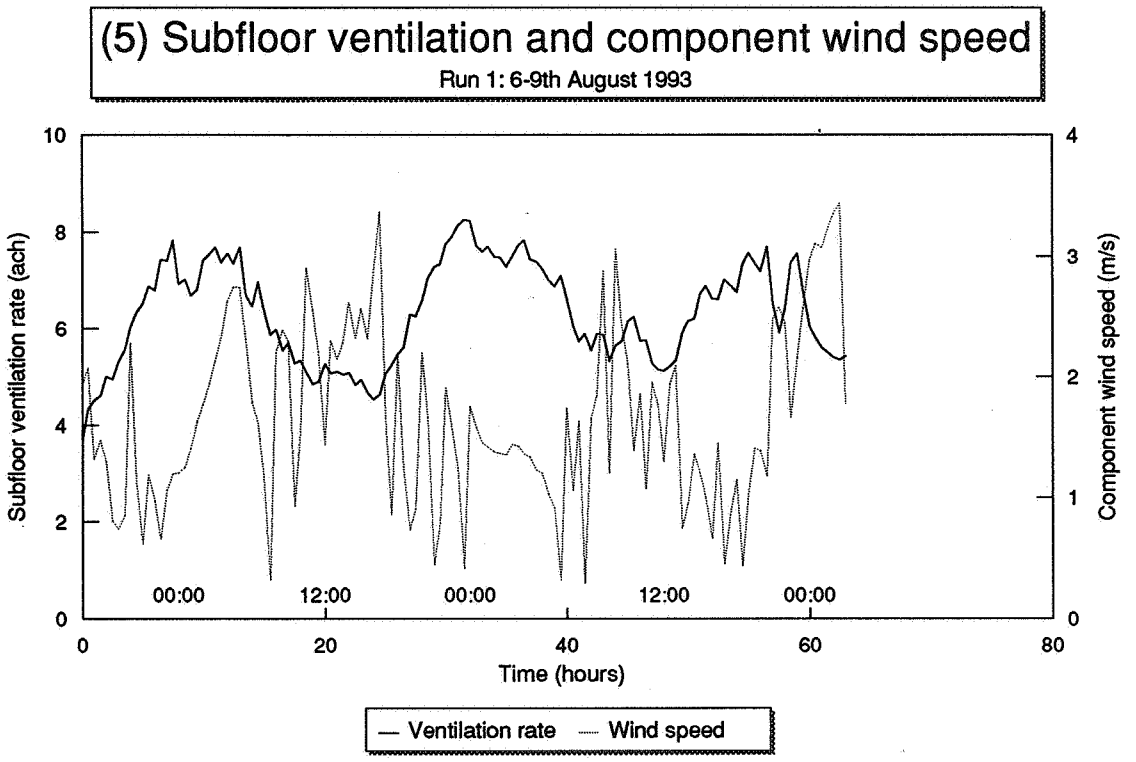
(5) Subfloor ventilation and component wind speed
Run 1: 6-9th August 1993
Subfloor ventilation rate (ach)
Component wind speed (m/s)
Time (hours)
00:00
12:00
00:00
12:00
00:00
— Ventilation rate
— Wind speed

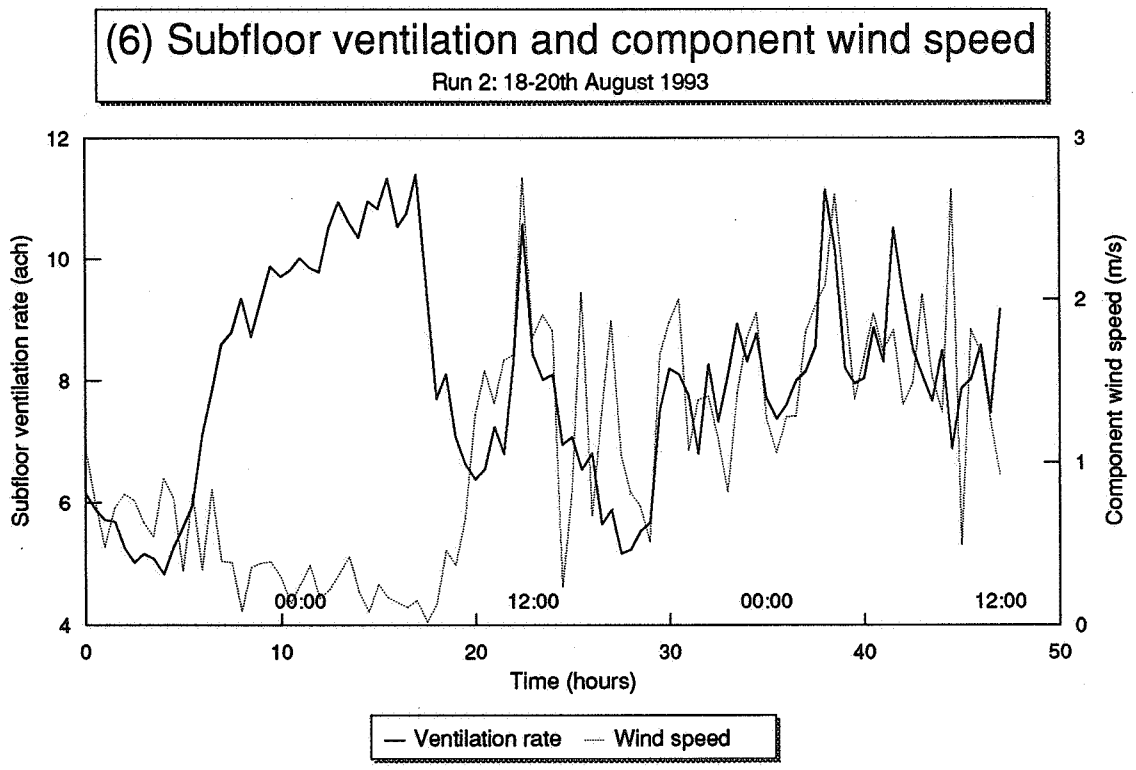
(6) Subfloor ventilation and component wind speed
Run 2: 18-20th August 1993
Subfloor ventilation rate (ach)
Component wind speed (m/s)
Time (hours)
00:00
12:00
00:00
12:00
— Ventilation rate
— Wind speed

The Role of Ventilation
15th AIVC Conference, Buxton, Great Britain
27-30 September 1994

Standardised Measurements of the Cooling Performance of Chilled Ceilings

F Steimle, B Mengede, K Schiefelbein

Universität Essen, Angewandte Thermodynamik und Klimatechnik, Universitätstr.15, 45141 Essen, Germany

Synopsis

One important aim for the development of new air conditioning systems is the reduction of the total energy consumption. This can be reached by separation of cooling and ventilation in air conditioning systems, because it is more effective to transport energy by using water systems instead of air to deliver cooling energy to the consumers. This strategie was the base for the development of several chilled ceilling systems during the last years, so that at present there are many different systems on the market.

One problem during the design period is to calculate the cooling performance of these systems depending on different operating conditions. So it is necessary for the companies to find characteristic data to describe the heat transfer of these elements. But an objective comparison of different systems and an accurate planning is only possible, if these data were investigated under comparable boundary conditions. Parallel to the Germany standard organisation (DIN) the working group "Heating and cooling surfaces" of the German FGK e.V., in which the leading manufacturing, planning and installation companies of chilled ceiling systems are represented, had outlined a guidline to guarantee standardized measurements under clearly defined boundary conditions. It is planed to discuss the main aspects of this guideline and the conditions for measurements of the cooling performance of open convective chilled ceiling systems.

List of symbols

A_a	[m^2]	active surface of the investigated chilled ceiling
C		regression coefficient
ε	[-]	emission coefficient
k_0	[W/m^2]	heat transfer coefficient from heat carrier to the surface
$\dot{M}$	[kg/s]	massflow of distribution medium
n		regression coefficient
$\dot{q}$	[W/m^2K]	heat-flux density
$\dot{q}_a$	[W/m^2K]	heat-flux density with structured surfaces
$\dot{q}_b$	[W/m^2K]	heat-flux density with closed surfaces
$\dot{Q}_H$	[W]	simulated cooling load
t_a	[°C]	ambient temperature
t_i	[°C]	initial temperature of the heat distribution medium
t_r	[°C]	return temperature of the heat distribution medium

t_A	[°C]	air temperature inside the testing chamber
t_R	[°C]	room temperature inside the testing chamber
t_0	[°C]	surface temperature at the chilled ceiling modul
$t_{0,m}$	[°C]	mean temperature at the surface of the chilled ceiling
Δt_0	[K]	logarithmic temperature gradient between surface and heat carrier
Δt_R	[K]	logarithmic temperature gradient between room and heat carrier

1. Introduction

During the last years the reduction of energy consumption in building became one of the most important aim for the development of new technologies. A significant share of energy consumption in non-residential buildings bases on the requirement of cooling and air conditioning. Due to energy saving issues its nessecary to develop new air conditioning and cooling strategies, which lead to an continious reduction of energy consumption.

One possible starting point for the development of these systems is the separation of cooling and ventilation in air conditioning systems, because it is more effective to transport energy by using water systems than to use only air to deliver the cooling energy to the rooms. This strategie was the basic for the development of hybrid systems. By using these systems, it is possible to reduce the ventilation rates to the minimum, which ensures dehumidification and guarantees an satisfying air exchange due to hygenic aspekts. The part of sensible cooling can be delivered to the room by induction-coil, heat exchangers with free convection or chilled structural elements in the room like chilled ceilings.

During the last few years many chilled ceiling systems were developed and in Germany they are nowadays often installed in combination with ventilation systems, which guarantees the necessary ventilation rate. The chilled ceilings can be installed as well in new as in retrofit comercial buildings. At the begining of this period, there was no guidline or technical standard available, which regulates or standardizes the measurement of cooling performance of chilled ceilings. So sometimes the given characteristic date for the design of these systems were related to different operating parameters like room temperature or mean temperature of the cold water, which is mainly used as transport medium to distribute the cooling energy within the building. Also it was possilble, that given data of cooling performance varied within a wide range for systems with nearly the same structure and design.

An accurade planning of these chilled ceiling systems during the design period and an objective comparison of different systems is only possible, if the characteristic data for the description of heat transfer and cooling performance were investigated under comparable and clearly defined boundary conditions. The demand of such a guidline, which guarantees an ojektive comparision of the cooling performance of different chilled ceiling systems, was recognized by the German FGK e. V., in which the leading manufacturing, planning and installation companies are reperesented. The workinggroup, which handels with "heating and cooling surfaces", had outlined a guidline, which guarantees the measurements of cooling performance of chilled ceilings at clearly defined boundary conditions.

2. Testing chamber and conditions for measurements

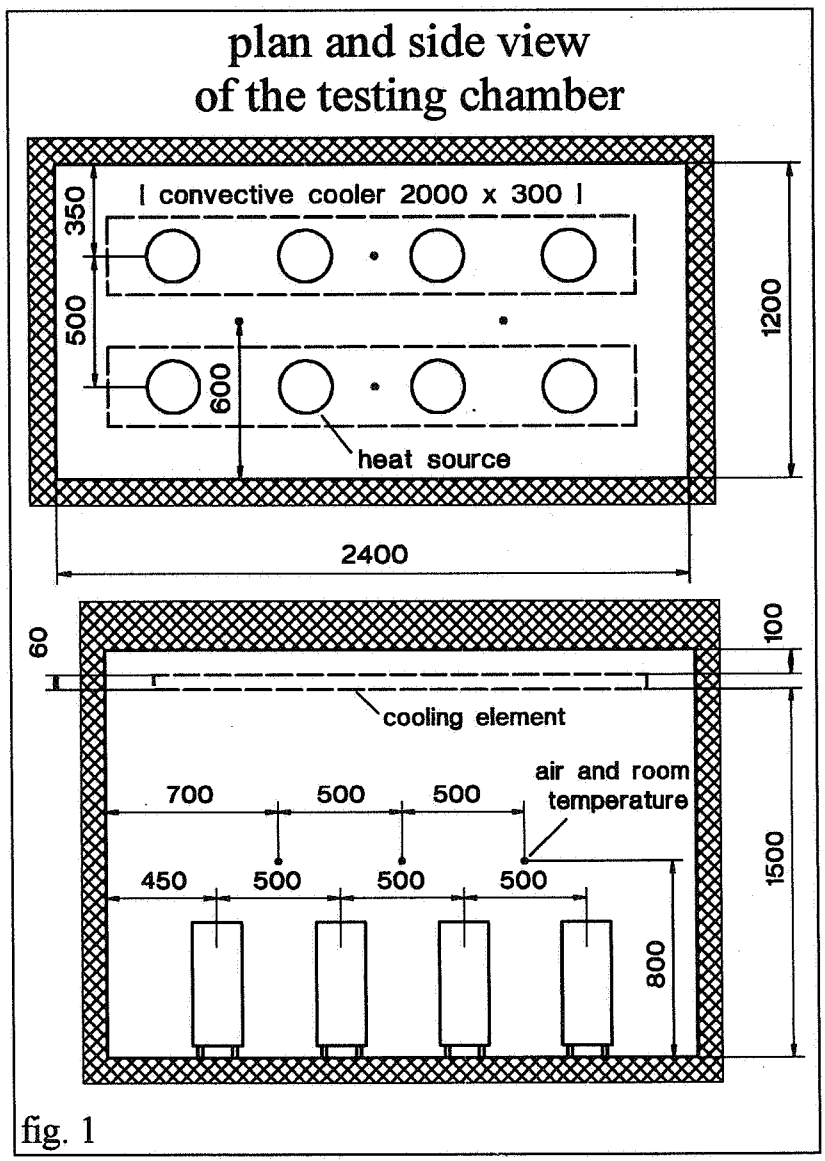

fig. 1

Chilled ceilings are installed in spaces with dimensions in a wide range. In practice chilled ceiling elements with fixed dimensions are combined to large surfaces. So a uniformed measurement is only possible at this ceiling elements, which are normaly available for only a few dimensions and applications as prefabricated moduls. The testing facility, that are explained in the guidline of the FGK e. V., bases on thermal measurements at these chilled ceiling elements with closed or open surfaces in a testing chamber as shown with plan and side view in fig. 1.

This chamber has to be built with a inside length of 2.4 m

and the inside width has to be 1.2 m. The chilled ceiling elements must be installed with a vertical clearance of 1.5 m. All elements of this testing chamber have to be well insulated. The thickness of insulation with a thermal conductivity less than 0.04 W/mK must be more than 0.1 m for walls and floor, for the ceiling the thickness has to be more than 0.2 m. The emission coefficient ε of the inside surfaces of the chamber must be higher than 0.9. Also it must be possible, that air circulates around the chamber while the temperature diffenence between the ambient air and air inside the testing chamber has to be less than 1 K. The reference temperature inside the chamber is the so called room temperature, which will be measured by a temperature sensor inside a black ball (diameter of 35 mm). For the investigation of cooling performance the share of active cooling moduls with closed surfaces has to be more than 70% of the total ceiling of the testing chamber. The rest of the surface has to be closed with a insulation material. The shown installation in Fig. 1 with two convective coolers (2000 x 300 mm) is not provided in this guidline. The cooling load will be simulated by 8 clearly defined cylindrical heat sources with a black surface ($\varepsilon > 0.9$).

In this testing chamber a lot of sensors have to be installed to get knowledge about the operating conditions of the chilled ceiling modules and the temperature distribution inside the testing chamber. The following list shows the variables and the allowed uncertainty of measurements.

measurement variable	unit	symbol	uncertainty of measurement
room temperature inside the testing chamber	[°C]	t_R	± 0.1 K
air temperature inside the testing chamber	[°C]	t_A	± 0.1 K
surface temperature at the chilled ceiling modul	[°C]	t_0	± 0.1 K
initial temperature of the heat distribution medium	[°C]	t_i	± 0.1 K
return temperature of the heat distribution medium	[°C]	t_r	± 0.1 K
ambient temperature	[°C]	t_a	± 0.1 K
massflow of distribution medium	[kg/s]	$\dot{M}$	± 0.1 kg/s
simulated cooling load	[W]	$\dot{Q}_H$	± 5 W
active surface of the investigated chilled ceiling	[m^2]	A_a	± 0.02 m^2

The room and air temperature inside the testing chamber have to be measured at at least 4 positions as marked in Fig. 1. Additional temperature sensors have to be installed at the

center of wall and bottom surfaces. The selection of 8 measurment points at the surface of the chilled ceiling must guarantee the measuring of a repersentive temperature distribution.

Each water temperature has to be measured by two seperate temperature sensors, while a difference of less than 0.05 K between these sensors is allowed. Otherwise they have to be exchanged.

The investigation of the characteristic of a chilled ceiling element includes at least 3 series of measurments with different initial temperatures of heat carrier medium. The rated temperature are 12, 14 and 16°C with a tolerance of ± 0.5 K, while the room temperature inside the chamber has to be 26°C ± 0.2 K. The cooling load simulated by the heat sources has to be regulated continiously from 0 to 100 % of their capacity, while the 4 heat sources in the centre can be switched symmetricaly.

parameter	standard deviation
t_i	0.1 K
t_r	0.1 K
$\Delta t_{i,r}$	0.05 K
t_a	0.2 K

During a period of at least one hour with stationary operating conditions 10 measurement points have to be determined to describe the cooling performance of the chilled ceiling elements. During this period the standard deviations of some parameters are limited as shown in the list. If the registrated data do not fulfil these requirements, the measurements have to be repeated. If the absolute difference between simulated absolute cooling load and cooling performance of the chilled ceiling is higher than 12 W, it is not allowed to use the data to describe the cooling performace. So the measurements have to be repeated.

3. Uniformed description of cooling performance

The guidline "thermal measurements at chilled ceilings" includes two different posibilities to descripe the cooling performance in a uniformed and comparable way.

The cooling performance of chilled ceilings with a smooth and plan surface can be descriped by a so-called "characteristic curve of the chilled ceiling", because the room itself has only a small effect on the cooling performance.

$$\dot{q} = k_0 \cdot \Delta t_0 \qquad \Delta t_0 = \frac{t_i - t_r}{\ln \frac{t_{0,m} - t_r}{t_{0,m} - t_i}}$$

The value k_0 can be explaind as a heat transfer coefficient from heat carrier to the surface and the Δt_0 is the logarithmic mean temperature gradient between heat carrier und mean representive temperature $t_{0,m}$ at the surface of the cilled ceiling. So the characteristic of such a chilled ceiling can be descriped clear by k_0.

In practice the surfaces of sutch chilled ceilings are not smooth, they are often structered with holes or breaks (not closed) and they are perfabricated with structered surfaces (not smooth). Chilled ceilings, which are not closed, can be investigated in the testing chamber too. In a first measurement series, the cooling performance $\dot{q}_a$ will be determined with openings in the ceiling. In a second measurment series the openings must be closed and the cooling performance $\dot{q}_b$ has to be determind once more. For these kind of chilled ceiling the value $\dot{q}_b$ is given as the cooling performance and the relation $\dot{q}_a/\dot{q}_b$ describes the increase of cooling performance because of the structured surface or opening within the ceiling. In the case of slight structered surfaces, the cilled ceiling can be handelt as a smooth one. But this is only allowed, if the relation between real active surface to the basal surface is less than 1.2.

Parallel to the "characteristic curve of the chilled ceiling" it is possible to describe the cooling performence of open and strong profiled cilled ceilings by using the so-called "room characteristic". In this case, the cooling performance depends on the ambient conditions in the room, in which the chilled ceiling has to be installed. The results of the measurements of cooling performance in the testing chamber can be described by

$$\dot{q} = C \cdot \Delta t_R^n \qquad\qquad \Delta t_R = \frac{t_i - t_r}{\ln \frac{t_R - t_r}{t_R - t_i}}$$

The parameters C and n have to be determined by a regression basing on the measured parameters and Δt_R, the logarithmic mean temperature gradient between heat carrier and room temperature as measured with the "black balls". This room characteristic can be used as well for open and structured ceillings as for closed ceilings with a smooth surface. So cooling performance of these different types of ceilings can be described by this equation and parameters C and n. A comparison of the cooling performance of different types of chilled ceiling can be done by the value of $\dot{q}$ for $\Delta t_R = 8$ K.

The evaluation of cooling performance of chilled ceilings by the shown room characteristic was primary developed for typs of ceilings, where heat transfer bases mainly on radiation and where convective shares are very low. The investigation of ceilings, where the heat transfer

bases mainly on convection, by using the testing chamber and the evaluation of cooling performance by the room characteristic is possible, if aditional parameters will be met. If active and non-active elements are combined to a ceiling, the share of active surface has to be more than 1 m^2. If cooling elements will be installed above a intermediate ceiling, they have to be investigated with the same type of intermediate ceiling in the testing chamber and the temperature distribution at the surface has to be measured too.

Investigations at free convective coolers, which are installed in the testing chamber as shown in Fig. 1, where carried out, to characterise the cooling performance and the effects on operating conditions and distibution of heat sources. During the first measurement series the effect of the heat carrier mass-flow on cooling performance was investigated. Five different flow rates of cold water (280 l/h, 330 l/h, 380 l/h, 430 l/h and 480 l/h) were adjusted at each of the two separate connected and measured coolers. The analysis of cooling performance includes the determination of two different "room charcteristics". The first one bases on the equiations as discribed in the guidline, where the cooling performance has to be related to the basal surface of the chilled ceiling (Fig. 2). The second "room charcteristic" bases on the cooling performance per length of cooler, so that the coefficient C varies. This value is often given by manufacturers of convective coolers to describe the cooling performance of their products.

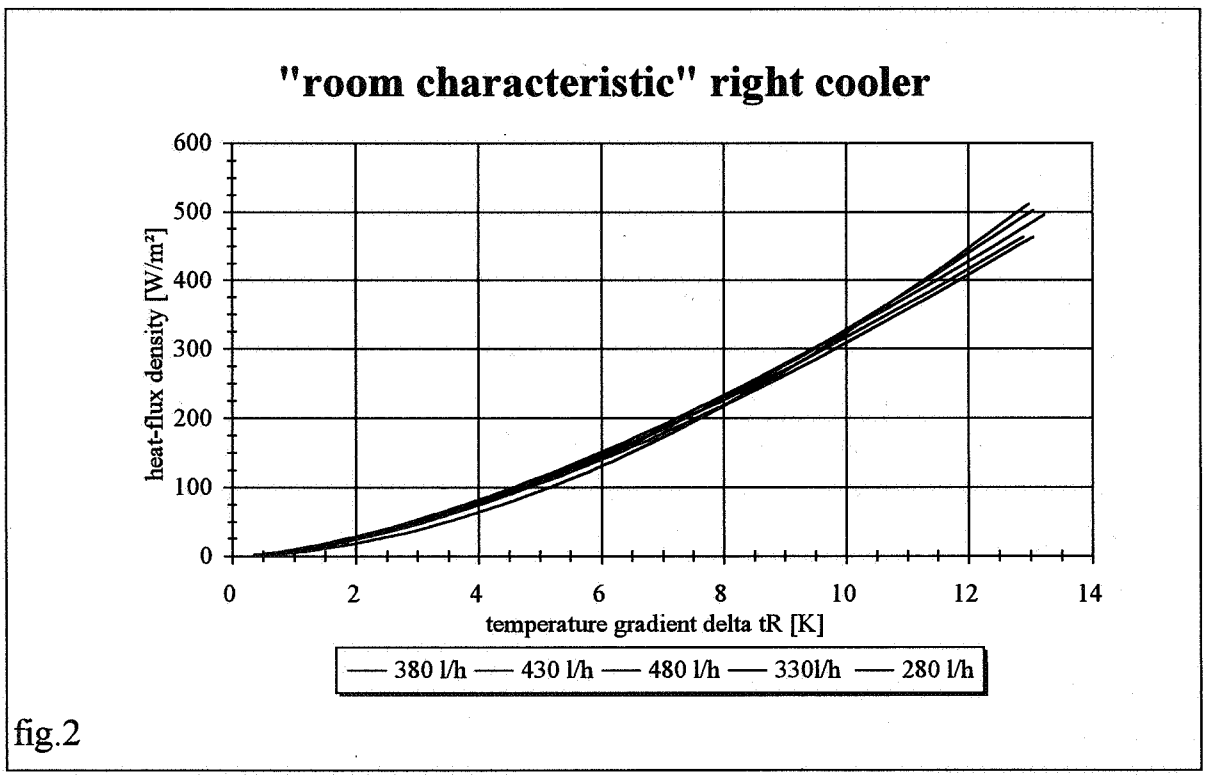

fig.2

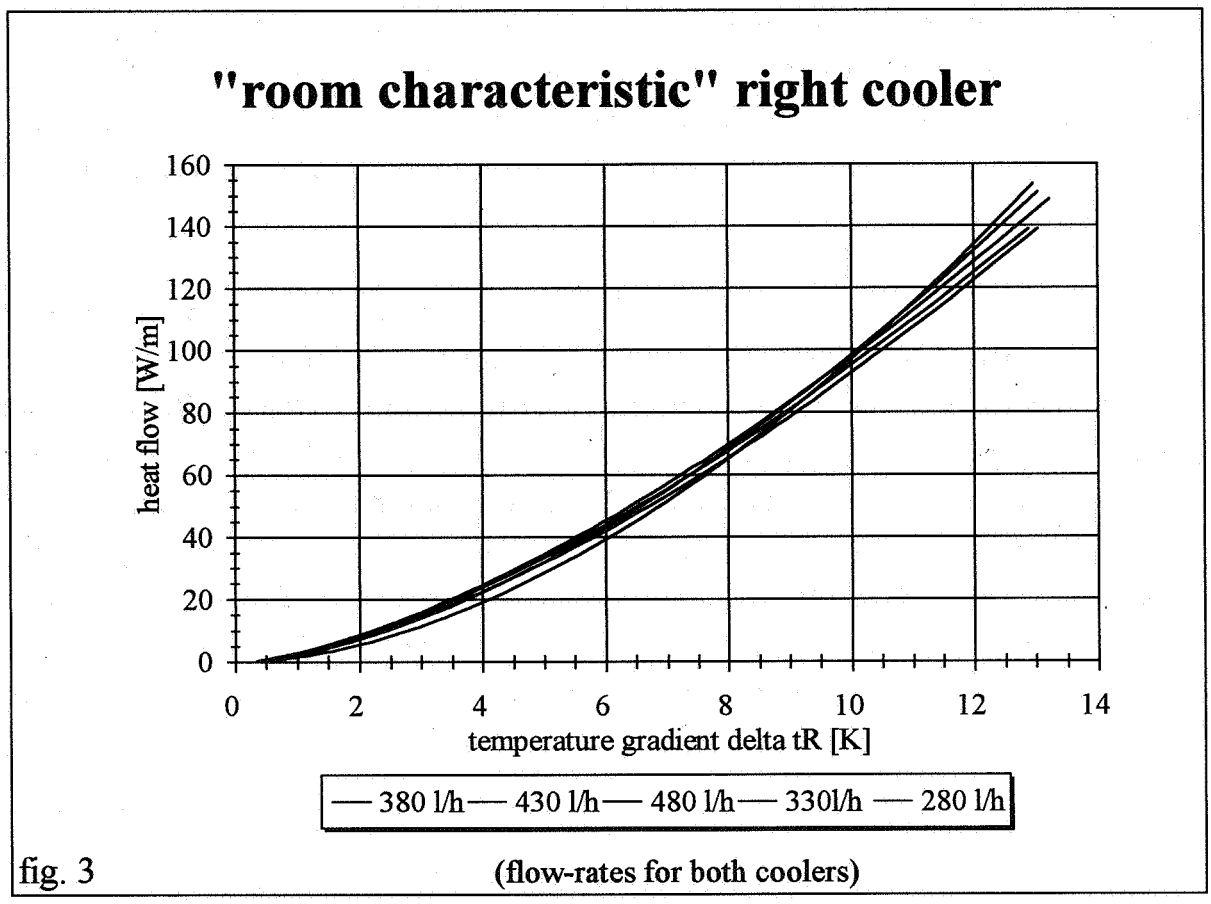

fig. 3 (flow-rates for both coolers)

The analysis of the measured series with different flow-rates shows, that the cooling performance varies only a little in the chosen range of flow-rates. The reason for this characteristic is the low gradient between cold water and room temperature because of the adjusted flow-rates and the low cooling performance. It can be estimated, that cooling performance increases at same logarithmic temperature gradients with the mass-flow of heat carrier. The deviation between estimated and investigated characteristic in the range of low temperature gradient can be related to the uncertainty of measurements and the regression.

Nevertheless the determined cooling performance of the convective coolers installed inside the testing chamber is much lower than the values, which can be reached in practise at the operating conditions. One reason for these lower cooling capacities during the measurements are the bad heat transfer conditions at the coolers in comparison to real operating conditions. Because the testing chamber is well insulated, the cooling load has to meet the cooling performance of the coolers. Because the basal surface of coolers and heat sources are nearly equal, the heat-flux densities in both layers are nearly equal too. Due to the arrangement of heat sources and convective coolers, natural convection of air at the coolers is reduced by the natural convection of the heat sources. The part of cooling performance by convection drops.

In practice coolers will not be installed above heat sources with nearly the same heat-flux density as the cooler. In practice the installation position of the free convective coolers inside the room depends on the given distribution of internal heat sources and solar gain. So the caused air flow pattern may have a positive effect on cooling performance, because the natural convection at the convective coolers can be forced.

The investigated "room characteristcs" of the right cooler by a heat-carrier flow rate of 165 l/h per cooler are shown in Fig. 4. During these mearsurements the effect of the distribution of the heat sources on cooling performance was investigateted while only one of the two installed coolers was active. The comparison of the "room characteristics" with heat sources below the active or inactive cooler shows, that the distribution of the heat sources has an effect on the cooling performance. The characteristic shows a slightly lower cooling performance of the right cooler with heat sources below the cooler than the characteristic with both coolers and heat sources. This effect can be related to the heat transfer conditions by radiation, because the share of surfaces with high temperatures was higher, when both coolers and all heat sources were active.

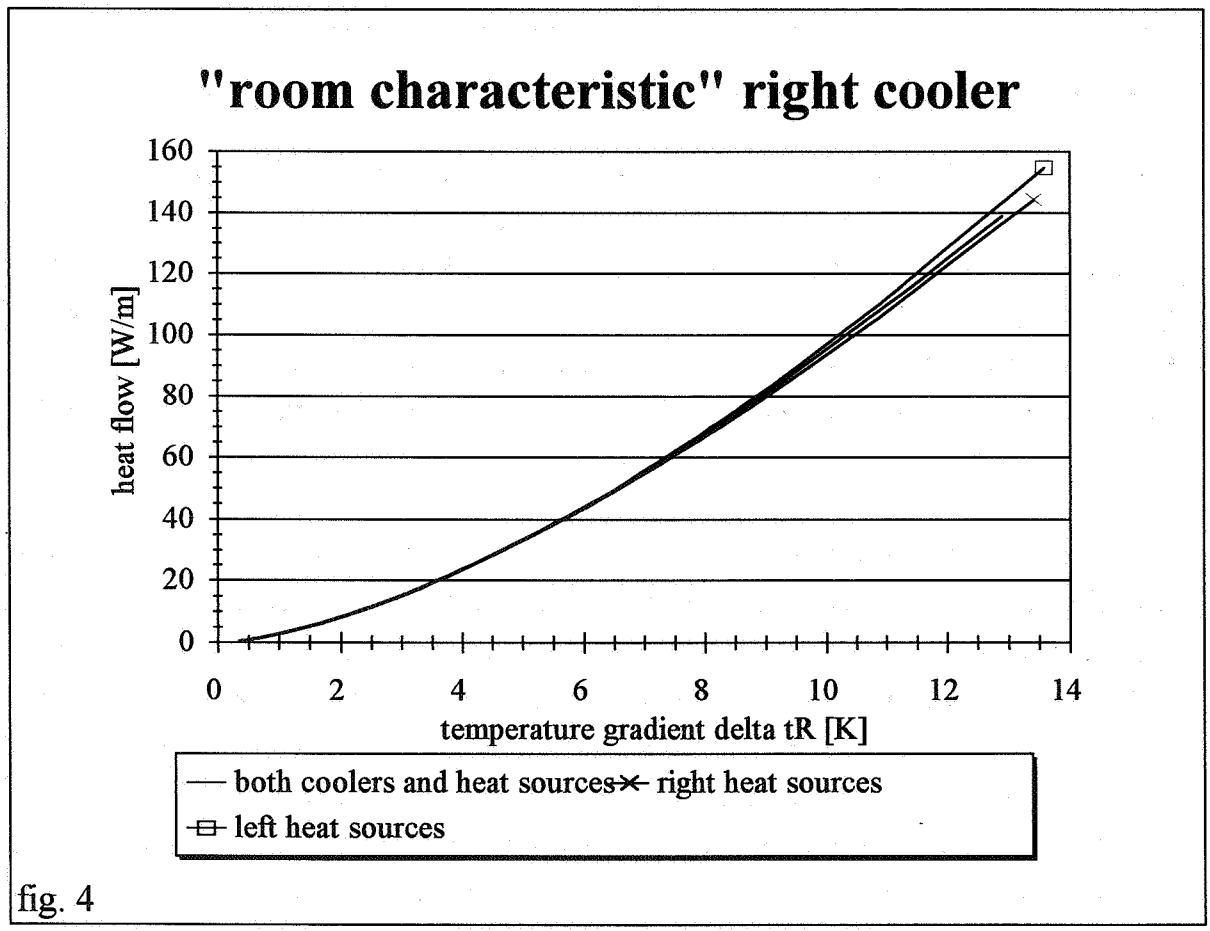

fig. 4

The investigation of the convective coolers with symmetric and different unsymmetric distributions of the heat sources has shown the estimated effects of the varied parameters on cooling performance. But in practice the cooling performance varies in a range, which is larger than determined on the base of the measurements in the testing chamber. Distribution of heat sources in relation to the cooler position, air flow pattern and type of intermediate ceiling have a significant effect on cooling performance, so that the investigation of these convective coolers in larger testing rooms with real headroom of 2.6 - 3 m may lead to smaller differences between investigations in a test room and installations in buildings.

5. Summary

The described guidline "thermal measurement at chilled ceilings" guarantees a uniformed measurement of cooling performance of chilled ceiling elements under clearly defined boundary conditions. Since these guidline was outlined, the range of cooling performance of systems, where the heat transfer bases mainly on radiation, investigated by several companies and institutes decreases. An objective comparison of different systems and a accurate planning is possible by using the characteristic data described in the guidline. But the certainty of the characteristic data basing on measurements in the testing chamber decreases, if the share of heat transfer by convection increases. The determination of cooling performance of free convective coolers should be investigated in larger testing chambers with realistic distributions of heat sources and positions of coolers.

6. Acknowledgement

The measurements were part of a research project, which was supported by the Bundesministerium für Forschung und Technologie under the contract number 0329399A.

The Role of Ventilation
15th AIVC Conference, Buxton, Great Britain
27-30 September 1994

Air Flow Through Smooth and Rough Cracks

H-G Kula, S Sharples

Building Science Research Unit, School of Architectural Studies, The University of Sheffield S10 2UJ

Synopsis

A series of laboratory experiments are described which investigated the effect of surface roughness on the air flow characteristics of simple, straight-through, no-bend cracks with smooth and rough internal surfaces. The crack thicknesses used in the study were 1.0, 1.5 and 2.0mm. The crack lengths, in the direction of flow, were 50.8mm and 76.2mm. For the rough cracks the roughness was simulated with two different grades of commercially available emery-cloth (grade 60 and 100). The experimental results were satisfactorily fitted to a quadratic relationship between Δp and Q of the form $\Delta p = AQ + BQ^2$ for both the smooth and rough crack data. The effect of roughness on the reduction of air flowing through a crack is also discussed.

1.0 INTRODUCTION

1.1 Background

The amount of air flowing in and out of an enclosure is greatly influenced by the size and distribution of the cracks contained within or around the surfaces which form the boundaries of the enclosure. It is desirable to know the flow characteristics of cracks so that, from a knowledge of the pressure drop across a crack, it is possible to calculate the air flowing through that crack. Much work to establish crack flow equations has been carried out in the last twenty years [Hopkins and Hansford (1974), Etheridge (1977), Baker *et al.* (1987), Fleury *et al.* (1990)]. However, most of the fundamental experimental studies associated with this area of research have tended to use idealised cracks made from smooth surface materials such as Perspex or steel. This arrangement may be a reasonable approximation for air flowing through the cracks found, for example, around window or door frames. In reality many building cracks are formed at the junctions of constructional elements such as concrete blocks or brickwork. Such elements may contain appreciable surface roughness, and it of interest to understand how degrees of roughness can influence the fundamental crack flow equations. The classic work by Nikuradse (1933), on pipes whose internal surfaces were coated with sand, dealt with a geometry where the separation between the surfaces was large compared to the size of the roughness elements. An excellent review of this and other relevant work is given by Kronvall (1980). Gardner and Tyrrell (1986) investigated what happened to the Nikuradse equations as the separation between rough plane surfaces was reduced. Their crack separations tended to be much larger than those investigated in this study. Gardner and Tyrrell observed that as the roughness elements came close enough together to overlap then an upper limit on the friction factor was achieved. For even smaller separations the friction factor started to fall.

1.2 Crack flow equations

The results from many experimental and theoretical studies suggest that the practical relationships for describing the flow of air through a crack may be categorised in one of two ways:

$$Q = kL(\Delta p)^n \qquad (1)$$

$$\Delta p = AQ + BQ^2 \qquad (2)$$

where Q = air flow through crack, m^3s^{-1}
k = flow coefficient, $m^3s^{-1}m^{-1}Pa^{-1}$
L = length of crack, m
Δp = pressure drop across crack, Pa
n = flow exponent
A,B = flow coefficients

Both the power-law (equation 1) and the quadratic form (equation 2) of the crack flow equation are widely used. The quadratic form has a stronger theoretical basis and is, unlike the power law, dimensionally homogeneous in that it obeys Reynolds law of similitude. In practice, for the range of pressure drops and air flows typically encountered across building cracks either equation will usually give good agreement with measured data - see, for example, Liddament (1987). One objective of this study was to see if this assertion held for flow through rough cracks. Therefore, all the measured data from the smooth and rough cracks were curve fitted to both power and quadratic forms of the crack flow equation.

2.0 EXPERIMENTAL METHOD

2.1 Equipment

For the laboratory experiments a well sealed wooden box with a volume of 1 m^3 was constructed. The front plate of the box accommodated a model crack with a crack length of 0.5m. The crack itself was assembled using two steel plates which could be set to simulate various crack thicknesses. Two sets of different steel plates breadths (length in flow direction) of 50.8 and 76.2 mm were tested. The steel plates are adjusted for each set of measurement to create crack thickness of 1.0, 1.5 and 2.0 mm.

Figure 1 shows the set-up of the depressurisation technique used for the smooth and rough crack measurements. A fan was used to draw air through the rig to maintain the desired pressure drop across the crack in the front plate of the box. Baker *et al.*(1987) found during their investigation that a shielding "box" used for protection against external pressure fluctuations in the laboratory e.g. doors closing was not necessary. Flow rates below 0.00167 m^3s^{-1} were measured with a commercially available laminar flow device. Flow rates above 0.00167 m^3s^{-1} were measured using an orifice plate constructed and calibrated according to BS 1042 (1964). The pressure drop across the crack was set by adjusting the bleed valve of the fan system. Flow measurements were taken at several pressure drops in the range 0 to 50 Pa when the readings on the manometers had become steady at each set point. To ensure that only the flow through the crack was considered in the analysis the crack was sealed over and a leakage test of the $1m^3$ box was performed. The flow through the leakage of the box was then subtracted from the overall flow in order to obtain the flow through the crack only.

The steel plates were altered to simulate different kinds of roughnesses. The roughnesses were simulated by attaching emery cloth to the upper and lower surfaces of the cracks. The emery cloths corresponded to grades of 60 and 100, with the 60 grade being the rougher of the two. The average peak heights of the grains for each of these grades were measured using a microscope. The results are shown in Table 1.

The thickness of the crack was defined as shown in Figure 2. The grains on the emery cloth block off some of the open area, thus the effective leakage area gets smaller the rougher the crack is. This way of defining the crack thickness set-up was chosen to make it possible to

compare the flows through the same crack with and without the roughness being present. The ambient conditions in the laboratory, dry and wet bulb temperature and the barometric pressure, were measured to enable the calculation of air density, air viscosity and kinematic viscosity.

Table 1 Peak heights of emery cloth grains

Grade of emery cloth	Average peak height (mm)
60	0.613
100	0.375

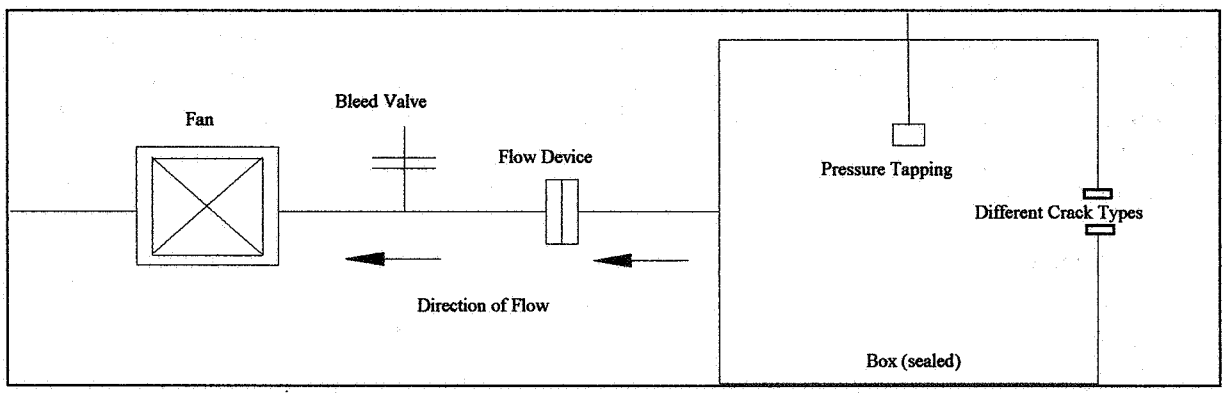

Figure 1 The Experimental Measurement Rig

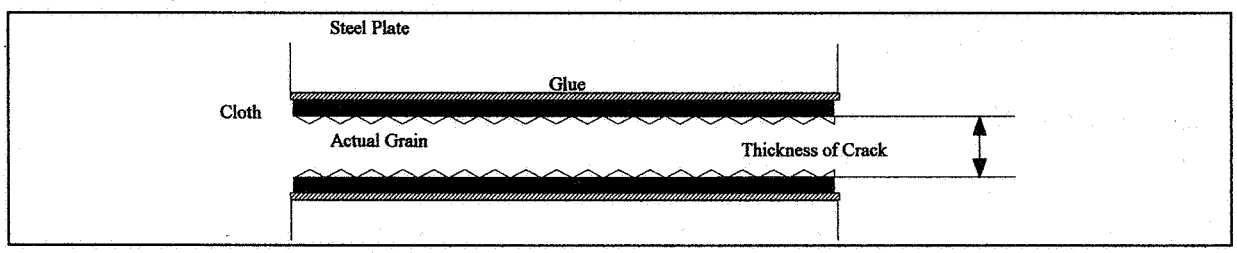

Figure 2 Measurement of the Rough Crack Thickness

3.0 RESULTS

3.1 Crack designation

Each crack used in the measurement programme had a designation code made up as:

Smooth or Rough -Crack length / crack thickness / grade of roughness

For example, a smooth 50.8mm long, 2.0mm thick crack would have the designation S50/2 while the same crack with the 60 grade emery cloth applied would be R50/2/60.

3.2 Smooth crack results

All the experimental measurements of air flow Q and pressure difference Δp were curve fitted to both the quadratic and power law forms of the crack flow equation. Table 2 gives the results of these fits and the r^2 correlation coefficient. It must be stressed that all the statistical results presented in the tables below are only strictly valid for the ranges of Q and Δp measured during the experiments. Both fits obviously provide excellent regression curves through the experimental data. The quadratic fit is seen to be consistently slightly better than the power law and was, therefore, the chosen approach for further analysis.

Table 2 Quadratic and power fits to the smooth crack data

Crack designation	Quadratic fit r^2	Power law fit r^2
S50/2.0	0.9999	0.9999
S50/1.5	0.9991	0.9974
S50/1.0	0.9946	0.9905
S76/2.0	0.9999	0.9984
S76/1.5	0.9991	0.9943

The regression coefficients for the quadratic fit are given in Table 3.

Table 3 Coefficients for regression fit $\Delta p = AQ + BQ^2$ for smooth crack data

Crack designation	A	B
S50/2.0	1117	703067
S50/1.5	3562	1578596
S50/1.0	14534	7986388
S76/2.0	2726	1113949
S76/1.5	7109	2430740

3.3 Rough crack results

The rough crack results were plotted graphically and these plots indicated that the relationship between Q and Δp could be described by a quadratic or power law curve fit. The correlations resulting from these curve fits are given in Table 4.

Table 4 Quadratic and power fits to the rough crack data

Crack Designation	Quadratic fit r^2	Power law fit r^2
R50/2.0/60	0.9995	0.9979
R50/1.5/60	0.9859	0.9749
R50/1.0/60	0.9184	0.9097
R50/2.0/100	0.9994	0.9947
R50/1.5/100	0.9992	0.9942
R50/1.0/100	0.9514	0.9362
R76/2.0/60	0.9988	0.9911
R76/1.5/60	0.9863	0.9767
R76/2.0/100	0.9999	0.9992
R76/1.5/100	0.9991	0.9937

As with the smooth crack data, both regressions give excellent fits to the data, with the quadratic equation again giving the slightly better r^2 value in each case. The regression coefficients for the quadratic fit are shown in Table 5.

Table 5 Coefficients for regression fit $\Delta p = AQ + BQ^2$ for rough crack data

Crack Designation	A	B
R50/2.0/60	4476	3780333
R50/1.5/60	11679	19122030
R50/1.0/60	30037	189480200
R50/2.0/100	2583	1456533
R50/1.5/100	4280	2252611
R50/1.0/100	33825	92263960
R76/2.0/60	7090	3887698
R76/1.5/60	20614	31179210
R76/2.0/100	6802	2197209
R76/1.5/100	12991	5420307

3.4 Comparison of smooth and rough crack results

The effect of the roughness on the air flow through the cracks is best understood by plotting the Q-Δp relationships for the smooth, 'rough 60' and 'rough 100' data for each individual crack, and these plots are shown in Figures 3 to 7. The actual reduction in the air flow as the crack becomes rougher may be expressed as :

$$flow\ reduction = [\ (Q_{smooth} - Q_{rough}) / Q_{smooth}\ ]\ x\ 100\%$$

The flow reductions at Δp values of 10 and 50 Pa are shown in Table 6

Table 6 Reduction in flow due to roughness

Crack type	Flow reduction 60 grade, 10Pa	Flow reduction 60 grade, 50Pa	Flow reduction 100 grade, 10Pa	Flow reduction 100 grade, 50Pa
50/2.0	63%	59%	38%	33%
50/1.5	72%	70%	17%	16%
50/1.0	69%	75%	64%	67%
76/2.0	53%	50%	46%	38%
76/1.5	69%	70%	54%	50%

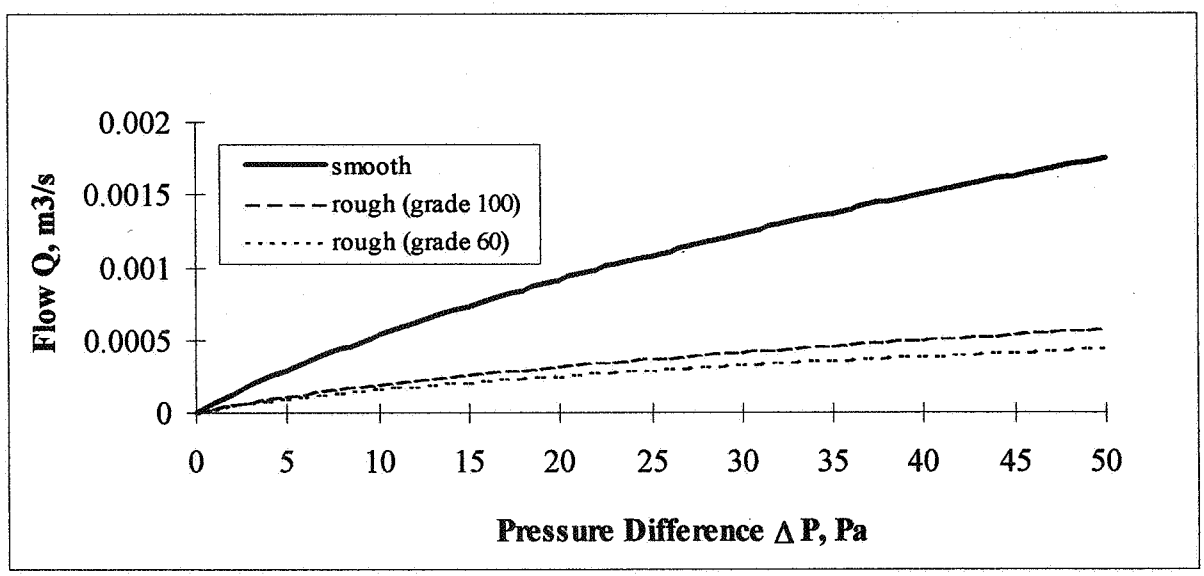

Figure 3. Smooth and Rough Flows for 50.8 x 1 mm Crack

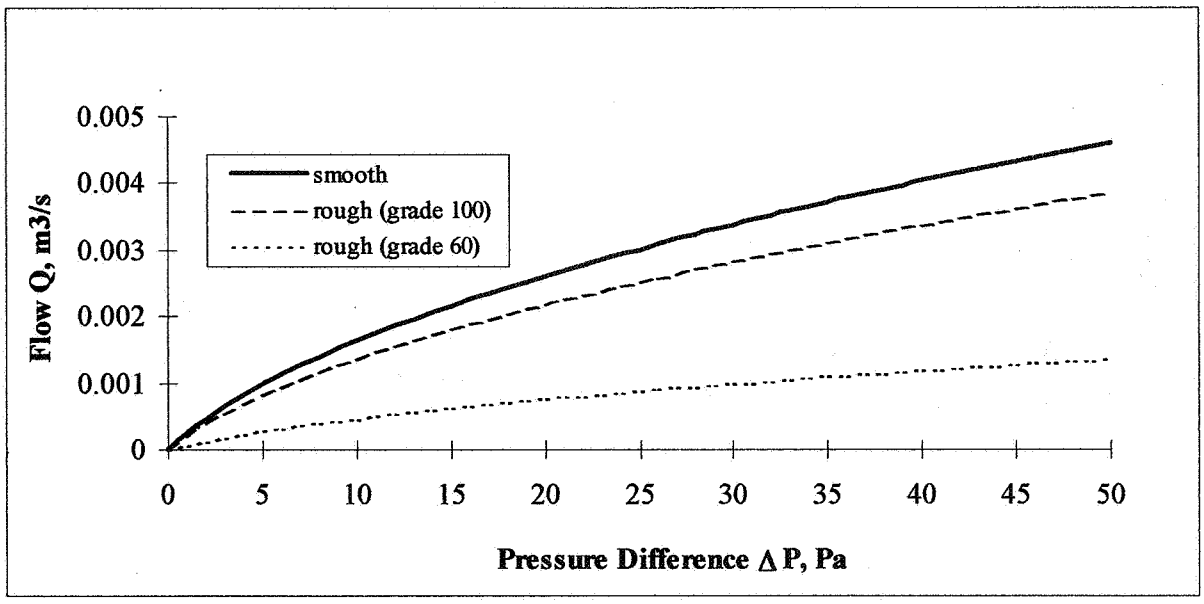

Figure 4. Smooth and Rough Flows for 50.8 x 1.5 mm Crack

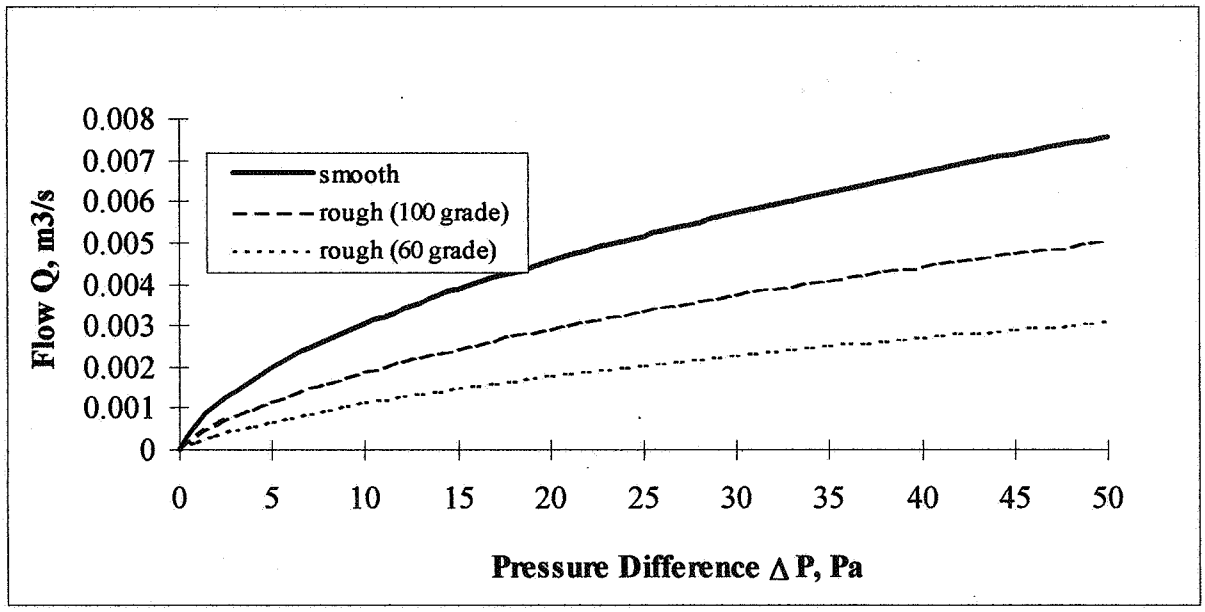

Figure 5. Smooth and Rough Flows for 50.8 x 2 mm Crack

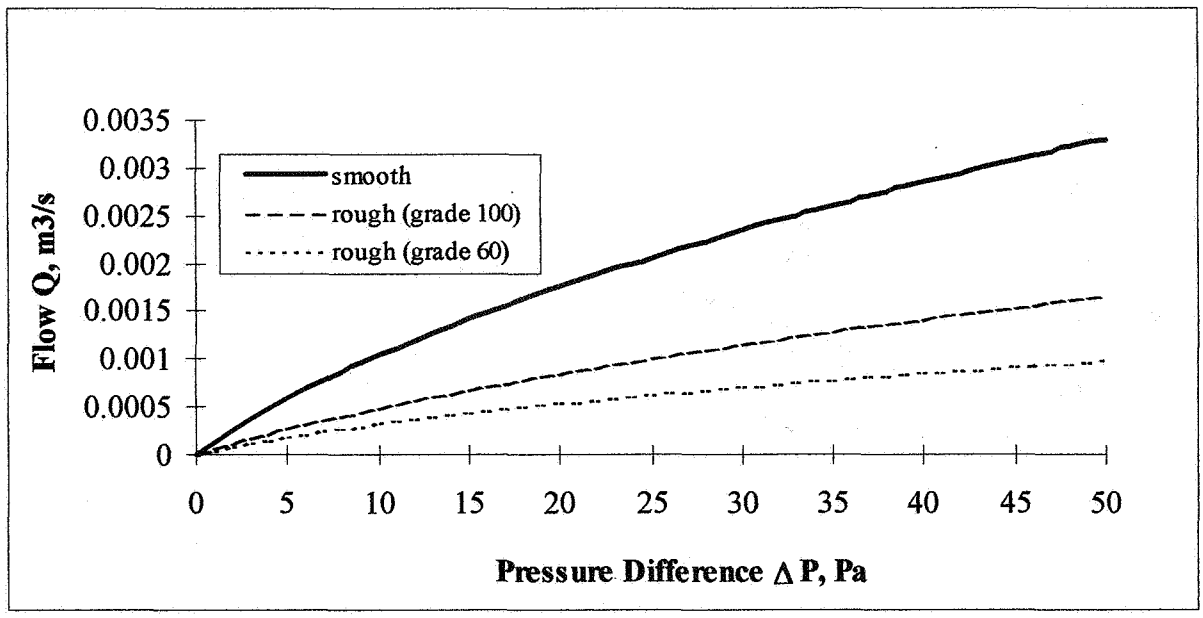

Figure 6. Smooth and Rough Flows for 76.2 x 1.5 mm Crack

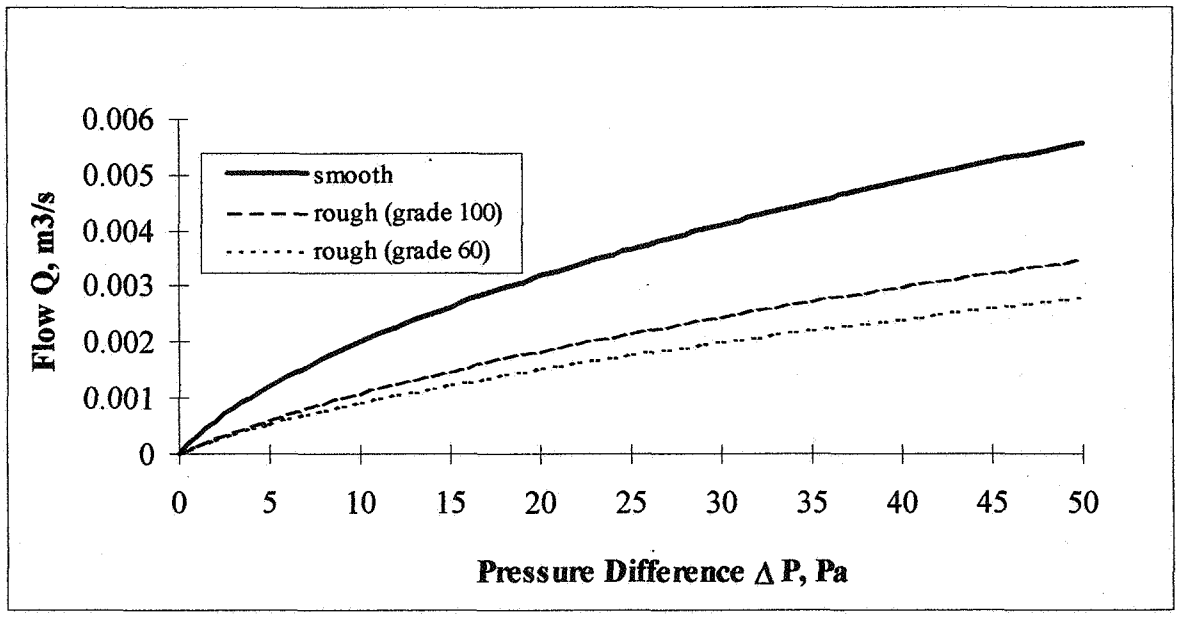

Figure 7. Smooth and Rough Flows for 50.8 x 2 mm Crack

4.0 DISCUSSION

Adding roughness to a crack can lead to a substantial reduction in the flow through that crack. Table 6 indicates that, for each crack, this reduction is fairly constant over the range of Δp used in this study. This suggests that if the roughness of a crack's surface can be

established then a constant may be applied to the smooth crack flow equation to obtain an estimate of the air flow through the rough crack. Table 6 also displays a very small flow reduction for the 50/1.5 crack with the 100 grade roughness. This may be an experimental mistake, although all measurements were repeated several times for all of the experiments. Another explanation is that the flow conditions for this configuration may be in the regime where the friction factor λ, as a function of the Reynolds number, is close to its minimum value. The work of Nikuradse on flow through pipes coated with uniform sand roughnesses, as described in Kronvall (1980), suggested that λ displays a minimum value at Re values around 2.5×10^3. It may be that an analogous situation exists for flow through rough cracks, but this study has not been extensive enough to allow this suggestion to be validated.

5.0 CONCLUSIONS

An investigation of the effect of crack surface roughness on air flow has been described. The main conclusions to be drawn are:

- crack flows through both smooth and rough cracks are well described by power law and quadratic forms of the crack flow equation, with the quadratic being slightly better
- the addition of even a small degree of roughness can greatly reduce the flow through a crack, compared to the smooth equivalent, for the same pressure difference
- the percentage flow reduction, for a given crack, over the range of pressure differences used in this study appears to have a fairly constant value
- it is tentatively suggested that there may be some configurations of flow and crack geometry and roughness which display a minimum in the friction factor.

Acknowledgements

The authors would like to thank the SERC (now EPSRC) for its financial support during this project and Garry Palmer and Mike Wright for their computing assistance.

References

Baker P H, Sharples S and Ward I C (1987) Air flow through cracks. *Building and Environment* **22** , 293-304

BS 1042 Part R (1964) Methods for the measurement of fluid flows in pipes; orifice plates, nozzles and venturi tubes.

Etheridge D W (1977) Crack flow equations and scale effect. *Building and Environment* **12**, 181-189

Fleury B A, Gadilhe A Y, Niard P and Chazelas J L (1990) Air flow through building slits and components. Proc 11th AIVC Conf., Belgrade, Italy, 389-399

Gardner G C and Tyrrell R J (1986) The flow resistance of experimental models of naturally occurring cracks. *Proc Inst. Mech. Engrs* **200**, No C4

Hopkins L P and Hansford B (1974) Air flow through cracks. *JIHHVE* **18**, 123-129

Kronvall J (1980) Air flow in building components. Report TVBH-1002, Division of Building Technology, Lund Institute of Technology, Lund, Sweden.

Liddament M W (1987) Power law rules - OK? Air Infiltration Review, 8(2), 4-6

Nikuradse J (1933) Strömungsgesetze in rauhen Rohren. *VDI-Forschungsheft 361*

The Role of Ventilation
15th AIVC Conference, Buxton, Great Britain
27-30 September 1994

Comparison of the Accuracy of Detailed and Simple Model of Air Infiltration

J-M Fürbringer

LESO-PB Departement d'Architecture, Ecole Polytechnique Fédérale de Lausanne, CH 1015 Lausanne, Switzerland

COMPARISON OF THE ACCURACY OF DETAILED AND SIMPLE MODELS OF AIR INFILTRATION

J.-M. FÜRBRINGER
LESO-PB, Département d'Architecture
Ecole Polytechnique Fédérale de Lausanne

CH - 1015 LAUSANNE, Switzerland

SYNOPSIS

Simulation is proving more and more important in building physics. Programs of different levels of complexity are today available for researchers and designers to model and plan buildings. But the accuracy of the output is not usually provided as a common result.

This paper is a short summary of a dissertation [1] focused on the accuracy of the simulation outputs as a function of the accuracy of the input parameters. This is a point which requires particular attention, so that the simulation outputs can be used with their confidence intervals; without these intervals, the use of the simulation output is risky. The following question is discussed in the paper : is the prediction of detailed models more accurate than that of simple models if the accuracy of their respective input parameters is taken into account ? There is a risk that inaccurate input data can invalidate attempts at exact simulation. For the studied case, the answer is that the detailed model has larger confidence intervals than the simple models in wind as well as stack dominated situations.

The result has been obtained by investigating models and measurement processes and determining their confidence intervals. Fractional factorial design has been used to estimate the partial derivatives of the models by the input parameters with an optimum number of simulations for the detailed multizone model COMIS and 4 simple models BREVENT, LBL, AIDA and TURBUL. A 6-zone family house was chosen as case of study because it allowed the comparison of the sensitivity of simple and detailed models.

SYMBOLS

a_o	constant effect	C_i	airtightness coefficient, [$m^3/s\ Pa^n$]
a_i	main effect	n_i	exponent, [-]
a_{ij}	interaction effect	Q_i	flow through the element i [m^3/s]
x_i	input parameter (standardised)	ΔP_i	pres. diff. through the element i, [Pa]
y	output parameter	N	number of tested parameters
$minX_i$	input parameter minima		
$maxX_i$	input parameter maxima		

1. INTRODUCTION

For researchers, the simulation saves time and money. But a simulation procedure which is not validated and whose sensitivity is unknown is risky. It is imperative to know the influence of the uncertainty of the input parameter on the output. It is important to know which are the critical parameters to be determined with the smallest possible confidence interval and the one which can be roughly estimated. Each year new models with each time more sophisticated

features are settled without any tools, and few study was available to assess their uncertainty level. At the age of the data base, data are used without handling of confidence intervals and the large majority of programs (for not saying all of them) has no tool to help the user to deal with the uncertainty of the input parameters.

From this standing point, we have tried with our study to make progress to solve this problem. We propose a method to analyse the sensitivity of simulation programs which is illustrated here. A tool was also set up to perform the analysis. This work was under taken in the frame of the IEA-ECB - Annex 23 "Multizone air flow modelling" [2, 3].

The questions which have motivated our work are :

1) Which are the confidence intervals of the output data of a simulation program taking into account the uncertainty on the input data and inversely which are the acceptable uncertainty on the input data to simulate the ventilation of a building within a given accuracy ?
2) Are the nodal and semi-empirical models, as COMVEN, more accurate than simple empirical models when the uncertainty of the input data is taken into account ?

We have also dealed a lot with the problem of discrepancies between measurements and simulations, but this work will not be reported here [1].

The usual tool systematically quoted when talking about sensitivity analysis is the Monte-Carlo Method. This random method allows with less than 100 runs the estimation of the global sensitivity of a program without having the possibility to determine which are the influent parameters. The other commonly quoted and used method is the "one factor at a time" method. This method is heavy to use and requests a considerable amount of simulations. More, it does not take into account the interaction effects which can occur between factors. After these depreciative comments, the reader has guessed that we want to make the apology of an alternative method : this is the factorial design method. Our study has also resulted to a comparison of factorial and Monte-Carlo design which can be synergetically combined [4].

Factorial design is a method settled in the 50's by chemists in the experimental domain. The main feature consists on extracting with a minimum number of experiments (runs) the maximum information. The method is also known as surface response method.

The aim of comparing simple against detailed model is not to eliminate the less accurates. Both types of models do not simulate exactly the same objects and the need in both of them is not in question. But from our point of view it appears risky to ignore, as it is done commonly, the problem of the confidence intervals of simulation results. This has ended in a despising regard of professionals to simulation and models to which it is reproached to give any desired answer. Under the deliberately polemic aspect of the comparison between two types of models which have convinced defenders, it lays the motivation of finding appropriate tools for given tasks.

2. FACTORIAL DESIGN METHOD

Factorial design has been used to calculate the confidence interval of the outputs and to evaluate their sensitivity to input inaccuracies. A comprehensive presentation of the factorial design can be found in [5], a short apology in [6,7]. The method consists on fitting an output y on a linear model corresponding to a Taylor series and which variables are the input parameters x_i :

$$y = a_0 + \sum_{i=1}^{N} a_i X_i + \sum_{i \neq j}^{N} a_{ij} X_i X_j + \ldots \qquad (1)$$

where N is the number of tested inputs.

The coefficients a_i are called main effects of the parameter X_i, and a_{ij} the conjugate effects of X_i and X_j. The values of the a_i and a_{ij} coefficients are determined by running the program with values of parameters selected to lead to a well conditioned system of equations with a minimum number of runs.

The fit is done on a given domain D of IR^N which is determined by the lowest and the highest values, $minX_i$ and $maxX_i$ that the tested input parameter X_i can take. Being given the linear model of equation 1, the best choice for optimising the number of runs and the condition of the system is a factorial design. This design is constituted by the points at the vertex of the domain D. The maximum number of points of simulation is then 2^N (full factorial design). If some coefficients a_i a_{ij} are of interest only a fraction of this full design can be selected (fractional design 2^{N-m}).

The choice of the linear model can be argued. Evidently physical phenomenon as complex as the air movements in a multizone building are seldom linear. But in one hand it is a suitable first step and in the other hand, it is possible to use non-linear metrics to linearize known non-linear input or output parameters.

The effects, corresponding to the first derivatives of the model are related to the local standard deviation $S_y(X_1,\ldots, X_i,\ldots)$ by the following equation :

$$(Sy(X_1,\ldots, X_i,\ldots))^2 = \sum a_i^2 + \sum a_{ij}^2 + \ldots \quad (2)$$

demonstrating that the effects are an interpretation of the standard deviation with the variation of the input. Equation (2) is also the point of comparison with Monte-Carlo Method usable to perform a rough sensitivity analysis.

The response which has been analysed is the mean age of air. The age of air τ is a matrix computed from the flow matrix Q as follows:

$$\tau = Q^{-1} V \quad (3)$$

where V is a diagonal matrix with the volume of the zones as elements. The mean age τ_j of air of a zone j is then :

$$\tau_j = \Sigma_j \tau_{ij} \quad (4)$$

3. Programs

One detailed model and 4 simple models have been investigated. The detailed model is COMVEN of COMIS [8, 9]. It is a nodal multizone model using a Newton-Raphson algorithm with 2 fixed relaxation coefficients to solve by iteration the system based on the mass conservation. The flow equation used to define cracks is the power law :

$$Q_j = C_j (\Delta P_j)^{nj} \quad (5)$$

The 4 simple models chosen for this study, BREVENT, LBL-model AIDA and TURBUL are of different types. The first two are used for the prediction of air renewal from pressurisation data [10, 11, 12]. Their simplicity makes their interest : both of them can be calculated by hand. AIDA is a nodal model for one zone [13]. It runs with an iterative algorithm simple enough to be implemented on a programmable pocket calculator. TURBUL is a monozone dynamic model settled to study wind turbulence effect on air renewal and test various algorithms of resolution in a dynamic process [14, 15]. Table 1 summarises they characteristics.

Table 1 : Caracteristics of the simple programs used in this study

Program	Comments
AIDA	Nodal monozone, iterative algorithm, implicit calculation of neutral level.
BREVENT	No calculation of neutral level. Air tightness uniformly distributed.
LBL	Calculation of neutral level. Air tightness uniformly distributed modelled by an equivalent leakage area. Wind, stack and mecanical induced ventilation calculated separatly.
TURBUL	implicit calculation of neutral level.

4. The case study

In the perspective of comparing detailed and simple models, a building suitable for both has been chosen. It is a test building of an Italian gas company. The plan is shown in figure 1 and the air flow network simulated with the detailed model COMVEN in figure 2. In table 2 are presented some data [16,17].

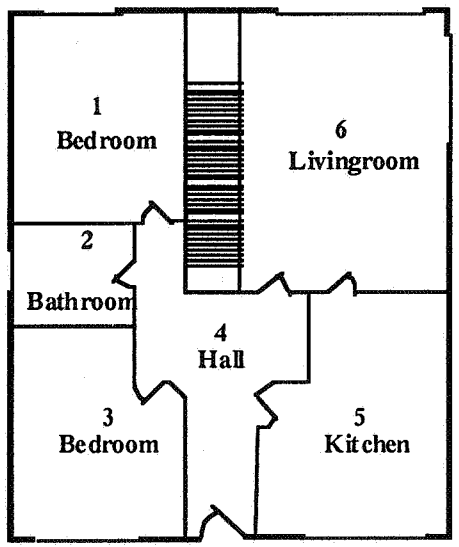

Figure 1 : Plan of the test building

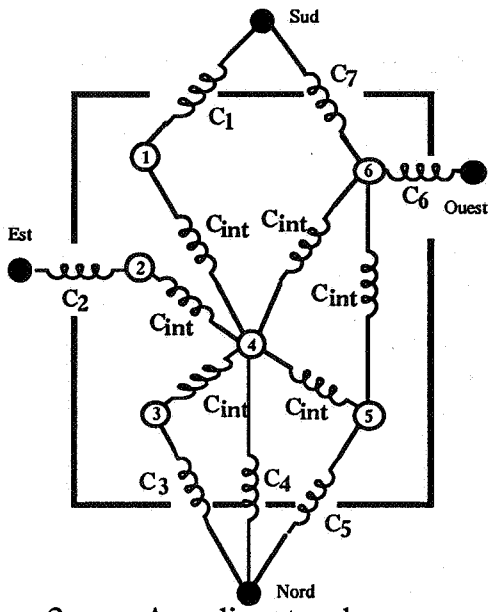

Figure 2 : Aeraulic network

Table 2 : Airtightness coefficients and related inaccuracies.

air tightness	[kg s^{-1} Pa^{-n}]	S(C)/C	Exponent	[-]	S(n)/n
C_1	0.018	24%	n_1	0.65	8%
C_2	0.0276	23%	n_2	0.39	13%
C_3	0.0048	24%	n_3	0.86	6%
C_4	0.0784	23%	n_4	0.54	10%
C_5	0.0252	23%	n_5	0.60	9%
C_6+C_7	0.0288	23%	$n_6 = n_7$	0.50	10%
C_{int}	0.0784	23%	n_{int}	0.54	10%

5. TEST AND RESULTS

The number of parameters being different for each model, different design have been used. Table 3 presents the features of the tests for each program. The comprehensive study includes analysis of the effect of each group of factors [1,16]. Here, for safe of concision, only general results are given. Detailed results and analysis will be published within the frame of Annex 23 of the IEA ECB&C. The results of two types of test are given here.

Table 3 : Detail of program tests.

Parameters	COMVEN	BREVENT	LBL	AIDA	TURBUL
Tested parameters	32	9	12	24	24
Design	$2^{(32-24)}$	$2^{(9-3)}$	$2^{(12-6)}$	$2^{(24-16)}$	$2^{(24-16)}$
Runs	64	64	64	256	256
Level of uncertainty :					
• air tightness(es)	±24%	±5%	±20%	±24%	±24%
• exponent(s)	±10%	±8%	±8%	±10%	±10%
• volume(s)	±10%	±10%	±10%	±10%	±10%
• temperatures	±0.5[°C]	±0.5[°C]	±0.5[°C]	±0.5[°C]	±0.5[°C]
• atmospheric pressure	±0.5%	-	-	-	-
• pressure coefficient	±50%	-	-	±50%	±50%
• wind speed	±5%	±5%	±5%	±5%	±5%
• heights	±1%	±5%	±5%	±1%	±1%
• terrain	-	±1	-	-	-
• wind exposure	-	±1	-	-	-

In a first step, the input parameters have been varied uniformly, with the same range of variation for each ones without relation with their actual and usual uncertainty. As example, all the parameter ranges have been fixed to 1% of their central value. The comparison is then done for the ratio between the standard deviation $S(\tau)$ of the mean age of air and the uniform standard deviation $S(X_i)$ of the input parameters. The results is shown in figure 3.

In a second step, the actual level of uncertainty has been used (cf table 3). This time the test has been performed for three different Archimede number. (The Archimède number is the ratio between wind and stack forces). The results are given in figure 4.

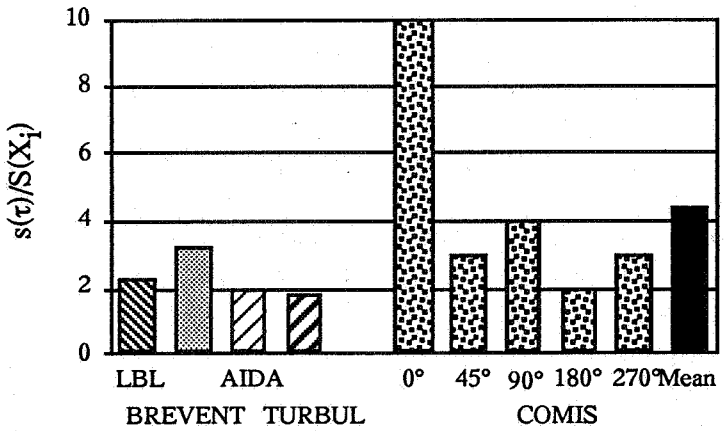

Figure 3 : Ratio between the standard deviation $S(\tau)$ of the mean age of air and the standard deviation $S(X_i)$ of the input parameters. Results obtained using different factorial designs for four simple models and COMVEN.

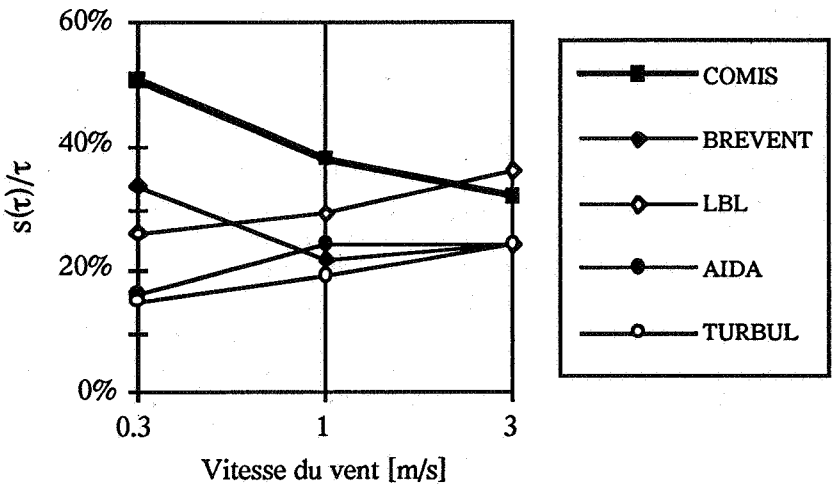

Figure 4 : Comparison of the variation of the mean age of air uncertainty as a function of the wind speed for considered models.

6. DISCUSSION

Comparing the uncertainty of simple model against the detailed model when using uniform ranges for the input (cf fig. 3), brings the following points :

- With same variation ranges for all the input parameters, the uncertainty ratio of simple or detailed model are of the same order of magnitude.
- For simple models, the confidence intervals of the nodal models (AIDA, TURBUL) are almost half the confidence intervals of the models of empirical conception (LBL, BREVENT).
- For the detailed model, there may be a large difference in sensitivity depending on the considered zone and the wind direction. There are critical situations for which the detailed

level of the model is not adapted to the accuracy of measurements. In these cases, the amplification of uncertainty between input and output data is about one order of magnitude. Except those critical situations, the uncertainty amplification ranges between 2 and 3.

The second step, when using actual uncertainty, drives to the following comments :

- The uncertainty got with the detailed model is greater than the uncertainty shown by the simple model. Remember that we are talking about the uncertainty coming from the input data and propagated trough the model. It is not question here of the accuracy of results, from the physical point of view, which must be determined by the validation process.
- The evolution of the uncertainty of the simple model with the wind speed is different from a model to another. This is attributed to the different options used to model wind effects.
- The model with a nodal conception have their uncertainty increasing with the wind speed.
- The model BREVENT has a maximal uncertainty when the wind dominates the thermal buoyancy. The LBL model has the inverse behaviour showing the smallest uncertainty at the equilibrium situation. For the latter, this is due to the use of indices for the terrain and the wind exposure. The minimal uncertainty for those indices, ±1, enlarge the output uncertainty of 10% each. Once these indices excepted, both models have the same behaviour with a light smaller uncertainty for the LBL model.
- A trend of homogeneity of uncertainty can be observed when the wind dominates ventilation process.

7. CONCLUSION

This study has shown the feasibility of a sensitivity analysis with a factorial design. The method has been illustrated for one building with five models. For these models, it has been shown that the amplification of the uncertainty between input and output data is almost two. Nevertheless there are considerable variations of sensitivity from a case to another. From one side, it has been shown for empirical model that the wind effect is more precise than the stack effect. For the detailed model COMVEN, those results are contradicted for some zones and some meteorological conditions. In those situations, the confidence intervals are so large that the numerical values can not be used. But those critical situations attest the existence of ventilation problems which must be detected and corrected. The possibility of simulating these situations, even inaccurately, is then interesting.

For simple models, it has been observed that the nodal ones (AIDA, TURBUL) present a smaller global sensitivity than the empirical ones (BREVENT, LBL) and this has been confirmed when taking into account the experimental uncertainties as variation ranges for the input data. The gap between the uncertainty of both model types is larger when stack effect dominates the ventilation process. This allows us to think that the localisation of leakages, which makes the difference between nodal model and others ends in more precise modelling.

More largely, take into account some features highlighted by our study but which have not been presented here, the following conclusions can be presented [1] :

- The enhancement of measurement techniques is imperative because of the dramatic amplification of the uncertainty during the simulation process.
- At the level of the empirical validation, it will not be possible to identify internal errors whose consequences are smaller than the model uncertainty (20% to 50%).

- The determination of the empirical model coefficients using a detailed model is not free of risk.
- Both types of models (simple or detailed) are interesting and related research must be continued. For global problems, as energy conservation, simple model are satisfactory.

8. REFERENCES

[1] Fürbringer J.M.: Sensibilité de modèles et de mesures en aéraulique du bâtiment à l'aide de plans d'expériences. Thèse No 1217, EPFL, Lausanne, 1994.

[2] Roulet C.A., Fürbringer J.M.: The evaluation of a multizone infiltration computer code, International Symposium on air flow in multizones structures, Budapest sept. 9 (1992).

[3] Fürbringer J.M.: Evaluation procedure using sensitivity analysis of model and measurement, International Symposium on air flow in multizones structures, Budapest sept. 9 (1992).

[4] Fürbringer J.M.: Comparison and combination of factorial and Montecarlo design in sensitivity analysis, submited to building and environment (1994).

[5] Box G. E. P., Hunter W. G., Hunter J. S.: Statistics for Experimenters, an Introduction to Design, Data Analysis and Model Building. John Wiley, New York, 1978.

[6] Box G. E. P.: The exploration and exploitation of response surfaces: some general considerations and examples. Biometrics, vol. 10, no 1 (1954).

[7] Gunter B. H.: How experimental design concepts can improve experimentation in the physical sciences. Computer in physics, vol 7, nº 3 May/Jun 1993.

[8] Feustel H.G., Allard F., Dorer V., Rodrigez Garcia E., Grosso M., Herlin M., Mingsheng L., Phaff H.C., Utsumi Y., Yoshino H.: Fundamentals of the Multizone Air flow Model - COMIS. AIVC TN 29, Coventry, UK, 1990.

[9] Feustel H.G., Allard F., Dorer V., Rodrigez Garcia E., Grosso M., Herlin M., Mingsheng L., Phaff H.C., Utsumi Y., Yoshino H.: COMIS 1.2 - user guide. Lawrence Berkeley Laboratory, Berkeley, USA, 1993.

[10] Awbi H.B.: Ventilation of buildings. E&FN SPON ed., London, GB, 1991

[11] Sherman M., Grimsrud D.T.: Infiltration-pressurisation correlation: simplified physical modelling. ASHRAE Semi-annual Meeting, Denver, USA, June 1980.

[12] Warren P.R., Webb B.C.: The relationship between tracer gas and pressurisation techniques in dwellings. Proc 1rst AIVC Conf 'Infiltration Measurement Technique', 1980.

[13] Liddament M.: AIDA-an air infiltration development algorithm. Air infiltration review, vol 11, no1, Dec. 1989.

[14] Fürbringer J.M.: Renouvellement d'air par une grande ouverture unique, analyse d'une méthode numérique dynamique, in IEA annex 20 final report, LESO-PB, EPFL, Lausanne, Switzerland (1992).

[15] Fürbringer J.M., Van de Maas J.: Suitable algorithms for calculating air renewal rate by pulsating air flow through a single large opening, submited to Building and Environment, (1994).

[16] Fürbringer J.M., Borchiellini R.: Technique of sensitivity analysis applied to an air infiltration multizone model, ASHRAE trans., june 93 conf.

[17] Girard M., Masoero M.: Determinazione sperimentale dell'entita dei ricambi d'aria nei locali ove operano apparecchi a gas. Proc. of ATIG italian national conference, Napoli, Nov., I, 1992.

ACKNOWLEDGEMENTS

This work, as participation to the IEA ECB Annex 13 "Multizone air flow modelling" is supported by the OFEN (National Office of Energy).

The Role of Ventilation
15th AIVC Conference, Buxton, Great Britain
27-30 September 1994

An Experimental and Theoretical Investigation of Airflow Through Large Horizontal Openings

J S Kohal, S B Riffat, L Shao

Building Technology Group, School of Architecture,
University of Nottingham, NG7 2RD United Kingdom

Synopsis

The work was concerned with measuring natural convection through a large horizontal opening of different sizes and shapes located between two rooms in a building. Airflow rates between the two rooms were measured using a tracer-gas decay technique. Room 1 was heated to various temperatures in the range 18°C to 33°C using thermostatically-controlled heaters; room 2 was unheated. A multi-point sampling unit was used to collect tracer-gas samples from each room. The concentration of SF_6 tracer was measured using an infra-red gas analyser. The heat and mass flow rates between the two rooms were calculated from the tracer-gas concentrations and temperature differences. The coefficient of discharge of the opening was found to be a function of the temperature difference between the two rooms. The mass flow rate was increased by increasing the area of the opening. The mass flow rate of a circular opening was in most cases higher than that of a square opening.

The work also describes CFD modelling of natural convection through horizontal openings. Results were compared with values obtained from experiment.

List of symbols

A = Cross-sectional area of the opening, (m^2)
A_i = The area perpendicular to U_i of individual cells within the opening, (m^2)
C_1 = Concentration of the tracer at time t in room 1, (ppm)
C_2 = Concentration of the tracer at time t in room 2, (ppm)
C_p = Specific heat of air, (J/kgK)
F = Volumetric flow rate, (m^3/s)
g = Acceleration due to gravity, (m/s^2)
H = Thickness of the partition containing the opening, (m)
M = Mass flow rate, (kg/s)
M_C = Mass flow rate of circular opening, (kg/s)
M_S = Mass flow rate of square opening, (kg/s)
q = Heat transfer rate, (W)
T = Mean absolute temperature of the two rooms, (°C or K)
T_1 = Average air temperature in room 1, (°C or K)
T_2 = Average air temperature in room 2, (°C or K)
ΔT = Average temperature difference between the two rooms, (°C or K)
U_i = The vertical component of air velocity at individual grid points within the opening, (m/s)
V_1 = Interior volume of room 1, (m^3)
V_2 = Interior volume of room 2, (m^3)
ρ = Average air density, (kg/m^3)
K = Coefficient of discharge
n = The number of grid points (or cells) within the span of the horizontal opening

1. Introduction

In recent years use of natural ventilation has become more widespread in order to minimise air conditioning and resulting emissions of greenhouse gases. Building services designers and architects require design tools for accurate prediction of air movement in buildings. Several advanced computer models such as ESP , BREEZE and COMIS have been developed for prediction of ventilation and interzone air movement in buildings. However, these models lack suitable algorithms for estimation of airflow through large horizontal openings, such as ventilation shafts and stairwells. Airflow through this type of opening has serious implications on energy saving, moisture and pollutant transfer, thermal comfort and control of fire and smoke.

A review of airflow through large openings carried out by Riffat (1) showed that little work has been published on interzonal convection through large horizontal openings. Brown and Solvason (2) have investigated airflow through small square openings in horizontal partitions. Riffat (3) has studied buoyancy-driven flow through a staircase in a house and Reynolds et. al (4) have developed a model for buoyancy driven flow in a stairwell. Advancements in tracer-gas technology allow scope for conducting extensive measurements to investigate airflow through openings. The results could be used to develop accurate algorithms for inclusion in existing mathematical models. The present paper provides the foundations for development of such algorithms.

2. Theory

2.1. Interzone airflows

Airflows in a two-zone system are shown in Fig. 1a. Air can infiltrate from outside the building into each room (F_{01} and F_{02}) and exfiltrate from each room to the outside (F_{10} and F_{20}). In addition, air can exchange between the rooms through a large horizontal opening (communication opening) in both directions (F_{12} and F_{21}). If one applies the tracer-gas material balances in each room, assuming that a steady state exists, the rate of change of tracer concentration in room 1 at time t is given by:

$$V_1 \frac{dC_1}{dt} = C_2 F_{21} - C_1 (F_{10} + F_{12}) \qquad (1)$$

Similarly, the rate of change of tracer concentration in room 2 at time t is given by:

$$V_2 \frac{dC_2}{dt} = C_1 F_{12} - C_2 (F_{21} + F_{20}) \qquad (2)$$

The other flow rates can be then determined using the continuity equation as follows:

$$F_{01} + F_{21} = F_{10} + F_{12} \qquad (3)$$

$$F_{02} + F_{12} = F_{20} + F_{21} \qquad (4)$$

The volumetric-balance equations can be solved using the theoretical technique based on the Sinden method (5). The method assumes that a multizone system may be represented by a series of cells of known and constant volume which are all connected to a cell of infinitely large volume, i.e., the outside space. The volumetric balance for each room can be expressed by a series of equations which can then be solved using matrices.

2.2 Interzone heat and mass transfer

Applying Bernoulli's equation, the mass flow rate through the opening is:

$$M = \rho A K \sqrt{\frac{\Delta T\, gH}{T}} \qquad (5)$$

The heat transfer flow between zone 1 and zone 2 through the opening is:

$$q = \rho A K C_p \sqrt{\frac{(\Delta T)^3\, gH}{T}} \qquad (6)$$

3. Material and method

Experiments were carried out using two rooms as shown in Fig. 1b. Room 1 is located downstairs and has dimensions 3.6m × 6m × 3.2m, (volume = 69m^3). Room 2 is located upstairs and has dimensions 3.6m × 11.7m × 3.2m, (volume = 135m^3). The two rooms are connected via a horizontal opening.

The dimensions of the opening were varied between 0.288 and 0.48 m^2 while the thickness was kept at 0.3m.

Room 1 was heated to various temperatures using thermostatically-controlled heaters. Room 2 was unheated. The temperature was measured at three different heights in each room using grids situated at the centre of the opening.

Airflow measurements were carried out using a single tracer-gas technique . Several tracer gases are available, but sulphur hexafluoride was chosen for this work since it has desirable characteristics in terms of detectability, safety, and cost and it has been used successfully in previous air movement studies. To estimate the airflow between the two rooms, two multi-point sampling systems were used. The first system was used to collect tracer-gas samples from room 1, while the second was used to collect samples from room 2. At the beginning of each test the communication door between the two rooms was closed and gaps between the door and its frame were sealed. This prevented heat and tracer-gas leakage prior to starting

the test. The tracer-gas was released in room 1, where it was mixed with air using an oscillating fan. To ensure that a uniform concentration had been achieved in room 1, samples were taken at ten sampling points in each room. After a mixing period of about 15 minutes, the communication door was opened. Samples were taken every 60 seconds for a total duration of 60 minutes. The concentration of SF_6 was measured using a BINOS 1000 analyser made by Rosemount Ltd, U.K. The temperature at various locations in each room was measured using thermocouples. The wind speed and direction were recorded during the test.

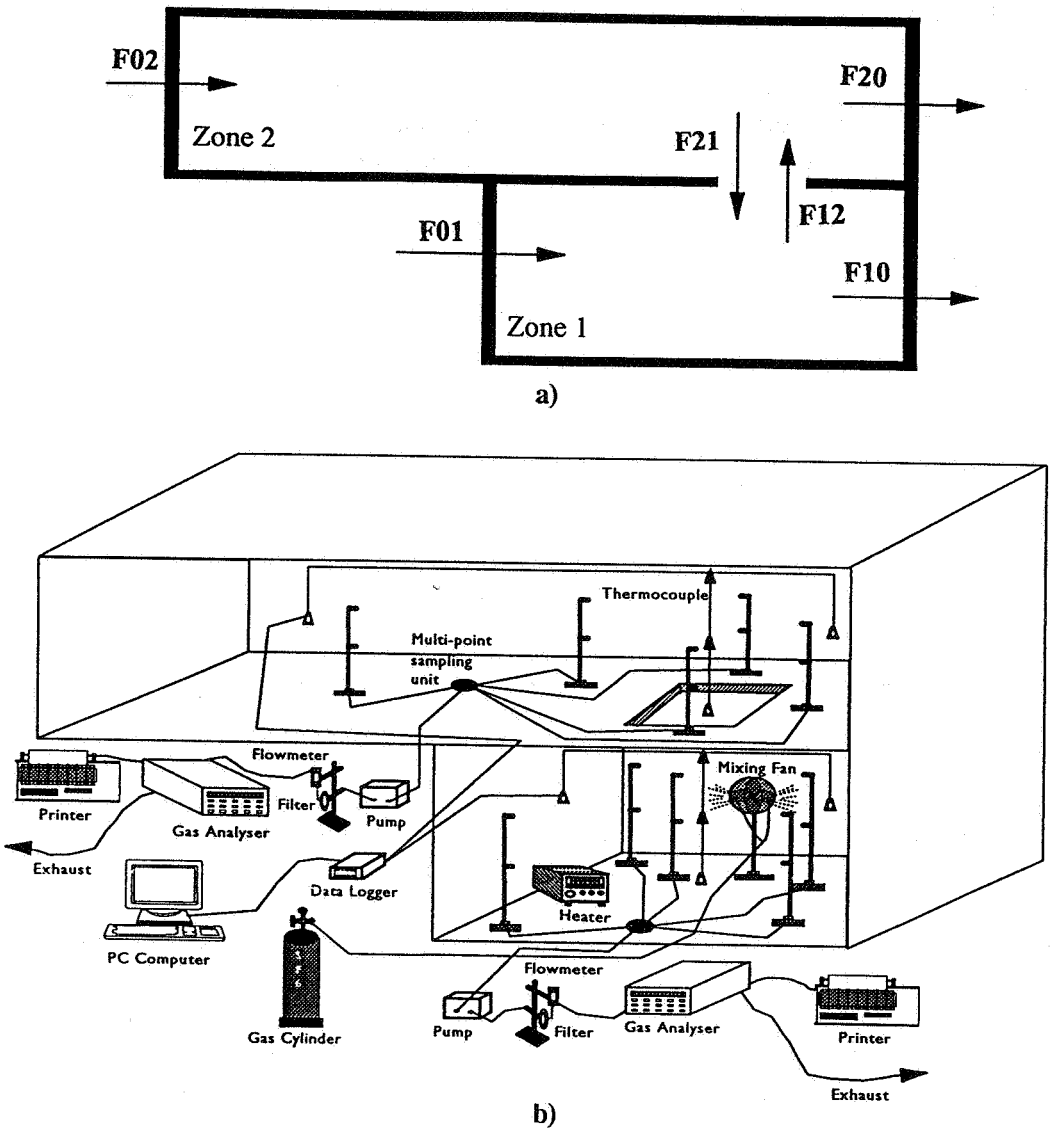

Fig. 1. Schematic of the rooms and instrumentation.

4. Results and discussion

The airflows between the two rooms were estimated from the tracer-gas concentration data using the method described in section 2.1. Several experiments were carried out for various temperature differences and opening sizes and square and circular cross-sections; only room 1 was heated to temperatures in the range 18°C to 33°C. Following this, the communication door was opened and temperature and tracer-gas concentration were monitored. The temperature in room 1 fell rapidly during the first 10 minutes and then decreased at a much slower rate. The temperature in room 2 increased during the first 10 minutes and then gradually stabilized at an almost constant value.

Fig. 2 shows an example of tracer-gas concentration against time for a temperature of 7.3 °C. To evaluate the coefficient of discharge, K for the horizontal opening, the airflow measured using the tracer-gas technique was divided by the theoretical airflow given by equation 5 (see section 2.2).

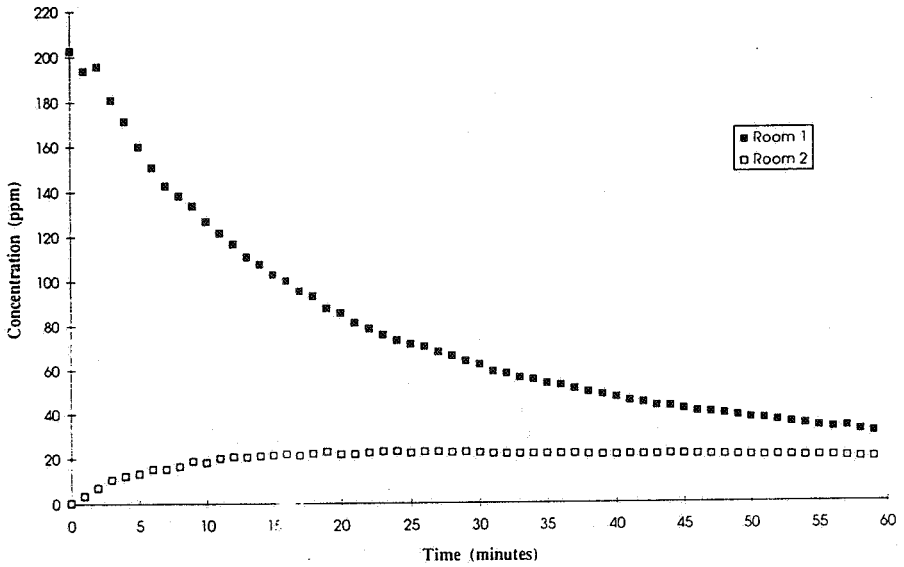

Fig. 2. Time dependency of tracer-gas concentration in rooms 1 and 2, ΔT = 7.3 °C, K = 0.46 square opening.

Fig. 3 shows the variation of M with $(\Delta T)^{0.5}$ for square and circular cross-section openings, respectively. The mass flow rate between the two rooms can be given in the form of a straight line (linear function of $(\Delta T)^{0.5}$) for each set of openings . The heat flow rate between the two rooms can be given in the form of a quadratic function of (ΔT) for each set of openings. (see table 1). The mass flow rate through the circular openings was generally higher than that through square openings.

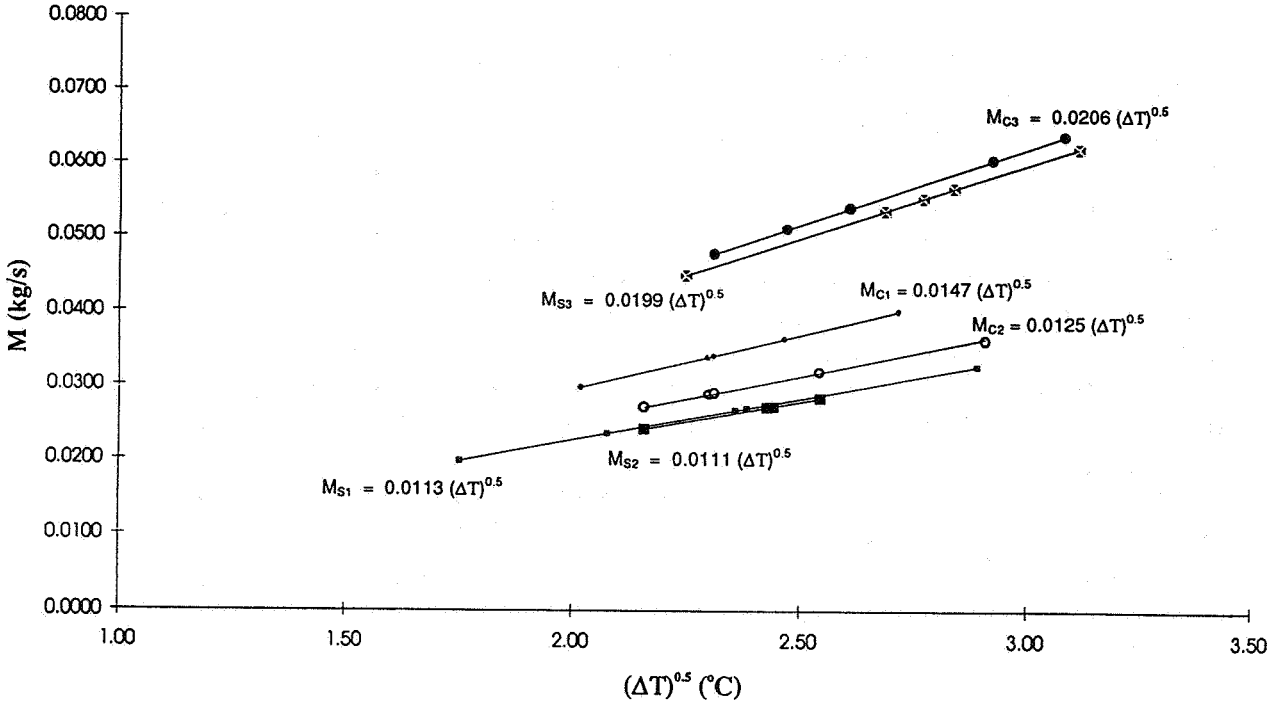

Fig. 3. Variation of mass flow rate with $(\Delta T)^{0.5}$ for two set of openings.

Table 1 shows the values of coefficient of discharge together with correlations for mass and heat flow rates. The coefficient of the discharge was found to be in the range 0.29 to 0.43 for circle openings and 0.26 to 0.35 for square openings depending on the temperature difference between the two zones.

OPENINGS		AREA (m^2)	K (Av.)	M (kg/s)	q (kW)
CIRCLE	C 1	0.28	0.43	$0.0147\ (\Delta T)^{0.5}$	$0.0147\ C_p\ (\Delta T)^{1.5}$
	C 2	0.36	0.29	$0.0125\ (\Delta T)^{0.5}$	$0.0125\ C_p\ (\Delta T)^{1.5}$
	C 3	0.48	0.36	$0.0206\ (\Delta T)^{0.5}$	$0.0206\ C_p\ (\Delta T)^{1.5}$
SQUARE	S 1	0.28	0.33	$0.0113\ (\Delta T)^{0.5}$	$0.0113\ C_p\ (\Delta T)^{1.5}$
	S 2	0.36	0.26	$0.0111\ (\Delta T)^{0.5}$	$0.0111\ C_p\ (\Delta T)^{1.5}$
	S 3	0.48	0.35	$0.0199\ (\Delta T)^{0.5}$	$0.0199\ C_p\ (\Delta T)^{1.5}$

Table 1. Correlations for mass and heat transfer rate for circular and square cross-section openings.

5. CFD Simulation

The CFD code FLUENT was used to simulate the buoyancy driven flow through horizontal openings by solving the Navier-Stokes equations. To predict the transient mass and energy transfer between building zones, the time dependent versions of the above equations were used. Because the information regarding the boundary condition of the test building was (e.g., wall temperature distribution/history, background leakage, wind environment) incomplete, it was not possible to simulate the test building. Instead two zones of simpler geometry were chosen for numerical simplicity (Fig.4). The two zones, both two-dimensional with a width of 3m and height of 2m, are connected via a horizontal opening in the partition (10cm in thickness). All the solid boundaries, i.e., walls, ceilings and floors were assumed to have a constant temperature of 10°C except the floor of the lower zone which was assigned the temperature of 27°C. A small opening was built into one of the side walls of the upper zone and the building was otherwise air tight. The Reynolds number was in the low region of 10^3-10^4 and to avoid over-prediction of heat and mass transfer, the turbulence models were not utilised. The computations were time dependent to deal with the temperature decay and the constantly varying flow field. Small time steps of around 1/10th of the characteristic time scale were used and at the end of each time step, the normalised residuals for the equations were around 10^{-6}. At the beginning of the tests, which last 800 seconds, the upper zone was a uniform air temperature of 10°C and the lower zone 27°C and the air in both zones was stationery. As the test proceedes, the mass and energy transfer between the two zones caused variations in air temperature and velocities which were recorded and subsequently analysed to obtain the temperature histories and air exchange rates between the two rooms.

Previous research has show that the buoyancy driven flow through horizontal openings is highly transient and occurs in intermittent pulses. Good agreement between CFD predicted flow rate and that based on experimental measurement has been obtained with a relative difference of 10.5% (6). In this study, the effect of the size of the horizontal opening on interzonal flow rate is examined, by computing there cases of buoyancy driven flow between two zones. The zones and boundary/initial conditions for the three cases are identical except the size of the horizontal opening which is assumed to be 1.0, 0.8 and 0.6 m wide.

Fig. 4 shows a typical flow pattern obtained from the CFD simulation. The arrows indicate the flow directions and flow velocities by using stems with lengths proportional to the local air speed. The flow pattern is dominated by vortices. A major vortex can be identified in the lower zone accompanied by three smaller, weaker ones. These eddies promote heat transfer and uniformity of temperature within the zone. The situation in the upper zone is similar, with two large eddies containing weaker, smaller eddies which prevent the thermal isolation of the central regions of the former. The air exchange between the two zones taking place at the horizontal opening is clearly shown by the velocity arrows in that region. Warmer air from the lower zone flows through the right half of the opening into the upper zone causing the temperature there to rise while cooler air moving downwards causes the temperature in the lower zone to fall. The vigorous

vortical movement induced by this air exchange keeps the temperature distribution virtually uniform in individual zones throughout the test duration of 800 s. The value of the air exchange rate is obtained using

$$M = \rho \sum_{i=1}^{n} |U_i| A_i /2 \qquad (7)$$

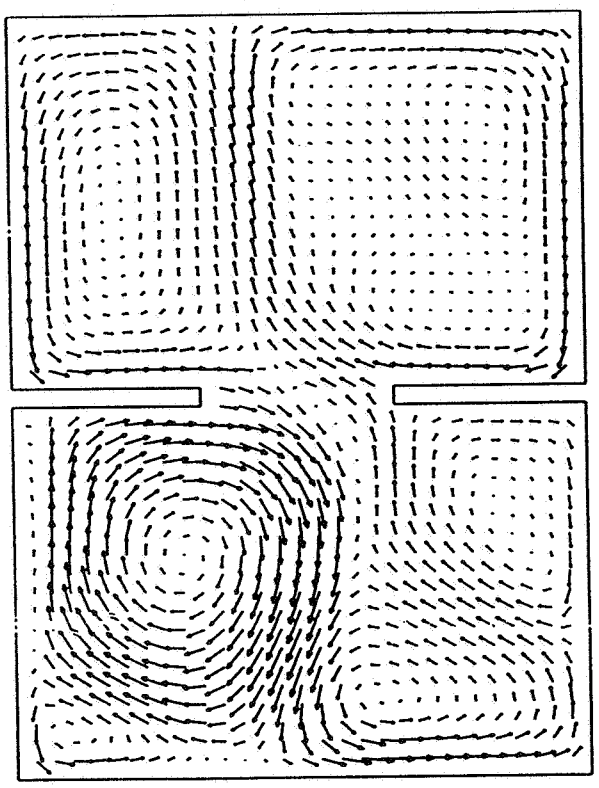

Fig. 4. CFD Simulation of flow pattern within two zones linked by a horizontal opening.

Fig. 5 shows the histories of air exchange rate of the three cases. Fig. 5(a) corresponds to the case with a horizontal opening of 0.6m wide and Fig. 5(b) and 5(c) correspond to openings of 0.8 and 1.0 m respectively. As can be seen, for all three cases the air exchange occurred in pulses, reaffirming the conclusions of previous research (6). On the other hand, the patterns and distribution of pulses for the three cases are quite different, which points to the random nature of buoyancy driven flow through horizontal openings. The average exchange rate over the 800-s duration are 0.010808 m^3/s, 0.011337m^3/s and 0.014897m^3/s for opening widths of 0.6m, 0.8m and 1.0m, respectively. This result agrees well with the analytical prediction of the effect of opening size on exchange rate, as shown by equation (5). The CFD prediction is not exactly linear as indicated by equation (5). This is probably due to the short averaging period and the random nature of the pulse flow through the openings.

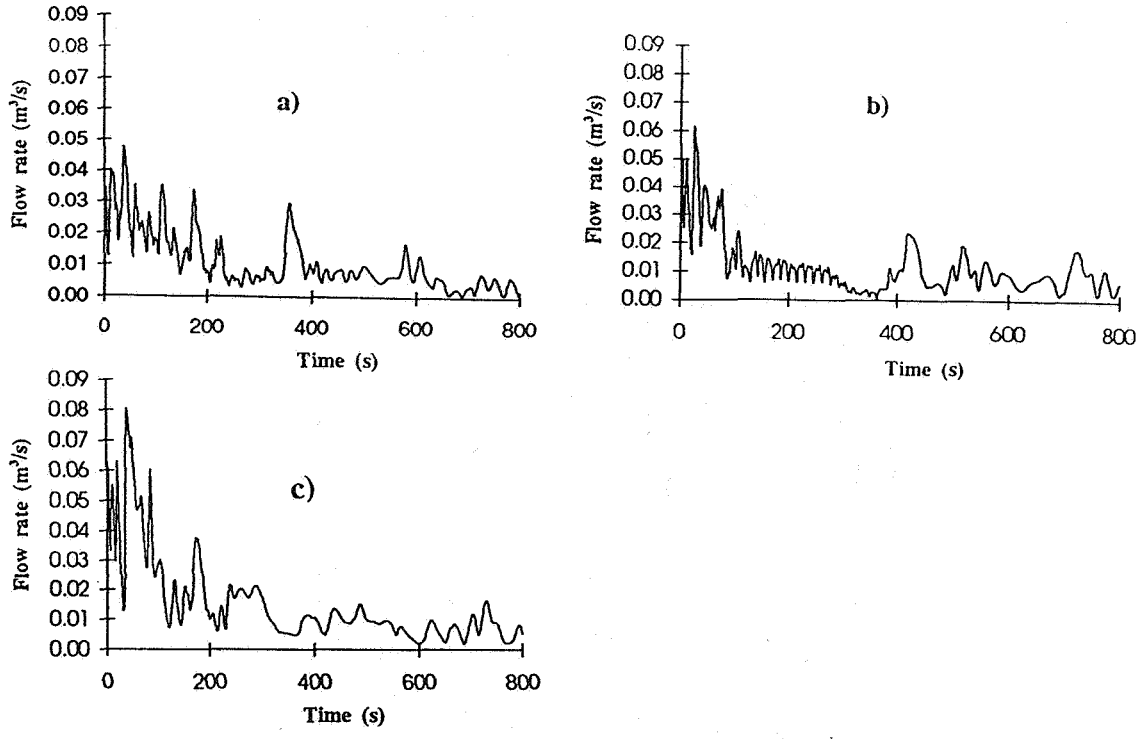

Fig. 5. Histories of air exchange through horizontal openings.

6. Conclusions

i) The experimental study shows that the average values of K is in the range 0.29 - 0.43 for circular openings and 0.26 - 0.35 for square openings depending on the interzonal temperature difference and size and shape of the opening.

ii) The heat and mass transfer through the opening was found to increase significantly with increasing temperature difference.

iii) Further work is required to examine the effect of the thickness of the opening on coefficient of discharge.

(iv) CFD simulation of buoyancy driven flow through horizontal openings has been carried out using the commercial software FLUENT. The transient velocity field was predicted using a time-dependent method. The CFD predictions agree with analytical findings that the exchange rate through the horizontal opening increases with the size of the latter. Furthermore, the results obtained reaffirm the finding of previous research that the buoyancy-driven flow occurs in random pulses through the horizontal opening.

References

1. RIFFAT, S. B. "Algorithms for Airflows Through Large Internal and External Openings"
Applied Energy, 40, 1991, pp171-188

2. BROWN, W.G.and SOLVASON, K.R. "Natural Convection Through Rectangular Openings in Partitions, Part 2: Horizontal Partitions"
Int. J. Heat and Mass Transfer, 5, 1962, pp869-78

3. RIFFAT, S. B. "Measurement of Heat and Mass Transfer Between the Lower and Upper Floors of a House"
International Journal of Energy Research, 13, 1989, pp231-241

4. REYNOLDS, A.R., MOKHTARZADEH, M.R. and ZOHRABIAN, A.,S. " The Modelling of Stairwell Flows"
Building and Environment, 23(2), 1988, pp63-66

5. SINDEN, F.W. " Multi-Chamber Theory of Air Infiltration"
Building and Environment, 23(2), 1978, pp21-8

6. RIFFAT, S. B., KOHAL, J. S. and SHAO, L. "Measurement and CFD Modelling of Buoyancy Driven Flows in Horizontal Openings"
ASHREA IAQ'94, St. Louis, Missouri, USA, 1994.

The Role of Ventilation
15th AIVC Conference, Buxton, Great Britain
27-30 September 1994

Algorithm for Interzonal Particle Flow Through Openings

K W Cheong, N Adam, S B Riffat

Building Technology Group, School of Architecture,
University of Nottingham, NG7 2RD United Kingdom

SYNOPSIS

Measurements of interzone airflow and movement of aerosol particles were carried out in an environmental chamber. SF_6 tracer gas and oil-smoke particles were used for this work. A series of measurements were conducted to investigate the effect of parameters such as interzone temperature difference and size of opening on the flow of aerosol particles. The particle deposition rate on the surfaces of the chamber together with algorithms for interzonal particle flow through the openings were determined. Results were compared with those obtained using the tracer-gas.

LIST OF SYMBOLS

A surface area of zone, (m^2)
A_x cross-sectional area of opening, (m^2)
A_m maximum area of opening, H = 0.5m and W = 0.7m, (m^2)
A_r ratio of A_x to A_m, (dimensionless)
d diameter of particle, (μm)
C_1 concentration of tracer-gas at time t in zone 1, ($\mu g/m^3h$ or ppm)
C_2 concentration of tracer-gas at time t in zone 2, ($\mu g/m^3h$ or ppm)
C_d coefficient of discharge, (dimensionless)
F volumetric flow rate, (m^3/s)
g acceleration due to gravity, (m/s^2)
H height of opening, (m)
I tracer-gas exchange rate, ($\mu g/m^3h$ or h^{-1})
P particle-exchange rate, ($\mu g/m^3h$ or h^{-1})
T mean absolute temperature of the two zones, (K)
ΔT average temperature difference between the two zones, (°C or K)
V volume of zone, (m^3)
W width of opening, (m)
α particle deposition rate, ($\mu g/m^2h$)

1. INTRODUCTION

Investigation of particulate pollutants in the indoor environment of residential and commercial buildings is important because of the potentially harmful effects on the health of the occupants. Indoor aerosol particles are not only associated with outdoor sources (e.g., automobile exhaust emissions, coal and oil combustion, road dust, etc.) but also arise from a number of indoor sources (e.g., cigarette smoke, building materials, personal products, etc.). Particulate pollutants in buildings can have harmful effects on the health of the occupants and studies have shown that indoor aerosol particles influence the incidence of sick building syndrome (1). Aerosol particles can deposit on surfaces of rooms or be transported between zones; this can have serious effects in hospitals and buildings used by pharmaceutical industries (2). Contamination of electronic equipment by particulate pollutants can significantly affect the reliability of equipment used by the micro-electronic industries (3,4). Soiling of collections in museum and galleries caused by the deposition of airborne particles is a topic under investigation by other researchers and studies have been carried out to establish means to reduce the soiling rate (5).

The concentration of indoor aerosol particles can be reduced by mechanical or natural ventilation. The ventilation rate is usually estimated using tracer-gas techniques. However, measurements based on these techniques are not sufficient to describe the removal of particles as particle deposition rate, particle type, source and concentration must be included to estimate the accurate exchange rate.

In this paper, a series of experiments were carried out based on buoyancy-driven air and particle flow through vertical openings in a two-zone chamber. The deposition of particles in the chamber was studied and algorithms for interzonal air and particle flow were established.

2. THEORY

Figure 1 shows a schematic diagram of a two-zone system. F_{01} and F_{02} show the infiltration from outside the chamber into each zone while F_{10} and F_{20} show the exfiltration of tracer-gas (e.g. SF_6) and particles (e.g. oil-smoke) from each zone to the outside. In addition, tracer gas and particles can exchange between the two zones through a doorway (communication opening) in the direction, F_{12} and F_{21}. If one applies the material balance in each zone, assuming that a steady state exists and that the concentration of tracer gas (or particles) is negligible, then the rate of change of tracer-gas (or particle) concentration in zone 1 at time t is given by:

$$V_1 \frac{dC_1}{dt} = -C_1(F_{10} + F_{12}) + C_2F_{21} \quad (1)$$

Similarly, the rate of change of tracer (or particle) concentration in zone 2 at time t is given by:

$$V_2 \frac{dC_2}{dt} = C_1F_{12} - C_2(F_{21} + F_{20}) \quad (2)$$

The other two flow rates can then determined using the continuity equations as follows:

$$F_{01} = F_{12} + F_{10} - F_{21} \quad (3)$$

$$F_{02} = F_{20} + F_{21} - F_{12} \quad (4)$$

Equations 1 - 4 may be solved using the theoretical technique described by Sinden (6). This method assumes that a multizone system may be represented by a series of cells of known and constant volume which are all connected to a cell of infinitely large volume, i.e., the outside space. The volumetric balance for each zone can be expressed by a series of equations which can then be solved using matrices.

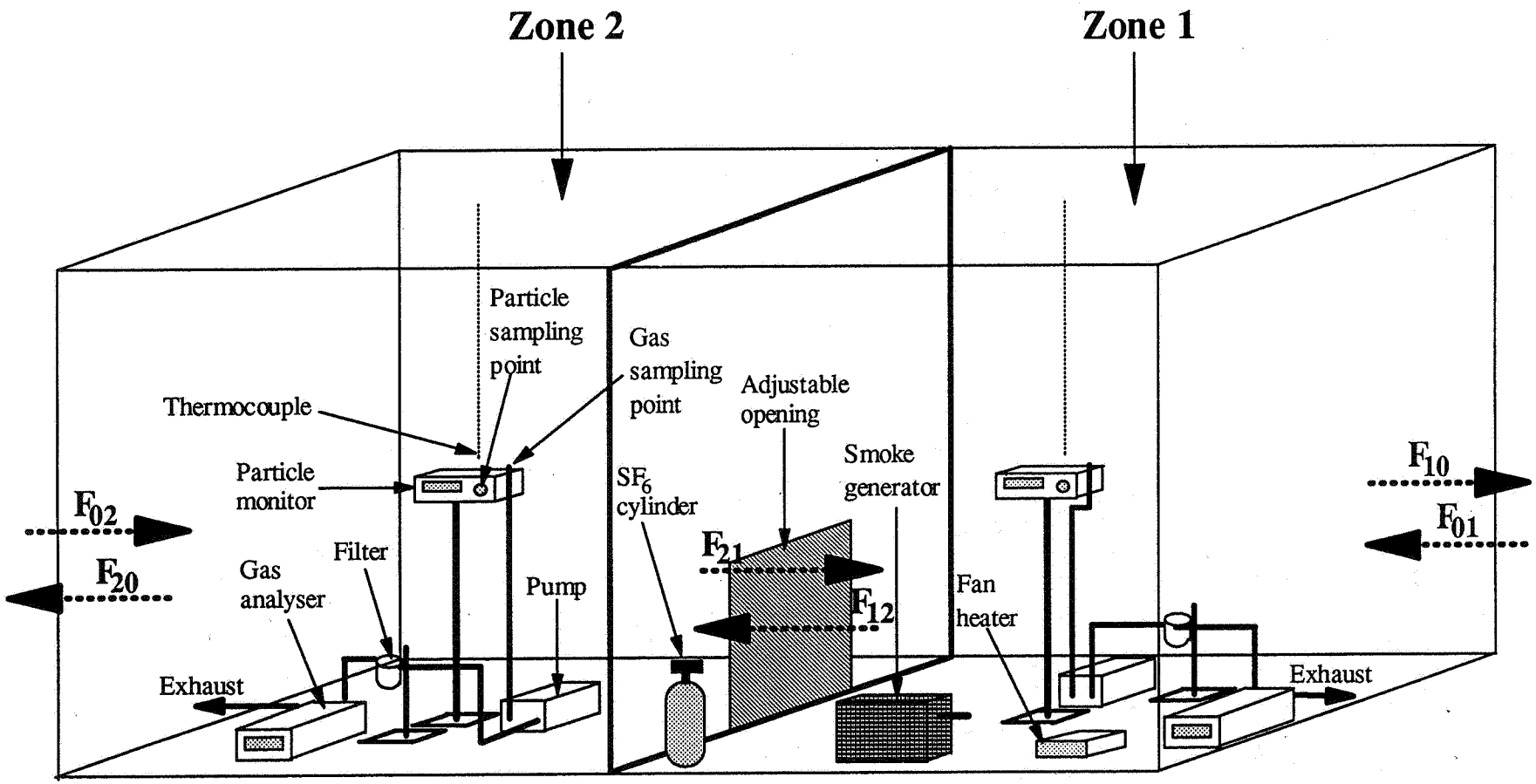

Figure 1 Schematic diagram of two-zone environmental chamber and its instrumentation

Shaw and Whyte (7) have given the volumetric discharge through an opening as:

$$F = C_d \frac{W}{3} \left[gH^3 \left(\frac{\Delta T}{T} \right) \right]^{0.5} \quad (5)$$

3. EXPERIMENTAL WORK

An environmental chamber consisting of two tightly-sealed zones was used for the experimental work (see Figure 1). The dimensions of each zone were 2.5m x 3m x 2.4m, (volume = $18m^3$) and these were connected by an opening with a sliding door. The height of the opening (H) could be adjusted by a pulley arrangement while the width (W) was fixed at 0.7m. The chamber was constructed from plywood sheet with a cavity insulated using polystyrene. Zone 1 was heated using a convector electric-heater; zone 2 was unheated. Temperatures were measured at the centre of the zone at mid-height locations using Ni/Cr/Al thermocouples.

Each experiment started with an initial release of SF_6 tracer-gas and oil-smoke particles into zone 1 with the sliding door between the two zones closed and gaps between the door and its frame sealed. This prevented leakage of tracer-gas and oil-smoke particles prior to the start of the test. An oscillating desk fan was used to assist mixing. After a mixing period of 1 hour, the desk fan was switched off and the sliding door was raised to a predetermined height. This was followed by simultaneous measurements of tracer-gas and oil-smoke particle concentration for both zones using an infra-red gas analyser type BINOS 1000 made by Rosemount Ltd., U.K. and an infra-red particle monitor type Grimm 1.100 manufactured by Grimm Ltd., Germany, respectively. Tracer-gas and oil-smoke samples were collected at the same locations as the thermocouples.

4. RESULTS AND DISCUSSION

4.1 Tracer-gas

The air flows between the zones were estimated using the concentration-decay technique. Several experiments were carried out for various temperature differences between the zones; only zone 1 was heated to temperatures in the range 18°C to 45°C. Following this, the sliding door was opened and both temperature and tracer-gas concentration were monitored. The sliding door was raised between 0.1m - 0.5m. The coefficient of discharge was found to correlate well with the area of the opening:

$$C_d = 1.36\, e^{-2.24A_r} \quad (6)$$

For W = 0.7m, g = $9.81 m/s^2$ and T = 300K and substituting equation (6) into equation (5) yields:

$$F = 0.057\, e^{-2.24A_r} \left[H^3 \Delta T \right]^{0.5} \quad (7)$$

4.2 Aerosol particles

SF_6 tracer-gas and oil-smoke particles were injected into zone 1. After a mixing period of 1 hour, simultaneous measurements of tracer-gas and oil-smoke particle concentration were performed using the infra-red gas analyser and particle monitor, respectively. Figure 3a and 3b show the variation of concentration of tracer-gas and smoke particles ($0.5\mu m < d < 5\mu m$) respectively with time for A_x= 0.1m x 0.7m and ΔT = 12.8K. The tracer-gas and particle curves were found to be simple exponential functions for all conditions.

The correlation between discharge coefficient and area of opening based on particle flow was determined:

$$C_d = 1.23\, e^{-1.42A_r} \tag{8}$$

The volumetric flow rate through opening was established by substituting equation (8) into equation (5) with W = 0.7m, g = 9.81m/s^2 and T = 300K:

$$F = 0.074\, e^{-1.42A_r}\, [H^3 \Delta T]^{0.5} \tag{9}$$

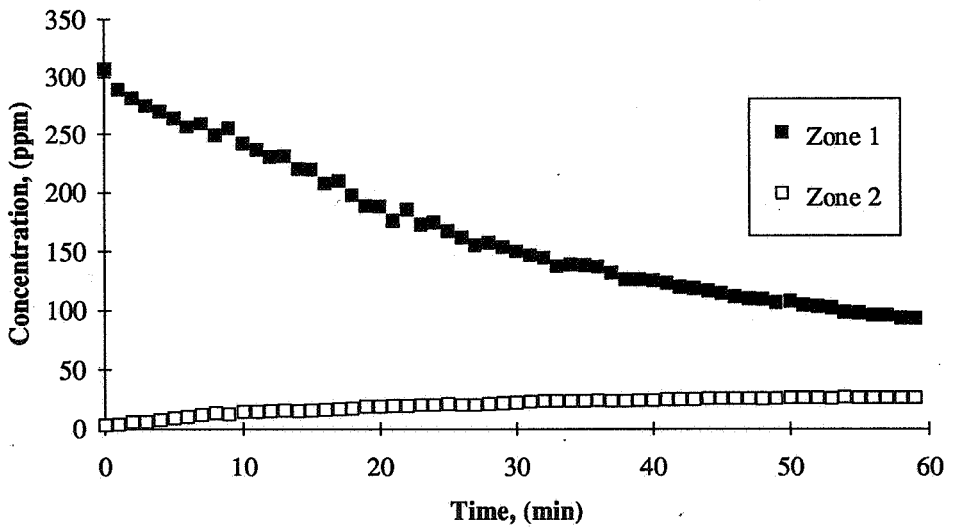

Figure 3a Variation of tracer-gas concentration with time in zone 1 and zone 2, H = 0.1m, ΔT = 12.8K

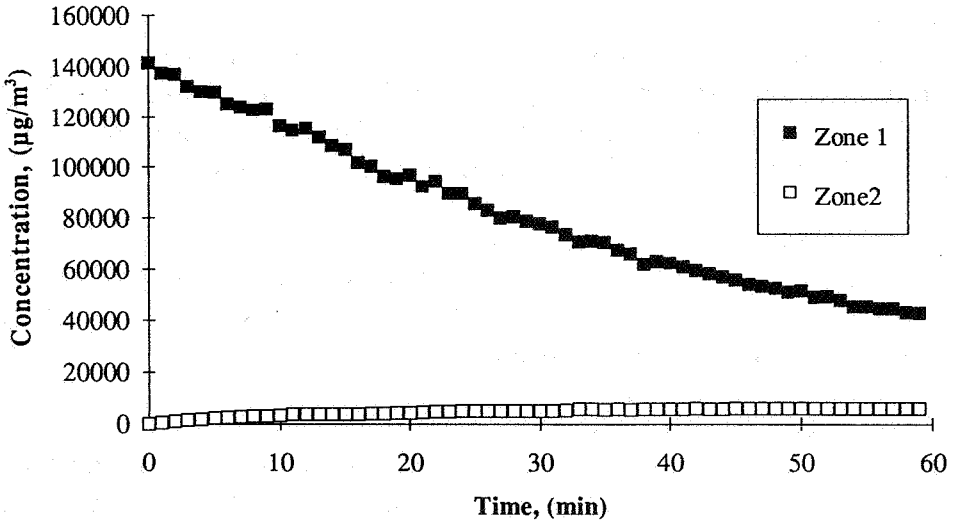

Figure 3b Variation of particle concentration with time in zone 1 and zone 2, $0.5\mu m < d < 5\mu m$, H = 0.1 m, ΔT = 12.8K

For A_r = 1, H = 0.5m and ΔT = 10K, the interzone airflow rates based on tracer-gas and particles were 24.4 m^3/h and 72 m^3/h, respectively. The particle exchange rates were found to be higher than tracer-gas exchange rates. The difference in tracer-gas and particle exchange rate is due to deposition (or adsorption effect) of particles on the surfaces of the environmental chamber. This was estimated using the following equation:

$$\alpha = (P-I) \times \frac{V}{A} \qquad (10)$$

Deposition of particles was found to be negligible in zone 1, (heated) and high in zone 2, (unheated). Thermophoresis might be partly responsible for deposition of particles as the warm particle came into contact with the cooler wall in the unheated zone. The deposition rates for particles ($0.5\mu m < d < 5\mu m$) in zone 2 for openings with areas $0.07m^2$, $0.21m^2$, $0.28m^2$ and $0.35m^2$ were in the range 2.77 - 9.78$\mu g/m^2h$, 4.30 - 64.64$\mu g/m^2h$, 12.48 - 32.07$\mu g/m^2h$ and 5.21 - 23.77$\mu g/m^2h$, respectively. This showed that the deposition of particles was random and independent of the area of opening. The coefficients of discharge based on tracer-gas and particles for openings with areas $0.07m^2$, $0.21m^2$, $0.28m^2$ and $0.35m^2$ were found to be 0.87, 0.35, 0.23 and 0.14, and 0.93, 0.52, 0.39 and 0.30, respectively. The coefficients of discharge based on particles were generally higher than those determined from tracer-gas measurements.

5. CONCLUSIONS

(i) The correlation between coefficient of discharge and cross-sectional area of opening was determined for tracer-gas and particles. Coefficient of discharge was found to vary with the area of opening and the coefficients of discharge based on particles were generally higher than those based on tracer-gas measurements.

(ii) Algorithms for interzonal particle and tracer-gas flow in a two-zone environmental chamber were established. The results showed that particle exchange rates were generally higher than tracer-gas exchange rates. This was due to the deposition effect of particles on the surfaces of the chamber.

(iii) The deposition rate in the heated zone is low compared with that in the unheated zone. This may be due to thermophoresis as warm particles were deposited on the cooler wall. In addition, the deposition rates of particles were found to be random.

ACKNOWLEDGEMENTS

The authors wish to thank the financial support of the Engineering and Physical Sciences Research Council (EPSRC).

REFERENCES

1. Turiel, I.
"Indoor air quality and human health"
Standford University Press, Standford, California, 1985.
2. Farrance, K. and Wilkinson, J.
"Dusting down suspended particles"
Building Services, Vol. 12, 1990, pp45-46.
3. Reagor B.T.
"Dust: What, Where, Why and How"
Proceedings National Communications Forum, Vol. 42, 1988, pp981-982.
4. Reagor B.T. and Russell C.A.
"A survey of problems in telecommunications equipment resulting from chemical contamination"
IEEE Trans Comp, Hybrids, Manuf Technol, Vol. 9, 1986, pp209-214.
5. Nazaroff W.W. and Cass G.R.
"Protecting museum collections from soiling due to the deposition of airborne particles"
Atmospheric Environment, Vol. 25A, No. 5/6, 1991, pp841-852.
6. Sinden F.W.
"Multi-chamber theory of air infiltration"
Building and Environment, Vol. 13, 1978, pp21-28.
7. Shaw B.H. and Whyte W.
"Air movement through doorways: the influence of temperature and its control by forced air flow"
Bldg Serv. Engrg, Vol 42, 1974, pp210-218.

The Role of Ventilation
15th AIVC Conference, Buxton, Great Britain
27-30 September 1994

Occupant Satisfaction and Ventilation Strategy - a case study of 20 public buildings

G Donnini*, V H Nguyen**, J Molina***

ADN Inc*, McGill University**, Concordia University***

Key words: Ventilation strategy, Occupant satisfaction

Summary: Occupant response in a good indicator of the effectiveness of a ventilation system. In a one-year study in the province of Quebec region, 20 public buildings were studied. Occupants were asked to answer questions on their perception of their environment and the ventilation at their workstation. Annual energy consumption for each building was recorded. The ventilation systems were studied as well as their rates; minimum outdoor air rates and average total air rates, at each workstation and at the ventilation system. Ventilation rates were plotted against energy consumption. Occupant satisfaction was plotted against ventilation rate and against energy consumption. It was found that as outdoor air rates at the work stations increased, the occupants perceived a better indoor air quality, a better ventilation, and a more constant ventilation frequency above 70 l/s/p. No trend was found from their perception of the air movement. As the total air supplied at the diffusers increased, the occupants perceived a better indoor air quality, a better ventilation, and a more constant ventilation frequency above 110 l/s/p. However, all these perceptions decreased to the original values above 130 l/s/p. No trend was found from their perception of the air movement. As the total air flow rates at the ventilation system increased, the occupants perceived a better indoor air quality, a better ventilation, a more constant ventilation frequency, and a better air movement above 200 l/s/p. However, all these perceptions decreased to the original values above 250 l/s/p. As the ventilation efficiency at the workstations increased from 27 to 70%, the occupants perceived a poor indoor air quality, an insufficient ventilation, and an irregular ventilation frequency above 25%. No trend was found from their perception of the air movement. As the maximum carbon dioxide concentration at the work place increased, the occupants perceived a worst indoor air quality above 800 ppm of CO_2, a worst air movement above 1000 ppm. The ventilation strategy resulting in the best perception from the occupants was of the type free cooling, with variable outdoor air supply, variable total air supply, and constant supply temperature.

TITLE: OCCUPANT SATISFACTION AND VENTILATION STRATEGY- A CASE STUDY OF 20 PUBLIC BUILDINGS

Introduction:

The occupant perception of the Indoor Air Quality and the Ventilation in 20 public buildings was sought through a survey by a building owner of 1500 commercial buildings in Canada. McGill University and ADN Inc. conducted this research whose objective is to seek which ventilation strategy satisfies best the majority of occupants. Twenty buildings were selected from across the province of Quebec, half from the cities of Montreal and Quebec, half in the countryside. The oldest building is 62 years old and the newest 6 years old. The tallest office building has 21 floors, the smallest 2 floors. There are a total of 8000 office workers in these 20 buildings that cover 350 000 m^2.

Methodology:

During the coldest months of winter 1991-1992 when fresh air rate was at its minimum rate, the field investigation was conducted by McGill University PhD students at 850 workstations (one out of 10 office workers) chosen by random to represent the building structure (perimeter and core), the office organizations (open plan versus closed offices) and the occupant population (temporary versus permanent workers, union versus management, female versus male, old versus young). At each workstation, a series of measurements was taken:

ventilation : fresh air ventilation rates (by decay of SF_6 tracer gas method) and total air rates (by balometer);

- contaminants: carbon monoxide, carbon dioxide (by direct reading infra-red instruments), formaldehyde, ozone, volatile organic compounds and total dust (the latter four contaminants were collected on appropriate media by sampling pumps following NIOSH official methods; the media was them analyzed in the chemical laboratory of McGill University by chromatography for chemicals and gravimetry for total dust);

- thermal parameters: ambient temperature, relative humidity, vertical gradient temperature, horizontal radiant temperature asymmetry and draft velocity (all these parameters were measured following the ASHRAE Standard 55-1981 specifications);

While a team of researchers was measuring at the workstations, a questionnaire was distributed to all the occupants of the buildings who were asked to answer the questions on the same day. The questionnaires were collected on the same day as the physical measurements.

Results and Discussion:

Indoor Air Quality: Results show that a two third majority of the occupant population was unsatisfied with the indoor air quality although most of the contaminant levels were below the recommended strict limits set by the American Society of Heating, Refrigerating and Air-Conditioning Engineers (standard 62-1989). The only contaminant that has relatively high concentrations is the Total Volatile Organic Compounds (or TVOC). The average measured TVOC concentration of 5000 $\mu g/m^3$ is in the discomfort range (3000 - 25000 $\mu g/m^3$) as defined by Dr.Molhave (3) in the European guidelines for Ventilation Requirements in Buildings (4). The TVOC concentrations may thus explain the high levels of dissatisfaction. Some TVOC measured values are in the toxic range (> 25000 $\mu g/m^3$) and are due to a single source: wet process photocopiers.

Thermal comfort: Occupant perception was very different from measured values. Average ambient temperature of 22.5 °C only satisfied 46% of the people, and for an average relative humidity of 37%, there was only 31% of satisfaction. And 60% of the occupants qualify the 0.09 m/s mean air speed as stagnant. Most of the measured values were within the ASHRAE standard 55-1981 and should satisfy 80% of the occupants. Analysis of the occupant responses show that it is not the actual measured values that are unsatisfactory but the variability of the thermal parameters. Humidity levels for example can vary from 5 to 35% within one day and temperature may jump from 20 to 26 °C in a few hours.

Occupant perception of Indoor Air Quality and Ventilation:

Questionnaire responses -- general: From the questionnaire responses, we notice that 44% of the occupants of all 20 buildings find the air ventilation to be insufficient, 45% of the occupants find it to be somewhat adequate, and 11% of the occupants find it to be adequate. In 6 of the 19 buildings, the questionnaire responses did not correspond to the measured data.

We also notice that 65% of the occupants are unsatisfied with the air quality, while 35% of the occupants are satisfied. In 2 of the 19 buildings, the questionnaire responses did not correspond to the measured data.

It was found 60% of the occupants find the frequency of ventilation to be irregular while 40% of the occupants find it to be constant.

Finally, 60% of the occupants found the air movement to be stagnant, 24% found the buildings had a good air movement, while 16% of the occupants found the air movement to be too drafty.

Outdoor air ventilation: We found that for 89 workstations tested, the mean outdoor air rate was 40 l/s/pers. The maximum outdoor air rate found was 375 l/s/pers while the minimum outdoor air rate was 1 l/s/pers (the standard deviation was 89 l/s/pers). For a confidence interval of 95% we found that the lowest value was 21 l/s/pers and that the highest value was 58 l/s/pers.

As the measured average outdoor air rate increased from 9 to 69 l/s/p, there was no change in responses from the occupants; they perceived the ventilation to be insufficient. The same phenomenon was noted when comparing the average measured outdoor air rate and the occupant perception of indoor air quality. They perceived the indoor air quality to be poor up until an outdoor air rate of 76 l/s/p. Their perception of the ventilation frequency also followed the same trend. The occupants felt the ventilation to be quite irregular with an outdoor air rate of less than 76 l/s/p. However, when comparing the occupants' perception of the air movement to the amount of outdoor air supplied, no trend was found.

Diffuser supply rate: We found that for 89 workstations tested, the mean diffuser supply rate was 80 l/s/pers and the standard deviation was 63 l/s/pers. For a confidence interval of 95% we found that the lowest value was 77 l/s/pers and that the highest value was 84 l/s/pers.

As the measured average diffuser supply rates increased from 31 to 111 l/s/pers , there was no change in the responses from the occupants; they perceived the indoor air quality to be poor. The same phenomenon was noted when comparing the average measured diffuser supply rates and the occupant perception of ventilation. They perceived the ventilation to be insufficient. Their perception of the ventilation frequency also followed the same trend. The occupants felt the ventilation to be insufficient. However, when comparing the occupants' perception of air movement to the average diffuser supply rate, no trend was found.

Total air flow: We found that for 89 workstations tested, the mean total air flow rates in the ventilation system was 123 l/s/pers and the standard deviation was 106 l/s/pers. For a confidence interval of 95% we fond that the lowest value was 102 l/s/pers and that the highest value was 144 l/s/pers.

As the measured average system supply rates increased from 11 to 194 l/s/pers, there was no change in responses from the occupants; they perceived the indoor air quality to be poor. The same phenomenon was noted when comparing the average measured supply rates and the occupants perception of ventilation. They perceived the ventilation to be unacceptable. The occupants felt the ventilation frequency to be irregular. However, when comparing the occupants' perception of the air movement to the average system supply rate, no trend was found.

Ventilation efficiency: We found that for 89 workstations tested, the mean ventilation efficiency at the workstations was 40% and the standard deviation was 20%. For a confidence interval of 95% we found that the lowest value was 37% and that the highest value was 43%.

As the measured average ventilation efficiency increased from 27 to 70%, there was no change in responses from the occupants; they perceived the indoor air quality to be unacceptable. The same phenomenon was noted when comparing the average ventilation efficiency measured and the occupants perception of ventilation They perceived the ventilation to be insufficient for an average ventilation efficiency between 27% to 70%. The occupants felt the ventilation to be quite irregular with an average ventilation efficiency higher than 27%. However, when comparing the occupants' perception of the air movement to the average ventilation frequency, no trend was found.

Carbon dioxide: We found that for 89 workstations tested, the mean arithmetic carbon dioxide concentration was 580 ppm and the standard deviation was 136 ppm. For a confidence interval of 95% we found that the lowest value was 575 ppm and that the highest value was 584 ppm.

As the measured maximum carbon dioxide concentration increased from 700 to 2200 ppm, there was no change in responses from the occupants; they perceived the indoor air quality to be poor. The same phenomenon was noted when comparing the maximum measured carbon dioxide concentration and the occupant perception of ventilation. They perceived the ventilation to be insufficient above 625 ppm. Their perception of the ventilation frequency also followed the same trend. The occupants felt the ventilation frequency to be irregular when the maximum carbon monoxide is higher than 625 ppm However, when comparing the occupants' perception of the air movement to the maximum carbon dioxide concentration, we noted that when the concentration of carbon dioxide is higher than 700 ppm the occupants perceived the air movement to be stagnant.

Conclusion:

This research study leads us to conclude that:

- office ventilation systems must be able to reduce Total Volatile Organic Compounds below the recommended 5000 $\mu g/m^3$ level;
- ventilation systems must provide stable ambient conditions of temperature and humidity within one day at the work stations;
- ventilation systems should be able to provide sufficient fresh outdoor air to reduce Carbon dioxide below the 650-700 ppm range.

The ventilation strategy resulting in the best perception from the occupants and based on above three conditions was of free cooling type, with variable outdoor air supply, variable total air volume and constant diffuser air temperature. The ventilation systems should be equipped with carbon dioxide and VOC monitors which would regulate the percentage of fresh air intake. These considerations will be taken into account in the design of future office building ventilation systems.

References:

1) American Society of Heating, Refrigerating and Air-Conditioning Engineers, Standards 55-1981 and 55-1992 "Thermal Environmental Conditions for Human Occupancy", Atlanta, GA, USA.

2) American Society of Heating, Refrigerating and Air-Conditioning Engineers, Standards 62-1989 "Ventilation for acceptable Indoor Air Quality", Atlanta, GA, USA.

3) Molhave, L. (1990) Volatile Organic Compounds, indoor air quality and health. Proceedings Indoor Air '90 in Toronto, Vol.5, 15-33.

4) Commission of the European Communities, Report no.11, "Guidelines for Ventilation Requirements in Buildings", EUR 14449 EN, 1992.

The Role of Ventilation
15th AIVC Conference, Buxton, Great Britain
27-30 September 1994

Natural Ventilation Strategies to Mitigate Passive Smoking in Homes

M Kolokotroni, M D A E S Perera

Building Research Establishment, Garston, Watford, Herts WD2 7JR, United Kingdom

SYNOPSIS

This paper investigates possible natural ventilation strategies to reduce exposure to environmental tobacco smoke (ETS) in dwellings. Particular attention is paid to the migration of tobacco smoke from the living room (usually the smoking room) to the bedrooms which may be occupied by children. This addresses an area of current concern regarding the possible association between passive smoking and adverse health conditions; in particular the link between parental smoking and respiratory illness in children.

The study used the multizoned airflow prediction program BREEZE to evaluate the movement of tobacco smoke from the smoking rooms to the bedrooms in typical detached, semi-detached and terraced dwellings for a variety of natural ventilation strategies. Typical smoking patterns were emulated and contaminant movements analysed, taking into account factors such as wind speeds and direction and air temperatures. Some of the results obtained were compared with limited full-scale measurements acquired elsewhere to provide the necessary confidence in the predictions.

Controlling pollutant concentration by ventilation can be an energy intensive process, especially during the heating and cooling season. Since almost all dwellings in the U.K. are naturally ventilated, providing optimum ventilation with minimum ventilation heat loss is of concern only during the heating season. Results from the study indicate three possible strategies to mitigate the effect of passive smoking in dwellings; two which could be used during the heating season and one for the remaining times of the year.

INTRODUCTION

Environmental Tobacco Smoke and Health Effects

In 1988 the UK Independent Scientific Committee on Smoking and Health published a report which concluded that there was "a small increase in the risk of lung cancer from exposure to environmental tobacco smoke." This increase was in the range of 10 to 30% and was calculated to amount to several hundred out of the current annual total of about 40,000 lung cancer deaths in the UK [1]. Reports with similar conclusions have also been published in other countries [2]. It is also believed that the impact of ETS on people with respiratory illnesses may be larger than the impact indicated by its carcinogenic effects [3]. ETS can impair the respiratory health of children. In particular, during a child's infancy, ETS is associated with increased prevalence of acute lower-respiratory tract infections such as bronchitis and pneumonia; also with increased prevalence of fluid in the middle ear, symptoms of upper respiratory tract irritation, a small but significant reduction in lung function and with additional episodes and increased severity of symptoms in children with asthma. ETS exposure is a risk factor for new cases of asthma in children who have not previously displayed symptoms. Finally, research [3, 4] indicates a linkage with other health effects including coronary heart disease and hazard to the foetus during pregnancy. For the above reasons, ETS is considered a most important contaminant of indoor air and 'no smoking' or 'restricted smoking' policies are established in many work and leisure environments. However, regulation cannot be imposed on people in their homes, although passive smoking is potentially as harmful in houses as in work places. The effect is considered to be more severe in babies, small children, young and old people.

In addition to these health effects, ETS in buildings has an energy cost through increased ventilation necessary to dilute and/or remove the pollutant. This cost is estimated [5] to be about 4500 million ECU/year in domestic buildings within the 14 countries participating in AIVC (approximately £3400 million//year).

ETS in houses

ETS distribution and removal in houses has received less attention than in commercial buildings. A recent field study on the distribution of ETS in homes [6] concluded that smoking in the home will expose non-smoking occupants to tobacco smoke throughout the home at levels which could represent a health threat. In addition, another study has demonstrated that high relative humidity (RH) levels increase perception of annoyance and nasal irritation from ETS [7]. Bearing in mind that RH levels are usually high in UK bedrooms, this finding has a direct consequence regarding the effect of ETS on non-smokers.

Approach used in the present study

In the UK, almost all dwellings are naturally ventilated. This paper addresses ways of minimising the effects of ETS in bedrooms using natural ventilation strategies. BREEZE, an airflow/contaminant multizoned computer model [8] was used to assist in this analysis. It was used to predict ETS contaminant concentrations within three typical UK house types and to assess the ETS risk in bedrooms.

ANALYSIS PROCEDURE

Computer Model

BREEZE is a suite of integrated and user-interactive computer programs to evaluate ventilation rates and inter-zonal airflows in buildings, from single-celled to large multi-storey, multi-celled buildings. The building is taken to consist of a number of inter-connected zones with air moving from zones at high pressure to those of low pressure. The pressure differences are set up both by the actions of wind on the external surface of the building and by the temperature difference between air inside and outside.

In BREEZE, the user describes the geometry of the building by drawing the plans of the building on screen. He then superimposes air paths onto these plans, each air flow path being a window, a door, a crack, a vent or a fan.

BREEZE also includes a contaminant analysis routine which, given a contaminant emission, employs an adaptive step-length method to determine cell concentration histories and determine the time weighted average (TWA) for user set-time intervals. Possible contaminant sources can include those from outside air, sources within rooms or pollutants released from surfaces. Adsorption and desorption by surfaces can also be addressed. User contaminant inputs include emission rate, initial concentration and adsorption characteristics.

Housing types

Three types of houses were used for the analysis; one detached, one semi-detached and one terraced house. These are typical housing units in the UK and they are all two-storey structures. Their size, layout and window areas have been taken from 'benchmark' buildings developed for thermal modelling [9]. The plans of the houses are shown in Fig 1. It can be seen that they differ in size, internal layout and exposure to outside elements.

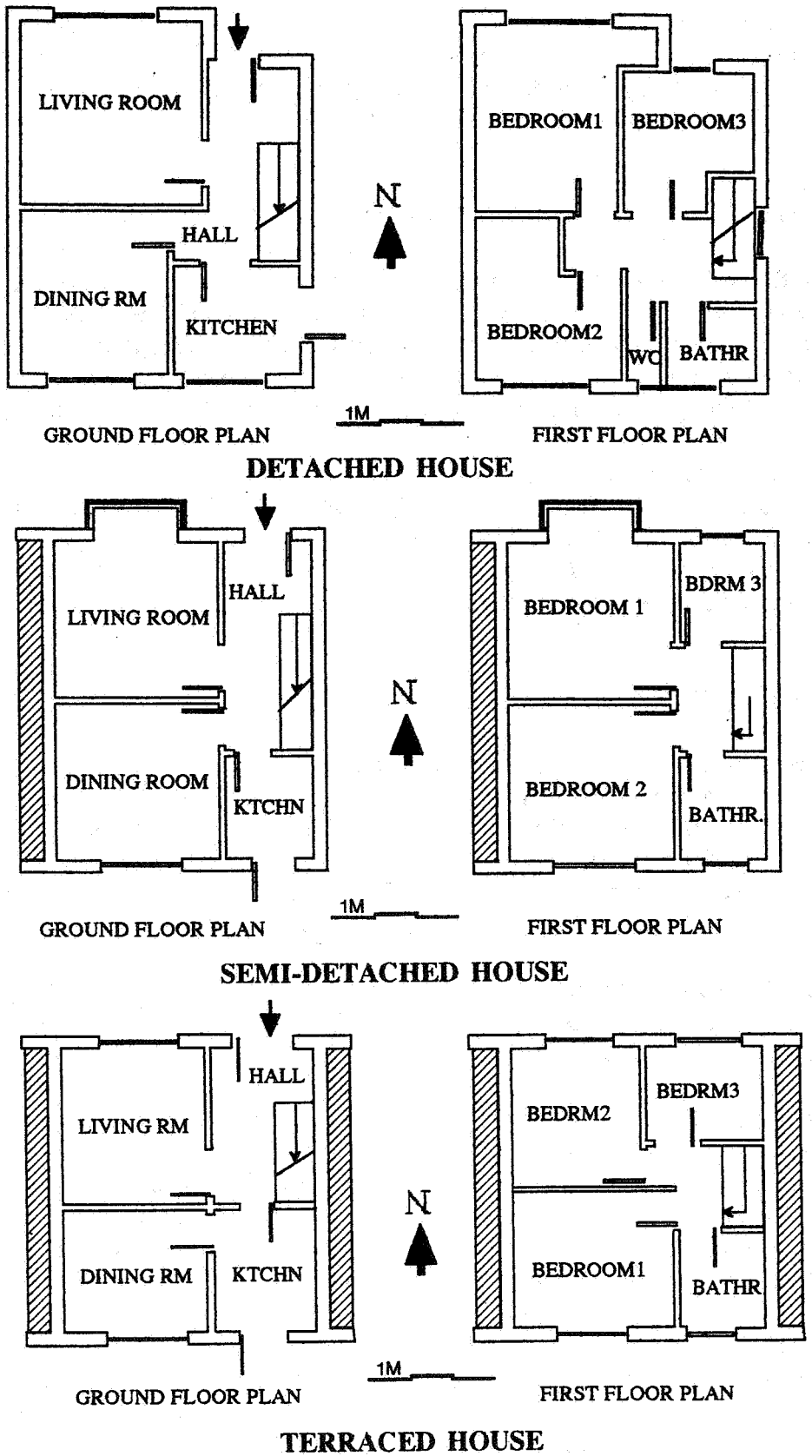

Figure 1: Floor plans of the detached, semi-detached and terraced housing types.

The ventilation strategies that were simulated fall into two categories:

a) preventing the spread of ETS from the source; and
b) diluting ETS concentration levels remote from source by fresh air ventilation.

Prevention (strategy a) is made possible by rapidly ventilating the smoking room, while dilution is carried out by removing the ETS that has migrated from the smoking room to the rest of the house. In these simulations, fresh air to remove and dilute is provided through external openable windows. Trickle ventilators, complying with the UK Building Regulations [10], are provided in each room of the house.

The following ventilation strategies were examined:

trickle ventilators; closed or open, upstairs or downstairs;
position of internal doors; closed or open;
opening windows;
operating extractor fans in the kitchen or bathrooms.

In all 21 simulations were carried out for each of the housing types (Table 1).

Table 1: House openings' configuration

Simulation Number	Windows	Internal doors	Trickle Ventilators
1	all closed	all closed	all open
2	all closed	all closed	all closed
3	all closed	all closed	closed upstairs
4	all closed	all closed	closed downstairs
5	all closed	s/r open	all open
6	all closed	b/r open	all open
7	all closed	b/r closed	all open
8	all closed	s/r closed	all open
9	all closed	all open	all open
10	all closed	all open	all closed
11	all closed	all open	closed upstairs
12	all closed	all open	closed downstairs
13	s/r open, ($0.1m^2$)	all closed	all open
14	b/r open. ($0.05m^2$)	all closed	all open
15	s/r open, ($0.1m^2$)	s/r closed	all open
16	s/r open, ($0.1m^2$)	b/r closed	all open
17	s/r open, ($0.1m^2$)	all open	all open
18	b/r open, ($0.05m^2$)	all open	all open
19	s/r + b/r open	s/r closed	all open
20	all closed	b/r closed	all open*
21	all closed	b/r closed	all open~

Note: s/r - smoking room, b/r - bedroom
* A fan is operated in the bathroom with extract flow rate 15 l/s
~A fan is operated in the kitchen with extract flow rate 30 l/s

Weather conditions

The outside air temperature was taken as 0°C to take into account winter conditions and the wind speed 4m/s. Wind from twelve equispaced directions were simulated for each of the ventilation strategies. Pressure coefficients were selected from a database available for UK houses [11]. Internal temperatures were fixed as 21°C in the living room, 20°C in all the other downstairs rooms and 17°C in the upstairs bedrooms.

Simulating cigarette smoking

Carbon monoxide (CO) and respirable particulate matter were used as markers for ETS. Although, these are two of the most important components in ETS, they are sometimes criticised as markers for ETS. This criticism usually refers to field studies where there is interference from other pollution sources [12]. However, this is not a problem in modelling.

The ETS simulation assumed light smoking by one adult in the household and, in this case, was represented by three cigarettes per hour being smoked in the living room (nominated as the smoking room) over a period of two consecutive hours. In this study we used an emission value of 34.4 mg/cigarette of particulate and CO together obtained from the EPA Indoor Air Database [13]. This is equivalent to an emission rate of 1.72 mg/min.

This study did not consider adsorption/desorption of ETS by internal surfaces although this does play an important part in ETS migration. However, it was considered that a useful investigation could still be undertaken to assess different ventilation strategies without including adsorption/desorption.

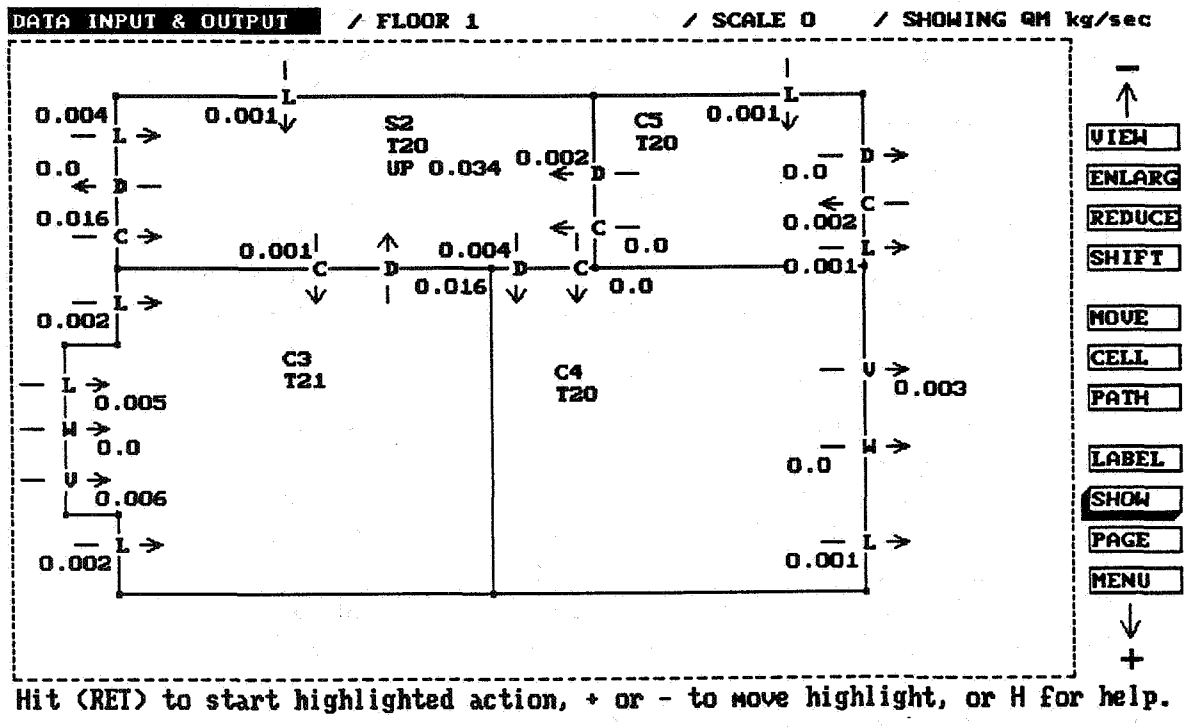

Figure 2: Graphical output from BREEZE. It shows the ground floor of the semi-detached house for one of the simulations.

SIMULATION RESULTS

Table 1 lists the ventilation strategies simulated. Figure 2 shows an example of the air flow results produced by BREEZE. The numbers indicate the air flow in kg and the arrows the direction of the flow. The symbols on the walls stand for doors (D), windows (W), ventilators (V), leakage (L) and crack (C). The symbols inside the rooms indicate a cell (C) or a stairwell (S). In addition the temperature of the rooms is shown (T).

BREEZE output also includes the pollutant concentrations from which TWA values are calculated and displayed. In these simulations, 15-minute TWAs of the combined concentration of CO and particulate matter were calculated for each of the simulations. Figure 3 shows examples of the individual simulation results for the twelve wind directions for the case of the terraced house.

Internal doors and windows closed

Figure 3a shows results from simulation # 1 with internal doors and external windows closed but with trickle ventilators open. The resulting air change rate for the whole house is 0.7 per hour, an average value for the 12 wind directions. ETS concentrations are highest for wind direction east to west with the smoking room facing north. The ETS concentration is high in the smoking room (average value 4 ppm with a minimum of 2 ppm for wind direction 0°(North), and a maximum of 5.5 ppm for wind direction 90° (east) and 270° (west). However, the concentration in the upstairs bedrooms is considerable lower, < 1 ppm in all cases (Fig 3a). Because of the high concentration in the smoking room ETS will migrate to the bedrooms long after smoking has ceased.

Internal doors open and windows closed

Figure 3b shows the results of simulation # 9 where all the internal doors were now opened. Compared to simulation # 1, the air change rate has increased by about 25% to 0.9 per hour. As a result, the ETS concentration in the smoking room is now reduced considerably to an average value of 1.5 ppm and in the bedrooms is lower than 1 ppm for all wind directions. As in the previous case, ETS concentration is greater for wind direction east to west with the smoking room facing north.

Smoking room window open

Figure 3c shows the results of simulation # 15 where the smoking room door is now closed and the window is kept slightly open. All other internal doors open are still kept open. The whole house air change rate has increased to 1.2 per hour. The ETS concentration in the smoking room is now less than 1 ppm for all wind directions and the concentration in the bedrooms becomes very small (less than 0.25 ppm in all cases).

Extractor fans

Figure 3d shows the results of simulation # 21 where an extractor fan with flow capacity of 30 l/s (as required by the 1990 Building Regulations for England and Wales for removal of excess humidity [10]) was operated in the kitchen during the 2 hrs that smoking took place in the living room. All windows in the house are assumed closed, trickle ventilators open and the bedrooms' doors closed to reduce migration of ETS. The ETS concentration in the living room is less than 1.5 ppm and the concentration in the bedrooms is very small.

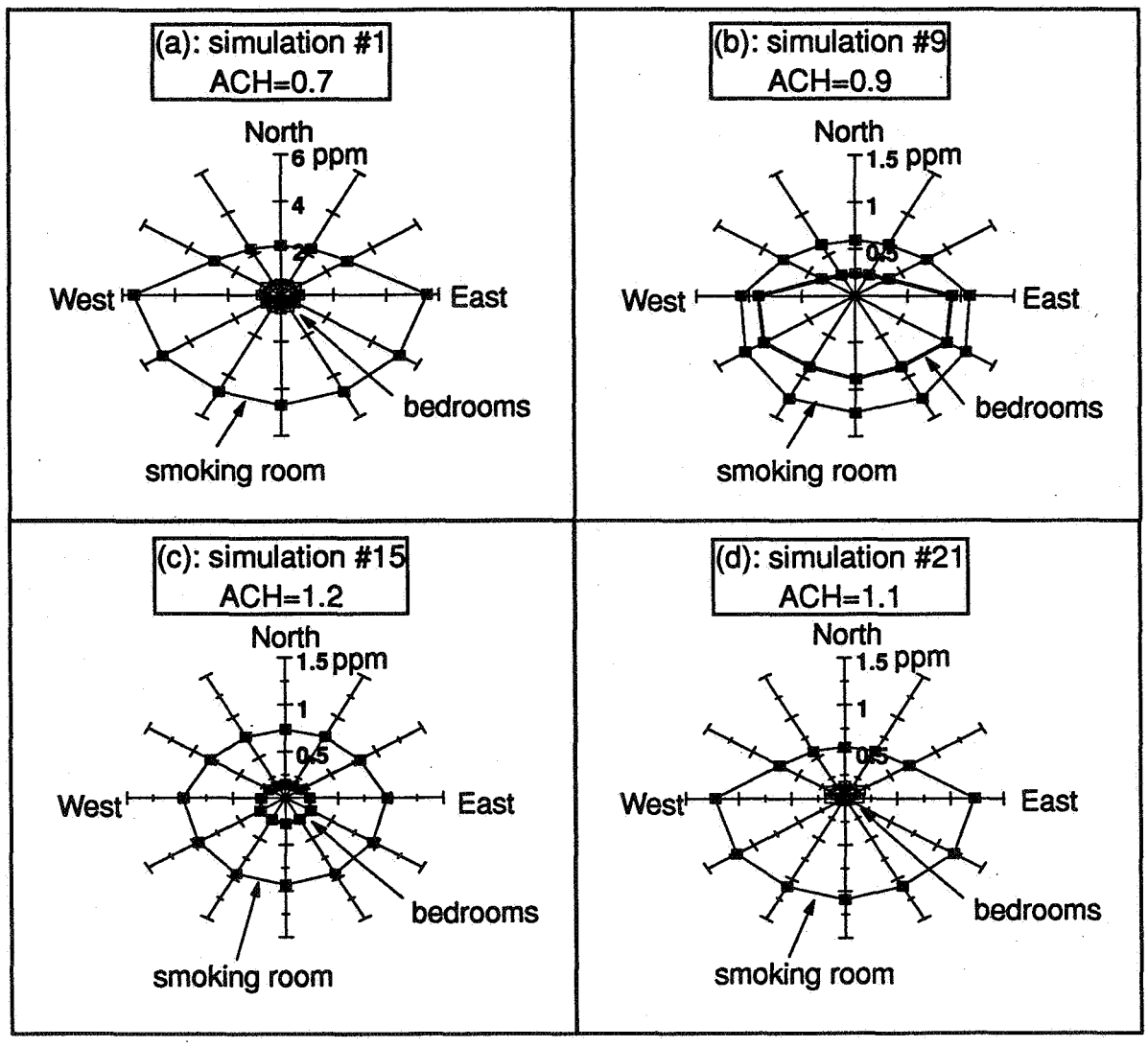

Figure 3: ETS concentration in the smoking room and the three bedrooms for 12 wind directions for four simulations. The wind speed is 4m/s, internal temperature 17-21°C and the external temperature 0°C.

Summary of simulation results

Figure 4 shows the mean TWAs for the 12 wind directions for all the simulations. The whole house predicted air change rate is shown on the graph. The lowest concentration of ETS is observed in the detached house and the highest in the terraced house. Air change rates are higher in the terraced house than in the detached. The higher concentration of pollutants could be attributed to the difference in their volumes, ie the pollutants are diluted more in the bigger volume of air of the detached house. Common sense suggests that smaller dwellings like flats and maisonettes might be more problematic. It should be noted that, many young families tend to live in smaller accommodation where babies might be exposed to higher ETS levels for similar smoking patterns. It is a similar problem to the one where high moisture levels are usually more evident in small densely occupied dwellings.

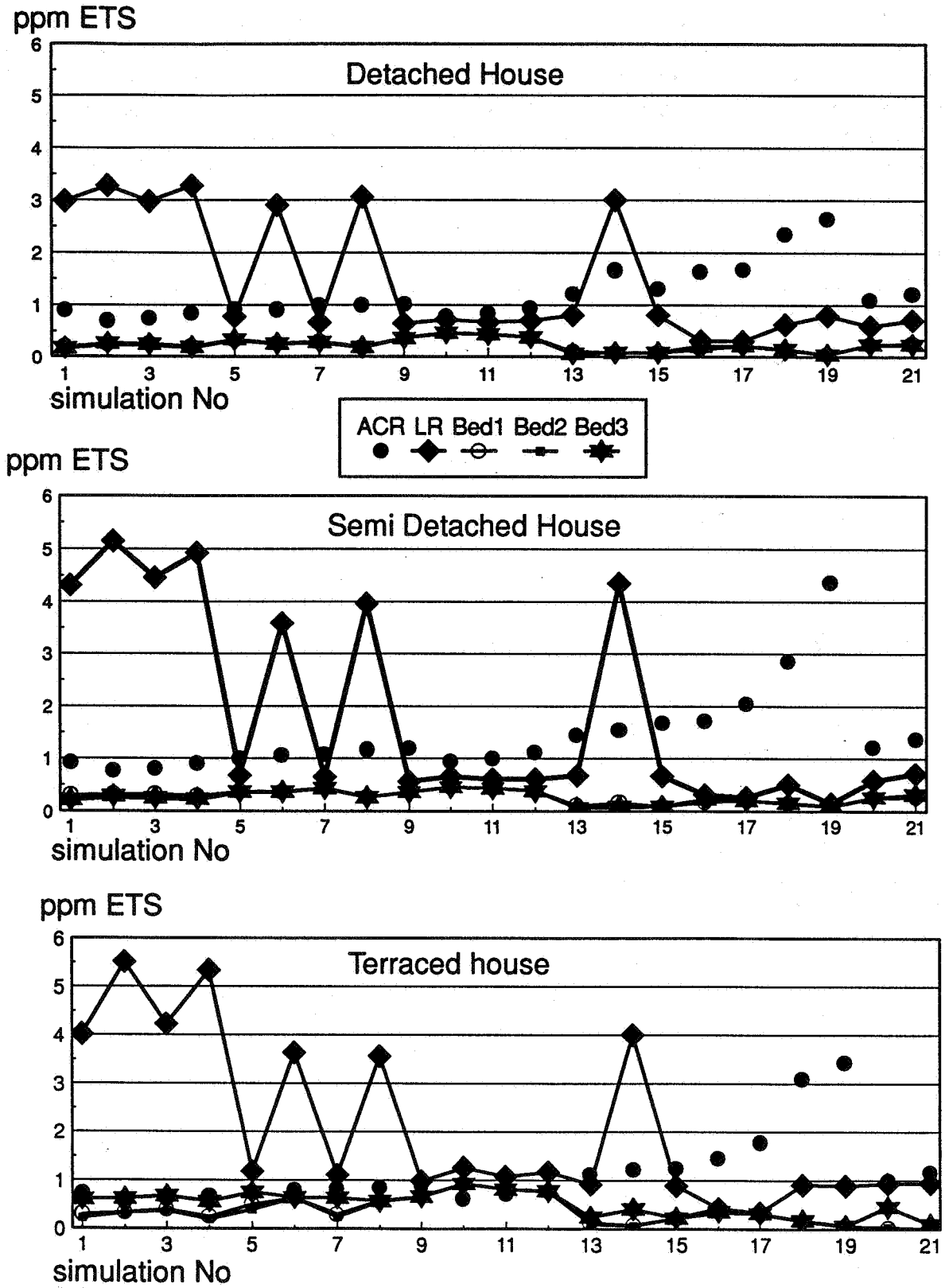

Figure 4: The average concentrations of ETS and air change rates for the three housing types for the 12 wind directions. The wind speed is constant at 4m/s, the external temperature 0°C and the internal temperature 17-21°C.

This suggests that measures that have been used to reduce problems associated with high moisture levels in homes could be also useful for the extraction of ETS pollutants. This strategy was investigated with simulations 20 and 21. It was found that using a (kitchen or bathroom) fan, the air change rate increased marginally (as expected) but that the ETS concentrations were considerably reduced; compared with simulations where the windows were kept closed. On average, kitchen or bathroom extract devices can more than halve the concentrations in the bedrooms.

However, these concentrations can be further reduced if windows are opened instead. There are exceptions such as when using the kitchen fan in the terraced house where concentrations are lower than in cases with open windows. This finding poses a dilemma as to which is the best approach and the choice would depend on external conditions (cold or warm days)

During warmer days, ETS levels can be kept low throughout (simulation no 19) by closing the smoking room door whilst opening windows in the smoking rooms and the bedrooms and leaving all other internal doors open. This will also provide enhanced ventilation for cooling.

Another interesting observation concerns the presence of trickle ventilators. Their effect could be seen in the smoking room for simulation 1 to 4. Opening the trickle ventilators affects the ETS concentration in the living room only marginally. Although the effect is shown to be small in this particular case, it might be significant for other internal pollutants such as metabolic CO_2 both in houses and commercial buildings.

Comparison with field studies

The results presented here were compared with measurements carried out in a recent field study of ETS in houses [6]. In that study, measurements were carried out with the doors of the house open. The air change rate was measured between 0.5-1.0 per hour and the smoking session lasted 4.5 hrs with a frequency of one cigarette every 20 to 30 mins. Particulate matter in the range of 330-500$\mu g/m^3$ (equivalent to 0.4-0.6 ppm) was measured. This is similar to simulations # 9 to 12 in our study where the particulate matter ranged between 0.2 and 0.45 ppm assuming a 1:2 split between CO and particulate matter.

Similarly, CO and respirable dust was measured in a range of renovated Dutch homes[15]. Respirable dust was found to be a problem in smokers' houses and measurements in the range of 2000 $\mu g/m^3$ (approximately 2.5 ppm) were observed in rooms where people smoke. This is certainly consistent with our simulations which indicate that particulate concentrations could range between 0.5 and 4.5 ppm during smoking in the smoking room and the concentration depends both on the pollutant removal strategy and on the ventilation rate.

CONCLUSIONS

This is the initial phase of a programme of the work for DOE Toxic Substances Division to investigate various simple natural ventilation strategies which could mitigate the effect of ETS on children in their bedrooms caused by tobacco smoking in the living room. The multizoned air flow and pollution transport software package BREEZE was used to simulate the transport and time-averaged concentration for various internal door and external opening configurations and a variety of external conditions to include different wind directions and temperature ranges.

We considered the impact of two obvious ventilation strategies to assess this evaluation process. The strategies considered here are;

a) isolation of the source and,

b) dilution of the contaminant.

In summary we can extract the key cases which provide us with alternative suitable strategies which are discussed below. Figure 5 shows the simulation results for the case of the terraced house.

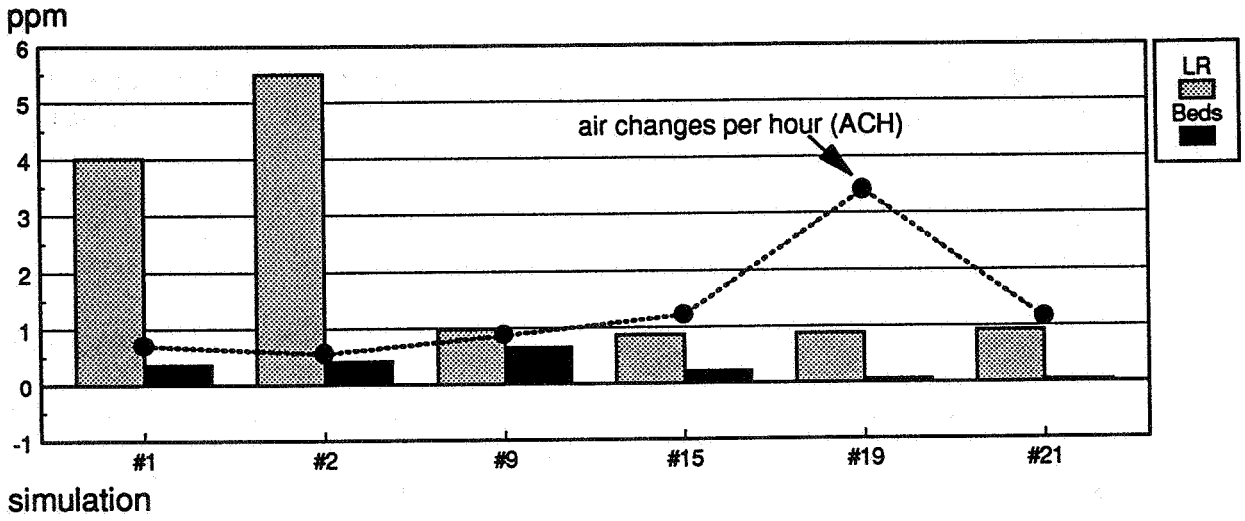

simulation	windows	internal doors	trickle vents	fans
1	closed	all closed	open	off
2	closed	closed	closed	off
9	closed	all open	open	off
15	s/r open	s/r closed	open	off
19	s/r+b/r open	s/r closed	open	off
21	closed	b/r closed	open	kitchen 30l/s

Figure 5: The ETS concentration levels in the terraced house for six alternative ventilation strategies

During the heating season, the best protection is to prevent the spread of ETS by opening the smoking room window slightly and closing the smoking room door. In this way, low concentrations of ETS are established in the smoking room and in the rest of the house. The position of the internal doors in the rest of the house does not have any significant effect on the migration of ETS. However, extract devices such as fans or passive stack ventilators usually installed for humidity control in the bathrooms and kitchens could be used

alternatively to reduce the concentration levels considerably without the uncomfortable effects of opening windows during cold days in winter. Using the kitchen fan appears to be more effective in smaller dwellings. In the larger house the bathroom or kitchen fan appear to be equivalent and produce relatively smaller changes. This is due to the large volume of air in the building which helps to dilute the ETS.

During warmer days, an alternative approach is to open the windows in the bedrooms, but still keeping the smoking room internal door closed and its window open. Higher air change rates will be created this way which will help to dilute the ETS further.

Acknowledgements
Thanks to Eric Solomon of Engineering Computations Ltd who prepared the data for the case-studies, Winnie Tse who ran some of the simulations and Martin Smith for useful advice on how to use BREEZE.

REFERENCES

1 The fourth report of the independent scientific committee on smoking and health - the Frogatt report, HMSO, 1988.
2 Environmental Protection Agency, Respiratory health effects of passive smoking: Lung cancer and other disorders, *EPA/600/6/90/006F*, December 1992.
3 Law M R, Buildings and Health, Part 3: Environmental tobacco smoke, *Building Research Establishment Note N168*, Garston, BRE,1992.
4 Ranson R, *Healthy housing: A practical guide*, E & F N Spon on behalf of the WHO, 1991.
5 Mansson L G and Svennberg S A , The influence of Indoor Tobacco Smoking on Energy Demand for Ventilation, *Proceedings 14th AIVC Conference on Energy Impact of Ventilation and Air Infiltration, Copenhagen, Denmark, 21-23 September 1993*. pp 325-336.
6 Löfroth G, Environmental tobacco smoke: multi-component analysis and room-to-room distribution in homes, *Tobacco Control*, 1993, 2 : 222-225.
7 Kay D L C, Heavner D, Nelson P R, Jennings R A, Eaker D W, Robinson J B, DeLuca P O and Risner C H, Effects of Relative Humidity on nonsmoker response to environmental tobacco smoke, *Proceedings Indoor Air '90, Volume 1: Human Health, Comfort and Performance, Toronto, 29 July- 3 August 1990*. pp275-280.
8 Building Research Establishment, *BREEZE 6.0, User Manual*, Garston, BRE, September 1993.
9 Allen E A and Pinney A A, Standard dwellings for modelling: details of dimensions, construction and occupancy schedules, *Technical Note 90/2, BEPAC*, July 1990.
10 The Building Regulations 1991, Part F, Ventilation, HMSO.
11 BRE Database
12 Guerin M R, Jenkins R A and Tomkins B A, *The Chemistry of Environmental Tobacco Smoke: Composition and Measurement*, Lewis Publishers, 1992.
13 Sparks L E, Indoor Air quality Model, *U.S. Environmental Protection Agency*, 1988.
14 ASHRAE Handbook - Fundamentals, Chapter 11 - Air Contaminants, SI Edition, 1989.
15 J F van der Wal, A M M Moons and H J M Cornelissen, Indoor air quality in renovated Dutch homes, *Indoor Air*, 4, 621-633 (1991).

The Role of Ventilation
15th AIVC Conference, Buxton, Great Britain
27-30 September 1994

Predicted and Measured Air Change Rates in Houses with Predictions of Occupant IAQ Comfort

T Hamlin* W Pushka**

* Buildings Group, Energy Efficiency Division
CANMET/NRCCan, Ottawa, Canada

** Research Division, Canada Mortgage and Housing Corp, Ottawa, Canada

Abstract

The purpose of this study was to test an Indoor Air Quality model on a variety of Canadian homes, and use this model to determine the optimal ventilation levels necessary to provide appropriate comfort levels.

The Indoor Air Quality model tested (the AQ1 program), was a single zone hour-by-hour model of air leakage, mechanical ventilation and pollutant concentration. Measured weekly air change rates were compared to the model's predicted rates, and sensitivity analysis' performed on a number of inputs. The model was exercised under a number of different conditions, and its limitations and reliability were investigated.

The AQ1 model was then applied to some current Canadian household characteristics. The relationship between air tightness and carbon dioxide concentrations in typical Canadian homes was calculated, and the ventilation requirements to provide a reasonable level of comfort in Canadian homes was estimated using carbon dioxide concentration as an indicator.

The AQ1 Model

The AQ1 program was designed to provide a quick algorithm with relatively few inputs, that would accurately describe hourly ventilation/infiltration rates and pollutant concentrations. The model uses a single zone method, whole building airtightness, hourly weather data and apparent pollutant source strengths to model indoor air quality. The program uses the AIM-2 infiltration model by Walker and Wilson to calculate natural infiltration (4), the fan model by Palmiter to calculate fan/air leakage interactions, and a pollutant concentration method as developed by Palmiter and Bond (7). A minimum temperature difference of two degrees was assumed to always exist during heating seasons to account for solar and internal gains. The stack effect pressure therefore can only go to zero for a house in airconditioning mode.

The pollutant model calculates concentration in accordance with the following equations. The effect of pollutant absorption and reemission is not accomodated, however, since the source strengths used are "apparent source strengths", the predicted concentrations will be correct for the same time base as the measurements. The apparent source strength is measured by taking simultaneous concentration and air change rate measurements. The equation used to calculate pollutant concentrations where the air-change rate is greater than 0.0001 is:

$$C_1 = C_0\, e^{-at} + S(1-e^{-at})/f$$

and

$$C_1 = C_0\, e^{-at} + S(1-a(0.5 + a/6))/V$$

if it is less.The average concentration for an hour is then;

$$C_{av} = (C_0-C_1)/a + S/f$$

if the air-change rate is greater than 0.0001/hr, and

$$C_{av} = (C_0+C_1)/2$$

if it is less. Thusly the concentration does not blow up severely at low air change rates.

Where C_1 is the new concentration (ppm).
C_0 is the original concentration (ppm).
a is the air change rate (h^{-1}).
t is time (hours).
S is the apparent pollutant emission rate (mL/h).
f is the flow rate (m^3/h).
V is the house volume (m^3).

The apparent pollutant emission rate is measured using simultaneous pollutant concentration and air change rate measurements. This apparent emission rate, therefore avoids the need to model absorption of non-emitting surfaces. The critical level of analysis was considered to be the concentration that occupants are exposed to.

The model simulates the control of mechanical ventilation, based on a schedule or the sensing of indoor/outdoor temperature differentials. This feature could also be used to simulate outdoor temperature controlledventilation or the opening of windows on a warm day. Imbalanced mechanical ventilation affects envelope presurres and this fan interaction effect of reducing air leakage is modelled.

Methodology

A total of 81 houses were chosen from 3 different studies (3), (5), and (6). The purpose of these studies varied from testing for VOCs (volatile organic compounds) to general indoor air quality. There was sufficient information on 81 of the houses to test the ventilation/infiltration aspects of the AQ1 model. House measurements had been taken for week long periods in January to April in 10 different cities across Canada.

An initial simulation was performed and after discounting for outliers, an adjusted R-squared value between expected and known PFT was determined. Sensitivity analysis and levels of error were determined for a number of variables, including wind effects, building altitude, set points, house heights and flue heights.

Since the data being tested had been gathered for purposes other than testing the AQ1 model, there were a number of uncontrolled factors contained in the measured data. Specifically, the air change rates would have changed due to the opening of windows on warm days, the opening of doors as people entered and exited the homes, the use of fireplaces, etc. It was felt that the largest variation would be due to the opening of windows on warm days, therefore, additional simulations were conducted using outdoor temperature controlled ventilation on the model to simulate this behaviour.

Using current Canadian housing characteristics, the AQ1 model was used to determine the relationship between air tightness and Carbon dioxide concentrations. House occupancies ranged from 1 to 6 people (within two standard deviations) and house sizes ranged from 300 to 800 m^2. Using the American Society of Heating Refrigeration and Air-Conditioning Engineers (ASHRAE) recommended 1000 ppm as a maximum concentration to maintain a reasonable 'comfort' level over time, minimum ventilation requirements were determined for the various occupancy and house size

ranges.

Discussion and Results

The refined simulation involved 80 houses. Opening of windows was simulated with an air change rate of 500m³/h when the differential between the outdoor and indoor temperatures was less than 5 Celsius. See Graph #1. The inverse airchange rate or turnover times predicted by the model were integrated over the measurement period in order to make the results comparable. Outliers were removed as it was not possible to verify the suspect model input parameters, leaving 72 houses. The standard error of estimate between the calculated and measured PFT values was found to be 0.1. This level of error is smaller than a the common ventilation rate target of one third air change per hour. It should also be remembered that the behaviour of the inhabitants is not known in the houses, therefore increasing the expected variance in the outcome.

Error levels were compared against different variables. It was found that a relationship existed between the level of error and wind speed. See Graph #2. It appears that the AQ1 model begins to break down at high wind speeds. However, with only five houses experiencing high wind speeds, a definitive conclusion cannot be made. This breakdown was expected in that local envelope pressures are highly variable due to wind turbulence, building shape, etc and local terrain shielding could also be highly variable.

Sensitivity analyses were conducted on a number of inputs. These included building height, flue height, heating set points, cooling set points, and elevation above sea level. It was found that 30% changes in these variables had less than a 10% change in the air change results.

The AQ1 model was then applied to some current Canadian household characteristics. The relationship between building leakage and carbon dioxide concentrations on a seasonal basis is described in Graph #3. In typical Canadian climate, the homes would not be heated from May to September. During this period the occupants would have the option of opening their windows to ventilate their homes, without affecting their heating costs. In the months outside of this period, the highest pollution concentration levels were found in the month of October.

ASHRAE recommends that in order to maintain reasonable comfort, carbon dioxide levels not exceed an average 1000 ppm. Using October as the worst case period, and with a continuous occupancy of three people, the number of hours in which a group of houses exceeded the 1000 ppm target in the month were calculated. The data was obtained from (1). Averages of building heights and air-tightness exponents were used for four age groups in three regions. The 50th, 75th and 90th percentile results were used. See Graph #4.

Conclusions

The AQ1 model was found to be reasonably accurate in determining the ventilation/infiltration levels in an average home. The standard error of estimate between the calculated and measured weekly airchange rates was found to be 0.1. This level of error is smaller than a theoretical target of 0.33 ach.

Houses in British Columbia are still very loose. However, recently built houses in Ontario and the Prairies have shown considerable increases in their air-tightness. Some of these houses would require mechanical ventilation in the spring and fall to keep carbon dioxide levels in a comfortable range.

References

(1) Cooper, K., Moffatt, P., Palmiter, L., "Indoor Air Quality Analysis for Detached Residences", CMHC research report, Ottawa, Canada, July 1992.

(2) Hamlin, T., Cooper, K., "Ventilation for Energy Efficiency and Optimum Indoor Air Quality", 13th AIVC Conference, Nice, France, September 1992.

(3) Hamlin, T., Forman, J., Lubun, M., "Ventilation and Airtightness in New, Detached Canadian Housing", ASHRAE Symposium paper, Indianapolis, U.S.A., June 1991.

(4) Walker, I.S., Wilson, D.J., "The Alberta Air Infiltration Model AIM-2", University of Alberta, Dept. of Mech. Eng. Report 71, Edmonton, Canada, January 1990.

(5) Dumont, R., Snodgrass, L., "Volatile Organic Compound Survey and Summarization of Results", Saskatchewan Research Council, Saskatoon, Canada, January 1992.

(6) Bowser Technical Inc., "Testing of Older Houses for Microbiological Pollutants", CMHC research report, Ottawa, Canada, December 1991.

(7) Palmiter, L., Bond, T., "Interaction of Mechanical Systems and Natural Infiltration", 12th AIVC Conference pp285-295, Ottawa, Canada, September 1991.

Graph #1 - PFT Measured vs. PFT Calculated

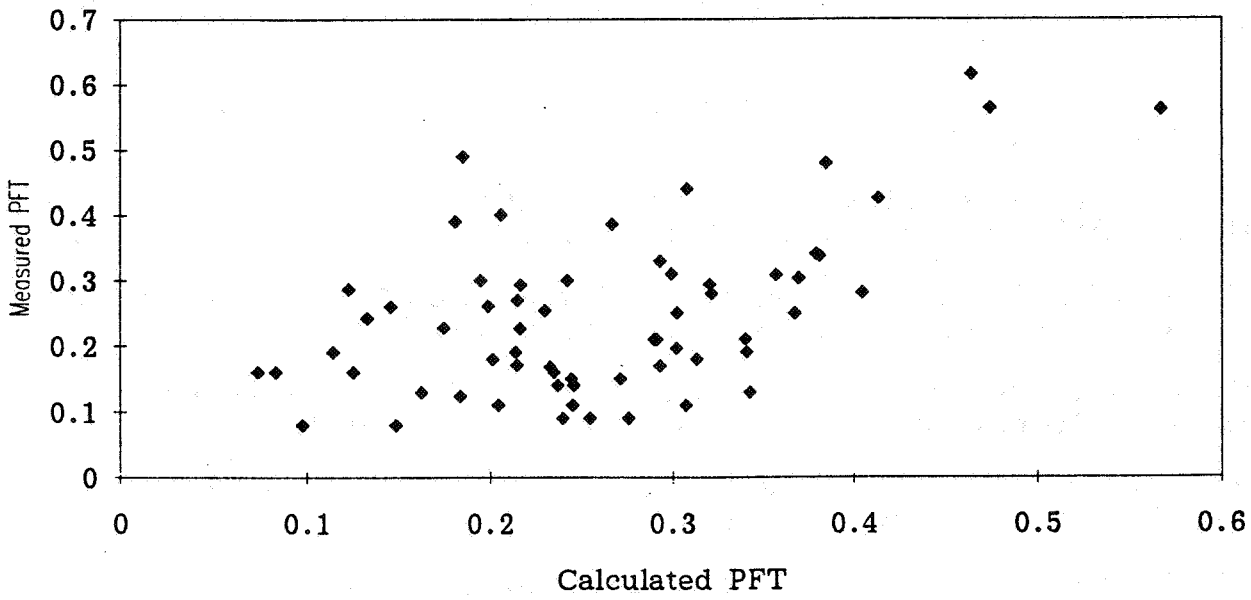

Graph #2 - Error vs. Wind Speed

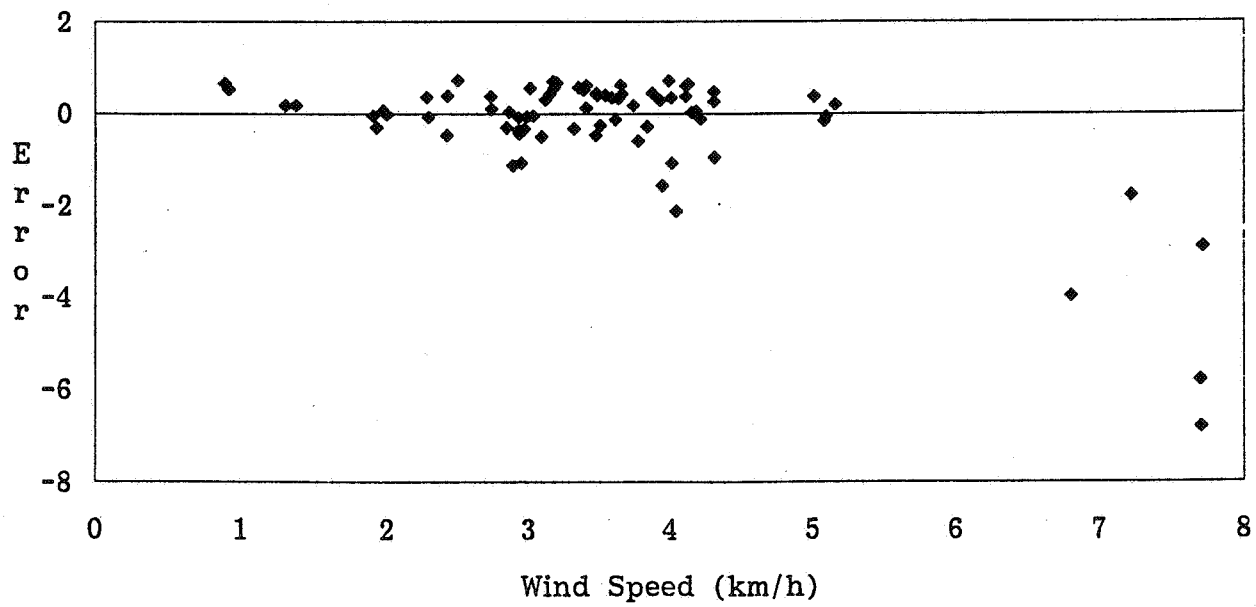

Graph #3 - Mean Pollutant Concentrations (ppm) where Ventillation Rates Range from 50 to 250 Cubic Meters per hour with a Full-Time Occupancy of 3 People

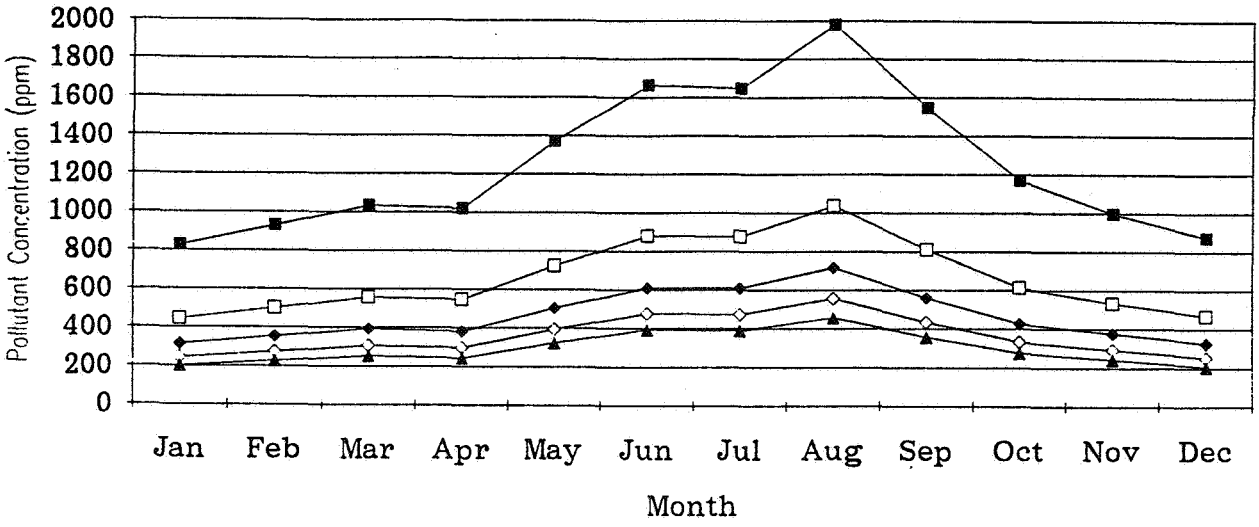

Graph #4 - Number of Hours in October where pollutant concentrations exceeded 1000ppm

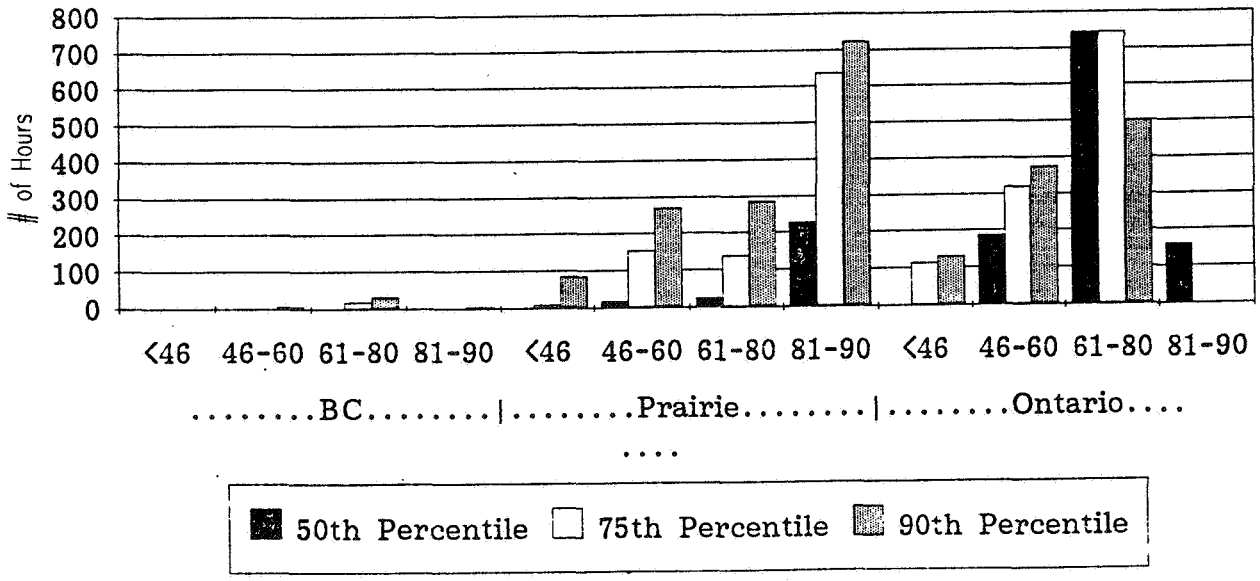

The Role of Ventilation
15th AIVC Conference, Buxton, Great Britain
27-30 September 1994

The Air Lock Floor

H J C Phaff, W F De Gids

TNO Building and Construction Research, P O Box 29,
NL 2600 AA Delft, The Netherlands

SYNOPSIS

The Air Lock Floor and the Pressure Ring are two effective measures for control of air flow directions between rooms or zones in buildings. They create a pressure hierarchy that controls spread of pollutants.
Here an example has been given for radon from a crawl space, odours from a bakery into a dwelling above and an isolation chamber with a leaky facade.
The Air Lock floor can operate with a 7 W fan and at the same time extract the normal dwelling ventilation flowrate. Used in the ground floor, the Air Lock Floor results in a warmer floor and contributes to energy savings. The now well ventilated, warmer and dryer crawl-space would make the use of wooden (plywood) floors possible with less risk of wood rot and mould growth.

1. INTRODUCTION

A large proportion of ventilation problems consists of air borne contaminant control in buildings. Reduction of pollutant sources always has the first priority. Air flow directions and optimal ventilation flow rates are second. In this paper only this second step is considered, assuming all possible actions for source reduction have been applied.

In most cases the spread of pollutants through buildings is totally determined by the entrainment of contaminants by air, moving in one room and from room to room.
This makes systems that control a sufficient pressure hierarchy between rooms very effective. The Air Lock Floor and the Pressure Ring are such systems. They both consist of combinations of existing techniques. But especially their combinations deliver unprecedented results.

Room to room diffusion of air borne concentrations through separation walls is often totally negligible and not taken into account here.
Dependent on the specific pollutant substance, in a small number of cases walls themselves might be the source of the pollutant. Then pressure can have a complicating effect on the source strength, which is not considered in this paper.

It is easy to say that a desired pressure hierarchy should be generated by a system and maintained at all conditions. Unfortunately in buildings where doors and windows will be opened and closed, or walls are leaky, large system air flow rates might be necessary to keep up the pressure differences. More over these necessary system air flow rates can change dramatically and very fast in time. On the other hand buildings, seen as a ventilation network of rooms of linked by cracks, doors, windows and (HVAC)systems, have an astounding level of self correction to disturbances. This is caused by the non linear relation between pressure over, and flow rate through the network links.

It all comes down to selecting the best place and kind of system to generate a pressure hierarchy, insensitive for disturbances. The Air Lock Floor and the Pressure Ring are thought to have good chances for this.

2. METHOD

The desired pressure hierarchy will have over pressure in rooms that are to be protected from pollutants. Polluted zones are kept at a low pressure, or if that is not possible they must be totally surrounded by a space or a connected series of spaces kept at low pressure. Pressures in the range of 1..10 Pa would be sufficient in most cases. Pressures over internal walls in low rise buildings rarely are larger than 10 Pa or one or more windows/doors are kept open at high wind.

High rise buildings are to be looked at separately as buoyancy pressures can amount approximately 0.04 Pa/(m.K). At 30 K temperature difference in a 100 m high building a pressure of 120 Pa could exist mostly subdivided into smaller fractions over a series of compartments.

The necessary flow rates at this 1..10 Pa totally depend on the leak of the walls over which the pressure should be maintained. Typical air leaks in room to room partition walls (as in dwellings) will yield flow rates in the order of magnitude of 0.02 m^3/s at 1..10 Pa. For outside walls this may be in the order of magnitude of 0.005 m^3/s per room at 1..10 Pa.

3. THE AIR LOCK FLOOR

The Air Lock Floor (ALF) was originally designed to prevent infiltration of crawl-space air in houses for a number of pollutants from the soil (moist, radon, soil pollution). It was developed and tested in the ventilation models (VenCon/COMIS). Figure 1 shows ALF in the dwelling. It consists of a number of parts and measures:

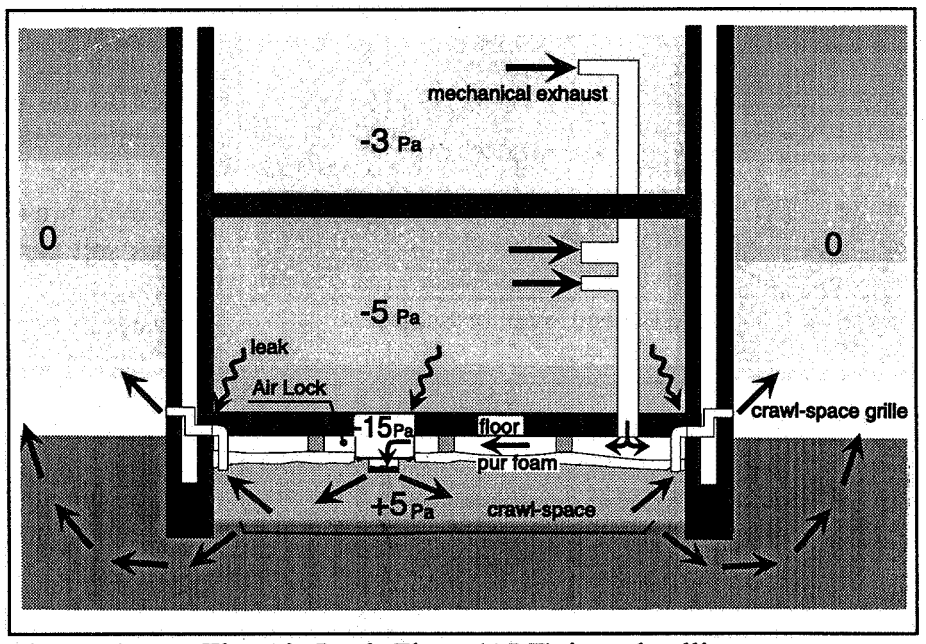

Figure 1 The Air Lock Floor (ALF) in a dwelling.

- a plastic foil over the crawl-space dirt floor (not airtight to the foundation walls)
- reduction of leaks in the floor to a total of less than 40 cm^2

- an airtight PUR insulation foam on a net, a few cm below the floor, airtight to the foundation walls, including the fan in a second crawl-space hatch.
- connection of the dwelling ventilation ducts to the cavity between the PUR layer and the floor.

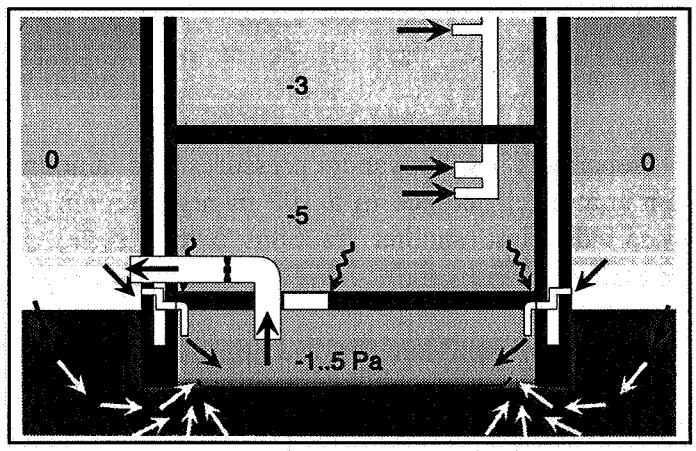

Figure 2 Crawl-space under pressure.

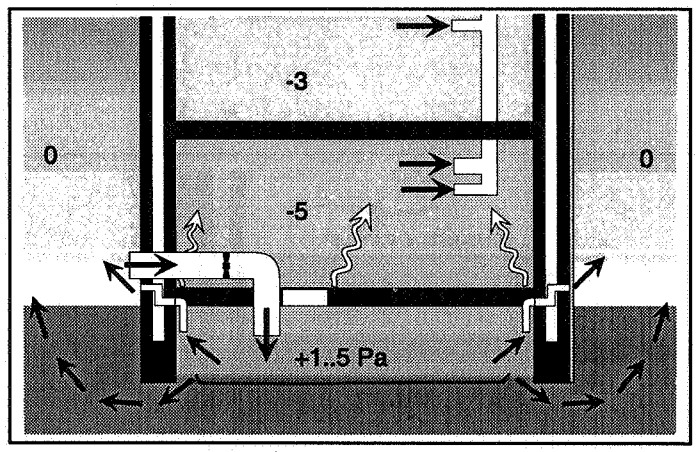

Figure 3 Crawl-space over pressure.

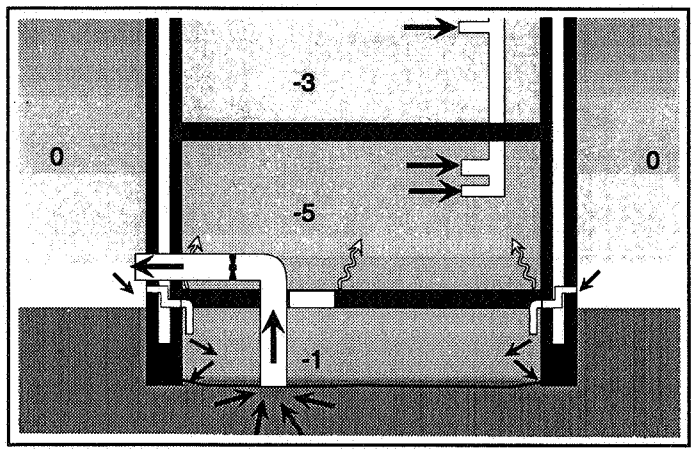

Figure 4 Sub Slab Depressurization.

Most floors in Holland are about or less leaky than 40 cm², but old houses or houses with wooden floors need extra attention and PUR-foam at the leaky parts.

The -10 Pa lower pressure in the Air Lock just below the original floor prevents any leak flow into the dwelling.
This -10 Pa serves as the driving force for the 'mechanical' dwelling exhaust ventilation. This bypass flow rate stabilizes the proper operation of ALF against any variation of the floor leak and increases the temperature below the floor close to the average dwelling temperature.

The dwelling ventilation flow rate is added to the crawl-space and dilutes concentrations a factor 3..10 .

The over pressure in the crawl-space forces soil gasses back into the soil.

The used mini-fan uses only 7 W for the radon reduction including the dwelling ventilation. Not many mechanical exhaust ventilation systems come close to this.
Noise of the fan is not noticeable, and in the prototype no sound insulation has yet been applied.

3.1. A combination of existing measures

In fact ALF is a combination of existing radon mitigation measures, but including the use of the dwelling

ventilation to boost the concentration reduction. An overview of existing measures is given by Henschel [HENSCHEL 1992].

Figure 2,3,4 show a crawl-space at under pressure, over pressure and the efficient sub slab depressurization method. ALF combines those three, and gets rid of disadvantages of the individual measures. Figure 2, the under pressure sucks more radon into the crawl-space and if anywhere the pressure hierarchy across the floor is not maintained, spread could be enhanced. Figure 3, the over pressure, would lead to very damp houses in Holland. Figure 4, the sub slab suction is effective but doesn't get rid of high radon concentrations at the foundation. Cracks (or diffusion from 30.000 Bq/m^3) there could spread radon.

3.2. Against radon from the soil

In a contract from VROM the Dutch Ministry of Housing, Environment and Town and Country Planning guided by the technical and financial control organisation NOVEM a test was made with a prototype of ALF in one house against radon according to figure 1.

The effectiveness of ALF is measured with SF_6 tracer gas injected in the crawl-space. With ALF in operation practically no spread into the dwelling occurs. The concentration in the house is than practically zero . ALF reduces the crawl-space concentration an additional 3 to 10 times, because the crawl-space ventilation is boosted by the dwelling ventilation flow rate which flows out through the crawl-space.

Some radon measurements were done but radon concentrations were low, about 15 Bq/m^3 in the living and the crawl-space. Therefore all radon reductions were calculated from the tracer gas measurements. It is expected that the extra flow through the crawl-space soil will result in an additional reduction of the radon transport, above the here calculated reduction.

ALF results in a warmer floor and can be operated with a 7 W mini-fan that also extracts the dwelling ventilation flow rate. This will yield some pay back.

Expectations.

According to the Dutch Base Document Radon (Basisdocument Radon) [VAAS 1991] the average contribution of soil radon amounts 60% of the concentration in Dutch dwellings. The tracer gas measurements show that the soil is totally eliminated by the ALF, resulting in a 60% radon reduction. Installation costs in existing dwellings are estimated US$ 1300 to $ 2000. A part of these costs can be compensated by the energy savings.

Alf will yield a large improvement in air quality (no more moist, radon, or other soil gasses from the crawl-space).

The less moist crawl-space could decrease the risk of wood rot for wooden (plywood) floor systems.

3.3. Against the spread of odours

In 1992 TNO was contacted in a long dispute between the occupant of a dwelling on floor 2..4 and the shop owner of a bakery and baker's business at the first floor (ground level). Baking smells, and heat infiltrated through the wooden floor into the dwelling. As most shops are at ground level, and many have dwellings, with different owners, on top, this is a very common problem. The dutch building codes demand gastight floors in this situation. But how tight is gastight, no one knows. And if known, it would not help as all floors leak (at least a bit).
It might be interesting to say that a gypsum board ceiling had already been placed under the wooden floor as fire retardant, but also it was thought to be gastight.

At TNO we 'smelled' our chance to apply the Air Lock Floor here, but the bakers advisor thought it would not be necessary.

The ceiling was removed and the wooden floor was sealed with several spray layers of PUR-foam. Half way leaks were made visible with smoke tubes to apply a final PUR-layer. A new gypsum board ceiling backed with a plastic foil was hung under the floor leaving a cavity between floor and gypsum of about 0.1 m .

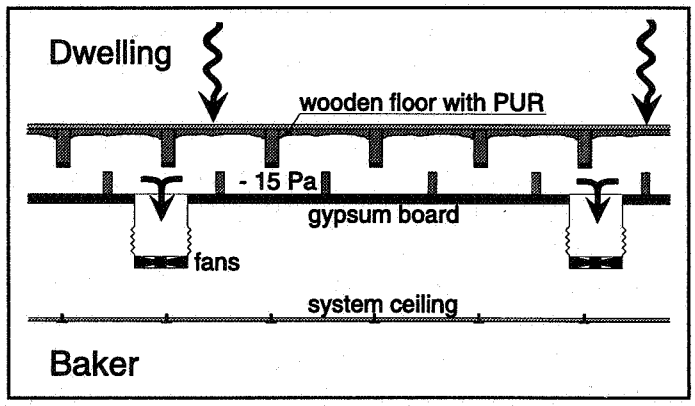

Figure 5 The Air Lock Floor principle in the floor between a bakery and a dwelling above avoids spread of smell.

Unfortunately for the baker, the smell complaints were not gone.

It didn't take much time to see where we could add our fans to create an ALF here and figure 5 shows the situation. An under pressure of 10..15 Pa could be created in the cavity under the floor. Smoke tests proved a reversed leak through the original wooden floor. Odours couldn't flow through the floor anymore.

It must be said that a large 0.3 m^3/s fan was necessary here because of large leaks at the facades between the walls and the gypsum board which had not been looked after carefully.

There still occurred some sporadic smell complaints that were caused by odours via the outside air. But during several visits of experts from the city building regulations and from TNO, things were very acceptable and greatly improved.
The occupant noticed that he had to make much more use of his heating system in winter.

4. THE PRESSURE RING

The pressure ring is a safe and simple construction that can be used for instance in hospitals and laboratories. A certain zone has to be kept at over or under pressure, but there is a leaky facade or neighbouring zone with varying pressure. Figure 6 shows a possible situation. In the protected room just behind the leaky facade a second facade is built. A duct with a larger cross section than the leak in the outside facade and the extra wall connects the newly formed pressure ring with the Lock at the corridor side of the room.

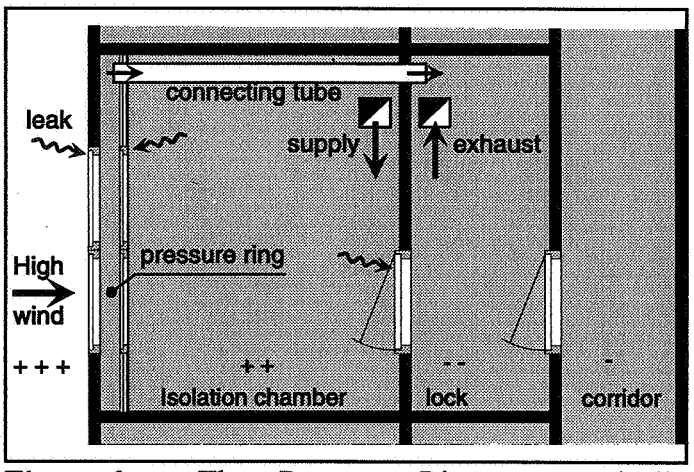

Figure 6 The Pressure Ring automatically protects the isolation chamber from infiltration through the facade.

5. CONCLUSION

The Air Lock Floor is a very promising but more complex system than existing measures. It prevents any infiltration from crawl-spaces into dwellings. It demands an accessible crawl-space with as little as possible separated compartments.

It can be operated with a very low power fan of 7 W.

The floor will get warmer, and in moderate/cold climates this will contribute to energy savings.

The principle of the Air Lock Floor could be used in many situations as the application in the ceiling of the ground floor of a baker's business indicates.

A construction quite similar as the Air Lock Floor is the Pressure Ring which eliminates unwanted leaks into a protected room, a hospital isolation chamber, or a laboratory room.

6. LITERATURE

HENSCHEL 1992 Henschel, D. Bruce. Indoor Radon Reduction in Crawl-space Houses: a Review of Alternative Approaches.

VAAS 1991 L.H. Vaas, H.B.Kal, P. de Jong en W. Sloof. Basisdocument radon. Rapport nr 710401014. RIVM Bilthoven 1991. (In Dutch)